

Preferred Posters – Symposium S5

Basic and translational aspects of tumour metabolism

PS5-01

**The acidotic metabolic microenvironment of tumors as a determinant for therapeutic efficacy and a challenge for functional imaging**

\*O. Thews

Martin-Luther-University Halle-Wittenberg, Julius-Bernstein-Institute of Physiology, Halle/Saale, Germany

The acidotic microenvironment in tumors results from the ability of tumor cells to perform glycolytic metabolism even under normoxia but also from an insufficient oxygen supply both leading preferentially to an extracellular acidosis. However, extra- and intracellular acidosis are known to activate numerous signaling pathways, such as MAP kinases, HIF-1 or CREB. However, the final acidosis sensing mechanism has not been fully understood today. Changes in these pathways not only modulate the transcriptional control in tumor and normal tissue cells but also the functional activity of cellular processes which, in return, affects the malignant progression or the efficacy of non-surgical treatment modalities. It has been shown that the extracellular acidosis enhances the metastatic potential of tumors in vivo even if the tumor cells have left the acidotic tissue and circulate in the blood (short term “memory” effect induced by acidic priming). Previous studies also demonstrated that low pH functionally activates active drug transporters, e.g. p-glycoprotein (Pgp), leading to a multidrug resistant phenotype. Here, the MAP kinases p38 and ERK1/2 play a key role in the cascade from pH sensing to Pgp activation. These results indicate the necessity of measuring metabolic parameters as well as the resulting cellular consequences in patients pre-therapeutically. With positron emission tomography (PET) it was possible to image non-invasively the acidosis induced Pgp activation leading to a reduced chemotherapeutic sensitivity of tumors. Using this techniques it is possible to adapt the therapeutic regime to the individual needs of the patient.

Supported by Deutsche Krebshilfe (grant 109136)

PS5-02

**Amino acids as metabolic target for the treatment of solid cancers - considerations and challenges**

\*L. Kunz-Schughart

TU Dresden, OncoRay - National Center for Radiation Research in Oncology, Dresden, Germany

Deprivation of single amino acids is a promising approach in metabolic anticancer therapeutics. Arginine, a semi-essential amino acid is for example targeted using the ar-

ginine-degrading enzyme arginine deiminase (ADI) which induced anti-proliferative effects, in particular in ASS-1 (argininosuccinate synthetase-1) auxotrophic cancers lacking ASS protein which converts citrulline to arginine. Other metabolic treatment strategies such as the application of recombinant human arginase are under development to enter clinical trial. Very recently, it has been shown that ASS-positive cancers may also be sensitive to ADI treatment and it was thus hypothesized that arginine starvation could in general sensitize cancer cells to chemo- and/or radiotherapy. Our first data in 2-D and/or 3-D culture models revealed that arginine starvation may indeed enhance the radiosensitivity of individual but not all ASS-positive cancer cells in vitro (colorectal and head & neck squamous carcinoma, glioblastoma). However, the mechanistic difference between responders and non-responders remains ambiguous. The challenges to study this phenomenon in vitro and for translation into animal studies and into the clinic will be discussed.

Beside arginine, restriction of methionine, an essential amino acid, has drawn lots of attention in metabolic anticancer therapy. However, in contrast to arginine, complete systemic deprivation is detrimental in humans and it remains a matter of debate if systemic reduction of this amino acid is sufficient in anti-cancer treatment when combined with other therapies. The presentation will give an overview about arginine and methionine as metabolic targets in cancer and will highlight important (patho)physiological concerns for the design of mechanistic studies.

PS5-03

**High lactate concentrations in head and neck squamous cell carcinoma and traumatized normal gingival tissue**

\*N. Voelxen<sup>1</sup>, T. Ziebart<sup>2</sup>, P. Knopf<sup>1</sup>, M. Henkel<sup>1</sup>, S. Walenta<sup>1</sup>, W. Wagner<sup>2</sup>, W. Mueller-Klieser<sup>1</sup>

<sup>1</sup>University Medical Center of the Johannes Gutenberg University, Institute for Pathophysiology, Mainz, Germany

<sup>2</sup>University Medical Center of the Johannes Gutenberg-University of Mainz, Department of Oral and Maxillofacial Surgery, Mainz, Germany

**Question:** Chronic accumulation of lactate in malignant tumor tissue is associated with increased malignancy and radio-resistance. For this study, biopsies of primary head and neck squamous-cell carcinoma (HNSCC) and of normal gingiva of the same patient were compared via metabolic profiling to healthy or metabolically stressed gingiva from cancer-free patients.

**Methods:** Cryobiopsies of 69 HNSCC-patients were used to determine ATP and lactate concentrations of tumor and normal gingiva via induced metabolic bioluminescence-imaging (imBi). Additionally, these metabolites were quantified in a collective of 43 healthy (non tumor-bearing) patients that were sub-divided into two groups according to the incidence of comorbidity (i.e. traumata: maxillary/mandibular fracture, dysgnathia).

**Results:** There were no significant differences in ATP concentrations detectable between tumor, normal gingiva of tumor-patients and gingiva from healthy patients. However,

comparing ATP concentrations from normal gingiva of tumor-patients to mucosa from healthy patients with and without traumata, significantly increased values were detectable in mucosa from healthy patients of both subgroups. Lactate concentrations were significantly increased in tumor tissue compared to normal gingiva of tumor-patients. Additionally, lactate concentration of gingiva from healthy patients with traumata was significantly enhanced compared to mucosa from patients without traumata.

**Conclusions:** We could demonstrate that lactate concentration in HNSCC correlates with primary tumor staging and nodal status. The presence of comorbidity, especially traumata, has an influence on the lactate concentration of healthy patients without cancer. Aim of this study is to identify metabolic parameters to improve early cancer diagnosis, allow predictions on the degree of malignancy and contribute to a personalized tumor therapy.

PS5-04

**Fractionated irradiation influences the tumor cell metabolism and mRNA expression of glycolytically relevant proteins in xenografts of head and neck cancer cell lines**

\*K. Goetze<sup>1</sup>, S. Meyer<sup>1</sup>, A. Yaromina<sup>2</sup>, D. Zips<sup>3</sup>, M. Baumann<sup>1,4</sup>, W. Mueller-Klieser<sup>1</sup>

<sup>1</sup>University Medical Center Mainz, Institute of Physiology and Pathophysiology, Mainz, Germany

<sup>2</sup>Technical University Dresden, OncoRay – National Center for Radiation Research in Oncology, Department of Radiation Oncology, Experimental Radiotherapy, Dresden, Germany

<sup>3</sup>University Hospital Tuebingen, Department of Radiation Oncology, Tuebingen, Germany

<sup>4</sup>Technical University Dresden, Experimental Center, Medical Faculty and University Hospital Carl Gustav Carus, Dresden, Germany

**Question:** Previous investigations on tumor xenografts of head and neck squamous carcinoma cells (HNSCC) suggest that metabolic changes during fractionated irradiation may limit the predictiveness of lactate for tumor radiosensitivity. Thus, the hypothesis of the current study was that tumor metabolism is influenced by a fractionated radiation scheme in HNSCC xenografts.

**Methods:** To investigate the effect of a clinically relevant fractionated irradiation scheme on tumor cell metabolism, xenografts of 4 HNSCC cell lines, which differed in their radiosensitivity were grown in nude mice. Tumor ATP and lactate content was analyzed with induced metabolic bioluminescence imaging (imBi) following 0, 3, 5, 10 and 15 fractions of radiation (fx). Using quantitative real time RT-PCR, changes in mRNA expression of 6 glycolytically relevant proteins (hk2, pfk2, gpi, pkm2, pdk1 and mct1) were measured at the same time points.

**Results:** In radiosensitive tumors UT-SCC-14 the expression patterns of 4 glycolytic enzymes (hk2, pfk2, pdk1 and mct1) was significantly increased after 3 fx, but decreased again to control levels after 10 fx. FaDu xenografts with an intermediate radioresistance showed a similar pattern. In contrast, two radioresistant cell lines (SAS and UT-SCC-5) showed no significant changes in mRNA expression over

the course of treatment. The changes in mRNA expression were accompanied by corresponding variations in ATP. Only radiosensitive and intermediately radioresistant xenografts (UT-SCC-14 and FaDu) showed a significantly reduced ATP content with increasing numbers of fx, whereas ATP was invariant in radioresistant xenografts (SAS and UT-SCC-5). Lactate content was reduced significantly in the course of radiation in 3 out of 4 tested tumor cell lines, which was unrelated to their radioresistance.

**Conclusion:** We have documented an impact of fractionated irradiation on mRNA expression and ATP content in radiosensitive but not in radioresistant tumors. Such radiosensitivity-related differentials in the early phase of radiation treatment could be exploited in the clinic for an individual adjustment of tumor therapy.

Supported by the DFG: MU 576/15-2, MU 576/17-1, BA 1433/4-2.

PS5-05

**Manipulation of tumor cell metabolism and its impact on radiosensitivity**

\*C. Fabian<sup>1</sup>, A. Siebers<sup>1</sup>, L. Binz<sup>1</sup>, D. Faber<sup>1</sup>, U. Sattler<sup>1</sup>, W. Mueller-Klieser<sup>1</sup>

<sup>1</sup>University Medical Center of the Johannes Gutenberg University Mainz, Institute of Physiology and Pathophysiology, Mainz, Germany

**Question:** Can manipulation of glycolysis and cellular respiration increase tumor cell sensitivity to radiotherapy? Methods: Two human ovarian cancer cell lines, IGROV-1 and OC316, were characterized according to their metabolic and radiobiological properties with and without addition of 2-deoxy-D-glucose (2DG, glycolytic inhibitor), of rotenone (ROT, respiratory chain blocker), or of 2DG and ROT in combination. Both cell lines were examined regarding their metabolic turnover rates using the Seahorse XF24/3 analyzer which allows for simultaneous extracellular measurements of oxygen consumption rates (OCR), acidification rates (ECAR) and carbon dioxide evolution rates (CDER) in vitro. Colony forming assays were accomplished from cells γ-irradiated with doses from 0-8 Gy. Induction and repair of double stand breaks were quantitatively evaluated through γH2AX foci 1 and 24 h after irradiation.

**Results:** OCR, ECAR, and CDER were significantly higher in OC316 compared to IGROV-1 cells. Non-toxic doses of 10 mM 2DG or 1 μM ROT, respectively, lead to a significant reduction of ECAR and OCR compared to control cells. Simultaneously γ-irradiation in combination with metabolic inhibitors resulted in a significant enhancement of radiation toxicity at a clinically relevant dose (2 Gy). The maximum decrease of clonogenic cell survival and the highest amount of γH2AX foci 1 and 24 h after irradiation were induced by treatment with 10 mM 2DG + 0.05 μM ROT in combination with γ-irradiation.

**Conclusion:** Since glycolysis is known to deliver scavengers of reactive oxygen species (ROS) and since an inhibition of the respiratory chain increases the forming of ROS, manip-

ulation of tumor cell metabolism may improve effectiveness of radiotherapy and therefore lead to a better outcome, especially in cases of metabolically highly active tumor cells. Supported by DFG SA 1749/3-1

**PS5-06**  
**Tumor metabolism - Characteristics and clinical consequences**

\*S. Walenta, W. Mueller-Klieser  
Medical Center of the Johannes Gutenberg University, Institute of Physiology and Pathophysiology, Mainz, Germany

Over the course of the development of a malignant tumor, the structure of the diseased organ changes fundamentally. The orderly composition of healthy tissue yields increasingly to a disordered, chaotic pattern. This results in extreme structural heterogeneity, which is shown, among other ways, by widespread destruction of the vascular architecture. The chaotic changes in tissue structure and vascular architecture additionally result in marked functional heterogeneity. Overall, this process creates a characteristic metabolic micro-milieu in tumor tissue, which is characterized, among other things, by marked hypoxic or anoxic areas, decreased extracellular pH, and an accumulation of lactate. The clinical significance of these changes is demonstrated by the fact that areas of the tumor that have been altered in this way show decreased sensitivity to various cancer therapies. Numerous clinical and experimental studies have shown that high lactate accumulation and increasing tumor hypoxia are associated with progression of the cancer, greater rates of metastasis and ultimately in reduced life expectancy for the patients. The pathophysiological factors just described affect the cellular physiology of the tumors, which is reciprocally related to genetic particularities of the tumor cells. Since Otto Warburg's classical experiments in the 1930s, high lactate production has been regarded as a typical, if not exclusive, characteristic of malignant tumors. Under hypoxic conditions, one can also find high lactate levels in normal tissues, but in most instances, restoration of normal oxygen levels results in a resumption of efficient mitochondrial respiration. However, most cancerous tumors have lost the capacity for this form of regulation, known as the Pasteur effect. Thus, even in the presence of adequate oxygen supplies, they obtain a portion of their metabolic energy through the breakdown of glucose to lactate by way of pyruvate. This is also termed aerobic glycolysis or the Warburg effect. A key question is whether and how these particularities of tumor metabolism can be exploited therapeutically. Which molecular mechanisms of tumor metabolism contribute to the development of radiation resistance in the tumor (see contribution by Fabian et al.)? Are there metabolic effects of tumors of the head and neck on the surrounding oral mucosa? Does the metabolic situation of the oral mucosa in these patients differ from that in the normal individual (see contribution by Voelzen et al.)? To what

extent does fractionated radiation therapy affect tumor metabolism and the expression of proteins relevant for glycolysis (see contribution by Goetze et al.)?

Poster Session I

Blood, immune system and stem cells

**P001**  
**Haematological evaluation in male rats following sub-chronic administration of aqueous crude extract of Parkia biglobosa leaves**

\*T. Ajibade, K. Soetan, S. Aina, Z. Sangodoyin  
University of Ibadan, Veterinary Physiology, Ibadan, Nigeria

Parkia biglobosa is an important multipurpose tree of West African Savannah land used traditionally, to treat a range of human and animal ailments. To evaluate the effects of sub-chronic administration of aqueous extract of the leaves of Parkia biglobosa in rats, twenty four male albino rats weighing between 120-200 g were distributed into four groups: A, B, C, and D containing 6 rats each. Aqueous extract of the leaves was administered to rats in groups B, C and D at doses of 100, 200 and 400 mgkg<sup>-1</sup> respectively for 21 consecutive days, while the rats in group A were administered distilled water (vehicle for extract) and served as control. After the treatment period, results of haematological evaluation revealed a dose dependent significant (p<0.05) decrease in the Packed cell volume of rats at all treatment levels. Likewise, haemoglobin concentration and red blood cell counts were also significantly decreased at the 200 and 400 mgkg<sup>-1</sup> doses. However, significant increase in total white blood cell count (WBC) was observed at the 400 mgkg<sup>-1</sup> dose. Changes observed in all analysed plasma biochemical parameters were not significant except for gamma glutamyl transferase, on which the extract caused a significant (p<0.05) increase at the 400 mgkg<sup>-1</sup> body weight dose. Moreover, mild portal congestion in the liver, mild renal cortical congestion in the kidney and moderate sub-capsular congestion in the testis were observed at the 400 mgkg<sup>-1</sup> dose. The study concludes that the extract is relatively safe provided that it is used judiciously at low doses.

**P002**  
**Purinergic signaling on leukocytes in the infarcted mouse heart**

\*N. Borg<sup>1</sup>, D. Friebe<sup>1</sup>, Z. Ding<sup>1</sup>, F. Bönner<sup>2</sup>, J. Schrader<sup>1</sup>  
<sup>1</sup>Heinrich-Heine-Universität, Molekulare Kardiologie, Düsseldorf, Germany  
<sup>2</sup>Universitätsklinikum Düsseldorf, Klinik für Kardiologie, Pneumologie und Angiologie, Düsseldorf, Germany

**Question:** Ecto-5'-nucleotidase (CD73; AMP → adenosine) on leukocytes is an important modulator in the healing process after myocardial infarction. AMP, the substrate of CD73, can be formed from the extracellular hydrolysis of ATP and NAD<sup>+</sup>. It is unknown, however, whether NAD<sup>+</sup>-degrading enzymes (CD157, CD38, ENPP1) are expressed on leukocytes

in the infarcted heart and which adenosine receptor subtype mediates the cardioprotective effect. **Methods:** Wild-type mice underwent 50 min occlusion of the left anterior descending artery (LAD) with subsequent reperfusion for 3 days. Leukocytes (APCs, granulocytes, T-cells) were isolated from heart and blood, and expression analysis of 28 genes involved in purinergic signalling was performed by qRT-PCR.

**Results:** We found that all enzymes involved in the degradation of extracellular NAD<sup>+</sup> were upregulated on myeloid antigen-presenting cells (APCs) after I/R. In contrast, the expression of the ATP receptor P2X7, which mediates apoptosis in the presence of high nucleotide concentration, was significantly down-regulated (basal: 0.019±0.011; I/R: 0.0054±0.004 AU; p<0.05). In granulocytes, the expression of connexins Cx37 and Cx43, P2X7, and the ectoenzymes CD38 and ENPP1 were upregulated after infiltration into the heart. Interestingly, the expression of the adenosine A2B receptor was significantly upregulated on cardiac APCs, granulocytes and T-cells which was not expressed on respective blood cell controls.

**Conclusions:** This study provides a first comprehensive overview on the expression of all relevant members of the purinergic signaling system on leukocytes during migration from the blood into the infarcted heart. Upregulation of the A2B receptor on leukocytes is likely to mediate pro-inflammatory effects and may play a key role in cardiac remodeling.

**P003**  
**Triggering of erythrocyte cell membrane scrambling by salinomycin**

\*M. Abaid, R. Bissinger, K. Jilani, F. Lang  
University of Tuebingen, Department of Physiology, Tübingen, Germany

**Question:** Salinomycin, a polyether ionophore antibiotic effective against a variety of pathogens, has been shown to trigger apoptosis of cancer cells and cancer stem cells. The substance is thus considered for the treatment of malignancy. Salinomycin compromises tumor cell survival at least in part by interference with mitochondrial function. Erythrocytes lack mitochondria but may undergo apoptosis-like suicidal cell death or eryptosis, which is characterized by scrambling of the cell membrane with phosphatidylserine-exposure at the erythrocyte surface. Signaling involved in the triggering of eryptosis include increase of cytosolic Ca<sup>2+</sup>-activity ([Ca<sup>2+</sup>]<sub>i</sub>). The present study explored, whether salinomycin stimulates eryptosis.

**Methods:** Phosphatidylserine-exposing erythrocytes were identified by measurement of annexin V binding, cell volume was estimated from forward scatter, hemolysis determined from hemoglobin release, and [Ca<sup>2+</sup>]<sub>i</sub> quantified utilizing Fluo3-fluorescence in flow cytometry.

**Results:** A 48 hours exposure to salinomycin was followed by a significant increase of Fluo3-fluorescence (≥10 nM), a significant increase of annexin-V-binding (≥5 nM), and a significant decrease of forward scatter (at 1-10 nM, but

not at 50 nM). The annexin-V-binding following salinomycin treatment was significantly blunted but not abrogated in the nominal absence of extracellular Ca<sup>2+</sup>.

**Conclusions:** Salinomycin triggers cell membrane scrambling, an effect at least partially due to entry of extracellular Ca<sup>2+</sup>.

**P004**

**Sphingosine kinase 1 negatively regulates platelet activation and thrombus formation**

\*E. Schmid<sup>1</sup>, P. Münzer<sup>1</sup>, B. Walker<sup>1</sup>, A. Fontinos<sup>2</sup>, M. Chatterjee<sup>2</sup>, P. Seizer<sup>2</sup>, T. Geisler<sup>2</sup>, M. Gawaz<sup>2</sup>, O. Borst<sup>1,2</sup>, F. Lang<sup>1</sup>

<sup>1</sup>University of Tuebingen, Department of Physiology, Tuebingen, Germany

<sup>2</sup> University of Tuebingen, Department of Cardiology and Cardiovascular Medicine, Tuebingen, Germany

**Question:** Sphingosine phosphate 1 (SP1) is a powerful regulator of platelet formation. Enzymes generating SP1 include sphingosine kinase 1. The present study thus explored the role of sphingosine kinase 1 in platelet formation and function.

**Methods:** Platelet count was obtained in gene-targeted mice lacking functional sphingosine kinase 1 (Sphk1<sup>-/-</sup>) and from their wild type littermates (Sphk1<sup>+/+</sup>). In isolated platelets P-selectin exposure (alpha granule secretion) was determined utilizing fluorescent antibodies in flow cytometry, ATP-release (dense granule secretion) utilizing a ChronoLume luciferin assay, platelet integrin activation utilizing fluorescent antibodies in flow cytometry, cytosolic Ca<sup>2+</sup> activity ([Ca<sup>2+</sup>]<sub>i</sub>) from Fura-2 fluorescence, aggregation using a luminoaggregometer and in vitro thrombus formation using a flow chamber with low (500 s<sup>-1</sup>) or high (1700 s<sup>-1</sup>) wall shear rates for 5 minutes.

**Results:** Platelet and RBC count were similar in Sphk1<sup>-/-</sup> and Sphk1<sup>+/+</sup> mice. However, increase of [Ca<sup>2+</sup>]<sub>i</sub>, collagen related peptide- and thrombin- induced P-selectin exposure (alpha granule secretion), ATP-release (dense granule secretion), platelet integrin activation, aggregation and in vitro thrombus formation were all significantly higher in isolated Sphk1<sup>-/-</sup> platelets than in isolated Sphk1<sup>+/+</sup> platelets. Bleeding time was similar in Sphk1<sup>-/-</sup> and Sphk1<sup>+/+</sup> mice. **Conclusions:** Sphingosine kinase 1 does not appreciably influence platelet formation but is a powerful negative regulator of platelet function counteracting degranulation, aggregation and thrombus formation.

**P005**

**Breakdown of phosphatidylserine asymmetry following treatment of erythrocytes with lumefantrine**

\*K. Alzoubi, M. Abed, F. Lang

University of Tuebingen, Department of Physiology, Tuebingen, Germany

**Question:** Lumefantrine, a commonly used antimalarial drug, is at least in part effective by inhibiting hemozoin formation in the parasite cell. The development of para-

sitemia and thus clinical course of malaria could further be favourably influenced by several substances triggering suicidal death or eryptosis of infected erythrocytes. Eryptosis is characterized by cell shrinkage and cell membrane scrambling leading to phosphatidylserine-exposure at the erythrocyte surface. Signaling involved in the triggering of eryptosis include increase of cytosolic Ca<sup>2+</sup>-activity ([Ca<sup>2+</sup>]<sub>i</sub>), formation of ceramide, oxidative stress and/or activation of p28 kinase. The present study explored, whether lumefantrine stimulates eryptosis.

**Methods:** Cell volume has been estimated from forward scatter, phosphatidylserine-exposure from annexin V binding, [Ca<sup>2+</sup>]<sub>i</sub> from Fluo3-fluorescence, reactive oxygen species from 2',7'-dichlorodihydrofluorescein-diacetate fluorescence, and ceramide abundance from binding of fluorescent antibodies in flow cytometry.

**Results:** A 24 hours exposure to lumefantrine (3 µg/ml) was followed by a significant increase of annexin-V-binding without significantly altering forward scatter, [Ca<sup>2+</sup>]<sub>i</sub>, ROS formation or ceramide abundance. The annexin-V-binding following lumefantrine treatment was not significantly modified by p38 kinase inhibitors SB203580 (2 µM) and p38 Inh III (1 µM).

**Conclusions:** Lumefantrine triggers cell membrane scrambling, an effect independent from entry of extracellular Ca<sup>2+</sup>, ceramide formation, ROS formation or p38 kinase activity.

**P006**

**Stimulation of erythrocyte cell membrane scrambling by mitotane**

\*P. Modicano<sup>1,2</sup>, J. Jacobi<sup>1</sup>, E. Lang<sup>1</sup>, R. Bissinger<sup>1</sup>, L. Frauenfeld<sup>1</sup>, C. Faggio<sup>2</sup>, M. Abed<sup>1</sup>, F. Lang<sup>1</sup>

<sup>1</sup>University of Tuebingen, Department of Physiology, Tuebingen, Germany

<sup>2</sup>University of Messina, Department of Biological and Environmental Sciences, S.Agata-Messina, Italy

**Question:** Mitotane (1,1-dichloro-2-[o-chlorophenyl]-2-[p-chlorophenyl]ethane), a cytostatic drug used for the treatment of adrenocortical carcinomas, is effective by triggering tumor cell apoptosis. In analogy to apoptosis of nucleated cells, eryptosis is the suicidal death of erythrocytes, which is typically paralleled by cell shrinkage and breakdown of cell membrane phosphatidylserine asymmetry with subsequent phosphatidylserine exposure at the erythrocyte surface. Eryptosis may be triggered by increase of cytosolic Ca<sup>2+</sup> concentration ([Ca<sup>2+</sup>]<sub>i</sub>). The present study tested, whether treatment of human erythrocytes with mitotane is followed by eryptosis.

**Methods:** [Ca<sup>2+</sup>]<sub>i</sub> was estimated from Fluo3 fluorescence, cell volume from forward scatter, phosphatidylserine exposure from annexin V binding, and hemolysis from hemoglobin release.

**Results:** Exposure to mitotane (≥ 5 µg/ml ≈ 16 µM) significantly increased [Ca<sup>2+</sup>]<sub>i</sub>, increased annexin V binding and triggered hemolysis, but did not significantly modify forward scatter. The effect on annexin V binding was significantly blunted in the absence of extracellular Ca<sup>2+</sup>.

Within 30 min Ca<sup>2+</sup> ionophore ionomycin (1 µM) decreased forward scatter, an effect virtually abolished in the presence of mitotane (15 µg/ml).

**Conclusions:** Mitotane increases [Ca<sup>2+</sup>]<sub>i</sub> with subsequent phosphatidylserine translocation. By the same token mitotane inhibits Ca<sup>2+</sup> induced cell shrinkage.

**P007**

**The Neuronal Calcium Sensor-1 in the immune system**

\*U. Hahn, B. Hawraa, E. Krause, O. Pongs, J. Rettig  
Saarland University, Physiology, Homburg, Germany

Our current work on calcium sensors focuses on the Neuronal Calcium Sensor-1 (NCS-1 aka Frequentin), a member of a growing family of highly conserved calcium binding proteins. While the cellular and subcellular distribution and the physiological role of NCS-1 in the nervous system of rodents has been investigated in detail using light and electron microscopy as well as immunohistochemistry, there are only few data on the distribution and functional role of NCS-1 in cells of the immune system.

Based on the findings that the vesicular trafficking and neuroendocrine secretion in neurons is influenced by NCS-1, and that the basic mechanisms of vesicle fusion in neurons and lymphocytes appear to be similar, we use a NCS-1<sup>-/-</sup> KO mouse line to investigate the functional role of NCS-1 in the immune system. We showed by immunoblots and PCR amplification that NCS-1 is expressed in naive CD8 T lymphocytes and is upregulated upon activation of these cells. In contrast, NCS-1 could not be detected in NK and B cells. To get a better understanding of the functional role in mouse cytotoxic T lymphocytes (CTL) we are currently fractionating activated CD8 cells by ultracentrifugation to localize NCS-1 in these cells.

Our first data show NCS-1 is expressed in naive CD8 T lymphocytes and is upregulated upon activation of these cells. NCS-1 shows a specific subcellular localization to the fractions which are presumed to include membranes from the Golgi/ER apparatus that play a key role in calcium regulated protein trafficking and cytoskeletal interactions.

**P008**

**Estramustine-induced suicidal erythrocyte death**

\*R. Bissinger<sup>1</sup>, P. Modicano<sup>1,2</sup>, L. Frauenfeld<sup>1</sup>, E. Lang<sup>1</sup>, J. Jacobi<sup>1</sup>, C. Faggio<sup>2</sup>, F. Lang<sup>1</sup>

<sup>1</sup>University of Tuebingen, Department of Physiology, Tuebingen, Germany

<sup>2</sup>University of Messina, Department of Biological and Environmental Sciences, S.Agata-Messina, Italy

**Question:** The nitrogen mustard derivative of estradiol-17β-phosphate estramustine is used for the treatment of prostate cancer. Estramustine may trigger suicidal death of cancer cells. Side effects of estramustine include anemia. At least in theory, estramustine could cause anemia by stimulation of eryptosis, the suicidal death of erythrocytes. Hallmarks of eryptosis include cell shrinkage, in-

creased cytosolic Ca<sup>2+</sup> activity ([Ca<sup>2+</sup>]<sub>i</sub>), ceramide formation and phosphatidylserine translocation to the outer leaflet of the cell membrane with phosphatidylserine exposure at the erythrocyte surface. Eryptosis is stimulated by increase of cytosolic Ca<sup>2+</sup> activity ([Ca<sup>2+</sup>]<sub>i</sub>). The present study explored whether estramustine triggers eryptosis.

**Methods:** [Ca<sup>2+</sup>]<sub>i</sub> was estimated from Fluo3 fluorescence, cell volume from forward scatter, phosphatidylserine exposure from annexin V binding, and hemolysis from hemoglobin release.

**Results:** A 24 h exposure to estramustine (≤ 100 µM) significantly increased [Ca<sup>2+</sup>]<sub>i</sub>, increased annexin V binding and increased hemoglobin release. The effect of estramustine on annexin V binding was significantly blunted by removal of extracellular Ca<sup>2+</sup>.

**Conclusions:** Estramustine stimulates both, eryptosis and hemolysis. The estramustine induced translocation of phosphatidylserine to the cell surface is at least partially due to increase of cytosolic Ca<sup>2+</sup> activity.

**P009**

**Hypoxia-inducible factor 1 in the course of retroviral infection**

\*T. Schreiber<sup>1</sup>, Y. Hüsecken<sup>1</sup>, K. Gibbert<sup>2</sup>, U. Dittmer<sup>2</sup>, S. Winning<sup>1</sup>, J. Fandrey<sup>1</sup>

<sup>1</sup>University Hospital Essen, Department of Physiology, Essen, Germany

<sup>2</sup>University Hospital Essen, Department of Virology, Essen, Germany

The transcription factor complex hypoxia-inducible factor 1 (HIF-1) plays a key role in adaptation of immune cells to hypoxic conditions during viral infections. To investigate the influence of myeloid HIF-1 deficiency in retroviral infections, we infected myeloid cell specific HIF-1 knockout mice with the murine Friend leukemia virus (FV). HIF-1 knockout as well as wild type mice developed a severe splenomegaly in the course of acute FV infection. Although we found an increase in the number of lymphocytes in the spleens of HIF-1 knockout mice compared to their counterparts 7 days after FV infection, there was no difference in spleen weight or viral load. 10 days post infection, spleen weight increased further in both groups. However, spleens in knockout mice appeared smaller than in wild types. Additionally, viral load was remarkably lower in HIF-1 knockout mice. The observed faster recovery from infection in knockout mice might be correlated with an increase in activated macrophages during the early course of infection that leads to an increase in lymphocyte numbers. Here, we showed that mice benefit from myeloid cell specific HIF-1 deficiency during acute retroviral infection. The underlying mechanism needs to be further elucidated.

**P010**

**Purinergic signaling on leukocytes infiltrating the LPS-injured lung**

\*D. Friebe, T. Yang, T. Schmidt, N. Borg, Z. Ding, J. Schrader  
Heinrich-Heine-University Düsseldorf, Department of Molecular Cardiology, Düsseldorf, Germany

Aim of this study was to examine the changes in the expression profile of multiple purinergic signaling molecules in leukocytes, particular different T cell subsets infiltrating the lung after acute lung injury (ALI).

Mice were challenged with intra-tracheal instillation of 3 µg/g LPS. After 3d and 7d blood, lung tissue and bronchoalveolar lavage (BAL) was collected. Immune cell subsets were isolated and analyzed using FACS. The expression profile of multiple purinergic molecules was then determined in different T cell subsets. Moreover, catabolism of the nucleotides ATP, NAD and cAMP by activated CD4+ T cells was evaluated by HPLC.

The ectoenzymes CD39 and CD73 showed an opposite expression pattern on myeloid and lymphoid cells in the uninjured lung. After ALI, the abundance of CD39 and CD73 was significantly increased on T cells derived from lung tissue and BAL compared to circulating T cells. T cell subsets from the lung expressed several ectoenzymes involved in the degradation of NAD such as Cd38, Cd157, Cd296 and Pc-1. Transcription of Cd38, Cd39, Cd73, Ent1, A2a receptor was significantly induced in T helper cells after ALI. Activated CD4+ T cells from the lung generated extracellular adenosine only from ATP and not from NAD or cAMP. T cells from the lung exhibit a unique expression pattern of purinergic molecules. The canonical pathway for adenosine production and an increased abundance of A2a receptor are likely to be important modulators of T cell function in the healing process after acute lung injury.

**P011**

**External regulators of the proteasome in human platelets**

\*K. Gruendler<sup>1,2</sup>, H. Mannell<sup>1</sup>, J. Pircher<sup>1</sup>, B. Krämer<sup>2</sup>

<sup>1</sup>Ludwig-Maximilians-Universität München, Walter Brendel Centre of Experimental Medicine, Munich, Germany

<sup>2</sup>Ludwig-Maximilians-Universität München, Medizinische Poliklinik, Munich, Germany

**Question:** The ubiquitin-proteasome systems (UPS) is the major degradatory pathway for proteins. It not only maintains protein quality control but is also involved in critical cellular processes such as apoptosis, antigen presentation and the development of neurodegenerative and vascular diseases. Recently a proteasome complex has also been identified in platelets, however its regulation and biological function are not well known. In this work, we focus on the regulation of the 20S and 26S proteasome in human platelets and aim to identify novel regulators of the platelet proteasome.

**Methods:** Platelets were isolated from healthy human donors and in vitro incubated. Gene expression analysis was performed by RNA sequencing technology and real-time

PCR. 26S and 20S proteolytic activity of the proteasome was analyzed by fluorescent peptide substrates (Boc-LL-VY-AMC, Boc-LSTR-AMC, Z-LLE-AMC). Quantification of polyubiquitinated proteins was assessed by ELISA and Western Blot.

**Results:** We initially demonstrated that most genes of the UPS and of the proteasome subunits are expressed in platelets. Chymotrypsin-, trypsin- and caspase-like activity of the 26S and 20S proteasome was quantified in lysed platelets. Interestingly, catalytic activity differed among the proteasome subunits while trypsin-like activity was the highest (3.1-fold increase versus chymotrypsin-like activity; n=3). Epoxomicin (1µM; 30min; n=3) robustly inhibited the platelet proteasome and resulted in a 1.52±0.32-fold increased accumulation of poly-ubiquitinated protein. Treatment of platelets with aspirin for one hour (0.5 to 5 mM, n=3) also inhibited proteasome activity significantly which is a novel function of aspirin. To mimic an infectious disease scenario, we incubated 1x10<sup>8</sup> platelets with 4x10<sup>6</sup> E. coli bacteria for 4h and detected increased activity of the proteasome (2.21±0.83-fold increase, n=3) and accelerated degradation of polyubiquitinated proteins (1.9-fold decrease, n=3). This effect was reversible with inhibition of the proteasome. Supporting these findings, platelets isolated from sepsis patients reveal an overexpression of the proteasome activating subunit PSME1 (2.7±0.7-fold increase, n=5).

**Conclusions:** We identified novel mediators that inhibit (e.g. aspirin) or activate (e.g. bacteria) the proteasome in platelets. This data may help in understanding the functional role of the proteasome in platelets, its role for platelet functions and platelet-related diseases.

**P012**

**Molecular mechanisms of particle detection, capture and engulfment by mouse macrophages**

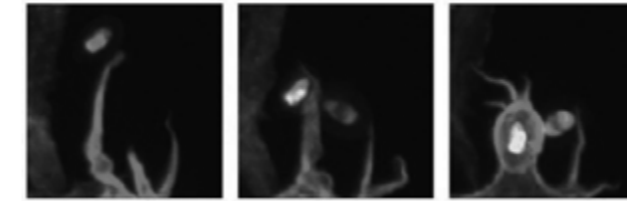
\*M. Horsthemke<sup>1</sup>, P. J. Hanley<sup>1</sup>, C. H. Brakebusch<sup>2</sup>, M. Bähler<sup>1</sup>

<sup>1</sup>Institut für Molekulare Zellbiologie, Westfälische Wilhelms-Universität Münster, Münster, Germany

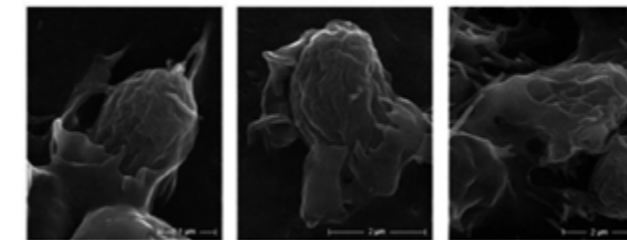
<sup>2</sup>University of Copenhagen, Biotech Research and Innovation Centre, Copenhagen, Denmark

Phagocytosis, the receptor-mediated ingestion of particles > 0,5 µm, is a specialist function restricted to professional phagocytes such as macrophages and neutrophils. This function is critical for the clearance of pathogens, such as bacteria and fungi, as well as for the removal of debris and senescent cells. Until recently, phagocytosis was thought to be a stochastic event, but now it is clear that cells can actively probe the environment. In this study, we used live-cell spinning disc confocal microscopy, superresolution structured illumination microscopy and scanning electron microscopy to image how macrophages, isolated from wt-mice and mice expressing the actin probe Lifeact-GFP, capture and ingest zymosan particles. First, we confirmed with Dectin-1(-/-) and Mannose receptor(-/-) mice that the process is mediated via Dectin-1. We found that a subset

of cells extended long tentacles which could „capture“ and envelope particles. We are currently investigating the role of the filopodia inducing RhoGTPase Cdc42 in phagocytosis.



Capture and engulfment of zymosan particles by filopodial extensions of macrophages. Lifeact-EGFP, green; zymosan-Texas Red, red



Scanning electron microscopy images of mouse macrophages fixed while engulfing zymosan particles. Zymosan, false-colored red

**P013**

**Suicidal erythrocyte death in end-stage renal disease**

\*M. Abed<sup>1</sup>, F. Artunc<sup>2</sup>, K. Alzoubi<sup>1</sup>, S. Honisch<sup>1</sup>, D. Baumann<sup>2</sup>, M. Föller<sup>1</sup>, F. Lang<sup>1</sup>

<sup>1</sup>University of Tuebingen, Department of Physiology, Tübingen, Germany

<sup>2</sup>University of Tuebingen, Department of Internal Medicine, Tübingen, Germany

**Question:** Anemia in end-stage renal disease (ESRD) results mainly from impaired erythrocyte formation following erythropoietin and iron deficiency. At least in theory, however, the anemia could partially be due to accelerated clearance of circulating erythrocytes because of suicidal erythrocyte death or eryptosis, which is characterized by phosphatidylserine exposure at erythrocyte surface. Triggers of eryptosis include increased Ca<sup>2+</sup>-concentration ([Ca<sup>2+</sup>]), reactive oxygen species (ROS) and ceramide. The present study explored whether and how ESRD influences eryptosis. **Methods:** Blood was drawn from healthy volunteers (n=20) and ESRD patients (n=20) prior to or after hemodialysis. Phosphatidylserine-exposure was estimated from annexin-V-binding, [Ca<sup>2+</sup>], from Fluo3-fluorescence, ROS from 2',7'-dichlorodihydrofluorescein-fluorescence and ceramide utilizing fluorescein-isothiocyanate-conjugated antibodies in flow cytometry. Measurements were made in erythrocytes from freshly drawn blood and in erythrocytes from healthy volunteers exposed 24h to plasma from healthy volunteers or ESRD patients prior to and following dialysis. **Results:** Patients suffered from anemia (hemoglobin 10.1±0.5g/100 ml) despite 1.96±0.34% reticulocytes. The percentage of phosphatidylserine-exposing erythrocytes was significantly higher in ESRD patients (0.84±0.09%) than in healthy volunteers (0.43±0.04%) and

was significantly increased after a standard dialysis session (1.35±0.13%). The increase in phosphatidylserine exposure was paralleled by increase of [Ca<sup>2+</sup>], ROS and ceramide abundance. As compared to addition of plasma from healthy individuals, addition of predialytic but not of post-dialytic plasma from ESRD-patients increased phosphatidylserine exposure, [Ca<sup>2+</sup>], ROS and ceramide abundance. **Conclusions:** Both, dialysable components of uremic plasma and dialysis procedure, trigger eryptosis at least in part by increasing erythrocyte [Ca<sup>2+</sup>], ROS, and ceramide formation.

**P014**

**Frequency-dependent QT-analysis in human induced pluripotent stem cell derived cardiomyocytes in vitro using optogenetics**

\*H. Lapp, T. Brueggemann, D. Malan, P. Sasse

University of Bonn, Institute of Physiology 1, Bonn, Germany

The long QT syndrome (LQTS) is a severe inherited or drug-induced cardiac disorder that is characterized by abnormal long QT durations, arrhythmia and sudden cardiac death. LQTS are occurring because of prolonged action potential durations (APD) and there is a strong dependence of APD on beating frequency. Screening of LQTS-inducing drugs can be performed with cardiomyocytes by recording extracellular field potential durations (FPD) that provide an indirect measure of the APD using micro-electrode arrays (MEA). Unfortunately electrical stimulation on MEA has technical limitations such as corrosion of electrodes, electrolysis and stimulation artifacts. Therefore we have established an optogenetic stimulation method for frequency-dependent investigation of FPD in human cardiomyocytes. Purified cardiomyocytes derived from human induced pluripotent stem cells were transfected with an adeno-associated virus of the serotype 2/1 (6.6x10<sup>4</sup> particles/cell) to express Channelrhodopsin-2, a light-gated cation channel in fusion with mCherry. About 50% of cells expressed mCherry and in these patch clamp recordings showed light-induced inward currents and action potentials. Importantly, APD turned out to be very similar using 1 ms light pulses (115.1±19.8 ms, n=7), compared to electrical (2 ms, 1000 pA) stimulation (129.8±24.6 ms, n=10). Next, transfected cardiomyocytes were plated on MEA and global stimulation with 1 ms long light pulses (0.92 mW/mm<sup>2</sup>) induced synchronized field potentials on all 60 electrodes without conduction delay. This allowed averaging of field potentials from all electrodes and from multiple beats to obtain a global field potential for the analysis of FPD. We found a clear frequency-dependence with significant shortening of FPD at higher beating rates (1.5 Hz: 265±49 ms; 3 Hz: 214±16 ms, p=0.0018, n=9). Drug-induced LQTS was evoked by application of the hERG potassium channel blocker Sotalolol. Interestingly this prolonged FPD only at low (1-1.5 Hz) pacing rate (at 1 Hz to 129±12%, p=0.0048, n=4, at 1.5 Hz to 111±10%, p=0.0432, n=5) but not at high (2 Hz) frequencies (to 101±5%, p=0.3351, n=5).

In summary we present a new method for optogenetic pacing of human cardiomyocytes on MEA. This novel approach enables spatial averaging of synchronized field potentials and assessment of frequency-dependent effects of drug-induced or inherited LQTS in vitro.

**P015**

**Establishment of reporter cell lines for the characterization of brachyury and mesp1 expression during in vitro cardiomyogenesis**

\*L. Leitner, G. Weitzer

MFPL, Vienna, Austria

Heart disease is a leading cause of death worldwide. As the heart has a very low regenerative potential, the existence of cardiovascular progenitor cells (CVPCs) opens new perspectives on how to deal with disease and ageing. The transcription factors Brachyury and Mesp1 play an important role in cardiac determination and are therefore promising candidates to identify additional direct target genes involved in cardiomyogenesis. Wnt signaling pathway induces mesoderm formation and directly activates Brachyury. In order to characterize the Wnt signaling pathway and the expression pattern of Brachyury and Mesp1 during in vitro differentiation we have stably transfected an embryonic stem cell (ESC) line and a CVPC line with reporter plasmids. The in vitro differentiation model embryoid bodies (EBs) was used to investigate the expression of Brachyury, Mesp1 and Wnt signaling during early embryogenesis, whereas cardiac bodies (CBs) reflected the expression during cardiomyogenesis. The expression levels were reported either by flow cytometry analysis or by luminescence. We demonstrated the transient upregulation of Brachyury and Mesp1 at day 5 of ESC aggregation and showed that CVPC derived CBs were five days ahead in differentiation compared to EBs. Furthermore we validated the responsiveness of our reporter cell line to Wnt signaling, which could be further induced by the addition of a GSK-Inhibitor (CHIR 99021). Our experimental data foster the understanding of the transcriptional network regulating heart differentiation and will contribute to the improvement of strategies to efficiently differentiate CVPCs into fully functional cardiac muscle cells.

**P016**

**Generation of a CD73-BAC-EGFP reporter mouse to investigate MSCs in vivo**

K. Kimura, C. J. Fuegemann, M. Hesse, B. K. Fleischmann, \*M. Breitbart

University of Bonn, Physiology I, Bonn, Germany

Mesenchymal stem cells (MSCs) are multipotent cells residing in the bone marrow and other tissues. They can be easily isolated and enriched in culture by plastic adherence. While in vitro MSCs are well characterized by their immunophenotype and differentiation potential to mesen-

chymal lineages, the current understanding of their localization and function in vivo remain elusive. We therefore aimed to generate a transgenic mouse model in which MSCs are labeled by a live reporter gene. CD73, also known as ecto-5'-nucleotidase, is a membrane-bound enzyme catalyzing the dephosphorylation of AMP to adenosine. It is a well-established marker for MSCs with only moderate distribution in other mesodermal cell types. We confirmed high expression of CD73 in various MSC populations by FACS, immunostainings and PCR. Thus, a reporter vector expressing EGFP under control of the CD73 promoter was created from bacterial artificial chromosomes (BACs), and transgenic mice were generated. As expected from literature kidney and lung epithelium showed a strong fluorescent signal, proving specificity of the construct. Transgene expressing cells correlating with MSC features were visible in different tissues of embryonic and adult CD73-BAC-EGFP mice. In developing bones EGFP emerges at the sites of endochondral ossification, demonstrating osteogenic precursor cells. Stromal adventitial cells are labeled in bone marrow sinusoids and colocalize with haematopoietic progenitors. The expression in other organs like white fat, uterus, and liver showed a perivascular distribution pattern as it is predicted for MSCs in vivo. Furthermore, primary cultures from epiphysis, bone marrow, white fat, and uterus gave rise to adherent growing EGFP positive cells that were able to differentiate into mesenchymal lineages, underlining the residence of MSCs in various organs. We are currently characterizing the EGFP positive cells and aim to further identify the MSC niche in order to better understand the biology of these cells. Besides that, the transgenic mouse model can give insights into the physiological roles of CD73 in normal and pathologic processes.

**P017**

**Defining the impact of newborn neurons in the mouse olfactory bulb by combining optogenetics and in vivo calcium imaging**

\*C. Fois<sup>1</sup>, G. Kumar Pramanik<sup>1</sup>, A. Stroh<sup>1</sup>, B. Berninger<sup>2</sup>

<sup>1</sup>Focus Program translational Neuroscience, Institute for Microscopic

Anatomy and Neurobiology, Mainz, Germany

<sup>2</sup>Institute of Physiological Chemistry, Mainz, Germany

**Question:** Olfactory bulb (OB) represents one of the two areas where neurogenesis takes place in the adult mammalian brain. The functional relevance and the impact of the newborn neurons on the functional architecture of OB circuitry are still not understood.

**Methods:** We use a combination of 2-photon calcium imaging and specific optogenetic stimulation of newborn neurons to control and monitor their function and impact in the OB circuitry. Adeno-associated viruses encoding for ChR2 and ArchT were injected in the subventricular zone of anesthetized adult mice. The animals were perfused one month after the viral injection to perform confocal microscopy in slices. OGB-1, a fluorescent calcium indicator and SR101 (a specific astrocytes fluorescent dye) have been

injected in the OB of anesthetized adult mice and a 2-photon microscope has been used to visualize and monitor the olfactory bulb circuit in vivo.

**Results:** Confocal microscopy allowed us to identify opsin expressing cells in SVZ, rostral migratory stream and OB. In the OB granule and periglomerular cells where identified relying on their morphology and localization. Newborn neurons in the OB stably express the optogenetic actuators over periods of at least 7 months. By using a 2-photon microscope we were able to visualize a homogeneous staining of the OB superficial layers and we could also discriminate between neurons and astrocytes.

**Conclusions:** Based on these two findings we will study the impact of newborn neurons on spontaneous and odor evoked activity and define their impact on OB microcircuitry.

**P017b**

**Triggering of suicidal erythrocyte death by celecoxib**

\*A. Lupescu, R. Bissinger, K. Jilani, F. Lang

University of Tübingen, Tübingen, Germany

The selective cyclooxygenase-2 (COX-2) inhibitor celecoxib triggers apoptosis of tumor cells and is thus effective against malignancy. The substance is at least partially effective through mitochondrial depolarization. Even though lacking mitochondria, erythrocytes may enter apoptosis-like suicidal death or eryptosis, which is characterized by cell shrinkage and by phosphatidylserine translocation to the erythrocyte surface. Eryptosis may be triggered by increase of cytosolic Ca<sup>2+</sup>-activity ([Ca<sup>2+</sup>]<sub>i</sub>). The present study explored whether celecoxib stimulates eryptosis. Forward scatter was determined to estimate cell volume, annexin V binding to identify phosphatidylserine-exposing erythrocytes, hemoglobin release to depict hemolysis, and Fluo3-fluorescence to quantify [Ca<sup>2+</sup>]<sub>i</sub>. A 48 h exposure of human erythrocytes to celecoxib was followed by significant increase of [Ca<sup>2+</sup>]<sub>i</sub> (15 μM), significant decrease of forward scatter (15 μM) and significant increase of annexin-V-binding (10 μM). Celecoxib (15 μM) induced annexin-V-binding was blunted but not abrogated by removal of extracellular Ca<sup>2+</sup>. In conclusion, celecoxib stimulates suicidal erythrocyte death or eryptosis, an effect partially due to stimulation of Ca<sup>2+</sup> entry.

Cardiac functions I

**P018**

**Ampk1 deficiency counteracts gap junction remodelling following pressure overload**

\*J. Völk<sup>1,2</sup>, I. Alesutan<sup>1</sup>, F. Stoeckigt<sup>3</sup>, U. Primessnig<sup>4</sup>, S. Mia<sup>1</sup>, M. Sopjani<sup>1</sup>, M. Feger<sup>1</sup>, C. Munoz<sup>1</sup>, O. Borst<sup>1,5</sup>, M. Gawaz<sup>5</sup>, B. Metzler<sup>2</sup>, J. Schriekel<sup>3</sup>, F. Heinzel<sup>4</sup>, F. Lang<sup>1</sup>

<sup>1</sup>University of Tuebingen, Department of Physiology, Tübingen, Germany

<sup>2</sup>Medical University Innsbruck, Department of Medicine – Cardiology, Innsbruck, Austria

<sup>3</sup>University Hospital Bonn, Department of Medicine – Cardiology, Bonn, Germany

<sup>4</sup>Medical University Graz, Department of Medicine – Cardiology, Graz, Austria

<sup>5</sup>University of Tübingen, Department of Cardiology and Cardiovascular Medicine, Tübingen, Germany

**Introduction:** Adenosine-5'-monophosphate-activated protein kinase (Ampk) is activated in cardiac tissue under physiological and pathological stress. Ampk regulates various ion channels and transporters. Moreover, the Ampka1 isoform contributes to the cardiac remodelling following pressure overload by “transverse aortic constriction” (TAC).

Therefore, a role of Ampka1 on gap junction remodelling was investigated.

**Methods:** Pressure overload was induced by TAC in gene-targeted mice lacking functional Ampka1 (Ampka1<sup>-/-</sup>) and corresponding wild-type mice (Ampka1<sup>+/+</sup>). Electrophysiological investigation and epicardial mapping of Langendorff-perfused hearts was performed. Xenopus oocytes were injected with cRNA encoding Cx43 together with various AMPK and NEDD4-2 mutants. Further measurements were performed utilizing quantitative RT-PCR, immunoprecipitation, western blotting, confocal microscopy and dual-electrode voltage clamp.

**Results:** Ampka1<sup>-/-</sup> mice are partially protected against increased conduction inhomogeneity following TAC. After TAC procedure, conduction blocks >4ms were more frequently observed in Ampka1<sup>+/+</sup> mice as compared to Ampka1<sup>-/-</sup> mice. Without modifying Cx43 mRNA expression, TAC decreased Cx43 protein abundance and increased Cx43 ubiquitination in Ampka1<sup>+/+</sup> mice, both effects blunted in Ampka1<sup>-/-</sup> mice. In Xenopus oocytes, wild-type AMPKWT and constitutively-active AMPK<sup>R70Q</sup>, but not catalytically inactive AMPK<sup>ΔK45R</sup> down-regulated Cx43-mediated current as well as Cx43 membrane abundance. Coexpression of NEDD4-2 together with AMPK<sup>R70Q</sup> led to a profound decrease of Cx43-mediated current, which was blunted by co-expression of NEDD4-2<sup>S795A</sup> lacking an AMPK phosphorylation consensus sequence or of catalytically inactive NEDD4-2<sup>C962S</sup>.

**Conclusions:** Ampka1 promotes Cx43 remodelling in a NEDD4-2-dependent manner. Thus, Ampka1 activation may be of significant importance in the electrical remodelling of the failing heart.

**P019**

**Ampk1 deficiency ameliorates cardiac dysfunction following pressure overload**

\*I. Alesutan<sup>1</sup>, J. Voelkl<sup>1,2</sup>, F. Stoeckigt<sup>3</sup>, U. Primessnig<sup>4</sup>, S. Mia<sup>1</sup>, M. Sopjani<sup>1</sup>, M. Feger<sup>1</sup>, C. Munoz<sup>1</sup>, O. Borst<sup>1,5</sup>, M. Gawaz<sup>5</sup>, B. Metzler<sup>2</sup>, J. Schrickel<sup>3</sup>, F. Heinzel<sup>4</sup>, F. Lang<sup>1</sup>

<sup>1</sup>University of Tuebingen, Department of Physiology, Tuebingen, Germany

<sup>2</sup>University Innsbruck, Department of Medicine – Cardiology, Innsbruck, Austria

<sup>3</sup>University Hospital Bonn, Department of Medicine – Cardiology, Bonn, Germany

<sup>4</sup>Medical University Graz, Department of Medicine – Cardiology, Graz, Austria

<sup>5</sup>Department of Cardiology and Cardiovascular Medicine, University of Tuebingen, Tuebingen, Germany

**Question:** Adenosine-5'-monophosphate-activated protein kinase (Ampk) is considered to play an important role in cardiac ischemia, hypertrophy and failure. In failing hearts, an isoform shift from the predominant catalytic AmpkQuestion:2 subunit towards the AmpkQuestion:1 subunit was previously observed.

**Methods:** Pressure overload was induced by “transverse aortic constriction” (TAC) in gene-targeted mice lacking functional AmpkQuestion:1 (AmpkQuestion:1<sup>-/-</sup>) and corresponding wild-type mice (AmpkQuestion:1<sup>+/+</sup>). Cardiac function was evaluated by pressure-volume measurements and echocardiography. HL-1 cardiomyocytes were transfected with constitutively-active AmpkQuestion:1 (CAQuestion:1) and silenced with PkcQuestion:;, Prkaa1 or Prkaa2 siRNA. Further measurements were performed utilizing quantitative RT-PCR, ELISA, immunoprecipitation, western blotting, confocal microscopy and luciferase reporter assay.

**Results:** AmpkQuestion:1<sup>-/-</sup> mice are partially protected against decreased cardiac ejection fraction and increased enddiastolic pressure following TAC. TAC increased cardiac AmpkQuestion:1 protein abundance in AmpkQuestion:1<sup>+/+</sup> mice. TAC induced cardiac Nppa and Nppb mRNA expression and elevated BNP serum levels in AmpkQuestion:1<sup>+/+</sup> mice, effects mitigated in the AmpkQuestion:1<sup>-/-</sup> mice. TAC increased PkcQuestion: abundance at the myocardial intercalated discs, Erk5 protein abundance and Ap-1 target gene expression (c-Fos, Il6, Mapk7, Ncx1), effects ameliorated in AmpkQuestion:1<sup>-/-</sup> mice. Overexpression of CAQuestion:1 in HL-1 cardiomyocytes increased PkcQuestion: phosphorylation and PkcQuestion:-dependent Ap-1 transcriptional activity and target gene expression. Silencing of AmpkQuestion:1, but not AmpkQuestion:2 blunted the effect of angiotensin-II on Ap-1 target gene expression in HL-1 cardiomyocytes.

**Conclusions:** AmpkQuestion:1 deficiency attenuates TAC-induced cardiac functional deterioration. AmpkQuestion:1 effects involving PkcQuestion:-dependent mechanisms. Cardiac isoform shift of AmpkQuestion:2 to AmpkQuestion:1 may thus be pathophysiologically decisive in the failing heart.

**P020**

**The effect of urea acid on cardiac function and the role of arginine**

\*S. Klaus-Dieter, S. Rolf, W. Martin

JLU Gießen, Physiologisches Institut, Gießen, Germany

**Background:** Plasma levels of uric acid increase during renal failure and they correlate to poor cardiac function. Uric acid can directly modify arginase activity in endothelial cells and arginase expression and activity is associated with depressed cardiac function. However, there are no data analyzing direct effects of plasma relevant uric acid concentrations, as they occur in renal failure, on cardiac function. Here, the effect of uric acid concentrations ranging between 0-10 mg/dl on load-free cell shortening was investigated. This allows to study the effect of uric acid independent of endothelium-dependent effects. Furthermore, its potential relationship to arginine metabolism was analyzed to establish a mechanistic link.

**Methods:** Isolated adult rat ventricular cardiomyocytes were cultured for 24 h in the presence of uric acid (0.0 - 10.0 mg/dl) to mimic the situation of chronically elevated uric acid concentrations. Thereafter, cells were electrically stimulated at 2 Hz and cell shortening was monitored by a cell edge detection system. Arginine consumption was inhibited by either inhibition of NO-producing enzymes with L-NAME or ETU and by inhibition of arginine metabolizing enzymes and downstream targets of arginase (Nor-NOHA and NPS). Depletion of arginine pools was attenuated by administration of L-arginine with D-arginine administration in controls. Calcium transients during electromechanical coupling were determined in FURA-2-AM loaded cells.

**Results:** Uric acid caused a concentration-dependent depressive effect on load-free cell shortening. At 10 mg/dl cell shortening was reduced by 20.4%. This effect of uric acid was accompanied by a paradoxical increase of calcium transients indicating calcium-desensitisation. The negative contractile effect was not accompanied by different expression of eNOS and arginase. However, inhibition of NOS with L-NAME or ETU effectively restored basal contractile activity, while inhibition of arginase with Nor-NOHA and of its downstream target polyamine metabolism partially restored the contractile responsiveness. Collectively, these data suggest that intensive arginine consumption and possibly depletion of intracellular arginine pools are responsible for cardiodepressive effects of uric acid. This hypothesis was tested by administration of L-arginine to replenish the arginine pool. L-Arginine restored cardiac function in the presence of uric acid in a concentration-dependent manner. However, the non-proteinogenic amino acid D-arginine did not affect cardiac function under the same conditions.

**Conclusion:** Plasma relevant concentrations of uric acid as they are found in renal failure impair load free cell shortening of adult ventricular cardiomyocytes by depletion of arginine pools in cardiomyocytes. Arginine seems to be required for regular calcium-sensing, in example of troponin C, which normally determines calcium sensitivity. Collectively these data argue for a direct cardiodepressive effect of high plasma concentrations of uric acid.

**P021**

**Less-invasive transverse aortic banding in mice for hypertrophy studies**

\*L. Schröder, Q. Tian, L. Kaestner, P. Lipp

Molecular Cell Biology, Saarland University, Homburg, Germany

Cardiac hypertrophy is a critical accompanying symptom associated with many cardiovascular diseases. To study the multifactorial processes involved, the use of surgically induced in vivo models became a standard method, especially aortic banding. In the conventionally used transverse aortic constriction (TAC) model, the survival rate is a serious problem, especially in the context of combined models, such as genetic modification, which could already impair the basic health status of the mice. Therefore, we adapted a novel, minimally invasive aortic banding, MTAB procedure (Martin et al. 2012). In this surgery, the access is located cranially of the sternum, avoiding the entering of the pleural space. This circumvents both the risk of a lethal pneumothorax and pleural infection. Additionally, artificial ventilation and intubation is redundant and time under anesthesia is reduced. Furthermore, it is less harmful to the animal. After surgery, the heart can be imaged in vivo by cardiac sonography, to assess the onset of change in cardiac morphology and performance during hypertrophy development. At the end point of observation, cardiac myocytes can be isolated, and T-tubules are imaged by confocal microscopy. T-Tubular regularity is assessed by Fourier-Analysis to gain a quantitative measure. After an initial survey (>20 mice), we have a clear evidence that the survival rate with MTAB is much higher compared to conventional TAC (70%, vs. 50%), with a tendency for a higher survival rate of female mice vs. male mice. Furthermore, we are able to correlate the ultrasonic hypertrophy data to the T-tubular properties.

**P022**

**Antagonizing aldosterone reduces cardiac effects of SPRED2 deficiency only partially**

\*A. M. Augustin, M. Ullrich, M. Abeßer, K. Schuh

University of Wuerzburg, Institute of Physiology, Wuerzburg, Germany

**Question:** SPRED (Sprouty-related proteins with an EVH1 domain) proteins are inhibitors of the pro-hypertrophic Ras/ERK-MAPK pathway and are expressed in the heart. SPRED2 KO mice show a variety of arrhythmias and ECG abnormalities, eventually caused by hyperactivation of the HPA axis and hyperaldosteronism. Based on these results, we explored the effect of the aldosterone antagonist Eplerenone, applied in the management of chronic heart failure to restore cardiac function.

**Methods & Results:** In SPRED2 KO mice, quantification of Western blots did not show compensatory up-regulation of SPRED1 and revealed activated MAPK- and Akt pathways in KO hearts. ECG recordings of WT and KO mice at rest revealed a significantly elevated heart rate in SPRED2 KO mice (+48.02 bpm; p<0,05). Eplerenone treatment (100 mg/

kg/day) reduced the heart rate in both groups and adjusted the frequency of KOs to that of WT mice (471.99 vs. 452.84 bpm, n.s.). Both QRS complex duration (+1.7 ms, p<0.05) and QRS area were increased in KO mice, in this case not reversible, neither by Eplerenone treatment nor by stimulation with isoproterenol (bolus 2mg/kg). In line with these data, the heart weight/body weight ratio was elevated (WT:4.5 vs. KO:6.7 mg/g; p<0.001) and it raised the question whether there might be also structural variances in cardiac tissues of KO mice influencing electrical conduction. Sirius red stainings to estimate cardiac fibrosis demonstrated elevated collagen content in KO hearts, which was incompletely reduced after Eplerenone treatment (6.1 to 1.6%, WT: 0.9 to 0.5%). Upon Eplerenone medication the T time-voltage area declined in WT and in KO mice (WT:-0.82 vs. KO:-1.08 ms\*mV) but, interestingly, the T area change upon isoproterenol administration appeared to be opposing: WT T area was reduced slightly (2.23 to 2.10 ms\*mV), while the KO T exceeded (1.96 to 3.43 ms\*mV). A similar effect was observed in Eplerenone treated mice, but less obvious (WT:1.41 to 1.23; KO:0.88 to 1.71 ms\*mV). The TP interval appeared to be shortened in KO mice (WT:49 vs. KO:35 ms) and to respond to Eplerenone treatment (WT:43 vs. KO:41 ms).

**Conclusion:** The effects of SPRED2-deficiency in mice could not be completely reversed by treatment with aldosterone antagonists. While some of the parameters responded to the medication, others were aldosterone-independent. This led us to the assumption that some cardiac effects are direct consequences of the genetic ablation. However, some of the pathophysiological effects, e.g. fibrosis in SPRED2 hearts, were influenced positively. We conclude that the hyperaldosteronism, which appears to accompany SPRED2-deficiency, enhances the SPRED2<sup>-/-</sup> phenotype but cannot be seen as causative for all cardiac symptoms associated with this gene ablation.

**P023**

**Humoral transfer of remote ischemic preconditioning's protection from donor pigs in vivo to an in vitro bioassay of isolated perfused recipient rat hearts**

\*C. Schulte, A. Skyschally, G. Heusch, P. Kleinbongard

University of Essen Medical School, Institute for Pathophysiology, Essen, Germany

**Question:** Brief episodes of ischemia/reperfusion in a remote organ reduce myocardial infarct size. However, the transfer of protection from the remote ischemic/reperfused organ to the heart is still not understood. Here we address the transfer of a blood-borne cardioprotective factor from a donor pig undergoing a remote ischemic preconditioning (RIPC) protocol and subsequent myocardial ischemia/reperfusion to an isolated perfused recipient rat heart undergoing global ischemia/reperfusion.

**Methods:** Anesthetized pigs were subjected to either RIPC (4 cycles of 5 min hindlimb occlusion/5 min reperfusion) or placebo. Plasma was separated from arterial blood samples collected 60 min after RIPC or placebo, respectively, and

stored at -80°C. Myocardial ischemia was induced by 60 min occlusion of the left anterior descending coronary artery (LAD) with subsequent 180 min reperfusion. Isolated rat hearts were mounted on a Langendorff apparatus and perfused at a pressure of 75 mmHg with Krebs-Henseleit-buffer before undergoing 30 min global ischemia and 120 min reperfusion. Pig plasma was added to the Krebs-Henseleit-buffer (1:10) for 8 min before and for 5 min after global ischemia. Infarct size in the pig heart and the isolated rat heart was determined by TTC.

**Results:** In pigs, infarct size was 22.1±3.5% with RIPC and 47.6±5.5% with placebo (mean±SEM; p<0.05). Plasma from RIPC pigs reduced infarct size in the isolated rat hearts to 25.9±1.9% versus 39.3±2.3% (mean±SEM; p<0.05). Infarct size of the isolated recipient rat hearts correlated to that of the donor pigs (r=0.74; n=12).

**Conclusion:** After RIPC in pigs, a cardioprotective, humoral signal can be transferred to an in vitro bioassay of isolated rat hearts.

**P024**

**Ischemic post-conditioning uncouples β-adrenoceptors in the post-ischemic heart**

\*R. Schreckenber<sup>1</sup>, P. Ferdinandy<sup>2</sup>, R. Schulz<sup>1</sup>, K.-D. Schlüter<sup>1</sup>

<sup>1</sup>Institute of Physiology, JLU-Gießen, Gießen, Germany

<sup>2</sup>University of Szeged, Department of Biochemistry, Szeged, Hungary

**Background:** Until now different strategies have been developed to protect post-ischemic myocardium against tissue injury and structural remodeling induced by ischemia/reperfusion injury. The most effective methods known, are ischemic pre-conditioning (IPC) and ischemic post-conditioning (IPoC). To what extent this protection also leads to a better prognosis in the long term depends fundamentally on its effect on the subsequent reconstruction processes. An important component in the course of cardiac remodeling is the specific receptor-mediated signalling of the post-ischemic heart, which is affected in very different ways by both the IPC and IPoC protocols. The aim of the current study is to clarify to what extent the effect of IPC and IPoC impacts receptor stunning and thus cardiac remodeling in the long-term.

**Methods:** Isolated adult rat hearts were saline perfused in Langendorff mode and underwent a 45 min no-flow ischemic protocol followed by 2 h of reperfusion (I/R). Where ever indicated, hearts were protected by an ischemic pre-conditioning (IPC) or ischemic postconditioning protocol (IPoC), (each group n=8). 30 min after reperfusion, hearts were stimulated by the beta-adrenoceptor agonist isoprenaline (ISO, 10 nM) for 10 min. Long-term effects of IPC and IPoC on receptor stunning and cardiac remodeling were analysed in vivo using an occlusion/reperfusion model. After inducing ischemia, the animals were monitored for 7 days. The remodeling of the signal transduction was subsequently investigated by stimulating β-adrenergic receptors using a Working Heart Model.

**Results:** In the post-ischemic myocardium, ISO caused a significant but transient improvement of cardiac perfor-

mance in either hearts treated by I/R or IPC. However, the response was blunted in the group of hearts undergoing IPoC. Ornithine decarboxylase (ODC), the rate limiting enzyme of the polyamine metabolism, and ANP were induced by ISO in hearts of I/R or IPC, but again not in hearts undergoing IPoC. One week after the myocardial infarction ISO still had no effects on the inotropy. The vasodilating effects on coronary vessels as well as the positive chronotropic effects were, however, still present. In the left ventricle the expression of the beta1 adrenergic receptor was reduced after a myocardial infarction, but not influenced by IPC or IPoC. **Conclusion:** IPoC leads to a specific and selective remodelling of beta-adrenoceptor signalling as indicated by reduced inotropic stimulation and loss of ODC/ANP activation with a simultaneously preserved relaxation of coronary vessels.

**P025**

**Evidence of hypoxia and Wilms' tumor 1 influencing EMT in epicardial cells byregulating Amiloride binding protein 1**

\*K. Kirschner, J. Braun, H. Scholz

Institut für Vegetative Physiologie, Charité - Universitätsmedizin Berlin, Berlin, Germany

Putrescine is a polyamine, which is important for normal cell growth and division as well as differentiation. After myocardial ischemia putrescine levels are increased. Cellular levels of putrescine are controlled by its methabolizing enzyme ornithine decarboxylase (Odc1) as well as its degrading enzyme Abp1. In this study a 10-fold increase of Abp1 transcripts was observed 24 h after surgery in the hearts of rats with myocardial infarction compared to sham-operated animals (t-test, P<0.001, n=5). Odc1 expression was not significantly changed. For this purpose, adult rats were subjected either to left coronary artery ligation or sham-surgery, and Abp1 and Odc1 mRNA was measured by real-time RT-PCR. Consistently, exposure of rats to 8 % O<sub>2</sub> for 6 hours caused a 2.5-fold increase of Abp1 mRNA in the hearts (t-test, P<0.05, n=7) with no significant changes of Odc1 transcripts. Abp1 mRNA levels were also significantly increased 30-fold (t-test, P<0.05, n=5) in mouse embryonic epicardial cells cultured at 1 % O<sub>2</sub> for 36 h. Inhibition of Abp1 by aminoguanidine at normoxia leads to an increase of E-cadherin mRNA and reduced levels of vimentine and N-cadherin mRNA in mouse embryonic epicardial cells. Indicating a role for Abp1 in EMT of epicardial cells. Interestingly Abp1 expression in mouse embryonic epicardial cells is not only regulated by hypoxia, but also by the transcription factor Wilms' tumor 1 (Wt1). Wt1 is one of the key regulators of EMT in epicardial cells. In this study we could identify Abp1 as a transcriptional target of Wt1. Abp1 mRNA was reduced to 5 % (t-test, P<0.001, n=5) in mouse embryonic epicardial cells after vivo-morpholino knock-down of Wt1. Abp1 and Wt1 are co-expressed in the epicardium of the developing heart. Wt1 binding sites in the Abp1 promoter could be identified and verified by luciferase promoter assays, electromobility shift assays and chromatin immuno-

precipitation. In conclusion, cardiac expression of Abp1 is regulated by Wt1 and is stimulated in response to hypoxia and myocardial infarction. It is suggested that enhanced Abp1 expression has a role in tissue remodelling after myocardial ischemia through increased EMT.

**P026**

**Myocardial ischemia acutely affects titin phosphorylation and cardiac myocyte stiffness**

\*S. Kötter<sup>1</sup>, C. Andresen<sup>1</sup>, J. Albrecht<sup>1</sup>, A. Gödecke<sup>1</sup>, M. Kuhlmann<sup>2</sup>, G. Heusch<sup>3</sup>, M. Krüger<sup>1</sup>

<sup>1</sup>Heinrich-Heine Universität Düsseldorf, Herz- und Kreislaufphysiologie, Düsseldorf, Germany

<sup>2</sup>European Institute for Molecular Imaging, Münster, Germany

<sup>3</sup>Universitätsklinikum Essen, Institut für Pathophysiologie, Essen, Germany

**Question:** Titin based passive stiffness is an important determinant of myocardial passive stiffness. Titin stiffness is modulated by changes in the relative expression levels of the cardiac titin isoforms N2BA (3.2-3.7 MDa) and N2B isoform (3.0 MDa) and is further modified by phosphorylation. Myocardial ischemia (MI) is known to activate several protein kinases, including PKCα, thereby regulating the onset and extent of cell injury and death. Here, we tested whether myocardial ischemia induces changes in titin phosphorylation and affects its elastic properties.

**Methods:** We analyzed titin phosphorylation and titin-based passive stiffness in four models of MI: (I) isolated Langendorff-perfused mice hearts, 20' global I/30' reperfusion (R); (II) Adult mice hearts with 3 days LAD ligation or (III) 10 days permanent LAD ligation; (IV) Pig heart 55' LAD ligation/10' and 120' R. Titin phosphorylation was tested by Western blot using phospho-specific antibody targeting Ser11878 in titin's PEVK domain ( ). Passive stiffness was measured using isolated skinned cardiac myocytes.

**Results:** In all investigated models titin PEVK phosphorylation was significantly increased by 25-45%. Significant changes occurred within 20' after beginning ischemia (I) and persisted even after 10 days (III). Isoform composition was unchanged in the acute MI models (I, IV), but shifted to a higher N2B amount in mice hearts 3 days after LAD ligation (III). Consistent with increased titin PEVK phosphorylation passive myocyte stiffness was significantly elevated by the ischemic insult.

**Conclusion:** Titin-based passive stiffness is rapidly increased upon myocardial ischemia and may play an important role in the development of myocardial dysfunction.

**P027**

**Activation of the cardiac renin-angiotensin system by NOS1 triggers age-related contractile dysfunction via NOX-dependent oxidative stress**

M. Villmow, U. Klöckner, \*U. Rueckschloss

Martin Luther University Halle, Julius Bernstein Institute of Physiology, Halle, Germany

Previously, we showed that calcium decay was slowed and calcium sensitivity of myofilament ATPase activity was reduced in aged wild-type ventricular myocytes. Consequently, kinetics of contraction/relaxation was decelerated. We attributed this contractile dysfunction of aged ventricular myocytes to an increased superoxide formation by upregulated cardiac NADPH oxidases (NOX2/NOX4). Question: Since NOS1 is also upregulated in aged murine hearts, we wondered whether NOS1 could play a role in cardiac aging. Methods: We analyzed isolated ventricular myocytes from young (2-4 months) and aged (24-26 months) wild-type and NOS1<sup>-/-</sup> mice, respectively. Contractions (sarcomere shortening, MyoCam system), calcium transients (Indo-1 fluorescence) and myofilament ATPase activity (blebbistatin-sensitive phosphate generation) were evaluated. Expression of NADPH oxidase subunits and components of the cardiac renin-angiotensin system were quantified (real-time PCR). Results: We found that age-dependent contractile dysfunction does not occur in ventricular myocytes from NOS1<sup>-/-</sup> mice. Calcium homeostasis and calcium sensitivity of myofilament ATPase activity are unchanged with aging. This can be explained, at least partially, by the finding that cardiac NOX expression and NADPH oxidase activity are not increased with age in NOS1<sup>-/-</sup> mice. The renin-angiotensin system is a well-known inducer of NADPH oxidase-dependent radical formation. We show that renin, the enzyme that catalyses the rate-limiting step within the cascade, is age-dependently induced in hearts of wild-type mice but not of NOS1<sup>-/-</sup> mice. Conclusion: We conclude that upregulation of NOS1 contributes to oxidative stress in aged myocytes via activation of the intra-cardiac renin-angiotensin system that in turn induces NOX expression. Increased NADPH oxidase-dependent superoxide formation then interferes with the contractile function of aged murine ventricular myocytes.

**P028**

**Conditional and selective activation of the Gq pathway in the heart and its impact on cardiac function in vivo**

\*E. Kaiser<sup>2</sup>, J. Wess<sup>2</sup>, Q. Tian<sup>1</sup>, L. Schröder<sup>1</sup>, L. Kaestner<sup>1</sup>, P. Lipp<sup>1</sup>

<sup>1</sup>Molecular Cell Biology, Saarland University, Medical Faculty, Homburg, Germany

<sup>2</sup>National Institute of Diabetes and Digestive and Kidney Diseases, Laboratory of Bioorganic Chemistry, Bethesda, United States

Gq/G11 mediated pathways are involved in the induction of myocardial hypertrophy and arrhythmia, although the specific impact of Gq signaling on the mammalian heart is not fully understood. Obstacles are the complex interaction with G11 protein-mediated pathways and the ubiquitous expression of Gq protein-coupled receptors. In addition nearly all endogenous agonists do not exclusively induce Gq mediated signaling. We therefore aim to examine how Gq activation alters cardiac physiology by inducing Gq receptor activation specifically in cardiomyocytes. We investigate a novel transgenic mouse line, expressing the designer-receptor Gq-RASSL (receptor solely activated by synthetic ligand) controlled by the MCK promoter. In

these animals the Gq pathway can be selectively activated in striated muscle cells including cardiomyocytes through injection of the synthetic ligand CNO (Clozapine-N-Oxide). Cardiac function was studied in-vivo by telemetric devices (DatasciTM) and we found that Gq-RASSL mice develop immediate cardiac arrhythmias in a CNO dose-dependent manner. This development was simultaneous to an increase in the mean aortic pressure. Interestingly, isolated ventricular myocytes only displayed benign responses to a robust CNO dose and did not develop cellular arrhythmogenic events. Mice expressing Gq-RASSL are a valuable tool to study the effect of Gq activation on cardiomyocytes under in-vivo conditions. Our results demonstrate the complex role of Gq mediated pathways in the heart, both on the short time course by contributing to life threatening arrhythmia and on a longer time scale by their genomic effects in the development of cardiac hypertrophy.

**P029**

**No evidence for autophagy in left ventricular myocardium with protection by remote ischemic preconditioning in patients undergoing coronary artery bypass grafting**

\*N. Gedik, G. Heusch, P. Kleinbongard  
University of Essen Medical School, Institute for Pathophysiology, Essen, Germany

Remote ischemic preconditioning (RIPC) by repeated brief limb ischemia/reperfusion episodes reduces infarct size. In our prior studies, activation of the signal transducer and activator of transcription 5 (STAT5) in left ventricular (LV) myocardium at early reperfusion was associated with protection by RIPC. Autophagy, i.e. removal of dysfunctional cellular components through lysosomes, has been suggested as a mechanism of cardioprotection. We have now analyzed, whether or not the protection by RIPC is associated with enhanced autophagy in LV myocardium of patients undergoing coronary artery bypass graft (CABG) surgery. CABG surgery patients were randomly assigned to undergo RIPC (3 cycles of 5 minutes of blood pressure cuff inflation/5 minutes deflation) or placebo (cuff uninflated) before skin incision (n=10/10). Transmural myocardial biopsies were taken from the LV perfusion territories before cardioplegia (baseline) and at early reperfusion. RIPC-induced protection was confirmed by reduced serum troponin I postoperatively (194±17 versus 709±129 ng/ml x 72 h, p=0.002). In LV biopsies, Western blotting for phosphorylation of beclin-1 and protein expression of autophagy-related gene 5-12 complex (Atg5-12), light chain 3B (LC3B), parkin and sequestosom 1 (p62) was performed. The phosphorylation of STAT3, STAT5 and extracellular signal-regulated protein kinase 1/2 (ERK1/2) was used as a positive reference to indicate protein kinase activation by ischemia/reperfusion. Immunoreactivities of phospho-proteins were normalized to their respective total proteins and protein expressions to Ponceau-S-staining, respectively. The phosphorylation of STAT3 and ERK1/2 was greater at early reperfusion with placebo and RIPC (≥2.7-fold versus baseline, p≤0.05). The phosphorylation of STAT5 at early

reperfusion was greater with RIPC than placebo (2.2-fold, p=0.02). In contrast, the signals of all analyzed autophagy proteins did not differ between baseline and early reperfusion and also not between RIPC and placebo, respectively. Protection through RIPC in patients undergoing CABG surgery is not associated with enhanced autophagy in LV myocardium at early reperfusion.

Supported by the Heinz-Horst Deichmann-Stiftung and Hans und Gertie Fischer-Stiftung.

Cell biology and signal transduction I

**P030**

**Probing the cis-arrangement of tight junction proteins claudin-1 and claudin-3 within strands**

\*S. Milatz<sup>1</sup>, J. Piontek<sup>1</sup>, J. Schulzke<sup>2</sup>, M. Fromm<sup>1</sup>, D. Günzel<sup>1</sup>  
<sup>1</sup>Institute of Clinical Physiology, Charité – Universitätsmedizin Berlin, Berlin, Germany  
<sup>2</sup>Department of Gastroenterology, Div. of Nutritional Medicine Charité – Universitätsmedizin Berlin, Berlin, Germany

**Question:** Claudins form a large family of tight junction (TJ) proteins featuring four transmembrane regions (TM1 to 4), two extra- and one intracellular loop and intracellular N- and C-terminals. They form continuous and branched TJ strands by homo- or heterophilic interaction to each other within the same membrane (cis-interaction) and with claudins of the opposing lateral cell membrane (trans-interaction).

**Methods:** In order to elucidate the molecular organization of TJ strand formation, we analyzed the cis-interaction of two abundant prototypic proteins. Human claudin-1 and claudin-3, fused to ECFP or EYFP at the N- or C-terminus, were expressed in the TJ-free cell line HEK 293. By Förster/Fluorescence Resonance Energy Transfer (FRET) analysis, the distances of claudin N- and C-termini integrated in homopolymeric strands composed of claudin-3 or of heteropolymeric strands composed of claudin-1 and claudin-3 were determined.

**Results:** There was only marginal influence of C-terminal manipulation on TJ strand formation. TMs1-4 and 4-4 within homo- and hetero-oligomers are almost equidistant and TM1 is adjacent to two or more other TMs1. This indicates that superordinate claudin cis-complexes are at least trimeric and bring three TMs1 into a closer proximity than TMs4.

**Conclusion:** Results reveal the existence of a second mode of interaction beside the interaction mode responsible for dimerization. It applies to both homo- and heterophilic interaction of claudin-3 and suggests that the basic cis-unit

is asymmetrically arranged. Our data provide novel insight in cis-strand arrangement of a prototype claudin and may be of general relevance for other claudins.

**P031**

**What can we learn from viruses to increase the efficiency of gene therapy?**

A. Meyring-Wösten<sup>1</sup>, I. Liashkovich<sup>1</sup>, W. Hafezi<sup>2</sup>, J. Kühn<sup>2</sup>, \*V. Shahin<sup>1</sup>  
<sup>1</sup>University of Münster, Institute of Physiology II, Münster, Germany  
<sup>2</sup>University of Münster, Institute of Medical Microbiology, Münster, Germany

All transport between the cytosol and the nucleus is mediated highly selectively by nuclear pore complexes (NPCs). Their selectivity can become an insurmountable hurdle for exogenously applied therapeutic macromolecules. Many viruses naturally overcome the NPC barrier. Therefore, gene therapy often utilizes viral particles as nano-carriers for exogenous therapeutic macromolecules. Viral gene therapy, however, frequently leads to severe adverse effects. We intend to elucidate the mechanisms underlying controlled release of viral DNA at the NPC in order to design new non-viral approach for intranuclear DNA delivery. For this purpose, we developed a comprehensive experimental strategy combining nano-imaging and biochemical methods. Here, we apply Herpes simplex virus type 1 (HSV-1) as an ideal example. HSV-1 contains its long 145kbp DNA in a capsid which is merely 125 nm in size. The capsid shields and targets the DNA specifically to the NPC. Only at the NPC, the capsid releases the DNA for nuclear delivery. The underlying mechanisms of this multi-step process remain unresolved. In this work we follow the fate of HSV-1 DNA in the process of transit across the NPC. Our results indicate an involvement of hydrophobicity for capsid opening. Furthermore, the DNA is released as a single thread. It likely penetrates the NPC in this conformation. It is compacted by host intranuclear proteins once it reaches the interior of the nucleus. Our proposed experimental strategy can be extended to other viruses. Moreover, our observations may help design potent non-viral based nano-carriers for gene therapy.

**P032**

**Genetic ablation of KATP channels protects murine beta-cells against nutrient stress**

\*R. Wagner<sup>1</sup>, A. Edalat<sup>1,2</sup>, B. Schittenhelm<sup>1</sup>, V. Kähny<sup>1</sup>, M. Düfer<sup>2</sup>, A. Ktorza<sup>3</sup>, J. Bryan<sup>4</sup>, P. Krippeit-Drews<sup>1</sup>, G. Drews<sup>1</sup>  
<sup>1</sup>Institute of Pharmacy, Department of Pharmacology, Clinical Pharmacy and Toxicology, Tübingen, Germany  
<sup>2</sup>Institute of Pharmaceutical and Medicinal Chemistry, Department of Pharmacology, Münster, Germany  
<sup>3</sup>Division de recherches, IdRS, 11, Suresnes, Paris, France  
<sup>4</sup>Pacific Northwest Diabetes Research Institute, Seattle, United States

**Question:** Excessive fuel intake is critically involved in the development of type-2 diabetes mellitus. KATP channels are essential for beta-cell function and are regulated by nutrients via mitochondrial metabolism. We proved the concept that genetic ablation of KATP channels (SUR1-KO) prevents impairment of beta-cell function induced by overnutrition or interference with mitochondrial function in vivo and in vitro.

**Methods:** [Ca<sup>2+</sup>]<sub>c</sub> was determined by fura-2 fluorescence and glucose-stimulated insulin release (GSIS) by radio-immunoassay. High fat diet (HFD) was applied to WT and SUR1-KO mice for 12 weeks. Morphometric analysis was carried out by insulin and glucagon immunostaining.

**Results:** WT mice on HFD became glucose-intolerant whereas SUR1-KO mice did not (n=8-9 mice/genotype). Morphometric analysis indicated higher proportion of beta-cells in WT islets compared to SUR1-KO islets of HFD-fed mice. In SUR1-KO islets HFD did not alter beta-cell mass but reduced alpha-cell number which may represent compensatory mechanisms. In vitro nutrient stress was induced by NPA (3-nitropropionic acid) which inhibits succinate dehydrogenase and by glucolipotoxicity (GLT; 25 mM glucose, 150 μM palmitate). NPA concentration-dependently inhibited GSIS in WT islets but not in islets of SUR1-KO mice (n=6 mice/genotype). GLT impaired the glucose-induced Ca<sup>2+</sup> signal only in WT beta-cells (n=3 mice/genotype). The protective effects of the SUR1-KO could be mimicked in WT mice by the KATP channel inhibitor gliclazide.

**Conclusion:** Our data show that ablation of KATP channels protects SUR1-KO mice against alimentary overload in vivo and in vitro. Targeting these channels may be a new strategy to protect beta-cells against nutrient stress.

**P033**

**Influence of Ca<sup>2+</sup> influx on mitochondrial activity of mouse pancreatic beta-cells**

\*C. Bauer<sup>1</sup>, A. Edalat<sup>2</sup>, M. Düfer<sup>2</sup>, P. Krippeit-Drews<sup>1</sup>, G. Drews<sup>1</sup>  
<sup>1</sup>Institute of Pharmacy, Department of Pharmacology, Clinical Pharmacy and Toxicology, Tübingen, Germany  
<sup>2</sup>Institute of Pharmaceutical and Medicinal Chemistry, Department of Pharmacology, Münster, Germany

**Question:** Pancreatic beta-cells respond to a primary stimulus with oscillations in electrical activity, cytosolic calcium concentration [Ca<sup>2+</sup>]<sub>c</sub>, and insulin secretion. A rise in [Ca<sup>2+</sup>]<sub>c</sub> leads to Ca<sup>2+</sup> influx into mitochondria, however, the consequences are controversial. Ca<sup>2+</sup> influx periodically depolarises mitochondria, thus lowering ATP production. This is part of a negative feedback, leading eventually to oscillations described above. By contrast, Tarasov et al. (Pflügers Arch, 2013) assume that mitochondrial Ca<sup>2+</sup> accumulation leads to a Ca<sup>2+</sup>-dependent increase in activity of FAD- or NADH-coupled dehydrogenases and in turn to an enhancement of ATP synthesis. **Methods:** [Ca<sup>2+</sup>]<sub>c</sub> was measured by fura-2, mitochondrial membrane potential (ΔΨ) by rhodamine 123 and FAD and NAD(P)H by autofluorescence. **Results:** FAD and NAD(P)H autofluorescence changed, when dehydrogenases were activated by



increases in glucose concentration from 0.5 to 4 and 15 mM. The FAD signal (n=11) did not alter when  $[Ca^{2+}]_c$  (n=8) (and subsequently  $[Ca^{2+}]_m$ ) was increased by tolbutamide (100  $\mu$ M, 4 mM glucose) or decreased by nifedipine (5  $\mu$ M, 15 mM glucose/100  $\mu$ M tolbutamide). The NAD(P)H signal (n=16) was decreased in response to a rise in  $[Ca^{2+}]_m$  and vice versa. This is ascribed to alterations in  $\Delta\Psi$  (n=10) as a  $Ca^{2+}$ -induced influence on NADH-coupled dehydrogenases should have the opposite effect.

**Conclusion:** The activity of mitochondrial dehydrogenases of beta-cells are independent of changes in  $[Ca^{2+}]_m$ .  $Ca^{2+}$ -induced changes in the NAD(P)H signal are a consequence of changes in respiratory chain activity. Increases in dehydrogenase activity are the sole result of fuel consumption independent from  $[Ca^{2+}]_m$ .

**P034**

**C2A domain of synaptotagmin-7 as regulator of fusion pore expansion during the post-fusion stage of lamellar body exocytosis in alveolar type II epithelial cells**

\*K. Neuland, N. Sharma, M. Timmler, P. Miklavc, O. H. Wittekindt, P. Dieltl, M. Frick

University of Ulm, Institute of General Physiology, Ulm, Germany

In regulated exocytosis  $Ca^{2+}$  is the key element controlling multiple steps during the exocytic pre- and post-fusion stages. We already described a „fusion-activated“  $Ca^{2+}$ -entry (FACE) via vesicular P2X4 receptors. Fusion pore expansion and vesicle content release are regulated by FACE (PNAS, 2011 Aug 30;108(35):14503-8). But the question how this locally restricted  $Ca^{2+}$  signal is translated into mechanical force promoting fusion pore expansion remained. Members of the synaptotagmin family that localize to secretory vesicles have been found to promote fusion pore expansion via  $Ca^{2+}$  binding to C2 domains. It was the aim of this study to test whether synaptotagmin and in particular  $Ca^{2+}$ -binding to one or both C2 domains could form a molecular link between FACE and fusion pore expansion in ATII cells. Synaptotagmin-7 was identified as the  $Ca^{2+}$ -binding isoform predominantly expressed in primary ATII cells using RT-PCR and western-blotting. Immunofluorescence confirmed its localization on LBs. In functional studies overexpressing wt synaptotagmin or synaptotagmin with defects in  $Ca^{2+}$ -binding to either the C2A or C2B domain we investigated changes in fusion pore diameters. Dissecting FACE from global elevations of intracellular  $Ca^{2+}$  we found that an intact C2A domain accelerates fusion pore expansion following FACE. Interestingly, however, overexpression of wt synaptotagmin-7 exerted an inhibiting effect on LB fusion in presence of  $Ca^{2+}$  and this effect depended on an intact C2A domain. Defects in  $Ca^{2+}$ -binding to the C2B domain did not influence LB fusion or FACE-dependent fusion pore expansion. In summary our results suggest that the C2A domain of synaptotagmin-7 is the major determinant of FACE-dependent fusion pore expansion during the post-fusion stage of lamellar body exocytosis and potentially provides the link between FACE and fusion pore expansion in LB exocytosis.

**P035**

**The IGF binding protein-5 is a novel downstream signaling molecule of the Wilms' tumor suppressor WT1**

\*M. Müller, A. Bondke Persson, K. Kirschner, P. Persson, H. Scholz  
Institut für Vegetative Physiologie, Charité Universitätsmedizin Berlin, Berlin, Germany

The Wilms' tumor gene, WT1, encodes a zinc finger transcription factor that functions as a tumor suppressor and a key regulator of kidney development. Recent findings indicate that WT1 is also necessary for maintaining normal bone integrity in the adult organism. In the present study, we aimed at identifying novel candidate targets of WT1 in these tissues. An initial genome-wide cDNA microarray analysis revealed a close correlation between the mRNA levels of WT1 and insulin-like growth factor binding protein-5 (IGFBP-5), which has a critical role in osteogenesis. WT1 and IGFBP-5 proteins were co-localized by immunohistochemistry in the kidney and bone of embryonic rats and mice. Silencing of WT1 by siRNA transfection of a murine mesonephros-derived cell line reduced IGFBP-5 mRNA levels by approximately 80% (real-time RT PCR) compared to transfection with a non-targeting siRNA. Accordingly, IGFBP-5 transcripts and protein levels were increased significantly in osteosarcoma cells expressing the transcriptionally active WT1(-KTS) protein. In contrast, the WT1(+KTS) isoform, which has a presumed role in mRNA processing rather than in transcriptional regulation, did not significantly change IGFBP-5 expression in osteosarcoma cells. Consistent with these experimental data, four predicted WT1 binding sites were disclosed in the first intron of the human IGFBP-5 gene by bioinformatic analysis. In conclusion, these findings indicate that IGFBP-5 may act as a novel downstream effector of WT1 during kidney and bone formation.

**P036**

**The Long non-coding RNA n342419 (Mantis) is an important component for the homeostasis of the vascular system**

\*M. S. Leisegang<sup>1</sup>, C. Fork<sup>1</sup>, Y. Ponomareva<sup>2</sup>, S. Uchida<sup>2</sup>, R. P. Brandes<sup>1</sup>

<sup>1</sup>Goethe-University Frankfurt, Institute for Cardiovascular Physiology, Frankfurt am Main, Germany

<sup>2</sup>Goethe-University Frankfurt, Institute for Cardiovascular Regeneration, Frankfurt am Main, Germany

Long non-coding RNA (lncRNA) is a very plastic and poorly understood class of non-coding RNA. It is broadly defined as transcribed, but not translated, RNA molecules greater than 200 nucleotides in length and can be classified in three major groups: structural, repressive and activating with a wide variety of important functions. Here, we took advantage of the Exon-array technique to analyze up- or down-regulated lncRNAs in response to a specific histone demethyltransferase knockdown in human umbilical vein endothelial cells (HUVEC). We studied a series of lncRNA candidates on the potential contribution to the homeostasis of the vascular system in a broad diversity of stimuli and focused on n342419, an uncharacterized lncRNA,

which we have termed Mantis according to its secondary structure. Interestingly, Mantis consists of four exons and its genomic position is intronic antisense to the Annexin A4 gene. Among the cell types we have analyzed, the lncRNA was expressed highest in HUVEC. Moreover, Mantis is a mRNA-like lncRNA showing PolyA, splicing and nuclear fractionation, but the majority of the lncRNA seems only conserved in the primate lineage. Down-regulation revealed that Mantis maintains endothelial cell homeostasis. Furthermore, it attenuated the TNF $\alpha$ -induced inflammatory activity, reduced the serum-induced proliferation rate and decreased the expression of TNF $\alpha$ -induced genes. Importantly, tube formation on matrigel and spheroid outgrowth of HUVEC were greatly attenuated after knockdown of Mantis. Collectively, our data demonstrate that Mantis is a novel element in angiogenesis-related processes in endothelial cells.

**P037**

**Temporal behaviour of cellular H<sup>+</sup> buffering**

\*M. Dietrich<sup>1</sup>, J. Hauth<sup>2</sup>, P. Lang<sup>2</sup>, J. W. Deitmer<sup>1</sup>

<sup>1</sup>TU Kaiserslautern, General Zoology, Kaiserslautern, Germany

<sup>2</sup>Fraunhofer Institut für Techno- und Wirtschaftsmathematik (ITWM), Kaiserslautern, Germany

The  $[H^+]$  is a potent modulator of several physiological processes. Thus, the regulation of cytosolic  $[H^+]$  is of central importance for the cell and the pH has to be maintained in a narrow range. One fundamental mechanism to maintain pH, besides the transport of acid/base equivalents across the cell membrane, is the buffering of cytosolic  $H^+$ . The degree to which protons are buffered is quantified by the buffer capacity (or buffer strength or power). M. Koppel & K. Spiro, (Biochem. Zeitschr. 65, 1914) and D.D. van Slyke, (J. Biol. Chem. 52, 1922) independently defined the buffer capacity  $\beta$  as the additive inverse of the differential quotient given by the infinitesimal amount of acid S divided by the actual infinitesimal change in pH:  $\beta = -dS/dpH$ . Until now, the definition was only used for steady state buffering (instantaneous buffering assumed for the intrinsic buffering). In the case that the buffering is not instantaneous (for the  $CO_2/HCO_3^-$  buffer system), two different buffer capacities can be defined:  $\beta_{dyn}$  for the dynamic reaction system and  $\beta_{eq}$  for the corresponding equilibrated system. While the last value corresponds to the classical buffer capacity, the last one is by itself less informative. More interesting is its rate of change with respect to time, given by the time derivative  $\beta'_{dyn} = d\beta_{dyn}/dt$ , which can be seen a quantitative measure how fast the buffering occurs under non-steady-state conditions. We will show in *Xenopus laevis* oocytes that  $\beta'_{dyn}$  can be modulated without effecting  $\beta_{eq}$ . Such a modulator is e.g. carbonic anhydrase II (CAII) in the presence of the  $CO_2/HCO_3^-$  buffer system.

Supported by the Deutsche Forschungsgemeinschaft (DE 231/24-1,2), and CMCM of the Land Rheinland-Pfalz.

**P038**

**Real 3D stochastic particle (H<sup>+</sup>) simulations**

\*J. Hauth<sup>1</sup>, \*M. Dietrich<sup>2</sup>, J. W. Deitmer<sup>2</sup>, P. Lang<sup>1</sup>

<sup>1</sup>Fraunhofer Institut für Techno- und Wirtschaftsmathematik (ITWM), Kaiserslautern, Germany

<sup>2</sup>TU Kaiserslautern, General Zoology, Kaiserslautern, Germany

The control and regulation of the intracellular pH is of pivotal importance for every living organism. To keep the  $pH_i$  at a constant level, the cell can bind or release protons from molecular binding sites. This process is called  $H^+$  buffering. Buffering was so far often measured in equilibrium, but the dynamic development over time has not been considered. We recently developed a new dynamic buffering concept, which considers both the amplitude and the time course of  $H^+$  buffering. To gain more knowledge about the dynamics of proton buffering we set up a mathematical model of the processes involved in  $H^+$  buffering. Since we have not found any adequate and efficient tool which allows the in-silico simulation of reaction-diffusion processes in cells with complex three-dimensional geometries, we developed a method which is based on a stochastic approach (in contrast to the common PDE solvers), and which consists of a combination of a Monte Carlo particle simulation and an additional Importance Sampling step, which allows the infinite reuse of already sampled paths. This additional step makes the method extremely efficient. Simulations can be done by factors faster than real-time. We used this tool to simulate the pH dynamics in an oocyte and in an astrocyte-like shape of model cell with a highly complex geometry. The computation time was compared with a state of the art partial differential equation (PDE) solver. Supported by the Deutsche Forschungsgemeinschaft (DE 231/24-1,2), and CMCM of the Land Rheinland-Pfalz.

**P039**

**ATP-Synthase and 3-Phosphoglycerate dehydrogenase (Phgdh) are new interaction partners of Akt1 in mouse hearts**

\*N. Blasberg, M. Reinartz, A. Gödecke

Cardiovascular Research, Düsseldorf, Germany

**Question:** Akt1 is a protein kinase that mediates manifold functions in cardiac growth, metabolism and apoptosis. To investigate novel Akt1 signal transduction pathways, we examined protein interactions of Akt1 in HEK293 cells and mouse hearts by tandem affinity purification (TAP) and mass spectrometry (MS).

**Methods:** Screening for Akt1 interacting proteins was performed by TAP and MS using Akt1-TAP-TAG transfected HEK293 cells for establishment of the method and transgenic mice with cardiac-specific expression of TAP-tagged Akt1. To quantify purified proteins we used Silac (Stable isotope labelling by amino acids in cell culture) in HEK293 cells and stable isotope dimethyl labelling of peptides purified from mouse hearts. For verification of candidates Proximity Ligation Assay (PLA) was used in HEK293 cells and isolated adult cardiac myocytes.

**Results:** Quantification of TAP-isolated proteins revealed that Heat shock protein 90 (Hsp90), Hsp70 and Hsp71 form stable complexes with Akt1, indicated by a high shifted ratio towards heavy labeled peptides. Other proteins like Sarcoplasmic/endoplasmic reticulum calcium ATPase (Serca), Actin, ATP-Synthase and Phgdh seemed to interact more transiently with Akt1. ATP-Synthase and Phgdh were verified as interaction partners of Akt1 by PLA in adult cardiac myocytes.

**Conclusion:** Quantitative TAP/MS analysis in HEK293 cells and transgenic mice revealed new Akt1 interacting proteins. Identification of ATP-Synthase as interaction partner illustrates that Akt1 plays a role in regulating energy supply of the cell. Interaction of Akt1 with Phgdh points out functions of Akt1 in anabolic cell metabolism.

**P040**

**The biological actions of R/S 11,12-epoxyeicosatrienoic acid in endothelial cells are Gas dependent**

\*Y. DING<sup>1</sup>, T. Frömel<sup>1</sup>, S. Offermanns<sup>2</sup>, I. Fleming<sup>1</sup>

<sup>1</sup>Johann Wolfgang Goethe University, Frankfurt am Main, Germany

<sup>2</sup>Max-Planck-Institute for Heart and Lung Research, Department of Pharmacology, Bad Nauheim, Germany

Cytochrome P450 (CYP)-derived epoxides of arachidonic acid i.e. the epoxyeicosatrienoic acids (EETs) are important lipid signalling molecules involved in the regulation of vascular tone and angiogenesis. Since many of the actions of 11,12-EET are dependent on the activation of protein kinase (PK) A, the existence of a cell surface Gas coupled receptor has been postulated. Here, we used the 11,12-EET-induced, PKA-dependent translocation of transient receptor potential (TRP) C6 channels as well as EET-induced angiogenesis to screen for a putative EET receptor in endothelial cells. TRPC6 was overexpressed in primary human umbilical vein endothelial cells (HUVEC) or a related cell line (HUV-EC-c) and TRPC6 translocation to the plasma membrane following EET-stimulation was assessed by confocal microscopy. Stimulating HUVEC or HUV-EC-c with 11,12-EET led to the translocation of TRPC6 channels from the Golgi apparatus to caveolae, this could be only reproduced by R/S-11,12-EET while not S/R-11,12-EET and ±14,15-EET. This response was sensitive to the EET-antagonists 14,15-EEZE and miconazole as well as the cyclic AMP analogue Rp-cAMPs. In HUV-EC-c cells siRNA directed against Gas abolished the 11,12-EET-induced translocation of TRPC6 but was without effect in cells stimulated with forskolin or Sp-cAMPs. In accord with previously report showing that 11,12-EETs can initiate angiogenesis, we found that the reduction of Gas-levels resulted in a significant lower total tube length in primary HUVEC. Taken together, our results suggest that a Gas-coupled receptor in the endothelial cell membrane responds to R/S 11,12-EET, mediate the PKA-dependent translocation and activation of TRPC6 channels and tube formation.

**P041**

**Decreased store operated Ca<sup>2+</sup> entry in dendritic cells isolated from mice expressing PKB/SGK-resistant GSK3**

\*J. Yan, E. Schmid, E. Shumilina, F. Lang

University of Tuebingen, Department of Physiology, Tübingen, Germany

**Question:** Dendritic cells (DCs) are regulated by glycogen synthase kinase GSK3, which fosters a proinflammatory DC phenotype. GSK3-activity is suppressed by protein kinase B (PKB) and serum and glucocorticoid inducible kinase (SGK). The present study explored whether PKB/SGK-dependent GSK3 $\alpha,\beta$ -activity impacts on Ca<sup>2+</sup> signaling in DCs.

**Methods:** DCs were isolated from gsk3<sup>KI</sup> and respective wild-type (gsk3<sup>WT</sup>) mice, [Ca<sup>2+</sup>]<sub>i</sub> estimated from Fura2 fluorescence and protein abundance of store operated Ca<sup>2+</sup> (SOC) channel subunits Orai1, STIM1, STIM2 as well as Ca<sup>2+</sup>-binding protein calbindin D28k determined by Western blotting.

**Results:** Thapsigargin-induced Ca<sup>2+</sup>-release from intracellular stores (CRIS) and SOC-entry were significantly blunted by GSK3-inhibitor SB216763 (10 $\mu$ M, 30min), but significantly lower in gsk3<sup>WT</sup> than in gsk3<sup>KI</sup>DCs. Orai1, STIM1 and STIM2 protein abundance was significantly lower and calbindin D28k abundance significantly higher in gsk3<sup>KI</sup> than in gsk3<sup>WT</sup>DCs. The activity of both, K<sup>+</sup>-dependent and K<sup>+</sup>-independent Na<sup>+</sup>/Ca<sup>2+</sup>-exchangers was significantly increased in gsk3<sup>KI</sup> DCs.

**Conclusion:** The present observations point to a dual role of GSK3 in the regulation of Ca<sup>2+</sup> in DCs. The increase of [Ca<sup>2+</sup>]<sub>i</sub> following CRIS and SOC entry is blunted by acute inhibition of GSK3. However, expression of PKB/SGK-resistant GSK3 $\alpha,\beta$  downregulates the increase of [Ca<sup>2+</sup>]<sub>i</sub> following CRIS and SOCE, an effect at least partially due to downregulation of Orai1, STIM1 and STIM2 expression as well as upregulation of Na<sup>+</sup>/Ca<sup>2+</sup>-exchangers activity and calbindin D28k expression.

**P042**

**Glycogen synthase kinase 3 controls hepatic triglyceride synthesis**

\*A. Fajol, H. Chen, B. Zhang, F. Lang, M. Föller

University of Tuebingen, Department of Physiology, Tübingen, Germany

**Question:** Glycogen synthase kinase 3 (GSK3) is involved in PI3-kinase-dependent insulin signaling. GSK3 is phosphorylated at Ser21 (GSK3 $\alpha$ ) and Ser9 (GSK3 $\beta$ ) and thereby inactivated by protein kinase B (PKB/Akt), an effector kinase of PI3-kinase signaling. Hepatic glycogen synthesis does not depend on GSK3 phosphorylation. Here, we explored the role of PI3-kinase-dependent phosphorylation of GSK3 in hepatic triglyceride synthesis.

**Methods:** Mice expressing a mutated form of GSK3 $\alpha$  which is not phosphorylatable by PKB/Akt (gsk3<sup>KI/KI</sup>) were compared to wild type mice (gsk3<sup>wt/wt</sup>). The mice were analysed before and after 10-12 weeks of high-fat diet. Serum triglyceride and cholesterol levels were determined by a clinical chemistry analyser, serum leptin by ELISA and

hepatic gene expression by qRT-PCR. Oil red staining was used to identify fatty liver.

**Results:** The serum triglyceride and total cholesterol levels were significantly lower and the serum GPT activity higher in untreated gsk3<sup>KI/KI</sup> mice compared to gsk3<sup>wt/wt</sup> mice. Transcript levels of CD36 gene encoding for a fatty acid transporter and of monoacylglycerol-O-acyltransferase (Mogat) 1 gene were drastically reduced in gsk3<sup>KI/KI</sup> mice compared to gsk3<sup>wt/wt</sup> mice. Following 10-12 weeks of high-fat diet, the serum leptin concentration was markedly lower in gsk3<sup>KI/KI</sup> mice than in gsk3<sup>wt/wt</sup> mice. In line with that subcutaneous and perirenal fat mass were significantly smaller in gsk3<sup>KI/KI</sup> mice compared to gsk3<sup>wt/wt</sup> mice. Oil red staining revealed hepatic steatosis in gsk3<sup>wt/wt</sup> mice but not in gsk3<sup>KI/KI</sup> mice.

**Conclusion:** PI3-kinase-induced inactivation of GSK3 controls triglyceride utilization and hepatic triglyceride synthesis and is important for triglyceride storage by adipose tissue.

**P043**

**Inhibition of PI3-kinase leads to apoptosis in TGF $\beta$ -stimulated cardiomyocytes of rat**

\*J. Heger, B. Warga, R. Schulz, G. Euler

Institute of Physiology, Giessen, Germany

**Question:** Apoptosis is involved in the transition of compensated hypertrophy to heart failure which is associated with increased TGF $\beta$  expression. We have shown in former studies that TGF $\beta$ -induced apoptosis needs SMAD transcription factors and NO. To identify further signaling molecules in this apoptosis pathway we analyzed, if PI3-kinase (PI3-K) may be involved in TGF $\beta$ -induced apoptosis.

**Methods:** Therefore, isolated adult cardiomyocytes of rat were stimulated with TGF $\beta$ 1 (1ng/ml) in presence of the PI3K inhibitor Ly294002 (10  $\mu$ M).

**Results:** After six hours caspase 3/7 activity increased significantly, that could be blocked with Ly294002. Moreover, chromatin condensation was analyzed and here again TGF $\beta$ -induced apoptosis could be inhibited with Ly294002 as well as with Wortmannin (100nM), another PI3K inhibitor. While TGF $\beta$  increased NO formation, inhibition of PI3-K could not reduce NO production. Since TGF $\beta$  stimulation results in activation of SMADs, SMAD binding activity was measured in EMSAs. TGF $\beta$ -induced increase in SMAD activation could be blocked with Ly294002. Furthermore, the increased expression of the apoptosis gene DAPK1 under TGF $\beta$  could be reduced by inhibition of PI3-K.

**Conclusion:** TGF $\beta$  induces apoptosis in adult cardiomyocytes. While NO formation is not mediated by PI3-K, we could demonstrate that SMAD binding activity as well as expression of apoptosis gene DAPK1 is depending on PI3-K. We could show that PI3-K is involved in the classical TGF $\beta$  signaling pathway and apoptosis induction in adult cardiomyocytes of rat.

**P044**

**Physiology and pathophysiology of ATPases in aldosterone secretion**

\*J. Stindl<sup>1</sup>, P. Tauber<sup>1</sup>, D. Penton<sup>2</sup>, C. Sterner<sup>1</sup>, I. Tegtmeier<sup>1</sup>, F. Beuschlein<sup>3</sup>, M. Reincke<sup>3</sup>, T. Williams<sup>4</sup>, P. Mulatero<sup>4</sup>, R. Warth<sup>1</sup>, S. Bandulik<sup>1</sup>

<sup>1</sup>University of Regensburg, Institute of Physiology, Regensburg, Germany

<sup>2</sup>Laboratories of Excellence, Ion Channel Science and Therapeutics, Nice, France

<sup>3</sup>Ludwig-Maximilians-Universität, Medizinische Klinik und Poliklinik IV, Munich, Germany

<sup>4</sup>University of Torino, Department of Medical Sciences, Torino, Italy

Aldosterone synthesis in adrenal glands is stimulated by angiotensin II and high plasma K<sup>+</sup>. Both factors induce membrane depolarization, activation of voltage-gated Ca<sup>2+</sup> channels, and an increase of cytosolic Ca<sup>2+</sup>, which triggers the expression of aldosterone synthase. Autonomous renin-independent production of aldosterone, so-called primary aldosteronism (PA), is found in 10% of the patients with essential hypertension of which one third have aldosterone producing adenomas (APAs). Somatic mutations of the alpha subunit (ATP1A1) of the Na<sup>+</sup>/K<sup>+</sup> ATPase are present in 5-6% of APAs. This study aimed at investigating the effects of mutants of ATP1A1 on intracellular Na<sup>+</sup> and pH homeostasis in adrenocortical cells. Primary cultured cells from patients with mutant ATP1A1<sup>L104R</sup> or ATP1A1<sup>V332G</sup> as well as HEK293 cells expressing mutant ATP1A1<sup>L104R</sup> or ATP1A1<sup>G99R</sup> displayed a pathological membrane depolarization. In adrenocortical NCI-H295R cells expressing the mutated ATP1A1 (L104R or V332G), Na<sup>+</sup> extrusion was only reduced after blocking the endogenous ATPase. In addition, BCECF fluorescence measurements showed that cytosolic pH balance was impaired after expression of the mutant ATP1A1. These data indicate that the adenoma-associated mutants ATP1A1<sup>L104R</sup> and ATP1A1<sup>V332G</sup> result in a gain-of-function phenotype that disturbs intracellular electrolyte and pH homeostasis.

Cell biology and signal transduction II

**P045**

**Extracellular acidosis affects the expression of pro-inflammatory mediators and signal transduction in monocyte- and macrophage-like cells**

\*A. Riemann, H. Wußling, B. Schneider, O. Thews

Martin-Luther-Universität Halle-Wittenberg, Julius-Bernstein-Institut für Physiologie, Halle/Saale, Germany

Extracellular acidosis can be present in different pathological conditions like inflammation, ischemia and solid tumors where it affects both cellular signaling and gene expression. Since mononuclear cells are involved in these diseases, the aim of the study was to analyze whether the monocytes/macrophages are affected by the acidotic environment and which signaling pathways are involved. Monocytic cell lines (THP-1, Mono Mac 6) and activated macrophage-like cells (PMA-differentiated THP-1, RAW264.7) were incubated at pH 7.4 or pH 6.6 for 3 h to study the effect of acidosis. Gene expression of COX-2, MCP-1, IL-1 $\beta$ , IL-6, TNF- $\alpha$ , iNOS and osteopontin as well as MAPK- and CREB phosphorylation were analyzed. Extracellular acidosis led to a decreased expression of COX-2 and MCP-1 in monocytes. In addition, the Mono Mac 6 cells exhibit reduced expression of IL-1 $\beta$ , IL-6 and osteopontin, while in THP-1 cells TNF- $\alpha$  expression was decreased. When THP-1 cells were differentiated to macrophage-like cells, no significant differences in gene expression were observed at pH 6.6. RAW264.7 macrophages displayed increased expression of COX-2, IL-1 $\beta$  and iNOS. These effects might be mediated by p38, since it is activated at pH 6.6 in this cell line, but not in THP-1 or Mono Mac 6 cells. MCP-1 expression was reduced similar to the monocytic cells. Taken together, acidosis affects the expression of different mediators of inflammation in dependency of the cellular differentiation. In monocytes several mediators were rather reduced, while in macrophages expression was increased at reduced pH.

**P046**

**The role of the actin capping protein (CapZ) for force development and force kinetics in skeletal myofibrils**

\*S. Rippl, M. Bitzer, S. Papadopoulos, M. Schroeter, G. Pfitzer, R. Stehle  
University of Cologne, Institute of Vegetative Physiology, Cologne, Germany

CapZ is the heterodimeric capping protein of the thin filament in the sarcomeres, the smallest contractile subunits of muscles. CapZ prevents actin polymerisation at the barbed end of the actin filament that is located at the Z-disc, a structural element that separates but also interconnects the sequence of sarcomeres in a myofibril. CapZ interacts with Z-disc proteins like nebulin and is suggested to participate in networks of mechanical linkage. We therefore hypothesized that CapZ and in particular its downreg-

ulation influences biomechanical parameters of the sarcomeres like passive and active tension and kinetics of force development and relaxation. To test this, we characterized the biomechanical properties of myofibrils from wildtype zebrafish larvae and zebrafish larvae that were manipulated by injection of morpholino modified antisense oligonucleotides. Those morpholinos are targeted to the mRNA of CapZ and should prevent its translation at the start site. The manipulated larvae, the morphants, exhibited reduced myofibrillar density but there were some myofibrils remaining that could be isolated and investigated. We analyzed the downregulation of the Z-disc protein CapZ with standard molecular methods like immunohistochemistry of myofibrils. Using a sophisticated setup for force measurements of small bundles of myofibrils or even of single myofibrils we determined maximum and passive force ( $F_{max}$ ,  $F_{pass}$ ), rate constants of force development kinetics ( $k_{ACT}$ ,  $k_{TR}$ ) and kinetics of relaxation ( $k_{REL}$ ). Our preliminary results indicate that despite the delayed development of larval somites, the myofibrils that are formed in the morphants are contractile and functional.

**P047**

**Age-dependent abundance of transcription factor Nuclear Factor of kappaB in human erythrocytes**

\*M. Ghashghaieinia<sup>1</sup>, J. Cluitmans<sup>2</sup>, F. Lang<sup>1</sup>, G. Bosman<sup>2</sup>, T. Wieder<sup>3</sup>

<sup>1</sup>University of Tübingen, Department of Physiology, Tübingen, Germany

<sup>2</sup>University of Nijmegen, Biochemistry, Nijmegen, Netherlands

<sup>3</sup>University of Tübingen, Dermatology, Tübingen, Germany

**Question:** Despite lacking nuclei, human erythrocytes possess large quantities of transcription factors of the NF $\kappa$ B-family (like NF $\kappa$ B p50 and NF $\kappa$ B p65). As reported earlier [Ghashghaieinia et al. 2011, Cell.Physiol.Biochem.27:45-54], treatment of human erythrocytes with the specific NF $\kappa$ B-inhibitors Bay 11-7082 and parthenolide leads to programmed death of the erythrocytes, i.e. eryptosis. The present study explored the connection between erythrocyte age and its possible influence on the abundance of the canonical NF $\kappa$ B family members.

**Methods:** Erythrocytes were drawn from healthy individuals and then divided into 5 fractions (fraction I to fraction V) utilizing density gradients. Fraction I comprised the youngest and fraction V the oldest erythrocyte population of each healthy volunteer. Then, the fractions were analyzed by Western Blot, and the amount of NF $\kappa$ Bs was determined by video-densitometry.

**Results:** Large differences were observed in NF $\kappa$ Bs abundance between the different fractions: whereas fraction I exhibited the highest NF $\kappa$ B level, fraction V showed the lowest level of NF $\kappa$ B. In contrast, both fractions contained similar amounts of  $\beta$ -actin. Even though possessing functional 20S proteasomes [Neelam et al. 2011, Exp.Biol. Med.236:580-591], some proteins including  $\beta$ -actin are protected in mature erythrocytes against proteolysis by other specific intraerythrocytic proteins and/or by structural properties (e.g. spacial configurations that mask ubiquitination sites), thus preventing their rapid degradation during

the erythrocytes' life span. Other proteins, like NF $\kappa$ Bs, however, are targeted to degradation depending on the age of the erythrocytes.

**Conclusions:** Erythrocytes harbour proteins which are stable, such as  $\beta$ -actin, or are rapidly degraded, such as NF $\kappa$ Bs.

**P048**

**A role for Rock1 and myosin light chain kinase in post-fusion compression of peri-vesicular actin coat in alveolar type II pneumocytes**

\*P. Miklavc, K. Ehinger, W. Close, T. Felder, P. Dietl, M. Frick

University of Ulm, Institute of General Physiology, Ulm, Germany

Exocytosis comprises a sequence of highly regulated steps leading to fusion of secretory vesicles with the plasma membrane, opening of a fusion pore and content release. Alveolar type II pneumocytes secrete surfactant, a lipo-protein substance which reduces surface tension in the lungs. Unlike soluble vesicle contents that readily diffuse from the vesicle lumen following fusion pore opening, additional mechanisms during the exocytic post-fusion phase are required for efficient secretion of poorly-soluble surfactant. Secretory vesicles in alveolar type II cells are coated with actin following vesicle fusion with the plasma membrane and subsequent compression of the actin coat is necessary for surfactant release. We have already demonstrated that myosin II is involved in actin coat compression, however detailed mechanisms of myosin II activation and coat compression were not clear. In the present study we used high-resolution life cell imaging to show that Rock1 and myosin light chain kinase (MLCK) are recruited to the secretory vesicles following fusion with the plasma membrane. Recruitment of Rock1 was preceded by transient activation of Rho GTPase on the fused vesicle. Inhibition of Rock1 significantly impaired full compression of fused vesicles without affecting initial compression. Inhibition of MLCK did not have a measurable effect on actin coat compression. Combined inhibition of Rock1 and MLCK completely blocked vesicle compression. Our data suggest that Rock1 and MLCK act via complementary pathways in activation of regulatory myosin II light chain and actin coat compression.

**P049**

**Subtype-specific voltage dependence of muscarinic receptors**

\*A. Rinne<sup>1</sup>, J. C. Mobarec<sup>2</sup>, P. Kolb<sup>2</sup>, M. Bünemann<sup>3</sup>

<sup>1</sup>Ruhr-Universität Bochum, Institut für Kardiovaskuläre Physiologie, Bochum, Germany

<sup>2</sup>Philipps-Universität Marburg, Institut für Pharmazeutische Chemie, Marburg, Germany

<sup>3</sup>Philipps-Universität Marburg, Institut für Pharmakologie und Klinische Pharmazie, Marburg, Germany

Muscarinic receptors (MR) are G protein-coupled receptors (GPCRs) which are voltage-sensitive. Because voltage ac-

tivates GqPCRs (e.g. M1R) but deactivates GiPCRs (e.g. M2R), it was proposed that the G protein class affected the outcome of voltage dependence. In this study we analyzed signaling of the M1R, M3R and M5R with fluorescence resonance energy transfer (FRET) microscopy and voltage clamp. To test whether Gq protein coupling influences voltage sensitivity, we expressed a biosensor that reports conformations of M1R in HEK 293 cells and analyzed Carbachol (CCh)-induced receptor activation at -90 mV and at +60 mV. Depolarization caused activation of M1R, which was not abolished after uncoupling of Gq proteins with GT-PyS. A FRET assay that reports activation of Gq was used to compare the voltage dependencies of M1R, M3R and M5R. Notably, voltage dependence was subtype-specific: Depolarization caused either activation (M1R) or deactivation of the receptors (M3R or M5R). Voltage sensitivity of MR was also ligand-specific: M3R displayed deactivation (CCh) or activation (Pilocarpine) at +60 mV. Computational docking studies predicted different molecular binding modes for each agonist and guided us to select key point mutations in the orthosteric binding site of muscarinic receptors. Further docking of mutant M3R predicted a novel "Pilocarpine-like" binding mode for CCh and indeed, the mutated receptor was activated by voltage in live cell experiments. Together, these results imply that a mechanism of voltage sensitivity of GqPCRs resides in the receptor protein without the requirement of G protein coupling.

**P050**

**Matrix stiffness-dependent change of endothelial cell phenotype**

\*T. Gloe, L. Devermann

Med. Fak. Mannheim, Heidelberg-University, CBTM, KPhys, Mannheim, Germany

**Introduction:** It is a long known fact that endothelial cells (EC) from different vascular beds show different phenotypes. However, up to date it is studied insufficiently how such differences are established and whether EC might change their phenotype even after terminal differentiation. In this study, we tried to address that question and draw the hypothesis that, similar to stem cells, the phenotype of EC might be dependent on the elastic properties of the extracellular matrix e.g. the vascular wall. Recent results showed that EC release proteases which in turn might modify extra cellular matrix. Therefore, we paid special interest on cellular phenotypes and signaling responses induced by changes in the matrix stiffness. Since during vascular remodeling processes, proteases are often recruited and seem to be critically involved in generation and maintenance of signaling cascades of adaptive vascular remodeling, we proposed that due to those proteolytic activities the matrix stiffness is altered and influences EC phenotype.

**Methods and Results:** To investigate acute signaling effects induced by proteolytic matrix degradation, EC were grown on plastic dishes coated with fibronectin and subsequently exposed to elastase (0.3 to 0.5U/ml). As soon as 2-5min after elastase treatment EC changed morphology

and showed a substantial reorganization of focal adhesion sites. In order to verify that matrix elasticity was the effective signal, EC were seeded on matrix-coated polyacrylamide gels exhibiting increasing stiffness (Young's modulus from 10 to 100kPa). Parallel to matrix flexibility, EC showed changes in morphology from a flat and spread phenotype to a more rounded and contracted, verifying that EC are constantly pulling on their adhesion sites. Additionally, soft and flexible matrix gels gradually induced apoptosis (tunnel- and annexin assay). The rate of apoptosis was further increased if cells seeded on different strong matrices were additionally exposed to elastase.

**Conclusion:** These results indicate that although the overall composition is not changed, proteolysis of the matrix induces distinct signaling induced by changes of the focal arrangement of matrix receptors. Thus, fragmentation of matrix proteins changes the microarchitecture and show modulator properties for adhesion dependent signaling leading to apoptosis (anoikis). This in vitro culture regime might serve not only as a model system to study development and progression of vascular aneurysms but also of arteriosclerosis and high blood pressure.

**P051**

**The Wilms' tumor suppressor Wt1 regulates Gata4 gene expression through activation of a distal enhancer element**

\*M. Klockziem<sup>1</sup>, L. J. Rudigier<sup>1</sup>, M. Klar<sup>2</sup>, K. M. Kirschner<sup>2</sup>, C. Dame<sup>2</sup>, H. Scholz<sup>1</sup>

<sup>1</sup>Charité-Universitätsmedizin Berlin, Institut für Vegetative Physiologie, Berlin, Germany

<sup>2</sup>Charité-Universitätsmedizin Berlin, Klinik für Neonatologie, Berlin, Germany

Mutations in the human genes encoding the transcription factors GATA4 and WT1 are associated with developmental disorders, particularly of the heart and the genitourinary system. Moreover, inactivation of either Gata4 or Wt1 causes similar cardiac and urogenital defects in mice. Yet, several genes have been identified as common downstream targets of both transcription factors. Thus, we addressed the question of whether a direct link exists between Wt1 and Gata4 in that the two molecules mutually regulate each other. We co-localized Gata4 and Wt1 proteins by immunohistochemistry in epicardial cells of the embryonic murine heart (e12.5) and in the developing gonads of both sexes. Wt1-deficient mice (Wt1<sup>-/-</sup>) expressed significantly lower Gata4 mRNA levels in the heart and gonads compared to their wild-type littermates. Suppression of Wt1 by RNA interference lowered Gata4 expression in cultured cells, which were derived from the murine gonad/mesonephros region. To further dissect the underlying molecular mechanism, we performed reporter gene assays on the Gata4 promoter and a distal enhancer element that directs Gata4 expression to the lateral mesoderm. Notably, Wt1 had no effect on the Gata4 promoter, but significantly activated the conserved region 2 (CR2) of the mesodermal Gata4 enhancer. Binding of Wt1 to this enhancer region was confirmed by chromatin immunoprecipitation assay.

In conclusion, our findings demonstrate that Gata4 acts downstream of Wt1 during gonad development. Moreover, Wt1 directly contributes to Gata4 expression by regulating the activity of the mesodermal Gata4 enhancer.

**P052**

**Effect of steroids on paracellular barrier function in lung epithelia**

\*F. Kielgast, H. Schmidt, M. Frick, P. Dietl, O. H. Wittekindt  
Ulm University, Institute of General Physiology, Ulm, Germany

We investigated the effect of the glucocorticoids Dexamethasone and Hydrocortisone as well as the mineralocorticoid Aldosterone on NCI-H441 lung epithelia cell layers cultivated at Air-Liquid Interface (ALI). Dexamethasone (Dex) and Hydrocortisone (HyCo) increased transepithelial resistance (TEER). This increase was sensitive to glucocorticoid receptor antagonist Mifepristone but not to the mineralocorticoid receptor antagonist Spironolactone. Aldosterone did not increase TEER compared to untreated control cells. Diffusionpotential measurements revealed a Dexamethasone and Hydrocortisone dependent increase in Cl<sup>-</sup> selectivity of tight junctions (TJ). An expression screening of TJ and TJ-associated protein transcripts revealed that exclusively Claudin 8 (Cldn8) expression was depending on glucocorticoids. Cldn8 expression was upregulated at [Dex] of 1nM and reached its maximum at [Dex] of 100 nM and above. A biphasic response of Cldn8 expression was observed for HyCo. Cldn8 down-regulation was observed for [HyCo] ranging between 10 and 100 nM. Up-regulation of Cldn8 expression was observed for [HyCo] 100 nM and above. This gives evidence for a glucocorticoid dependent increase of barrier function and paracellular Cl<sup>-</sup> selectivity of airway epithelia via upregulation of Cldn8. Our findings support the hypothesis that glucocorticoids not only support resorptive transport via upregulation of ENaC but also via increasing Cldn8 expression and hence supporting paracellular Cl<sup>-</sup> transport and preventing backleakage of Na<sup>+</sup>.

Supported by BIU D.5007 to OW.

**P053**

**Function of BAG-3 in cardiac and skeletal muscle**

\*A. Ooms<sup>1</sup>, A. Ulbricht<sup>2</sup>, J. Höhfeld<sup>2</sup>, D. O. Fürst<sup>2</sup>, M. Hesse<sup>1</sup>, B. K. Fleischmann<sup>1</sup>

<sup>1</sup>Institute for Physiology I, Bonn, Germany

<sup>2</sup>Institute for Cell Biology, Bonn, Germany

The key symptom of muscular dystrophies, progressive muscle weakness, is caused by mutations in genes encoding Z-disk proteins. The co-chaperone BAG3 (Bcl-2 associated athanogene 3) is strongly expressed in cross striated muscles and colocalizes with Z-disks. It plays a key role in turnover of muscle-proteins (Ulbricht et al., 2012) and blocks apoptosis through interaction with Bcl-2 in leuke-

mic cells (Liu et al., 2009). A mutation in the human BAG3 gene leading to an amino acid exchange (P209L) causes severe dominant childhood muscular dystrophy, cardiomyopathy and respiratory insufficiency (Selcen et al., 2009). To get deeper insights into pathological mechanisms of this disease we generated stable embryonic stem cell (ESC) lines with cardiomyocyte specific overexpression of either BAG3-EGFP or BAG3(P209L)-EGFP. In most cardiomyocytes derived from BAG3-EGFP expressing ESCs BAG3 localized to Z-disks, whereas in 2/3 of the cardiomyocytes expressing BAG3(P209L)-EGFP aggregation of BAG3 and Z-disk disruption was observed. In a transgenic mouse line overexpressing BAG3-EGFP, BAG3 stringently localized to and intercalated disks and Z-disks as proven by co-localization with the Z-disk proteins  $\alpha$ -actinin, Myopodin and Filamin C. Overexpression of BAG3(P209L)-EGFP in transgenic mice led to formation of BAG3(P209L) positive aggregates. Besides the above mentioned strategies, we have also designed an approach to express the BAG3-EGFP and BAG3(P209L)-EGFP transgenes in different organs: We have knocked in a cassette for inducible overexpression of BAG-3(P209L)-EGFP using the Cre-loxP-system in the Rosa26-locus of mouse ESCs. This mouse line will help us to unravel the pathomechanism(s) of BAG3(P209L)-associated myofibrillar myopathy in skeletal and cardiac muscle.

**P054**

**Establishment of a novel system for in vivo detection of cardiomyocyte apoptosis**

\*K. Martinez Lagunas, B. Fleischmann, M. Hesse

Institute for Physiologie I, University Hospital of Bonn, Bonn, Germany

Apoptosis, the programmed cell death, is thought to play an important role in cardiovascular diseases. However, the exact role of apoptosis in origin and progression of heart disease is still poorly understood. We aim to address this question by establishing a novel system for the in vivo detection of apoptosis. This is based on a secreted Annexin V (sA5) protein fused to yellow fluorescence protein (YFP) under control of the ubiquitous CAG promoter. The sA5-YFP protein is secreted into the extracellular space and once the cell is undergoing apoptosis, sA5-YFP binds phosphatidylserine residues, which are exposed on the outer leaflet of the membrane of apoptotic cells. In this way, apoptotic cells are labeled and identified based on sA5-YFP fluorescence signals. We generated transgenic mESCs stably expressing sA5-YFP, induced apoptosis and analyzed fluorescence signals by fluorescence microscopy and time lapse imaging. Accumulation of sA5-YFP was observed at the cell membrane of apoptotic cells by an increase in YFP-fluorescent intensity over time. Also a transgenic mouse line was generated from the CAG-sA5-YFP mESC line. As apoptosis is present during embryonic development, E8 embryos were isolated and analyzed by fluorescence macroscopy as a proof of concept. YFP fluorescent signals were observed as expected, thus proving the functionality of the system. In future experiments we will further characterize this transgenic mouse line at different stages

of development to ensure specificity of the fluorescence signal. Our long term aim is to detect apoptosis rates after myocardial infarction in the adult mouse heart to unravel the potential contribution of apoptosis to heart disease.

**P055**

**Investigating PI(3,4)P<sub>2</sub>-3-phosphatase activity of Ciona intestinalis voltage sensitive phosphatase in Xenopus laevis oocytes and Chinese hamster ovary cells using fluorescent phosphoinositide probes**

S. Mertelmeyer, A. Mavrantoni, D. Oliver, \*C. Halaszovich

Philipps-Universität Marburg, Institut für Physiologie, Marburg, Germany

The Ciona intestinalis voltage sensitive phosphatase (Ci-VSP) is generally considered to be a PI(4,5)P<sub>2</sub>/PI(3,4,5)P<sub>3</sub>-5-phosphatase in-vivo, while 3-phosphatase activity could be demonstrated in-vitro using the isolated catalytic domain of Ci-VSP. A recent study demonstrates PI(3,4)P<sub>2</sub>-3-phosphatase activity of Ci-VSP expressed in Xenopus laevis oocytes (Kurokawa et al, 2012, PNAS). This is in contrast to our previous findings obtained in Chinese hamster ovary (CHO) cells (Halaszovich et al., 2009, JBC). Therefore we set out to re-evaluate Ci-VSP's specificity in oocytes as well as CHO cells. TAPP1-PH-GFP was used as the PI(3,4)P<sub>2</sub> sensor, its membrane binding was quantified using fluorescence microscopy (confocal laser scanning microscopy for oocytes, TIRF microscopy for CHO cells). The membrane voltage of oocytes was controlled using the two-electrode voltage-clamp technique, for CHO cells the patch-clamp technique was used. In oocytes, we failed to demonstrate 3-phosphatase activity against PI(3,4)P<sub>2</sub> but reliably detected production of this phosphoinositide species, presumably reflecting PI(3,4,5)P<sub>3</sub>-5-phosphatase activity of heterologously expressed Ci-VSP as well as endogenous VSPs. However, in Ci-VSP expressing CHO cells we could detect a reduced increase, albeit no decrease in TAPP1-PH-GFP binding to the cell membrane at high voltages. This reduction probably reflects PI(3,4)P<sub>2</sub> phosphatase activity and not reduced PI(3,4,5)P<sub>3</sub>-5-phosphatase activity. In conclusion, our findings show an overall production of PI(3,4)P<sub>2</sub> over the whole voltage range studied. Therefore we presume that under physiological conditions the PI(3,4,5)P<sub>3</sub>-5-phosphatase activity of Ci-VSP outweighs its PI(3,4)P<sub>2</sub>-3-phosphatase activity.

Supported by University Medical Center Giessen and Marburg (UKGM 32/2011 MR) to C.R.H. and Deutsche Forschungsgemeinschaft (SFB593 TP A12) to D.O.

**P056**

**The FRET based cAMP-sensor Epac as a tool to characterize Gi/o-coupled receptor activation**

\*J. Straub, U. Storch, T. Gudermann, M. Mederos y Schnitzler

Walther-Straub-Institut für Pharmakologie und Toxikologie, München, Germany

The FRET-technique can be used to elucidate the function and regulation of GPCRs. To investigate the functional differences of distinct GPCR-subtypes ( $G_{i/o}$ ,  $G_s$ ) we performed a fluorescent approach with a cAMP-sensitive reporter coupled to a FRET-pair, the ECFP/EYFP-flanked cAMP sensor Epac. This cAMP reporter is commonly used to detect cAMP increases upon  $G_s$ -PCR activation. We intended to assess the method on  $G_{i/o}$ -protein activation. For this, HEK293 cells transiently over-expressing the  $G_{i/o}$ -protein coupled adrenergic  $\alpha_{2A}$  receptor and the cAMP sensors EYFP-Epac1-ECFP or EYFP-Epac2-ECFP were analyzed. The cells were pretreated with either IBMX, forskolin or bromo-cAMP and subsequently stimulated with the agonist noradrenaline which caused an increase in FRET signals corresponding to a decrease of cAMP levels. Furthermore, we replaced the ECFP by mTurquoise2, which gave higher quantum efficiency, photostability and strictly single-exponential fluorescence decay. In addition, EYFP was exchanged by mVenus to obtain less sensitivity to pH- and Cl<sup>-</sup>-changes. Testing the new mVenus-Epac1/2-mTurquoise sensors with the  $G_s$ -protein coupled adrenergic  $\beta_2$  receptor confirmed their functionality. To underline our results, electrophysiological whole cells recordings were performed with HEK293 cells over-expressing  $G_{i/o}$ -protein coupled 5-HT<sub>1B</sub> receptors and Kir3.1/Kir3.2 or Kir3.1/Kir3.4 channel complexes that are activated by  $\beta\gamma$  dimers of  $G_{i/o}$ -proteins following receptor activation. Stimulation of the 5-HT<sub>1B</sub> receptor with serotonin resulted in profound current increases. Our findings indicate that a FRET based approach using the cAMP sensor Epac is comparable to an electrophysiological technique as a tool to monitor  $G_{i/o}$ -protein activation.

**P057**

**Paracellular transport through healthy and cystic fibrosis bronchial epithelial cell lines - do we have a proper model?**

\*N. Molenda<sup>1</sup>, K. Urbanova<sup>1</sup>, D. Günzel<sup>2</sup>, H. Schillers<sup>1</sup>

<sup>1</sup>Universitätsklinikum Münster, Institut für Physiologie II, Münster, Germany

<sup>2</sup>Charité, Institute of Clinical Physiology, Berlin, Germany

For investigation of cystic fibrosis transmembrane conductance regulator (CFTR) dependent disease cell lines representing healthy (16HBE14o-) and cystic fibrosis epithelium (CFBE41o-) are widely used. Additionally CFBE clones overexpressing wtCFTR or mutant (delF508) CFTR are now available. Question: Are these cell lines a proper model to investigate CFTR influence on epithelial transport? Methods: Paracellular fluorescein fluxes were measured in all those cell lines under control and CFTR-stimulating conditions. The morphology of the intercellular junction of monolayers was determined by ZO-1 staining. Claudins-3, -4, -5 and -7 were investigated by western blots and immunostaining. Results: Under control conditions all four cell lines show similar paracellular fluorescein flux. Only 16HBE14o- cell monolayers increased fluorescein flux upon CFTR stimulation. 16HBE14o- cells are smaller and have more complex cell-cell contacts than CFBE41o- and its overexpressing clones.

In consequence they should have higher solute flux or other tight junctions (TJ) composition. We found that claudins-4, -5 and -7 expression comparable, but claudin-3 expression was considerably stronger in 16HBE14o- cells than in the three CFBE41o- cell clones. It is known that claudin-3 has a tightening effect on the paracellular pathway. Conclusions: Cell size, TJ morphology and claudin-3 expression of 16HBE14o- and CFBE41o- cells is clearly different. Overexpression of wtCFTR or delF508 CFTR in CFBE41o- does not influence neither claudins expression nor paracellular transport. We conclude, that those cells are not a proper model to investigate CFTR's regulatory function on epithelial transport.

**P058**

**Surfactant secretion in LRRK2 knock-Out rats: Changes in lamellar body morphology and rate of exocytosis**

\*K. Ehinger<sup>1</sup>, P. Miklavc<sup>1</sup>, K. E. Thompson<sup>1</sup>, N. Hobi<sup>1,2</sup>, D. R. Shimshak<sup>3</sup>, M. Frick<sup>1</sup>

<sup>1</sup>University of Ulm, Institute of General Physiology, Ulm, Germany

<sup>2</sup>Innsbruck Medical University, Department of Physiology and Medical Physics, Innsbruck, Austria

<sup>3</sup>Novartis Pharma AG, Novartis Institutes for BioMedical Research, Basel, Switzerland

Leucine-rich repeat kinase 2 (LRRK2) is involved in the pathogenesis of various diseases including Parkinson disease, morbus Crohn, leprosy and cancer. LRRK2 is suggested to participate in various cell biological processes such as vesicular trafficking, transcription, autophagy and lysosomal pathways. Recent histological studies of lungs of LRRK2 knock-out (LRRK2 -/-) mice revealed significantly enlarged lamellar bodies (LBs) in alveolar type II (ATII) epithelial cells. LBs are large, lysosome-related storage organelles for pulmonary surfactant, which is released into the alveolar lumen upon LB exocytosis. Here, we used high-resolution, subcellular live-cell imaging assays to investigate whether similar morphological changes can be observed in primary ATII cells from LRRK2 -/- rats and whether such changes result in altered LB exocytosis. Similarly to the report in mice, ATII cells from LRRK2 -/- rats contained significantly enlarged LBs (>50% volume increase). Stimulation of ATII cells with ATP elicited LB exocytosis in a significantly increased proportion of cells from LRRK2 -/- animals. LRRK2 -/- cells also displayed increased intracellular Ca<sup>2+</sup> release upon ATP treatment and significant triggering of LB exocytosis. These findings suggest that LRRK2 -/- affects exocytic response in ATII cells via modulating intracellular Ca<sup>2+</sup> signaling. Post-fusion regulation of surfactant secretion was unaltered. Actin coating of fused vesicles and subsequent vesicle compression to promote surfactant expulsion were comparable in cells from LRRK2 -/- and wt animals. Surprisingly, surfactant (phospholipid) release from LRRK2 -/- cells was reduced following stimulation of LB exocytosis possibly due to impaired LB maturation and surfactant loading of LBs. In summary, our results suggest that LRRK2 -/- affects LB size, modulates intracellular Ca<sup>2+</sup> signaling and promotes LB exocytosis upon stimulation of ATII cells with ATP.

**P059**

**The effect of intracellular pH and redox state on the catalytic activity of voltage sensitive phosphatases**

\*A. Mavrantoni, D. Oliver, C. Halaszovich

Philipps University, Physiology, Marburg, Germany

Voltage Sensitive phosphatases (VSPs) are PI(4,5)P<sub>2</sub> phosphatases activated upon membrane depolarization. They have been cloned from species like *Ciona intestinalis* (Ci-VSP), *Xenopus laevis* (XI-VSP1, XI-VSP2), *Danio rerio* (Dr-VSP) and human (hVSP1). VSPs are suggested to play a role in fertilization and development, where pH and redox state changes are known to occur. Moreover, in adults they are found to be expressed in different tissues including kidney, stomach, sperm and ovary that are also known to undergo pH changes. Here we investigated the effect of intracellular pH and oxidation on VSP activity. We used whole-cell patch clamping to control the membrane potential and TIRF microscopy to monitor the depletion of PI(4,5)P<sub>2</sub>. We show that acidification of the cell's interior resulted in increased PI(4,5)P<sub>2</sub> depletion and a shift of the voltage dependence towards more negative potentials. The gating mechanism of the enzyme, as demonstrated by measuring sensing currents, seemed to be unaffected. Similar effects were observed in all tested VSPs. Second we examined the effect of oxidation on VSPs' activity. We found that oxidation of Ci-VSP with H<sub>2</sub>O<sub>2</sub> demolished the phosphatase activity whereas the weak oxidation oxidizing agent Glutathione disulfide had no effect. Similarly the effect of the reducing agent Dithiothreitol is investigated. Thus we suggest that intracellular pH and redox state can play a role in the regulation of the activity of VSPs.

This work was supported by a research grant of the University Medical Center Giessen and Marburg (UKGM32/2011 MR) to C.R.H and by Deutsche Forschungsgemeinschaft (SFB593 TP A12) to D.O.

Cellular and molecular neuroscience I

**P060**

**Store-operated calcium entry maintains steady-state levels of ER calcium in neurons**

\*S. Samtleben, R. Blum

Institut für klinische Neurobiologie, AG Blum, Würzburg, Germany

**Methods:** Targeted-Esterase induced Dye loading (TED) is a method that supports the labeling of the ER calcium store with synthetic calcium indicators. TED depends on targeted expression of a carboxylesterase in the ER using lentiviral vectors. This carboxylesterase then releases low-affinity

calcium indicators in the ER, where they, upon binding of calcium ions, fluoresce. Here, we introduce new constructs for TED application and used them to visualize the ER distribution in cultured hippocampal neurons. Direct ER calcium imaging with the help of TED and cytosolic calcium imaging were used to monitor effects of calcium homeostasis at steady state.

**Results:** The ER of cultured hippocampal neurons is prominent in the cytosol and in dendrites, but not pronounced within synapses or axons. We observed a rapid and activity-independent loss of both cytosolic and ER calcium in cultured hippocampal neurons under calcium free conditions which recovered upon calcium addition. Both loss and recovery of calcium occurred in somatic regions and dendrites of the hippocampal neurons. Our results demonstrate that the loss of ER calcium by leak channels is not rescued from the cytosol by the activity of the SERCA (sarco-/endoplasmic reticulum calcium transport ATPase), but rapidly lost into the extracellular space. Only after re-addition of calcium to the neurons, ER calcium is rapidly restored.

**Conclusion:** The results point towards a fundamental role of SOCE under steady state conditions. SOCE mechanisms appear to maintain a constant basal calcium level in both the cytosol and the ER.

Funded by the DFG: BL567/3-1.

**P061**

**Activity-dependent apoptosis in dissociated neocortical cultures**

A. Sinning, \*O. Blanquie, H. Luhmann, K. Weir

University Medical Center of the Johannes Gutenberg University, Institute of Physiology, Mainz, Germany

Programmed cell death is a major event in the developing nervous system. In the human neocortex, apoptosis occurs mostly during the third trimester of gestation, while in rodents it mainly takes place during the first two postnatal weeks. We studied the developmental profile of apoptosis in different neuronal subpopulations using immunocytochemistry in dissociated cortical cultures from neonatal mice. We were particularly interested in two transient neuronal subpopulations, Cajal-Retzius neurons (CRNs) and subplate neurons, which both play a crucial role in neuronal migration, columnar development and early neuronal network activity. Our current data suggests that the time course and rate of postnatal apoptosis in vitro varies between neuronal subpopulations. Whereas about 60% of GABAergic neurons undergo apoptosis between DIV 6 and 12, the majority of CRNs (80 %) has already undergone apoptosis by DIV 9. These data are consistent with the situation described in vivo. Our group has previously shown that a decrease in electrical activity induces a rise in the overall rate of neuronal apoptosis. To further study the mechanisms of activity-dependent apoptosis in different neuronal subpopulations, we investigated whether a change in electrical activity has differential effects on apoptosis in distinct neuronal subpopulations. Pharmacological blockade of glutamatergic or GABAergic transmission is controlled by con-

comitant MEA-recordings and the subsequent effect on the apoptosis rate is analyzed at DIV 7 and 14. To conclude, this in vitro study will provide further insights into the mechanisms underlying neurodevelopmental activity-dependent apoptosis occurring in rodents as well as in humans.

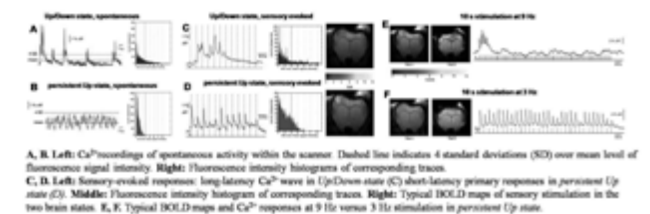
**P062**

**Combining fMRI with optical Ca<sup>2+</sup> recordings to define the impact of brain states on BOLD**

\*M. Schwalm<sup>1</sup>, L. Wachsmuth<sup>2</sup>, F. Schmid<sup>2</sup>, C. Faber<sup>2</sup>, A. Stroh<sup>1</sup>  
<sup>1</sup>Johannes Gutenberg-University Mainz, Institute of Microscopic Anatomy and Neurobiology - Research Group Molecular Imaging and Optogenetics, Mainz, Germany  
<sup>2</sup>University of Münster, Department of Clinical Radiology, Münster, Germany

**Question:** Furthering our understanding the neuronal underpinnings of fMRI, we implemented the combination of optical Ca<sup>2+</sup> recordings with BOLD fMRI in rat somatosensory cortex (S1) in two different brain states: persistent Up state characterized by high excitability upon sensory stimulation; and the oscillatory state of Up/Down state, resembling slow wave sleep. Optic-fiber-based Ca<sup>2+</sup> recordings enabled us to characterize those brain states and to monitor stimulation induced spiking activity. Varying stimulation frequencies and durations we explored the impact of suprathreshold activity on the BOLD response.

**Methods:** Oregon-Green-BAPTA-1 was injected in the cortex (S1) of anesthetized rats and an optical fiber was implanted. A custom made optical laser setup was used to excite the Ca<sup>2+</sup>-dye and to record changes in fluorescence. Different electric forepaw stimulation paradigms were conducted. Simultaneous fMRI (9.4 T) was performed. **Results:** During spontaneous activity in Up/Down state high-amplitude Ca<sup>2+</sup> waves were identified versus in persistent Up state only baseline fluctuations were detected. Sensory stimulation in Up/Down state did not lead to BOLD activation, despite the initiation of Ca<sup>2+</sup> waves. In persistent Up state, we recorded primary neuronal Ca<sup>2+</sup> responses and robust BOLD activation. BOLD response duration was dependent on the duration of electric stimulation, although Ca<sup>2+</sup> transients revealed fast adaptation: while at higher frequencies BOLD response was detected, the much longer neuronal spiking activity at lower frequencies did not reveal BOLD. **Conclusion:** Our data show a predominant contribution of sub-threshold neuronal activity to the BOLD response, thus it cannot be interpreted as a surrogate of neuronal spiking activity.



A, B: Left: Ca<sup>2+</sup> recordings of spontaneous activity within the scanner. Dashed line indicates 4 standard deviations (SD) over mean level of fluorescence signal intensity. Right: Fluorescence intensity histograms of corresponding traces.  
 C, D: Left: Sensory-evoked responses: long-latency Ca<sup>2+</sup> wave in Up/Down state (C) short-latency primary responses in persistent Up state (D). Middle: Fluorescence intensity histograms of corresponding traces. Right: Typical BOLD maps of sensory stimulation in the two brain states. E, F: Typical BOLD maps and Ca<sup>2+</sup> responses at 9 Hz versus 3 Hz stimulation in persistent Up state.

**P063**

**Influence of casein kinase 2 inhibition on afterhyperpolarisation potential in epileptic tissue**

\*H. Brehme, T. Kirschstein, R. Schulz, R. Köhling  
 Oscar-Langendorff-Institut für Physiologie, Rostock, Germany

**Aim:** The afterhyperpolarizing potentia – especially the medium (mAHP) and the slow part (sAHP) – following prolonged depolarizations is a major intrinsic mechanism of neuronal inhibition, powerfully dampening excitability for up to two seconds. Therefore, an altered sAHP function might be underlying neuronal hyperexcitability states, such as found in epilepsy. Here, we have investigated the impact of casein kinase 2 (CK2) on modulation of mAHP and sAHP in control and chronically epileptic tissue. **Methods:** Using the rat pilocarpine model of chronic temporal lobe epilepsy, we performed whole-cell patch-clamp recordings of acutely isolated CA1 pyramidal cells and field potential measurements on hippocampal slices.

**Results:** Chronic oral administration of the CK2 inhibitor 4,5,6,7-tetrabromotriazole (TBB) for 4 days prior to brain dissection caused a significant increase of the sAHP-mediated current in both control and epileptic tissues. In contrast, when TBB was acutely applied during patch-clamp recordings, sAHP remained unaltered, indicating that prolonged CK2 inhibition is required for sAHP augmentation. TBB had no influence on the mAHP mediated current. To test whether CK2 inhibition also has an anticonvulsive effect, we evoked recurrent epileptiform discharges (REDs) in hippocampal slice preparations by Mg<sup>2+</sup> removal. Importantly, chronic oral TBB administration abolished REDs induced by 0-Mg<sup>2+</sup>, suggesting that CK2 inhibition indeed has anticonvulsive and perhaps antiepileptogenic properties.

**Conclusions:** Our data demonstrate that CK2 inhibition augments the sAHP, which may point towards a novel mechanism of action of anticonvulsant drugs.

**P064**

**Mutant α-synuclein enhances firing frequencies in dopamine substantia nigra neurons by oxidative impairment of A-type potassium channels**

\*M. Subramaniam, J. Roeper  
 Goethe University Frankfurt, Neurophysiology, Frankfurt, Germany

Parkinson disease (PD) is a synucleinopathy resulting in the selective degeneration of highly vulnerable substantia nigra (SN) dopamine (DA) neurons. Mutations or wildtype overexpression of the α-synuclein gene (SNCA) impose a high risk for developing familial or sporadic forms of PD. While multiple pathways have been identified how α-synuclein leads to cell death, but preceding functional changes in SN DA neurons are unknown. We characterized the electrophysiological in vivo properties of identified SN DA neurons in anaesthetized mice using in vivo extracellular single-unit recordings combined with the juxtacellular labeling technique. In young-adult A53T-SNCA mice (3-4 month), we identified about 30% higher mean in vivo firing rates in SN DA neurons compared to age-matched

controls. This hyperexcitability phenotype dramatically increased with age indicated by about 90% higher mean in vivo firing frequencies of SN DA neurons in middle-aged (8-10 month) A53T-SNCA mice compared to age-matched controls. As no differences in mean firing rates were observed in DA neurons in the ventral tegmental area (VTA) from middle-aged mice, these changes were selective for SN DA neurons. The hyperexcitability phenotype was also partially conserved in synaptically isolated SN DA neurons in vitro. The spontaneous discharge frequencies of middle-aged A53T-SNCA mice were about 40% faster compared to age-matched controls. Regarding the key pacemaker channels controlling discharge frequencies in SN DA neurons, we identified about 40% smaller maximal A-type potassium (K) conductances, both in standard whole-cell and in nucleated outside-out recordings in SN DA neurons from middle-aged A53T-SNCA mice. Selective inhibition of A-type K channels with 400µM 4-aminopyridine completely occluded the genotype differences in middle-aged SN DA neurons, indicating that the identified changes in A-type channel conductances are sufficient to explain the A53T-SNCA induced phenotype. The protein expression of Kv4.3 channels, which are known to constitute the A-type K channels in DA SN neurons, in A53T-SNCA mice showed an increase in the total protein content that was further confirmed using immuno-gold electron microscopy. We show that the Kv4 channels are regulated by redox-dependent mechanism, rendering them dysfunctional, thereby resulting in decreased functional channels, while the expression of the channel per se on the membrane is increased. Together, we have identified a redox-sensitive acquired dysregulation of Kv4 channels in the DA SN neurons of A53T-SNCA mice that leads to increased in vivo firing frequency, much ahead of neurodegeneration.

**P065**

**Cotransmission of GABA and glycine in neurons of the respiratory centre**

\*S. Besser<sup>1</sup>, J. Rahman<sup>2</sup>, M. Sicker<sup>1</sup>, I. Milenković<sup>3</sup>, R. Rübsamen<sup>3</sup>, U. Winkler<sup>1</sup>, S. Hülsmann<sup>2,4</sup>, J. Hirrlinger<sup>1,5</sup>  
<sup>1</sup>Carl-Ludwig-Institute for Physiology, Leipzig, Germany  
<sup>2</sup>Centre of Physiology and Pathophysiology, Department of Neurophysiology and Cellular Biophysics, Göttingen, Germany  
<sup>3</sup>Institute of Biology, Department of Zoology and Neurobiology, Leipzig, Germany  
<sup>4</sup>DFG Research Center for Molecular Physiology of the Brain (CMPB), Göttingen, Germany  
<sup>5</sup>Max-Planck-Institute for Experimental Medicine, Department of Neurogenetics, Göttingen, Germany

In the central nervous system fast inhibitory neurotransmission is mediated by glycine and gamma-aminobutyric acid (GABA). Contradicting Dale's principle, cotransmission of these two transmitters from a single neuron has recently been observed in many different brain regions. However, while the corelease of GABA and glycine offers a wide spectrum of signalling variations, the role of cotransmitting neurons is not well understood. Our research is focused on

GABA and glycine cotransmitting interneurons in the respiratory centre in the brain stem, the Pre-Bötzinger-Complex, where inhibitory synaptic transmission is crucial for the patterning of the respiratory rhythm. Using electrophysiology, single cell RT-PCR and immunohistochemistry, we show that numerous neurons in the Pre-Bötzinger-Complex of mice transmit by both GABA and glycine. In addition, the quantitative analysis of different developmental stages revealed a decrease of cotransmitting neurons from P4 to P14, whereas the number of glycinergic neurons increased, indicating a developmental shift to glycinergic transmission. Experiments using advanced mouse genetic tools are currently ongoing to identify the fate of cotransmitting neurons as well as to define their functional relevance.

**P066**

**Developmental switch in the influx-release topography at the active zone of the parallel-fiber to Purkinje neuron synapse**

\*D. Baur, J. Eilers, H. Schmidt  
 Carl-Ludwig-Institute for Physiology Leipzig, Leipzig, Germany

The coupling distance between presynaptic Ca<sup>2+</sup> channels and the sensor for vesicular release is a key determinant of speed and reliability of synaptic transmission (1). Recently, it was shown that mature parallel-fiber (PF) to Purkinje neuron (PN) synapses, conventional small cortical synapses, operate at tight nanodomain coupling (2+ signals were not different between maturation stages, we observed differential effects of the slow and fast exogenous Ca<sup>2+</sup> chelators EGTA and BAPTA (4), respectively, on release in young and mature synapses, indicating that coupling in young synapses is significantly less tight and less homogenous than in the adult. This was accompanied by reduced transmitter release probability (adult: p<sub>r</sub> = 0.22 ± 0.07; young: p<sub>r</sub> ≤ 0.05) and increased paired-pulse facilitation in young synapses (adult: PPR = 2.0 ± 0.3; young: PPR = 2.5 ± 0.5; at 50 ms interstimulus interval). These data suggest that a substantial functionally relevant rearrangement of the influx-release topography occurs during postnatal development of PF to PN synapses.

- (1) Bucurenciu et al., Neuron, 2008
- (2) Schmidt et al., Curr Biol, 2013
- (3) Fedchyshyn and Wang, J Neurosci, 2005
- (4) Adler et al., J Neurosci, 1991

Supported by a faculty scholarship to DB and the DFG grant SCHM1838/1-1

**P067**

**Morphological, neurochemical and electrophysiological analysis of GFP-expressing interneurons**

\*T. Riedemann, B. Sutor  
 Institute of Physiology, LMU München, Physiological Genomics, München, Germany

We investigated the morphological, neurochemical and electrophysiological properties of EGFP-expressing GABAergic interneurons (GIN) in the mouse cingulate cortex. Electrophysiological recordings were performed on GIN located in layer II/III. Biocytin was added to the intracellular recording solution for further morphological and neurochemical analysis of the cells. We analyzed passive and active membrane properties, time course of action potentials, discharge behavior and synaptic input and found these parameters to be very similar in all 47 recorded neurons. Following electrophysiological characterization, GIN morphology and neurochemistry was examined. The injected biocytin was visualized by Alexa 594. Morphological reconstructions were performed with the help of a Zeiss LSM710 laser scanning microscope. Z-stacks (mean range: 150  $\mu\text{m}$ ) of each neuron were collapsed onto a single plane. In contrast to their electrophysiological properties, the morphological features of GIN (i.e. number of primary processes, soma size, existence of dendritic spines, axonal projections) proved quite variable. Neurochemical markers of interest were calretinin and calbindin, since earlier experiments revealed that close to a 100% of GIN express somatostatin while parvalbumin expression could never be detected. Additionally, calbindin, calretinin and confirmation of GFP expression was examined on a few optical planes centered around the soma of cells. Out of 47 neurons, 8 were positive for GFP only, 33 were positive for GFP and calretinin and 6 were positive for both, calretinin and calbindin. These results show that the genetically homogeneous GIN population of the mouse cingulate cortex comprises different phenotypic subgroups.

**P068**

**Molecular regulation of  $\text{Ca}^{2+}$ -dependent neurotrophin secretion in hippocampal neurons by CAPS1**

\*R. Eckenstaler, T. Munsch, T. Brigadski, V. Leßmann

Otto von Guericke University, Medical Faculty, Institute of Physiology, Magdeburg, Germany

The mammalian neurotrophin brain-derived neurotrophic factor (BDNF) is an important regulator of a variety of brain functions including neuronal development and synaptic plasticity. The protein is stored in secretory granules and released in an activity-dependent manner. Although the activity-dependent release of BDNF is assumed to be a key element for the induction of synaptic plasticity processes in neurons, the molecular mechanisms of secretory granule exocytosis in neurons largely remained elusive. We have now investigated the relevance of priming factor CAPS1 for the release of BDNF-containing secretory granules in dissociated hippocampal neurons from mice. The cells were transfected with plasmids coding for BDNF-GFP and shRNA directed against CAPS1. Depolarization-induced secretory granule release was analysed by monitoring the intragranular GFP-fluorescence intensity using time-lapse video microscopy. In addition, the role of CAPS1 during transmitter release from synaptic vesicles was analysed by destaining of styryl dye FM1-43. While density and size of synaptic

boutons was unaffected by CAPS1 knockdown, the rate of transmitter release was significantly reduced. In addition, fusion pore opening of secretory granules and the amount of BDNF release was affected after CAPS1 knockdown. Although the average size of single secretory granules and their BDNF-GFP loading was unchanged by CAPS1 knockdown, the intragranular pH value was significantly higher in hippocampal neurons transfected with CAPS1-shRNA. The present results suggest that endogenous CAPS1 plays an important role in regulating both, synaptic vesicle exocytosis as well as secretory granule exocytosis and that CAPS1 has an additional function in regulating intragranular pH.

**P069**

**Role of ATP-sensitive potassium current ( $I_{\text{KATP}}$ ) for intrinsic firing activity of immature entorhinal cortex neurons**

M. S. Lemak<sup>1,2</sup>, A. Draguhn<sup>1,3</sup>, \*A. V. Egorov<sup>1,3,2</sup>

<sup>1</sup>University of Heidelberg, Institute of Physiology and Pathophysiology, Heidelberg, Germany

<sup>2</sup>Institute of Higher Nervous Activity and Neurophysiology, Russian Academy of Sciences, Moscow, Russia

<sup>3</sup>Bernstein Center for Computational Neuroscience (BCCN), Heidelberg/Mannheim, Germany

Intrinsic firing properties of individual neurons change during postnatal maturation. This may be important for the development of coordinated network activity. Therefore, we investigated maturation of intrinsic firing behavior of developing medial entorhinal cortex (mEC) neurons. We have previously shown that layer III (LIII) principal neurons of the immature mEC of rats display at least two distinct intrinsic firing patterns: spontaneous prolonged bursts and regular firing (Sheroziya et al. 2009). Burst discharges involve  $\text{Ca}^{2+}$ -sensitive non-specific cationic currents ( $I_{\text{CAN}}$ ), persistent  $\text{Na}^+$ -currents ( $I_{\text{Nap}}$ ), and  $\text{Ca}^{2+}$ -activated  $\text{K}^+$ -currents ( $I_{\text{AHP}}$ ). We have now studied the contribution of the ATP-sensitive potassium current ( $I_{\text{KATP}}$ ) in generation of intrinsic bursts and in modulation of regular firing activity. Whole-cell recordings were performed from mEC LIII neurons in horizontal brain slices obtained from rats at postnatal day (P)6-P13. Burst discharges were prolonged by the IKATP blockers tolbutamide (300  $\mu\text{M}$ ) and glibenclamide (1  $\mu\text{M}$ ). Accordingly, activators of IKATP strongly suppressed bursts (diazoxide, 100  $\mu\text{M}$ ; NN414, 25  $\mu\text{M}$ ). Regular firing activity was modulated in a frequency-dependent manner: discharges at ~6-10 Hz were enhanced by tolbutamide while slower activity (~1-3 Hz) was largely resistant. Diazoxide, in contrast, preferentially suppressed low frequency regular firing (1-3 Hz). Western blot analysis of Kir6.2 (a major subunit of the IKATP channel) showed significant expression of this protein in the immature EC which was developmentally downregulated from P0 to P25. We suggest that IKATP plays an important role in modulation of intrinsic firing properties of immature mEC LIII neurons.

Supported by BMBF (01DJ12061, RUS 11/015; 01GQ1003A, BCCN), Germany.

**P070**

**Testosterone excites hypothalamic histaminergic neurons controlling wakefulness**

\*W. Baumgärtel, O. Sergeeva

Heinrich-Heine-Universität, Düsseldorf, Germany

Testosterone is the male sex hormone responsible for the development of the masculine habitus during embryogenesis, the sexual maturation as well as the maintenance of male reproductive function in adulthood. Testosterone regulates not only endocrinium and metabolism but also active waking. We investigate now the expression of androgen receptor (AR) and functional correlates of this expression in hypothalamic neurons controlling wakefulness. The histaminergic tuberomamillary nucleus (TMN) of the posterior hypothalamus controls important components of arousal such as cognition, energy expenditure and body temperature. Using transgenic mouse model expressing a red fluorescent protein under control of the histidine decarboxylase promoter we visualize and select histaminergic (HA) neurons for the ex-vivo patch-clamp experiments and for immunohistochemistry. The majority of HA neurons from the ventral subdivision of TMN (TMNv) are immunopositive for AR (65% in adolescent and 89% in mature adult mouse). Testosterone (0.1-1  $\mu\text{M}$ ) increases the firing rate of 40% of adolescent HA neurons recorded in slices, an effect abolished by the AR antagonist flutamide. A similar response to testosterone is found in juvenile cultured HA neurons grown on microelectrode array (MEA). At concentrations >1  $\mu\text{M}$  testosterone enhances the apparent macroscopic desensitization of current responses to a saturating GABA concentration by decreasing the exponential decay time constant (to 65 $\pm$ 21% of control in the presence of testosterone 10  $\mu\text{M}$ ). This action of testosterone resembles previously described action of bile steroids, which also enhance apparent desensitization of GABA-currents and thus can decrease GABAergic inhibition promoting neuronal excitation. We conclude that AR but not the GABAAR mediates physiological actions of testosterone in TMN.

**P071**

**The active zone ultrastructure matches the functional neuronal gradient at the Drosophila neuromuscular junction**

\*N. Ehm<sup>1</sup>, S. van de Linde<sup>2</sup>, T. Holm<sup>2</sup>, M. Heckmann<sup>1</sup>, M. Sauer<sup>2</sup>, R. J. Kittel<sup>1</sup>

<sup>1</sup>University of Würzburg, Institute of Physiology, Department of Neurophysiology, Würzburg, Germany

<sup>2</sup>University of Würzburg, Department of Biotechnology & Biophysics, Würzburg, Germany

By employing super-resolution microscopy at the Drosophila melanogaster neuromuscular junction (NMJ) we developed an experimental approach to analyse Bruchpilot (Brp; Wagh et al., 2006), a key component of the cytomatrix associated with the active zone (CAZ), in a quantitative manner. Combining these data with electrophysiology enabled us to correlate specific functional synaptic determinants with the number of AZs, their Brp content and the

ultrastructural distribution of Brp within the CAZ. A major determinant of short-term synaptic plasticity is the probability of neurotransmitter release ( $p_{\text{vr}}$ ). Interestingly, previous studies suggested a non-uniformity of pvr at the glutamatergic Drosophila NMJ with larger  $\text{Ca}^{2+}$  signals and correspondingly higher pvr at the terminal boutons (Guerrero et al., 2005; Peled and Isacoff, 2011). However, an ultrastructural gradient matching the proposed functional diversity has not been identified. Focusing on this intrinsic property, we analysed the ultrastructural organisation of Brp within the CAZ along wildtype NMJs by dSTORM (direct Stochastic Optical Reconstruction Microscopy; Heilemann et al., 2008). Building on our previous correlation of ultrastructural and functional data we were able to resolve a clear gradient of both CAZ size and the number of Brp molecules per CAZ along a glutamatergic neuron. With the largest values at terminal boutons, this structural diversity closely matches the functional gradient.

References:

Guerrero et al., (2005). Nat Neurosci 8:1188-1196; Peled ES, Isacoff EY (2011). Nat Neurosci 14:519-526.; Heilemann et al., (2008). Angew Chem Int Ed 47:6172-6176.; Wagh et al., (2006). Neuron 49:833-844.

**P072**

**Ultrafast action potentials and vesicle recruitment mediate kilohertz signaling at a central synapse**

A. Ritzau-Jost, I. Delvendahl, A. Weyhersmüller, \*N. Byczkiewicz, J. Hirlinger, H. Schmidt, J. Eilers, S. Hallermann

Medical Faculty, University of Leipzig, Carl-Ludwig-Institute for Physiology, Leipzig, Germany

Information processing within milliseconds is important during evolution, but the underlying mechanisms remain unclear. Presynaptic cerebellar mossy fiber bouton (cMFB) contact dozens of postsynaptic granule cell (GC) and can fire action potentials with ~1 kHz frequency in vivo. Here, we analyze high-frequency signaling at individual cMFB-GC connections with paired recordings and demonstrate reliable neurotransmission at 1 kHz. Presynaptic action potentials are ultrafast (half-width ~100  $\mu\text{s}$ ), show little broadening during bursts at up to 1.5 kHz frequency, and efficiently open  $\text{Ca}^{2+}$  channels. Analyzing basal parameters of transmitter release reveals a subset of vesicles tightly coupled to  $\text{Ca}^{2+}$  channel and ultrafast vesicle recruitment. Postsynaptic GCs generate slightly slower action potentials (half-width ~190  $\mu\text{s}$ ) at up to 1 kHz frequency and process cMFB firing up to 1.5 kHz linearly. Thus, our results demonstrate that ultrafast action potentials and vesicle recruitment enable signaling up to kHz frequencies from single boutons to dozens of postsynaptic partners.

**P073**

**Dynamics of intracellular ATP in brain cells**

\*U. Winkler<sup>1</sup>, P. Seim<sup>1</sup>, A. Trevisiol<sup>2</sup>, Y. Enzbrenner<sup>1</sup>, A. S. Saab<sup>2,3</sup>, K.-A. Nave<sup>2</sup>, J. Hirrlinger<sup>1,2</sup>

<sup>1</sup>Carl-Ludwig-Institute for Physiology, University of Leipzig, Leipzig, Germany

<sup>2</sup>Max-Planck-Institute for Experimental Medicine, Department of Neurogenetics, Göttingen, Germany

<sup>3</sup>Institute of Pharmacology & Toxicology, University of Zurich, Zurich, Switzerland

Brain function crucially depends on an appropriate supply of energy and failure of a sufficient supply of energy as e.g. during stroke will very quickly severely impair proper activity of this vital organ. However, while the consequences of energy depletion during pathophysiological events have well been documented, much less is known about physiological dynamics in energy load of brain cells. ATP is the major energy carrier of cells and changes in the intracellular ATP concentration have been postulated to contribute to cellular signalling. Therefore, we have addressed intracellular ATP in astrocytes and neurons in primary culture as well as in acutely isolated tissue preparations by time-lapse microscopy using a genetically encoded fluorescent sensor for ATP expressed by either transient transfection or driven by cell-type specific promoters in transgenic mice. Both major ATP producing pathways, glycolysis and mitochondrial respiration, contributed to maintenance of ATP in astrocytes. ATP in astrocytes decreased after application of the neurotransmitter glutamate dependent on the activity of glutamate transporters, while other neurotransmitters had only minor effects. Also neurons showed an activity dependent modulation of intracellular ATP levels. These results confirm the hypothesis that intracellular ATP levels are indeed subject to fast and reversible changes during physiological activity of at least two types of brain cells and open up the avenue for further studies addressing factors which affect regulation of ATP.

**P074**

**Recruitment of BDNF/TrkB signaling in hippocampal mossy fiber LTP depends on stimulation frequency used for LTP induction**

\*E. Edelmann<sup>1</sup>, A. Jahn<sup>1</sup>, S. Schildt<sup>1</sup>, V. Leßmann<sup>1,2</sup>

<sup>1</sup>Institute of Physiology, Otto-von-Guericke University Magdeburg, Magdeburg, Germany

<sup>2</sup>Center of Behavioral Brain Sciences (CBBS), Magdeburg, Germany

The neurotrophin brain-derived neurotrophic factor (BDNF) is a major regulator of synaptic plasticity in the CNS. Its role in hippocampal plasticity is best studied at Schaffer Collateral - CA1 synapses, while the role of BDNF in mossy fiber (MF-) LTP is still not clear. MF-LTP exhibits some unique features of plasticity (i.e., frequency facilitation and NMDA receptor independent presynaptic expression). By means of acute inhibition of BDNF/TrkB signaling (either with the tyrosine-kinase inhibitor k252a or with the BDNF scavenger

ger TrkB-Fc), and chronic ~50% reduction of BDNF protein levels in heterozygous BDNF knockout mice, we now investigated the requirement of BDNF signaling in MF-LTP induced with different induction protocols. We established field potential recordings in the CA3 region of acute slices from 8-10 weeks old, male C57Bl/6J mice. MF-signals were identified on the basis of the pronounced short-term plasticity and frequency facilitation. MF-LTP was induced in the presence of 50µM DL-APV by a 50Hz stimulation protocol (3x 50Hz) and blocked by bath application of TrkB-Fc or k252a, or by chronic reduction of BDNF. The residual MF-LTP seemed to be mediated by BDNF independent mechanisms. NMDA receptor dependent LTP at adjacent CA3-CA3 synapses, induced with a similar LTP protocol, was not dependent on BDNF signaling. Since BDNF has been shown to be recruited in a stimulus dependent manner in CA1 LTP, we established two further MF-LTP protocols (3x25Hz and 3x100Hz), which lead to similar robust potentiation. However, neither the 25Hz nor the 100Hz induced MF-LTP was inhibited in the presence of k252a, suggesting Trk-independent expression of LTP. This is, to our knowledge, the first study focusing on acute BDNF effects in MF-LTP. Taken together, our results suggest that BDNF is critically involved in the expression mechanism of MF-LTP when induced with a mild 50Hz stimulation protocol, but not when MF-LTP is induced with either lower or higher frequencies of stimulation.

This work is supported by the Schram-Stiftung and by CBBS/EFRE.

**P075**

**Endocytosis defects and disturbed vesicle pool dynamics induced by human autoantibodies targeting amphiphysin SH3 domain**

\*C. Werner<sup>1,2</sup>, M. Pauli<sup>3</sup>, M. Heckmann<sup>3</sup>, K. V. Toyka<sup>2</sup>, E. Asan<sup>4</sup>, C. Sommer<sup>2</sup>, C. Geis<sup>1,2,5</sup>

<sup>1</sup>Hans-Berger Dept. of Neurology, Jena, Neurology, Jena, Germany

<sup>2</sup>Dept. of Neurology, University of Wuerzburg, Wuerzburg, Germany

<sup>3</sup>Dept. of Physiology, University of Wuerzburg, Wuerzburg, Germany

<sup>4</sup>Dept. of Anatomy, University of Wuerzburg, Wuerzburg, Germany

<sup>5</sup>Integrated Research and Treatment Center, Center for Sepsis Control and Care (CSCC), Jena University Hospital, Jena, Germany

Paraneoplastic Stiff person-Syndrome (pSPS) is a central nervous system (CNS) autoimmune disorder characterized by autoantibodies (AB) targeting the endocytic protein amphiphysin. Previously we could provide evidence of AB induced disturbed GABAergic inhibition at the spinal level in an animal model of pSPS.

Here, we focused on investigating AB-induced structural changes in GABAergic synapses with electron microscopy (EM) in rat spinal cord slices and super-resolution microscopy (dSTORM) in primary neurons at different activation patterns. EM revealed a structural endocytosis defect with disturbed clathrin mediated endocytosis (CME) which leads to fast consumption of clathrin coated vesicles and vesicles in general in the pSPS animal model at

high activity. Detailed quantitative analysis of GABAergic synapses using dSTORM microscopy shows a defect in CME that leads to a switch to clathrin independent endocytosis. This type of endocytosis prevalently produces vesicles equipped with the vesicular SNARE (v-SNARE) synaptobrevin (syb) 7 instead of the isoform syb-2 which is the predominant v-SNARE in healthy synapses. Further, cluster analysis, and individual bouton signal quantification reveals that clustering of endophilin, an interaction partner of amphiphysin that is also involved in CME, is reduced following application of anti-amphiphysin AB and sustained stimulation. The uncoating factor synaptojanin is more dispersed during low synaptic activity after AB application but its abundance at presynaptic terminals is comparable to controls. Together, these results indicate that anti-amphiphysin AB lead to a presynaptic endocytic defect in GABAergic synapses that is characterized by a switch to clathrin independent endocytosis with distinct presynaptic molecular reorganization.

**P076**

**The motorprotein Prestin and Caveolin associate in distinct membrane microdomains**

\*A. Feuer, C. Köhne, D. Oliver

Physiology, Neurophysiology, Marburg, Germany

Prestin (SLC26a5) is a membrane-spanning protein essential for sensitive hearing. It is almost exclusively expressed in the lateral membrane of the outer hair cells (OHCs) in the mammalian cochlea. Here it functions as the motor protein. It changes its conformation according to membrane potential and thereby the over-all length of the OHC, a process termed somatic electromotility necessary for fine-tuning of frequency-selectivity. Prestin displays a specific distribution in the lateral membrane in OHCs, possibly enabling its unique function. It localises to distinct clusters that are thought to be cholesterol-rich membrane compartments identified by microdomain markers. Determinants of Prestins membrane localisation remain unknown. The question that arises is how Prestin is spatially constrained to the lateral domain of the membrane. What other proteins play a role in the transmission of power from Prestin to the membrane, finally leading to change of the overall-length of OHCs?

To understand Prestins clustering in the OHC lateral wall, we search in a heterologous expression system for prestin-associated proteins first by using high-resolution optical microscopy. We found that Prestin and Caveolin-1 showed a strong co-localisation. In addition, protein biochemical approaches demonstrate an association of Caveolin-1 and Prestin. Last, using electrophysiological techniques in CHO cells co-expressing Prestin and Caveolin we found a decrease in Prestins non-linear charge transfer, possibly reflecting reduced electromotility. These data suggest that Caveolin-1 contributes to the protein complex that is involved in Prestins localisation in clusters in membrane microdomains. This cluster formation might be relevant to enable Prestins function as motorprotein in OHCs.

**P077**

**Gastrocnemius-soleus contractile characteristics in the G93A-SOD1 ALS mouse model**

\*P. Dibaj, E. D. Schomburg, H. Steffens

MPI, Experimentelle Medizin, Göttingen, Germany

SOD1 mutations cause the fatal motor neuron disease familial ALS. Diverse pathophysiological mechanisms in the pre-clinical stage of SOD1G93A mouse model of ALS have been described, primarily leading to a selective vulnerability of fast-fatigable motor axons before appearance of clinical signs. Accordingly, an early decline of the contractile force has been observed in isolated fast-twitch but not slow-twitch hind limb muscles in SOD1G93A mice. In this study we analysed, in SOD1G93A mice, contractile characteristics of the muscle gastrocnemius-soleus (GS) which comprises fast-twitch and slow-twitch fibres. Attenuation of GS force appeared during the development of clinical signs, but not before. Similarly, fusion of GS twitches at relatively low stimulation frequencies was observed during the clinical course of SOD1G93A. Analysis of the amplitude course of tetanic twitches during stimulation rates of increasing frequencies, however, revealed a gradual shift of the response pattern over time towards higher frequencies in SOD1G93A mice, already beginning in pre-clinical mice. Additionally, the peak amplitude during the response course at high stimulation frequencies was higher in ctrl mice than in pre-clinical mice. Detailed analysis of single twitch configuration revealed a slower decay in SOD1G93A mice. This delayed relaxation of GS fibres was already observed in pre-clinical mice. Thus, analysis of the contractile pattern over time as well as of the twitch configuration of the mixed muscle GS has provided a distinctive aspect between ctrl and pre-clinical SOD1G93A mice. Future research will show whether these pre-clinical changes are also detectable in ALS patients.

**P078**

**Exceptional biomechanical properties of peripheral myelinated nerve fibers: Implications for neuropathies**

\*G. Rosso<sup>1</sup>, I. Liashkovich<sup>1</sup>, P. Young<sup>2</sup>, B. Gess<sup>2</sup>, V. Shahin<sup>1</sup>

<sup>1</sup>Institute of Physiology II, Münster, Germany

<sup>2</sup>Department of Neurology - University of Münster, Münster, Germany

The physiologically crucial central nervous system (CNS) of the human body is naturally very well protected. The bones of the skull and the spinal column create a hard physical barrier that protects the delicate nervous system from injury. The peripheral nervous system (PNS) on the other hand is equally crucial yet widely assumed to be far less protected. However, the PNS is permanently exposed to a variety of substantial mechanical stresses like shear, tension, compression and physiological through inflammation. Hence, our hypothesis is that the PNS must be inherently self-protective and that natural biomechanical resilience of the PNS is critical for its function. To check this hypothesis we designed an appropriate experimental strategy. It is based on simultaneous combination of confocal fluores-



cence microscopy and atomic force microscopy. Using this strategy it becomes possible to precisely and simultaneously study the physiological and biomechanical integrity of isolated, both nerves and nerve fibers. Here, we deal with nerve fibers. Peripheral nerve fibers from both wild type mice and mice with a peripheral neuropathy (homozygous *pmp22<sup>-/-</sup>*) were tested. Exposure of wild type mice fibers to incremental mechanical compression ranging from light to substantial (fully squeezed) reveals the following: The fibers maintain their physiological integrity in all conditions and fully restore their original shape upon relief from compression. The fairly thin basal lamina (nano-scale) of the Schwann cells is found out to be the major contributor to the astonishing biomechanical properties of peripheral nerve fibers. This is particularly astonishing bearing in mind that the tested fibers have diameters ranging from 5  $\mu\text{m}$  to 10  $\mu\text{m}$ . The same investigations carried out on fibers from *pmp22<sup>-/-</sup>* mice reveal that their physiological and biomechanical integrity is substantially impaired. Interestingly, the structural arrangement of the Schwann cell basal lamina is also significantly altered. In conclusion, the PNS is self-protective at the single nerve fiber level. The Schwann cell basal lamina confers astonishing biomechanical integrity to the nerve fibers, which is critical to their function. Consequently, altered structural arrangement of the basal lamina and impaired biomechanics has direct implications for peripheral neuropathies.

**P078b**  
**Enhanced glutamatergic innervation in surviving dopamine substantia nigra neurons in a 6-OHDA mouse model of Parkinson disease**

\*A. Kreuzer, A. Prinz, J. Roeper  
 Goethe Universität Frankfurt, Frankfurt, Germany

The clinical core symptoms of Parkinson disease (PD) are tightly linked to the progressive degeneration of dopamine substantia nigra (DA SN) neurons. It is however unclear, how the increasing loss of affects the synaptic and intrinsic properties of surviving DA SN neurons.

To investigate the electrophysiological properties of surviving SN DA neurons with intact axonal projections to striatum, we combined retrograde tracing with in vitro patch clamp recordings in an unilateral hydroxydopamine (6-OHDA) mouse model. The partial degeneration of SN DA neurons in adult (>12 weeks old) C57Bl6 mice was induced by unilateral infusion of 6 $\mu\text{l}$  (2 $\mu\text{g}/\mu\text{l}$ ) of 6-OHDA. Neurons with intact axonal connections to striatum were identified by injection of red fluorescent retrobeads (RB) within the ipsilateral striatum (2-4 days before in vitro recordings and 3 weeks post-lesion). RB-containing neurons were filled with neurobiotin during recordings and later immunostained for TH to verify their DA identity.

For immunocytochemical experiments, VGLUT1 and VGLUT2 Antibodies (1:1000) were utilized and the number of respective immuno-positive terminals was calculated using ImageJ.

For optogenetic experiments control or 6-OHDA lesioned animals were infused with 1 $\mu\text{l}$  AAV5-CamKIIa-hChR2(H134R)-EYFP into the STN. Light evoked (470 nm) EPSCs in SN DA neurons were recorded after 3 weeks using single pulse stimulation (1,5 ms) of varying intensity.

We found that miniature excitatory postsynaptic currents (mEPSCs) in the surviving SN DA neurons occurred with significantly, about 3-fold higher frequencies compared to controls. In contrast, mEPSC amplitudes and kinetics were unchanged. Fluorescent immunostaining showed that VGLUT2 positive terminals were significantly increased, also about 3-fold, in SNc of lesioned animals, while the number of VGLUT1 positive terminals was unaffected by the lesion. Furthermore, the stimulation of infused AAV5-ChR2 into the STN of lesioned mice resulted in significantly higher maximum amplitudes of light evoked EPSCs in surviving DA SN neurons compared to those in controls.

These results suggest enhanced glutamatergic neurotransmission in SN DA neurons surviving in a striatal 6-OHDA lesion model. Consistently, the mean mEPSC frequencies, the numbers of VGLUT2 positive terminals and the maximal amplitudes of optogenetically evoked EPSCs all showed 3-fold increase. Currently, we are working towards the complete neuroanatomical identification of the sources of this altered glutamatergic inputs to surviving DA SN neurons.

**Renal functions I**

**P079**  
**Hyperaldosteronism in  $K_{Ca}1.1$  channel  $\beta_2$ -subunit knockout mice**

\*C. Larsen, M. Sorensen, H. Praetorius, J. Leipziger  
 Aarhus University, Dept. of Biomedicine, Aarhus C, Denmark

Whole body  $K^+$  homeostasis depends on matching  $K^+$  excretion to the daily  $K^+$  intake.  $K^+$  is excreted via the colon and the kidney, the latter handling the majority of the total  $K^+$  excretion. Aldosterone is an important regulator of both renal and colonic  $K^+$  excretion. Renal  $K^+$  secretion depends on 2 apical  $K^+$  channels, ROMK and  $K_{Ca}1.1$ , while colonic  $K^+$  secretion depends on apical  $K_{Ca}1.1$  channels. We have

acquired a novel global knockout mouse for the  $\beta_2$ -subunit of the  $K_{Ca}1.1$  channel, which is the only  $K_{Ca}1.1$   $\beta$ -subunit expressed in murine colonic epithelium. The  $\beta_2$  KO mice have increased plasma aldosterone. Primary hyperaldosteronism is characterized by low plasma  $K^+$ , low renin and hypertension.  $\beta_2$  KO mice have normokalemia and low renin, indicating a secondary cause of hyperaldosteronism. The low renin in  $\beta_2$  KO mice indicates that a  $K^+$  handling deficiency, rather than hypotension, is causing the hyperaldosteronism. BK channel-dependent colonic  $K^+$  secretion was not disturbed in  $\beta_2$  KO mice. In contrast, urinary  $K^+$  excretion was reduced in  $\beta_2$  KO mice ( $P=0.06$ ,  $n=5$ ), suggesting that  $\beta_2$  KO mice have a reduced capacity for renal  $K^+$  secretion. mRNA expression of the  $\beta_2$  subunit has previously been found in rabbit cortical collecting ducts, where expression is increased by  $K^+$  loading and reduced by  $K^+$  depletion. These data indicate an important function of the  $\beta_2$  subunit of the  $K_{Ca}1.1$  in renal  $K^+$  excretion.

Supported by the Lundbeck foundation.

**P080**  
**The role of soluble guanylate cyclase in renal hemodynamics and autoregulation**

M. Dautzenberg<sup>1</sup>, A. Kahnert<sup>2</sup>, J.-P. Stasch<sup>2</sup>, \*A. Just<sup>1</sup>  
<sup>1</sup>Universität Freiburg, Physiologisches Institut, Freiburg, Germany  
<sup>2</sup>BAYER Pharma AG, Cardiology/Hematology Research, Wuppertal, Germany

Endogenous nitric oxide (NO) importantly impacts on baseline renal blood flow (RBF), glomerular filtration (GFR), and RBF autoregulation. The major signaling target of NO is thought to be soluble guanylate cyclase (sGC), but sGC-independent NO signaling pathways have also been postulated. We studied the effect of pharmacological activation of soluble guanylate (sGC) by cinaciguat on baseline RBF, GFR, and RBF autoregulation, as well as the extent to which sGC-signaling accounts for the effects of endogenous NO on RBF autoregulation. Arterial pressure (AP), heart rate (HR), RBF, GFR, and RBF autoregulation were studied in anesthetized rats during iv. infusion of cinaciguat. AP, HR, RBF, and autoregulation were also studied after elimination of endogenous NO by NO-synthase (NOS) inhibition. Cinaciguat reduced AP, increased HR, tended to elevate RBF, did not change GFR, and slightly reduced filtration fraction. RBF autoregulatory efficiency and the myogenic response in autoregulation were slightly depressed. NOS-inhibition expectedly increased AP, reduced RBF, and augmented the myogenic response in RBF autoregulation. Cinaciguat restored AP, RBF, and myogenic response by 77%, 78%, and 90% back to normal. In vehicle controls, in which the hypotension observed during cinaciguat was reproduced by aortic compression, changes of RBF and autoregulation induced by NOS-inhibition were not reversed. We conclude that sGC activation by cinaciguat leaves RBF and GFR well maintained despite hypotension and only slightly impairs autoregulation. The ability to normalize RBF autoregulation

and the renal myogenic response after L-NAME indicates that this influence of endogenous NO is mediated predominantly via sGC.

**P081**  
**Calcium measurement in renin producing cells in situ**

\*D. Steppan, A. Kurtz  
 University of Regensburg, Institute of Physiology, Regensburg, Germany

The protease renin is produced and stored in huge lysosome related organelles in juxtaglomerular cells of the kidney. It is secreted by mechanism similar to compound exocytosis triggered by the cyclic-AMP signaling pathway. Calcium appears to play a rather unusual role in the control of renin secretion as it is thought to inhibit renin secretion i.e. exocytosis in juxtaglomerular cells. This concept about the unusual role of calcium has mainly been derived from indirect evidence, since so far no data is available on calcium handling in juxtaglomerular cells in situ.

In order to obtain more direct insight into the regulation of intracellular calcium concentration in renin secreting cells, we have established an experimental model that allows to trace the intracellular concentration of calcium in renin secreting cells using the fluorescent calcium indicator fura-2. For this purpose we microdissected glomeruli with attached afferent arterioles from kidneys of mice harbouring a BAC chromosome with GFP under the control of the Ren-1 gene promoter. Thus GFP fluorescence identifies all cells actively expressing the renin gene. In pilot experiments with adult kidneys we detected GFP fluorescence in juxtaglomerulars only. After microdissection of glomeruli renin expressing cells became clearly visible by intense GFP fluorescence. Glomeruli with GFP fluorescence were selected by hand using a Zeiss Stereo Discovery.V8 stereomicroscope and transferred into a perfusion bath, where they were loaded with fura-2 AM. Fura-2 fluorescence could be well separated from endogenous GFP fluorescence. It is therefore possible to use microdissected glomeruli and its renin expressing cells for calcium measurement. For measurement we used a Zeiss Axiovert 200 fluorescence microscope and the Metafluor 6.2r2 software. We found that angiotensin II (100nM) and ATP (100 $\mu\text{M}$ ) elicited calcium transients followed by sustained elevations of the intracellular calcium concentration in GFP-positive cells. Notably other glomerular cells, which could not be distinguished between capillary endothelial cells, podocytes or mesangial cells frequently responded to ATP but not to angiotensin II. In summary we present a novel approach to directly measure intracellular calcium concentration in defined renin producing cells of the kidney. Combining results from those calcium measurements with results on renin secretion from isolated perfused mouse kidneys may be a promising approach to understand the yet mysterious role of calcium in the control of renin secretion.

**P082**  
**Upregulation of voltage-gated K<sup>+</sup> channel Kv1.3 by klotho protein**

\*S. S. Ajay<sup>1</sup>, C. Munoz<sup>1,2</sup>, A. Almilaji<sup>1</sup>, Z. Hosseinzadeh<sup>1</sup>, E. Shumilina<sup>1</sup>, F. Lang<sup>1</sup>

<sup>1</sup>University of Tuebingen, Department of Physiology, Tuebingen, Germany

<sup>2</sup>University of Zurich, Institute of Physiology and Zurich Center for Integrative Human Physiology (ZIHP), Zurich, Switzerland

**Question:** Klotho, a transmembrane protein, can be cleaved off and then act as a hormone or an enzyme with β-glucuronidase or sialidase activity. Klotho protein is known to regulate different ion channels and transporters. Klotho deficiency leads to early appearance of age-related disorders and premature death. Heavily glycosylated membrane proteins and thus potential targets for klotho include the voltage-gated K<sup>+</sup> channel Kv1.3, which modulates membrane excitability in many cell types. The present study explored whether Klotho influences the activity of Kv1.3.

**Methods:** cRNA encoding Kv1.3 was injected into *Xenopus laevis* oocytes and Kv1.3 expressing *Xenopus* oocytes were further treated with recombinant human Klotho protein with or without β-glucuronidase inhibitor D-saccharic acid 1,4-lactone monohydrate (DSAL) or sialidase inhibitor 2,3-didehydro-2-deoxy-N-acetyl neuraminic acid (DANA). Kv1.3 currents were measured in two electrode voltage clamp experiments.

**Results:** Treatment with recombinant human Klotho protein up-regulates Kv1.3 depending currents, an effect reaching statistical significance after 12 h and 24 h after addition of klotho protein. The upregulating effect of the Klotho protein on Kv1.3 current was abrogated in the presence of DSAL or DANA.

**Conclusions:** Klotho is a novel and powerful regulator of the potassium voltage-gated K<sup>+</sup> channel Kv1.3.

**P083**  
**JAK3 sensitivity of renal 1α hydroxylase expression, 1,25(OH)<sub>2</sub>D<sub>3</sub> formation and phosphate metabolism**

\*A. Umbach<sup>1</sup>, B. Zhang<sup>1,2</sup>, A. Fajol<sup>1</sup>, Z. Hosseinzadeh<sup>1</sup>, S. K. Bhavsar<sup>1</sup>, T. Bock<sup>2</sup>, R. Kandolf<sup>2</sup>, B. J. Pichler<sup>3</sup>, M. Föller<sup>1</sup>, F. Lang<sup>1</sup>

<sup>1</sup>University of Tuebingen, Department of Physiology, Tuebingen, Germany

<sup>2</sup>University of Tuebingen, Department of Molecular Pathology, Tuebingen, Germany

<sup>3</sup>University of Tuebingen, Department of Radiology, Tuebingen, Germany

**Question:** Calcitriol (1,25(OH)<sub>2</sub>D<sub>3</sub>), a powerful regulator of phosphate metabolism and hormone participating in the regulation of the immune response, is generated by 1α hydroxylase (1αH) in kidney and macrophages. Renal 1αH expression is suppressed by Klotho and FGF23, the expression of which is in turn stimulated by 1,25(OH)<sub>2</sub>D<sub>3</sub>. IL-12 regulates 1αH expression through transcription factor interferon regulatory factor-1 (IRF-1). INFγ-sensitive signaling includes Janus kinase 3 (JAK3). A role of JAK3 in the regulation of 1αH expression and mineral metabolism has, however, never been shown. Thus, the impact of JAK3 deficiency on 1,25(OH)<sub>2</sub>D<sub>3</sub> formation and phosphate metabolism was analysed.

**Methods:** In mice lacking JAK3 (jak3<sup>-/-</sup>) and wild type mice (jak3<sup>+/+</sup>) transcript levels of renal 1αH (CYP 27B1) and IRF-1 were determined by RT-PCR. Klotho expression by Western blotting, serum 1,25(OH)<sub>2</sub>D<sub>3</sub>, IL-12, PTH and FGF23 concentrations by immunoassays and serum, fecal and urinary phosphate concentration by photometry.

**Results:** Serum IL-12 levels as well as renal IRF-1 and 1αH transcript levels were significantly higher in jak3<sup>-/-</sup> mice than in jak3<sup>+/+</sup> mice. Moreover, serum 1,25(OH)<sub>2</sub>D<sub>3</sub> and FGF23 levels were elevated in jak3<sup>-/-</sup> compared to jak3<sup>+/+</sup> mice. Intestinal phosphate absorption as well as absolute and fractional renal phosphate excretion were higher in jak3<sup>-/-</sup> mice than in jak3<sup>+/+</sup> mice.

**Conclusions:** JAK3 is a powerful regulator of 1αH expression and JAK3 deficiency leads to marked derangement of phosphate metabolism.

**P084**  
**Prevention of accelerated tissue calcification and aging of klotho-hypomorphic mice by NH<sub>4</sub>Cl treatment**

\*C. Leibrock<sup>1</sup>, I. Alesutan<sup>1</sup>, J. Voelkl<sup>1</sup>, D. Michael<sup>1</sup>, E. Schleicher<sup>2</sup>, Z. Kamyabi-Moghaddam<sup>3</sup>, L. Quintanilla-Martinez<sup>3</sup>, M. Kuro-o<sup>4</sup>, F. Lang<sup>1</sup>

<sup>1</sup>University of Tuebingen, Department of Physiology, Tuebingen, Germany

<sup>2</sup>University of Tuebingen, Department of Internal Medicine, Tuebingen, Germany

<sup>3</sup>University of Tuebingen, Department of Pathology, Tuebingen, Germany

<sup>4</sup>University of Texas, Southwestern Medical Center at Dallas, Department of Pathology, Dallas, United States

**Question:** Klotho, a protein inhibiting 1,25(OH)<sub>2</sub>D<sub>3</sub>-formation and regulating mineral metabolism, counteracts age-related disorders. Klotho-hypomorphic mice (kl/kl) suffer from excessive plasma 1,25(OH)<sub>2</sub>D<sub>3</sub>- and CaHPO<sub>4</sub>-concentrations, leading to severe soft tissue calcification, volume depletion, early appearance of numerous age related disorders and dramatically decreased life span. The calcification involves stimulation of osteoinductive signaling. The present study explored whether calcification, ageing and life span of kl/kl mice could be modified by NH<sub>4</sub>Cl intake.

**Methods & Results:** NH<sub>4</sub>Cl added to drinking water (15 g/l) prevents soft tissue and vascular calcification without significantly affecting plasma concentrations of 1,25(OH)<sub>2</sub>D<sub>3</sub>, Ca<sup>2+</sup> and phosphate in male kl/kl mice. All male NH<sub>4</sub>Cl treated kl/kl mice survived >700 days, whereas none of the untreated male kl/kl mice survived >95 days. NH<sub>4</sub>Cl treatment similarly increased average life span of female kl/kl mice (from 84±4 to 355±46 days). NH<sub>4</sub>Cl treatment restored fertility of male but not female kl/kl mice. NH<sub>4</sub>Cl treatment significantly decreased plasma aldosterone and ADH concentrations as well as aortic transcript levels of osteoinductive Pit1, osteogenic transcription factors Msx2 and Cbfa1, alkaline phosphatase and senescence-associated molecules Pai-1, p21 and Tgfb1 in male kl/kl mice. Similarly, in human aortic smooth muscle cells, NH<sub>4</sub>Cl treatment (500 μM) reduced phosphate-induced mRNA expression of Pit1, MSX2, CBFA1, alkaline phosphatase as well as Pai-1, p21 and Tgfb1.

**Conclusion:** NH<sub>4</sub>Cl is a powerful inhibitor of osteogenic signaling, tissue calcification and accelerated aging of klotho-hypomorphic mice.

**P085**  
**Distribution of phosphorylated CREB in the mouse kidney**

\*I. Schwarzensteiner, B. Kurt, A. Kurtz

University of Regensburg, Physiology, Regensburg, Germany

The nuclear abundance of phosphorylated CREB (pCREB) protein is considered as an indirect indicator of endogenous protein kinase A activity on the one hand and as an indirect indicator of the potential transcriptional activity of pCREB-triggered genes on the other. So far there exists only little information about nuclear pCREB abundance in the vascular, glomerular and tubular compartments of the kidney. We therefore first analyzed pCREB distribution in normal mouse kidneys. Since renin gene expression and renin secretion are considered to be essentially regulated by the cAMP-signaling pathway, we further analyzed pCREB immunoreactivity in renin producing cells in different activity states of the renin-angiotensin-aldosterone system. For this purpose, we performed costainings of pCREB with renin and with structural markers for distal (calbindin) and proximal (megalin) tubules, arterioles (α smooth muscle actin) and the collecting duct (aquaporin-2) together with nuclear staining (DAPI). We found that about 20% of proximal and distal tubule cells stained positive for pCREB. 30% of all glomerular cells stained positive for pCREB. 45% of renin cells and preglomerular arteriolar smooth muscle cells showed strong nuclear staining for pCREB, respectively, in normal kidneys. Collecting duct cells showed a gradual increase of costaining with pCREB from the cortex (50%) over medullary regions (60%) to the papilla (90%). In kidneys with stimulated renin expression which was induced by feeding the mice a low salt diet, colocalization of pCREB with renin increased to 65% whilst nuclear staining of pCREB in smooth muscle cells decreased to 30%. The percentage of pCREB positive tubule cells increased to 40%. The papillary portion of the collecting duct showed a decrease in coexpression with pCREB to 50%. All other structures showed no significant changes. Our data show that nuclear pCREB abundance is, in fact, different between the various structures of the kidney. There is a strong colocalization with the water resorption capability of collecting ducts, what is in good accordance with the regulation of aquaporin-2 gene expression and the intracellular aquaporin-2 trafficking by the cAMP-signaling pathway. Over-average pCREB immunoreactivity in renin cells is also in accordance with the particular role of the cAMP-signaling pathway in the control of renin cell function. We therefore suggest that determination of nuclear pCREB abundance in the kidney can be used as one indicator for the activity of the cAMP-signaling pathway of kidney cells in physiological, pathophysiological and pathological states.

**P086**  
**Tamoxifen-inducible Cx40 cell specific Vhl deletion induced erythropoietin production in the kidney**

\*K. Gerl<sup>1</sup>, B. Kurt<sup>1</sup>, L. Miquero<sup>2</sup>, A. Kurtz<sup>1</sup>

<sup>1</sup>University of Regensburg, Physiology, Regensburg, Germany

<sup>2</sup>Universite de la Mediterranee, Developmental Biology, Marseille, France

Based on previous evidence that conditional deletion of von Hippel-Lindau protein (pVHL) in renin-expressing juxtaglomerular cells of the kidney suppresses renin expression and induces erythropoietin expression, we wondered if this striking endocrine shift is developmentally programmed or if it can also be induced in the normal adult kidney. To address this question we used a tamoxifen-inducible Cre deleter under the control of the connexin 40 gene promoter, as connexin 40 is strongly expressed by juxtaglomerular cells. Thus we generated Vhl<sup>fl/fl</sup> x Cx40<sup>tam-Cre</sup> mice, to induce Cx40 cell specific pVHL deletion at a particular time by tamoxifen supply. Vhl<sup>+/+</sup> x Cx40<sup>tam-Cre</sup> litters served as controls. Both genotypes were fed a special chow containing tamoxifen at the age of four weeks. Determination of hematocrit (hct) values of Vhl<sup>fl/fl</sup> x Cx40<sup>tam-Cre</sup> mice showed pronounced polycythemia that was caused by elevated red blood cell counts. Control litters had normal hct values. The stimulated erythropoiesis was paralleled by elevated plasma EPO concentrations. To search for the origin of EPO, we determined EPO mRNA expression in several organs, since Cx40 is apart from the kidneys also expressed to a significant extent in the arterial endothelium, in lung or heart. Amongst these organs we only found elevated EPO-mRNA levels in the kidneys. Renin mRNA levels as well as plasma renin concentrations were significantly reduced in these Vhl<sup>fl/fl</sup> x Cx40<sup>tam-Cre</sup> mice. Although not yet definitively confirmed, our data might suggest that deletion of pVHL in juxtaglomerular cells of adult kidneys induces EPO and suppresses renin expression.

**P087**  
**Stress-induced expression and function of the long non-coding WISP1 transcript lncWISP1 in human renal cells**

I. Hennemeier, M. Gekle, \*G. Schwardt

Institut für Physiologie, Halle, Germany

Non-coding sequences make up only a small fraction of DNA in prokaryotes. Among eukaryotes, as their complexity increases, the proportion of their DNA that does not code for protein increases, too. These non-coding sequences have been considered as junk, but research of the last years showed that they have crucial importance in physiological as well as pathophysiological processes. Today it is known that 76 % of the human genome is transcribed into RNA but only 3 % of the genome is translated into proteins. In our studies using human renal cells (RPTEC, HEK293 and HK2), we have identified a novel long non-coding transcript of Wnt1 inducible signaling pathway protein 1, named lncWISP1. The expression of lncWISP1 is induced by the profibrotic mycotoxin ochratoxin A (OTA), the

PKC-activator PMA and the NO-donor SNAP in HEK293 cells. Furthermore, IncWISP1 is transcribed in an ERK/MEK-dependent manner, is nuclear enriched and uses an alternative promoter compared to its parent gene WISP1. In a first approach to study the influence of IncWISP1 on cell function, IncWISP1 was overexpressed and pathway specific RT2 Profiler PCR arrays were performed. They showed that an excess of IncWISP1 alters the expression of genes involved in fibrotic and malignant events. In contrast, IncWISP1 overexpression does not influence cell survival determined by apoptosis, necrosis and total protein content. In summary therefore, IncWISP1 seems to act on cell homeostasis without disturbing cell survival in a so far unknown manner.

**P088**

**NH<sub>4</sub>Cl treatment mitigates renal fibrotic response following unilateral ureteral obstruction**

\*M. Feger, J. Voelkl, T. Pakladok, S. Mia, I. Alesutan, F. Lang  
University of Tuebingen, Department of Physiology, Tuebingen, Germany

Question: Ammonium chloride (NH<sub>4</sub>Cl) treatment confers protective effects against deterioration of experimental renal failure. Furthermore, NH<sub>4</sub>Cl interferes with signaling leading to vascular damage by 5/6 nephrectomy. The present study investigated whether NH<sub>4</sub>Cl treatment influences the pro-fibrotic signaling following unilateral ureteral obstruction (UUO) model of renal fibrosis. Methods: UUO was induced in C57Bl6 mice with or without NH<sub>4</sub>Cl treatment and seven days after the obstructive injury, kidney tissues were harvested for tissue analysis. Protein expression was determined by western blotting and the mRNA levels by quantitative RT-PCR. Results: Following UUO, expression of the fibrosis markers  $\alpha$ -smooth muscle actin, type I collagen and fibronectin increased in the obstructed kidney tissues, effects significantly attenuated following NH<sub>4</sub>Cl treatment. Moreover, UUO induced renal mRNA expression of Tgfb1, an effect again blunted by NH<sub>4</sub>Cl treatment. In accordance, the protein abundance of Tgf $\beta$ -activated kinase 1 (Tak1) was increased by UUO, an effect ameliorated by NH<sub>4</sub>Cl treatment. Furthermore, UUO increased NF-kB protein abundance. NH<sub>4</sub>Cl treatment mitigated the effects of the obstructive injury, and both, the cytoplasmic and nuclear Nf-kB protein levels were higher in the obstructed kidney tissues of untreated mice as compared to NH<sub>4</sub>Cl treated mice. The expression of NF-kB target genes Il6, Tnfa and Pai-1 was stimulated by UUO, effects again ameliorated by NH<sub>4</sub>Cl treatment. Conclusions: Ammonium chloride mitigates the effects of obstructive injury on renal fibrosis, Tgfb1 production and NF-kB signalling in the UUO model, indicating that NH<sub>4</sub>Cl treatment might be beneficial in renal fibrotic disease.

**P089**

**Ampk $\alpha$ 1 deficiency attenuates renal fibrotic response following unilateral ureteral obstruction**

\*S. Mia, I. Alesutan, M. Feger, T. Pakladok, A. Meissner, J. Voelkl, F. Lang  
University of Tuebingen, Department of Physiology, Tuebingen, Germany

Question: AMP-activated protein kinase (Ampk) acts as a metabolic stress sensor and its activation plays a role in several renal disease models. Recently, isoform specific actions of the Ampk $\alpha$  subunit were described. Therefore, the role of the Ampk $\alpha$ 1 subunit was investigated in the unilateral ureteral obstruction (UUO) model of renal fibrosis. Methods: UUO was induced in Ampk $\alpha$ 1-deficient mice (Ampk $\alpha$ 1<sup>-/-</sup>) and corresponding wild-type mice (Ampk $\alpha$ 1<sup>+/+</sup>). Seven days after the obstructive injury, protein expression was determined by western blotting and the mRNA levels by quantitative RT-PCR. Results: After UUO treatment, renal Ampk $\alpha$ 1 protein abundance was increased in the obstructed kidney tissues from Ampk $\alpha$ 1<sup>+/+</sup> mice as compared to the contralateral non-obstructed kidney tissues. Increased Ampk $\alpha$  and ACC phosphorylation following UUO were suppressed in the obstructed kidney tissues from Ampk $\alpha$ 1<sup>-/-</sup> mice as compared to Ampk $\alpha$ 1<sup>+/+</sup> mice. More importantly, the elevated protein and mRNA expression of  $\alpha$ -smooth muscle actin and type I collagen in the obstructed kidney tissues from Ampk $\alpha$ 1<sup>+/+</sup> mice were ameliorated in the obstructed kidney tissues from Ampk $\alpha$ 1<sup>-/-</sup> mice. UUO treatment further led to an increased renal Tak1 and Erk5 protein abundance, effects which were blunted in the Ampk $\alpha$ 1<sup>-/-</sup> mice. In addition, the increased mRNA levels of the Ap-1 target genes: Il6 and c-Fos in the kidney tissues from Ampk $\alpha$ 1<sup>+/+</sup> mice after obstruction were mitigated in the Ampk $\alpha$ 1<sup>-/-</sup> mice. Conclusions: Ampk $\alpha$ 1 deficiency ameliorates the fibrotic response following UUO. Thus, Ampk $\alpha$ 1 contributes to the pro-fibrotic signaling leading to renal tissue fibrosis in obstructive nephropathy.

**P090**

**Purinergic P<sub>2</sub>X channels are mechanotransducing elements in podocytes**

\*A.-L. Forst, V. S. Olteanu, T. Gudermann, M. Mederos y Schnitzler, U. Storch  
Walther Straub Institut, Munich, Germany

Podocytes are visceral epithelial cells lining the glomerular basement membrane thereby fulfilling an important role in the kidney filtration. Hypertension and the resulting increase in mechanical load to podocytes are believed to result in podocyte damage. However, the molecular identity of the proteins sensing the mechanical force is completely unknown. It has been speculated whether the classical transient receptor channel type 6 (TRPC6) in complex with the MEC-2 homologue podocin and possibly other slit-membrane protein could form a mechanosensitive channel complex in podocytes. Here, we report that podocytes indeed respond to mechanical stretch with increased inward cation current densities in electrophysiological whole-cell measurements that are not mediated by TRPC6

since podocytes isolated from TRPC6 knock-out mice responded to mechanical stretch in a similar way as control podocytes. By using the G-protein inhibitor GDP- $\beta$ S in the pipette solution, we could rule out an involvement of mechanosensitive G<sub>q/11</sub>-protein coupled receptors. Instead, the observed currents could be reduced by using the specific purinergic P<sub>2</sub>X<sub>4</sub> channel blocker 5-BDBD in electrophysiological measurements as well as in fluorimetric calcium recordings. Quantitative RT-PCR confirms expression of several purinergic receptor channels including P<sub>2</sub>X<sub>2</sub> and P<sub>2</sub>X<sub>4</sub>. We could show that podocytes indeed respond to extracellularly perfused ATP with similar inward currents as observed with hypotonic solution. Moreover, we found out that hypoosmotically induced membrane stretch leads to release of ATP which subsequently activates P<sub>2</sub>X channels thereby determining mechanosensitivity of podocytes.

**P091**

**The effect of LRRK2 depletion on vitamin D adaptation**

\*F. Simona, N. Hernando, C. A. Wagner  
UZH, Physiology, Zürich, Switzerland

Leucine-rich repeat kinase 2 (LRRK2) is a multidomain protein mutated in patients with Parkinson's disease. LRRK2 mRNA is widely expressed and is highly abundant in the kidney but little is known about its function. In mice, depletion of LRRK2 resulted in downregulation of the renal sodium-phosphate cotransporter NaPi2a (Slc34A1) as well as of the vitamin D activating hydroxylase (Cyp27b1) and upregulation of the inactivating one (Cyp24a1). The aim of this study was to test the implication of LRRK2 in the metabolism of phosphate (Pi) and vitamin D. For that, wild type (LRRK2<sup>+/+</sup>) and LRRK2-depleted (LRRK2<sup>-/-</sup>) mice were fed during 48 h with either high (HVD) or low vitamin D (LVD) diets, both containing high Pi. The expression of NaPi2a protein was downregulated in LRRK2<sup>-/-</sup> as compared with LRRK2<sup>+/+</sup>. In both genotypes there was a tendency for reduced expression of the cotransporter on HVD. Cyp27b1 mRNA was reduced in LRRK2<sup>+/+</sup> fed with HVD compared with LVD. This downregulation was blunted in LRRK2<sup>-/-</sup>. Cyp24a1 mRNA increased in the groups fed with HVD, although upregulation was more moderate in LRRK2<sup>-/-</sup> than in LRRK2<sup>+/+</sup>. The vitamin D receptor (VDR) that in LRRK2<sup>+/+</sup> mice fed with HVD was upregulated at both RNA and protein level, remained unchanged in LRRK2<sup>-/-</sup> mice. Immunohistochemistry showed similar localization of VDR in the nucleus of LRRK2<sup>-/-</sup> and LRRK2<sup>+/+</sup> mice. In conclusion, LRRK2<sup>-/-</sup> mice showed reduced sensitivity to dietary vitamin D (as indicated by the blunted adaptation of Cyps and VDR) what indirectly may affect the proper expression of NaPi2a.

**P092**

**SPAK and OSR1 dependent down-regulation of renal outer medullary K<sup>+</sup> channel ROMK1**

\*J. Borras, B. Elvira, C. Munoz, E. Shumilina, F. Lang  
University of Tuebingen, Department of Physiology, Tuebingen, Germany

**Question:** The kinases SPAK (STE20/SPS1-related proline/alanine-rich kinase) and OSR1 (oxidative stress-responsive kinase 1) participate in the regulation of the NaCl cotransporter NCC and the Na<sup>+</sup>,K<sup>+</sup>,2Cl<sup>-</sup> cotransporter NKCC2. The kinases are regulated by WNK (with-no-K[Lys]) kinases. Mutations of genes encoding WNK kinases underly Gordon's syndrome, a monogenic disease leading to hypertension and hyperkalemia. WNK kinases further regulate the renal outer medullary K<sup>+</sup> channel ROMK. The present study explored, whether SPAK and/or OSR1 similarly modify the activity of ROMK1. **Methods:** ROMK1 was expressed in Xenopus laevis oocytes with or without additional expression of wild-type SPAK, catalytically inactive SPAK<sup>KD</sup>, wild type OSR1, or catalytically inactive OSR1<sup>KD</sup>. Channel activity was determined utilizing dual electrode voltage clamp and ROMK1 protein abundance in the cell membrane utilizing chemiluminescence of ROMK1 containing an extracellular hemagglutinin epitope (ROMK-HA). **Results:** ROMK1 activity was significantly down-regulated by wild type SPAK but not by SPAK<sup>KD</sup>. Similarly, ROMK1 activity was significantly down-regulated by wild type OSR1, but not by OSR1<sup>KD</sup>. According to chemiluminescence, wild type SPAK but not SPAK<sup>KD</sup> decreased ROMK-HA protein abundance in the cell membrane. Similarly, ROMK-HA protein abundance was significantly down-regulated by wild type OSR1 but not by OSR<sup>KD</sup>. **Conclusions:** ROMK1 protein abundance and activity are down-regulated by SPAK and OSR1.

Vascular functions and circulation I

**P093**

**Reduced microRNA levels contribute to platelet hyperactivity in diabetes: role of calpain**

\*A. Elgheznawy, L. Shi, I. Wittig, H. Laban, U. Pohl, A. Mann, V. Ramiariboavonjy, I. Fleming  
Institute for Vascular Signalling, Centre for Molecular Medicine, Frankfurt am Main, Germany

MicroRNA-223 (miR-223) is currently of particular interest as although it is highly expressed in healthy platelets, circulating miR-223 levels (presumably derived from platelets) are decreased in subjects with type 2 diabetes and myocardial infarction. The aim of this study was to determine how decreased miR-223 levels affect platelet function and

why platelet miR-223 levels are attenuated in diabetic individuals. MiR-223 deletion in mice (miR-223<sup>-/-</sup>) resulted in dysregulated platelet function versus wild-type littermates but demonstrated a phenotype similar to platelets from diabetic patients. Moreover, miR-223<sup>-/-</sup> mice and diabetic patients had large platelet aggregates formation and delayed clot retraction. Proteomic analysis revealed the increased expression of kindlin-3 and coagulation factor XIIIa (FXIIIa) in miR-223<sup>-/-</sup> platelets. A similar dysregulation of both proteins was detected in platelets from diabetic patients, and was linked to the increased expression of  $\beta$ 1 and  $\alpha$ 2 integrins. Reporter gene assays revealed that  $\beta$ 1 integrin and FXIIIa are directly targeted by miR-223. Indeed, a  $\alpha$ 2 $\beta$ 1 integrin antagonist prevented the formation of large aggregates, while FXIIIa inhibition normalized the clot retraction process. Dicer degraded in platelets from diabetic patients compared to healthy donors indicating why platelet miRNA levels were decreased. We found that Dicer was a calpain substrate in platelets and that calpain inhibition prevented Dicer cleavage in diabetic mice. Correspondingly, treating diabetic mice with a calpain inhibitor prevented the upregulation of  $\beta$ 1 integrin, kindlin-3 and FXIIIa. These results indicate that calpain inhibition may be one means of normalizing platelet microRNA processing in diabetes as well as platelet function.

**P094**  
**Contractile response of vasoactive substances is mediated by EGFR transactivation in vascular smooth muscle cells**

\*D. Bethmann<sup>1</sup>, B. Schreier<sup>1</sup>, M. Hünerberg<sup>1</sup>, S. Mildenerberger<sup>1</sup>, S. Rabe<sup>1</sup>, M. Gekle<sup>1</sup>, S. Rupp<sup>2</sup>

<sup>1</sup>Martin-Luther-Universität, Julius-Bernstein-Institut für Physiologie, Halle (Saale), Germany

<sup>2</sup>Martin-Luther-Universität, Pharmakologie und Toxikologie, Halle (Saale), Germany

**Question:** The EGFR plays an important role in cell proliferation, differentiation and survival. Moreover, it seems to be involved in the development of cardiovascular diseases. The EGFR can be activated either by its classical ligands or by vasoactive substances, like endothelin-1, epinephrine or angiotensin-II, a process called transactivation. Here we determine the contribution of the EGFR in vascular smooth muscle cells (VSMC) to vasoconstriction/-dilation induced by different vasoactive substances.

**Methods:** Therefore we used mice with a specific, inducible deletion of EGFR in VSMC. 56 days after induction with tamoxifen aortic rings of wildtype and knockout animals were mounted onto Mulvany myographs and force generation ( $\Delta F$ ) as well as velocity of force development ( $\Delta F / \Delta T$ ) was measured.

**Results:** Upon stimulation with serotonin or KCl no difference in  $\Delta F$  or  $\Delta F / \Delta T$  was observed, indicating that aortic rings from wildtype and knockout animals can generate the same force upon adequate stimulation. Norepinephrine, phenylephrine or angiotensin-II induced a significantly smaller increase in force in knockout than in wildtype animals, supporting the hypothesis that EGFR might increase

blood pressure via transactivation. In contrast, endothelin-1 induced a stronger reaction in knockout compared to wild-type aortic rings, while there was no difference observed upon addition of either isoprenaline, S-Nitroso-N-acetyl-DL-penicillamine (NO-donor) or carbamoylcholine chloride (carbachol).

**Conclusions:** In summary, we were able to show that transactivation of the VSMC-EGFR via endothelin-1, angiotensin-II or  $\alpha$ -adrenergic agonists plays a significant albeit differential role in aortic vasoconstriction, whereas  $\beta$ -adrenergic or NO-mediated vasodilation was not affected. Further studies will have to address the underlying molecular mechanisms.

**P095**  
**The AMPK $\alpha$ 2 subunit is crucial for myeloid cell-mediated post-ischemic revascularization**

\*R. Abdel Malik, N. Zippel, P. Seifert, B. Fißthaler, I. Fleming  
 Insitute for Vascular Signalling, Goethe University, Frankfurt, Germany

Immune cells play a key role in regulating angiogenesis through the production and release of a wide range of pro-angiogenic mediators. Given that the AMP-activated protein kinase (AMPK) positively regulates angiogenesis, we investigated the consequences of deleting the  $\alpha$ 2 subunit in myeloid cells (AMPK $\alpha$ 2<sup>ΔMy</sup>) on vascular repair as well as macrophage and neutrophil function. Wild-type and AMPK $\alpha$ 2<sup>ΔMy</sup> mice were subjected to femoral artery ligation and the recovery of blood flow (laser Doppler), capillary density (immunohistochemistry) as well as immune cell infiltration (flow cytometry) were determined. Recovery of blood flow after hindlimb ischemia was significantly impaired (80%) in AMPK $\alpha$ 2<sup>ΔMy</sup> versus the wild-type littermates. In addition, AMPK $\alpha$ 2<sup>ΔMy</sup> mice showed significantly reduced capillary density and decreased myeloid cell infiltration into the ligated limb. Mechanistically, the deletion of the AMPK $\alpha$ 2 subunit increased the mRNA expression levels of TNF- $\alpha$  and IL-1 $\beta$  in LPS-stimulated polymorphonuclear cells (PMN). On the other hand, SDF-1 $\alpha$  and MMP-9 gene expression were significantly decreased. In bone marrow derived and M2 polarized macrophages from AMPK $\alpha$ 2<sup>ΔMy</sup> mice mRNA levels of FIZZ-1 and VEGF were also down regulated. These results indicate that the AMPK $\alpha$ 2 plays a crucial role in regulating the inflammatory state and angiogenic potential of myeloid cells promoting vascular repair in vivo.

**P096**  
**Modulation of angiogenesis by the fatty acid amide hydrolase (FAAH)**

\*S. Köster<sup>1</sup>, S. Rieck<sup>1</sup>, S. Vosen<sup>1</sup>, M. Matthey<sup>1</sup>, J. Meyer<sup>2</sup>, S. Schmitz-Valckenberg<sup>2</sup>, B. Fleischmann<sup>1</sup>, D. Wenzel<sup>1</sup>

<sup>1</sup>University of Bonn, Institute of Physiology I, Bonn, Germany

<sup>2</sup>Department of Ophthalmology, University of Bonn, Bonn, Germany

**Question:** Previous studies have demonstrated that the endocannabinoid anandamide (AEA) and its metabolites are biologically active in the vasculature and can regulate vascular tone. We therefore wondered, whether FAAH-dependent AEA degradation also plays a role in angiogenesis.

**Methods:** To examine angiogenesis in vitro different sprouting assays were used: a transgenic murine Flt-eGFP embryonic stem cell system, a Matrigel assay using human umbilical vein endothelial cells (HUVEC) and an aortic ring assay. We determined proliferation and apoptosis by Ki67 or annexin V staining, respectively. Cell migration was tested in a scratch assay. Finally the results were verified in vivo in a model of choroidal neovascularisation (CNV).

**Results:** The pharmacological FAAH inhibitor URB597 similar as the FAAH substrate AEA and its metabolically stable analogue Met-AEA strongly reduced vessel formation in different in vitro angiogenesis assays. The specificity of URB597 was confirmed by an aortic ring assay using FAAH<sup>-/-</sup> mice that also demonstrated less angiogenesis compared to wild-type rings. The underlying mechanism could be attributed to attenuated endothelial cell proliferation and migration while there was no effect on apoptosis. To test the relevance of this signalling pathway for angiogenesis in vivo we used a CNV model and recent experiments suggest that there is reduced neovascularisation in FAAH<sup>-/-</sup> mice upon injury.

**Conclusion:** Thus, FAAH is a crucial modulator of angiogenesis as its inhibition reduces endothelial cell proliferation and migration. This pathway may be also interesting for the design of a novel anti-angiogenic therapy against tumor growth and/or eye diseases (i.e. wet age-related macular degeneration).

**P097**  
**Cardiovascular response to NO donors in mice deficient in NO-GC**

\*D. Groneberg, A. Schlembach, A. Friebe  
 Universität Würzburg, Physiologie, Würzburg, Germany

The NO/cGMP cascade is essential for the regulation of many physiological functions in the cardiovascular system and it is also involved in the pathophysiology of several cardiovascular diseases. One of the main vascular factors involved in the regulation of blood pressure is nitric oxide (NO). Target of NO is the NO-sensitive guanylyl cyclase (NO-GC) which is expressed in different cell types in the cardiovascular system (e.g. smooth muscle cells, cardiomyocytes and nerve system). The stimulation of the NO/cGMP cascade is used pharmacologically for the treatment of coronary heart disease; substances commonly used are compounds such as glycerol trinitrate (GTN) or isosorbide dinitrate which are thought to act by increasing NO concentration and activation of NO-GC. We have previously shown that complete knockout of NO-GC (GCKO) in mice led to an increase in systolic blood pressure (+30 mmHg) and loss of NO responsiveness of vascular smooth muscle. Smooth muscle-specific KO mice for NO-GC (SM-GCKO) showed an increase in systolic blood pressure and loss

of NO responsiveness of vascular smooth muscle identical to that seen in general GCKO mice. In order to find out the relative contribution of different cell types expressing NO-GC in the cardiovascular system, we here used catheter measurements to compare the effect of different NO donors (GTN and DEA-NO) on blood pressure and heart rate in vivo. In WT mice, both GTN and the radical NO donor DEA-NO reduced systolic blood pressure and increased heart rate indicating the contribution of the baroreceptor reflex. The deletion of NO-GC in mice (GCKO) abrogated both effects. We are currently investigating mice lacking NO-GC in smooth muscle cells and cardiomyocytes.

**P098**  
**AT1B and CysLT1 receptors act together as mechanosensors determining myogenic tone**

\*U. Storch, S. Blodow, T. Gudermann, M. Mederos y Schnitzler  
 Ludwig-Maximilians-Universität, Walther-Straub-Institut für Pharmakologie und Toxikologie, München, Germany

G<sub>q/11</sub>-protein coupled receptors like angiotensin II AT<sub>1B</sub> receptors are considered as mechanosensors in vascular smooth muscle cells (VSMCs) mediating myogenic vasoconstriction. Unexpectedly, we found a hyper-reactivity of AT<sub>1A</sub> and AT<sub>1B</sub> receptor double gene-deficient (AT<sub>1AB</sub><sup>-/-</sup>) murine mesenteric arteries in the low pressure range up to 70 mmHg and a decreased myogenic tone at higher pressures up to 120 mmHg analyzing myogenic tone ex vivo. A gene expression array and a qPCR approach revealed high mRNA expression levels of cysteinyl leukotriene 1 receptor (CysLT1R) in AT<sub>1AB</sub><sup>-/-</sup> compared to wild-type mesenteric arteries. Pharmacological blockade of CysLT1Rs with pranlukast significantly reduced myogenic tone not only in AT<sub>1AB</sub><sup>-/-</sup> but also in wild-type arteries suggesting that these receptors are generally involved in myogenic vasoconstriction. Furthermore, in wild-type arteries additional blockade of AT<sub>1</sub> receptors with candesartan resulted in an additive reduction of myogenic tone. To analyze whether CysLT1Rs are intrinsically mechanosensitive calcium imaging experiments were performed with Fura-2 loaded HEK293 cells over-expressing CysLT1Rs and with isolated mesenteric VSMCs. Hypoosmotically induced membrane stretch caused calcium transients that were significantly reduced by pranlukast. Moreover, the G<sub>q/11</sub> protein inhibitor YM254890 was used to analyze the involvement of G<sub>q/11</sub> proteins in myogenic vasoconstriction and led to a severe reduction of myogenic tone comparable to the reduction induced by pranlukast plus candesartan demonstrating that myogenic tone is mainly mediated by G<sub>q/11</sub> proteins following AT<sub>1</sub> and CysLT<sub>1</sub> receptor activation.

**P099**  
**Jarid1b maintains endothelium-dependent relaxation and is essential for angiogenesis**

\*C. Fork<sup>1</sup>, L. GU<sup>1</sup>, S. Uchida<sup>2</sup>, Y. Ponomareva<sup>2</sup>, R. P. Brandes<sup>1</sup>  
<sup>1</sup>Kardiovaskuläre Physiologie, Frankfurt am Main, Germany  
<sup>2</sup>Cardiovascular Regeneration, Frankfurt am Main, Germany

Epigenetic regulation involves histone methylation and the methylation state of these DNA binding proteins is dependent on histone methyl-transferases but also by demethylases. Histone H3 is one of the most frequently modified histones. Methylation at H3-lysine-4 (H3K4me3) is located in promoter region, increases gene expression whereas removal of this histone mark silences transcription. We hypothesized that a low H3K4 methylation state is involved in the maintenance of a normal quiescent endothelial phenotype. To identify factors controlling H3K4 methylation in human umbilical vein endothelial cells (HUVECs), H3K4 demethylases were screened. As a highly expressed H3K4 demethylase, Jarid1b was identified by PCR and Western blot analysis. To uncover potential functions of Jarid1b, RNAi experiments were performed. Knockdown of Jarid1b by shRNA in HUVECs attenuated angiogenic sprouting, tube formation and cell migration in the scratch wound assay. Importantly, also 2-4(4-methylphenyl)-1,2-benzisothiazol-3-(2H)-one, a pharmacological Jarid1b inhibitor, diminished the angiogenic capacity of endothelial cells. To clarify the importance of Jarid1b function in the vascular system, Jarid1b knockout mice were studied. As global knockout of the gene is embryonic lethal, tamoxifen-inducible conditional knockout mice were generated. After knockout of Jarid1b, endothelial sprout outgrowth from aortic segments was attenuated. Moreover, Jarid1b diminished the acetylcholine-induced endothelium-dependent relaxation whereas the SNP-induced endothelium-independent relaxation was not affected. As basal NO release was not altered by Jarid1b knockout, alterations in the muscarinic receptor pathway were analyzed. Exon-array technique indeed revealed that Jarid1b maintains cholinergic receptor mRNA level. Conclusion: Jarid1b maintains endothelial angiogenic capacity in part by controlling endothelial cell receptor expression.

**P100**  
**Platelet and monocyte adhesion to endothelial cell-tethered ultra-large von Willebrand factor multimers is shear stress, P-selectin and nitric oxide-dependent**

\*J. Koffler<sup>1</sup>, J. Elrod<sup>1</sup>, S. Grässle<sup>2</sup>, V. Huck<sup>2</sup>, S. W. Schneider<sup>2</sup>, A. H. Wagner<sup>1</sup>, M. Hecker<sup>1</sup>

<sup>1</sup>Institute for Physiology and Pathophysiology, University of Heidelberg, Division of Cardiovascular Physiology, Heidelberg, Germany

<sup>2</sup>Medical Faculty Mannheim, University of Heidelberg, Department of Experimental Dermatology, Mannheim, Germany

**Question:** Von Willebrand Factor (vWF) plays a crucial role in primary hemostasis. Platelet-vWF interaction may facilitate leukocyte diapedesis in inflammation. The co-stimulatory CD40 ligand (CD40L)-CD40 receptor dyad plays an important role in rendering atherosclerotic plaques prone to rupture resulting in thrombus formation. Platelets may also contribute to early plaque formation by an as yet ill-defined mechanism. We investigated whether CD40L-induced ultra-large vWF (ULVWF) multimers deposition on the luminal aspect of an endothelial cell (EC) monolayer not only elicits ULVWF multimer-platelet string formation but also enables

platelet-monocyte interaction at arterial flow.

**Methods:** Human umbilical vein ECs were grown in a parallel plate flow chamber until confluent, perfused at 2.5 or 10 dyn/cm<sup>2</sup> shear stress and exposed to histamine or soluble CD40L (sCD40L). Freshly isolated platelets and monocytes from whole blood were labeled with fluorescent dyes and superfused over the EC monolayer. Platelet and monocyte adhesion to ULVWF multimers was monitored by live cell imaging. In addition, ECs genotyped for the T-786C single nucleotide polymorphism (SNP) of the endothelial nitric oxide (NO) synthase gene (NOS-3) were cultured under static conditions or exposed to 3 dyn/cm<sup>2</sup> of shear stress followed by quantification of vWF release and deposition using a modified ELISA.

**Results:** Platelet CD40L and sCD40L elicited both a prominent deposition of ULVWF multimers on the luminal EC surface to which platelets adhered forming sting like structures. Interestingly, platelet adherence was flow-dependent with 4-times more platelets adhering to ULVWF multimers at 10 dyn/cm<sup>2</sup> compared to 2.5 dyn/cm<sup>2</sup>. Furthermore, monocyte recruitment under flow was dependent on the presence of platelets adhering to the ULVWF multimers and abolished by neutralizing P-selectin. Moreover, ECs derived from homozygous carriers of the T-786C SNP of the NOS-3 gene revealed a significant increase in vWF release and deposition on the EC surface as compared to the other two genotypes.

**Conclusion:** Thus (platelet) CD40L interacting with human ECs evokes deposition of ULVWF multimers to which platelets and monocytes adhere despite fast flow. A genetically determined NO deficit augments this ULVWF multimer deposition hence potentially contributing to an enhanced EC-monocyte interaction in the early phase of atherosclerosis.

**P101**  
**TGFβ/SMAD-signaling in hypoxic/reoxygenated microvascular endothelial cells**

\*I. Sniegon, J. Heger, R. Schulz, G. Euler  
Justus-Liebig-Universität, Physiologisches Institut, Gießen, Germany

Under different pathophysiological conditions, as after myocardial infarction, the growth factor TGFβ is increased in hearts and contributes to cardiac remodeling. Since there are various cell types in the heart that can serve as a source of TGFβ, we now analyzed if cardiac endothelial cells can release bioactive TGFβ under hypoxic/reoxygenated conditions and which signaling pathways are induced by TGFβ. Microvascular endothelial cells were isolated from rat hearts and exposed to hypoxia (Hx) for 1 hour and reoxygenated (Rx) up to 24 hours. To verify that hypoxic conditions were efficiently generated in the hypoxic chamber, expression of HIF-1α was tested. Indeed, after 1 h of hypoxia HIF-1α increased by 92 ± 32 % vs. normoxic controls (n=7, p<0.05). These hypoxic conditions induced an increase in TGFβ1-mRNA expression after 2 h of reoxygenation (Rx). Enhancement of the TGFβ1-precursor protein expression was increased significantly after 15

min. and 24 h Rx (n=21, p<0.05). In order to analyse, if the increase of TGFβ precursor protein results in enhancement of bioactive TGFβ1, we analysed activation of SMAD transcription factors, as classical signaling molecules of TGFβ. An increase in phosphorylation of SMAD2 to 130 ± 15% (n=13, p<0.05) was found after 2h Rx. This effect was abolished by incubation of endothelial cells with ALK5 receptor blocker SB431542 (1µM). In addition to SMAD2 phosphorylation enhanced phosphorylation of SMAD1/5 was also detected. This could be blocked by the ALK2/3-receptor blocker LDN193189 (1 µM). To analyse if the TGFβ release after hypoxia/reoxygenation may contribute to endothelial/mesenchymal transition we looked at αSMA and FSP1 expression. Indeed, protein expression of αSMA and FSP1 increased after Hx/Rx. However, this mRNA induction could neither be blocked by the ALK5-receptor SB431542 nor by TGFβ1-neutralizing antibodies. In conclusion, under hypoxic conditions endothelial cells release TGFβ1. This can activate SMAD2 by phosphorylation via the ALK5 receptor and SMAD1/5 via the ALK2/3 receptor. However, the enhanced FSP-1 expression after Hx/Rx, which is indicative for endothelial/mesenchymal transition, was independent of the TGFβ1-release.

**P102**  
**Deficiency of non-endothelial eNOS causes hypertension in mice**

\*T. Suvorava<sup>1</sup>, J. Stegbauer<sup>2</sup>, M. Thieme<sup>2</sup>, S. Pick<sup>1</sup>, C. Rump<sup>2</sup>, T. Hohlfeld<sup>1</sup>, G. Kojda<sup>1</sup>

<sup>1</sup>University Hospital Düsseldorf, Pharmacology, Düsseldorf, Germany

<sup>2</sup>University Hospital Düsseldorf, Nephrology, Düsseldorf, Germany

**Question:** We sought to investigate whether endothelial-specific targeting of endothelial NO-synthase (eNOS) in eNOS-deficient mice (eNOS-KO) normalizes vascular reactivity and blood pressure (BP).

**Methods and Results:** A double transgenic strain expressing eNOS exclusively in the vascular endothelium has been generated (eNOS-Tg/KO). Expression of eNOS was evaluated in aorta, myocardium, kidney, brain stem and skeletal muscle by western blot and real-time PCR. Organ bath studies revealed a complete normalization of aortic reactivity to acetylcholine, phenylephrine and the NO-donors S-nitroso-N-acetyl-D,L-penicillamine and diethylamine/nitric oxide in eNOS-Tg/KO. Function of eNOS in resistance arteries was demonstrated by acute i.v. infusion of acetylcholine and the NOS-inhibitor L-arginine methyl ester (L-NAME). Acetylcholine decreased mean arterial pressure in all strains but eNOS-KO responded significantly less sensitive than eNOS-Tg/KO and C57BL/6. Likewise, acute i.v. L-NAME application elevated MAP in C57BL/6 and eNOS-Tg/KO, but not in eNOS-KO. Voluntary exercise training similarly increased aortic eNOS protein expression and phosphorylation at Ser1177 in C57BL/6 and eNOS-Tg/KO suggesting a normal response of re-expressed eNOS to shear. In contrast to these findings, mean, systolic and diastolic BPs in eNOS-Tg/KO remained significantly elevated and similar

to values of eNOS-KO. Chronic treatment with L-NAME increased systolic BP to the level of eNOS-KO only in C57BL/6, but had no effect on hypertension in eNOS-KO and eNOS-Tg/KO.

**Conclusions:** The blood pressure lowering eNOS-mediated local vasodilator activity in resistance vessels alone cannot compensate for the lack of the non-endothelial eNOS-dependent component in the regulation of BP. These data establish the necessity of functional non-endothelial eNOS expression for physiologic BP regulation.

**P103**  
**Feeling for filaments - a dynamic cortical actin web controls endothelial function**

\*C. Kronlage, J. Fels

Institute of Physiology II, University of Muenster, Muenster, Germany

The release of the vasodilator nitric oxide (NO) is a hallmark of endothelial function. The activity of the endothelial NO-synthase is known to depend on the mechanical properties of the topmost layer underneath the plasma membrane (known as the cell cortex). Recent work indicates that cortical actin dynamics mediates this effect: When the cell cortex softens, submembranous f-actin depolymerizes and increases eNOS activity. A direct visualization of submembranous actin dynamics, however, is still missing. Therefore, we applied combined atomic force microscopy (AFM) and confocal imaging to directly visualize the dynamics of the cortical actin web in living endothelial cells. AFM-based imaging allows high resolution topography mapping of the cell surface as well as the underlying structures. Simultaneous confocal microscopy of f-actin (by lifeact-EGFP) was used for 3-dimensional imaging of the actin cytoskeleton. Topography maps reveal a coarse and a fine meshwork of submembranous filaments. The coarse mesh - that matches the lifeact-fluorescence - appears to be rather stable and can be tracked over extended periods of hours. However, the fine meshwork is highly dynamic showing rapid alteration. Low concentrations (50nM) of the f-actin-disrupting drug cytochalasin D, known to induce cortical softening and to increase NO-release, thin out the fine mesh in the AFM-images. Fine mesh F-actin thus represents the functionally relevant structure of the endothelial cortex in terms of mechanics and endothelial function.

**P104**  
**Endothelial surface layer function is regulated by CFTR**

\*W. Peters, H. Oberleithner, H. Schillers

University of Münster, Institute of Physiology II, Münster, Germany

The endothelial surface layer (ESL), formed by the glycocalyx and adsorbed plasma proteins, is a crucial part of the endothelium and an important regulatory interface between blood and tissue. The thickness and stiffness of this layer corresponds to its function (soft and thick ESL = healthy vessels) but the regulation of these two param-

eters is unclear. Recent results indicate that activators of CFTR modulate ESL properties. CFTR, a chloride channel and regulator of membrane transport proteins is not only expressed in epithelial cells but is also found in vascular endothelium. In this study, we investigated the role of CFTR in the regulation of ESL-height and ESL-stiffness by means of an atomic force microscope. Force-distance measurements were used to determine ESL-thickness and stiffness of cultured aortic GM7373 cells under physiological conditions. The presence of CFTR in these cells was shown by immunostaining. The activity of CFTR was modulated with polyphenols (CFTR-activators), NPPB and CFTR(inh)-172 (CFTR-inhibitors). We show that activation of CFTR is followed by ESL-swelling i.e. an increase in ESL-thickness (+66%) and a decrease in ESL-stiffness (-63%). This effect is prevented in presence CFTR inhibitors. As the ESL is a highly hydrated polyanionic biogel, it is likely that the ESL-swelling is induced by a local change in ion concentration induced by CFTR activation. It is concluded that (a) ESL properties are regulated by endothelial transport processes and (b) CFTR plays a role in endothelial physiology.

**P105**

**Acute effects of high sodium concentrations on the endothelial glycocalyx in vitro and in vivo**

\*M. Wisdorf, K. Kusche-Vihrog, V. Drüppel, W. Peters

Institute of Physiology II, University of Muenster, Muenster, Germany

In vitro a small increase in extracellular sodium concentration chronically stiffens endothelial cells and was shown to damage the endothelial glycocalyx (eGC), a negatively charged biopolymer which covers the surface of the endothelial cells. Here we tested the hypothesis if high sodium concentrations have also acute effects on endothelial cells in vitro and in vivo. Therefore, human endothelial cells (EA.hy926) were exposed to high sodium concentration (150 mM) or low sodium concentration (130 mM) for (i) 30 minutes and for (ii) 24 hours. To test if the eGC is shedded due to different sodium concentrations a Syndecan-1 ELISA was performed. In addition the stiffness and height of the eGC was determined by nanoindentation measurements with the Atomic Force Microscope (AFM). For in vivo studies mice were given either 200 µl of tap water or double isotonic sodium solution (274 mM) and after 30 minutes of digestion time, in situ endothelial eGC stiffness and height were measured in ex vivo aorta preparations. Chronically, Syndecan-1 concentrations were increased after treatment with high sodium concentrations in comparison to low sodium concentrations. However, an acute application of high sodium concentrations revealed no effect on the eGC. Also stiffness and height of the eGC were unaffected in the acute experiments. More importantly, these results could be confirmed in vivo. It can be concluded that high sodium concentrations only affect the eGC chronically whereas an acute presence, e.g. after a meal, has no direct effects on the eGC.

**P106**

**Genetic ablation of regulator of G-protein signaling 5 inhibits collateral growth during arteriogenesis**

\*C. Arnold<sup>1</sup>, A. Feldner<sup>2</sup>, L. Pfisterer<sup>1</sup>, M. Hödebeck<sup>1</sup>, K. Troidl<sup>3</sup>, G. Genové<sup>4</sup>, T. Wieland<sup>5</sup>, M. Hecker<sup>1</sup>, T. Korff<sup>1</sup>

<sup>1</sup>Heidelberg University, Institute of Physiology and Pathophysiology, Heidelberg, Germany

<sup>2</sup>German Cancer Research Center, Vascular Signaling and Cancer, Heidelberg, Germany

<sup>3</sup>Max-Planck-Institute for Heart and Lung Research, Department of Pharmacology, Bad Nauheim, Germany

<sup>4</sup>Karolinska Institutet, Medical Biochemistry and Biophysics, Stockholm, Sweden

<sup>5</sup>Heidelberg University, Experimental and Clinical Pharmacology and Toxicology, Heidelberg, Germany

Consequences of peripheral artery disease include progressive occlusion of large conductance arteries such as the femoral artery. Perfusion of the tissue distal to the occlusion site can be restored by enlargement of preexisting collateral arterioles. This beneficial arterial remodeling process is referred to as arteriogenesis. However, mechanisms underlying arteriogenic remodeling remain elusive. Arteriosclerosis-mediated obstruction of arteries are mimicked in mice by occluding the femoral artery. Immunofluorescence analyses of cross sections of growing collateral arterioles revealed that the abundance of the regulator of G-protein signaling 5 (RGS5) is increased in vascular smooth muscle cells (SMCs). RGS proteins are endogenous G-protein inhibitors which terminate signaling cascades which control SMC contractile responses to regulate vascular tone. In vitro analyses of human arterial SMCs showed elevated RGS5 protein levels after exposure to biomechanical stretch or nitric oxide - determinants promoting the onset of arteriogenesis. Moreover, RGS5 blocked  $G_{\alpha_{q/11}}$ -mediated intracellular calcium mobilization in SMCs but facilitated  $G_{\alpha_{12/13}}$ -mediated RhoA activation. The latter has already been proven to be essential for arteriogenesis. In line with this, collateral growth was severely impaired in rgs5-deficient mice. This was accompanied by a blockade of SMC proliferation, diminished RhoA activation and the inability of these cells to acquire a synthetic phenotype during arteriogenesis. Collectively, these findings suggest that an increase in RGS5 abundance in SMCs shifts G-protein signaling from  $G_{\alpha_{q/11}}$ -mediated calcium-dependent contraction towards  $G_{\alpha_{12/13}}$ -mediated RhoA activity. This mechanism may play a critical role in activating SMCs and establishes RGS5 as a novel determinant of arteriogenesis.

**P107**

**5' adenosine monophosphate-activated protein kinase (ampk) induces vasodilation by dually acting on smooth muscle membrane potential and calcium pumps**

\*H. Schneider<sup>1,2</sup>, K. M. Schubert<sup>1,2</sup>, S. Blodow<sup>1,2</sup>, S. Erdogmus<sup>3</sup>, M. Mederos y Schnitzler<sup>3</sup>, T. Gudermann<sup>3</sup>, U. Pohl<sup>1,2</sup>

<sup>1</sup>Ludwig Maximilians University, Walter Brendel Centre of Experimental Medicine, Munich, Germany

<sup>2</sup>Munich Cluster for Systems Neurology (SyNergy), Munich, Germany

<sup>3</sup>Ludwig Maximilians University, Walther Straub Institute of Pharmacology and Toxicology, Munich, Germany

**Question:** The metabolic syndrome is characterized by impaired glucose tolerance and disturbances in blood lipids. These changes can be partly corrected by AMPK activation in skeletal muscle. However, the metabolic syndrome also has a vascular component reflected by arterial hypertension. It is still unclear whether AMPK also impacts microvascular arterial tone, which is a major control element for perfusion, glucose uptake in skeletal muscle and blood pressure.

**Methods:** We used isobaric preparations of hamster resistance arteries supplying skeletal muscle. Diameter and intracellular calcium upon AMPK activation were recorded simultaneously. Vascular smooth muscle cells (VSMC) of the same type of vessel were isolated and subjected to patch clamp analysis. Furthermore, changes in VSMC membrane potential upon AMPK activation were registered in intact arteries via sharp microelectrodes.

**Results:** Two structurally unrelated AMPK activators (A-769662, PT-1) dose-dependently dilated NE-precontracted microvessels, accompanied by a parallel decrease in intracellular free calcium. AMPK activated  $BK_{Ca}$  potassium channels in isolated VSMC. Accordingly, we could show a hyperpolarization (30 mV) in intact precontracted vessels by AMPK stimulators. Surprisingly, inhibition of  $BK_{Ca}$  had only minor effects on AMPK-induced dilation and calcium decrease in intact small vessels. On the contrary, inhibition of SERCA by thapsigargin significantly reduced both effects. Combined  $BK_{Ca}$  and SERCA inhibition abolished all AMPK effects.

**Conclusion:** AMPK dilates microvessels by activation of  $BK_{Ca}$  and SERCA. The latter seems to be the more powerful component. AMPK-linked vasodilation could therefore account for a decrease in systemic blood pressure and explain increased glucose uptake by skeletal muscle via improved perfusion.

Transporters I

**P108**

**The Na/Cl cotransporter NCC is stimulated by high phosphate diet and FGF23**

\*A. Daryadel, I. Rubio Aliaga, J. Loffing, C. Wagner

University of Zurich, Institute of Physiology, Zurich, Switzerland

The thiazide-sensitive  $Na^+-Cl^-$  cotransporter (NCC, SLC12A3), which is expressed on the apical membrane of epithelial cells lining the distal convoluted tubule, plays a key role in renal salt reabsorption and determination of systemic blood pressure. Herein we report that diets with high and low phosphate content regulate NCC phosphorylation and alter the abundance of total NCC protein in a time-dependent manner (12 hours till 5days) in mouse kidney. High phosphate diet increased expression of total NCC and stimulated phosphorylation of NCC as early as 12 hours after induction of diets. High phosphate diet caused also an increase in circulating Parathyroid hormone, FGF23, and a transient increase in  $1,25\text{ OH}_2$  vitamin D3. Additionally, mice with elevated FGF23 levels, phosphaturia and hypophosphatemia due to a mutation in PheX showed also higher expression and phosphorylation of NCC. The expression of other  $Na^+$  transporters like as NHE3, NKCC2 and ENaC remained unchanged by dietary phosphate intake or in PheX mice, suggesting that the regulation is specific for NCC. Thus, high phosphate intake stimulates NCC expression likely via FGF23 and may present a link how intake of phosphate increases the risk for hypertension and cardiovascular disease.

**P109**

**The role of RhoGTPase Cdc42 in regulation of arginine transport mediated by human cationic amino acid transporters (hCAT)**

\*J. Bender-Sigel, T. Stenger, A. Rotmann, E. I. Closs

University Medical Center of the Johannes Gutenberg, Pharmacology, Mainz, Germany

**Introduction:** Human cationic amino acid transporters (hCAT) are a family of multimembrane spanning proteins that mediate the transport of cationic amino acids through the plasma membrane. Our earlier results have demonstrated that activation of protein kinase C by PMA leads to an internalization of these transporters. In the present study, we investigated if the RhoGTPase RhoA, Rac1, or Cdc42 are involved in internalization of hCAT proteins.

**Methods:** [3H]-arginine transport studies in *Xenopus laevis* oocytes expressing different hCAT isoforms. Internalization of hCAT-2A was quantified by biotinylation of cell surface proteins and subsequent Western blot analyses of the biotinylated fraction.

**Results:** Co-expression of the constitutive active form of Cdc42 (V12) with individual hCAT isoforms in *Xenopus laevis* oocytes lead to a pronounced reduction in transport

activity compared to oocytes expressing the respective hCAT isoform alone. In contrast to Cdc42, RhoA had no effect on hCAT-1 or -2A activity. Rac1 reduced transport mediated by either transporter by 30-40%. The isoforms hCAT-2A, -2B and -3 were more sensitive to Cdc42 inhibition than hCAT-1. Biotinylation of cell surface domains and subsequent separation of the biotinylated protein fraction and Western blot analyses revealed that Cdc42 induced a reduction of hCAT-2A in the plasma membrane, but did not change total cellular hCAT-2A protein content. Preincubation of hCAT-2A-expressing *X. laevis* oocytes with TcdB 10463 or 1470 toxins that inhibit all three RhoGTPases or Rac1 and Cdc42 respectively, prevented the PKC-mediated reduction of transport activity of hCAT-2A.

**Conclusion:** RhoGTPases act downstream of PKC in reduction of arginine transport mediated by hCAT-2A.

#### P110

##### Mutation of a single threonine in the cytoplasmic N-terminus disrupts trafficking of the renal betaine/GABA transporter during hypertonic stress

\*E. Schweikhard<sup>1,2</sup>, S. Kempson<sup>3</sup>, G. Burckhardt<sup>4</sup>, J. Bonner<sup>3</sup>, C. Ziegler<sup>1,2</sup>, B. Burckhardt<sup>4</sup>

<sup>1</sup>MPI of Biophysics, Structural Biology, Frankfurt, Germany

<sup>2</sup>University, Biophysics II, Regensburg, Germany

<sup>3</sup>Indiana University School of Medicine, Department of Cellular & Integrative Physiology, Indianapolis, United States

<sup>4</sup>University Medical Center, Institute of Systemic Physiology and Pathophysiology, Göttingen, Germany

Within the potential range -90 to 0 mV, superfusion of *Xenopus* oocytes with 1 mM GABA or betaine produced inward currents in oocytes expressing the renal betaine/GABA transporter (BGT1). At -60 mV the KM was 0.02 mM for GABA and 0.18 mM for betaine. GABA-sensitive currents were diminished after 30 min preincubation with 100 nM PMA or 31 μM DOG, activators of protein kinase C (PKC). Staurosporine blocked the response to DOG. Four potential phosphorylation sites on BGT1 were mutated to alanine by site-directed mutagenesis. Three mutants (T235A, S428A, S564A) evoked normal GABA-sensitive currents but currents in oocytes expressing T40A were greatly diminished. [3H]GABA uptake was determined in HEK 293 cells expressing EGFP-tagged BGT1 with the same mutations. T235A, S428A and S564A showed normal upregulation of GABA uptake after hypertonic stress over night, and downregulation by PMA was normal compared to native EGFP-BGT1. In contrast, GABA uptake by T40A showed no response to hypertonicity or PMA. Confocal microscopy of the EGFP-BGT1 mutants expressed in MDCK cells, grown on glass or filters, revealed that T40A was present in cytoplasm after 24 h hypertonic stress while the other mutants and native EGFP-BGT1 were primarily in the plasma membrane. All four mutants co-migrated with native EGFP-BGT1 on western blots suggesting they are full length proteins. In conclusion, T235, S428, and S564 are not involved in downregulation of BGT1 by PKC activators. However,

T40 near the N terminus may be part of a hot spot important for normal trafficking or insertion of BGT1 at the plasma membrane.

#### P111

##### Characterization of the transporter SLC41A3 in HEK293 transgenic cell line

\*L. Mastrototaro, G. Sponder, J. Aschenbach, M. Kolisek

Institute of Veterinary-Physiology, Free University, Molecular Physiology, Berlin, Germany

Magnesium is the second most abundant cation within the cell and plays an important role in many intracellular biochemical and physiological processes, such as protein synthesis or neuromuscular excitability. Deficiency of this essential metal is implicated in many diseases, ranging from hypertension to bone disorders. The 41<sup>st</sup> family of solute carrier superfamily comprises three members, including the Na<sup>+</sup>/Mg<sup>2+</sup> exchanger SLC41A1. However, not much is known about the function of SLC41A2 and there is literally no information available on SLC41A3 in peer-reviewed literature. Here we used HEK293 cells overexpressing SLC41A3 upon tetracycline induction. Induced cells demonstrated an increased ability to transport Mg<sup>2+</sup> in and out of the cell, based on measurements using the Mg<sup>2+</sup>-sensitive, fluorescent dye mag-fura2 in influx and efflux mode. Furthermore we demonstrated the ability of SLC41A3 to form protein complexes of higher molecular order by using blue native electrophoresis and in vivo chemical cross-linking of the complexes. We also identified the cellular localization of the protein. In conclusion we propose SLC41A3 to be involved in Mg<sup>2+</sup> transport (influx and efflux) and to form protein complexes of higher order. Identities of the binding partners, however, remain to be determined. As predicted in silico, we can also conclude that SLC41A3 is a membrane protein but based on our data we are not able to address its exact cellular topology. Membrane topology also awaits its examination.

#### P112

##### The role of glycine transporter 2 in neurotransmission in inhibitory auditory synapses

\*M. Fuhr, E. Friauf

TU Kaiserslautern, Animal Physiology/Biology, Kaiserslautern, Germany

The glycinergic projection from the medial nucleus of trapezoid body (MNTB) to the lateral superior olive (LSO) in the auditory brainstem is perfectly suited to investigate short term plasticity at inhibitory synapses. As MNTB neurons are known for prolonged high frequency outputs/spiking we are interested in the performance of MNTB-LSO synapses under such conditions. Furthermore we address the contribution of glycine transporter 2 GlyT2, as the key presynaptic replenishing machinery, during neurotransmission. In acute coronal slices of P10-12 wild-type (WT) and GlyT2<sup>-/-</sup> mice, electrical activation of MNTB axons was combined with patch-clamp

recordings of LSO neurons. In addition to continuous stimulation (60 s), the stimulation protocol contained patterns where gaps of silence were induced to mimic natural inputs. Peak amplitudes of evoked inhibitory postsynaptic currents (eIPSC) were determined. eIPSC amplitudes of WT showed frequency-dependent short term depression (STD) upon continuous stimulation (to 45-55% within the first 10 s) and a steady state level around 30%. In GlyT2<sup>-/-</sup> mice, STD was drastically stronger, and steady state level decreased to 0%. Introducing gaps diminished STD to 40-60% in WT, but not in GlyT2<sup>-/-</sup> mice. Furthermore, the absolute eIPSC amplitude in GlyT2<sup>-/-</sup> animals was reduced. Analysis of fidelity showed drastic deficits in neurotransmission in GlyT2<sup>-/-</sup> mice. Our results demonstrate a high reliability of the MNTB-LSO synapse, which is increased when gaps of silence are introduced and decreased when glycine reuptake via GlyT2 is abolished genetically. We conclude that persistent presynaptic replenishment of glycine by GlyT2 is crucial for sustained neurotransmission in MNTB-LSO synapses.

#### P113

##### Generation of mice expressing red fluorescent protein-tagged sodium phosphate cotransporter type IIa

\*J. Ruminska<sup>1</sup>, M. Patti<sup>1</sup>, A. Voller<sup>1</sup>, S. Bourgeois<sup>1</sup>, I. C. Forster<sup>1</sup>, E. Hummler<sup>2</sup>, J. Biber<sup>1</sup>, N. Hernando<sup>1</sup>, C. A. Wagner<sup>1</sup>

<sup>1</sup>University of Zurich, Institute of Physiology, Zurich, Switzerland

<sup>2</sup>University of Lausanne, Département de Pharmacologie et de Toxicologie, Lausanne, Switzerland

Homeostasis of inorganic phosphate (Pi) is essential for several vital functions. Sodium phosphate cotransporter type IIa (NaPi-IIa) is located in the brush border membrane (BBM) of the renal proximal tubule and it is the main player in the control of Pi homeostasis in mice. The amount of NaPi-IIa at the BBM is under the control of several hormones and factors including parathyroid hormone (PTH), fibroblast growth factor 23 (FGF-23) and dietary intake of Pi. With the generation of mice expressing NaPi-IIa tagged with red fluorescent protein (RFP) we aim at developing a novel mouse model to examine the trafficking of NaPi-IIa within the renal proximal tubule cells in real time and space. This model will also help us to better understand events underlying the insertion and retrieval of NaPi-IIa from the brush border membrane. In addition, we may characterize the sensing mechanism(s) to changes of Pi. We have generated RFP-NaPi-IIa constructs containing the RFP at three different locations of the cotransporter, the very N-terminus, within the N-terminal tail and within the big extracellular loop. Control experiments in opossum kidney cells and in *Xenopus laevis* oocytes to analyze the cotransporter polarization, PTH sensitivity and Na<sup>+</sup>-dependent cotransport activity respectively, suggested that the RFP at the very N-terminus and within the N-terminal tail does not disturb greatly proper expression, regulation and function. Kinetic characterization however revealed Pi and Na<sup>+</sup> activation indices within the expected wild type tolerance only for the RFP within the N-terminal tail. Consequently, this insertion site is being

used to produce transcription activation-like endonucleases (TALENs) and the targeting vector for the generation of transgenic mice.

#### P114

##### Role of the electrogenic sodium-bicarbonate cotransporter (NBCe1) and carbonic anhydrase II (CAII) for cytosolic H<sup>+</sup> buffering of mouse cortical astrocytes

\*S. M. Theparambil, J. W. Deitmer

University of Kaiserslautern, Kaiserslautern, Germany

Intra- and extracellular H<sup>+</sup> concentration is strictly maintained by chemical buffering of H<sup>+</sup> and active transport of acid/base equivalents. The CO<sub>2</sub>/HCO<sub>3</sub><sup>-</sup> is the major buffer in biological systems, and its efficacy is dependent on the activity of the enzyme carbonic anhydrase (CA). The electrogenic sodium bicarbonate transporter (NBCe1, SLC4A4) is one of the major HCO<sub>3</sub><sup>-</sup> transporters involved in pH<sub>i</sub> regulation in many tissues. We have used primary cultured mouse cortical astrocytes, which express both NBCe1 and intracellular CAII. We have employed intracellular H<sup>+</sup> imaging using confocal microscopy with H<sup>+</sup>-sensitive fluorescence probe BCECF and compared the activities of NBCe1 and CAII in wild-type mice with astrocytes prepared from mice deficient in NBCe1 or CAII. We found that NBCe1 greatly suppresses the butyric acid-induced intracellular acidification, and hence contributes to the total effective H<sup>+</sup> buffering capacity. We also found that CAII not only slows the butyric acid-induced acidification, but also contributes to the NBCe1-mediated increase in effective H<sup>+</sup> buffering capacity, presumably by accelerating the formation of HCO<sub>3</sub><sup>-</sup>, which is then transported by NBCe1 into the cells. Our results challenge the classical view of cellular H<sup>+</sup> buffering and suggest that effective physiological H<sup>+</sup> buffering is attributed not only to physicochemical processes, but also to transport of HCO<sub>3</sub><sup>-</sup> across the cell membrane.

Supported by the Deutsche Forschungsgemeinschaft (DE 231/24-1,2)

#### P115

##### Mouse organic cation transporter 1 determines properties and regulation of basolateral organic cation transport in renal proximal tubules

\*E. Schlatter<sup>1</sup>, P. Klaassen<sup>1</sup>, V. Massmann<sup>1</sup>, S. K. Holle<sup>1</sup>, D. Guckel<sup>1</sup>, B. Edemir<sup>1</sup>, H. Pavenstädt<sup>2</sup>, G. Ciarimboli<sup>1</sup>

<sup>1</sup>Universität Münster, Medizinische Klinik D, Exp. Nephrologie, Münster, Germany

<sup>2</sup>Universitätsklinikum Münster, Medizinische Klinik D, Münster, Germany

The proximal tubule of mouse kidney expresses mOCT1, mOCT2 and much less mOCT3. Therefore, mOCT-mediated transport across the basolateral membrane of proximal tubules reflects properties of at least mOCT1 and mOCT2. Here we unraveled substrate affinities and modulation of

transport activity by acute regulation by protein kinases on mOCT1 and mOCT2 separately and compared these findings with those from isolated proximal tubules of male and female mOCT2<sup>-/-</sup> mice. These data are also compared to our previous data on isolated tubules from wild type and mOCT1/2 double knockout (mOCT1/2<sup>-/-</sup>) mice. OCT-mediated transport in proximal tubules of mOCT2<sup>-/-</sup> mice was only 20 % lower compared to those isolated from wild type mice. While mOCT1 was regulated by all five pathways examined (PKA, PKC, p56lck, PI3K, CaM), mOCT2 activity was modulated by PKA, p56lck, and CaM only, however, in the same direction. As mOCT mediated transport across the basolateral membrane of mOCT2<sup>-/-</sup> mice expressing only mOCT1 and to a small amount mOCT3 was identical to that observed for tubules isolated from wild type mice and to that observed for HEK293 cells stably expressing mOCT1, mOCT1 represents the relevant paralog for OCT-dependent organic cation transport in the mouse kidney. Gender does not play a major role in expression and activity of renal OCT-mediated transport in the mouse. In conclusion, using proximal tubules of mOCT-deficient mice and mOCT paralogs expressed in HEK293 cells we demonstrate that acute kinase dependent regulation of mouse organic cation transport is dominated by mOCT1, the main paralog expressed in mouse kidney. There is apparently only a small quantitative gender dependence of OCT transport in the mouse. These specific properties of organic cation transport in the mouse which differ significantly from the human and even rat orthologs underlines the importance of studies on human OCTs. When findings from such animal systems should be transferred to the human situation in pharmacological or toxicological studies this fact has to be considered seriously. Supported by Deutsche Forschungsgemeinschaft CI 107/4-1.

**P116**  
**The human organic cation transporter 3 is a sensor for extracellular histamine concentrations by basophils**

\*G. Ciarimboli, R. Al-Monajjed, R. Schröter, H. Pavenstädt, E. Schlatter  
Universitätsklinikum Münster, Exp. Nephrologie, Med. Klinik D, Münster, Germany

The secretion of the important inflammatory mediator histamine by basophils is accompanied by translocation of tetraspanin CD63 in the plasma membrane. Using a split-ubiquitin yeast-two-hybrid-system, pull-down and FRET experiments, we found a direct interaction of CD63 with the human organic cation transporter 3 (hOCT3), a membrane transporter able to translocate histamine. We here demonstrate that hOCT3 is expressed together with CD63 at mRNA and protein level in basophils isolated from human blood. Down- and up-regulation of CD63 expression stimulated and inhibited, respectively, the function of hOCT3 expressed in HEK-cells measured by microfluorimetry using the fluorescent organic cation 4-4-dimethylaminostyryl-N-methylpyridinium as tracer. Biotinylation experiments showed that CD63 overexpression decreased hOCT3 expression in the plasma membrane, suggesting

that CD63 influences membrane trafficking of OCT3. We compared histamine secretion of bone marrow cells (BM) from WT and CD63<sup>-/-</sup> mice under IL-3 incubation, a maneuver known to stimulate histamine secretion by basophils. IL-3 induced a significant higher increase of histamine levels as measured by an ELISA in BM supernatants from CD63<sup>-/-</sup> (11±1 ng/10<sup>6</sup> cells/24 h, n = 3) compared to WT mice (4±0.3 ng/10<sup>6</sup> cells/24 h, n = 3). Blocking hOCT3 with its substrate 1-methyl-4-phenylpyridinium (MPP<sup>+</sup>, 1 mM) significantly increased histamine secretion induced by IL-3 from human basophils (64±0.6 and 72±0.3 ng/ml without and with MPP<sup>+</sup>, respectively). Taken together, these data suggest that the physiological function of hOCT3 in basophils is to mediate re-uptake of histamine, in this way controlling extracellular histamine concentration and probably functioning as a sensor mediating histamine biosynthesis negative feedback. Supported by the Deutsche Forschungsgemeinschaft (DFG CI 107/4-2).

**P117**  
**Absence of Slc26a9 results in altered tracheobronchial anion transport and high mortality in neonate mice**

\*X. Liu<sup>1</sup>, B. Riederer<sup>1</sup>, P. Anagnostopoulou<sup>2</sup>, T. Li<sup>1</sup>, B. Rausch<sup>1</sup>, J. Duerr<sup>2</sup>, M. Soleimani<sup>3</sup>, M. Mall<sup>2</sup>, U. Seidler<sup>1</sup>

<sup>1</sup>Hannover Medical School, Gastroenterology, Hannover, Germany  
<sup>2</sup>University of Heidelberg, Center for Translational Lung Research and Division for Pediatric Pulmonology, Heidelberg, Germany  
<sup>3</sup>University of Cincinnati, Division of Nephrology and Hypertension, Cincinnati, United States

**Question:** The anion transporter Slc26a9 is highly expressed in lung and stomach. We observed an excess perinatal mortality in Slc26a9<sup>-/-</sup> neonate mice, but the underlying cause is unknown.

**Methods:** the dead pups were collected, genotyped, and examined histologically. Slc26a9 and CFTR mRNA expression was measured by qPCR in microdissected lung. Slc26a9<sup>-/-</sup>, CFTR<sup>-/-</sup>, and WT neonatal trachea were studied electrophysiologically in Ussing chambers.

**Results:** Dead pups were Slc26a9<sup>-/-</sup> in >95%. Volume density measurements revealed a strong excess of tracheal and bronchial mucus in the Slc26a9<sup>-/-</sup> pups. Slc26a9 as well as CFTR mRNA expression was significantly higher in the distal than proximal airways, and significantly higher in neonatal than adult mice. The amiloride-insensitive, bumetanide-sensitive short circuit current (Isc) was higher in neonatal Slc26a9<sup>-/-</sup> than WT trachea, but lower in neonatal CFTR<sup>-/-</sup> than WT trachea. Surprisingly, forskolin (FSK) + IBMX elicited a significantly higher Isc response (ΔIsc) in neonatal Slc26a9<sup>-/-</sup> than WT trachea. This difference was abolished by preincubation with the CFTR inhibitor CFTRinh172.

**Conclusions:** Neonatal Slc26a9-deficient trachea displayed a higher electrogenic anion secretory rate than WT, and this difference was abolished by CFTR inhibition. The early death of Slc26a9<sup>-/-</sup> pups may be related to problems with airway liquid absorption rather than lack of secretion.

**P118**  
**Role of Na<sup>+</sup>HCO<sub>3</sub><sup>-</sup> cotransporter NBCe1 (Slc4a4) in colonic pH<sub>i</sub> regulation and anion transport**

\*X. Liu<sup>1</sup>, Q. Yu<sup>1</sup>, B. Riederer<sup>1</sup>, D.-A. Tian<sup>2</sup>, B. Tuo<sup>3</sup>, C. Aalkjaer<sup>4</sup>, G. Shull<sup>5</sup>, U. Seidler<sup>1</sup>

<sup>1</sup>Hannover Medical School, Hannover, Germany  
<sup>2</sup>Tongji Medical College, Huazhong University of Science & Technology, Wuhan, China  
<sup>3</sup>ZunYi Medical College, Gastroenterology, ZunYi, China  
<sup>4</sup>University of Aarhus, Aarhus, Denmark  
<sup>5</sup>University of Cincinnati, Cincinnati, United States

**Question:** The electrogenic Na<sup>+</sup>-HCO<sub>3</sub><sup>-</sup> cotransporter NBCe1 (Slc4a4) is strongly expressed in intestinal epithelium, but the physiological role is need to be elucidated. **Methods:** We used miniaturized Ussing chambers and fluorescent pH-indicator BCECF-loaded colonic crypts to study the importance of NBCe1 in pH<sub>i</sub> control, HCO<sub>3</sub><sup>-</sup> as well as anion (Cl<sup>-</sup> and HCO<sub>3</sub><sup>-</sup>) secretory rates Slc4a4 KO and WT mice.

**Results:** Steady state pH<sub>i</sub> and pH<sub>i</sub>-recovery was significantly lower in proximal and distal colonic surface/cryptal mouth cells but not in and colonic crypt base cells, which also displayed high expression levels of the electroneutral NBCn1 (Slc4a7) (and was significantly lower in slc4a7-deficient colonic crypt cells). Forskolin-stimulated HCO<sub>3</sub><sup>-</sup> secretory rates were similar between WT and KO mucosa in all intestinal segments. The Cl<sup>-</sup>-dependent luminal alkalization rate, which is a function of the anion exchanger slc26a3 (DRA) expressed in the colonic surface cells, were strongly decreased after carbonic anhydrase inhibition in the NBCe1-deficient but not the WT colonic mucosa. **Conclusions:** In the intestine, the electrogenic NBCe1 is a mechanism to counteract surface enterocyte acid loads that occur with absorptive processes, but is not important for agonist-induced electrogenic HCO<sub>3</sub><sup>-</sup> secretion, possibly because the concomitant K<sup>+</sup> channel activation reduces the driving for electrogenic Na<sup>+</sup>-HCO<sub>3</sub><sup>-</sup> cotransport.

**P119**  
**pH-dependent substrate uptake via organic anion transporters 1, 2, and 3 (OAT1, 2, 3)**

\*B. C. Burckhardt, Y. Hagos, G. Burckhardt  
Institut für Vegetative Physiologie und Pathophysiologie, Göttingen, Germany

**Question:** Renal proximal tubular organic anion secretion involves the organic anion transporters 1, 2, and 3 and plays an important role in metabolite, xenobiotic, and drug excretion. Here, we tested the pH dependence of OAT1, 2, and 3, and the possible involvement of histidines. **Methods:** HEK293 cells stably transfected with the human OAT1, 2, or 3 were used to demonstrate uptake of PAH, cGMP, and ES while varying extracellular pH (pH<sub>o</sub>). **Results:** For OAT1, 2, and 3, substrate-dependent uptake was higher at acidic than at alkaline pH, was not dependent on the degree of ionization of the substrate and on bicarbonate. In the presence of the protonophore, carbonyl cyanide m-chlo-

rophenylhydrazone (CCCP), substrate-mediated uptake was still larger at pH<sub>o</sub> 6.4 than at pH<sub>o</sub> 7.4, indicating that not the pH-difference across the membrane, but an acidic pH<sub>o</sub> stimulated substrate uptake. At a given pH<sub>o</sub>, neither nigericin (leading to intracellular acidification) nor monensin (introducing intracellular alkalization) affected substrate uptake, indicating that variation of intracellular pH did not influence substrate uptake. Uptake was strongly reduced in the presence of diethylpyrocarbonate (DEPC), a histidine reagent, suggesting that histidines might be involved in pH-dependent transport. **Conclusions:** The increased substrate uptake at acidic pH<sub>o</sub> is not due to substrate proton cotransport or to substrate hydroxyl ion exchange, but rather to protonation/deprotonation of functionally important histidine residues. Mutational analysis of histidines will follow to identify those histidines responsible for the pH-dependence of substrate uptake by OAT1, 2, and 3.

Oxygen metabolism / hypoxia / ROS I

**P120**  
**Dimethylfumarate attenuates cerebral edema formation during ischemic stroke by protecting the blood-brain barrier integrity**

\*R. Kunze, A. Urrutia, H. Liu, S. Reischl, T. Korff, H. H. Marti  
University of Heidelberg, Institute of Physiology and Pathophysiology, Heidelberg, Germany

**Question:** Phase III clinical trial clearly demonstrated that dimethyl fumarate (DMF) reduces relapse rate and the time to disability progression in patients suffer from multiple sclerosis. Similar, in a murine multiple sclerosis model DMF decreased neuronal damage by oxidative stress. As oxidative stress is also a hallmark of ischemic stroke pathogenesis, we aimed to analyze if DMF treatment is also effective for stroke therapy.

**Methods:** After treatment with DMF mice were subjected to transient occlusion of the middle cerebral artery followed by reperfusion period. Infarct and edema volume were quantified with histological methods. In vitro ischemic conditions were generated by exposing cells to oxygen-glucose deprivation (OGD). Gene expression in cells and tissue was analyzed by real-time PCR and Western Blotting. Immunofluorescence techniques were used to determine subcellular localization and expression of proteins.

**Results:** In brain capillary endothelial cells, astrocytes and cerebral tissue in vivo DMF promoted the antioxidant NF-E2-related factor 2 (Nrf2) pathway. DMF-treated endothelial cells showed sustained membrane localization of the



interendothelial junction proteins Zonula occludens (ZO)-1 and vascular endothelial (VE)-cadherin upon OGD. Astrocytes and endothelial cells responded to OGD with an increased expression of pro-inflammatory factors, which was suppressed in the presence of DMF. Systemic pre-treatment of mice with DMF significantly reduced cerebral edema formation and prevented subcellular delocalization of interendothelial junction proteins during the acute phase after stroke.

**Conclusion:** DMF treatment could be a promising clinical strategy against not only ischemic stroke, but also other neurological diseases associated with blood-brain barrier dysfunction such as Alzheimer's disease.

**P121**

**Inhibition of HIF prolyl-4-hydroxylases by FG-4497 reduces brain tissue injury and edema formation during ischemia**

\*S. Reischl<sup>1</sup>, L. Li<sup>1</sup>, G. Walkinshaw<sup>2</sup>, L. A. Flippin<sup>2</sup>, H. H. Marti<sup>1</sup>, R. Kunze<sup>1</sup>

<sup>1</sup>University, Institute of Physiology and Pathophysiology, Heidelberg, Germany

<sup>2</sup>FibroGen Inc., San Francisco, United States

**Question:** Stroke causes acute ischemic cell death by oxygen and nutrient depletion and initiates blood-brain barrier malfunction, which leads to further tissue damage. Several studies showed that pharmacological stabilization of hypoxia inducible transcription factors (HIFs) conferred neuroprotection during ischemic stroke. This study aimed to evaluate if inhibition of prolyl hydroxylase proteins (PHD) which control HIF stability by FG-4497 improves stroke outcome regarding infarct size and edema formation.

**Methods:** Transient and permanent middle cerebral artery occlusion (MCAO) were used as short- and long-term stroke models. FG-4497 was administered as pre- and post-treatment. Infarct and edema size was quantified by histological methods. Ischemic conditions were generated in vitro by exposing cells to oxygen-glucose-deprivation (OGD). Cell viability was monitored by Live/Dead assay (Invitrogen). Gene expression in cells and tissue was quantified by Western Blot and real-time PCR. Immunohistochemical stainings were used to localize tight junction proteins.

**Results:** FG-4497 administration increased Hif-1 $\alpha$  protein abundance in cerebral tissue, brain derived endothelial cells and astrocytes. VEGF and Epo mRNA expression was upregulated accordingly. Survival of HT-22 neuronal cells under OGD was significantly improved under FG-4497 treatment. Infarct size and edema formation was significantly reduced in mice pre-treated with a single dose of FG-4497 in the tMCAO model. Single post-treatment in the permanent occlusion model also reduced infarct size at 7 days after occlusion. Tight-junction gap formation in the penumbra region was significantly reduced in FG-4497 treated animals undergoing stroke.

**Conclusion:** PHD inhibition by FG-4497 could be a promising clinical strategy to prevent cerebral ischemic damage by direct neuroprotection and prevention of vascular leakage.

**P122**

**Influence of the Nrf2 activator oltipraz and the SOD mimetic tempol on beta-cell viability and insulin secretion**

\*J. Schultheis<sup>1</sup>, A. Edalat<sup>1</sup>, P. Krippel-Drews<sup>2</sup>, G. Drews<sup>2</sup>, M. Düfer<sup>1</sup>

<sup>1</sup>Institut für Pharmazeutische und Medizinische Chemie, Münster, Germany

<sup>2</sup>Institut für Pharmakologie, Klinische Pharmazie und Toxikologie, Tübingen, Germany

**Question:** Oxidative stress in pancreatic beta-cells contributes to the development of type-2 diabetes mellitus (T2DM). Therefore, reducing oxidative stress at a prediabetic stage should help to conserve beta-cell mass and function. We investigated whether increasing antioxidative defence capacity by the Nrf2 activator oltipraz or the superoxide dismutase mimetic tempol are suited to maintain beta-cell function and viability.

**Methods:** Islets were isolated from C57Bl/6 mice. Cell death was measured by TUNEL assay. Oxidative stress was induced by H<sub>2</sub>O<sub>2</sub> or glucolipotoxic conditions (33 mM glucose/10  $\mu$ M TO-901317). Insulin release was quantified by a radioimmunoassay.

**Results:** Tempol (1 mM, 15 min preincubation) protected against oxidant-induced (100  $\mu$ M H<sub>2</sub>O<sub>2</sub>, 1h, n=6) impairment of glucose-stimulated insulin secretion (GSIS), but not against H<sub>2</sub>O<sub>2</sub>-provoked (25-50  $\mu$ M, 2 h, n=5-7) cell death. Oltipraz (10  $\mu$ M, overnight) prevented H<sub>2</sub>O<sub>2</sub>-evoked reduction of GSIS (n=7). Concerning apoptosis, oltipraz protected beta-cells against a low concentration of H<sub>2</sub>O<sub>2</sub> (25  $\mu$ M, 2 h, n=5), but was ineffective in the presence of 50  $\mu$ M H<sub>2</sub>O<sub>2</sub> (n=9). Culturing beta-cells in glucolipotoxic medium for 7 d significantly increased cell death. In the presence of oltipraz this harmful effect was markedly attenuated (n=3).

**Conclusion:** These data point out that mimicking superoxide dismutase protects GSIS, but not cell mass against oxidative stress. Oltipraz which upregulates the entire antioxidant defense system preserves beta-cell function and viability suggesting that targeting Nrf2 can serve as a promising strategy to counteract beta-cell damage in T2DM.

**P123**

**Remodeling of the actin cytoskeleton in hypoxia: An emerging role for ArhGAP29**

\*J. Peters, M. Vogler, S. Vogel, S. Krull, L. Swain, D. Katschinski, A. Ziesenis

Georg-August-University Göttingen, University Medical Center, Cardiovascular Physiology, Göttingen, Germany

Cells can adapt to hypoxia by various mechanisms. Yet, hypoxia-induced effects on the cytoskeleton-based cell architecture are not well understood. We observed that L929 fibroblasts cultivated in hypoxia (1% O<sub>2</sub>) showed striking morphological differences as compared to cells cultivated under normoxic conditions (20% O<sub>2</sub>) including the appearance of prominent actin filaments. It has been shown in different cell types that hypoxia influences members of the Rho family of GTPases which are master regulators of the actin cytoskeleton. RhoGTPases cycle between an active

GTP-bound state and an inactive GDP-bound state. This cycle is regulated by GEFs (guanine nucleotide-exchange factors), GAPs (GTPase activating proteins) and GDIs (guanine nucleotide-dissociation inhibitors). However, the mechanisms of hypoxia-specific Rho regulation are largely unexplored. Here we show that ArhGAP29 (Rho GTPase activating protein 29) is induced in hypoxia in a HIF-1 $\alpha$  dependent manner. As ArhGAP29 has GAP activity towards RhoA and is involved in regulating non-muscle myosin-light chain phosphorylation levels we currently analyze its role in hypoxia induced cytoskeletal remodeling and contraction.

**P124**

**Quantitative proteomic analysis of the plasma membrane protein composition in hypoxia**

M. Wottawa, \*J. Böttger, M. von Ahlen, D. Katschinski

Georg-August-University Göttingen, University Medical Center Göttingen, Cardiovascular Physiology, Göttingen, Germany

A variety of different proteins are present in the plasma membrane which are involved in regulating cell shape, motility, cell-matrix interactions and cell signaling. The composition of membrane proteins is highly variably and reflects for example adaption mechanisms to environmental changes. Oxygen availability is an important factor in the cell environment. Hypoxia can occur in pathophysiological conditions like solid tumor development or tissue ischemia. To analyze changes in the plasma membrane protein composition after 6 hours hypoxia compared to normoxia we performed a SILAC (Stable-Isotope-Labeling-with-Amino-acids-in-Cell-culture) screen followed by mass spectrometry using the breast cancer cell line MDA-MB 231 and primary rat fibroblasts. The protein expression was measured in a forward (20% O<sub>2</sub> heavy labeled vs. 1% O<sub>2</sub> light labeled amino acids) and a reverse (1% O<sub>2</sub> light labeled vs. 20% O<sub>2</sub> heavy labeled amino acids) experiment and the ratios of heavy to light amino acids were analyzed.

Studying the MDA-MB 231 cells by mass spectrometry we identified 2481 different proteins in the membrane fraction. Out of these just 2.7% were more abundant and 10% were less abundant in the plasma membrane after hypoxia. In primary rat fibroblasts we identified 2645 different proteins. In sharp contrast to the MDA-MB 231 cells, in fibroblasts 5.2% of the identified proteins were more abundantly found in the plasma membrane and just 1.1% showed a decreased expression. Our preliminary data suggest a cell type specific membrane composition in response towards hypoxia. We are currently testing the differences and consequences in organizing the plasma membrane in tumor cells and fibroblasts.

**P125**

**Neuronal HIF prolyl-4-hydroxylase 2 knockout attenuates cerebral tissue injury in the sub-acute phase after ischemic stroke**

\*L. Li, R. Kunze, H. H. Marti

University of Heidelberg, Institute of Physiology and Pathophysiology, Heidelberg, Germany

**Question:** Hypoxia-inducible factors (HIFs) mediate the endogenous adaptive responses to hypoxia. The protein stability of HIF- $\alpha$  subunits is tightly regulated by HIF prolyl-4-hydroxylase domain (PHD) proteins. Neuron-specific deletion of PHD2 has been previously shown to be neuroprotective in the early acute phase upon ischemic stroke. In contrast, its impact on post stroke long-term recovery is still ambiguous.

**Methods:** Neuron-specific PHD2 knockout mice were subjected to permanent occlusion of the distal middle cerebral artery using electrocoagulation. Infarct volume was calculated with Nissl staining 7 days after stroke onset. Immunohistological methods were applied to analyze post stroke neurogenesis, astrogliosis and leukocyte infiltration.

**Results:** Neuron-specific PHD2 ablation significantly attenuated the cerebral cortical infarct volume. The number of the infarct core infiltrating monocytes/microglia was reduced in PHD2 deficient mice in comparison to wild type littermates. Furthermore, PHD2 deficient mice showed significant less reactive astrocytes (astrogliosis) within the peri-infarct region. By contrast, proliferation of neural precursor cells along the subventricular zone after ischemia was not different between wild type and PHD2 knockout mice.

**Conclusion:** Our findings suggest that neuronal PHD2 deletion not only increases resistance of neurons against ischemic conditions in the acute phase upon stroke, but may also improve cellular processes initiated in the sub-acute phase that contribute to the long-term recovery from ischemic stroke.

**P126**

**Cellular localisation of NADPH oxidases in rat renal resistance arteries**

\*N. Basler<sup>1</sup>, T. Schlüter<sup>1</sup>, R. Schlüter<sup>2</sup>, R. Rettig<sup>1</sup>, O. Grisk<sup>1</sup>

<sup>1</sup>University of Greifswald, Institute of Physiology, Karlsburg, Germany

<sup>2</sup>University of Greifswald, Institute of Microbiology, Greifswald, Germany

**Question:** NADPH oxidase (Nox)-generated reactive oxygen species (ROS) carry signals that regulate vascular tone and remodeling. Their role for regulating artery function differs between artery segments and vascular beds of different organs. The localisation of Nox isoforms in renal resistance arteries (RA) is currently unknown. We investigated Nox-isoform localisation in RAs and compared our findings with isolated aortic cell populations.

**Methods:** Cellular Nox localisation in rat renal resistance arteries, isolated aortic fibroblasts, endothelial (EC) and vascular smooth muscle (VSMC) cells was analyzed by transmission electron and confocal laser scanning micros-

copy. Nox activity was determined by lucigenin enhanced chemiluminescence. **Results:** In agreement with data from other vascular beds RA showed Nox1 and 2 localised to VSMC cytoplasm and Nox4 localised to both VSMC cytoplasm and nuclei. Nox1 was also present in RA VSMC nuclei. Studies in isolated aortic cells confirmed the nuclear localisation of Nox1 in VSMCs while ECs and fibroblasts were devoid of nuclear Nox1. Membrane and nuclear fractions from rat renal tissue showed ROS formation attributable to Nox activity while Nox activity was absent in cytosolic fractions.

**Conclusion:** Nox localisation in RAs is similar to other vascular beds. In addition to Nox4 also Nox1 is expressed in VSMC nuclei. Nuclear Nox is active and leads to ROS formation. Nox1 may play a VSMC-specific role in vascular nuclear signaling under physiological and pathological conditions.

**P127**

**Amyloid precursor protein protects hippocampal network function against acute hypoxia in vitro**

\*D. Hefter<sup>1</sup>, S. Weyer<sup>2</sup>, U. Müller<sup>2</sup>, A. Draguhn<sup>1</sup>

<sup>1</sup>Universität Heidelberg, Institut für Physiologie und Pathophysiologie, Heidelberg, Germany

<sup>2</sup>Universität Heidelberg, Institut für Pharmazie und Molekulare Biotechnologie, Heidelberg, Germany

**Question:** There is strong evidence for a role of amyloid precursor protein (APP) in the cellular response to hypoxia. We lack, however, any understanding of the underlying mechanisms. Since the hippocampus is one of the brain areas most susceptible to hypoxia as well as to Alzheimer's disease, we studied the effects of hypoxia in acute slices from wild-type and APP deficient mice.

**Methods:** We compared horizontal brain slices from wild-type, APP-KO, and mice expressing only the extracellular soluble fragment of APP (sAPP $\alpha$ -KI). Local field potential and intracellular recordings, and calcium imaging were performed in CA1. After recording baseline activity, slices were exposed to a five-minute period of hypoxia (nominally oxygen-free extracellular solution). Recordings were continued for 40 min following hypoxia. After the experiment, slices were further incubated for four hours, fixed and analyzed for cell damage.

**Results:** Synaptic transmission as well as spontaneous network oscillations disappeared rapidly during hypoxia. Activity recovered partially or completely following reoxygenation. However, slices from APP-KO mice showed an increased probability of hypoxic spreading depression (HSD) as well as impaired recovery from hypoxia as compared to wild-type slices. These deficits were abolished by bath application of the L-Type calcium channel (LTCC) blocker nifedipine (10 $\mu$ M). Slices from sAPP $\alpha$ -KI mice also showed a higher risk of HSD, but recovered better than APP-KO.

**Conclusions:** We conclude that APP is beneficial for recovery of CA1 function following a hypoxic insult. The mechanisms involve regulation of intracellular calcium levels.

The protective effect is, at least partially, mediated by the sAPP $\alpha$  domain.

**P128**

**Expression of the cellular oxygen sensor PHD2 correlates with radiation sensitivity in different cancer cell lines**

\*M. Nagel<sup>1</sup>, J. Dunst<sup>2</sup>, R. Depping<sup>1</sup>, F. K. Kosyna<sup>1</sup>

<sup>1</sup>University of Lübeck, Institute of Physiology, Lübeck, Germany

<sup>2</sup>University Medical Center Schleswig-Holstein, Clinic for Radiotherapy, Lübeck, Germany

The human prolyl-4-hydroxylase domain (PHD) proteins 1-3 function as major regulators of the oxygen sensor machinery. In normoxia the hypoxia-inducible factor (HIF)- $\alpha$  subunits are hydroxylated by the three PHD isoforms, however PHD2 is the key player in HIF-1 $\alpha$  regulation. This prolyl hydroxylation leads to recognition by von Hippel-Lindau tumor suppressor protein (pVHL), ubiquitination and proteasomal degradation of HIF- $\alpha$ . Recently, the expression of PHDs in human tumors has been investigated in different studies showing that their role in cancer is cell and cancer type-specific. The three PHD isoforms are overexpressed in cancers of the breast, prostate, pancreas and head and neck region. In contrast, immunohistochemical studies in renal cell carcinoma and follicular lymphomas revealed decreased staining of PHDs. The aim of our study was to examine the relation between expression of PHD2 and radioresponsivity in vitro. Therefore, we treated wildtype, PHD2-deficient and PHD2-overexpressing cells with ionizing radiation in doses from 2 to 6 Gray and evaluated clonogenic survival. Our results demonstrate a correlation between PHD2 expression and radiation-induced apoptosis in different human cancer cell lines and extend previous observations on PHD2. These data suggest PHD2 as a promising target for novel anti-cancer therapy.

**P130**

**The NADPH Oxidase Nox4 exists in macromolecular complexes within the cell**

\*K.-K. Prior<sup>1</sup>, I. Wittig<sup>2</sup>, R. P. Brandes<sup>1</sup>

<sup>1</sup>Goethe University Frankfurt, Institute for Cardiovascular Physiology, Frankfurt am Main, Germany

<sup>2</sup>University of Frankfurt, Functional Proteomics, SFB815 Core Unit, Frankfurt am Main, Germany

NADPH Oxidases are important sources of reactive oxygen species. Among them, Nox4 is unique as it is not localized on the plasma membrane, has constitutive activity and predominantly generates H<sub>2</sub>O<sub>2</sub>. We hypothesize that these features and specific signaling properties of Nox4 are a consequence of so far unidentified Nox4-interacting proteins. We used complexome profiling, a novel proteomic approach, combining blue-native electrophoresis (BNE), quantitative mass spectrometry and hierarchical clustering to identify Nox4-containing macromolecular complexes. Samples were obtained from HEK293 cells stably over-

expressing Nox4 or mouse kidneys that show high basal Nox4 expression. BNE was performed from subcellular fractions after different solubilization techniques. Using mild detergents, Nox4 was observed in complexes of sizes more than one megadalton in HEK293 cells overexpressing human Nox4 and Nox4-YFP, respectively, as well as in mouse kidney. Less mild detergents like Triton X-100 or dodecyl- $\beta$ -D-maltoside destroyed these complexes, explaining why Nox4-interacting proteins cannot be discovered by immunoprecipitations from such extracts. Complexome profiling identified over 20 candidate proteins interacting with Nox4, of which the majority resides in the endoplasmic reticulum. Among them were DDRGK domain-containing protein 1 and sphingosine-1-phosphate lyase 1, which may tether Nox4 to this compartment and link to migration, proliferation and cell death. Some of the candidates (thioredoxin-related transmembrane protein or peroxiredoxine-4) are known to be redox-sensitive, raising the possibility that Nox4 forms "redox-signalling hot spots". Our results suggest that endogenous Nox4 forms macromolecular complexes which may locally control the redox milieu and protein function, and might link it to specific physiological functions.

**P131**

**HIF mediated induction of WISP-2 contributes to attenuated breast cancer progression**

\*J. H. Fuady<sup>1</sup>, M. R. Bordolij<sup>1,2</sup>, I. Abreu-Rodriguez<sup>1</sup>, G. Kristiansen<sup>3</sup>, D. P. Stiehl<sup>1,4</sup>, D. Hoogewijs<sup>1</sup>, R. H. Wenger<sup>1</sup>

<sup>1</sup>University of Zurich, Institute of Physiology, Zurich, Switzerland

<sup>2</sup>Harvard Medical School, Developmental Biology, Boston, United States

<sup>3</sup>University Hospital Bonn (UKB), Institute of Pathology, Bonn, Germany

<sup>4</sup>Novartis Institutes for Biomedical Research, Basel, Switzerland

**Question:** One hallmark of tumour cells is the ability to adapt to conditions of low oxygen concentration (hypoxia). The major mechanism crucial to this adaptation process is via hypoxia-inducible factors (HIFs). Transcriptionally active HIF-1 and HIF-2 heterodimers regulate overlapping sets of target genes, however only few HIF-2 specific target genes are known. We investigated Wnt-1 induced signalling protein 2 (WISP-2) and its regulation by HIF-2 $\alpha$ . We aim to comprehensively study the molecular mechanism of HIF-2 $\alpha$ -dependent transcriptional induction of WISP-2 as well as the functional consequences of HIF-2 $\alpha$ -dependent regulation of WISP-2 under hypoxic conditions.

**Methods:** Reporter gene assays were employed to investigate the contribution of conserved regions within the WISP-2 promoter in its HIF-2 $\alpha$ -dependent regulation. Stable WISP-2 knockdown MCF-7 cells were generated using expression vectors encoding different short hairpin RNA (shRNA) sequences targeting WISP-2. Cellular proliferation, colony formation, mobility and invasion assays were performed to study the functional consequences of hypoxic WISP-2 regulation.

**Results:** Our results show that the HIF-2 $\alpha$ -dependent induction of WISP-2 in breast cancer cells is mediated by

two, phylogenetically only partially conserved, functional hypoxia-responsive elements (HRE) located upstream of the transcriptional start site. We confirmed the role of WISP-2 in cell proliferation and tumorigenesis and our data suggest a role of WISP-2 as anti-invasive factor in breast cancer. Both the tumorigenic and anti-invasive properties of WISP-2 are HIF-2 $\alpha$ -dependent.

**Conclusion:** WISP-2 is a HIF-2 $\alpha$ -dependent target gene and HIF-2 $\alpha$  plays a role in maintaining a low invasive tumour type by inducing WISP-2 expression.

**P132**

**Modulation of oxygen-regulated erythropoietin expression**

\*F. Storti<sup>1</sup>, S. Santambrogio<sup>1</sup>, L. Crowther<sup>1</sup>, M. R. Kauffmann<sup>1</sup>, I. Abreu-Rodriguez<sup>1</sup>, T. Otto<sup>2</sup>, J. Fandrey<sup>2</sup>, W. G. Forssmann<sup>3</sup>, R. H. Wenger<sup>1</sup>, D. Hoogewijs<sup>1</sup>

<sup>1</sup>University of Zurich, Institute of Physiology, Zürich, Switzerland

<sup>2</sup>University of Duisburg-Essen, Institute of Physiology, Essen, Germany

<sup>3</sup>Medical School Hannover, Clinic of Immunology and Rheumatology, Hannover, Germany

**Question:** Erythropoietin (Epo), the key hormone regulating red blood cells homeostasis, is mainly produced in the adult kidney in response to hypoxia and anemia. Hypoxia-inducible Epo transcription is controlled by distinct regulatory sequences in liver and kidney. These regions flank the Epo coding sequence on both sides, but while the liver-inducible element in the 3'-region is well established, the kidney-inducible element (KIE) in the 5'-region remains unexplored. We aim to use in vitro approaches to investigate the modulation of Epo production at different levels.

**Methods:** We employ available Epo-expressing cell models to characterize a novel distal hypoxia responsive element (HRE) located upstream of the Epo gene, within the KIE, using reporter gene and chromatin immunoprecipitation assays. Moreover, we are screening a collection of peptides derived from human haemofiltrates to identify potential factors influencing the HIF (hypoxia-inducible factor) pathway and, possibly, Epo expression.

**Results:** We identified and functionally validated a novel distal 5' HRE regulating inducible HIF-2-dependent Epo expression, likely representing the thus far uncharacterized KIE. Additionally, we identified peptide fractions influencing the HIF pathway in both directions and we are currently sub-fractionating positive hits to determine single peptides responsible for the effect.

**Conclusions:** Our study is the first to functionally characterize an HRE within the enigmatic KIE and provides the basis for further studies on tissue-specific Epo expression. The screening of the peptide collection explores Epo regulation by humoral factors, representing another hitherto poorly understood layer of Epo modulation.

Glia cells

**P133**  
**Complex regulation of a kainate receptor trafficking by NDRG**

\*V. Matschke, G. Seebohm, N. Strutz-Seebohm  
Institute for Genetics of Heart Diseases (IfGH), Department of Cardiovascular Medicine, Münster, Germany

The human nervous system is composed of a variety of cells including neuronal and glial cells. Astrocytes, the most abundant glial cells, not only play supportive roles in brain function but also play an active role in modulating neuronal function. Among their tasks is the regulation of neuronal excitation by controlling the extracellular potassium homeostasis and removing excess glutamate through glutamate transporters. The functional role of glutamate receptors, especially of the kainate receptors, in astrocytes has not yet been satisfactorily clarified. The glutamate receptor of the kainate family, GluK2, which is expressed in neurons and astrocytes, is under tight regulation of the PI3-kinase-SGK (SGK1) pathway as shown in neurons. In the present study, we analyse the effect of SGK1 on GluK2 in astrocytes and demonstrate that the proteins N-myc downstream regulated genes, NDRG1 and NDRG2, themselves have no effect on GluK2 current amplitudes in heterologous expressed ion channels. However, when NDRG2 is coexpressed with GluK2 and SGK1, the stimulating effect of SGK1 on GluK2 is inverted. Therefore, NDRG2 seems to be a regulator for GluK2 function. Preliminary results indicate the same regulatory mechanism in rat astrocyte cultures. These findings suggest a novel GluK2 modulating function by NDRG2 in astrocytes.

**P134**  
**Examination of NG2 and S100B co-localization in hippocampal glia in the mouse brain**

\*B. Moshrefi-Ravasdjani<sup>1</sup>, G. Seifert<sup>2</sup>, C. Steinhäuser<sup>2</sup>, C. Rose<sup>1</sup>, P. Dublin<sup>1</sup>  
<sup>1</sup>Heinrich-Heine Universität, Düsseldorf, Germany  
<sup>2</sup>Bonn University, Bonn, Germany

NG2 proteoglycan expressing glia, also known as polydendrocytes, have recently been shown to be a new subtype of glial cells in the vertebrate brain. Originally described as OPCs (oligodendrocyte precursor cells), they have later been found to feature several characteristics not expected from mere progenitor cells. However, as research on this cell type is only emerging, its functions and overall characteristics remain to be described in full detail. Recent work in EYFP knock-in mice (Karram et al. 2008, Genesis 46, 743-757) revealed that NG2 cells differ in expression levels of certain proteins, one of which is the "astrocytic" calcium binding protein S100B. In this transgenic mouse model, NG2+ cells were detected using an EYFP reporter construct controlled by the endogenous NG2 promoter.

In the present work, we studied the cellular expression of NG2 and S100B in the hippocampus of Balb/c mouse brains by applying the respective antibodies in immunohistochemical double-stainings. Stainings were analysed by confocal laser scanning microscopy as well as structured illumination microscopy (SIM). We found co-localizations of both antibodies, indicating the untypical co-expression of both proteins in one cell. The percentage of NG2-positive cells which also expressed S100B increased from 9% at P10 to about 25% at P26-32. Our results thus confirm the suggested heterogeneity of NG2 glia in the mouse brain. Furthermore, our data indicate that the occurrence of this heterogeneity in the hippocampus depends on the postnatal age and may thus be developmentally regulated.

We thank J. Trotter, Mainz, for providing us with NG2/EYFP mice.

**P136**  
**Transfer of exosomes from oligodendrocytes to neurons**

\*D. Fröhlich<sup>1</sup>, C. Frühbeis<sup>1</sup>, W. P. Kuo<sup>1</sup>, W. Möbius<sup>2</sup>, S. Goebbels<sup>2</sup>, K.-A. Nave<sup>2</sup>, A. Schneider<sup>2</sup>, M. Simons<sup>2</sup>, M. Klugmann<sup>3</sup>, J. Trotter<sup>1</sup>, E.-M. Krämer-Albers<sup>1</sup>  
<sup>1</sup>Johannes Gutenberg University, Molecular Cell Biology, Mainz, Germany  
<sup>2</sup>Max Planck Institute of Experimental Medicine, Göttingen, Germany  
<sup>3</sup>University of New South Wales, Sydney, Australia

**Introduction:** Exosomes are small membranous vesicles of endocytic origin, which are released by almost every cell type and have been implicated to play important roles in intercellular communication. We have recently discovered that oligodendrocytes secrete exosomes containing a distinct set of proteins as well as mRNA and microRNA. Intriguingly, oligodendroglial exosome release is stimulated by the neurotransmitter glutamate indicating that neuronal electrical activity controls glial exosome release. In this study we examined the role of exosomes in neuron-glia communication and its implications in glial support.

**Results:** To analyze the transfer of oligodendroglial exosomes to neurons, we exposed cultured cortical neurons to fluorescently labeled oligodendroglial exosomes. Indeed, cultured cortical neurons internalized and accumulated oligodendroglial exosomes in the neuronal cell soma in a time-dependent manner. Addition of endocytosis inhibitors or expression of dominant negative dynamin interfered with neuronal exosome internalization indicating that exosome uptake is mediated by clathrin-dependent endocytosis. Furthermore, neuronal internalization of exosomes resulted in functional retrieval of exosomal cargo in vitro and in vivo upon stereotactic injection of exosomes.

**Conclusion:** Taken together, our results represent a proof of principle of exosome transmission from oligodendrocytes to neurons suggesting a new route of horizontal transfer in the CNS.

**P137**  
**Argonaute proteins in oligodendrocytes**

\*C. Müller, H. Luhmann, R. White  
University Medical Center Mainz, Institute of Physiology, Mainz, Germany

Argonaute proteins (Agos) are key players in microRNA-dependent translational inhibition of mRNAs. Together with microRNAs and additional factors they form the miRNA induced silencing complex (miRISC). Ago-dependent translational inhibition via miRNAs is essential for temporal or local control of protein synthesis. In oligodendrocytes the most abundant myelin protein MBP is transported as mRNA in hnRNP A2-containing RNA granules towards the cell periphery, where localised translation takes place and is regulated by the Src kinase Fyn (Müller et al., 2013). Fyn is activated at the axon-glia contact site by neuronal signals and phosphorylates hnRNP A2. This leads to the release of granular proteins and MBP mRNA, thereby allowing translation initiation (Krämer-Albers and White, 2011). Oligodendrocyte differentiation is regulated by various small RNAs (Budde et al., 2010; Dugas et al., 2010) and MBP translation in particular is dependent on the small non-coding RNA 715 (Bauer et al., 2012). We therefore suggest that Ago proteins also play an important role in translational inhibition of specific myelin mRNAs. But how is a target mRNA translationally reactivated when protein is needed? Which signal leads to the dissociation of the miRISC from the target mRNA? It was recently discovered that the phosphorylation of a conserved tyrosine on Position 529 in human Ago2 abolishes miRNA binding (Rudel et al., 2011). This tyrosine phosphorylation might be a general regulatory step in translational modulation of individual mRNAs. We investigated if Ago proteins are downstream targets of Fyn in oligodendrocytes and if Ago proteins are involved in hnRNP A2-dependent transport of MBP mRNA.

**P138**  
**Translational regulation and function of myelin associated oligodendrocytic basic protein**

\*I. Schäfer, H. Luhmann, R. White  
University Medical Center of the Johannes Gutenberg University Mainz, Institute of Physiology, Mainz, Germany

Oligodendrocytes are the myelinating glial cells of the central nervous system (CNS). CNS myelination requires the synthesis of large amounts of myelin proteins such as myelin basic protein (MBP), proteolipid protein (PLP) and myelin-associated oligodendrocytic basic protein (MOBP). The non-receptor tyrosine kinase Fyn is important in the axon-glia signal transduction leading to MBP synthesis and myelination (Krämer-Albers and White, 2011). Mediated by the cis acting A2RE element and hnRNP A2 binding, MBP mRNA is transported in RNA granules in a translationally silenced state to the axon-glia contact side. Active Fyn leads to a release of this translational repression by phosphorylating hnRNP A2 (White et al., 2008). Four of the seven MOBP mRNAs expressed by oligodendrocytes contain a common region in their 3'UTR which is similar to the

MBP A2RE. Like MBP, those MOBP isoforms are distributed throughout compact myelin (Montague et al., 2006). That leads us to the question if Myelin-associated oligodendrocytic basic proteins containing an A2RE are translationally regulated by Fyn kinase like MBP? MOBP expression follows that of MBP and PLP and is limited to densely myelinated regions. Instead of being one of the intrinsic elements initiating the process of sheath compaction at the cytoplasmic aspect of the myelin membrane it seems to be more likely that MOBP plays a role in maintaining the integrity of the myelin sheath (Yoshikawa et al., 2001; Yool et al., 2002). So we are also interested in getting a better understanding on a functional benefit of the different MOBP splice variants for oligodendrocytes.

**P139**  
**Astrocytic Na<sup>+</sup> influences extracellular GABA/glutamate balance in the neocortex**

\*S. Kirischuk, P. Unichenko  
University Medical Center of the Johannes Gutenberg University Mainz, Institute of Physiology, Mainz, Germany

In the CNS, glutamatergic neurotransmission proceeds with high temporal and spatial resolutions. Synaptically released glutamate diffuses through the synaptic cleft and activates postsynaptic receptors, eliciting a postsynaptic current. Glutamate effects on receptors are terminated by diffusion and by the actions of glutamate transporters (EAATs). Glial EAATs strongly contribute to glutamate removal, and synaptically-activated, glutamate transporter-mediated currents (STCs) can be recorded. In this study, STCs elicited by local electrical stimulation in cortical layer 4 were recorded from layer 2/3 astrocytes. When low [Na<sup>+</sup>]<sub>i</sub> (5 mM) intra-pipette solution was used, STCs demonstrated paired-pulse facilitation (PPF) at short (<250 ms) inter-stimulus intervals (ISIs) and paired-pulse depression (PPD) at longer ISIs. Elevation of intra-pipette [Na<sup>+</sup>]<sub>i</sub> to 20 mM, i.e. close to its physiological value, reduced PPF of STCs at short ISIs, while PPD at longer ISIs was not affected. STC decay kinetics were slowed in the presence of high [Na<sup>+</sup>]<sub>i</sub>. Exogenous GABA increased astrocytic [Na<sup>+</sup>]<sub>i</sub>, reduced the mean STC amplitude, decreased PPF at short ISIs, and slowed STC kinetics. All GABA-induced changes were blocked by NO-711 and SNAP-5114, GABA transporter (GATs) antagonists. GAT blockade decreased PPF at short ISIs under control conditions, provided low [Na<sup>+</sup>]<sub>i</sub> intra-pipette solution was used. Dialysis of single astrocyte with low [Na<sup>+</sup>]<sub>i</sub> solution increased the amplitude and reduced paired-pulse ratio of evoked field potentials recorded in the vicinity of the astrocyte. Thus, endogenous GABA can influence EAAT functioning via GATs and astrocytic [Na<sup>+</sup>]<sub>i</sub> modulates the short-term plasticity of STCs and in turn the efficacy of glutamate removal.

**P140**

**Loss of NG2 exacerbates secondary brain damage following traumatic injury in mice**

\*C. Huang<sup>1</sup>, D. Sakry<sup>2</sup>, A. Sebastiani<sup>1</sup>, K. Engelhard<sup>1</sup>, J. Trotter<sup>2,3</sup>, M. K. E. Schäfer<sup>3,1</sup>

<sup>1</sup>University Medical Center, Johannes Gutenberg-University Mainz, Department of Anesthesiology, Mainz, Germany

<sup>2</sup>Johannes Gutenberg-University Mainz, Department of Biology, Mainz, Germany

<sup>3</sup>Research Center for Translational Neurosciences (FTN) of the Johannes Gutenberg-University Mainz, Mainz, Germany

The chondroitin sulfate proteoglycan NG2 is expressed by oligodendrocyte precursor cells (OPCs), also termed NG2+ cells. These cells have been implicated in the pathophysiology of acute and chronic brain injuries but the function of NG2 protein therein is unclear. This in vivo study examined wild-type and NG2-knockout mice following experimental traumatic brain injury (TBI) at 2 days and 7 days after lesion. The NG2 encoding gene *cpsg 4* was up-regulated at both time points in the injured brain of wild-type mice. Histopathological brain damage and immunoglobulin G extravasation were increased at 7 dal in NG2-knockout mice. Moreover, an increased neurological severity score from 3 to 7 dal was observed compared to WT mice. Examination of different cell subpopulations revealed more GFAP-positive astrocytes and less infiltrating T cells at perilesional sites in NG2-KO mice at 7 dal. No differences were observed for OPCs and microglia compared to WT. Gene expression analyses showed no differences in the pro-inflammatory cytokines IL-1 $\beta$ , IL-6 and TNF $\alpha$ . However, PCR array screening revealed marked up-regulation of the chemokine Cxcl13 that was exclusively observed in NG2-KO mice after TBI. This in vivo study demonstrates exacerbated histopathological and neurological signs in NG2-knockout mice following TBI. Our findings suggest a beneficial function of NG2 during secondary brain damage progression. The obtained results provide evidence that NG2 contributes to the control of astrogliosis, the presence of T cells and CXCL13 expression in the injured brain.

**P141**

**Impact of extracellular ion concentration and osmolarity on the migration of oligodendrocyte progenitor cells**

\*N. Schwering<sup>1</sup>, L. Bösche<sup>1</sup>, I. D. Dietzel<sup>2</sup>, P. Happel<sup>1</sup>

<sup>1</sup>Ruhr Universität Bochum, Rubion, Bochum, Germany

<sup>2</sup>Ruhr Universität Bochum, Molecular Neurobiochemistry, Bochum, Germany

The saltatory migration of Oligodendrocyte Progenitor Cells (OPCs) consists of well coordinated cycles of protrusion and retraction, showing a local cell body swelling towards the direction of movement prior to accelerated migration (Happel et al. 2013). The occurrence of this swelling suggests that various ion fluxes across the cell membrane play a role in OPC migration as already reported for various migrating cells (Schwab 2007). Here we investigated whether different osmolarities of the culture medium affect the

migration of OPCs. We investigated the random migration of OPCs in three different culture media with osmolarities of 230 mOsm, 280 mOsm and 320 mOsm. We found that OPCs showed a decreased migration in the culture medium with the highest osmolarity. Furthermore, it is known that ion channels of the TRP family are involved in the cell migration machinery of various cell types (recently reviewed by Pla & Gkika, 2013). To test whether ion channels of the TRP family are involved in OPC migration, we observed the random migration of OPCs in the presence of the unspecific blocker 2-APB as well as in the presence of ruthenium red, which is, among others, a competitive inhibitor of TRPV1. In presence of the blockers, the migration of OPCs was severely reduced. Although the molecular mechanisms remain to be worked out in detail, our findings support the hypothesis that ion fluxes as well as TRP channels are involved the orchestration of OPC migration.

**P142**

**A novel pathway in glia controls Tyramin homeostasis in the Drosophila CNS**

A. de Visser, A. Dadak, \*B. Altenhein

Johannes Gutenberg-University Mainz, Institute of Genetics, Mainz, Germany

The nervous system of all higher eucaryotes is composed of neurons and glial cells, both of which come in very different morphological shape and physiological properties. Heterogeneity among glial cells is widely accepted, yet functionally only poorly understood. We use *Drosophila* as a model to investigate the genetics behind cell fate decisions and specification events of glial cells during neurogenesis as well as gain insights into the functionality of distinct populations of glial cells. In this project we focussed on a population of glia that are referred to as longitudinal or interface glia which resemble astrocyte-like properties. We analysed a set of genes that are exclusively expressed in these glial cells. Among these genes, CG31235 which we termed *nazgul* (*naz*), encodes an oxidoreductase of so far unknown substrate specificity. Mutations of the *naz* gene or cell specific knock-down in glia leads to behavioural phenotypes such as deficits in motor performance. We have evidence that *Naz* is part of a metabolic pathway that is responsible for the homeostatic control of the neurotransmitter Tyramin. Tyramin is synthesized from Tyrosine and together with Octopamine serve as neuromodulators and transmitters in both vertebrates and invertebrates. In order to be metabolized in glia, Tyramin released from neurons needs to be transported across the plasmamembrane. We hence screened for transmembrane transporters and discovered that the *Drosophila* excitatory amino acid transporter 1 (EAAT1) most likely fulfils this task. Lack of either *Naz* or EAAT1 show elevated Tyramin levels in the CNS and similar phenotypes in behavioural assays.

**P143**

**Role of the natriuretic peptide/guanylyl cyclase/cyclic GMP system in retinal glia cells for physiological and pathological vascularization**

\*S. Hupp, H. Oberwinkler, B. Gassner, M. Kuhn

University of Würzburg, Physiology I, Würzburg, Germany

**Background:** During retinal vascularization, the reciprocal feedback between neurons, astrocytes, pericytes and endothelial cells is crucial for proper radial patterning. Also microglia are known to play a pivotal role in this event through secretion of pro-angiogenic factors. Natriuretic peptides (ANP, BNP and also CNP) and their shared cGMP-forming guanylyl cyclase (GC-A and GC-B) receptor are expressed by different retinal vascular, neuronal and glial cells, suggesting local modulatory actions on vessel growth and/or permeability.

**Methods:** We compared physiological postnatal retinal vascularization in mice with global (GC-A KO) or conditional, endothelial- or astrocyte-restricted deletion of GC-A and respective control mice. In preliminary experiments we addressed microglial activation under hypoxic conditions in vivo and in vitro. Additionally, we studied pathological neoangiogenesis in oxygen-induced retinopathy (OIR), a disease model for diabetic retinopathy and retinopathy of prematurity.

**Results:** Five days after birth, physiological vasculogenesis was markedly delayed in GC-A KO as compared to wildtype control mice. In contrast, pathological neoangiogenesis was severely enhanced in GC-A KO mice. Surprisingly, EC- and astrocyte GC-A KO mice did not resemble these phenotypes under physiological conditions. However, during relative hypoxia astrocytes via GC-A seem to attenuate tuft formation, whereas deletion of the receptor in EC seems to be beneficial.

**Conclusions:** NPs, via GC-A, exert dual actions on retinal angiogenesis: stimulation of physiological vascularization, and attenuation of pathological, hypoxia-driven neovascularization. These effects are not mediated by endothelial cells. Our future studies will be directed to further dissect the role of astrocytes, microglia and pericytes in the protective angiogenic actions of the NP/GC-A system. Supported by SFB 688.

Exercise / pulmonary functions / applied physiology

**P144**

**Influence of moderate exercise training on carotid-baroreflex functioning and autonomic pattern in young mildly hypertensive and normotensive men**

\*E. Izdebska<sup>1</sup>, J. Izdebski<sup>2</sup>, L. Czerwoszcz<sup>3</sup>

<sup>1</sup>Medical University of Warsaw, Department of Experimental & Clinical Physiology, Warsaw, Poland

<sup>2</sup>National Center of Sports Medicine, Warsaw, Poland

<sup>3</sup>Medical Research Center, Polish Academy of Sciences, Warsaw, Poland

Autonomic balance and baroreflex functioning are altered in hypertension. We investigated the effects of 3-month moderate exercise training on carotid baroreflex sensitivity (gain, CBRG) and response latency (CBRL) in 30 mild hypertensive (HT, n=30, 23±0.9 years) and 30 matched normotensive men (NT, n=30, 23±0.5 years). We tested the hypothesis that moderate exercise training shortens the CBRL elicited by carotid baroreceptor stimulation by application of negative pressure bilaterally on the carotid areas in the neck (NS), in 10 mmHg steps from -10 to -60 mmHg. We measured the CBRL from the onset of neck suction to the maximal R-R interval (RRI) or to the minimal value of total peripheral resistance (TPR) during the suction time. Additionally, we calculated the gain of the response (maximum change in RRI or TPR divided by NS). We recorded continuously: arterial blood pressure (BP) by Finapres method, heart rate (HR) by ECG, and stroke volume (SV) by impedance reography. The RRI variability (HRV) indices were measured by spectral method. 3-month moderate exercise training decreased significantly BP and TPR in HT and increased the cardiac CBRG in both groups; the increase was greater in HT; vasomotor CBRG did not change significantly after training in both groups. In the pre-training period, HT exhibited longer latencies than NT. After training, we observed in HT and NT significant shortening of cardiac CBRL, by 19% vs. 21% respectively. The shortening of vasomotor CBRL was greater in HT compared to NT: 22% and 11% respectively. The intrasubject positive correlation between basal TPR and vasomotor CBRL was observed (r = 0.4, p < 0.01), suggesting implication of arterial compliance. The autonomic pattern changed from sympathetic to vagal predominance. Our findings suggest that antihypertensive hemodynamic effects of moderate exercise training are associated with readjustment of autonomic cardiovascular control system.

**P145**

**Oxygen Enriched Air: Is it bad for the diver?**

\*A. Zenske<sup>1</sup>, J. D. Schipke<sup>2</sup>, W. Kähler<sup>3</sup>, A. Koch<sup>3</sup>, A. Stirban<sup>4</sup>, M. Krüll<sup>5</sup>

<sup>1</sup>Klinikum Landshut, Landshut, Germany

<sup>2</sup>University Hospital Düsseldorf, Research Group Experim Surgery, Düsseldorf, Germany

<sup>3</sup>SchiffMedInst der Marine, Kiel, Germany

<sup>4</sup>Profil, Metabolic Research Institute, Neuss, Germany

<sup>5</sup>Medical Institute Berlin-Marathon, Berlin, Germany

**Background:** The increasing depth increases the pO<sub>2</sub> while diving. Usage of oxygen enriched air (=Nitrox) additional increases pO<sub>2</sub> and thus, the oxidative stress. In parallel, pN<sub>2</sub> is decreased thereby decreasing potential narcotic N<sub>2</sub> effects Aim: Investigate whether increasing O<sub>2</sub> and reducing N<sub>2</sub> exerts effects on pulmonary function, elastic properties of blood vessels, cognitive competence, and bubble formation.

**Volunteers and Methods:** 25 divers (~40ys) performed one dive with air and another with Nitrox40 (max. 25m and 40min). Before and after the dive, pulmonary function (MasterScreen-IOS, CareFusion) and flow mediated dilatation (FMD; Periflux5000, Perimed) were assessed. Cognitive competence was assessed during the dive, and bubbles in the internal jugular vein (Doppler) were counted 30, 60, and 90 min after the end of the dive.

**Results:** Diving with Nitrox40 lead to an increase of the peripheral pulmonary resistance by 19% (air: +9%), reduced the FMD by 29.5% (air: unchanged), improved memory and alertness, and reduced bubble formation by 15 and 50%, respectively.

**Discussion:** Nitrox is increasingly used by recreational divers, in particular by dive guides. Our results suggest that the increased oxidative stress impairs small pulmonary air ways as well as the venous endothelium. On the other hand, cognitive competence is better preserved with less narcotic N<sub>2</sub>-effects and less N<sub>2</sub>-bubbles are formed.

**Conclusion:** Under the conditions of this study, Nitrox40 exerts both advantages and disadvantages. As disadvantages might accumulate over time, dive pauses should be allowed for injured organic tissue to recover.

**P146**

**Quantification of cell-free DNA from capillary plasma in treadmill running tests**

\*S. Breitbach, C. Magallanes, B. Sterzing, S. Tug, P. Simon

Johannes Gutenberg-Institute Mainz, Department of Sports Medicine, Rehabilitation and Prevention, Mainz, Germany

**Introduction:** Concentrations of cell-free DNA (cfDNA) increase significantly after acute exercise and return to baseline within 1-2 hours of recovery. We established a direct real-time PCR for the measurement of cfDNA from unpurified capillary plasma, which facilitates the investigation of cfDNA accumulations due to exercise.

**Methods:** 13 male handball players and 13 male triathletes performed an incremental treadmill test. Four participants performed further continuous running tests for up to 30 min

at the velocity at the individual anaerobic threshold (V<sub>IAT</sub>). Capillary samples were collected from the fingertip pre, during and several times post exercise.

**Results:** In the incremental treadmill test, cfDNA concentrations increased 9.8-fold and nearly paralleled the kinetics of lactate. Significant elevations of cfDNA and lactate appeared after the 10 km/h and 12 km/h stage, respectively. cfDNA concentrations correlated well with lactate, heart frequencies, oxygen consumption, energy expenditure and Borg values (0.710 ≤ r ≤ 0.808). No significant difference existed between handball players and triathletes with regard to the concentrations or the kinetics of cfDNA. In the continuous running tests, lactate levels remained constant from 10 min of running at the V<sub>IAT</sub> until exercise cessation, while cfDNA concentrations increased 18-fold within this interval.

**Discussion:** cfDNA accumulations might be triggered by stress hormones that already increase at intensities below the anaerobic threshold, and be released through the mechanism of NETosis. DNase concentrations might play a role in the clearance of cfDNA. Analyses of cfDNA might yield physiologically relevant conclusions on aerobic or intermittent exercise, where other metabolites like lactate would not provide respective information.

**P147**

**Long-term respiratory muscle endurance training in patients with myasthenia gravis**

\*B. Raßler<sup>1</sup>, S. Hallebach<sup>1</sup>, S. Freitag<sup>1</sup>, I. Baumann<sup>2</sup>, P. Kalischewski<sup>2</sup>

<sup>1</sup>University of Leipzig, Carl-Ludwig-Institute of Physiology, Leipzig, Germany

<sup>2</sup>Neurological Practice, Leipzig, Germany

Myasthenia gravis (MG) is characterized by reduced muscle endurance and is often accompanied by respiratory complications. Improvement of respiratory function is therefore an important objective in MG therapy. A previous study demonstrated that respiratory muscle endurance training (RMET) over four weeks increased respiratory muscle endurance of MG patients to about 200 % of baseline. The purpose of the present study was to establish a maintenance training program and to test its effects over seven months. Ten patients with mild to moderate MG participated in the training group (TG). During the first month, they performed five training sessions per week. For the following 6 months, training frequency was reduced to five sessions per two weeks. Myasthenia score, lung function and respiratory endurance were determined prior to training, after the first month and after 4 and 7 months. Five patients served as controls (CG). They did not perform RMET but were tested in the same way as patients in TG. RMET significantly improved myasthenia symptoms, maximum inspiratory muscle force (P<sub>Imax</sub>) and respiratory endurance time (RET). In contrast, no significant improvement was observed in CG. In TG, myasthenia score improved from 0.63 ± 0.1 to 0.44 ± 0.1 (p<0.001), P<sub>Imax</sub> increased from 7.3 ± 0.4 to 8.4 ± 1.0 kPa (p=0.002), and

RET increased from 8.8 ± 1.4 to 24.2 ± 3.4 min (p<0.001). In conclusion, this RMET maintenance program is feasible and is significantly beneficial for MG patients.

**P148**

**Bone metabolic responses to bed rest in young and older men**

\*J. Rittweger<sup>1</sup>, J. Bühlmeier<sup>2</sup>, P. Frings-Meuthen<sup>1</sup>, N. Mohorko<sup>3</sup>, R. Pisot<sup>3</sup>, B. Simunic<sup>3</sup>

<sup>1</sup>Institute for Aerospace Medicine, Space Physiology, Köln, Germany

<sup>2</sup>Institut für Ernährungs- und Lebensmittelwissenschaften, Ernährungsphysiologie, Bonn, Germany

<sup>3</sup>University of Primorska, Institute for Kinesiology Research, Koper, Slovenia

**Background and Hypothesis:** It is well known that immobilization, through reductions of musculoskeletal forces, leads to bone loss. This is well established for clinical conditions, such as stroke, spinal cord injury as well as for spaceflight and disuse models, such as experimental bed rest. Age is another condition that predisposes to bone loss, which is intimately linked to fractures in the elderly population. Bone turn-over is known to be reduced in the elderly, and animal studies suggest a blunted response of bone to mechanical stimuli at old age, and that old age might 'shield' against immobilization-reduced bone loss. Whether this applies also to humans is currently unknown. The aim of the present study therefore was to compare bone metabolic responses to bed rest in a group of young (23.4 (SD 2.9) Years, n=7) and older men (59.1 (SD 2.5) Years, n=8). It was hypothesized that bone metabolic responses would be generally blunted in older men.

**Methods:** A 14-day bed rest study was organized in the Orthopaedic hospital in Ankaran, Slovenia. Blood samples and 24-hour urine collections were obtained at baseline, on the 2<sup>nd</sup>, 5<sup>th</sup>, 10<sup>th</sup> and 14<sup>th</sup> day of bed rest, and on the 7<sup>th</sup> and 14<sup>th</sup> day of recovery. Urinary concentrations of the resorption markers CTX and NTX were assessed by ELISA, serum levels of the bone formation marker P1NP by RIA, and serum calcium levels were assessed by flame photometry. Linear mixed effects models were designed and run with the R statistical software package.

**Results:** All bone formation and resorption marker levels were substantially lower in the old than in the young subjects at baseline (P < 0.01). P1NP decreased by 21.6 (SE 9.7)% during bed rest in the young group only (P = 0.042), but not in the older group. The enhancement in P1NP that was seen after re-ambulation in the older group (P < 0.001) was not seen in the young group. Urinary NTX excretion was increased by 74.2 (SE 9.9)% during bed rest (P < 0.001), without any group differences (P = 0.62). Serum calcium levels were marginally affected by bed rest, with a the young group depicting a moderate increase from 2.44 (SE 0.03) mM at baseline to 2.53 (SE 0.04) mM during bed rest.

**Discussion:** The present study has replicated the expected result of a mitigated bone turnover in older men, as compared to young men. Although the moderate decline in bone formation that was seen in young men was obliterated

in the older group, both groups depicted very similar responses in bone resorption. It therefore seems that the older human skeleton retains most of its potential to lose bone in response to immobilization.

**P149**

**Exercise acutely changes titin phosphorylation and cardiac myofilament stiffness**

\*A.-E. Müller<sup>1</sup>, F. Suhr<sup>2</sup>, M. Kreiner<sup>1</sup>, P. Lassak<sup>1</sup>, S. Kötter<sup>1</sup>, W. Bloch<sup>2</sup>, M. Krüger<sup>1</sup>

<sup>1</sup>Heinrich-Heine-Universität Düsseldorf, Herz- und Kreislaufphysiologie, Düsseldorf, Germany

<sup>2</sup>Sporhochschule Köln, Institut für Kreislaufforschung und Sportmedizin, Köln, Germany

Titin-based myofilament stiffness is largely modulated by phosphorylation of its elastic I-band regions N2-Bus (decreases passive stiffness, PT), and PEVK (increases PT). Here, we tested the hypothesis that exercise acutely changes titin phosphorylation and modifies myofilament stiffness. Adult rats were exercised on a treadmill for 15min, untrained animals served as controls. Titin phosphorylation was determined by Western blot analysis using phosphospecific antibodies to Ser4099 and Ser4010 in the N2-Bus region (PKG and PKA-dependent), and to Ser11878 in the PEVK region (PKC-dependent). Passive tension (PT) was determined by step-wise stretching of isolated skinned cardiomyocytes to sarcomere length from 1.9-2.6µm. In cardiac samples titin N2Bus phosphorylation was significantly decreased by 40% at Ser4099, however, no significant changes were observed at Ser4010. PEVK phosphorylation at Ser11878 was significantly fivefold increased, suggesting an exercise-induced increase in PKCα activity. Consistent with the changes in titin phosphorylation passive stiffness of the cardiomyocytes was significantly increased. Surprisingly, in skeletal samples from acutely exercised animals we detected a significant decrease in PEVK phosphorylation at Ser11878 by 60% and a reduction in PKCα activity. Experiments are currently underway to test how titin-based PT is affected in skinned skeletal myocytes. In summary, our data show that a single exercise bout of 15 min. acutely affects titin phosphorylation, but has opposite effects on cardiac and skeletal muscle tissue. The observed changes in titin stiffness could play an important role in adapting the passive and active properties of the myocardium and the skeletal muscle to increased physical activity.

**P150**

**Circulating microRNAs as biomarkers for recombinant human erythropoietin (r-HuEPO) doping detection**

\*G. Wang<sup>1</sup>, \*E. Neuberger<sup>2</sup>, S. Perikles<sup>2</sup>, J. Durussel<sup>1</sup>, J. D. McClure<sup>1</sup>, M. W. McBride<sup>1</sup>, Y. P. Pitsiladis<sup>3</sup>

<sup>1</sup>University of Glasgow, Glasgow, United Kingdom

<sup>2</sup>Johannes Gutenberg University of Mainz, Mainz, Germany

<sup>3</sup>University of Brighton, Brighton, United Kingdom

Administration of recombinant human erythropoietin (rHuEpo) improves performance and hence is subject to abuse by athletes. The detection of rHuEpo doping remains a major challenge at present. The aim of the current study was to investigate whether circulating microRNA (miRNA) can be used for detecting r-HuEpo doping. Twenty trained males received rHuEpo injections of 50 IU·kg<sup>-1</sup> body mass every two days for 4 weeks. Blood was obtained 2 weeks before, during and 4 weeks after administration. For this pilot analysis, plasma miRNA expression was assessed at selected time points using the Affymetrix GeneChip 3.0 and the miScript 384 HC PCR Array (Qiagen). For the Affymetrix microarray data, GC content adjustment was carried out prior to background correction and quantile normalization. For the Qiagen PCR Array data, raw C<sub>T</sub> values exported from the RQ manager were firstly normalized to the spike-in control (i.e. cel-miR-39-3p), then to the mean of commonly expressed miRNAs with a C<sub>T</sub> < 35 prior to formal analysis. 1733 human miRNAs are present on the GeneChip 3.0. Eighty-two of the 1733 miRNAs were commonly expressed across all samples and 773 miRNAs were found in at least one sample. Six miRNAs showed significant fold changes following r-HuEpo, with 5 miRNAs up-regulated (fold change ranging from 2.03-3.07, P < 0.05) and 1 miRNA down-regulated (fold change: 2.56, P = 0.042). Out of 372 human miRNAs present (Qiagen), 205 human miRNAs were detected in all samples and 164 miRNAs were found in at least one sample. Two miRNAs were differentially expressed (fold changes: 3.4 - 3.84, P ≤ 0.03) following r-HuEpo. For significantly expressed miRNAs identified by both methods, 6 common miRNAs were found to be either predicted or validated miRNAs potentially involved in Epo signalling pathways. Analysis of identified miRNAs in the remaining samples will be required in order to determine whether circulating miRNAs can be effectively used for r-HuEpo doping detection. miRNAs isolated from red blood cells before and after r-HuEpo are also currently being analysed using next generation sequencing.

**P151**  
**Nox4 maintains exercise induced neovascularization**

\*J. Vogel, K. Schröder  
Institut für Kardiovaskuläre Physiologie, Universität Frankfurt, Frankfurt, Germany

The NADPH oxidase Nox4 is involved in hypoxia associates angiogenesis, like vascular remodeling of the hypertrophic heart or blood flow recovery after hindlimb ischemia. As Nox4 is a stress-inducible enzymatic source of hydrogen-peroxide we wondered whether or not Nox4 contributes to angiogenesis in none disease models as well. Exercise represents such a situation of hypoxia in healthy subjects. Beside angiogenesis exercise modulates the composition of slow and fast twitch fibers in skeletal muscles. We hypothesize that Nox4 is involved in exercise induced angiogenesis and thereby contributes to muscle fiber-switch in skeletal muscle. We studied skeletal capillary density in wildtype (WT) and Nox4-knockout (Nox4<sup>-/-</sup>) mice

in forced endurance and voluntary exercise models. In WT animals exercise results in an increase in capillary density and capillary-to-fiber ratio as measured by indirect immunofluorescence of CD31 in soleus and gastrocnemius. This increase is accompanied by a higher number of type IIA fast-twitch fibers in the skeletal muscle. In Nox4<sup>-/-</sup> mice exercise-mediated neovascularisation was not observed. However exercise induced muscle fiber-switch of Nox4<sup>-/-</sup> is comparable to that observed in WT mice. Quantitative PCR analysis revealed that exercise-induced elevation in vascular endothelial growth factor (VEGF) expression as seen in WT is not present in Nox4<sup>-/-</sup> mice. In contrast the expression of the metabolism switch representative PGC1α was similar in WT and Nox4<sup>-/-</sup> mice. These data suggest that Nox4 maintains exercise-induced elevation in VEGF expression in murine skeletal muscle and thereby contributes to neovascularization while muscle fiber switch is Nox4 independent.

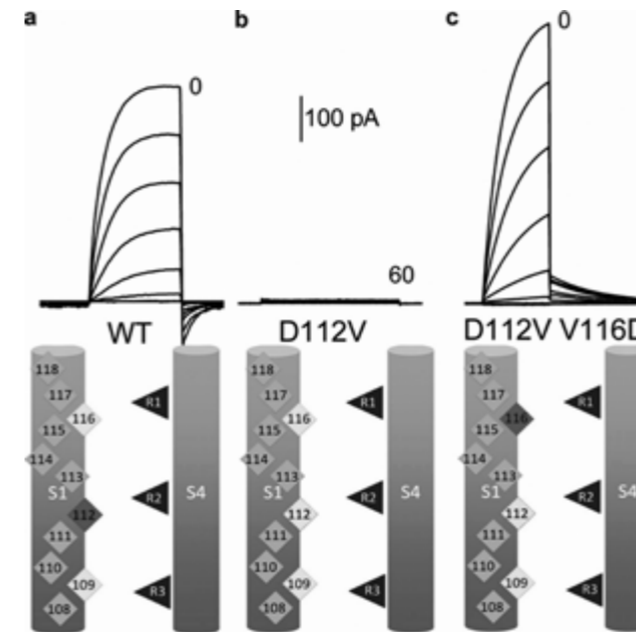
Ion channels I

**P152**  
**Peregrination of the selectivity filter delineates the pore of the human voltage gated proton channel**

\*B. Musset  
Forschungszentrum-Jülich, ICS-4 Zelluläre Biophysik, Jülich, Germany

Extreme selectivity is crucial to all proton conducting molecules, including the human voltage gated proton channel, hHV1, because the proton concentration is 10<sup>6</sup> lower than that of other cations. Here we use "selectivity filter scanning" to elucidate the molecular requirements for proton specific conduction in hHV1. Aspartate 112, in the middle of the S1 transmembrane domain is an essential part of the selectivity filter in WT channels. After neutralizing D112 by mutation (D112A), we introduced aspartate at each position along S1 from 108 to 118, to search for "second site suppressor" activity. Surprisingly, most mutants lacked even the anion conduction exhibited by D112A. Proton conduction was restored only at position 116, confirming that aspartate is crucial to hHV1 proton selectivity. With aspartate at position 109, anion conductance was observed, as with D112A. Evidently, aspartate must face the pore directly to enable conduction, and the S1 helix is not free to rotate when aspartate does not face the pore. Glutamate at position 116 also produced proton specificity, indicating leeway in the required chain length. The three positions that permitted conduction all line the pore in our homology model, supporting the model and clearly delineating

the conduction pathway. That the selectivity filter functions when shifted to a new position refines our understanding of proton selectivity.



**P153**  
**Cisplatin reduces voltage gated calcium channel currents in small dorsal root ganglion neurons**

\*M. Leo, \*T. Hagenacker  
University Hospital Essen, Germany, Dep. of Neurology, Essen, Germany

Neurotoxic effects of cisplatin, which is part of cancer treatment has been linked to disturbance of the intracellular calcium homeostasis. Recent studies provide evidence for primary extracellular source of this increase of cytosolic calcium. Voltage gated calcium channels (VGCC) and thermoreceptors (TRP) conduct calcium ions and have been shown to be dysregulated by platinum compounds. Dorsal root ganglion (DRG) neurons were prepared from three weeks old Wistar rats and cultivated for 24 h. VGCC currents were isolated in cultured dorsal root ganglion neurons of rats using the whole cell patch clamp method and Ba<sup>2+</sup> as charge carrier. VGCC currents were only isolated in small diameter neurons (<25µm). Cisplatin reduces dose-dependently (0.01-50µM) peak VGCC currents after acute application. 0.1µM leads to reduction of 19,31% 700 sec after administration of the drug. 5µM reduces the current by 43,21% after 700 sec. Subtype isolation provide evidence for differential effects of cisplatin on N-type, P/Q-type, L-type and T-type channel currents. While acute application of cisplatin reduces VGCC currents, incubation of DRG neurons with cisplatin (1-5µM) increase the mean VGCC currents suggesting an overexpression of VGCC channels after platin administration. These results provide evidence for an essential role extracellular calcium in DRG neurons as main cause for neurotoxicity of platinum based

cancer curing chemotherapy. Future studies are planned to identify the main carrier of VGCC and TRP channels responsible for the increase in intracellular calcium to open up new possibilities to reduce neurotoxic side effects of platinum based drugs.

**P154**  
**Volume regulation by anoctamins**

\*L. Sirianant, J. Ousingsawat, P. Wanitchakool, R. Schreiber, K. Kunzelmann  
University of Regensburg, Physiology, Regensburg, Germany

Volume regulation is an intrinsic property of any living cell. An increase in intracellular osmolytes or decrease in extracellular osmolarity leads to cell swelling, which is counteracted immediately by activation of K<sup>+</sup> and Cl<sup>-</sup> currents, releasing KCl to the extracellular space. Anoctamin 1 (Ano1; TMEM16A) has recently been identified as the important Ca<sup>2+</sup> activated Cl<sup>-</sup> channel (CaCC) expressed in a wide range of tissues and was found together with other anoctamins to support cellular volume regulation and regulatory volume decrease (RVD). However, the biophysical properties of Ano1 and its Ca<sup>2+</sup> sensitivity made it an unlikely candidate for the classical volume regulated anion channel VRAC. We present evidence that full activation of RVD and VRAC in HEK293 cells and lymphocytes requires the presence of physiological extracellular Ca<sup>2+</sup> concentrations. Anoctamins are broadly expressed which makes them good candidates for VRAC. We analyzed mRNA expression of the ten anoctamins in a large number of tissues and cell lines and found that almost all human and murine cell types express Ano6, 8, 9, and 10. Whole cell currents induced by hypotonic cell swelling were measured using a patch pipette filling solution with a cytosolic-like ion composition, and physiological extracellular Ca<sup>2+</sup> concentrations, allowing direct comparison of ion current and volume measurements. When overexpressed in HEK293 cells Ano6, 9, and 10 but not Ano8 enhanced RVD and VRAC as well as apoptotic whole cell currents induced by staurosporine. The data suggest broadly expressed Ano6, 9, and 10 as possible candidates for swelling activated ion channels.

**P155**  
**Overexpression of Gαi1 in atrial myocytes interrupts GIRK current activation by functionally removing M2-receptors**

\*M.-C. Kienitz, L. Pott, E. Mintert-Jancke  
Ruhr-Universität, Institut für Physiologie, Bochum, Germany

G protein-activated inward-rectifying K<sup>+</sup> (GIRK) channels comprised of Kir3 subunits are canonically opened by direct ("membrane-delimited") interaction with βγ subunits released from heterotrimeric G proteins upon activation of a GPCR. In atrial myocytes channel Kir3.1/Kir3.4 complexes are controlled by vagally released acetylcholine via muscarinic M<sub>2</sub> receptors (M<sub>2</sub>-R). Evidence has been provided, primarily from reconstitution experiments in the Xenopus

oocyte expression system, that G $\alpha$ -subunits, beyond their role as G $\beta\gamma$  donors, are important for forming signalling complexes (GPCR-G $\alpha\beta\gamma$ -Kir3.1/Kir3.x). The major finding in support of this hypothesis is a positive correlation between the expression level of G $\alpha_{v_o}$  and the amplitude of receptor-activated GIRK current and a reduction in agonist independent current ( $I_{\text{basal}}$ ), which was assumed to reflect scavenging of free G $\beta\gamma$ <sup>1</sup>. In the present study we overexpressed Gai1 in rat atrial myocytes using adenoviral gene transfer. This had no effect on  $I_{\text{basal}}$  but reduced ACh-activated current ( $I_{\text{K(ACh)}}$ ) and slowed its activation. These effects were analogous to reducing expression of M<sub>2</sub>-R by siRNA or physiological down regulation<sup>2</sup>. This suggested that overexpressed G $\alpha_{v_o}$  associate with endogenous GPCRs, resulting in complexes devoid of  $\beta\gamma$  subunits. To test for this hypothesis, G $\alpha_{v_o}$ , expressed as a fusion construct with a different GPCR species (A1-adenosine), resulted in an increased amplitude and activation rate of ACh-induced current, demonstrating that the fusion construct assembles with G $\beta\gamma$  and is fully functional. More importantly, in myocytes expressing this construct, amplitude and activation rate of  $I_{\text{K(ACh)}}$  were not different from native or mock-infected cells, in support of the above "hijack-hypothesis". A rescue of the native features of  $I_{\text{K(ACh)}}$  was also achieved by overexpressing G $\alpha_{v_o}$  in combination with the M<sub>2</sub>-R. Conclusions: These data demonstrate that surplus G $\alpha_{v_o}$  subunits interrupt G $\beta\gamma$ -signaling rather than facilitating formation of GPCR-G $\alpha\beta\gamma$ -Kir3.1/Kir3.4 complexes.

<sup>1</sup>Rubinstein et al. (2009) J. Physiol. 587:3473-91 2 Rinne et al. (2009) Methods Mol Biol. 515:107-23

**P157**  
**Analysing dependence of KCNQ1/KCNE1 K<sup>+</sup> channel current (IKs) on ATP in CHO cells using a FRET-sensor for ATP**

<sup>\*</sup>D. Vladimirova, L. Pott, M.- C. Kienitz  
Ruhr-Universität, Institut für Physiologie, Bochum, Germany

Voltage-activated K<sup>+</sup>-channels composed of KCNQ1/KCNE1 subunits, carrying the  $I_{\text{Ks}}$  current in cardiac myocytes, are dependent on the concentration of phosphatidylinositol 4,5-bisphosphate (PIP<sub>2</sub>) in the plasma membrane and on the concentration of cytosolic ATP by two distinct mechanisms<sup>1</sup>. Experimental depletion of cellular ATP also affects PIP<sub>2</sub> and vice versa. To clearly distinguish between effects related to either PIP<sub>2</sub> or ATP on  $I_{\text{Ks}}$ , tools for monitoring concentrations both signalling molecules are required. Simultaneous patch-clamp and FRET measurements in cells co-expressing the switchable phosphatase Ci-VSP and a PIP<sub>2</sub>-FRET sensor revealed a component of  $I_{\text{Ks}}$  inhibition directly correlated to dynamic PIP<sub>2</sub>-depletion. A second component of  $I_{\text{Ks}}$  inhibition was independent of rapid changes in PIP<sub>2</sub> and could be mimicked by dialyzing the cell with ATP-free pipette solution, supporting the notion that the second component results from intracellular ATP-depletion. In the present study we explored a novel genetically-encoded FRET-sensor for ATP based on a bacterial F<sub>o</sub>F<sub>1</sub>-ATP synthase (ATeam<sub>2</sub>). Simultaneous patch-clamp and FRET measurements in cells coexpressing Ci-

VSP and ATeam show that the second, slow component of  $I_{\text{Ks}}$  inhibition reflects changes in intracellular ATP upon Ci-VSP activation. This component of  $I_{\text{Ks}}$  inhibition was prevented by the non-hydrolysable ATP analogue AMP-PNP, indicating that direct binding of ATP to the KCNQ1/KCNE1 channel is required for channel activation.

<sup>1</sup> Li et al (2013) PNAS 110:18922-7 2 Imamura et al (2009) PNAS 106:15651-6

**P158**  
**Interaction between purinergic receptors and Ca<sup>2+</sup>-dependent Cl<sup>-</sup> channels**

<sup>\*</sup>M. Klapperstück<sup>1</sup>, M. Stolz<sup>2</sup>, S. Detro-Dassen<sup>2</sup>, G. Schmalzing<sup>2</sup>, F. Markwardt<sup>1</sup>

<sup>1</sup>Martin-Luther-Universität Halle-Wittenberg, Medizinische Fakultät, Halle, Germany

<sup>2</sup>RWTH Aachen University, Molecular Pharmacology, Aachen, Germany

The P2X7 receptor (P2X7R) is an ATP-gated nonselective Ca<sup>2+</sup> permeable cation channel, which for example is found coexpressed with the TMEM16A(a)/anoctamin-1 (Ano-1) anion channel in secretory epithelia. The Ano-1 channel is activated by increase in the intracellular Ca<sup>2+</sup> concentration. To screen for a possible physical interaction between the P2X7R and Ano-1, we coexpressed His-tagged and StrepII-tagged versions of the P2X7R and the Ano-1 in *Xenopus* oocytes and purified the proteins under non-denaturing conditions. Besides we investigated by using the two-microelectrode voltage-clamp technique whether the coexpressed channels are functionally coupled.

Indeed, coexpression of Ano-1 with the P2X7R led to a significant and sustained augmentation of the ATP-induced current compared to the current mediated by the singly expressed P2X7R. This Ano-1-dependent current increase was diminished in Ca<sup>2+</sup>-free extracellular solution, by buffering the oocyte cytosol with BAPTA or by the coapplication of the anion channel blockers niflumic acid or carbenoxolone with ATP. In contrast to the sustained P2X7R-mediated activation of the Ano-1 current, increasing the intracellular Ca<sup>2+</sup> concentration by activating the co-expressed G-protein-coupled P2Y1 receptor (P2Y1R) or by a Ca<sup>2+</sup> ionophore produced only a transient increase in the Ano-1-mediated anion conductance. Biochemically we did not observe a co-purification of the Ano-1 with the P2X7R or the P2Y1R by immunoprecipitation or Strep-Tactin purification, even when weak protein-protein interactions were stabilized by chemical cross-linking. This indicates that the P2X7R-mediated or the P2Y1R-mediated stimulation of Ano-1 is not mediated by a direct protein-protein-interaction. We conclude that P2X7R stimulation may permanently activate Ano-1, a process which may be of relevance for the time course of stimulus-secretion coupling in secretory epithelia.

**P159**  
**Expression of anoctamins in retinal pigment epithelial cells**

<sup>\*</sup>R. Schreiber, L. Sirianant, K. Kunzelmann

Universität Regensburg, Institut für Physiologie, Regensburg, Germany  
The family of the Ca<sup>2+</sup> activated Cl<sup>-</sup> channels Anoctamin (Ano) consists of ten different proteins (Ano1-Ano10). It was shown that Anoctamins are related to two several cellular functions. Ano1 is the Ca<sup>2+</sup> activated Cl<sup>-</sup> channel in secretory cells, like pancreas acinar epithelia cells, salivary glands or enterocytes. Additionally expression of Ano1 promotes cell proliferation and migration of tumor cells. Ano6 plays a crucial role in Ca<sup>2+</sup>- dependent scrambling of membrane phospholipids in platelets, red blood cells and lymphocytes. Our study indicates that Ano6 produces an outwardly rectifying Cl<sup>-</sup> current during cell swelling and apoptotic cell death. The function of Anoctamins in retinal pigment epithelial cells (RPE) is unknown. Expression studies by RT-PCR are suggesting strong expression of Ano6 and Ano10 mRNA in human, bovine and mouse native RPE cells and in the RPE cell line hTERT RPE1. Culturing of hTERT RPE1 under serum free conditions induces formation of primary cilium. Immunocytochemistry suggests expression of Ano10 on the basis of the primary cilium. Intracellular Ca<sup>2+</sup> concentration increases during cell swelling and upon stimulation with the acetylcholine receptor agonist carbachol. These results suggest involvement of Ano6 and Ano10 in cell volume regulation and on acetylcholine receptors dependent pathways of RPE cells.

**P160**  
**The role of Epac2 in bile acid-stimulated insulin secretion**

<sup>\*</sup>E. Heider<sup>1</sup>, P. Krippeit-Drews<sup>1</sup>, M. Düfer<sup>2</sup>, G. Drews<sup>1</sup>

<sup>1</sup>Institute of Pharmacy, Department of Pharmacology, Clinical Pharmacy and Toxicology, Tübingen, Germany

<sup>2</sup>Institute of Pharmaceutical and Medical Chemistry, Department of Pharmacology, Münster, Germany

**Question:** The aim of the study was to test whether Epac2 (Exchange protein directly activated by cAMP 2) plays a role in the bile acid-mediated regulation of glucose homeostasis via farnesoid X receptor (FXR).

**Methods:** Experiments were performed with beta-cells from wild-type (WT) and Epac2-knockout (KO) mice, respectively. Ion currents were measured with the patch-clamp technique; the cytosolic Ca<sup>2+</sup> concentration [Ca<sup>2+</sup>]<sub>c</sub> was determined by fura-2.

**Results:** Taurochenodeoxycholate (TCDC) and the synthetic FXR agonist GW4064 (500nM respectively) enhanced [Ca<sup>2+</sup>]<sub>c</sub> in beta-cells of WT mice (n=13-18). Interestingly, GW4064 did not alter [Ca<sup>2+</sup>]<sub>c</sub> in beta-cells of Epac2-KO mice (n=22). The Epac-selective cAMP analog Sp8 (1 $\mu$ M) evoked an elevation of [Ca<sup>2+</sup>]<sub>c</sub> in WT beta-cells (n=23) but not in Epac2-KO beta-cells (n=17) indicating that Epac activation augments [Ca<sup>2+</sup>]<sub>c</sub> in beta-cells. We further tested whether the K<sub>ATP</sub> channel density is altered in beta-cells of Epac2-KO mice. Whole-cell K<sub>ATP</sub> current measurements revealed a significant decrease in K<sub>ATP</sub> channel density in beta-cells lacking Epac2 (n=15-22). To investigate if the

sensitivity of the K<sub>ATP</sub> channel is modified by FXR activation, we tested different  $K_{\text{ATP}}$  concentrations in the pipette solution in the absence and presence of GW4064. The FXR agonist increased  $K_{\text{ATP}}$  sensitivity of the channels in WT beta-cells but not in Epac-KO beta-cells (n=5-11).

**Conclusion:** The experiments provide evidence for a link between bile acid signaling and the activation of Epac2 which seems to increase K<sub>ATP</sub> channels sensitivity towards  $K_{\text{ATP}}$ . It is suggested that FXR stimulation activates Epac2 which in turn decreases K<sub>ATP</sub> channel activity.

**P161**  
**Modulation of beta-cell function by the atrial natriuretic peptide**

<sup>\*</sup>S. Undank<sup>1</sup>, H. Nakagawa<sup>2</sup>, K. Völker<sup>2</sup>, B. Gaßner<sup>2</sup>, H. Oberwinkler<sup>2</sup>, P. Krippeit-Drews<sup>1</sup>, M. Düfer<sup>3</sup>, M. Kuhn<sup>2</sup>, G. Drews<sup>4,1</sup>

<sup>1</sup>Institute of Pharmacy, Department of Pharmacology, Toxicology and Clinical Pharmacy, Tübingen, Germany

<sup>2</sup>Institute of Physiology, Würzburg, Germany

<sup>3</sup>Institute of Pharmaceutical and Medicinal Chemistry, Department of Pharmacology, Münster, Germany

<sup>4</sup>Pharmazeutisches Institut, Pharmakologie, Toxikologie und Klinische Pharmazie, Tübingen, Germany

**Question:** Recent studies suggest that the cardiac hormone ANP (atrial natriuretic peptide) is an important regulator of metabolism. It may provide a link between cardiovascular and metabolic dysregulation in obesity and prediabetes. The aim of the present study was to investigate the effect of ANP on beta-cell stimulus-secretion coupling.

**Methods:** Ion currents and the membrane potential (Vm) of mouse beta-cells were measured with the patch-clamp technique and the microelectrode array system (MEA), respectively. Cytosolic Ca<sup>2+</sup> concentration [Ca<sup>2+</sup>]<sub>c</sub> was determined by fura-2 and mitochondrial membrane potential ( $\Delta\psi$ ) by Rh-123. Protein expression in pancreatic islet lysates was assessed by Western blotting.

**Results:** ANP (10 nM) decreased the open probability of the KATP channel in beta-cells of C57BL/6N (n=17) and GC-A<sup>fllox/fllox</sup> mice (n=5). This effect was absent in mice with specific deletion of the GC-A receptor in beta-cells (Rip-Cre<sup>+/-</sup> GC-A<sup>fllox/fllox</sup>) (n=5). ANP did not influence DY (n=60), indicating that it does not affect ATP production. In accordance with closure of KATP channels, ANP increased glucose-induced electrical activity (n=6-15). Determination of specific current density (n=33-34) as well as Western blotting (n=6) revealed no significant difference in the number of KATP channels in beta-cells of Rip-Cre<sup>+/-</sup> GC-A<sup>fllox/fllox</sup> mice and their wild type littermates. In the presence of stimulatory glucose concentration, [Ca<sup>2+</sup>]<sub>c</sub> was elevated by ANP (10 nM) in beta-cells of both genotypes (n=29), possibly due to the involvement of the natriuretic peptide receptor-C. **Conclusion:** These results provide evidence that ANP exerts specific actions in the endocrine pancreas and that the hormone is involved in the regulation of beta-cell function.

**P162**

**Mechanically induced stretch of native pulmonary epithelium activates both KATP and KCNQ channels**

\*K. Richter<sup>1</sup>, W. Clauss<sup>1</sup>, M. Fronius<sup>1,2</sup>

<sup>1</sup>Justus-Liebig-University, Giessen, Institute of Animal Physiology, Dept. Molecular Cell Physiology, Giessen, Germany

<sup>2</sup>University of Otago, Department of Physiology, Dunedin, New Zealand

**Objective:** The pulmonary epithelium (PE) is permanently exposed to mechanical forces due to breathing movements, although little is known about the impact of mechanical forces on transepithelial ion transport processes. Since transepithelial ion transport is an essential function of epithelial cells, the aim of this study was to investigate the impact of mechanical forces on ion transport processes with a focus on K<sup>+</sup> channel activity in native PE.

**Methods:** Freshly dissected *Xenopus laevis* lungs were used for transepithelial short-circuit current (I<sub>sc</sub>) recordings in a modified Ussing chamber. Hydrostatic pressure (HP; 5 cm fluid-column) was introduced to the tissue to apply stretch. The influence of HP on K<sup>+</sup> channel activity was determined with specific inhibitors (HMR1098, glibenclamide: ATP-sensitive K<sup>+</sup> channel (K<sub>ATP</sub>) inhibitor; XE-991: KCNQ channel inhibitor). For investigation of the basolateral membrane, tissues were apically permeabilized by using the pore forming agent nystatin.

**Results:** Apical application of HP to unpermeabilized epithelia led to a pressure-induced current decrease (17.6 ± 2%). This effect was prevented by apical application of HMR1098 and glibenclamide indicating a mechanosensitive activation of apically localized K<sub>ATP</sub>. Conversely, application of HP on apically permeabilized epithelia resulted in a current increase (39.2 ± 6%). This effect was abolished by basolateral application of XE-991, indicating a mechanosensitive activation of basolaterally localized KCNQ channels. RT-PCR experiments confirmed expression of KCNQ1 and K<sub>ATP</sub> subunit transcripts.

**Conclusion:** We demonstrate a direct impact of mechanical forces on K<sup>+</sup> channels in native pulmonary epithelia. HP activates apically localized K<sub>ATP</sub> as well as basolaterally localized KCNQ channels.

**P163**

**A family of prokaryote cyclic-nucleotide modulated ion channels**

\*J. Kusch<sup>1</sup>, M. Brams<sup>2</sup>, R. Spurny<sup>2</sup>, C. Ulens<sup>2</sup>

<sup>1</sup>Universitätsklinikum Jena, Physiologie II, Jena, Germany

<sup>2</sup>KU Leuven, Department of Cellular and Molecular Medicine, Leuven, Belgium

**Question:** Cyclic nucleotide-modulated ion channels belong to the superfamily of six-transmembrane domain voltage-gated K<sup>+</sup> channels. Whereas CNG (cyclic-nucleotide gated) channels are only weakly voltage dependent and activated by the binding of cyclic nucleotides, HCN (hyperpolarization-activated and cyclic-nucleotide modulated) channels activate upon hyperpolarizing voltages and are

only modulated by cyclic-nucleotide binding. At the structural level, insight into these channels is limited to crystal structures of the HCN and spHCN C-terminal portion, including the cyclic-nucleotide binding domain (CNBD) and the C-linker, which connects the CNBD to the transmembrane portion, and to a prokaryote cyclic nucleotide-gated channel (MloK1), lacking the C-linker. To advance our structural understanding of this ion channel family, we investigated bacterial homologs as candidates for large-scale expression and future structural studies.

**Methods:** We used molecular biological and biochemical techniques, to investigate the expression of five different HCN/CNG channel homologs in *E.coli*. Additionally, we applied electrophysiological and optical techniques to a SthK-GFP fusion construct expressed in *Xenopus laevis* oocytes to describe membrane trafficking and functional properties.

**Results:** We identified two homologs that could be expressed at a whole-cell fluorescence level of ~40% compared to KcsA-GFP. We found that dodecylmaltoide or undecylmaltoide are suitable detergents to solubilize these channels in a tetrameric monodisperse state. Optical and functional tests showed that SthK-GFP is expressed in *Xenopus laevis* oocytes. Patch-clamp recordings in inside-out macropatches revealed that this homolog is potassium selective and requires the binding of cyclic nucleotides for activation.

**Conclusions:** Together, these data pave the way for future functional and structural studies on prokaryote HCN and CNG channel homologs.

**P164**

**Gadolinium, released by gadolinium-containing contrast-agents, decreases the activity of human epithelial Na<sup>+</sup>-channels**

\*F. Knoepp<sup>1</sup>, W. Clauss<sup>1</sup>, M. Fronius<sup>1,2</sup>

<sup>1</sup>Justus-Liebig-University Giessen, Institute of Animal Physiology, Giessen, Germany

<sup>2</sup>University of Otago, Department of Physiology, Dunedin, New Zealand

**Question:** Gadolinium-containing contrast-agents, commonly used for magnetic-resonance-imaging (MRI) can provoke adverse-effects like acute urinary urgency, hypotension or pulmonary edema. These effects are directly related to a decreased salt- and water-reabsorption. A decisive role in maintaining the salt- and water-homeostasis plays the epithelial Na<sup>+</sup>-channel (ENaC) which is expressed in various epithelial and nonepithelial tissues. An interference of the contrast-agents with ENaC-activity could deliver an explanation for the above-mentioned adverse-effects, considering that the contrast-agents got in direct proximity to ENaC-expressing tissues, e.g. during excretion by the kidneys. Therefore it was examined, whether the contrast-agent gadolinium-diethylenetriaminepentaacetic-acid (Gd-DTPA), resp. its core-cation gadolinium (Gd<sup>3+</sup>) interferes with human ENaC and thereby affect its activity.

**Methods:** Human αβγENaC was expressed in *Xenopus laevis* oocytes and transmembrane currents were recorded by Two-Electrode-Voltage-Clamp measurements.

**Results:** Gd-DTPA, applied in a concentration which is used for radiological MRI diagnostics (7.5mM), significantly decreased ENaC activity (19±2%), whereas the chelator DTPA alone showed no effect. This suggests that released Gd<sup>3+</sup> is responsible for decreasing ENaC-activity. Applying solely Gd<sup>3+</sup> (0.1mM) showed comparable effects - ENaC-currents were reduced by 17±1%. Further, Gd<sup>3+</sup> significantly increased the halfmaximal inhibition-coefficient (IC<sub>50</sub>) for amiloride from 79±5nM to 114±4nM, but did not affect self-inhibition of ENaC (control: 32±8%; Gd<sup>3+</sup>: 33±7%). The histidine-modifying compound DEPC completely prevented the Gd<sup>3+</sup>-induced ENaC inhibition, arguing for histidines as potential binding-sites for Gd<sup>3+</sup>. **Conclusions:** Gd<sup>3+</sup>, released from Gd<sup>3+</sup>-containing contrast-agents, directly interacts with human ENaC and decreases its activity. This finding provides an explanation for adverse-effects of Gd<sup>3+</sup>-containing contrast-agents as observed in patients.

**P165**

**Atrio-ventricular conduction disorder caused by a mutation in the popeye domain containing protein Popdc2**

\*S. Rinné<sup>1</sup>, B. Ortiz<sup>1</sup>, B. Stallmeyer<sup>2</sup>, S. Zumhagen<sup>2</sup>, E. Schulze-Bahr<sup>2</sup>, N. Decher<sup>1</sup>

<sup>1</sup>Philipps-University Marburg, Vegetative Physiology, Marburg, Germany

<sup>2</sup>Institute for Genetics of Heart Diseases (IfGH), Department of Cardiovascular Medicine, Münster, Germany

Popeye domain containing (Popdc) proteins harbour three transmembrane domains. The carboxyterminal part is localized to the cytoplasm and contains the Popeye domain involved in cAMP binding. We have previously described that Popdc proteins modulate the two-pore-domain potassium channel TREK-1. Popdc proteins recruit TREK-1 channels to the plasma membrane leading to increased current amplitudes. This modulation of TREK-1 is abolished in the presence of high levels of cAMP. Popdc proteins are preferentially expressed in skeletal and heart muscle. We have also shown that transgenic mice deficient for Popdc2 develop stress-induced sinus bradycardia. Here, we report a heterozygous Popdc2 mutation in monozygotic twins presented with third-degree atrio-ventricular block (AVB III°). While classical arrhythmia genes did not harbour mutations, we have identified a nucleotide exchange leading to a premature stop within the Popeye domain of Popdc2. The transcript with the premature stop and the truncated protein were detected in leucocytes and fibroblasts of the index patient, indicating that the expression of the mutant allele is not hindered by nonsense-mediated mRNA decay or proteolytic degradation. We have characterized the truncation mutant using a wide range of methods, including electrophysiological recordings, chemiluminescence assays, fluorescence microscopy, quantitative PCR and molecular modelling. We found that the Popdc2 mutation causes an altered TREK-1 channel regulation. But most importantly, using a functional co-expression screen, we have

identified another cardiac ion channel to be modulated by Popdc2. Dysregulation of this channel by the truncated Popdc2 protein is most likely the primary cause of the conduction disorder observed in our patients.

**P166**

**The influence of the auxiliary subunit TRIP8b on pacemaker channels in thalamocortical system**

\*M. Zobeiri<sup>1</sup>, P. Bista<sup>1</sup>, D. M. Chetkovich<sup>2</sup>, H. C. Pape<sup>1</sup>, T. Budde<sup>1</sup>

<sup>1</sup>Institute of Physiology I, Westfälische Wilhelms-Universität, Münster, Germany

<sup>2</sup>Davee Department of Neurology and Clinical Neurosciences and Department of Physiology, Northwestern University, Chicago, United States

**Question:** The present study was conducted to determine how dysregulation of hyperpolarization-activated and cyclic nucleotide-gated (HCN) channels due to the lack of expression of tetratricopeptide repeat-containing Rab8b-interacting protein (TRIP8b), an auxiliary subunit of HCN channels which contributes to the surface expression and gating of these channels, can contribute to the pathophysiology of absence epilepsy and thalamic oscillatory activity.

**Methods:** Voltage dependency and kinetics of hyperpolarization-activated inward currents (I<sub>h</sub>) were compared in whole cell patch clamp recordings from thalamocortical neurons (TC) of the ventrobasal thalamic complex (VB) and posterior thalamic nucleus (PO), as well as neurons in layer V of the somatosensory cortex (S1) of epileptic TRIP8b null mice (TRIP8b<sup>-/-</sup>) and the non-epileptic wild type (C57Bl/6J) between ages p14 - p25.

**Results:** I<sub>h</sub> was characterized by significantly lower current amplitude and density at -130 mV in TRIP8b<sup>-/-</sup> as compared to the wild type control mice. Analysis of the I<sub>h</sub> steady states activation curves demonstrated a significant shift in voltage-dependency towards more hyperpolarization in all three investigated regions of TRIP8b<sup>-/-</sup>. The TC neurons of VB and Po in TRIP8b<sup>-/-</sup> mice also showed a more hyperpolarized resting membrane potential compared to control animals.

**Conclusion:** The hyperpolarizing shift in resting membrane potential of thalamic relay neurons in TRIP8b<sup>-/-</sup> mice might increase the probability of burst activity from the resting membrane potential. Moreover, down-regulation of I<sub>h</sub> in cortical neurons might increase the excitability of this region, possibly due to an increased input resistance of these cells.

**P167**

**Involvement of the second transmembrane domain of human P2X7 receptors in permeation and gating**

\*A. Pippel<sup>1</sup>, M. S. Stolz<sup>2</sup>, G. Schmalzing<sup>2</sup>, F. Markwardt<sup>1</sup>

<sup>1</sup>Julius-Bernstein-Institute for Physiology, Martin-Luther-University Halle-Wittenberg, Halle/Saale, Germany

<sup>2</sup>Molecular Pharmacology, RWTH Aachen, Aachen, Germany



Immune cells like B-cells and macrophages express P2X7-receptors at the cell membrane. These receptors are ATP-dependent cation channels which are involved in modulation of immune and inflammatory processes. P2X7 receptors are homotrimers of subunits with intracellularly located N- and C-termini, two transmembrane domains and a large extracellular domain comprising the ATP-binding site. We performed single cysteine scanning mutagenesis of amino acids in the second transmembrane domain (TM2) of human P2X7 receptors (hP2X7), a region which is supposed to be involved in pore opening and ion permeation of other P2X receptor channels. *Xenopus laevis* oocytes were injected with cRNAs of the different hP2X7 constructs and ATP-dependent currents were measured using two microelectrode voltage clamp and patch clamp techniques. Only the hP2X7 receptor construct S342C displayed the anticipated sustained reduction of the ATP-induced current after application of the sulfhydryl group modifying cationic reagent MTSEA, probably by blocking the ion channel pore. Six other cysteine mutants between I331C and G345C were found to irreversibly increase the ATP-dependent ion current after MTSEA application. Single channel recording revealed that the stimulatory effect of MTSEA was due to an increase of the open probability. At four of these constructs near S342 the single channel current amplitude was decreased by MTSEA. This indicated an additional partial open channel block. However, the prevailing effect of the increased open probability results in stimulation of macroscopic currents by MTSEA. We conclude that the TM2 region between I331C and G345C is simultaneously involved in permeation and gating of P2X7 receptor channels.

**P168**  
**Pathophysiology of the p.A167V Mutation of KCNJ10 in mammalian cells**

\*E. Tondorf<sup>1</sup>, A. Ratermann<sup>1</sup>, F. Scherl<sup>1</sup>, E. Humberg<sup>1</sup>, M. Reichold<sup>1</sup>, D. Bockenbauer<sup>2</sup>, A. Zdebik<sup>2</sup>, R. Kleta<sup>2</sup>, R. Warth<sup>1</sup>

<sup>1</sup>University of Regensburg, Institute of Physiology, Regensburg, Germany

<sup>2</sup>University College London, Nephrology and Physiology, London, United Kingdom

Mutations of the inwardly rectifying K<sup>+</sup> channel KCNJ10 (Kir4.1) cause the autosomal recessive EAST (or SeSAME) syndrome that is characterized by epilepsy, ataxia, sensorineural deafness, and salt wasting tubulopathy. In renal distal tubules, KCNJ10 dimerizes with KCNJ16 to form basolateral K<sup>+</sup> channels. Here, we investigated the functional consequence of the disease-related p.A167V mutation of KCNJ10 in mammalian cells. When expressed in CHO cells, KCNJ10 wildtype homomers showed mildly inwardly rectified K<sup>+</sup> currents, which were only slightly reduced by the mutation A167V. The membrane potentials of CHO cells expressing A167V homomers were not different from CHO cells expressing KCNJ10 wildtype homomers (~90 mV). In contrast to the mild phenotype of homomeric channels, co-expression of the A167V mutant with KCNJ16 led to very small residual K<sup>+</sup> currents while co-expression of

wildtype KCNJ10 with KCNJ16 led to large inwardly rectified K<sup>+</sup> currents. In parallel, the membrane potential of cells co-expressing A167V/KCNJ16 was depolarized to ~-40 mV compared to ~-80 mV in cells expressing wildtype heteromers. In cell-attached patch clamp experiments on HEK cells co-expressing A167V and KCNJ16, the open probability was strongly reduced. In excised inside-out patches of such cells, channel activity was virtually absent and could not be activated by alkaline pH. In conclusion, the KCNJ10 mutation A167V causes a mild functional impairment of homomeric channels. When co-expressed with KCNJ16, the A167V mutation almost abolished the K<sup>+</sup> current. Therefore, the heteromer-specific loss-of-function appears relevant in the pathophysiology of EAST patients carrying the A167V mutation.

**P169**  
**Evaluating the functional impact of subunit positions in heterotetrameric olfactory CNG channels**

\*J. Schirmeyer, N. Wongsamitkul, G. Ehrlich, T. Zimmer, V. Nache, K. Benndorf

University Hospital Jena, Institute of Physiology II, Jena, Germany

Cyclic nucleotide-gated (CNG) ion channels, key components in the sensory transduction of vision and smelling, are non-selective cation channels, activated by binding of cAMP or cGMP. Heterotetrameric CNG channels of olfactory sensory neurons are composed of two CNGA2 subunits, one CNGA4 and one CNGB1b subunit.

We address the functional role and the arrangement of the different subunits in the heterotetrameric channel. Therefore we designed the possible 12 tetrameric concatamers. Ligand-dependent channel activation of macroscopic currents was examined using the inside-out configuration of the patch-clamp method after expression in *Xenopus* oocytes. All concatamers showed robust expression with current amplitudes comparable with heterotetrameric channels formed by monomeric subunits (685 ± 144 pA, n = 27). However, the current amplitudes were slightly different between individual concatamers, e.g. 207 ± 47 pA (n = 9) for A4-A2-A2-B1b compared to 701 ± 100 pA (n = 29) for A4-B1b-A2-A2 (P < 10<sup>-4</sup>). For all concatamers concentration-activation relationships with either cAMP or cGMP were approximately similar to that for native channels. However, the Hill coefficients for cAMP (~1.5) were consistently smaller than for cGMP (~1.8). Notably, there was no difference for the same cyclic nucleotide among all concatamers. However, a moderate difference between the EC<sub>50</sub> values either for cAMP or cGMP was observed. B1b-A2-A4-A2 seems to be the most and A2-A2-B1b-A4 the least ligand-sensitive channel (cAMP: 1.83 ± 0.13 μM versus 4.29 ± 0.36 μM, P < 10<sup>-6</sup>, cGMP: 0.61 ± 0.06 μM versus 1.14 ± 0.04 μM, P < 0.002). Apparently all arrangements of the subunits are possible, indicating that the functional specificities inferred by the individual subunits do not critically depend on the nature of the neighbor subunits.

**P170**  
**The regulation of the cardiac L-type Ca<sup>2+</sup> current by corticosteroids does not involve altered transcription of the ion channel subunits α<sub>1c</sub> or β<sub>2</sub>**

\*E. Rudakova, M. Wagner, A. Schauer, T. Volk

Institut für Zelluläre und Molekulare Physiologie, Friedrich-Alexander-Universität Erlangen-Nürnberg, Erlangen, Germany

Corticosteroids have been shown to increase the L-type Ca<sup>2+</sup> current (I<sub>CaL</sub>) in cardiomyocytes in vitro by activation of the mineralocorticoid receptor (MR). Since activated MRs serve as a transcription factor, we investigated to what extent the upregulation of I<sub>CaL</sub> in isolated rat cardiomyocytes is caused by an increased mRNA expression of the L-type Ca<sup>2+</sup> channel α- and β-subunits. I<sub>CaL</sub> was assessed in isolated rat left ventricular cardiomyocytes by whole-cell patch-clamp after 24h incubation with control solution or dexamethasone (1 μM) + insulin (100 nM). Under control conditions, the amplitude of I<sub>CaL</sub> remains stable during the 24h of primary culture. 24h incubation with dexamethasone + insulin increased I<sub>CaL</sub> (at 0 mV) by 49% (-1.2 ± 0.9 pApF<sup>-1</sup>, n=15, p < 0.001) compared to control (-8.2 ± 0.6 pApF<sup>-1</sup>, n=15). mRNA expression levels of the L-type Ca<sup>2+</sup> channel α<sub>1c</sub> and β<sub>2</sub> subunits were investigated using real-time RT-PCR after 0, 3, 6 and 24h incubation of isolated myocytes under control conditions and with dexamethasone + insulin; expression levels were normalized to the expression of GAPDH. The expression of both subunits decreased after 24 h down to 40% (α<sub>1c</sub>) respectively 65% (β<sub>2</sub>) of initial value and was not significantly affected by dexamethasone + insulin treatment at each time point tested (n=8). In contrast, the expression of Per-1 mRNA, which is known to be regulated by corticosteroids, increased fivefold after 6h treatment with dexamethasone + insulin. We conclude that the increase in I<sub>CaL</sub> induced by dexamethasone + insulin does not involve altered transcription of the L-type Ca<sup>2+</sup> channel α<sub>1c</sub>- or β<sub>2</sub>-subunits.

**P171**  
**Expression of δβγENaC at the plasma membrane is reduced by mutating two putative phosphorylation sites at the N-terminus of δENaC**

S. Haerteis, \*S. Wallner, C. Korbmacher, R. Rauh

Friedrich-Alexander-Universität Erlangen-Nürnberg (FAU), Institut für Zelluläre und Molekulare Physiologie, Erlangen, Germany

**Question:** The epithelial sodium channel (ENaC) is the rate limiting step for transepithelial sodium transport in sodium absorbing tissues, e.g. the aldosterone-sensitive distal nephron or respiratory epithelia. ENaC is believed to form a heteromeric channel composed of three homologous subunits α, β, and γ (βγENaC). In humans, a δ-subunit can replace the α-subunit, but little is known about the physiological role and regulation of δβγENaC. We previously reported that δβγENaC is activated by intracellular cAMP in *Xenopus laevis* oocytes (Acta Physiol 201 [Suppl. 682] (2011): P279). The aim of the present study was to identify relevant phosphorylation sites. **Methods:** Human wild-type or mutant δβγENaC was expressed in *Xenopus laevis*

oocytes. A chimeric δ<sub>1-538</sub>α<sub>562-669</sub>ENaC subunit was generated using Gibson Assembly® Cloning Kit (NEB). Point mutations were generated by site-directed mutagenesis. Channel function was assessed by measuring <sup>125</sup>I-amiloride (100 μM)-sensitive whole-cell current (ΔI<sub>ami</sub>) with the two-electrode voltage-clamp technique. Intracellular cAMP was elevated by 3-isobutyl-1-methylxanthine (IBMX, 1mM) and forskolin (1μM). Biotinylated cell surface and whole cell protein expression were detected by PAGE and Western blot analysis. **Results:** Raising intracellular cAMP by IBMX/forskolin increased ΔI<sub>ami</sub> of δβγENaC expressing oocytes by ~ 60 %. Replacing the C-terminus of δENaC with that of αENaC (δ<sub>1-538</sub>α<sub>562-669</sub>) did not diminish the stimulatory effect of cAMP indicating that the effect of cAMP is not mediated by the C-terminus of δENaC. In silico analysis (<http://elm.eu.org/>) of the N-terminus of δENaC revealed four putative glycogen synthase kinase 3 β (GSK3β) phosphorylation sites: T15, S19, T61, T65. Mutating these residues to alanine (δT15A/S19A, δT61A/T65A, δT15A/S19A/T61A/T65A) to prevent phosphorylation or mutating them to glutamate (δT15E/S19E, δT61E/T65E, δT15E/S19E/T61E/T65E) to mimic phosphorylation did not affect the stimulation of ΔI<sub>ami</sub> by cAMP. However, baseline ΔI<sub>ami</sub> was reduced by ~ 80 % in δT61E/T65EβγENaC expressing oocytes. In good agreement with this finding, cell surface and whole cell protein expression of δT61E/T65EβγENaC was reduced. **Conclusion:** Our results suggest that phosphorylation of T61 and T65 at the N-terminus of δENaC is not involved in the regulation of δβγENaC by cAMP. However, our data indicate that mutating these sites affects channel synthesis and channel expression at the cell surface.

**P172**  
**Characterization of the olfactory CNG-channel gating at the single-channel level**

\*N. Wongsamitkul<sup>1</sup>, V. Nache<sup>1</sup>, R. Schmauder<sup>1</sup>, M. Eberhard<sup>2</sup>, N. Wiesener<sup>1</sup>, K. Benndorf<sup>1</sup>

<sup>1</sup>Jena University Hospital, Institute of Physiology II, Jena, Germany

<sup>2</sup>Heinrich Heine University Medical Center & Biological Medical Research Center, Düsseldorf University Hospital, Dept. of Experimental and Clinical Hemostasis, Hemotherapy and Transfusion Medicine, Düsseldorf, Germany

Cyclic nucleotide-gated (CNG) channels play a significant role in the sensory transduction in the olfactory and visual system. CNG channels open in response to the binding of cyclic nucleotides (cAMP or cGMP). Native CNG channels are heterotetramers composed of three different subunits: two CNGA2, one CNGA4 and one CNGB1b. It has been shown that the dose-response relation of heterotetrameric channels is shallower and shifted to lower cGMP concentrations compared to homotetrameric channels. To gain further insight into the gating mechanisms of the CNGA2:A4:B1b channel and the functional characteristics of the modulatory CNGA4 and CNGB1b subunits, we performed a detailed analysis of single-channel kinetics in inside-out single-channel patches. We expressed CNGA2, CNGA2+CNGA4, CNGA2+CNGB1b and CNGA2+CN-

GA4+CNGB1b channels in *Xenopus* oocytes and the currents were recorded in the presence of different ligand concentrations at +100 mV.

The following single-channel parameters were considered: single-channel amplitude, single-channel noise, open probability as well as open and closed times. The single-channel current was  $\sim 1.3 \pm 1.06$  pA for the CNGA2+CNGA4+CNGB1b channels and  $\sim 5.7 \pm 0.9$  pA for the CNGA2 channels. Notably, in the heterotetrameric channels, the observed small level of  $\sim 1.3 \pm 1.06$  pA consistently superimposed with very short larger levels, suggesting that the heterotetrameric channel reaches only very briefly the conductance state of the homotetrameric CNGA2 channel. For homotetrameric channels, the open-time histograms were compared with the predictions of the C4L-\*O4L Model derived from ligand binding and activation gating in macroscopic currents (Nache et al., Nat. Commun., 2013). For the heterotetrameric channels new kinetic models are proposed.  $P_o$  at saturating [cGMP] was close to unity for all tested channels with the exception of CNGA2+CNGA4 channels, where  $P_o$  was significantly reduced. The presented data contribute to a better understanding of the role of the CNGA4 and CNGB1b subunits in the heterotetrameric channels and improves our present knowledge about the role of the CNGA2:A4:B1b channels in the olfactory signal transduction.

## Ion channels II

### P173

#### Electrophysiological evidence for PAR2-mediated stimulation of TRPV4 in the *Xenopus laevis* oocytes expression system

\*S. Sostegni<sup>1</sup>, A. Diakov<sup>1</sup>, P. McIntyre<sup>2</sup>, N. Bunnett<sup>3</sup>, C. Korbmacher<sup>1</sup>, S. Haerteis<sup>1</sup>

<sup>1</sup>Friedrich-Alexander-Universität Erlangen-Nürnberg (FAU), Institut für Zelluläre und Molekulare Physiologie, Erlangen, Germany

<sup>2</sup>RMIT University, Health Innovations Research Institute, Bundoora, Australia

<sup>3</sup>Monash University, Monash Institute of Pharmaceutical Sciences, Melbourne, Australia

TRPV4 is a non-selective cation channel of the vanilloid group of TRP (transient receptor potential) ion channels. It has been implicated in diverse pathophysiological processes but its role and mechanisms of activation remain incompletely understood. Proteases that cleave protease-activated receptor 2 (PAR<sub>2</sub>) have been shown to sensitize TRPV4 (Poole et al., J Biol Chem, 2013). This may be

relevant in pathophysiological conditions associated with protease activation, e.g. in inflammation. The aim of the present study was to further investigate the electrophysiological properties of human TRPV4 and its PAR<sub>2</sub>-mediated stimulation. Whole-cell currents were measured in *Xenopus laevis* oocytes expressing TRPV4, PAR<sub>2</sub> or TRPV4/PAR<sub>2</sub> using the two-electrode voltage-clamp technique. Single-channel recordings were performed using the outside-out configuration of the patch-clamp technique. The synthetic TRPV4 activator GSK1016790A (50 nM) and the selective inhibitor HC067047 (100 nM) were used as tools to activate and inhibit TRPV4 currents, respectively. PAR<sub>2</sub> was activated by trypsin (8 nM) or the PAR<sub>2</sub> agonists 2-Furoyl LIGRL-NH<sub>2</sub> (10 μM) or SLIGRL-NH<sub>2</sub> (100 μM). In outside-out patches from TRPV4 expressing oocytes typical TRPV4 channels were detected with a single-channel inward conductance for Na<sup>+</sup> and an outward conductance for K<sup>+</sup> of 112 pS and 82 pS, respectively. Moreover, we demonstrated that GSK1016790A activates TRPV4 currents mainly by increasing the number of active channels in the patch. Using the two-electrode voltage-clamp technique, we demonstrated a concentration and time dependent activation of TRPV4 by GSK1016790A. Importantly, in co-expression experiments (TRPV4/PAR<sub>2</sub>) we showed that activation of PAR<sub>2</sub> by trypsin or by PAR<sub>2</sub> agonists increased TRPV4 currents several fold. Pre-incubation of oocytes co-expressing TRPV4/PAR<sub>2</sub> with BAPTA-AM (100 μM) to buffer intracellular calcium prevented PAR<sub>2</sub>-mediated activation of an endogenous calcium-activated chloride current but did not reduce TRPV4 stimulation. In conclusion, we established functional expression of PAR<sub>2</sub> and TRPV4 in the oocyte expression system and demonstrated that PAR<sub>2</sub> activation by trypsin increases TRPV4 currents. Interestingly, the observed stimulatory effect of PAR<sub>2</sub> activation on TRPV4 is independent of intracellular calcium. Additional studies are needed to determine the calcium independent signalling pathway responsible for PAR<sub>2</sub>-mediated TRPV4 stimulation. Our results indicate that the oocyte system is a powerful approach for detailed studies of mechanisms by which TRP channels are regulated.

### P174

#### Elucidating the role of the modulatory subunits in olfactory CNG-channels

\*V. Nache<sup>1</sup>, N. Wongsamitkul<sup>1</sup>, M. Eberhard<sup>2</sup>, R. Schmauder<sup>1</sup>, N. Wiesener<sup>1</sup>, T. Zimmer<sup>1</sup>, K. Benndorf<sup>1</sup>

<sup>1</sup>Jena University Hospital, Institute of Physiology II, Jena, Germany

<sup>2</sup>Düsseldorf University Hospital, Department of Experimental and Clinical Hemostasis, Hemotherapy and Transfusion Medicine, Düsseldorf, Germany

Cyclic nucleotide-gated (CNG) channels play an important role in the olfactory and visual signal-transduction cascades. CNG channels are heterotetramers composed of three homolog subunits of which only one type, the CNGA2 subunit, can form functional homotetrameric channels when expressed in heterologous systems. CNGA4 and CNGB1b subunits only modulate the function of the

heterotetrameric channels. The individual contribution of these subunits to the activation process and their physiological role has not been elucidated so far. Herein, the role of the modulatory subunits was analysed in detail by measuring on the one hand ligand binding and gating in macroscopic patches, thereby using patch-clamp fluorometry, and on the other hand the gating kinetics at different cGMP concentrations in single channels. The results show that the CNGA4 and CNGB1b subunit confer to the heterotetrameric channel faster binding and activation as well as unbinding and deactivation. By coexpressing either CNGA4 or CNGB1b subunits with CNGA2 subunits containing disabled binding domains, we observed significant cGMP binding only to the CNGA4 but not to the CNGB1b subunit. At the single-channel level we studied heterotetrameric channels containing besides CNGA2 subunits either a CNGA4 or a CNGB1b subunit. Evaluated were the single-channel conductance, the open probability,  $P_o$ , as well as closed and open times. The single-channel current amplitude was independent of the cGMP concentration, being  $1.5 \pm 0.07$  pA for CNGA2:A4 and  $4.5 \pm 0.04$  pA for CNGA2:B1b channels.  $P_o$  at saturating [cGMP] was close to unity for CNGA2, CNGA2:A4:B1b, and CNGA2:B1b channels but significantly smaller for CNGA2:A4 channels. Notably, CNGA2:A4:B1b channels reached for only very short sojourns the large and dominating conductance state of the homotetrameric CNGA2 channel. Our results provide new insight into the contribution of the CNGA4 and CNGB1b subunit to the gating of olfactory CNG channels and improve our understanding regarding their role in the olfactory transduction. Possible physiological implications are discussed.

### P175

#### Depolarization-induced attenuation of somatic GABAergic responses

\*R. Chen, H. Luhmann, W. Kilb

Johannes Gutenberg University, Mainz, Germany

Depolarization-induced suppression of inhibition is a well-known mechanism for short-time plasticity and is mainly mediated by the endocannabinoid system acting on pre-synaptic neurotransmitter release. Here we demonstrate that depolarization also induced short-time plasticity of somatic GABA responses. We performed whole-cell patch-clamp recordings from CA3 pyramidal neurons of juvenile mice to investigate the influence of a 5 s depolarization to 0 mV on GABAergic responses induced by a focal application of 20 μM GABA to the cell soma. GABA application induced an inward current that was transiently reduced by  $34.9 \pm 4.7$  % after the depolarization. GABA responses returned to baseline levels within 30-60 s. The depolarization-induced suppression of GABA responses was unaffected by 10 mM EGTA in the pipette solution or in nominally Ca<sup>2+</sup>-free solutions, suggesting that it is independent of a Ca<sup>2+</sup> influx. In addition, the depolarization-induced suppression of GABA response was unaffected in the presence of 0.5 μM TTX. However, lidocaine (5 mM) in the bath-

ing solution or its derivative QX-314 (5 mM) in the pipette solution, as well as bath application of Cs<sup>+</sup> or Cs<sup>+</sup>-based pipette solution, abolished the depolarization-induced suppression of GABA responses, suggesting an involvement of a K<sup>+</sup> conductance in the depolarization-induced suppression of GABA response. However, the transient change of GABA responses after depolarization was not accompanied by a decrease of input resistance, demonstrating that an indirect effect via space-clamp does not contribute to our observation. In summary our results demonstrate that sustained depolarization can influence GABA receptors by a yet unknown mechanism.

### P176

#### Functional assessment of murine epithelia cell lines as a basic model system in Cystic Fibrosis research

\*K. Tomczak<sup>1</sup>, N. Bangel-Ruland<sup>1</sup>, C. U. Cotton<sup>2</sup>, W.-M. Weber<sup>1</sup>

<sup>1</sup>University of Muenster, Institute of Animal Physiology, Muenster, Germany

<sup>2</sup>Case Western Reserve University, Departments of Pediatrics and Physiology and Biophysics, Cleveland, United States

**Question:** Human primary epithelial cell cultures and immortalized cell lines are a common tool for the study of the underlying defects in the frequent human genetic disease Cystic fibrosis (CF). However, their use is highly limited in functional studies and therefore, new cell lines need to be validated for electrophysiological measurements. In this study the established murine cell lines mSEC1-CF (S498X mutation) and mSEC1-nonCF were analyzed for the use in transepithelial current measurements for a project involving functional CFTR correction by Sleeping Beauty (SB)-based CFTR vectors and CFTR-specific Zinc Finger Nucleases (ZFN).

**Methods:** First, we performed genotyping by PCR analysis of DNA extracts from mSEC1-nonCF and mSEC1-CF cells to assure correct genotype expression. Afterwards, we analysed the functional phenotype by electrophysiological measurements in Ussing chamber experiments. We characterized the CFTR secretion in the cells using a CFTR activating cAMP cocktail and the CFTR specific inhibitor CFTRinh172. Furthermore, we identified the CFTR protein expression by Western blot analysis.

**Results:** The genotyping analysis showed that both cell lines express the right genotype and the electrophysiological Ussing chamber measurements demonstrated the appropriate functional phenotype for both cell lines. Moreover, we were able to identify a suitable antibody to detect CFTR in mouse cells.

**Conclusions:** The murine cell lines mSEC1-CF and mSEC1-nonCF cells reflect the CF and nonCF situation and are well suitable for the ongoing studies using the two novel strategies (SB and ZFN) for a long long-term therapeutic transgene expression.

P177

**Breaking new ground for cystic fibrosis therapy: CFTR-mRNA restores defect Cl-transport**

\*N. Bangel-Ruland<sup>1</sup>, K. Tomczak<sup>1</sup>, E. Fernández Fernández<sup>1</sup>, C. Rudolph<sup>2</sup>, J. Rosenecker<sup>2</sup>, W.-M. Weber<sup>1</sup>

<sup>1</sup>University of Muenster, Institute of Animal Physiology, Muenster, Germany

<sup>2</sup>University of Munich, Department of Pediatrics, Munich, Germany

**Question:** Cystic fibrosis (CF) is the most frequent lethal genetic disease caused by a defective gene coding for the cystic fibrosis transmembrane conductance regulator (CFTR). The most common mutation inducing CF is  $\Delta F508$ . In the past it became obvious that several mostly DNA based gene therapy approaches failed to correct CFTR symptoms in the airways of CF patients. We developed a new strategy to restore CFTR protein function using optimized wtCFTR-mRNA. We aimed the question if the transfection of human respiratory epithelial cells with this wtCFTR-mRNA is functional and effective.

**Methods:** We used primary cultured human nasal epithelial (HNE) cells and the human bronchial epithelial cell line CFBE41o- that stably expresses  $\Delta F508$ -CFTR and carried out transepithelial Ussing chamber measurements after transfection with optimized wtCFTR-mRNA. We confirmed the electrophysiological data using immunofluorescence and protein biochemical approaches.

**Results:** Transfection of the CFBE41o- cells with wtCFTR-mRNA restored cAMP-induced CFTR currents similar to the values seen in control cells (16HBE14o-). Using immunofluorescence approaches we demonstrated that a considerable amount of CFTR is located at the apical surface or nearby regions in the CF cells after transfection. Western blot analyses of wtCFTR-mRNA transfected CFBE41o- cells confirmed these findings. Furthermore, we demonstrated physiological relevance by using primary cultured HNE cells and showed a nearly doubled increase in cAMP-stimulated CFTR current after transfection.

**Conclusion:** The results of the present study provide evidence that mRNA transfection of cystic fibrosis airway epithelial cells could be capable of restoring CFTR function defective in the airways of CF patients.

P178

**TRPC1 and TRPC6 channels - Important players in hypoxia-mediated activation of pancreatic stellate cells**

\*N. Nielsen<sup>1</sup>, K. Kondratska<sup>2</sup>, N. Prevarskaya<sup>2</sup>, A. Schwab<sup>1</sup>

<sup>1</sup>Institute of Physiology II, Münster, Germany

<sup>2</sup>INSERM U.1003, Lille, France

Pancreatic cancer is characterized by the presence of an excessive amount of connective tissue primarily formed by pancreatic stellate cells (PSCs). This elevation in connective tissue leads to a hypoxic and acidic tumor microenvironment. We postulate that PSCs get activated by a hypoxic and acidic tumor microenvironment. This response triggers signaling pathways involving intracellular Ca<sup>2+</sup> transients mediated by TRPC channels, which have already been linked to

cell migration, chemotaxis and hypoxia in other cell types. We profiled the expression of TRPC1-7 in PSCs with qPCR, revealing the highest level for TRPC1 and TRPC6 channels. We then investigated their role in PSCs isolated from TRPC1<sup>-/-</sup> and TRPC6<sup>-/-</sup> mice. Using video microscopy we monitored the chemokinetic response of PSCs to PDGF in 3D matrices and the chemotactic response on a 2D matrix. Further, PSCs were incubated with 1% O<sub>2</sub> or with dimethylglyoxaline (DMOG) to analyze the effect of hypoxia. In the presence of PDGF, migration velocity of PSCs increased, cell translocation distance almost doubled, and the PSCs efficiently chemotaxed in a gradient of PDGF. Within a hypoxic and acidic 3D matrix TRPC6<sup>-/-</sup> PSCs failed to increase their migration velocity, while WT and TRPC1<sup>-/-</sup> PSCs did so. This observation was confirmed on 2D surfaces in chemically induced hypoxia, which also increased migration velocity and translocation of WT PSCs. This activation was almost absent in TRPC1<sup>-/-</sup> and TRPC6<sup>-/-</sup> PSCs. Additionally, hypoxia increased TRPC1 protein expression (~2 fold). We can therefore conclude that TRPC1 and TRPC6 are involved in PSCs response to hypoxia.

P179

**Upregulation of hERG K<sup>+</sup> channels by B-RAF**

\*T. Pakladok<sup>1</sup>, Z. Hosseinzadeh<sup>1</sup>, A. Almilaji<sup>1</sup>, A. Lebedeva<sup>1,2</sup>, E. Shumilina<sup>1</sup>, I. Alesutan<sup>1</sup>, F. Lang<sup>1</sup>

<sup>1</sup>University of Tuebingen, Department of Physiology, Tuebingen, Germany

<sup>2</sup>Institute of Experimental Medicine, Department of Immunology, St. Petersburg, Russia

**Question:** Human ether-a-go-go related-gene K<sup>+</sup> channels (hERG) participate in the regulation of tumor cell proliferation and apoptosis. HERG channel activity is up-regulated by growth factors. Kinases sensitive to growth factor signaling include the serine/threonine protein kinase B-RAF. The present study thus explored whether B-RAF influences hERG channel expression and activity.

**Methods:** hERG channels were expressed in Xenopus oocytes with or without wild-type B-RAF, hERG channel activity was determined utilizing dual-electrode voltage clamp and hERG protein abundance in the cell membrane was analysed utilizing confocal microscopy and chemiluminescence. Moreover, in rhabdomyosarcoma RD cells the effect of B-RAF inhibitor PLX-4720 on hERG-mediated current was quantified by whole-cell patch clamp and hERG cell surface protein abundance by utilizing biotinylation of cell surface proteins and flow cytometry.

**Results:** Co-expression of wild-type B-RAF in hERG-expressing Xenopus oocytes significantly increased hERG channel activity and hERG channel protein abundance in the cell membrane. Treatment for 24 hours of B-RAF and hERG-expressing Xenopus oocytes with PLX-4720 (10  $\mu$ M) significantly decreased hERG-mediated currents. Similarly, in rhabdomyosarcoma RD cells, treatment for 24 hours with PLX-4720 significantly decreased hERG cell membrane protein abundance and hERG-mediated currents. **Conclusions:** B-RAF is a powerful regulator of hERG channel activity and cell surface hERG protein abundance.

P180

**Dose and time dependency of functional CFTR expression due to wtCFTR-mRNA transfection**

\*E. Fernández Fernández, N. Bangel-Ruland, K. Tomczak, W.-M. Weber

University of Muenster, Institute of Animal Physiology, Muenster, Germany

**Question:** Cystic fibrosis (CF) is the most common life-threatening inherited disease in the Caucasian population. It is caused by genetic defects in the cystic fibrosis transmembrane conductance regulator gene (CFTR). CFTR encodes for a cAMP-regulated chloride channel located in the apical membrane of polarized epithelial cells. In the forefront we successfully restored Cl<sup>-</sup> secretion in human CF epithelia cells using optimized wtCFTR-mRNA. In the present study we assess the minimal mRNA concentration that is needed for a proper functional CFTR expression. Furthermore, we determined the persistence of the CFTR expression over a period of 48h.

**Methods:** We used primary cultured human nasal epithelial (HNE) cells and carried out transepithelial Ussing chamber measurements after transfection with optimized wtCFTR-mRNA. We reduced the wtCFTR-mRNA amount stepwise to determine the minimal concentration that is needed for the most efficient restoration of the functional chloride secretion. Furthermore, the duration of the CFTR expression is evaluated 24 and 48h after transfection.

**Results:** In Ussing chamber experiments we showed an increase in the cAMP-stimulated CFTR current 24 and 48h after wtCFTR-mRNA transfection in HNE cells. This current could also be inhibited by the specific CFTR blocker CFTRinh172. A reduction of the used mRNA dose (0.6  $\mu$ g/cm<sup>2</sup>) resulted in a proper functional chloride secretion.

**Conclusions:** From these data, we conclude that it is possible to sustain the successful restoration of the defective CFTR function even by a reduction of the wtCFTR-mRNA concentration and to extend the duration of the CFTR expression over a time period of 48h.

P181

**A novel HCN2 pacemaker channel interaction partner modulates surface expression and channel conductivity**

\*N. Silbernagel<sup>1</sup>, M. Walecki<sup>1</sup>, S. Rinné<sup>1</sup>, N. Decher<sup>1</sup>

<sup>1</sup>Philipps-University of Marburg, Institute of Physiology und Pathophysiologie-Vegetative Physiologie, Marburg, Germany

Hyperpolarization-activated cyclic nucleotide-gated (HCN) channels are primarily expressed in the sino-atrial node and in neuronal tissue. Their currents named I<sub>p</sub>, I<sub>h</sub> or I<sub>q</sub> play a major role in generating spontaneous pacemaker activity. HCN channel trafficking and gating are modulated by cAMP, PIP<sub>2</sub> and the auxiliary subunit Trip8b. In our study we have identified a novel HCN channel modulating protein using a split-ubiquitin yeast-two-hybrid screen with HCN2 and a human brain cDNA library. Further yeast-two-hybrid assays and pull-down experiments confirmed the protein-protein interaction with HCN2. Electrophysiological recordings and luminometric surface expression assays showed concen-

tration dependent effects on current amplitudes and voltage-dependence of HCN2 channel activation. In particular low concentration of the novel HCN interaction partner increase conductivity of the channel. The accessory protein modulates current densities via an interaction with the N-terminus of HCN1 and HCN2, whereas no interaction and channel modulation was observed for HCN4. Fluorescence imaging experiments after co-transfection in COS-7 cells revealed a strong co-localization of the subunit with HCN2 and a delay in HCN2 channel surface expression. We conclude that the novel accessory protein identified in our yeast-two-hybrid screen has a regulatory effect on the cellular distribution and the conductance of HCN2 channels.

P182

**Relationship between activation of the epithelial sodium channel and water reabsorption after apical volume expansion in airway epithelia**

\*H. Schmidt<sup>1</sup>, C. Michel<sup>1</sup>, F. Kielgast<sup>1</sup>, D. Neubauer<sup>2</sup>, K. Thompson<sup>1</sup>, M. Frick<sup>1</sup>, B. Mizaikoff<sup>2</sup>, P. Dietl<sup>1</sup>, O. H. Wittekindt<sup>1</sup>

<sup>1</sup>Ulm University, Institute of General Physiology, Ulm, Germany

<sup>2</sup>Ulm University, Institute of Analytical and Bioanalytical Chemistry, Ulm, Germany

Apical volume expansion (AVE) is shown to activate the epithelial sodium channel (ENaC) via inducing proteolytic cleavage of its  $\gamma$ -subunit. We aimed on the question to which extend the modulation of ENaC activity effects water resorption after AVE in lung epithelia. Water resorption was investigated by the novel D<sub>2</sub>O dilution method and ENaC activity was measured in Ussing chamber experiments.

Water resorption after AVE can be divided in an early low or non resorptive phase (LRP) and a late high resorptive phase (HRP). LRP lasted 4 h or 2 h after AVE with resorption rates of almost zero or 0.7  $\pm$  0.4  $\mu$ l/h\*cm<sup>2</sup> in NCI-H441 cells and human tracheal epithelial cells (hTEpC), respectively. During HRP resorption rate was 1.7  $\pm$  0.1  $\mu$ l/h\*cm<sup>2</sup> in H441 cells and 2.8  $\pm$  0.1  $\mu$ l/h\*cm<sup>2</sup> in hTEpC. Onset of HRP in H441 cells did not depend on AVE volume. Resorption stopped when apical volume was reduced to 11.1  $\pm$  0.6  $\mu$ l/cm<sup>2</sup>. ENaC was maximally activated 20 min after AVE. When AVE was 75  $\mu$ l/cm<sup>2</sup> ENaC remained activated even 16 h after AVE. An AVE of 15  $\mu$ l/cm<sup>2</sup> did not result in maximally activated ENaC and activity returned to basal levels at 16 h after AVE. We hypothesize that ENaC activation is not the major trigger of the onset of HRP. However, offset of HRP is associated with ENaC inactivation.

Supported by BIU D.5007 to OW

P183

**TRPM7 is a potential diagnostic marker and therapeutic target in stroke patients**

\*C. Eider<sup>1</sup>, W. Jessen<sup>1</sup>, K. Gröschel<sup>2</sup>, F. Birklein<sup>2</sup>, D. Prawitt<sup>1</sup>

<sup>1</sup>Johannes Gutenberg University Medical Centre, Molecular Pediatrics, Centre for Pediatrics and Adolescent Medicine, Mainz, Germany  
<sup>2</sup>Johannes Gutenberg University Medical Centre, Department of Neurology, Mainz, Germany

**Background and Question:** TRPM7 is a member of the transient receptor potential melastatin-like (TRPM) subfamily of TRP-ion channels. This ion channel is ubiquitously expressed as a bifunctional protein, consisting of both a functional ion channel proportion and a N-terminal atypical Ser/Thr  $\alpha$ -kinase. TRPM7 participates in many physiological and pathophysiological cellular aspects, including  $Mg^{2+}/Ca^{2+}$ -homeostasis, proliferation, neurotransmitter release, migration and cell adhesion. TRPM7 is also known to be a keyplayer in the ROS-induced neuronal cell death after ischemic insults. In vitro and in vivo experiments in rats and cultured neuronal cells showed that TRPM7 and the TRPM7 mediated ion currents are highly overexpressed after ischemic insults and trigger apoptosis in these neuronal cells. Affected neurons could be rescued by abolishing TRPM7 expression or suppressing of TRPM7 currents. Stroke or ischemic insults are often caused by a thrombus that, similar to the mentioned experiments, abolishes the normal blood flow needed to supply the brain and the neurons with oxygen and nutrients. It is tempting to speculate, that TRPM7 could also be upregulated in these thrombi and the adjacent neuronal cells.

**Methods:** We consequently analyze the TRPM7 expression in the material which we obtained from surgical thrombectomies after establishing a reliable RNA extraction and qRT-PCR protocol.

**Results:** We present our preliminary data of this ongoing study and the potential correlation between TRPM7 expression in the analyzed material and the outcome for the patient.

**Conclusion:** Our data suggest that TRPM7 could be a promising target for the preventive treatments in Apoplex cerebri patients.

**P184**

**The endogenous expression of anoctamins 2 and 4 in the eye**

\*S. Keckeis<sup>1</sup>, N. Reichhart<sup>1</sup>, D. Salchow<sup>1</sup>, V. M. Milenkovic<sup>2</sup>, O. Strauß<sup>1</sup>  
<sup>1</sup>Charité Universitätsmedizin Berlin, Berlin, Germany  
<sup>2</sup>University Medical Centre, Regensburg, Germany

Anoctamins are a family of transmembrane proteins with recently identified ion channel function, e.g. anoctamin-2, which functions as a  $Ca^{2+}$ -dependent  $Cl^-$  channel in photoreceptors. We explored the role of anoctamins in the eye by means of whole-cell patch-clamp techniques and immunocytochemistry. In the fresh tissue, RT-PCR showed expression of ANO2 and ANO4 in the retinal pigment epithelium (RPE) and in lens cells. Staining of both the juvenile human lens cells and cells of the human RPE cell line ARPE-19 against ANO4 confirmed the ANO4 expression in the plasma membrane. Staining of mouse retina against ANO4 revealed a more precise localization in the basolateral

membrane of the RPE. Immunocytochemical experiments against ANO2 showed the same results. We performed whole-cell patch-clamp experiments with the ARPE-19 cells and human lens cells. In ARPE-19 cells, the application of the  $Ca^{2+}$ -ionophore ionomycin under  $K^+$ -free and intracellular low  $Cl^-$  conditions led to an increase in membrane conductance accompanied with a depolarization of the membrane potential. The current showed a reversal potential of +6.09 mV. Preliminary data in lens cells showed a comparable increase in the membrane conductance in response to  $Ca^{2+}$  elevation by ionomycin application. Since cells depolarized under intracellular low  $Cl^-$  concentration we can rule out the effect as a  $Cl^-$  channel; due to the  $K^+$ -free conditions maxi-K channels were not involved in this current response. These data and previous publications let us suspect that the current was a  $Ca^{2+}$ -dependent cation current carried by ANO4.

**P185**

**Characterization of  $Ca^{2+}$  currents and  $Ca^{2+}$  transients in cultured neonatal mouse spiral ganglion neurons**

\*T. Eckrich, F. Stephani, V. Scheuer, K. Blum, S. Münkner, J. Engel  
 Saarland University, Biophysics, Homburg, Germany

Spiral ganglion neurons (SGNs) transmit the entire auditory information transduced by hair cells to the brain. Myelinated type I SGNs contact inner hair cells, establish precise 1 to 1 connections and comprise 95% of all SGNs. SGNs express somatic, dendritic and axonal (presynaptic) voltage-activated  $Ca^{2+}$  channels. In mature, hearing mice their  $Ca^{2+}$  currents are mediated by L-, P/Q-, N-, R- and T-type channels (Lv et al., J Neurosci 2012), but very little is known about the  $Ca^{2+}$  channel composition in neonatal (pre-hearing) SGNs. We recorded  $Ca^{2+}$  currents in cultured neonatal SGNs using whole cell patch-clamp experiments. And found that mouse SGNs are myelinated as early as postnatal day 2. Patch-clamp recordings were possible after culturing SGNs for several days.  $Ca^{2+}$  currents were isolated from large  $K^+$  and  $Na^+$  currents using various blockers and were mediated by L- and non-L pore-forming  $\alpha 1$  subunits. In order to estimate if culturing of SG tissue affects the contribution of  $Ca^{2+}$  channel subtypes, we performed  $Ca^{2+}$  imaging. Somatic  $Ca^{2+}$  transients ( $\Delta F/F_0$ ) could be elicited by applications of a depolarising 70 mM  $K^+$  solution and were abolished in  $Ca^{2+}$ -free extracellular solution. Furthermore, the application of Nimodipine and Mibefradil largely reduced depolarization-induced increases in  $\Delta F/F_0$ , indicating that somatic  $Ca^{2+}$  channels were mostly L- and T-type. Altogether, we have established a culture method allowing for patch-clamp recordings in neonatal mouse SGNs. Using  $Ca^{2+}$  imaging we were able to estimate cell culturing effects on  $Ca^{2+}$  channel subtypes.

Funding: DFG PP1608, DFG SFB 1027, DFG SFB 894

**P186**

**Mechanism of slow repriming of voltage-gated Na channels by Lidocaine**

V. Gawali, P. Lukacs, R. Cervenka, L. Rubi, X. Koenig, K. Hilber, \*H. Todt  
 Medical University of Vienna, Dpt. of Neurophysiology & Neuropharmacology, Vienna, Austria

**Question:** Local anaesthetics (LA) exert their action by prolongation of the time course of repriming of voltage-gated Na channels after repolarization of the action potential. This may result from slow drug-dissociation from fast inactivated states or, alternatively, from stabilization of a native slow inactivated state ( $I_M$ , Chen ZH et al. J Physiol. 524:37). We sought to determine the nature of the high affinity state for LA binding by investigating mutations that produce different amplitudes of  $I_M$ .

**Methods:** The C-terminal part of transmembrane S6 segment of domain IV (DIV-S6) is an important determinant of inactivation gating and LA block. We performed serial cysteine scanning mutagenesis of positions 1575-1586 in DIV-S6 of rNav1.4 channels and investigated the relationship between changes in mutation-induced alterations of  $I_M$  and respective changes in LA-induced prolongation of recovery. The constructs were expressed in TsA201 cells and studied by means of whole-cell patch-clamp technique. We examined the time course of recovery from fast and slow inactivation produced by 50 ms and by 10 s conditioning pulses to -20 mV, respectively.

**Results:** The LA Lidocaine (500  $\mu M$ ; LIDO) significantly slowed recovery from fast inactivation in all tested constructs except F1579C. The time constant of LIDO - induced slow recovery was ~ 150 ms. Under LIDO-free conditions a similar time constant of slow recovery was found most constructs following 10 s depolarization, presumably reflecting recovery from native  $I_M$ . However, the fraction of channels recovering from  $I_M$  ( $F-I_M$ ) varied greatly among the tested constructs. LIDO significantly increased  $F-I_M$  in most constructs. Interestingly, there was a significant negative correlation between  $F-I_M$  without LIDO and the LIDO-induced increase in  $F-I_M$  ( $R^2=0.91$ ; P), i.e. LIDO was most effective in increasing  $F-I_M$  if  $F-I_M$  under drug-free conditions was low. This was most evident with the mutation M1585C in which  $F-I_M$  was 0 under LIDO-free conditions but increased to  $0.73 \pm 0.02$  with LIDO.

**Conclusion:** The data suggest that in the tested constructs slow recovery with LIDO reflects slow dissociation from fast inactivation rather than recovery from  $I_M$ . Funding support: Austrian Science Fund W1232-B11

**P187**

**The impact of human glutamate receptor 2 autoantibodies on  $\alpha$ -amino-3-hydroxy-5-methyl-4-isoxazolepropionic acid receptor mediated synaptic transmission**

\*H. Haselmann<sup>1,2</sup>, B. Grünewald<sup>1,2</sup>, C. Geis<sup>1,2</sup>  
<sup>1</sup>Hans-Berger-Klinik für Neurologie, Universitätsklinikum Jena, Jena, Germany  
<sup>2</sup>Integrated Research and Treatment Center, Center for Sepsis Control and Care (CSCC), Jena University Hospital, Jena, Germany

**Question:** Autoantibodies to  $\alpha$ -amino-3-hydroxy-5-methyl-4-isoxazolepropionic acid receptors (AMPA) were recently described in the sera of patients with limbic encephalitis suffering from memory dysfunction, seizures, psychotic episodes, and reduced consciousness. Here, we purified autoantibodies from plasma exchange material of a patient with limbic encephalitis. The patient IgG fraction showed high specificity to glutamate receptor 2 (GluR2) subunit which is crucial for AMPAR function, most importantly for calcium permeability. Thus, patient autoantibodies may interfere with excitatory synaptic transmission and long-term-potential (LTP).

**Methods & Results:** We used a combination of electrophysiological measurements and imaging methods to reveal the influence of autoantibodies against GluR2 subunits on a molecular basis. Electrophysiological measurements showed impairments in short-term plasticity of dentate gyrus granule cells of hippocampal brain slices after incubation with human IgG. Furthermore the effects of autoantibodies on synaptic transmission of cultured hippocampal neurons were investigated by single synapse stimulation by glutamate iontophoresis. Incubation experiments with patient IgG showed a decrease in GluR2 containing synaptic boutons in cultured hippocampal neurons after 24 hours.

**Conclusion:** In conclusion, human autoantibodies targeted to the AMPAR GluR2 subunit may influence fast excitatory synaptic transmission by reducing surface expression of GluR2 subunit containing AMPAR.

**P188**

**Salt-bridge formation of three highly conserved aminoacids during gating in rASIC1a**

\*K. Augustinowski, S. Gründer  
 RWTH Aachen, Physiology, Aachen, Germany

Acid-sensing ion channels belong to the Degenerin/Epithelial sodium channels. They are expressed in the nervous system and are activated by protons. Previous work has shown that His72, His73 and Asp78 influence the gating mechanism if mutated. The crystal structure of the trimeric cASIC1 indicates that His73 of one subunit could form a salt-bridge with Asp78 from an adjacent subunit. To assign the formation of a salt-bridge to a particular state of gating (closed, open, desensitized) of rASIC1a, we used the double-mutant cycle analysis. We mutated the three amino acids to alanine, individually and in pairs, and determined the activation and deactivation constants with a piezo-driven application system, to assure a solution exchange less than 2 ms. Furthermore we used two-electrode voltage clamp (TEVC) experiments, to determine the pH values for half-maximal activation and time constants of desensitization and recovery. To confirm these findings, we introduced cysteine side-chains at positions 72, 73 and 78 and modified cysteines by MTS-reagents. Modification significantly reduced the current responses of H73C and D78C. The treatment of the cysteines with MTS-reagents at different states of gating corroborates the close position of these aminoacids. Additionally, the treatment of H73CD78C with

hydrogen peroxide and the reducing reagent DTT gave further evidence for the interaction of these aminoacids in the closed state. This study provides first evidence that these three highly conserved aminoacids interact during channel gating by building a salt-bridge.

**P189**

**Effects of mutations and putative regulatory proteins on the activity of TRPM1 channels**

\*F. Schneider, M. Behrendt, J. Oberwinkler  
Philipps-University Marburg, Institute for physiology and pathophysiology, Marburg, Germany

TRPM1, a tetrameric non-selective cation channel and the founding member of the Transient-Receptor-Potential-Melastatin channel group, is expressed on the post-synaptic side of the sign-inverting synapse between photoreceptor cells and the dendritic tips of ON-bipolar cells in the mammalian retina. Glutamate released from photoreceptor cells into the synaptic cleft triggers an intracellular G-protein coupled signaling cascade in ON-bipolar cells which leads to an inhibition of TRPM1. Since direct interaction partners and the course of the signaling cascade are not completely elucidated it is also not understood how loss-of-function mutations of TRPM1 lead to Congenital Stationary Night Blindness (CSNB). We therefore asked why mutations in TRPM1 lead to CSNB and how the activity of TRPM1 is regulated. In a heterologous expression system we studied the impact of mutations on the biophysical characteristics of TRPM1 channels and the interaction with signaling proteins, e.g.  $\beta/\gamma$ -subunits and RGS-proteins in calcium-imaging and patch-clamp experiments. Out of three examined mutations in TRPM1, two do not lead to a functional channel whereas one (p.A1068T) was still active, although it is associated with a CSNB-phenotype in mice. This mutation lies in the so called LYAMEIN-motif which is a part of the pore region and discriminates TRPM1 from its closely related homolog TRPM3. Our preliminary data indicate that this mutation leads to an increased constitutive activity of this channel. Furthermore we identified a region of TRPM1 that is necessary for its inhibition by G-protein coupled receptors.

**P190**

**Molecular basis for anion selectivity in claudin-17-based paracellular channels**

M. P. Conrad, D. Günzel, J. Piontek, M. Fromm, \*S. M. Krug  
Charité - Universitätsmedizin Berlin, Institute of Clinical Physiology, Berlin, Germany

**Question.** Tight junctions (TJ) regulate the transport of solutes and water through the paracellular pathway. Claudins are a family of tetraspan TJ-proteins with two extracellular loops (ECL1 and -2). Claudin-17 (Cldn17) forms a paracellular channel and is one of two known claudins with distinct anion selectivity. Its main abundance is in the proximal

nephron. The molecular determinants of its anion selectivity are yet unknown and were characterized in this study.

**Methods.** MDCK C7 cells, a kidney cell line genuinely devoid of Cldn17, were stably transfected with 3xFLAG-tagged mutant or wild-type Cldn17. Using site-directed mutagenesis, we introduced single amino acid substitutes in ECL1 and -2. Expression and localization were validated by WB and IF staining. Charge selectivity was obtained from dilution potentials measured in Ussing chambers.

**Results.** While vector controls exhibited cation selectivity, wtCldn17-transfected MDCK C7 cells switched to anion selectivity. Charge-reversing (K65E), charge-neutralizing (K65A) and charge-maintaining (K65R) mutations at lysine 65 led to loss of anion selectivity. Furthermore, in ECL1 mutations R31E, E44A and E48Q/K also abolished anion selectivity of Cldn17, whereas charge-neutralizing mutations (R45, R56, R59 and R61) had no effect. In ECL2, position H154, but not Y149, was identified to contribute to anion selectivity.

**Conclusion.** In ECL1, positions R31, E44, E48 and K65 are crucial for anion selectivity of cldn17. Contrary to the assumption that only ECL1 establishes charge selectivity, we report for the first time that position H154 within ECL2 influences charge selectivity. Thus, both ECLs are essential determinants for charge selectivity of a claudin channel.

**P190b**

**Function of Ca<sub>v</sub>2.3 Ca<sup>2+</sup> channels in sinoatrial impulse conduction**

\*E. Tevoufouet<sup>1</sup>, M. Dibué<sup>1,2</sup>, F. Neumaier<sup>1</sup>, J. Hescheler<sup>1</sup>, F. Nguemo<sup>1</sup>, T. Schneider<sup>1</sup>

<sup>1</sup>Institute of Neurophysiology, Köln, Germany

<sup>2</sup>University Hospital, Heinrich-Heine-University, Department of Neurosurgery, Düsseldorf, Germany

**Background:** Faultless impulse generation and conduction from the sinoatrial node (SAN) is a prerequisite for a normal heartbeat in mammals, representing a complex and vital function involving multiple ionic channels. While the function of L- and T-type Ca<sup>2+</sup> channels is well established in the heart, little is known about the role of the Ca<sub>v</sub>2.3 Ca<sup>2+</sup> channels in this organ.

**Objective:** To investigate the role of Ca<sub>v</sub>2.3 Ca<sup>2+</sup> channels in impulse conduction in the SAN using the isolated perfused heart technique, electrocardiograms of Ca<sub>v</sub>2.3-deficient control mice were evaluated focusing on P-wave indices. **Results:** Critical evaluation of P-wave indices and morphology in isolated perfused hearts mice from both genotypes revealed a significantly lower P-wave amplitude (PWA) in Ca<sub>v</sub>2.3-deficient hearts under baseline conditions (p = 0.013). Although no significant difference was found when the P-wave slope (PWS) was compared between control and Ca<sub>v</sub>2.3-deficient hearts even after application of 100  $\mu$ M Ni<sup>2+</sup>, control hearts exhibited a clear tendency towards a steeper slope (p = 0.074), therefore a higher probability for a more rapid depolarization than Ca<sub>v</sub>2.3-deficient hearts. **Conclusion:** Ablation of Ca<sub>v</sub>2.3 Ca<sup>2+</sup> channels in mice impairs impulse conduction in the SAN. Our

results suggest a potential function of Ca<sub>v</sub>2.3 channels in SAN function, probably related to action potential conduction.

**P191**

**Role of HIF in the inflammatory response at the alveolar epithelium and macrophages**

\*K. Velineni<sup>1,2</sup>, E. Baloglu<sup>1,2</sup>, H. Mairbaeurl<sup>1,2</sup>

<sup>1</sup>University of Heidelberg, Internal Medicine VII, Heidelberg, Germany

<sup>2</sup>German Center for Lung Research (DZL-TLRC-H), Heidelberg, Germany

**Question:** Alveolar macrophages release mediators upon stimulation with bacterial toxins, which inhibit fluid reabsorption from the alveolar space, increase barrier leakage, and cause pulmonary edema and alveolar hypoxia, which further impairs barrier function. Hypoxia can also cause a pro-inflammatory response. Here we test whether hypoxia aggravates the pro-inflammatory response in alveolar epithelial cells and whether this increased response involves HIF.

**Methods:** Rat primary alveolar epithelial cells (AEC), in which HIF-1 $\alpha$  and HIF-2 $\alpha$  was silenced, were co-cultured with rat alveolar macrophages (M $\phi$ ), stimulated with LPS, and kept in normoxia or hypoxia (1.5%, O<sub>2</sub>) for 24h. Trans-epithelial electrical resistance (TEER), short circuit current (ISC), NO production, and cytokine mRNA expression were measured in AEC.

**Results:** Our results indicate that AEC hypoxia aggravated the decrease in TEER and Na<sup>+</sup>-transport induced by M $\phi$ -LPS. Effects on permeability and Na-transport were not affected by HIF silencing. Inhibition was prevented when AEC were treated with iNOS and ERK-1/2 inhibitors, indicating that it is likely caused by NO formed by AEC. MM-LPS media from which nitrite was removed by dialysis did not induce nitrite formation by ATEC cells and partially prevented Na- transport inhibition in ATEC cells.

**Conclusion:** Exposure with M $\phi$ -LPS increased the m-RNA expression of cytokines in AEC. Hif-2 $\alpha$  silencing decreased mRNA expression of TNF- $\alpha$  in normoxia and hypoxia but not IL-6 and iNOS. These results indicate that signals from stimulated macrophages induce a pro-inflammatory response in alveolar epithelium, which is enhanced by hypoxia. The increased permeability and the decreased ion transport in normoxic and hypoxic AEC exposed to stimulated macrophages seems to be caused by NO produced in response to enhanced cytokine expression in AEC involving ERK1/2 dependent signaling, part of which might depend on HIF-2 $\alpha$ .

**P192**

**Best's disease and the cellular behaviour of mutant bestrophin-1**

\*M. Markowski, N. Reichhart, O. Strauss

Charite - Universitätsmedizin, Experimentelle Ophthalmologie, Berlin, Germany

The retinal pigment epithelium (RPE) expresses bestrophin-1, an integral protein of the basolateral membrane. Mutations of Bestrophin-1, the BEST1 gene product, are associated with an inherited autosomal dominant form of macular degeneration. The molecular pathology of mutant BEST1 is not understood. As RPE cells tightly interact with photoreceptors it can be assumed that Morbus Best is caused by a malfunction of the RPE, resulting from BEST1 mutations. In addition to its function as Cl<sup>-</sup>-channel bestrophin-1 is known to interact with Ca<sub>v</sub>1.3 L-type channels, a function which opens a new route to understand the disease. To address the question whether mutant bestrophin-1 influences the regulation of voltage-dependent L-Type Ca<sup>2+</sup>-channels we analyzed the electrophysiological properties of Ba<sup>2+</sup>-currents from in chinese hamster ovary (CHO) cells expressed L-type channels. Ca<sup>2+</sup>-channel subunits (Ca<sub>v</sub>1.3, the  $\alpha$ 2 $\delta$  and  $\beta$ <sub>4</sub>-subunit) were co-expressed with mutant bestrophin-1: T6P, F305S, R218C, F80L. Quantification of surface expression by means of confocal microscopy revealed trafficking defects of the four mutants. Furthermore, the presence of mutant Bestrophin-1 also resulted in a reduced surface expression of the L-type channel subunits Ca<sub>v</sub>1.3 and  $\beta$ <sub>4</sub>. We verified our findings of trafficking defects in polarized porcine RPE cells, where bestrophin-1 and Ca<sub>v</sub>1.3 channels are endogenously expressed. In the presence of mutant bestrophin-1, electrophysiological properties of Ba<sup>2+</sup>-currents through Ca<sub>v</sub>1.3/ $\beta$ <sub>4</sub> channels were not changed. Our results may represent a first step towards the understanding how molecular mechanisms may lead to photoreceptor degeneration.

## Poster Session II

### Cardiac functions II

#### P193

##### Cardiac remodelling in a p38-MAPK-knockout mouse model

\*K. Bottermann<sup>1</sup>, J. Stegbauer<sup>2</sup>, S. Mende<sup>2</sup>, S. Stamer<sup>2</sup>, A. Gödecke<sup>1</sup>

<sup>1</sup>Heinrich-Heine University Düsseldorf, Cardiovascular Physiology, Düsseldorf, Germany

<sup>2</sup>Heinrich-Heine University, Nephrology, Düsseldorf, Germany

**Question:** p38 MAPK is activated downstream of AngiotensinII in cardiomyocytes and vascular smooth muscle cells and is critically involved in cardiac hypertrophy and remodelling. The exact molecular mechanisms remain to be elucidated.

**Methods:** A knockout of p38 in vascular smooth muscle cells and in cardiomyocytes was induced expressing cre under control of the SM22 promotor. Measurement of cardiac function and arterial blood pressure was performed in 12 week old male mice (SM22 cre p38 flox, cre- p38flox as control) at basal conditions and after treatment with Angiotensin II (1µg/kg/min) over 14 days.

**Results:** Echocardiographic characterization of KO and control mice revealed no significant differences in cardiac function under basal conditions. (EF: SM22 cre p38 flox: 57 ± 12%, n=13, cre-: 60 ± 7%, n=11). Mean arterial pressure tended to be higher in KO mice (MAP: 109±2 mmHg, n=6) in comparison to control mice (MAP: 103±2 mmHg, n=5). Treatment with AngII resulted in a severe dilated cardiomyopathy in KO-mice with a dramatic reduction in cardiac pump function to 20 ± 3% ejection fraction already 48h after onset of AngII-treatment. Concurrently mean arterial blood pressure in KO-mice dropped to 86±13 mmHg after AngII-treatment. Control mice developed a typical AngII-induced hypertension (MAP 125±4 mmHg) and cardiac hypertrophy.

**Conclusion:** p38MAPK is a critical mediator of cardiac protection against AngII-induced cardiac hypertrophy and remodelling. If these effects are due to higher afterload or direct AngII-signaling in cardiomyocytes is a central element of further analyses.

#### P194

##### Precise spatio-temporal modulation of cardiac pacemaker activity by optogenetic GS stimulation

\*P. Makowka, T. Brueggemann, T. Beiert, M. Hesse, P. Sasse

Institute of Physiology 1, University of Bonn, Bonn, Germany

The G<sub>s</sub>-signaling cascade is important for the physiological regulation of beating frequency and contractility of the heart. This signaling pathway is normally activated by pharmacological stimulation of G<sub>s</sub>-protein coupled β<sub>1</sub>-receptor, but this approach has low spatial and temporal precision due to the diffusion of agonists. To stimulate the G<sub>s</sub>-signaling cascade by light with high spatio-temporal precision

we used the optogenetic protein JellyOp, a light-sensitive and directly GS-coupled receptor (Bailes HJ et al. PLoS One, 2012). G4 embryonic stem cells were genetically engineered to co-express JellyOp and EGFP under control of the ubiquitous chicken β-actin promoter. These cells were used for in vitro differentiation into cardiomyocytes within embryoid bodies (EBs) as well as to generate a transgenic mouse line. Spontaneously beating EBs contained α-actinin and EGFP expressing cardiomyocytes and were analyzed at day 10 of differentiation by infrared (760 nm) video microscopy. Brief illumination (20 sec, 470 nm, 111.5 nW/mm<sup>2</sup>) increased beating frequency to 432±42 % of baseline (n=7) with a subsequent decrease to initial beating rates after termination of illumination. The lowest effective light intensity was 9.1 nW/mm<sup>2</sup> resulting in a frequency increase to 207±27 % of baseline. Similar to dose-response-curves of receptor agonists, light-induced acceleration of beating showed a sigmoid dependence on light-intensity with a half maximal light intensity of 20.8 nW/mm<sup>2</sup>. Direct comparison to pharmacological G<sub>s</sub>-activation showed that peak frequencies were reached significantly faster using illumination (18.9 ± 1.7 s) than upon application of the β-receptor agonist isoprenaline (80.4 ± 9.3s) (Stimulation time: 120 sec, 470 nm, 308.5 nW/mm<sup>2</sup>, 1 µM isoprenaline, p < 0.0001, n=9) and that both approaches induced similar maximal frequencies. Hearts from JellyOp transgenic mice showed EGFP expression in cardiomyocytes and were analyzed ex vivo using Langendorff perfusion. Brief (100 ms) illumination (537 µW/mm<sup>2</sup>) of the right atrium led to an almost instantaneous (delay ~300 ms) acceleration of sinus rhythm to ~120%. The increase in beating rate was highly reproducible and depended on the applied light intensity. In summary optogenetic JellyOp activation in cardiomyocytes in vitro and in the intact heart enables stimulation of the G<sub>s</sub>-signaling pathway with high temporal precision. This approach will be useful to further investigate temporal and site-specific effects of physiological and pathophysiological G<sub>s</sub>-activation.

#### P195

##### Intercellular communication in stem cell-derived cardiomyocytes

I. C. Marcu<sup>1</sup>, A. Illaste<sup>1</sup>, C. Lansche<sup>2</sup>, \*N. D. Ullrich<sup>2,1</sup>

<sup>1</sup>University of Bern, Department of Physiology, Bern, Switzerland

<sup>2</sup>University of Heidelberg, Institute of Physiology and Pathophysiology, Heidelberg, Germany

Structural and functional coupling between neighbored cardiomyocytes is compulsory for the formation of a functional syncytium and required for barrier-free signal transmission across the myocardium. In the heart, intercellular communication operates at two levels: electrical coupling is responsible for the rapid action potential propagation and synchronization of contraction, and metabolic coupling enables chemical connection between adjacent cells: free passage of ions, metabolites and small second messenger molecules. Both functions require expression of gap junctional proteins, which in the ventricular myocyte

are mainly represented by connexin-43 (Cx43) forming hexameric hemichannels and assembling across membranes of cell neighbours to build a gap junction channel. Recent advances in the generation of stem cell-derived cardiomyocytes (SC-CMs) raise new hope for the development of cell-based therapies for cardiac diseases including cell implantation into damaged myocardium. However, the physiological characteristics of these newly generated cardiomyocytes need to be intensively evaluated before functional integration of these cells into the adult heart may be assumed. In this project, we investigated the properties of intercellular communication and the quality of cell-to-cell coupling in different SC-CMs. Using embryonic and induced pluripotent SC-CMs, we compared coupling properties in cell pairs with neonatal cardiomyocytes and the cardiac HL-1 cell line. Electrical stimulation of a patch-clamped myocyte allowed us to study electrical signal transmission and initiation of excitation-contraction coupling in the paired cell. Ca<sup>2+</sup> transients were visualized by fluo-3 and changes in fluorescence intensities were recorded in the line-scan mode of a laser-scanning confocal microscope. Metabolic coupling quality was assessed by evaluating temporal transfer of a gap junction-permeant dye between cell pairs. Differences in the expression pattern of Cx43 were analyzed in immunocytochemical reactions. We discovered that in comparison with native cardiomyocytes, Cx43 expression levels are significantly reduced in SC-CMs. Despite intact electrical coupling between cell pairs and temporally synchronized generation of Ca<sup>2+</sup> transients upon stimulation, metabolic coupling was significantly slowed and less efficient in SC-CMs compared with native myocytes reminding of the coupling properties of HL-1 cells, which are known for weak coupling. Increase in fluorescence in the coupled cells was 0.27±0.03 in neonatal CMs, 0.08±0.01 in SC-CMs and in HL-1 cells 0.08±0.01 ΔF/F<sub>0</sub> normalized to contact area at 120 s of dye transfer. In summary, SC-CMs present cardiac-like functional properties at the level of intercellular communication, but metabolic coupling via gap junctions is significantly less developed in these cells. This might be due to the poor cardiogenic maturation of SC-CMs and needs to be seriously considered before any therapeutic applications of these cells.

#### P196

##### Cyclic GMP enhancing therapy promotes titin phosphorylation and corrects high cardiomyocyte passive stiffness in heart failure with preserved ejection fraction

\*N. Hamdani<sup>1</sup>, K. Bishu<sup>2</sup>, M. M. Redfield<sup>2</sup>, W. A. Linke<sup>1</sup>

<sup>1</sup>Ruhr University Bochum, Cardiovascular Physiology, Bochum, Germany

<sup>2</sup>Mayo Clinic, Cardiovascular Division, Rochester, United States

**Background:** Heart failure with preserved ejection fraction (HFpEF) is a major cause of morbidity and mortality. The main pathophysiological alterations in HFpEF are increased left ventricular (LV) stiffness and abnormal relaxation, resulting in impaired LV filling. In the present study we aimed to examine whether titin phosphorylation and

stiffness are affected by PKG activation in vivo. We examined how a dog model with hypertension and diastolic dysfunction responds to agents that enhance cGMP-PKG signaling, in terms of altered titin phosphorylation status and cardiomyocyte passive stiffness.

**Methods and Results:** Isolated permeabilized cardiomyocytes from dog left ventricular (LV) biopsies at baseline (untreated, n=5) and after injection of sildenafil (n=7), followed by BNP (n=7), were attached to a force transducer and the passive length tension relationship (F<sub>passive</sub>) was measured between 1.8 and 2.4 µm sarcomere length (SL) before and after administration of protein kinase (PK) A, PKG, and calcium/calmodulin-dependent protein kinase-IIδ (CaMKIIδ). We assessed the phosphorylation of titin by gel electrophoresis using SYPRO Ruby (total protein) and ProQ Diamond (phospho-protein) stain and immunoblotting using phosphoserine-specific antibodies to titin N2Bus and PEVK. Compared to untreated cardiomyocytes, F<sub>passive</sub> was significantly reduced with sildenafil, which was maintained with BNP. Ex-vivo administration of PKG lowered F<sub>passive</sub> of untreated cardiomyocytes to the levels measured in sildenafil and BNP samples; additional administration of PKA did not affect F<sub>passive</sub>. Furthermore, CaMKIIδ lowered F<sub>passive</sub> of untreated cardiomyocytes, but did not affect F<sub>passive</sub> of cardiomyocytes from sildenafil and BNP samples. Total titin phosphorylation was low in untreated samples, but significantly increased with sildenafil and BNP. Sildenafil and BNP samples showed higher phosphorylation than untreated samples at titin PEVK and N2Bus sites known to be targeted by PKA, PKG, and CaMKIIδ.

**Conclusions:** Acute cGMP enhancing therapy with sildenafil and BNP improves LV diastolic function through correction of a phosphorylation deficit of I-band titin, thereby reducing cardiomyocyte passive stiffness.

#### P197

##### The cardiac proteome changes with protein degradation in aging

\*F. Koser, M. Hecker, O. Drews

Institute of Physiology and Pathophysiology, University of Heidelberg,

Division of Cardiovascular Physiology, Heidelberg, Germany

**Introduction:** Aging hearts are subject to structural and functional changes, which are associated with an increased incidence of cardiac disease. Investigation of molecular changes to gain insights in potential causative mechanisms mostly focus on protein expression while assuming changes in synthesis. In contrast, we studied whether alterations in the ubiquitin-proteasome system, which degrades up to 90% of all intracellular proteins, may contribute to altered protein expression in aging hearts.

**Objective:** Aim of the study was to investigate whether alterations in the proteome of aging hearts is accompanied by changes in proteasome function. **Methods & Results:** Cardiac proteomes of young versus old, male mice (17±1 vs. 113±9 weeks; n=5) were compared by 2-D electrophoresis. More than 10 highly abundant proteins were significantly increased in aged hearts. These proteins were

identified via the utilization of proteomics databases as essential structural and functional proteins (e.g. myosin light chain 1, myoglobin). The results suggest major structural and functional changes although at macroscopic level the heart weight and heart weight to body weight ratio were not altered. The observations made at proteome level were matched by changes in cardiac proteasome activities. In aging hearts, the ATP-dependent chymotrypsin-like 26S proteasome activity was 85% higher ( $p < 0.01$ ). Analyses of 20S proteasome activities and assembly were not significantly different, indicating that elevated 26S proteasome activity is potentially regulated by 26S assembly (19S+20S) or post translational modifications. In conclusion, altered expression of structural and functional proteins in aging hearts is affected by distinct changes in targeted protein degradation as well.

**P198**  
**Age-dependent effects of hyperbaric hyperoxia on cardiovascular function**

T. Wunderlich<sup>1</sup>, W. Kähler<sup>1</sup>, P. Radermacher<sup>1,2</sup>, J. Witte<sup>1</sup>, \*A. Koch<sup>1</sup>  
<sup>1</sup>German Naval Medical Institute, Maritime Medicine, Kronshagen, Germany  
<sup>2</sup>University of Ulm, Ulm, Germany

**Question:** Hyperoxia is known to influence cardiovascular function, but it's unknown, if there are differences between younger and older persons. The aim of this study was, to monitor changes in Flow mediated Dilatation (FMD) as a measure of peripheral endothelial function and parameters of myocardial diastolic function in younger and elderly volunteers, before and after exposures to hyperbaric hyperoxia.

**Methods:** 30 young, healthy, (26±6years) and 28 older males (52±8years) were enrolled. Both groups were exposed to standard Hyperbaric Oxygenation protocol (90min., 240kPa oxygen). FMD and echocardiography were done directly prior and after exposures with focus on diastolic function.

**Results:** Parameters of diastolic function changed as follows: E/A-Ratio significantly increased in the younger (1,46±0,35 to 1,68±0,34), remained unchanged in the elderly (0,98±0,33 to 0,99±0,32), e'/a'-Ratio, significantly increased in the younger (2,11±0,54 to 2,32±0,63), and less pronounced in the elderly (0,98±0,42 to 1,09±0,47). E/e'-Ratio increased in the younger (3,34±0,74 to 3,55±0,79) and decreased (4,04±1,25 to 3,84±0,86) in the elderly. Deceleration-time increased highly significant in both groups, whereas IVRT remained unchanged. Heart Rate decreased in both groups significantly. The FMD<sub>sys+diast</sub> decreased in both groups ( $p < 0.0001$ ).

**Conclusion:** Hyperoxia influences FMD negatively in both groups, but more severe in the elderly. The influence of hyperoxia on myocardial diastolic function is different: changes point towards improved compliance only in the younger. Left ventricular changes in preload due to resorption atelectases

may play a role, and a preexisting impaired diastolic function in the elderly might be causative for their fail in myocardial compensation.

**P199**  
**The costameric protein Ahnak is regulated by physical exercise in heart and skeletal muscle**

\*F. Suhr<sup>1,2</sup>, W. Bloch<sup>1</sup>, I. Morano<sup>2</sup>  
<sup>1</sup>Institute of Cardiovascular Research and Sport Medicine, Department of Molecular and Cellular Sport Medicine, Cologne, Germany  
<sup>2</sup>Max Delbrück Centre for Molecular Medicine, Department of Molecular Muscle Physiology, Berlin, Germany

**Question.** Costameric proteins provide a functional unit by linking Z-discs to the sarcolemma thus allowing heart and skeletal muscle tissues to adapt to mechanical impacts. Defective regulations of costameric proteins consequently result in disorganized heart and skeletal muscle structures. Physical exercise validly induces mechanical impacts on muscle tissues and their mechanosensitive costameres. Interestingly, it has not been determined, yet, whether exercise and the type of muscle contraction regulates the costameric protein Ahnak in both heart and skeletal muscle. However, these questions are of a very high relevance, as we demonstrated recently that Ahnak determines muscle rigidity ex vivo and thus directly influences the adaptational potential of muscle tissue towards mechanical stress.

**Methods.** Sprague Dawley-rats have been assigned to the following groups: Con (sedentary control), Level (level running, 6 wks/5d\*wk-1/30min\*d-1/20m\*min-1/0° incline), and Downhill (downhill running, see Level, but -20° incline). Heart, soleus and Edl muscles were dissected after the last training bout. Ahnak was investigated by means of western blot and immunofluorescence.

**Results.** We found the highest absolute Ahnak levels in Sol, followed by heart and Edl. Furthermore, Ahnak is regulated by exercise in both heart and skeletal muscle while the type of muscle contraction seems to have a critical influence.

**Conclusion.** We show for the first time that exercise and importantly the type of muscle contraction has a significant influence on the costameric Ahnak protein. These data might provide a new understanding of the impact and functional consequences of different contractions types in mechanobiological adaptations of heart and skeletal muscles.

**P200**  
**The type of skeletal muscle contraction specifically regulates mechanosensitive players in the heart**

\*F. Suhr, W. Bloch  
<sup>1</sup>Institute of Cardiovascular Research and Sport Medicine, Department of Molecular and Cellular Sport Medicine, Cologne, Germany

**Question.** Mechanosensitive proteins, e.g. integrin-linked kinase/pinch/parvin (IPP) complex, regulate adaptations in

the heart towards physiological and pathological demands, e.g. exercise or pressure overload. These adaptations are downstream processed by IPP-specific signaling pathways. Skeletal muscles can exert both concentric and eccentric muscle contractions and it was demonstrated that eccentric muscle contractions could be beneficial in exercise-based therapies of cardiac disease patients. However, the underlying molecular mechanisms are unknown. Here, we asked the question whether the type of muscle contraction has a significant influence on the expression levels of IPP members in the heart what could serve a potential hypothesis to explain different outcomes in exercise-based cardiac adaptations.

**Methods.** Sprague Dawley-rats have been assigned to the following groups: Con (sedentary control), Level (level running, 6 wks/5d\*wk-1/30min\*d-1/20m\*min-1/0° incline), and Downhill (downhill running, see Level, but -20° decline). Heart muscles were dissected after the last training bout. IPP members and signaling pathways were investigated by means of western blot and immunofluorescence.

**Results.** We found that Level (concentric) training induced significantly higher levels of IPP members and signaling molecules, such as pAktS473, compared to Con and Downhill (eccentric) training. No differences were found between Con and Downhill training with respect to IPP regulation. IPP members were mainly localized beneath the cardiomyocyte sarcolemma.

**Conclusion.** These data demonstrate that concentric and eccentric muscle contractions induce different mechanical demands in the heart why cardiomyocytes adapt distinctly at the molecular level. Our findings could pave the way for an explanation of different outcomes in heart muscle adaptation induced by physiological and also pathological loading situation.

**P201**  
**Optical trapping reveals a 3-fold increase in stiffness of the myosin head as the molecular basis for increased active force by the FHC-related mutation R723G in the β-cardiac myosin heavy chain**

C. Werkman<sup>1</sup>, N. Hahn<sup>1</sup>, A. Francino<sup>2</sup>, F. Navarro-Lopéz<sup>2</sup>, T. Kraft<sup>1</sup>, W. Steffen<sup>1</sup>, \*B. Brenner<sup>1</sup>  
<sup>1</sup>Hannover Medical School, Molecular and Cell Physiology, Hannover, Germany  
<sup>2</sup>University of Barcelona, Hospital Clinic, Barcelona, Spain

**Background.** Missense mutations in the β-cardiac myosin heavy chain (β-MyHC) are the most frequent cause of Familial Hypertrophic Cardiomyopathy (FHC). For such missense mutations both mutant and wildtype β-MyHCs are co-incorporated into the contractile apparatus, and the direct functional effects of such mutations are thought to trigger development of the FHC-phenotype. In an earlier study on skinned fibers from M. soleus biopsies of affected patients we found the converter mutation R723G to increase force generation and fiber stiffness.

**Question.** We hypothesized that the increase in active force is caused by an increase in the stiffness of the mu-

tated myosin head. Detection and quantification of such an increase in head stiffness in fiber studies, however, is complicated by compliance in actin and myosin filaments, as well as non-equal and variable co-expression of mutant and wildtype protein in the tissue samples.

**Method.** In the present study we directly measured stiffness of individual myosin heads isolated from M. soleus tissue samples of affected patients using the three-bead optical trapping assay. Since each assay contained both mutant and wildtype myosin heads stiffness of individual heads with and without the R723G mutation could directly be compared. We imposed triangular-shaped stage displacements on the three-bead trapping assay and determined head stiffness from the difference between imposed stage displacements and resulting bead displacements with the compliance of the links between actin filament and trapped beads determined by the variance-Hidden-Markov method (Smith et al., Biophys J 2001).

**Results.** We found two populations of head domains, one with a head stiffness of 0.39±0.24 pN/nm the other with an about 3-fold higher stiffness. The low value is close to our previous optical trapping with β-MyHC (0.38±0.06 pN/nm; Brenner et al., JMRCM 2012). Thus, the myosin head with the R723G mutation has an about 3-fold higher stiffness than the wildtype myosin head.

**Conclusions.** Our data show that the FHC-related missense mutation R723G causes a 3-fold increase in the stiffness of the myosin head domain, i.e., a 3-fold higher resistance to elastic distortion. Since muscle force at the molecular level results from elastic distortion of the myosin heads by the structural changes in the working stroke, the increased head stiffness, i.e., the increased resistance to elastic distortion of myosin heads with mutation R723G explains the increased active force that we had observed in our earlier study on isolated fibers from soleus muscle fibers of FHC-patients with mutation R723G (Seeböhm et al., Biophys J 2009).

**P202**  
**Familial hypertrophic cardiomyopathy: Malignant β-myosin mutation Arg453Cys increases force generation by altering cross-bridge cycling kinetics**

\*T. Kraft<sup>1</sup>, J. Rose<sup>1</sup>, J. Montag<sup>1</sup>, D. List<sup>1</sup>, W. J. McKenna<sup>2</sup>, B. Brenner<sup>1</sup>  
<sup>1</sup>Hannover Medical School, Molecular and Cell Physiology, Hannover, Germany  
<sup>2</sup>University College London, Institute of Cardiovascular Science, London, United Kingdom

In Familial Hypertrophic Cardiomyopathy (FHC) about 1/3 of genotyped patients carries mutations in the β-myosin heavy chain (β-MyHC), the myosin isoform of the ventricle and of slow skeletal muscle fibers. We analyzed the effects of the β-MyHC-mutation R453C on contractile properties of slow skeletal muscle fibers of a severely affected FHC patient to characterize its effect on acto-myosin function and assess its possible role for development of the FHC-phenotype. We found that with mutation R453C isometric force was about 12% higher, rate constant of

force redevelopment ( $k_{tr}$ ) was 15% faster, isometric AT-Pase activity was 10% higher and tension cost was essentially unchanged. Together with only slightly higher fiber stiffness in rigor, a main part of the increase in isometric force appears to be due to an increase in  $f_{app}$ , the rate constant for transition of cross-bridges into force generating states. Quantification of the ratio of mutated vs. wildtype  $\beta$ -MyHC-mRNA in the muscle tissue revealed a fraction of about 36% R453C-mRNA. If at the protein level a similar fraction of mutated MyHC is present, as we had found in other FHC-mutations, about a third of the  $\beta$ -myosin heads in the sarcomeres carry R453C. Thus, force contribution of the mutated myosin head population is about 40% increased. A larger variability in  $pCa_{50}$  among individual mutated fibers vs. control fibers for this and other FHC-mutations suggests unequal expression of mutated myosin in individual muscle fibers. In the FHC-myocardium, unequal expression of mutated myosin in individual cardiomyocytes could cause imbalanced force generation and thus trigger functional impairment.

#### P203

##### Early stimulating and late inhibiting effects of lipoteichoic acid on adult cardiomyocyte contractility and calcium-transients

\*N. Mutig<sup>1</sup>, C. Geers-Knoerr<sup>1</sup>, B. Piep<sup>1</sup>, A. Pahuja<sup>1</sup>, B. Brenner<sup>1</sup>, A. D. Niederbichler<sup>2</sup>, T. Kraft<sup>1</sup>

<sup>1</sup>Hannover Medical School, Molecular and Cell Physiology, Hannover, Germany

<sup>2</sup>HELIOS Klinikum Berlin-Buch, Department für Handchirurgie und Plastische Chirurgie, Berlin, Germany

Cardiac dysfunction has been implicated to play a key role in pathophysiology and outcome of septic disorders which frequently occur in critical care patients. Reduced cardiac pump function and loss of peripheral resistance are two of the major mechanisms contributing to organ hypoperfusion and death. Major pathogenic factors in sepsis are lipopolysaccharide (LPS) of gram-negative bacteria and lipoteichoic acid (LTA) of gram-positive bacteria. We hypothesized that LTA contributes to cardiac failure in sepsis by directly affecting cardiomyocyte function. In the present work we set out to characterize the effects of LTA on contractile properties and calcium-transients of isolated adult rat cardiomyocytes. Exposure of cardiomyocytes to LTA for 1h increased the amplitude of calcium-transients to 130% and the contraction amplitude to 142% at 1Hz stimulation frequency. The maximum velocities of increase and decay of the calcium-transients and the relengthening of the sarcomeres were accelerated after LTA incubation. Interestingly, after exposure of cardiomyocytes to LTA for 24h, the LTA-effect on cardiomyocyte contractility was reversed. Sarcomere shortening and relaxation velocities as well as amplitudes and rates of rise and decay of calcium-transients were significantly depressed after 24h incubation with LTA compared to non-treated controls. Our experiments indicate that LTA most likely affects calcium-handling of the cardiomyocytes. At a reduced extracellular

calcium concentration (0.9 mmol/L) resembling the clinical situation in septic patients, the early stimulating effects of LTA incubation were exacerbated. Functionally, the initial stimulating effect of LTA with increased contractility of the cardiomyocytes may be the in vitro reflection of an early hyperdynamic phase of gram-positive sepsis. The reduced contractility observed after 24 hours exposure to LTA may reflect in vitro a late hypodynamic phase as it is also found in the myocardium of patients with septic disorders.

#### P204

##### Titin-isoform analysis in human embryonic stem cell (ESC) derived cardiomyocytes

\*A. Fomin<sup>1</sup>, M. Tiburcy<sup>2</sup>, W.-H. Zimmermann<sup>2</sup>, W. A. Linke<sup>1,2</sup>

<sup>1</sup>Ruhr University Bochum, Department of Cardiovascular Physiology, Bochum, Germany

<sup>2</sup>University Medicine Göttingen, Heart Center, Göttingen, Germany

**Rationale:** Human embryonic stem cell (ESC) derived cardiomyocytes have great potential for basic and applied research; however, they are notoriously immature. Cardiac titin, the giant protein of the myocytes, undergoes dramatic changes in the isoform expression pattern during perinatal heart development, from long and compliant fetal N2BA (3.7 MDa) via intermediate-size neonatal N2BA to short and stiff adult N2B (3.0 MDa). Therefore, the cardiac titin-isoform composition could be a useful readout to help judge the maturation of human ESC-derived cardiomyocytes. Here, we aimed to derive a method to detect titin protein isoform expression in these cells. We hypothesized that ESC-derived cardiomyocytes cultured in 3D as Engineered Heart Muscle (EHM) under mechanical load may produce a more mature titin-isoform pattern than ESC-derived cardiomyocytes not engineered into EHM.

**Methods:** Cardiomyocytes were differentiated from human ESCs and directly used for titin analysis or cultivated for an additional 10 days in a 3D collagen I matrix under mechanical load as Engineered Heart Muscle (EHM). EHM cultures were enzymatically digested; cellular proteins were solubilized and analyzed by gel electrophoresis in low-concentrated SDS-polyacrylamide gels strengthened with agarose.

**Results:** Compared with human adult heart muscle, which expressed ~40% N2BA (~3.3 MDa) and 60% N2B (3.0 MDa) isoforms, we detected only a long fetal N2BA-isoform (3.7 MDa) in ESC-derived cardiomyocytes. Culture of EHM under mechanical load did not alter this fetal titin-isoform pattern, suggesting that these cardiomyocytes are not yet fully differentiated.

**Conclusions:** Titin isoforms can be identified in human stem cell derived cardiomyocytes and could potentially be used as readout for monitoring sarcomeric maturation.

### Cell biology and signal transduction III

#### P205

##### Investigation of erythropoietin receptor activation in living cells by Förster resonance energy transfer microscopy

\*A. Bernardini, U. Brockmeier, J. Fandrey

University of Duisburg-Essen, Institute of Physiology, Essen, Germany

**Question:** The erythropoietin receptor (EpoR) has been claimed to be present in non-erythroid cells, particularly in cancer cells. The antibodies used so far, however, have been shown to be highly unspecific. Additionally it has never unambiguously been shown that EpoR forms homodimers in the membrane of non-erythroid cells which is the prerequisite for activity. The goal of this study is therefore to investigate EpoR homodimerization in living cells and show whether these homodimers are functionally active or not.

**Methods:** To investigate the EpoR homodimerization, we employed Förster resonance energy transfer (FRET) microscopy. We used fusion constructs of EpoR with cyan (ECFP) and yellow fluorescent protein (EYFP) to transfect different cell lines and FRET microscopy on live cells to detect dimerization of both chimeras. FRET only occurs over very short distances (<10 nm). Therefore positive FRET levels are evidence for dimerization. It is known that the EpoR dimer exhibits a conformational change during ligand binding. Such a change would induce a change in the observed FRET efficiency upon the addition of Epo and could therefore serve as evidence for receptor activation in live cells.

**Results:** We confirmed receptor homodimerization in living cells via FRET. The highest FRET efficiencies were observed when the fluorophores were inserted near the transmembrane domain. No FRET signal was observed with constructs that were labelled near the intracytoplasmic tail suggesting a separation of the C-terminal domains that is larger than 10 nm. Constructs that exhibit positive FRET however do not show any changes upon ligand addition.

**Conclusion:** The homodimerization of EpoR monomers in living cells of different lines provides evidence that non-erythroid cells are able to form EpoR homodimers if the receptor is expressed at a sufficient level. The question whether these constructs are functionally active remains open. Failure to detect FRET with the C-terminally labelled constructs may be caused by separation of the C-terminal tails that is unfavorable for FRET.

Supported by European Commission under the 7th Framework Programme (FP7-HEALTH-2011-single-stage Grant Agreement Number 282551EpoCan) to Joachim Fandrey. This report reflects only the authors' views, and the European Community is in no way liable for any use that may be made of the information contained herein.

#### P206

##### A novel membrane targeting of nPKC via cAMP-Epac reducing global Ca<sup>2+</sup> mobilization

\*X. Hui, G. Reither, L. Kaestner, P. Lipp

University of Saarland, Institute for Molecular Cell Biology, Homburg (Saar), Germany

The activation of the two ubiquitous families of protein kinases, Protein Kinase A (PKA) and Protein Kinase C (PKC), was currently thought of being independent with virtually no overlap. PKA activity was evoked by cAMP via stimulation of Gas proteins, while Ca<sup>2+</sup> and/or DAG activated PKC isoforms via stimulation of G $\alpha_q$  protein. Additionally, how exactly the major subfamily of PKC, novel PKCs ( $\delta$ ,  $\epsilon$ ,  $\eta$ ) decode lipid signals into phosphorylation events is still unclear. We applied confocal imaging of living cells expressing protein kinase C-fluorescent protein fusion constructs and revealed that activation of G $\alpha_q$  resulted in recruitment of the novel PKC $\delta$  to the membrane of the endoplasmic reticulum (ER). We further demonstrated that PKC $\delta$  translocation was driven by a novel G $\alpha_q$ -cAMP-EPAC-RAP-PLC $\epsilon$  pathway resulting in specific DAG production at the membrane of the ER. Specific membrane targeted phosphorylation sensors revealed that directed translocation of PKCs resulted in phosphorylation activity confined to the target membrane. Specific stimulation of PKC $\delta$  not only caused its accumulation at the ER membrane but also phosphorylation of the InsP<sub>3</sub> receptor and dampening of global Ca<sup>2+</sup> signalling as shown by graded flash photolysis of caged-InsP<sub>3</sub>. Our data demonstrates a novel signalling pathway enabling differential decoding of incoming stimuli into PKC isoform specific membrane targeting. Such a signalling network significantly enhances the versatility of cAMP signalling, demonstrates the possible interconnection between the PKA and PKC pathways, and provides novel and elementary understanding and insights into physiological and pathological cellular responses.

#### P207

##### Characterisation of CapZ deficient zebrafish larvae utilising a novel force measurement technique

\*M. Bitzer<sup>1</sup>, J. Eckhardt<sup>1</sup>, A. Habermann<sup>2</sup>, M. Schroeter<sup>1</sup>, S. Papadopoulos<sup>1</sup>, A. Frangakis<sup>2</sup>, G. Pfister<sup>1</sup>, R. Stehle<sup>1</sup>

<sup>1</sup>University of Cologne, Institute for Vegetative Physiology, Cologne, Germany

<sup>2</sup>Goethe Universität Frankfurt, Frankfurt Molecular Life Science Institute, Frankfurt am Main, Germany

In this study we addressed the question, whether the z-disc actin capping protein CapZ is crucial for myogenesis and for muscle contractility of zebrafish larvae. Zebrafish larvae were manipulated by injecting one of three different morpholino modified antisense oligonucleotides suppressing the expression of the beta-subunit of CapZ. Knockdown of CapZ in the injected larvae (CapZ-Morphants) was tested by Western Blot analysis and indirect immunohistochemistry of larval muscle tissue (monoclonal mAb 1E5.25.4 against capping protein -beta -1). Sarcomere ultrastructure



was investigated by electron microscopy. A novel method for measuring force transients induced by electrical stimulation (EFS) of zebrafish larvae was established. All three different CapZ-Morphants exhibited a similar phenotype showing developmental delay, reduced mobility and a malformation of the body axis. No CapZ immunoreactive protein band was detected in the Western Blots of two of the three approaches. Indirect immunohistochemistry of the larvae revealed a CapZ signal at the Z-discs and the myosepta of the larval trunk and tail region. Notably, EM images showed reduced myofibrillar density and delayed sarcomerogenesis. Morphants (n=15) generated EFS induced twitch-forces ranging from 0mN to 0,5mN which were significantly lower than the forces of controls (n=19) ranging from 1mN to 1,25mN. Our study suggests that CapZ might play a role in myogenesis in early zebrafish development. For the first time we show force measurements of zebrafish larvae in natural conditions.

**P208**

**The epsin N-terminal homology (ENTH) domain as sensitive reporter for PI(4,5)P<sub>2</sub> in physiological pathways**

\*M. G. Leitner<sup>1</sup>, B. U. Wilke<sup>1</sup>, Y. Kosimons<sup>1</sup>, C. R. Halaszovich<sup>1</sup>, O. Dominik<sup>1</sup>  
<sup>1</sup>Institute for Physiology, Philipps University Marburg, Marburg, Germany

The activation of Gq protein-coupled receptors couples extracellular signalling to cell physiology via phospholipase C-β (PLC-β)-dependent hydrolysis of phosphatidylinositol-(4,5)-bisphosphate (PI(4,5)P<sub>2</sub>). Since PI(4,5)P<sub>2</sub> regulates the activity of most membrane proteins, experimental assessment of phosphoinositide concentrations is crucial to elucidate the magnitude of PLC-β-dependent PI(4,5)P<sub>2</sub> depletion in physiological pathways. PI(4,5)P<sub>2</sub> levels can be monitored with PI(4,5)P<sub>2</sub> recognition domains coupled to fluorescent proteins, but established sensors exhibit some limitations: the Pleckstrin homology domain of PLC<sub>β1</sub> (PLC<sub>β1</sub>-PH) recognises also PLC-downstream messengers which limits estimations of actual PI(4,5)P<sub>2</sub> depletion, and the PI(4,5)P<sub>2</sub> affinity of Tubby-Cterm presumably is too high to detect PI(4,5)P<sub>2</sub> changes in cells. These caveats warrant the establishment of more valuable PI(4,5)P<sub>2</sub> sensors.

We took advantage of a recent study that introduced epsin N-terminal homology (ENTH) domain with chemical modifications as PI(4,5)P<sub>2</sub> reporter, and evaluated Epsin1-ENTH-GFP as translocation sensor for physiologically-relevant PI(4,5)P<sub>2</sub> changes. Using genetically-encoded tools to manipulate phosphoinositides, we found that, in contrast to in-vitro conditions, Epsin1-ENTH-GFP specifically bound to PI(4,5)P<sub>2</sub>. The PI(4,5)P<sub>2</sub> binding affinity was low which conferred highest sensitivity towards PI(4,5)P<sub>2</sub> level changes to Epsin1-ENTH-GFP. Epsin1-ENTH-GFP could be used to monitor PLC-β-mediated PI(4,5)P<sub>2</sub> depletion at agonist concentrations missed by other sensors, and also detected membrane-associated PI(4,5)P<sub>2</sub> elevations reliably. As overexpression of Epsin1-ENTH did not attenuate cellular signalling and did not affect cellular PI(4,5)P<sub>2</sub> homeostasis.

In summary, we propose Epsin1-ENTH-GFP as highly sensitive reporter for smallest PI(4,5)P<sub>2</sub> level changes in physiological pathways.

**P209**

**Defining the impact of optogenetic silencing of PV interneurons on barrel cortex micro-circuit activity by 2 photon Ca<sup>2+</sup> imaging**

\*P.-H. Prouvot, J.-W. Yang, G. Pramanik, A. Stroh  
 Institute for Microscopic Anatomy and Neurobiology, Research Group Molecular Imaging and Optogenetics, Mainz, Germany

**Question:** The somatosensory cortex of the rodent's whiskers (barrel cortex) is ideally suited as model for studying cortical computation and organization. Here, we aim at understanding the role of PV interneurons on microcircuit computation of sensory input.

**Methods:** To monitor micro-circuit activity in neurons from layer 2/3 of the barrel cortex we used bolus loading of the fluorescent Ca<sup>2+</sup> indicator OGB-1 AM. We monitored the changes in fluorescence in 20-100 cells simultaneously using a two photon microscope equipped with a resonant scanner at video rate. Simultaneous Local Field Potential (LFP) recordings allowed us to monitor the brain state. For optogenetics we injected P20 mice according to stereotactic coordinates with 300µl of a virus containing the floxed gene expressing ArchT in PV::Cre or wild type animals in order to achieve an expression specific to Parvalbumin positive interneurons or in a more general population. Cell-type specificity was confirmed by immunostainings.

**Results:** We achieved strong, membrane-bound expression of ArchT in WT animals, in PV::Cre animals expression was limited to Parvalbumin positive interneurons. In vivo Ca<sup>2+</sup> imaging and LFP recordings revealed spontaneous activity under light anesthesia. As a next step, sensory stimulation will be implemented.

**Conclusion:** We demonstrate the feasibility of the combination of 2-photon Ca<sup>2+</sup> imaging in combination with simultaneous optogenetic inhibition in mouse barrel cortex.

**P210**

**The influence of the ginger constituent 6-shogaol on intestinal barrier**

\*J. Lüttig<sup>1</sup>, R. Rosenthal<sup>2</sup>, M. Fromm<sup>2</sup>, J. Schulzke<sup>1</sup>  
<sup>1</sup>Department of Gastroenterology, Infectiology and Rheumatology, Charité, Berlin, Germany  
<sup>2</sup>Institute of Clinical Physiology, Charité, Berlin, Germany

We investigated the effects of 6-shogaol, a pungent component of ginger, on an intestinal model epithelium challenged with the proinflammatory cytokine tumor necrosis factor-α (TNF-α). We determined intestinal barrier function, the involved tight junction (TJ) proteins and signaling pathways. **Methods:** The human colon cell line HT-29/B6 which

forms confluent monolayers on permeable supports was challenged by pretreatment with TNF-α (250 U/ml, 24 h). Transepithelial resistance (TER) and permeability to the paracellular marker fluorescein were measured in Ussing chambers. We performed Western blotting and confocal laser-scanning microscopy to analyze the expression of TJ proteins and their cellular distribution. **Results:** TNF-α reduced TER by half and strongly increased fluorescein permeability compared to untreated controls. 6-shogaol-pretreated cells (100 µM, 2 h) showed a partial prevention of the TNF-α-induced TER decrease as well as of the fluorescein permeability rise. After treatment with TNF-α, the barrier-forming TJ protein claudin-1 was redistributed and the expression of the cation and water channel-forming TJ protein claudin-2 increased by activation of phosphatidylinositol-3-kinase signaling. 6-shogaol pre-incubation prevented the increase in claudin-2 expression by inhibition of the phosphatidylinositol-3-kinase (PI3K) signaling. In addition, we found that 6-shogaol averted the TNF-α-triggered phosphorylation of the transcription factor NFκB. The effects of 6-shogaol were mimicked by signal blockers of NFκB (BAY11-7082) and PI3K (LY294002).

**Conclusion:** 6-shogaol exerted anti-inflammatory effects by diminishing the TNF-α-induced claudin-1 disassembly and attenuating the TNF-α-mediated claudin-2 upregulation. Thus, the barrier-protective role of 6-shogaol in intestinal inflammation appears to be associated with both, the NFκB and the PI3K/Akt pathway.

**P211**

**Exogenous expression of VE-cadherin in invasive human breast cancer cell lines induces cell morphological changes and alteration in the mechanism of cell migration**

\*M. Rezaei<sup>1</sup>, A. Abu Taha<sup>1</sup>, B. Kemper<sup>2</sup>, H.-J. Schnittler<sup>1</sup>  
<sup>1</sup>Universitätsklinikum Münster, Institute of Anatomy and Vascular Biology, Münster, Germany  
<sup>2</sup>Universitätsklinikum Münster, Münster, Germany

Several pieces of evidence suggest that changes in cadherin expression play an important role in tumor progression. Surprisingly, a recent study showed that vascular endothelial specific cadherin expression (VE-cadherin) (Type II cadherin) is induced during epithelial-mesenchymal transition in mouse mammary tumor cells and in invasive human breast carcinomas. Furthermore, VE-cadherin expression in aggressive mouse tumor cell line promotes tumor progression by altering the TGF-beta signaling pathway. These findings have raised the possibility that VE-cadherin expression in human breast carcinomas contributes to the invasive phenotype. To determine whether VE-cadherin promotes human breast cancer invasiveness, we transduced MCF-7 and MDA-231 cell lines with VE-cadherin-EGFP and analyzed the effects on cell morphology and migration. Both cell lines don't express VE-cadherin. MCF-7 cell line retained several characteristics of differentiated mammary epithelium, including expression of E-cadherin (Type I cadherin) whereas MDA-231 cell line is poorly differentiated and expresses low level of E-cadherin. Exogenous expres-

sion of VE-cadherin in MCF-7 cells slightly downregulates E-cadherin expression and increases cell motility. However, its expression has no influence on the cells morphology and the mechanism of cell migration. In MDA-231 cells, VE-cadherin induces epithelial like morphology, an increase in β-catenin expression, and recruitment of β-catenin to adherens junctions. Interestingly, VE-cadherin expression in MDA-231 cells changes the individual non-directional migration of the cells in a scratch assay to collective unidirectional migration, the mechanism that may relevant for cancer invasion and metastasis. These results demonstrate that expression of VE-cadherin in invasive human breast cancer cells modulates the cell morphology, promotes motility and changes the mechanism of cells migration, the properties that may promote the metastatic potential of cancer cells.

**P212**

**A role of cortical acto-myosin dynamics in epithelial morphogenesis and plasma membrane organization**

C. Klingner<sup>1</sup>, A. V. Cherian<sup>1</sup>, \*J. Fels<sup>2</sup>, R. Wedlich-Söldner<sup>2,1</sup>  
<sup>1</sup>Cellular Dynamics and Cell Patterning, Max Planck Institute of Biochemistry, Martinsried, Germany  
<sup>2</sup>Institute of Cell Dynamics and Imaging, University of Muenster, Muenster, Germany

The cortical actin cytoskeleton plays a central role during morphogenesis, migration and barrier function of epithelial cells. During these processes, assemblies of actin filaments generate, sense and transmit mechanical forces. We have recently identified a novel actin organization at the apical surface of non-polarized epithelial cells, which exhibits rapid dynamics driven by an underlying non muscle myosin II network. The observed acto-myosin dynamics was characterized using optical flow, spatio-temporal correlation analysis and atomic force microscopy (AFM). We identified a global pulsatile contractility in the cortical acto-myosin web, which shifts between states of low and high activity. AFM-based quantification of this dynamic remodeling revealed a periodic softening/stiffening cycle of the cell cortex at a similar frequency to that seen for lateral acto-myosin reorganization. Interestingly, apical acto-myosin oscillations were mainly found in non-confluent cells and during cellular rearrangements such as wound healing or induction of epithelial-mesenchymal transition. Finally, we could show that apical acto-myosin organization and dynamics directly affected distribution and lateral mobility of integral plasma membrane proteins - either by actively moving proteins that were tethered to actin, or through (re-) organization of diffusion barriers. Taken together we identified a dynamic acto-myosin network on the apical surface of epithelial cells and characterized a novel aspect in the complex interplay between cellular organization and the mechanical forces acting on cells.

**P213**

**A novel transgenic approach for identification of cardiomyocytes and their cell cycle status in-vitro and in-vivo**

\*A. Raulf, H. Horder, C. Geisen, S. Grünberg, P. Freitag, B. Fleischmann, M. Hesse

University of Bonn, Physiology I, Bonn, Germany

The typical remodelling process after cardiac injury is scarring and compensatory hypertrophy. The limited regeneration potential of the adult heart is due to the post-mitotic status of cardiomyocytes (CMs), which are mostly binucleated. Nevertheless there is evidence for CM turnover in the adult heart, but the extent of this turnover is under debate. One technical limitation of the analyses is the unequivocal identification of CMs and of cell division.

In order to enable a clear identification of CM nuclei in-vivo, we have developed a transgenic mouse line in which a fusion protein of human histone 2B and the red fluorescence protein mCherry is specifically and persistently expressed in CM nuclei (αMHC-H2B-mCherry). This fluorescence label allows an investigation of CM portions in native tissue slices, which reflect the cellular composition of the heart. In this regard we analysed regional and developmental-stage dependent changes in the fraction of CM nuclei and CM binuclearity. We therefore chose time-points before, during and after terminal differentiation of the CMs (postnatal day 3 (P3), P7 and P56). Furthermore, we crossed the αMHC-H2B-mCherry with mice expressing the CAG-eGFP-anillin transgene (Hesse et al., 2012), which visualizes cell-cycle activity with a high resolution of M-phase. Using live monitoring of postnatal double-transgenic whole organ cultures, we investigate cell cycle variations in CMs in order to understand cell biological mechanisms that lead to their terminal differentiation. One strategy for regeneration of lost CMs is the application of substances that increase the regeneration potential of the heart. We established a novel screening assay for cell-cycle modifying substances in isolated, postnatal CMs of αMHC-H2B-mCherry/CAG-eGFP-anillin mice. As a proof of principle we are currently analyzing micro RNAs, which have been reported to induce cell cycle activity and cell division in CMs. The double transgenic mouse line can also be used to directly evaluate the effect of positively tested substances in-vivo.

**P214**

**Interleukin-1β mediated transcriptional downregulation of NHERF family PDZ adaptor protein PDZK1 in caco-2bbe cells**

M. Luo<sup>1,2</sup>, G. Chodisetti<sup>1</sup>, B. Riederer<sup>1</sup>, M. Menon<sup>3</sup>, M. Gaestel<sup>3</sup>, D. A. Tian<sup>2</sup>, K. Tachibana<sup>4</sup>, D. Takefumi<sup>4</sup>, \*S. Yervu<sup>1</sup>, U. Seidler<sup>1</sup>

<sup>1</sup>Hannover Medical School, Dept. Of Gastroenterology, Hepatology and Endocrinology, Hannover, Germany

<sup>2</sup>Tongji Medical School, Dept. of Gastroenterology, Wuhan, China

<sup>3</sup>Hannover Medical School, Institute for Biochemistry, Hannover, Germany

<sup>4</sup>Osaka University, Graduate School of Pharmaceutical Sciences, Osaka, Japan

**Question:** PDZK1 is an important PDZ adaptor protein of the NHERF family that interacts with a variety of membrane proteins in the intestine, liver and kidney, thereby stabilizing the proteins in the membrane and facilitating interaction with signalling molecules. We previously reported a strong decrease of PDZK1 expression in the inflamed murine and human intestine. In this study, we searched for the molecular mechanisms of inflammation-associated PDZK1 downregulation, using an in vitro Caco-2bbe cell culture model.

**Methods:** Promoter constructs for the PDZK1 promoter, as well as 5' deletion constructs, were transiently transfected into Caco-2bbe cells and their activity assessed by luciferase reporter gene assays. Real-time PCR and Western blots were performed to measure the mRNA and protein expression, respectively.

**Results:** Treatment of Caco-2bbe cells with Interleukin-1β (IL-1β) dose-dependently decreased PDZK1 promoter activity, as well as PDZK1 mRNA and protein expression in Caco2bbe cells. TNF-α and IFN-γ, alone, or in combination with IL-1β, did not show an additional inhibitory effect compared to IL-1β alone. 5'-deletion analysis of PDZK1 promoter reporter constructs showed that the base pairs -4689 to -3995 are responsible for the basal and IL-1β mediated inhibitory effect in Caco-2bbe cells. In silico analysis of the PDZK1 promoter sequence showed that this regions harbours the major transcription factor binding elements, for NF-κB, AP-1, SP-1 and retinoid X receptor alpha (RXR-α) proteins. The use of BAY11-7082 (NF-κB inhibitor) and BIRB (p38MAPK inhibitor) could not prevent IL-1β-mediated PDZK1 downregulation of promoter activity or protein expression, which indicated the involvement of other signalling cascades for the inhibitory effect of IL-1β on PDZK1 expression. Further studies utilizing real-time PCRs showed a downregulation of RXR-α transcription factor expression after IL-1β treatment in Caco-2bbe cells.

**Conclusions:** IL-1β downregulated PDZK1 protein expression in Caco-2bbe cells through transcriptional inhibition of PDZK1 promoter. The region between base pairs -4689 to -3995 in the PDZK1 promoter is important for both its basal expression and IL-1β mediated inhibition in Caco-2bbe cells. Initial results suggested that IL-1β might downregulate RXR-α and there by decreasing PDZK1 transcription.

**P215**

**15-deoxy-Δ<sup>12,14</sup>-prostaglandin J2 reinforces the anti-inflammatory capacity of endothelial cells with a genetically determined nitric oxide deficit**

\*I. Kadiyska, S. Yakubenia, M. Cattaruzza, M. Hecker

Heidelberg University, Cardiovascular Physiology, Heidelberg, Germany

Blood flow-generated shear stress (FSS) is the major determinant of endothelial nitric oxide (NO) synthase (NOS3) expression. In humans, a promoter variant of the NOS3 gene, the C-variant of the T-786C single nucleotide polymorphism (SNP), renders the gene insensitive to shear stress, resulting in a reduced endothelial capacity to generate NO. Consequently, individuals homozygous for the C-variant have a high risk of developing certain cardiovascular and rheuma-

toid diseases. However, there are at least two mechanisms by which insufficient NO production can be counteracted, one of which involves a multi-component pathway leading to an increased release of the anti-inflammatory prostanoicid 15-deoxy-Δ<sup>12,14</sup>-prostaglandin J2 (15d-PGJ2). FSS significantly up-regulated the expression of the two major rate-limiting enzymes for 15d-PGJ2 synthesis, cyclooxygenase-2 and lipocalin-type prostaglandin D synthase, solely in CC-genotype ECs. Moreover, only these cells released 15d-PGJ2 in response to FSS, and 15d-PGJ2 markedly suppressed monocyte pro-inflammatory activation. The anti-inflammatory activity of 15d-PGJ2 in activated monocytes may involve an induction of the Nrf2/anti-oxidant response element (ARE) pathway. We have found three ARE-like motifs in the human interleukin-1 beta (IL-1β) promoter region, suggesting that Nrf2 may act through an as yet unknown mechanism to repress the transcription of the IL-1B gene. Using chromatin immunoprecipitation and reporter gene analysis we are currently investigating the functional interaction between Nrf2 and the AREs in the IL-1β promoter. Despite an inadequate capacity to form NO, CC-genotype ECs reveal a robust anti-inflammatory phenotype due to an up-regulation of 15d-PGJ2 synthesis in response to FSS. Its inhibitory effect may involve a novel functional role for Nrf2 as a direct repressor of pro-inflammatory gene expression.

**P216**

**Phosphatidylinositol-(4,5)-bisphosphate clusters into functionally distinct plasma membrane microdomains**

\*V. Thallmair, M. Leitner, D. Oliver

Institut für Physiologie und Pathophysiologie, Department of Neurophysiology, Marburg, Germany

Phosphatidylinositol-(4,5)-bisphosphate (PI(4,5)P<sub>2</sub>), the most prominent plasma membrane phosphatidylinositol is implicated in various cellular functions including exo- and endocytosis, ion channel regulation and cytoskeleton anchoring. Additionally, PI(4,5)P<sub>2</sub> serves as substrate for the generation of the second messengers inositoltrisphosphate and diacylglycerol as well as phosphatidylinositol-(3,4,5)-trisphosphate. Given the many and diverse functions of PI(4,5)P<sub>2</sub>, spatial separation into membrane pools has been suggested as a putative measure to ensure specific signaling. Indeed, PI(4,5)P<sub>2</sub> dependent KCNQ and Kir channels, as well as the PI(4,5)P<sub>2</sub> sensors PLCδ1-PH-GFP and Tubby-GFP respond differently to depletion of PI(4,5)P<sub>2</sub> by activation of Gq-coupled receptors: Only KCNQ channels and PLCδ1-PH-GFP sense the activation of phospholipase C (PLC), suggesting the existence of distinct PI(4,5)P<sub>2</sub> pools which differ in their accessibility to PLC. Moreover, specific depletion of raft PI(4,5)P<sub>2</sub> inhibits KCNQ but not Kir ion channels, whereas depletion of non-raft PI(4,5)P<sub>2</sub> interferes with Kir but not with KCNQ channel activity. These results suggest co-clustering of KCNQ, muscarinic receptor 1 and PLC with a raft associated PI(4,5)P<sub>2</sub> pool, which excludes Kir channels. To further dissolve this raft PI(4,5)P<sub>2</sub> pool, an anchor library was

generated, which allows rapamycin-induced recruitment of PI(4,5)P<sub>2</sub> phosphatases to different microdomains of the raft fraction. In further experiments the impact of microdomain-specific PI(4,5)P<sub>2</sub> depletion on KCNQ and Kir channel activity as well as on PI(4,5)P<sub>2</sub> sensor dynamics will be analyzed. Studying the compartmentalization of PI(4,5)P<sub>2</sub> will help to understand PI(4,5)P<sub>2</sub> multifunctionality and regulation, a necessary step to further understand fundamental cellular processes.

**P217**

**The polarity protein Scribble is a positive regulator of inflammatory response in endothelial cells**

\*C. Kruse, K. Pálfi, R. P. Brandes, R. U. Michaelis

Goethe Universität, Inst. für Kardiovaskuläre Physiologie, Frankfurt a. M., Germany

The highly conserved epithelial protein and known tumour suppressor Scribble (Scrib) is part of a multiprotein complex, which is responsible for the development and maintenance of apical-basal and planar polarity of epithelial cells. Also vascular endothelial cells express Scrib where it controls directed endothelial cell migration and maintains angiogenesis, but further functions of the protein in the vascular system remain unclear.

Given the fact that Scrib depletion disrupts E-cadherin-mediated cell-cell adhesion and the plasticity of the epithelium, we hypothesize that Scrib has a central impact on lateral junctions and therefore on inflammatory signalling and permeability control in endothelial cells.

In Human Umbilical Vein Endothelial Cells (HUVEC) silencing of Scrib by siRNAs indeed lead to a reduced abundance of VE-cadherin at the lateral junctions shown by confocal microscopy. Hereupon we investigated the influence of Scrib on the cytokine-induced vascular cell adhesion molecule-1 (VCAM-1) and the intercellular adhesion molecule-1 (ICAM-1) by RT-PCR and Western blotting. Scrib knock-down by shRNAs revealed a diminished expression of the adhesion proteins. To flesh out the results, we could show a clearly reduced VCAM-1 expression in the endothelium of carotid arteries in LPS treated conditional Scribflox/flox-Cdh5-CreERT2 mice. To demonstrate the functional relevance of these data, we analysed monocyte adhesion to TNFα-treated HUVEC in the Ibidi perfusion system. Monocyte adhesion to Scrib-deficient endothelial cells was significantly reduced as compared to control cells. Taking together, these observations identify Scrib as a novel positive regulator of inflammatory signalling in endothelial cells. Inhibition of Scrib could be a strategy to enhance the anti-inflammatory effect of laminar flow on endothelial cell function.

P218

**Lipoxin A4 inhibits cAMP-dependent cell migration and ion transport in colonic epithelial cells**

\*M. I. Hollenhorst<sup>1,2</sup>, J. Roubineau<sup>3</sup>, V. Urbach<sup>1,3</sup>

<sup>1</sup>National Children's Research Centre, Dublin, Ireland

<sup>2</sup>Royal College of Surgeons, Dublin, Ireland

<sup>3</sup>INSERM, France

**Question:** Lipoxin A4 (LXA<sub>4</sub>) is an endogenous inflammation resolving molecule that has beneficial effects in inflammatory bowel diseases (IBD) and inflammation related cancer. However, its exact mechanisms of action in these conditions are not fully understood. Therefore, the aim of this study was to investigate the influence of LXA<sub>4</sub> on colonic cell migration and transepithelial ion transport.

**Methods:** Expression of the LXA<sub>4</sub> receptor FPR2 in the colonic epithelial cell lines T84 and HT29Cl.19A was analysed by western blot, flow cytometry and immunofluorescence experiments. LXA<sub>4</sub>-dependent ion current changes were elucidated with electrophysiological Ussing-chamber recordings of T84 cells. LXA<sub>4</sub>-dependent T84 cell migration was analysed with a Boyden chamber assay. KCNQ1 K<sup>+</sup>-channel expression in human colonic cancer biopsies was assessed with quantitative real-time PCR.

**Results:** We detected FPR2 protein in T84 and HT29Cl.19A cells. Application of LXA<sub>4</sub> (1nM, 10 nM or 100 nM, apical) did not alter baseline short circuit current or Ca<sup>2+</sup>-dependent ion transport in T84 cells, but reduced the cAMP-dependent current increase evoked by the adenylate cyclase activator forskolin (10 μM, apical). Presence of LXA<sub>4</sub> (1nM, 10 nM or 100 nM) decreased basal and forskolin-induced cell migration. Migration inhibition of LXA<sub>4</sub> and the KCNQ1 K<sup>+</sup>-channel inhibitor chromanol 293B (10 μM) were not additive. KCNQ1 expression was upregulated in human colonic cancer biopsies.

**Conclusions:** These results show that LXA<sub>4</sub> decreases cAMP-dependent ion transport and cell migration in T84 cells. These findings might be important for reducing osmotically driven excess fluid loss in IBD and for migration inhibition of cancerous colonic epithelial cells.

P219

**Morpholino-induced gene knockdown reveals functional cooperation between Gata4 and Wt1 transcription factors during gonadal development**

\*L. J. Rudigier, K. M. Kirschner, H. Scholz

Charité-Universitätsmedizin Berlin, Institut für Vegetative Physiologie, Berlin, Germany

Mutations in the human genes encoding the transcription factors GATA4 and WT1 cause malformations of the genitourinary system. Furthermore, mice with disrupted Gata4 or Wt1 genes are embryonic lethal and fail to develop gonads. To study the functional relationship between Gata4 and Wt1 proteins in gonad formation we combined a morpholino-induced gene knockdown technique with ex vivo embryonic organ cultures. Inhibition of Wt1 with antisense vivo-morpholino significantly reduced Gata4 transcripts in

cultured gonads of male but not of female murine embryos. Consistently, suppression of Wt1 by RNA interference lowered Gata4 transcripts in Sertoli cells of the testis and/ or in cells derived from the gonad/ mesonephros region. Gata4 and Wt1 proteins were co-localized in embryonic XY and XX gonads throughout development, and Wt1-deficient mouse embryos (Wt1<sup>-/-</sup>) of either sex contained significantly less Gata4 mRNA in their gonads than the wild-type and heterozygous littermates. Treatment of cultured XY and XX gonads with Wt1 and Gata4 antisense vivo-morpholinos markedly reduced cell proliferation and survival. Moreover, knockdown of Gata4 and Wt1, either alone or in combination, revealed that both factors cooperate to some extent in the control of genes involved in sex differentiation. These findings demonstrate that Gata4 acts downstream of Wt1 on target gene expression in the developing gonad. Moreover, morpholino-induced gene knockdown in embryonic organ culture provides a suitable tool for identifying transcription-regulatory networks in gonadal differentiation.

P220

**Acidosis activates transcription factors Nrf2 and CREB via p38 signalling in prostate cancer cells**

\*A. Ihling, M. Gekle, A. Riemann, B. Schneider, O. Thews

MLU Halle-Wittenberg, Julius-Bernstein-Institut für Physiologie, Halle (Saale), Germany

**Question:** An acidic environment is a major characteristic of many solid growing tumours and leads to altered intracellular signalling and cell phenotype. Acidosis enhances the formation of reactive oxygen species (ROS) which triggers MAPK phosphorylation. Nrf2 (nuclear factor erythroid 2-related factor 2) pathway is the major regulator of cytoprotective responses to endogenous and exogenous stresses caused by ROS. For this reason we investigated the effects of an acidic tumour-like microenvironment on Nrf2 pathway in rat R-3327 prostate cancer cells (AT1). Additionally we studied activation of cAMP-responsive element binding protein (CREB), a transcription factor that is downstream of MAPK signalling.

**Methods:** Cells were exposed either to a control (pH 7.4) or an acidic extracellular environment (pH 6.6) for 3 h. For investigation of nuclear translocation of Nrf2, cytoplasmic and nuclear fractions were prepared and subjected to immunoblot analysis. Phosphorylation of CREB was determined with phospho-specific antibodies.

**Results:** In AT1 cells extracellular acidosis led to an increased CREB phosphorylation and nuclear translocation of Nrf2. Blocking of p38 MAPK signalling pathway abolished the acidosis-induced phosphorylation of CREB and Nrf2 translocation into the nucleus.

**Conclusions:** The results demonstrate that the p38 MAPK pathway results in the downstream activation of transcription factors CREB and Nrf2, possibly in response to oxidative stress. An active Nrf2 pathway could sustain a favorable redox balance and upregulate antioxidative genes in cancer cells to promote their survival.

(Supported by the BMBF ProNet-T3)

P221

**The Cx43 induced migratory activity is associated with alterations of the cytoskeleton and may be due to Cx43/p21-activated kinase (PAK) interaction**

\*K. Pogoda, P. Kameritsch, U. Pohl

Walter-Brendel-Centre of Experimental Medicine/LMU-University of Munich, Cardiovascular Physiology, München, Germany

**Question:** Previously, we have shown in HeLa cells that Cx43 expression enhances cell migration in a channel independent, p38-mediated manner. Further, the enhanced migration was associated with enhanced filopodia formation which is an actin dependent process. Here we studied potential changes of the actin cytoskeleton as well as involvement of p38 upstream molecules in the control of migration.

**Methods:** Serum-starved HeLa cells expressing Cx43 or empty-vector transfected cells (CTL; expressing no connexins) were stimulated with 10% NBCS to elicit migration. Actin staining was performed using AF546-phalloidin. Actin polymerisation was measured after stimulation with 10% NBCS for 3h and staining of F-actin (AF546-phalloidin) and G-actin (AF488-DNAseI). Using immunoprecipitation (IP) we studied the potential interaction of Cx43 with the p38 upstream molecule PAK, the effector protein of Rac and Cdc42 (molecules affecting filopodia and lamellipodia formation).

**Results:** Cx43 expression altered the actin organisation in HeLa. Compared to HeLa-CTL, HeLa-Cx43 expressed significantly more filopodia per single cell (mean ± SEM: Cx43: 30±7 CTL: 12±3; n=4). Cx43 was expressed at intercellular contact areas but also in filopodia and filopodial structures connecting two cells. F-actin/G-actin ratio in the presence of 10% NBCS of HeLa-Cx43 cells was 31% higher than in HeLa-CTL (n=4). IP-studies revealed interaction of Cx43 with PAK (n=3).

**Conclusion:** Cx43 enhanced cell migration is associated with an altered actin composition in a way as seen in an increased number of filopodia. It is tempting to speculate that activation of PAK is enhanced after binding to Cx43, thereby mediating the p38 dependent enhancement of cell migration.

P222

**A computational approach to study the influence of axon location on signal integration in pyramidal neurons**

\*A. Yanez<sup>1</sup>, A. V. Egorov<sup>1</sup>, C. Thome<sup>1</sup>, T. Kelly<sup>2</sup>, H. Beck<sup>2</sup>, A. Draguhn<sup>1</sup>, M. Both<sup>1</sup>

<sup>1</sup>University of Heidelberg, Institute of Physiology and Pathophysiology, Heidelberg, Germany

<sup>2</sup>University of Bonn, Life and Brain Center, Bonn, Germany

Neuronal processing is classically divided into dendritic input, somatic integration and axonal output. In this view, neurons process information by receiving input from the dendrites, integrate it in soma and finally producing an output at the axon. The axon initial segment (AIS), where action potentials (AP) are initiated is usually located adjoining to the soma, although other configurations have been reported (Grubb 2011; Häusser, Stuart, Racca Sakmann 1995). Interestingly, we found that about 50 % of CA1 pyramidal neurons branch off from a basal dendrite rather than the soma. We used NEURON simulations of a biophysically realistic pyramidal CA1 neuron to see how this might affect the integration of synaptic input at such a dendrite compared to a simple dendrite. The axon of our study neuron was connected to an axon carrying dendrite (AcD) at a variable length from soma, and we studied whether the input from this dendrite was favored due to the bypassing of the soma. Our simulations show that although the essential properties of the neuron do not change, the input of the dendrite adjacent to the axons is highly favored, lowering both the threshold of action potential (AP) activation as well as the synaptic input required. Furthermore, we were also interested in studying how dendritic spikes (DS) were affected in this special morphology. These results suggest that an axon directly connected to a dendrite rather than the soma creates an asymmetric situation concerning the input to this dendrite and that this dendrite is highly favored with respect to others.

Supported by "la Caixa" and DAAD.

P223

**Distinct optogenetically evoked waveforms in hippocampal circuits provide information about assembly formation**

\*P. Geschwill<sup>1</sup>, M. Both<sup>1</sup>, K. Deisseroth<sup>2</sup>, A. Draguhn<sup>1</sup>

<sup>1</sup>Universität Heidelberg, Institut für Physiologie und Pathophysiology, Heidelberg, Germany

<sup>2</sup>Stanford University, Department of Bioengineering, Stanford, United States

**Question:** Transient formation of neuronal ensembles in various regions of the brain likely underlies mnemonic processes such as spatial memory generation. One defining feature of ensembles is the repetitive coordinated activity of defined sets of neurons. Many studies have tried to elu-

cidate the underlying mechanisms that govern this binding of distinct, scattered neurons into a functional ensemble. However, many questions about the spatiotemporal structure of memory-forming ensembles remain unanswered.

**Methods:** We activated subsets of hippocampal neurons in vitro, using optogenetic tools in conjunction with a pattern illumination system and custom-built spinning disk confocal optics. This system allows region specific optical stimulation of genetically targeted neurons expressing the light-gated ion channel channelrhodopsin-2 (ChR2). We characterized the virus-mediated expression of two ChR2 mutants, H134R and T159C, and compared their ability to evoke light induced network activity in three different biological preparations: dissociated primary hippocampal neurons (controlled by patch clamp recordings), organotypic slice cultures and acutely prepared hippocampal brain slices (controlled by local field potentials).

**Results:** Expression of optogenetic constructs in dissociated cells appeared to be highly dependent on virus serotype. In cells expressing ChR2, light illumination showed reliable responses in both voltage and current clamp recordings. Field potential recordings from cultured and acutely prepared brain slices revealed that region-specific optical activation of pyramidal cells elicits stable waveforms resembling a physiological type of network activity, so-called sharp wave-ripple complexes (SPW-R).

**Conclusions:** We conclude that pattern illumination grants many unprecedented possibilities for investigating neural circuits that possibly underlie memory formation.

**P224**

**Potential effect of low-frequency magnetic fields (LF-MFs) on mouse models of amyotrophic lateral sclerosis and Alzheimer's disease**

M. Liebl<sup>1</sup>, J. Windschmitt<sup>1</sup>, A.-K. Schäfer<sup>1</sup>, A. Besemer<sup>1</sup>, B. Pophof<sup>2</sup>, C. Behl<sup>1</sup>, <sup>\*</sup>A. Clement<sup>1</sup>

<sup>1</sup>University Medical Center Mainz, Institute for Pathobiochemistry, Mainz, Germany

<sup>2</sup>Federal Office for Radiation Protection, Salzgitter, Germany

Amyotrophic lateral sclerosis (ALS) and Alzheimer's dementia (AD) are devastating neurodegenerative diseases affecting different sets of neuronal populations. Although some ALS and AD cases are inherited, the vast majority of cases are sporadic. Therefore, environmental factors are discussed as potential risk factors. Several epidemiological studies investigated whether occupational and residential exposure to low-frequency magnetic fields (LF-MFs) increases the risk to develop ALS or AD. LF-MFs are generated by electrical current flow and can penetrate biological tissue. Some of these studies found a positive correlation between LF-MF exposure and disease. To investigate whether LF-MFs interfere with molecular pathways involved in ALS and AD, we exposed transgenic mice expressing mutant SOD1 and mutant APP, representing mouse models for ALS and AD, respectively, with LF-MFs (50 Hz, 1 mT) and compared them with sham-exposed animals. We examine potential effects of LF-MFs on the life

span, disease duration and learning behavior. Furthermore we compared RNA and protein levels of genes involved in proteostasis, markers for oxidative damage, glial activation and enzymatic activities between exposed and sham exposed mice to detect a potential influence of LF-MFs on ALS and AD.

This project is funded by the Federal Office for Radiation Protection

**P225**

**Molecular identity of Ca<sup>2+</sup> sensors for transmitter release at the developing calyx of Held**

<sup>\*</sup>O. Kochubey, R. Schneggenburger

École Polytechnique Fédérale de Lausanne (EPFL), Brain Mind Institute, Laboratory of Synaptic Mechanisms, Lausanne, Switzerland

In many CNS circuits, the functional properties of synapses can change drastically after initial formation of synapses, but the underlying molecular mechanisms are largely unknown. We used genetic deletions of presynaptic Ca<sup>2+</sup> sensor proteins in combination with molecular perturbations by virus-mediated expression and patch-clamp electrophysiological analysis at an identified auditory brainstem synapse, the calyx of Held, to study these mechanisms. In calyces after P12, the predominant Ca<sup>2+</sup> sensor for fast release is Synaptotagmin 2 (Syt2), since the release that remains in Syt2 KO mice is ~100 times slower and has significantly lower Ca<sup>2+</sup>-cooperativity in Ca<sup>2+</sup>-uncaging experiments (power ~1, versus ~4 in control). At P5-P6, however, a residual fast release component was observed in Syt2 KO mice, and aggregate release showed a mixed Ca<sup>2+</sup>-cooperativity of ~2. At even younger ages (P2-P3), we found no difference in release between Syt2 KO and control. Thus, an alternative fast Ca<sup>2+</sup> sensor might be present early in development, and Syt1 and Syt9 isoforms are obvious candidates. However, the residual fast release in young Syt2 KO mice was insensitive to shRNA mediated Syt1 knock-down, and remained in Syt9/Syt2 DKO synapses, while Syt9 was able to rescue fast release in Syt2 KO. In agreement with these functional findings, immunohistochemistry showed that: i) small VGLUT2 positive terminals at P2 were devoid of Syt2, which only appeared in growing calyces from ~P3-P4 onwards, and ii) Syt1 was largely absent from glutamatergic terminals and calyces at all ages studied. These experiments suggest a developmental Ca<sup>2+</sup> sensor isoform switch at an identified CNS synapse. Furthermore, they suggest that unknown Ca<sup>2+</sup> sensor proteins could drive fast release in recently formed synapses.

**P226**

**Dendritic inhibition via GABA<sub>A</sub> α5 subunit-containing receptors controls synaptic integration in CA1 pyramidal neurons**

<sup>\*</sup>J. Schulz<sup>1</sup>, A. Thomas<sup>2</sup>, M.-C. Hernandez<sup>2</sup>, J. Bischofberger<sup>1</sup>

<sup>1</sup>University of Basel, Department of Biomedicine, Basel, Switzerland

<sup>2</sup>F. Hoffmann-La Roche Ltd, Pharma Research and Early Development,

Discovery Neuroscience Department, Basel, Switzerland

Alpha5-containing GABA<sub>A</sub> receptors have been implicated in tonic inhibition, while their contribution to phasic synaptic inhibition remains more controversial. Recently, the α5-selective negative allosteric modulator (NAM) RO4938581 was shown to increase synaptic plasticity and improve spatial learning in a mouse model of Down syndrome (Martinez-Cue et al., 2013). Although this treatment has been suggested to reverse the over-inhibition found in Down syndrome, the precise cellular mechanisms remain obscure. Therefore, we investigated the effect of RO4938581 on neurons in mouse hippocampal brain slices. Tonic inhibition was evoked by bath-application of 5 μM GABA in the presence of 25 μM AP5 and 10 μM CNQX. Application of the α5-NAM (3 μM) reduced the GABA-dependent tonic currents (~25 pA) by about 25%. To study phasic inhibition, inhibitory postsynaptic currents (IPSCs) were evoked by stimulating locally in the dendritic layer or close to the soma. Slow dendritic IPSCs evoked in stratum lacunosum moleculare were significantly reduced to 64.4 ± 14.4% (n=5) after the application of 1 μM α5-NAM. In contrast, there was no reduction of somatic IPSCs evoked in stratum pyramidale. Remarkably, postsynaptic potentials evoked by coincident brief burst stimulation of the perforant path and Schaffer collaterals in the absence of glutamate receptor blockers were strongly increased by 48.7 ± 13.7% (n=9) after application of the α5-NAM (1 μM). These results indicate that dendritic α5-containing GABA<sub>A</sub> receptors contribute to both, phasic and tonic inhibition and thereby powerfully control postsynaptic integration in CA1 pyramidal cells.

Supported by the Roche RPF program.

**P227**

**Contribution of GABA to spontaneous waves of activity in developing mouse cerebral cortex**

<sup>\*</sup>K. Weir<sup>1,2</sup>, C. Easton<sup>2</sup>, A. Scott<sup>2</sup>, W. Moody<sup>2</sup>

<sup>1</sup>University of Mainz, Physiology, Mainz, Germany

<sup>2</sup>University of Washington, Neurobiology, Seattle, United States

During a period of early development, structures within the central nervous system of mammals generate spontaneous waves of electrical activity. This spontaneous activity is necessary for maturation of the CNS, including maturation of ion channel properties, formation of synaptic connections and neuronal migration. In the developing mouse cerebral cortex such waves occur between embryonic day 18 and postnatal (P) day 8, and manifest as increases in intracellular calcium and bursts of actions potentials in the majority of neurons in the cortex. We have developed a microfluidic multi-electrode array that is compatible with fluorescent imaging of intracellular calcium signals at single-cell resolution to study the spatial and temporal characteristics of these waves in P1-P5 coronal brain slices. In coronal slices, waves initiate in the ventral (piriform) cortex and are detected by twelve apertures placed along the ven-

tral-dorsal axis of the slice, and by simultaneous calcium imaging as the spread of the fluorescence signal along the same propagation axis. The signals from the dorsal cortex show a prominent low-frequency oscillation late in the signal that is not present in ventral cortex. The use of a genetic knockout of the major synthetic enzyme for GABA, GAD67, has also revealed that there is both a GABAergic and glutamatergic pacemaker present in the piriform cortex and that waves initiated by either pacemaker can be distinguished by their distinct electrical signatures.

**P228**

**All optical physiology - Investigating slow wave initiation by combining optogenetics and two-photon calcium imaging**

<sup>\*</sup>J. Döring, G. Pramanik, E. Rosales, A. Stroh

Universitätsmedizin Mainz, Mainz, Germany

**Question:** Here, we investigate an oscillatory neuronal population activity highly relevant to normal cognitive function, the slow oscillations, reflecting two different brain states - a depolarized Up state and a hyperpolarized Down state. Slow oscillations represent the characteristic activity patterns during sleep and many types of anesthesia. We applied 2-photon Ca<sup>2+</sup> imaging in combination with single-cell optogenetic stimulation to explore the initiation of slow waves on micro-circuit level.

**Methods:** AAVs encoding for C1V1mCherry were injected in layer 2/3 of mouse visual cortex. VGLUTII and GAD65/67 immunofluorescence was employed for the characterization of the opsin-expressing neurons. For in vivo Ca<sup>2+</sup> imaging, Oregon-Green-Bapta-1 (OGB 1) and the astrocytic label sulforhodamine 101 (SR 101) were pressure-injected in the C1V1-expressing region (V1). The Ca<sup>2+</sup> indicator was excited using a Ti:Sa laser at 800 nm, C1V1 was simultaneously excited using an Optical Parametric Oscillator (OPO) at wavelengths ranging at 1100-1300 nm.

**Results:** Strong, membrane-bound expression of C1V1mCherry was found in layer II/III of V1 14 days after injection, covering an area of 500 μm. Immunofluorescence revealed predominant expression of C1V1-mCherry in excitatory neurons. In vivo, we demonstrate simultaneous 2-photon Ca<sup>2+</sup> imaging and single cell 2-photon C1V1 excitation. **Conclusion:** We established an all-optical-physiology approach, no cross-talk of optogenetic stimulation/ optical imaging could be observed. This allows a causal exploration of the activity patterns required for the initiation of slow waves.

**P229**

**Characterizing Ca<sup>2+</sup> dynamics upon mechanical lesion in an astrocyte/neurosphere co-culture model**

<sup>\*</sup>E. Rosales Jubal<sup>1</sup>, A. Kraft<sup>2</sup>, Z. Barger<sup>3</sup>, S. Momma<sup>2</sup>, A. Stroh<sup>1</sup>

<sup>1</sup>Johannes Gutenberg University of Mainz, Institute of Microscopic Anatomy and Neurobiology - Research Group of Molecular Imaging and Optogenetics, Mainz, Germany

<sup>2</sup>Johann Wolfgang Goethe University Frankfurt, Institute of Neurology - Edinger Institute - Neuroscience Center, Frankfurt am Main, Germany

<sup>3</sup>University of Washington, Department of Biology, Seattle, United States

**Question:** How to characterize a traveling Ca<sup>2+</sup> wave in an astrocyte/neurosphere co-culture induced by acute lesioning?

**Methods:** Ca<sup>2+</sup> imaging in vitro on micro-circuit level allowed us to record the activity of astrocytic/neurosphere network in response to a mechanical lesion. Following previous work (Nauhaus et al 2009, 2012), we adapted the procedure to characterize the Ca<sup>2+</sup> wave in terms of velocity and recruitment of cell population with single-cell resolution. We fitted a line to the site of mechanical lesion and select the ROIs semi-automatically, afterwards we calculated the minimum distance to each ROI center of mass to the linear lesion and sort the ROIs according to those values. The highest value of the normalized fluorescence (dF/F) was defined as the maximum response from each cell, and the correlation between distance from the lesion and peak activity was assessed. Finally, the velocity of the Ca<sup>2+</sup> wave was obtained from the slope of the best fitting line to the latter relationship.

**Results:** We recorded an astrocytic Ca<sup>2+</sup> wave originating from the lesion and recruiting the entire network of both astrocytes and neurospheres. The analysis shows that more than 95% of cells are participating in the Ca<sup>2+</sup> wave. The average velocity of the astrocytic Ca<sup>2+</sup> wave ranged at 0.8 mm/sec.

**Conclusions:** This implementation of data analysis designed to capture population dynamics is suitable to analyse spatio-temporal patterns of activity in cellular networks.

### P230

#### Disturbed excitation-inhibition balance in a human embryonic stem cell-derived model for Tuberous sclerosis

\*K. Behr<sup>1</sup>, M. Vukcevic<sup>1</sup>, V. Costa<sup>1,2</sup>, S. Aigner<sup>2</sup>, R. Jagasia<sup>2</sup>, J. Bischofberger<sup>1</sup>

<sup>1</sup>University of Basel, Department of Biomedicine, Basel, Switzerland

<sup>2</sup>F. Hoffmann-La Roche Ltd, Pharma Research and Early Development, Basel, Switzerland

Mutations in the TSC2 gene coding for tuberin, a negative regulator of mTORC1, lead to mTORC1 hyperfunction and to Tuberous Sclerosis, characterized by cortical tuber formation, epilepsy and autism. From transgenic mouse models we know that TSC1 or TSC2 deletion results not only in brain malformations and seizures, but also in altered synaptic plasticity and disturbed learning and memory. To investigate the impact of TSC2-deletion directly in human neurons we used zinc-finger mediated genome editing to target the TSC2 gene in hESCs. After generating hESC clones with heterozygous or homozygous deletions of TSC2, cells were differentiated into neural stem cells and synaptically connected neuronal networks within 6-8 weeks in vitro. TSC2-deletion induced a hyperactivation of mTORC1 and increased protein translation as indicated

by hyperphosphorylation of S6 and 4EBP1. To investigate synaptic transmission we used whole-cell patch-clamp recordings, demonstrating that networks of human TSC2-/- neurons show a ~3-fold higher frequency of spontaneous synaptic currents compared to human control neurons. Similarly, the total synaptic charge was ~3-times larger. Recording miniature glutamatergic and GABAergic synaptic currents in the presence of TTX revealed that the excitation-inhibition balance was significantly changed with a 4-fold decrease in the rate of glutamatergic and a 7-fold increase in the rate of GABAergic synaptic currents. By contrast, kinetic properties of GABA and glutamate receptors as well as the amplitude of mEPSCs and mIPSCs appear to be unchanged. Taken together, TSC2-deletion disturbs synapse formation and excitation-inhibition balance in immature human neuronal networks.

Supported by the EU-AIMS and the Roche RPF-program.

### P231

#### Functional changes in GABAergic inhibition following focal cortical lesions

\*B. Imbrosci, A. Neitz, T. Mittmann  
University of Mainz, Mainz, Germany

Focal lesions in the cerebral cortex lead to profound alterations in the functional properties of the surviving cortical networks. In particular, a reduced strength of GABAergic transmission is classically considered one major cellular mechanism underlying neuronal hyperexcitability often developing following these pathological events.

In the present study, by using an in vivo-ex vivo model of laser-lesions in the rodent visual cortex, we provide several lines of evidence indicating that this conclusion may be an oversimplification. Changes in the inhibitory system were studied in the first week post-injury, in a cortical area located at around 1 mm distance from the lesion. Sham-operated animals were used as controls. Immunohistochemical analyses revealed no apparent signs of degeneration of GABAergic synaptic terminals. Patch-clamp recordings from layer 2/3 pyramidal neurons, in acute brain slices, disclosed a reduced frequency of miniature inhibitory postsynaptic currents (mIPSCs) post-lesion. These changes, accompanied by an increased PPR of evoked postsynaptic inhibitory currents (eIPSCs), suggest an impairment in phasic GABA release. Counteracting the reduced phasic GABA release we observed a prolongation in the kinetics of IPSCs as well as an enhancement of GABAA-receptor-mediated tonic inhibition. To further explore the effect of the lesion on inhibition we also performed extracellular measurements and patch clamp recordings from inhibitory cells in the GAD67-GFP knock-in mice line. Interestingly, our data revealed an elevated excitability in a large subpopulation of GABAergic cells that were identified, based on specific firing properties, as non fast-spiking (Non Fs) interneurons. In net contrast, fast-spiking (Fs), parvalbumin-expressing interneurons, displayed a reduction in the strength of their excitatory drive and therefore tended to

be hypoexcitable. Based on the outlined observations we propose a revision to the generally accepted notion that a cortical lesion simply leads to a reduction in the intracortical inhibitory strength. Our new findings rather suggest that the inhibitory strength following brain injuries may dynamically change depending on the brain state and on the activation level of certain interneuronal subtypes.

### P232

#### Role of the proteasome protein degradation system on synaptic function in a mouse model of traumatic brain injury in the somatosensory cortex

\*E. Le Priault<sup>1</sup>, B. Imbrosci<sup>1</sup>, A. Neitz<sup>1</sup>, C. Gölz<sup>2</sup>, S. Thal<sup>2</sup>, V. Felzen<sup>3</sup>, C. Behr<sup>3</sup>, K. Engelhard<sup>2</sup>, T. Mittmann<sup>1</sup>

<sup>1</sup>UMC of the University of Mainz, Institut of Physiology and Pathophysiology, Mainz, Germany

<sup>2</sup>UMC of the University of Mainz, Clinics of Anaesthesiology, Mainz, Germany

<sup>3</sup>UMC of the University of Mainz, Institute of Pathobiochemistry, Mainz, Germany

Traumatic brain injury (TBI) ranks upon the top 3 causes of mortality worldwide. TBI leads to brain tissue necroses as well as to secondary cellular and molecular processes, which may increase the primary damage. Aberrant functionality and expression of the ubiquitin proteasome system (UPS) has been implicated in the pathology of TBI. Certain studies pinpoint the fact that modulation of the proteasome activity might have neuroprotective effects after TBI, mainly via its positive influence on the completely shattered neuronal proteostasis of the injured brain. Here we used a controlled cortical impact (CCI) model of TBI in adolescent mice (between P18-P23) and investigated the potential contribution of the UPS for functional alterations of surviving neurons after 1-7 days post-injury. A biochemical assay detecting chymotrypsin-like protease activity of 20S proteasome disclosed a dramatic decrease of proteasome activity in the ipsilateral hemisphere after the lesion. The contralateral hemisphere was also effected, but less prominently. We also investigated the functional alterations induced by the CCI in acute brain slices from TBI-treated animals. We analyzed extracellular field potentials in the somatosensory cortex both in the injured hemisphere and in the hemisphere contralateral to the lesion by use of a 32-channel Multi-Electrode Array (MEA). Interestingly, we observed an altered short-term plasticity as measured by paired-pulse stimulation as well as an altered synaptic fatigue upon high frequency synaptic stimulation. These changes indicate alterations in the release probability of neurotransmitter at glutamatergic synapses in the vicinity of the injury. Next we investigated the potential contribution of the altered proteasome activity on the observed functional changes. Bath application of the specific inhibitor of the proteasome (MG132, 10µM) to slices of untreated animals indeed modulated the basal synaptic transmission. In conclusion, we observed an altered activity of the ubiquitin proteasome system following TBI, which potentially modulates the synaptic function of surviving neurons in somato-

sensory cortex. A better understanding of this interaction might help to develop future therapeutical treatments following TBI.

This work is supported by the Collaborative Research Centre 1080 (TP-A7 to K.E., T.M. and C.B) at the UMC of the Univ. Mainz.

### P233

#### SPRED-2 is involved in synaptic efficacy

\*M. Weber<sup>1</sup>, M. Ullrich<sup>2</sup>, K. Schuh<sup>2</sup>

<sup>1</sup>Johann Wolfgang Goethe University of Frankfurt, Institute of Physiology II, Frankfurt am Main, Germany

<sup>2</sup>Julius-Maximilian-University of Wuerzburg, Institute of Physiology I, Wuerzburg, Germany

SPRED-2 is one of the Sprouty-related proteins (SPREDs) inhibiting the Ras/Raf/MAP-kinase cascade and is strongly expressed in neurons. In previous studies we found that SPRED-2 knock-out (KO) mice show, among other changes, obsessive-compulsive disorder (OCD) and reduced anxiety in the elevated plus maze. In the current study SPRED-2 KO mice showed an increased synaptic efficacy compared to wild-type animals (WT). This effect was observed in two distinct brain regions related to anxiety and OCD, namely the lateral amygdala and putamen. More precisely, the excitatory postsynaptic current (EPSC), elicited by presynaptic fibre stimulation with 1 mA, was significantly increased in both regions. In lateral amygdala neurons, stimulation of thalamic afferences elicited an EPSC with 121.3 ±44.5 pA in WT (n=8) and 279.51 ±40.89 pA in KO (n=9; p=0.02). In the putamen, stimulation of corpus callosum fibres innervating the putamen elicited an EPSC with 31 ±4.95 pA in WT and 63.3 ±11.8 pA in KO (both n=5; p= 0.04). Further data, measured in the lateral amygdala, point to a presynaptic localisation of these changes: Firstly, the paired pulse ratio (EPSC2/EPSC1, 50 ms interstimulus interval) was reduced from 0.44 ±0.08 in WT (n=8) to 0.19 ±0.05 in KO (n=9; p= 0.02). Secondly, the frequency of miniature synaptic currents was also reduced from 0.32 ±0.08 in WT (n=8) to 0.12± 0.05 in KO (n=9; p= 0.04). Although, in both regions additional postsynaptic changes occurred, they rather attenuate synaptic responses. In the amygdala, amplitudes of miniature synaptic currents were 21.44 ±1.07 pA in WT (n=8) compared to 17.1 ±1.24 pA in KO (n=9; p= 0.02). In the putamen, especially in the negative potential range, the whole cell current increased: at -130 mV voltage clamp we measured -684 ±80.08 pA in WT (n=6) and -1020 ±91.59 pA in KO (n=5; p=0.02). The reversal potential of this additional current was -79 mV, indicating an increase in potassium current of the inward rectifying type. We conclude that SPRED-2 is involved in tuning synaptic efficacy in putamen and lateral amygdala, which may explain the strong changes in behaviour of SPRED-2 KO mice.

**P234****The role of the JAK/STAT pathway in synaptic plasticity**

\*L. Hildebrandt-Einfeldt<sup>1,2</sup>, C. Nicolas<sup>1</sup>, S. Peineau<sup>1,3</sup>, M. Amici<sup>1</sup>, M. Zhuo<sup>4</sup>, B.-K. Kaang<sup>4</sup>, S. M. Fitzjohn<sup>1</sup>, Z. A. Bortolotto<sup>1</sup>, K. Cho<sup>1</sup>, G. L. Collingridge<sup>1,4</sup>

<sup>1</sup>University of Bristol, MRC Centre for Synaptic Plasticity, Bristol, United Kingdom

<sup>2</sup>Johannes Gutenberg University of Mainz, Institute of Physiology, Mainz, Germany

<sup>3</sup>INSERM, Paris, France

<sup>4</sup>Seoul National University, Department of Brain and Cognitive Sciences, Seoul, Korea

The Janus kinase (JAK)/signal transducer and activator of transcription (STAT) pathway is linked to many physiological processes such as cell proliferation, differentiation and development. The cellular and molecular mechanism by which the JAK/STAT pathway could be involved in neuronal function is still not known. The JAK/STAT pathway can be activated by distinct types of cytokines, growth factors, and protein tyrosine kinases and its main role is the regulation of gene expression. Four JAK and seven STAT isoforms are known, but just JAK2 and STAT3 are highly expressed in the brain. Using a combination of biochemistry, pharmacology and genetic approaches, we could show that this pathway plays an important role in the induction of NMDA-receptor dependent long-term depression (NMDAR-LTD) in the hippocampus of juvenile Wistar rats. Pharmacological inhibition of JAK blocks the induction of NMDAR-LTD at CA1 synapses in the hippocampus. This effect is highly selective since the same treatment has no effect on LTP, on the activity-dependent reversal of LTP, and on LTD, induced by the activation of metabotropic glutamate receptors. In addition, a knockdown of JAK2 blocks the induction of NMDAR-LTD. The effects of JAK2 on NMDAR-LTD are mediated via STAT3, and pharmacological inhibition or knockdown of STAT3 also blocks the induction of NMDAR-LTD. Furthermore, low-frequency stimulation causes activation and nuclear translocation of STAT3. Interestingly, we find that the nuclear translocation of STAT3 is not required for NMDAR-LTD. In summary, we could show that the JAK/STAT pathway is a key player in synaptic plasticity.

**P235****SPRED2 - a critical regulator of synaptic protein expression and of behavior?**

\*M. Ullrich<sup>1</sup>, M. Weber<sup>2</sup>, A. Post<sup>3</sup>, S. Popp<sup>3</sup>, H. Guerrero<sup>1</sup>, K. Schuh<sup>1</sup>

<sup>1</sup>University of Würzburg, Institute of Physiology, Würzburg, Germany

<sup>2</sup>Zentrum der Physiologie, Frankfurt, Germany

<sup>3</sup>University of Würzburg, Würzburg, Germany

**Question:** Recently, we demonstrated that SPRED2 is indispensable for appropriate regulation of hormonal homeostasis. We showed that SPRED2, by down-regulating MAPK signaling via inhibition of ERK phosphorylation, suppresses Ets-dependent activation of the CRH promoter and thus reduces CRH transcription and release. Vice versa, SPRED2 KO mice show increased hypothalamic CRH mRNA levels

and release, eliciting elevated downstream hormone secretion, including ACTH, corticosterone, and aldosterone. Excessive stress hormone release from the HPA axis is often associated with behavioral and mood disorders, as reflected by the obsessive grooming of SPRED2 KO mice, which was associated with self-inflicted skin lesions. Therefore, we investigated how SPRED2 ablation affects behavior, emotional state, brain structure and functions.

**Methods and Results:** A set of behavioral standard tests with SPRED2 KO mice and WT littermates, including elevated plus maze, open field and light dark box, indicated a changed anxiety behavior in SPRED2 KOs, which correlated with increasing age and the incidence of compulsive grooming. In order to investigate synaptic transmission from thalamic nerve fibers to the amygdala, a brain region related to anxiety and obsessive compulsive disorders (OCD), we performed electrophysiological measurements on acute brain slices. Thereby, we detected elevated excitatory postsynaptic currents (EPSCs), indicating an augmented synaptic transmission from thalamus to amygdala. Subsequent expression studies by RT-PCR and Western blot revealed that amygdala mRNA and protein levels of postsynaptic glutamate receptors mGluR2 and mGluR5, and PSD95 were up-regulated, whereas the presynaptic bassoon was down-regulated. Reflected by dysregulated protein expression, these data suggest counter-regulating mechanisms between presynaptic and postsynaptic activities. Because the antidepressant fluoxetine, a selective serotonin reuptake inhibitor, is a common drug for the treatment of mood disorders, we tried to rescue the excessive grooming by oral fluoxetine treatment. Fluoxetine was administered at a dose of 20 mg/kg/day within white chocolate and for the duration of four weeks. Photo documentations on day 0, 14, and 28 demonstrated a reduced severity and occurrence of self-inflicted lesions. In line, video documentations also indicated a reduced grooming behavior after fluoxetine treatment, which further underlines the existence of a mood disorder in our SPRED2 KOs.

**Conclusions:** Taken together, we demonstrated that SPRED2 deficiency results in obsessive compulsive grooming and in altered anxiety behavior, which is associated with increased synaptic transmission from thalamus to amygdala and can be rescued by fluoxetine treatment. Increased synaptic transmission is accompanied by altered expression of pre- and postsynaptic proteins in the amygdala. Thus our study for the first time indicates a causal context between SPRED2, MAPK signaling, and OCDs and suggests novel functions of SPRED2 in the brain.

**P236****Filamentous actin in cortical dendrites of the living mouse visualized by superresolution**

\*H. Steffens, K. I. Willig, S. W. Hell

MPI for Biophysical Chemistry, Dept. NanoBiophotonics, Goettingen, Germany

Filamentous (F-) actin is one of the proteins important for growth of dendritic spines, anchoring of postsynaptic receptors and modulation of synaptic activities. It is self

evident that actin dynamics is best studied in vivo. Confocal microscopy and 2-Photon Laser Scanning microscopy provide excellent tools to study the dynamics of fluorescently labelled proteins in 3D. However, these methods are diffraction limited, i.e. best optical resolution of these tools is between 250 and 400 nm. The recently developed Stimulated Emission Depletion (STED) microscopy provides a tool to go beyond the diffraction barrier. Time lapse STED imaging of actin in dendrites and spines of the molecular layer of the visual cortex of the living mouse provided detailed insight of spine dynamics. F-actin was labelled with fluorescent markers (eYFP) by transfection of pyramidal cells with viral vectors (Semliki Forest virus, SFV; Adeno-associated virus, AAV). We could image the dendritic structures with a resolution of around 50 to 60 nm (raw data), down to  $z = -40 \mu\text{m}$  below the brain surface, despite the sources of manifold tissue motion. Time lapse imaging visualized the high dynamics of dendritic spines in the adult brain, which might reflect the plasticity of the brain. The results show also that in vivo STED microscopy is capable to provide insights into the dynamics of the protein-based machinery within its natural environment.

**P237****Neuron type-specific impact on formation and propagation of hippocampal sharp wave ripples**

\*G. Caliskan<sup>1</sup>, I. Müller<sup>2</sup>, A. Winkelmann<sup>2,3</sup>, J. O. Hollnagel<sup>1</sup>, A. Rösler<sup>1</sup>, O. Stork<sup>2</sup>, U. Heinemann<sup>1</sup>, J. C. Meier<sup>3</sup>

<sup>1</sup>Charité Universitätsmedizin-Berlin, Inst. for Neurophysiology, Berlin, Germany

<sup>2</sup>Otto-von-Guericke-University, Institute of Biology, Magdeburg, Germany

<sup>3</sup>Max Delbrück Center for Molecular Medicine, RNA editing and Hyperexcitability Disorders Helmholtz Group, Berlin, Germany

**Question:** Explicit memories are transferred from the transitory memory storage in the hippocampus to the cortical mantle. Sharp wave-ripple (SPW-R) activity in the hippocampus likely contributes to this process by replay of previously stored information in a select ensemble of neurons. Although SPW-Rs have been studied extensively, the role of glycine and its receptors in SPW-R modulation has not been investigated. RNA splicing of GlyR  $\alpha 3$  determines presynaptic expression of the RNA-edited  $\alpha 3$  receptors (Winkelmann et al., 2014) leading to a gain-of-function of glutamatergic or parvalbumin-positive neurons in genetically modified mice and phenotypes associated with hyper-excitability and cognitive dysfunction or anxiety, respectively. Here, we studied neuron type-specific impact on hippocampal SPW-Rs using these two mouse lines for cell type-specific glycinergic enhancement of neuronal function.

**Methods:** Mice with targeted presynaptic expression of a gain-of-function glycine receptor (GlyR) RNA variant were used. Field potential recordings of SPW-Rs were obtained from CA3 and CA1 of horizontal hippocampal slices.

**Results:** Mice with GlyR expression in parvalbumin-positive synapses showed reduced ripple amplitude and increased ripple frequency as well as ripple probability per

sharp wave (SPW), while mice with GlyR expression in principal neurons (Camk2a) showed no significant alterations. Incidence of SPW-Rs was higher in CA3 and CA1 in mice with GlyR expression in parvalbumin-positive synapses, and SPW propagation from CA3 to CA1 was facilitated due to increasing signal to noise ratio in CA3 of these animals.

**Conclusion:** Our study identifies a critical role for parvalbumin-positive interneurons in regulation of SPW-R formation and CA3-to-CA1 propagation.

**P238****Effects of blood-brain barrier dysfunction on response to antiepileptic drugs in the hippocampus**

\*U. Heinemann<sup>1</sup>, S. Salar<sup>1</sup>, A. Maslarova<sup>1</sup>, K. Lippmann<sup>1</sup>, J. Nichtweiss<sup>1</sup>, I. Weissberg<sup>2</sup>, L. Sheintuch<sup>2</sup>, A. Friedman<sup>2</sup>, W. Kunz<sup>3</sup>

<sup>1</sup>Charité Universitätsmedizin Berlin, Institute of Neurophysiology, Berlin, Germany

<sup>2</sup>Ben-Gurion University of the Neg, Zlotowski Center of Neuroscience, Department of Physiology and Cell Biology, Faculty of Health Sciences, Beersheba, Israel

<sup>3</sup>University of Bonn, Department of Epileptology, Medical Center, Bonn, Germany

**Question:** Pharmacoresistance is affecting 30 % of epileptic patients and the ratio increases infocal and partial epilepsies. Recent studies indicate that blood-brain barrier dysfunction is common among patients with pharmacoresistant epilepsy. We hypothesized that the presence of interstitial albumin, the most abundant protein in serum, may contribute to pharmacoresistance either by buffering of the antiepileptic drugs or by leading to transcriptional changes that may in turn affect the drug efficacy.

**Methods:** Seizure-like events were induced by 4-Aminopyridine in acute rodent entorhinal cortex-hippocampus slices. Extracellular field potential recordings were performed in entorhinal cortex layer III/IV in order to evaluate the effects of the standard antiepileptic drugs (phenytoin, valproic acid, carbamazepine and phenobarbital) in the presence of acute albumin or 24 hrs after its application. Unbound drug concentrations were quantified by ultrafiltration and high-pressure liquid chromatography.

**Results:** Antiepileptic drugs failed to suppress seizure-like events in the presence of albumin. This effect was not seen in rodents that were pretreated with albumin 24 hrs before the experiments suggesting the acute buffering effect of albumin on antiepileptic drugs.

**Conclusions:** A dysfunctional blood-brain barrier with acute extravasation of albumin could contribute to pharmacoresistance. The choice of an antiepileptic drug with low albumin-binding affinity may help in seizure control.

**P239****Effects of blood-brain barrier dysfunction on plasticity changes in the hippocampus**

\*S. Salar<sup>1</sup>, E. Lapilover<sup>1</sup>, U. Heinemann<sup>1</sup>, A. Friedman<sup>2</sup>

<sup>1</sup>Charité Universitätsmedizin Berlin, Institute of Neurophysiology, Berlin, Germany

<sup>2</sup>Zlotowski Center of Neuroscience, Ben-Gurion University of the Negev, Department of Physiology and Cell Biology, Faculty of Health Sciences, Beersheba, Israel

**Question:** Dysfunction of the blood-brain barrier has been shown to play a role in epileptogenesis following brain insult via leakage of serum albumin and transforming growth factor beta signalling. Expressional changes after activation of that signaling pathway suggested to be related with alterations of the network excitability in the brain. We therefore evaluated the effect of brain exposure to serum albumin on homo- and heterosynaptic plasticity in the hippocampal network.

**Methods:** Extracellular recordings were performed in acute rodent entorhinal cortex- hippocampus slices, from stratum radiatum and stratum pyramidale of CA1 area. Albumin was applied intraventricularly 24 hrs before slicing in order to assess the effect of robust transcriptional changes following the application. Schaffer collaterals were activated for homosynaptic plasticity experiments. Temporoammonic pathway stimulation or alveus stimulation, both in combination with Schaffer collateral stimulation were used to evaluate the heterosynaptic plasticity changes.

**Results:** Following repetitive high frequency temporoammonic pathway stimulation, Schaffer collateral-induced potentials were no longer reduced but enhanced in amplitude. Low frequency temporoammonic pathway stimulation failed to induce long term depression following albumin treatment. There was no difference in the heterosynaptic interactions following combined Schaffer collateral and alveus stimulation but following alveus low frequency stimulation, Schaffer collateral-induced popspikes were slightly potentiated compared to the slight depression in the controls.

**Conclusions:** These findings showed that following exsudation of albumin there are significant alterations in synaptic plasticity that might represent the transformation of the healthy tissue following an initial insult into a hyperexcitable state.

#### P240

##### Interleukin-1 $\beta$ induces pCreb in neurons of dorsal root ganglia

\*G. Segond von Banquet, C. König, J. Patzer, H.- G. Schaible  
Jena University Hospital, Institut of Physiology I, Jena, Germany

In the course of an antigen-induced arthritis (AIA) in knee joints of rats we found an increasing expression of the transcription factor Creb (cAMP response element-binding protein) in dorsal root ganglion neurons (DRG) mainly in the chronic phase of inflammation. Phosphorylated Creb (pCreb) is usually associated with the induction of neuronal plasticity. Here we investigated which mediators and cascades may be involved in this pCreb activation. To identify the critical inductor of pCreb we first analyze whether the proportion of pCreb positive neurons changes in sections

of DRGs during AIA under therapy with etanercept, infliximab or anakinra. Therapy with etanercept or infliximab (inhibitors of TNF $\alpha$  action) had no effect, but after therapy with anakinra (an interleukin-1 receptor antagonist) the pCreb formation was significantly reduced. To investigate the effect of interleukin-1 $\beta$  in more detail DRG-neurons in culture were incubated with IL-1 $\beta$  for 1 to 60 min. Thereafter the cells were either fixed and the expression of pCreb was analyzed with immunocytochemical methods or the cells were lysed, the proteins extracted, separated by SDS-PAGE and finally blotted to a PVDF-membrane. Using specific antibodies the expression of pCreb, pStat3, pErk1/2, pAkt and p38 were visualized. We found that all analyzed factors were induced in DRG-neurons after IL-1 $\beta$  treatment. A nuclear expression of pCreb was also found in fixed cultured DRG-neurons after IL-1 $\beta$  treatment, but not in satellite-cells or other accompanying cells in the culture. Our study has shown that IL-1 $\beta$  but not TNF $\alpha$  is critical involved in the induction of pCreb in DRG-neurons. Beside pCreb IL-1 $\beta$  treatment activates a multitude of intracellular cascades in DRG-neurons. We conclude therefore that DRG-neurons may be a significant target for IL-1 $\beta$  actions and that IL-1 $\beta$  is possibly associated with the neuronal plasticity which causes chronic pain in arthritis.

#### P241

##### TNF $\alpha$ -induced spinal hyperexcitability involves Interleukin-6 dependent processes

\*C. König, C. Möller, H.- G. Schaible, A. Ebersberger  
Institute of Physiology/Neurophysiology, Jena, Germany

Spinal application of Tumor-Necrosis-Factor  $\alpha$  (TNF $\alpha$ ) enhances the responses of spinal cord neurons to innocuous and noxious mechanical stimulation of the normal knee joint. During the development of knee joint inflammation, spinal hyperexcitability can be prevented by the TNF $\alpha$ -neutralizing compound Etanercept® or blockage of its TNF $\alpha$ -receptor type I (TNFRI). The hyperexcitability during established inflammation could not be reversed by Etanercept®. Interestingly, spinal Interleukin-6 (IL-6) levels increased following TNF $\alpha$  application and concomitant application of IL-6, IL-6 soluble receptor (IL-6sR), and TNF $\alpha$  did not differ from the effect of TNF $\alpha$  alone on spinal hyperexcitability. We used in-vivo electrophysiology measurements to explore whether IL-6 is involved in the TNF $\alpha$ -induced increase of spinal cord neuronal activity upon mechanical stimulation of the knee, ankle, and paw. During co-application of TNF $\alpha$  together with soluble-glycoprotein 130 (sgp130), absorbing freely available IL-6, no increases of responses of spinal cord neurons upon innocuous and noxious stimulations were observed. To explore the source of IL-6, we applied TNF $\alpha$  together with the common microglia-inhibitor Minocycline. In the presence of Minocycline we observed a significant reduction of the TNF $\alpha$ -induced enhancement of spinal neuronal activity upon mechanical stimulation of the normal knee joint, ankle, and paw. These results suggest that TNF $\alpha$  might exert its neuronal effects in the spinal cord

at least in part by an interaction with IL-6. Thus TNF $\alpha$  may be an important trigger of the release of IL-6 from glia cells.

## Cognitive and behavioural neuroscience

#### P243

##### Acute and sub-acute muscle inflammation change bilateral segmental reflex transmission from fine muscle afferents in the feline spinal cord

\*E. D. Schomburg<sup>1</sup>, H. Steffens<sup>1</sup>, P. Dibaj<sup>1,2</sup>, T. Sears<sup>1,2,3</sup>

<sup>1</sup>Institute of Physiology, Goettingen, Germany

<sup>2</sup>Max-Planck-Institute of Experimental Medicine, Dpt. of Neurogenetics, Goettingen, Germany

<sup>3</sup>University of London, King's College, Dpt. of Physiology, London, United Kingdom

**Question:** Longer lasting proprioceptive nociceptive inputs may require other motor reactions than the standard flexion reflex combined with a crossed extensor reflex.

**Methods:** In high spinal cats bilateral reflex effects of group III/IV muscle afferents, activated by i.a. injection of KCl into the gastrocnemius-soleus (GS) muscle were investigated during acute carrageenan induced myositis and sub-acute myositis induced by Freund's adjuvant (FA). Reflex transmission was investigated by monosynaptic reflex testing.

**Results:** Under all conditions the ipsilaterally evoked reflex pattern strictly followed a flexion reflex pattern. However, the reflex effects crossing to the contralateral side did not follow a general extension reflex pattern. In the control experiments only 15% of tests with chemically activated group III/IV muscle afferents induced a contralateral inhibition of the flexor posterior-biceps-semitendinosus (PBSt) and less than half of the tests induced a contralateral facilitation of GS. After induction of an acute myositis by carrageenan transiently facilitatory reflex effects to PBSt from the pre-treated side to the to the un-treated contralateral side increased. During FA induced sub-acute myositis a bidirectional predominance of crossing facilitatory but no inhibitory effects from group III/IV muscle afferents to PBSt occurred and no longer any crossing facilitatory but in half of tests inhibitory effects on GS occurred. The bilaterally determined number of lumbar spinal interneurons with increased c-fos proto-oncogene expression largely reflected the described reflex effects.

**Conclusions:** Under the condition of sub-acute myositis group III/IV do no longer induce any signs of a crossed extension reflex but a bilateral flexion reflex pattern instead.

#### P244

##### Spatiotemporal properties of neuronal assemblies in mice thalamocortical slices

\*J. Mordel, V. Reyes-Puerta, W. Kilb, H. J. Luhmann  
Institut für Physiologie, Mainz, Germany

The rodent barrel cortex with its anatomically distinguishable functional columnar organization is extensively used to investigate the properties of somatosensory information processing. Despite detailed information about response properties of single neurons and the synaptic circuitry, the exact mechanisms by which this sparse network encodes tactile information has not been resolved yet. To elucidate spatiotemporal dynamics of neuronal assemblies, we performed electrophysiological recordings in acute mice thalamocortical slices using perforated microelectrode arrays and stimulated thalamocortical afferents with bipolar tungsten electrodes. These experiments revealed that the first evoked spikes occurred in putative inhibitory neurons in layer 4 (L4) of the principal column (latency:  $2.9 \pm 2.5$  ms), followed by spikes in excitatory neurons in L2/3 ( $4.4 \pm 3.4$  ms), L5 ( $5.2 \pm 0.5$  ms) and L6 ( $7.1 \pm 2.2$  ms). Putative excitatory neurons did not show a significantly different latencies between layers. Excitatory and inhibitory L4 neurons also exhibited the highest firing probability following stimulation. Coprobability of firing revealed high correlation between activity in L4 neurons of the principal barrel and L4 and L6 neurons of the same column, as well as L4 and L2/3 neuron of the adjacent column. Specific assemblies of co-activated neurons containing on average  $5.9 \pm 0.1$  spikes repeated with high probability over trials. Interestingly, putative inhibitory L4 and L5 neurons of the principal and adjacent columns participated in most of these patterns. The present results suggest that sensory information may be encoded within the barrel cortex in spatially confined assemblies involving preferentially barrel and infragranular layers neurons.

#### P245

##### How thoughts give rise to action - Conscious motor intention activates target-specific motor circuits

\*R. Köhling, V. R. Zschorlich  
Universitätsmedizin Rostock, Oscar-Langendorff-Institut für Physiologie, Rostock, Germany

The present study shows evidence for conscious motor intention in motor preparation prior to movement execution. We demonstrate that conscious motor intention of directed movement, combined with minimally supra-threshold transcranial magnetic stimulation (TMS) of the motor cortex, determines the direction and the force of resulting movements, whilst a lack of intention results in weak and omni-directed muscle activation. We investigated changes of consciously intended goal directed movements by analyzing amplitudes of motor-evoked potentials of the forearm muscle, flexor carpi radialis (FCR), and extensor carpi radialis (ECR), induced by transcranial magnetic stimulation over the right motor cortex and their motor

outcome. 14 right-handed subjects were asked to develop a strong intention to move their left wrist (flexion or extension), without any overt motor output at the wrist, prior to brain stimulation. Our analyses of hand acceleration and electromyography showed that during the strong motor intention of wrist flexion movement, it evoked motor potential responses that were significantly larger in the FCR muscle than in the ECR, whilst the opposite was true for an extension movement. The acceleration data on flexion/extension corresponded to this finding. Under no-intention conditions again, which served as a reference for motor evoked potentials, brain stimulation resulted in undirected and minimally simultaneous extension/flexion innervation and virtually no movement. These results indicate that conscious intentions govern motor function, which in turn shows that a neuronal activation representing an “intention network” in the human brain pre-exists, and that it functionally represents target specific motor circuits. Until today, it was unclear whether conscious motor intention exists prior to movement, or whether the brain constructs such an intention after movement initiation. Our study gives evidence that motor intentions become aware before any motor execution.

**P246**

**Living human brain: Slow (DC) potentials**

\*E.-J. Speckmann<sup>1,2</sup>, A. Gorji<sup>1,2</sup>

<sup>1</sup>Institut für Physiologie I, Münster, Germany

<sup>2</sup>University, Neurophysiology, of Muenster, Germany

DC potentials of the brain comprise sustained displacements of the baseline as well as fluctuations between 0 Hz and 100 Hz including the frequency range of the conventional EEG. Neurons, glial cells and blood-brain barriers forming functional units may act as a compound generator of DC potentials. Several investigations both on animal and man have already shown that recordings of DC potentials of the brain provide an objective access to the understanding of higher brain functions as well as pathophysiology of different neurological disorders. The slow components of neocortical DC potential shifts reflect changes in the level of excitation and excitability of the cortex. Epileptiform field potentials, either focal or generalized discharges, are always associated with characteristic deviations of the DC potential in different animal model of epilepsy. Negative DC fluctuation was also observed accompanied by ictal discharges in human brain. In animal experiments, a reduction of the oxygen content of the brain evokes negative DC displacements in both in vivo and in vitro models. The same negative DC deflections were reported in patients suffering from hypoxic brain injuries. Spreading depression, a negative DC deflection, has been shown to play crucial role in aura phase of migraine and cerebrovascular diseases. Psychophysiological studies revealed that DC potentials are highly sensitive to different information processing and to personal characteristics. It seems promising to extend DC potentials studies to provide further insights into mechanisms of brain function and dysfunction.

**P247**

**Saffron extract and Crocin have beneficial effects on oxidative stress damage and spatial learning and memory deficits induces by chronic stress in rat**

\*B. Ghadrdoost<sup>1</sup>, A. A. Vafaei<sup>2</sup>, A. Rashidipour<sup>2</sup>

<sup>1</sup>Rajaie cardiovascular research center, Tehran, Iran

<sup>2</sup>Semnan University of Medical Sciences, Laboratory of Learning and Memory, Research Center and Department of Physiology, Semnan, Iran

**Introduction:** Chronic stress has been reported to induce oxidative damage of the hippocampus. A few studies have shown that Crocus Sativus L., commonly known as saffron and its active constituent Crocin have beneficial effects on oxidative stress damage.

**Material and Methods:** The present work was designed to study the protective effects of saffron extract and Crocin in oxidative stress damage of the hippocampus by chronic stress. Rats were injected with daily dose of saffron extract (30 mg/kg) or Crocin (15 and 30 mg/kg) during a period of 21 days chronic restraint stress (6h/day). Then for determine the changes of the oxidative stress parameters following chronic stress, the levels of the lipid peroxidation product malondialdehyde (MDA), the total antioxidant reactivity (TAR), as well as antioxidant enzyme activities glutathione peroxidase (GPx), glutathione reductase (GR) and superoxide dismutase (SD) were measured in the hippocampus.

**Results:** Treatments with saffron extract or Crocin modulate the ability of chronic stress to oxidative stress damage. In the stressed animals receiving saffron extract or Crocin, levels of MDA, and the activities of GPx, GR, and SD were significantly higher and the TAR capacity were lower than those of the stressed animals receiving vehicle, respectively.

**Conclusion:** Finally, these observations indicate that saffron and its active constituent Crocin can prevent chronic stress-induced oxidative stress damage of the hippocampus and that using these substances may be useful in pharmacological alleviation of oxidative damage.

Keywords: Chronic stress; Spatial memory; Saffron; Crocin; Oxidative stress; Rats

**P248**

**Sensory-evoked and spontaneous gamma and spindle bursts in neonatal rat motor cortex**

\*S. An, W. Kilb, H. J. Luhmann

Institute of Physiology and Pathophysiology, Johannes Gutenberg-University, Mainz, Germany

Self-generated neuronal activity originating from subcortical regions drives early spontaneous motor activity, which is a hallmark of the developing sensorimotor system. However, whether the primary motor cortex (M1) contributes to these early movements and whether movement-induced sensory information is already in the immature animal represented in M1 are currently unknown. To address these questions we analyzed spontaneous and forepaw stimula-

tion-induced activity in rat primary somatosensory cortex (S1) and M1 in vivo at postnatal day 3-5 using voltage-sensitive dye imaging (VSDI), simultaneous extracellular multi-electrode recordings and registrations of forepaw motor activity. We observed that tactile forepaw stimulation induced spindle bursts in S1 and gamma and spindle bursts in M1. About 50% of the spontaneous gamma and spindle bursts in M1 were driven by early motor activity and ~30% of the M1 bursts triggered forepaw movements. Inhibition of S1 attenuated evoked and spontaneous M1 activity. Focal electrical stimulation of layer V neurons in M1 mimicking physiologically relevant 40 Hz gamma or 10 Hz spindle burst activity elicited forepaw movements. We conclude that M1 is involved in somatosensory information processing already during early development. M1 is mainly activated by tactile stimuli triggered by preceding spontaneous movements, which reach M1 via S1. In contrast, only a minority of M1 activity transients directly trigger motor responses. We suggest that both spontaneously occurring and sensory evoked gamma and spindle bursts in M1 contribute to the maturation of corticospinal and sensorimotor networks required for the refinement of sensorimotor coordination.

**P249**

**Monitoring of network activity and behavioral correlates in freely moving neonatal and pre-juvenile rodents: a methodological approach**

\*S. Schildt, I. L. Hanganu-Opatz

Center for Molecular Neurobiology, University Medical Center Hamburg-Eppendorf, Developmental Neurophysiology, Hamburg, Germany

Coordinated patterns of electrical activity emerge in all cortical areas early in life. They have a discontinuous structure and have been hypothesized to actively contribute to the refinement of neuronal networks and the maturation of specific behavior. For example, oscillatory coupling within neonatal prefrontal-hippocampal networks appears to be necessary for the development of recognition memory in juvenile rats. However, all available experimental evidence originates from head-fixed and mainly anesthetized pups and therefore, monitors the sleep-related patterns of activity. The networks interactions in freely moving animals are currently unknown. For their assessment, we developed a new method for recording unit activity and local field potentials from the prefrontal cortex (PFC) in relationship with the behavioral development of neonatal and pre-juvenile rat pups. For this, custom-designed tetrodes were implanted into the PFC of male and female pups at postnatal day (P) 5. The patterns of prefrontal oscillatory activity were analyzed based on their occurrence, amplitude and spectral frequency from P7 to P21 and related to the (i) developmental milestones, (ii) emergence of circadian rhythms, (iii) exploratory behavior, and (iv) recognition memory. Anatomical investigation confirmed the position of electrodes and the safety of the recording method for the correct brain

development. Monitoring the ontogeny of network interactions in relationship to the early behavioral abilities allows better understanding of the functional cortical maturation.

Supported by the DFG (Emmy Noether Program and SFB936, B5)

**P250**

**Scaling of precision grip forces in a grip-lift task is influenced by probabilistic information about object weight**

\*J. P. Kuitz-Buschbeck<sup>1</sup>, L. Trampenau<sup>2</sup>, K. Zeuner<sup>2</sup>, T. van Eimeren<sup>2</sup>

<sup>1</sup>Christian Albrechts Universität, Physiologisches Institut, Kiel, Germany

<sup>2</sup>Neurologie UKSH, Kiel, Germany

**Question:** Dexterous manipulation of objects involves predictive scaling of the forces applied by the fingers. When an object is grasped and lifted, the entire weight sensation is not perceptible until lift-off. The development of the grip and lift forces applied by the fingers prior to lift-off therefore relies on memory representations of the object's weight. Motor prediction errors occur when the object is unexpectedly light or heavy, resulting in force overshoot or undershoot. We examined whether probabilistic information about object weight influences force scaling.

**Methods:** A precision grip-lift paradigm was established where visual cues predict an object's weight only to a certain degree. Subjects repetitively grasped and lifted a small block equipped with force transducers with the thumb and index finger of the right hand. A linear motor varied the object's weight from trial to trial, between light (260 g), medium (600 g), and heavy (1400 g). Just before each lift, visual cues provided probabilistic information about the upcoming weight (e.g. 75% 260g and 25% 600g).

**Results:** The probabilistic cues influenced force development in healthy volunteers. When e.g. the medium weight (600 g) was grasped and lifted, the peak grip force rate (around lift-off) was higher when the cue indicated that the object might be heavier, and lower when the cue suggested that it might be lighter. This effect was reduced in patients with Parkinson's disease.

**Conclusion:** Scaling of manipulative forces in a precision grip-lift task is influenced by cues that provide probabilistic information about object weight.

**P251**

**Cross-frequency coupling between Theta and Gamma oscillations is impaired in APP-deficient mice**

\*X. Zhang<sup>1</sup>, S. Weyer<sup>2</sup>, U. Müller<sup>2</sup>, J. Brankack<sup>1</sup>, A. Draguhn<sup>1</sup>

<sup>1</sup>Universität Heidelberg, Institut für Physiologie und Pathophysiologie, Heidelberg, Germany

<sup>2</sup>Universität Heidelberg, Institute of Pharmacy and Molecular Biotechnology, Heidelberg, Germany

**Question:** The amyloid precursor protein (APP) plays a key role in Alzheimer's disease (AD), but the physiological function of APP remains unknown. Recent studies have



demonstrated morphological alternations and behavioral deficits in aged APP-KO mice. However, APP functions at network level are not well studied.

**Methods:** Here we recorded local field potentials in parietal cortex, prefrontal cortex and dorsal hippocampus of freely moving control and APP-KO mice. Cross frequency coupling between theta phase and gamma amplitude was calculated for two different vigilant states: active waking and rapid-eye movement sleep (REM).

**Results:** In parietal cortex, cross frequency coupling (CFC) is impaired during both active waking and REM sleep in APP-KO mice. In hippocampus, CFC is also decreased during both vigilant states in APP-KO mice. In prefrontal cortex, theta band power is decreased during active waking; however, CFC is not altered in APP-KO mice. Cross-regional coupling between dorsal hippocampus and prefrontal cortex is also attenuated in APP-KO mice in comparison to control mice.

**Conclusions:** Our findings suggest supporting evidence at network level which may contribute to cognitive impairments in APP-KO mice.

**P252**

**Low-repeat STDP paradigms induce dopamine sensitive plasticity in acute hippocampal slices**

\*E. Cepeda<sup>1</sup>, V. Leßmann<sup>1,2</sup>, E. Edelmann<sup>1</sup>

<sup>1</sup>Institute of Physiology, Otto-von-Guericke University Magdeburg, Physiology, Magdeburg, Germany

<sup>2</sup>Center of Behavioral Brain Sciences (CBBS), Magdeburg, Germany

The dopaminergic system has an essential role in integration of novelty and reward memories in the hippocampus. Nevertheless, the modulation of synaptic plasticity by Dopamine (DA) in the hippocampus is still not well understood. The spike timing dependent plasticity (STDP) paradigm is one of the most physiological protocols to induce synaptic plasticity consisting of repetitive activation of pre- and postsynaptic spikes with a specified time delay ( $\Delta t$ ). Consequently, timing-dependent long-term potentiation (t-LTP) is generated when presynaptic precedes postsynaptic spiking, whereas timing-dependent long-term depression (t-LTD) is induced when postsynaptic precedes presynaptic spiking. Our study aimed at elucidating the neuromodulatory role of DA in STDP at Schaffer collateral-CA1 synapses in acute hippocampal slices from mice. We found successful induction of t-LTP when one presynaptic action potential (AP), leading to an excitatory postsynaptic potential (EPSP), was combined with one postsynaptic AP (1EPSP/1AP) with a  $\Delta t = +10\text{ms}$  at low frequency (0.5Hz). Different numbers of pairing repeats were successful (6, 12, 25, 50 and 70 repeats). The respective t-LTP magnitudes were:  $2.04 \pm 0.3$  (1EPSP/1AP\_6X),  $(1.47 \pm 0.2)$ , (12X),  $1.37 \pm 0.1$  (25X),  $1.29 \pm 0.1$  (50X) and  $1.55 \pm 0.2$  (70X), respectively, while a 1EPSP/1AP\_3X protocol showed no t-LTP ( $1.06 \pm 0.2$ ); not significantly different from unpaired control experiments ( $0.95 \pm 0.1$ ). Surprisingly, the 1EPSP/1AP\_6X protocol showed the highest magnitude of plasticity, and it was sensitive to dopamine D1-like receptor antagonism

(SCH23390), suggesting that endogenous DA might be required for STDP in hippocampus Schaffer collateral-CA1 synapses with this low repeat protocol. In the future we will employ this physiologically highly relevant low repeat STDP paradigm a, to investigate dopaminergic function in hippocampal synaptic plasticity.

**P253**

**A young pilocarpine model for epilepsy**

\*C. Wormuth, A. Papazoglou, M. Weiergräber

Federal Institute for Drugs and Medical Devices, Cellular and Systemic Neurophysiology, Bonn, Germany

Epilepsy is a neurological disorder that is characterized by involuntary spontaneous seizures. Temporal lobe epilepsy (TLE) is a complex partial epilepsy in which patients experience recurrent epileptic seizures emerging mainly from the hippocampus and amygdala of the uni- and/or bilateral temporal lobes of the brain. The pilocarpine animal model mimics both the underlying aetiology and symptoms of TLE. This includes: i) seizure foci in the hippocampus; ii) a latent period as a seizure-free time before phenotype manifestation iii) hippocampal sclerosis. The model is very common in adult rats and induces chronic epileptic seizures in an already consolidated brain. Our study goal is to electrophysiologically and pharmacologically shed light on why epileptic children have a high tolerance to bromide and why adults generally have severe side effects. Therefore, we developed a juvenile rat model which reconstructs epilepsy in children. Epilepsy was induced in rat pups at different ages, with different pilocarpine doses, variable durations of treatment and diazepam doses. Based on survival rates and seizures, a protocol was selected for further validation. EEG was recorded at 30, 60 and 120 days after treatment in the hippocampal CA1 region and motorcortex for 3-7 days and seizures were analyzed with a Seizure Detection Module (NeuroScore, DSI). We conclude that our model is easy to use and yields the desired outcome. It presents seizures in the hippocampus and motorcortex on a reproducible manner. Mortality rates are as low as 10-20% while 70-90% of the survival animals present an epileptic phenotype. The model can be used to mimic epilepsy in children and for testing antiepileptic drugs such as bromide.

**P254**

**Pathophysiology of long-term cognitive deficits in a mouse model of polymicrobial sepsis**

\*B. Grünewald<sup>1,2</sup>, H. Haselmann<sup>1,2</sup>, S. Lindig<sup>1,3</sup>, M. Bläß<sup>1</sup>, R. Klaus<sup>1</sup>, C. Geis<sup>1,2</sup>

<sup>1</sup>Jena University Hospital, Integrated Research and Treatment Center, Center for Sepsis Control and Care (CSCC), Jena, Germany

<sup>2</sup>Jena University Hospital, Hans-Berger Department of Neurology, Jena, Germany

<sup>3</sup>Hans-Knöll-Institute, Jena, Germany

**Question:** Sepsis-associated encephalitis (SAE) is a common neurological complication affecting up to 70% of patients diagnosed with bacteremia. Survivors of severe sepsis often suffer from debilitating cognitive and behavioral problems. The underlying mechanisms are yet poorly understood and effective treatment is lacking.

**Methods:** The peritoneal contamination and infection model (PCI) with subsequent antibiotic treatment was used as a model polymicrobial sepsis. Surviving animals were tested for anxiety-related behavior, spatial learning and aversion learning. Synaptic function and plasticity were analyzed in acute hippocampal brain slices via field potential recording and induction of long-term potentiation in Schaffer-collateral CA1 pathway. Further gene expression analysis and immunohistochemistry were used to identify potential molecular mechanisms.

**Results:** Surviving animal showed no general abnormalities after recovery of 6 weeks. However, using standardized behavioral analysis, we found increased anxiety related behavior and a reduced learning performance in PCI-animals. Accordingly, long-term potentiation in the Schaffer-collateral CA1 pathway was reduced in sepsis-surviving animals. Gene expression analysis revealed dysregulation of early growth response transcription factors (Egr1-4) and activity-regulated cytoskeleton-associated protein (Arc) which are major regulators of synaptic plasticity by scaling postsynaptic insertion of AMPA-receptors.

**Conclusions:** Mice after PCI show reduced long-term learning performance resembling cognitive impairments in human sepsis survivors. Abnormal brain function after polymicrobial infection might be caused by dysfunction of glutamatergic synapses.

**P255**

**Functional prefrontal-VTA interactions in a transgenic mouse model of schizophrenia**

\*S. Duvarci, J. Roeper

Goethe University Frankfurt, Neurophysiology, Frankfurt, Germany

Schizophrenia is a debilitating psychiatric disease causing cognitive, social and emotional dysfunction. Dysregulation in the dopaminergic control of brain circuits, including prefrontal cortex and striatum, plays a key role in the cognitive and motivational impairments of this disease. Yet, how this dysregulation is manifest at the level of individual dopamine neurons and the neural networks in which they are embedded is poorly understood. Genetic mouse models of schizophrenia are likely to be of crucial importance in this effort, because they allow the use of invasive recording techniques that can monitor the activity of individual neurons in freely behaving animals. In this study, we examine how a pathophysiological mechanism of schizophrenia - overexpression of dopamine D2 receptors in the striatum - alters the activity of midbrain dopamine neurons. To this end, neural activity is recorded from mice that are genetically engineered to selectively and reversibly control dopamine D2 receptor overexpression in the striatum. The

alterations in the activity of midbrain dopamine neurons, as well as their coordination with the prefrontal cortex during cognitive tasks, are currently investigated.

**P256**

**Repeated transcranial magnetic stimulation relieves pain in fibromyalgia patients: An electrophysiological approach to evaluate pain**

\*A. H. Ansari<sup>1,2</sup>, R. Mathur<sup>2</sup>, S. Jain<sup>2</sup>, K. Mukherjee<sup>2</sup>, K. Mukherjee<sup>2</sup>

<sup>1</sup>Nepalgunj Medical College, Physiology, Chisapani, Nepal

<sup>2</sup>All India Institute of Medical Sciences, Physiology, New Delhi, India

Fibromyalgia (FM) is characterized by chronic, diffuse musculoskeletal pain and fatigue with muscle stiffness, anxiety and depression, disturbed sleep, irritable bowel syndrome, restless leg syndrome, memory and concentration problems. Altered pain perception due to abnormal pain modulation system and central sensitization has been reported in FM. The aim of this study was to investigate the role of transcranial magnetic stimulation (TMS) in pain associated symptoms and its effects on pain modulation system in female FM patients. The patients were randomized into TMS and sham groups. TMS patients received TMS (0.5 Hz, 80% of motor threshold) at right dorsolateral prefrontal cortex in 8 trains of 5 min at 5 min interval /5 days/week for four weeks, sham group received sham TMS with same modality. The Rill reflex and diffuse noxious inhibitory controls were recorded at basal, immediately and two weeks after exposure. For sucrose challenge test, blood samples were collected in luteal phase before and after 4 weeks exposure, each time 8 blood samples were collected, first two samples at interval of 10 min then at interval of 5 min after 25% sucrose ingestion for six times, LH levels were analyzed. The results showed that exposure to TMS in FM patients (n=76) may cause improvement in pain and associated symptoms. Sucrose challenge test was abnormal in fibromyalgia patients. The Rill threshold and latency were significantly lower than healthy controls (n=46) which increased after TMS exposure showing beneficial effects of TMS but not after sham exposure.

**P257**

**Multisensory development in rodents critically depends on early unisensory inputs prior to the first cross-modal experience**

\*K. Sieben<sup>1</sup>, B. Röder<sup>2</sup>, I. L. Hanganu-Opatz<sup>1</sup>

<sup>1</sup>University Medical Center Hamburg-Eppendorf, Developmental Neurophysiology, Hamburg, Germany

<sup>2</sup>University of Hamburg, Biological Psychology and Neuropsychology, Hamburg, Germany

Real-world perception of environment and optimal behavior relies on integration of information from multiple senses. Multisensory interactions have recently been demonstrated in putatively unisensory neocortical regions including the primary cortices. While the acquisition of some multisensory

sory functions and maturation of cross-modal integration in single neurons of high order convergence regions critically depend on multisensory experience during defined periods, the developmental mechanisms of cross-modal processing in primary sensory cortices are still unknown. We assessed the development of visual-somatosensory interactions and their behavioral correlates by performing extracellular recordings of network activity in primary sensory cortices (somatosensory and visual) in vivo and testing the cross-modal novelty recognition in pigmented rats. Similar to adult animals, juvenile rats with no cross-modal experience (retina light sensitive, eyes closed, no whisking) displayed supra-additive augmentation of evoked responses and phase reset of network oscillations in response to cross-modal light and whiskers stimulation. Adult rats experiencing neonatal tactile deprivation showed diminished cross-modal evoked responses and novelty discrimination. These neural and behavioral deficits resulted from decreased density of direct visual-somatosensory connections, which underlay the abnormal synchrony and directionality of cross-modal interactions. Thus, unimodal experience is a prerequisite for the development of cortico-cortical interplay underlying multisensory functions.

**P258**

**Role of neuronal subtypes in the prefrontal-hippocampal network during a touch screen based working memory task**

\*A. de Mooij - van Malsen, W. Nissen, L. Ansel, A. Foggetti, T. Schiffelholz, N. Scheel, P. Wulff

CAU Kiel, Institute of Physiology, Dept. of Neurobiology, Kiel, Germany

**Questions:** Schizophrenia, with a prevalence rate of about 1%, is characterized by a complex blend of positive, negative and cognitive symptoms. However, which mechanisms are underlying cognitive deficits is still largely unknown. One problem is that most tests for working memory in animal models to a certain degree lack translationability to human psychiatric tests.

**Methods:** Our project is focused on studying neuronal networks involved in working memory. We make use of Cre-recombinant mouse strains combined with AAV-mediated gene transfer into particular subareas of the prefrontal-hippocampal network to silence specific neuronal subtypes and analyze their function. By utilizing a novel paradigm in touch screen chambers for mice, we intend to unravel the function of the intricate neuronal connections between the hippocampus and prefrontal cortex in working memory. For this, we use innovative touch screens for which we have developed our own behavioral working memory task with high translationability to human tests. By combining this and other established working memory tests with immunohistochemical and tracing studies, as well as in vitro and in vivo electrophysiology, we aim at increasing our understanding of the processes and brain networks involved in functional memory formation.

**Results:** Our preliminary data show that mice are indeed capable of learning the challenging cognitive tasks as we have developed them. Variation between mice is mainly

based on differences in motivational aspects and learning speed. Future experiments will elucidate the functional role of specific parts of the neuronal network.

**Conclusions:** The touch screen working memory task combined with in vivo electrophysiology and neuronal subtype silencing in specific brain areas has the capacity of being of crucial importance in the identification of neuronal subtype functioning within complex cortical networks involved in working memory deficits.

**P259**

**Influence of casein kinase-2 inhibitor to seizure frequency and seizure severity in a rodent model of chronic epilepsy**

\*R. Bajorat, J. Kuhn, E. Goßla, D. Goerß, K. Porath, R. Koehling

University Medicine Rostock, Oscar Langendorff Institut für Physiologie, Rostock, Germany

A single pilocarpine-induced status epilepticus (SE) results in a chronic state of spontaneous recurrent seizures resembling human temporal lobe epilepsy as one of the most common epilepsies in adults. Hyperexcitability and abnormal synchronisation of neuronal transmission play an important role in the initiation of epileptic activity and the generation of ictal discharges. Hippocampal CA1 neurons show an afterhyperpolarising potential (AHP), which is essentially involved in the regulation of cellular excitability. The AHP comprises 3 parts, of which the middle component is generated by small-conductance Ca<sup>2+</sup>-activated K<sup>+</sup> (SK) channels. Evidence from experimental and modelling studies indicates that an increase of AHPs suppresses excitability of the neuronal network. The aim of investigation to test whether oral application of casein kinase-2 inhibitor (TBB), known to increase SK currents in vitro, would lead to suppression of seizures in vivo. A prolonged SE was induced by a single pilocarpine injection in 30-day-old rats (Pilo-rats). Control rats received saline instead of pilocarpine. SE resulted in a chronic state of spontaneous recurrent seizures. A telemetric EEG system was used for continuous long-term video-EEG monitoring of Pilo- and control rats. After recording a baseline EEG to determine the pattern of distribution and the mean frequency of seizures (2 to 3 weeks), TBB was applied orally for 3 weeks, and then discontinued with ongoing monitoring for another 3 weeks minimum. Afterwards, expression levels of mRNA and protein of SK2-channel were determined by real-time PCR and western blot analysis. For this, regions of the hippocampus were dissected, and mRNA or protein were extracted. As housekeeping controls, S18 and β-actin were used. In CA1 region of hippocampus there, was a highly significant difference in SK2 expression levels in the Pilo-group between TBB-treated and untreated animals. With TBB, SK2-channel expression was up regulated in Pilo-rats to the level of controls without seizures. This notwithstanding, close to half of Pilo-rats showed a significant increase of seizure-frequency after starting TBB-treatment, and a further increase during the period of wash-out of TBB. The other Pilo-rats did not show significant differences between seizure-frequencies during the different recording

periods (baseline, TBB-treatment, wash-out). We conclude that although TBB treatment is able to normalise SK channel expression in epileptic rats and to reduce excitability in vitro, it is not sufficient to alter seizure emergence in vivo.

Methods and teaching

**P260**

**Characterization of Asante NaTRIUM Green for wide-field and confocal sodium imaging in situ**

\*N. Gerkau, K. Kafitz, C. Rose

Heinrich-Heine-University, Institute of Neurobiology, Düsseldorf, Germany

The inward-directed electrochemical sodium gradient enables sodium-based electrical signalling, and energizes nutrient uptake and ion homeostasis. Because sodium is thus essential for neuronal function, methods for reliable detection of sodium signals are needed. Up to now, SBFI, a UV-excitabile dye, is commonly used. SBFI, however, is prone to bleaching and cannot be employed in confocal microscopy. The recently developed sodium indicator Asante NaTRIUM Green (ANG, maximal absorption 500 nm) may serve as an alternative, but little is known about its properties. We studied the suitability of ANG1 and ANG2 as compared to that of SBFI for intracellular sodium imaging in astrocytes and neurons. The membrane-permeable AM-forms of the dyes were bolus-loaded in the CA1 region of acute mouse hippocampal slices. With wide-field and confocal imaging, both ANG forms exhibited bright fluorescence emission from intracellular regions, implying efficient uptake and de-esterification of the dye. ANG emission did not appreciably decay over time even with prolonged excitation and imaging periods, indicating minor bleaching and high photo-stability. In situ calibrations showed that the sodium sensitivity of ANG1 follows Michaelis-Menten kinetics and revealed a K<sub>d</sub> ~34 mM. Upon short bath application of glutamate or perfusion with potassium-free saline, fluorescence emission rose reversibly, indicating that ANGs reliably reports increases in intracellular sodium under these conditions. Our results thus show that ANGs are well suited for wide-field and confocal imaging of intracellular sodium. They may thus represent an additional valuable tool for the investigation of intracellular sodium homeostasis and signalling.

Supported by DFG (Ro2327/6-1)

**P261**

**Determination and compensation of the series resistance during whole-cell patch-clamp recordings: application of the phase-sensitive method**

\*B. Sutor<sup>1</sup>, F. Rucker<sup>1</sup>, T. Riedemann<sup>1</sup>, H.- R. Polder<sup>1,2</sup>

<sup>1</sup>Institute of Physiology, LMU München, Physiological Genomics, München, Germany

<sup>2</sup>npi electronic, Tamm, Germany

The series resistance (RS) is a systematic error associated with whole-cell patch-clamp recordings from excitable and non-excitabile cells. The voltage drop across RS deteriorates both the determination of membrane conductances and the measurement of the signals' frequency responses. In order to determine RS during an experiment, we made use of the possibility to measure R<sub>s</sub> by means of an active bridge circuit. During current-clamp recordings, the neutralization of the electrode's capacity and the balancing of the bridge circuit was performed by using the phase-sensitive method introduced by Park et al. (J. Neurosci. Meth. 8: 105, 1983). A short (1 - 2 ms) sine wave current with frequencies in the range from 3 to 7 kHz was injected into the cells. In a first step, the electrode's capacity was neutralized by adjusting the capacity compensation of the amplifier (ELC-03XS or SEC 10L, npi, Tamm, Germany) until the voltage response was in phase to the current signal. This procedure was monitored on an X - Y - screen by displaying the corresponding Lissajous figure. In a second step, the bridge circuit was balanced by minimizing the slope of the residual Lissajous figure. The R<sub>s</sub> value determined in this way provides the basis for the R<sub>s</sub> compensation performed in the voltage-clamp recording mode. Recordings from cell models, from neurons and from astrocytes show that the bridge circuit-based R<sub>s</sub> determination can be performed with high accuracy (error: 2 - 3%) and that R<sub>s</sub> can be compensated by up to 90% during patch-clamp recordings.

**P262**

**Single-cell juxtacellular recording and transfection technique**

\*T. Brigadski, J. Daniel, V. Leßmann

Otto-von-Guericke-University, Institute of Physiology, Magdeburg, Germany

Genetic modifications and pharmacological studies enable the analysis of protein function in living cells. While many of these studies investigate the effect of proteins by bulk administration or withdrawal of the protein in complex cellular networks, understanding the more subtle mechanisms of protein function requires fine-tuned changes on a single cell level without affecting the balance of the system. In order to analyse the consequences of protein modification at the single cell level we have developed a single cell transfection method in the loose patch configuration, which allows juxtacellular recordings of neuronal cells prior to juxtacellular transfection. CA1 pyramidal neurons were selected

based on morphological and electrophysiological criteria. Using a patch clamp amplifier which allows sensitive recordings of action currents in the loose seal mode as well as electroporation with high voltage electrical stimulation the identified neurons were transfected with a combination of specific nucleotides, e.g. siRNA and a plasmid coding for GFP for later cell retrieval. Two days after transfection, whole-cell patch clamp recordings of transfected cells were performed to analyse electrophysiological properties. Action potential firing and synaptic transmission of single electroporated CA1 pyramidal cells were comparable to untransfected cells. Our study presents a method which enables identification of neurons by juxtacellular recording prior to single cell juxtacellular transfection, allowing subsequent analysis of morphological and electrophysiological parameters several days after the genetic modification.

**P263**  
**Ca<sup>2+</sup> measurements in red blood cells with fluorescence lifetime imaging microscopy**

\*J. Schweizer, B. Sauer, L. Kaestner, P. Lipp  
Saarland University, Institute for Molecular Cell Biology, Homburg / Saar, Germany

The ubiquitous messenger Ca<sup>2+</sup> is associated with a variety of physiological and pathophysiological processes in red blood cells (RBCs) (Bogdanova et al. 2013). Although the average Ca<sup>2+</sup> content of RBCs can be measured the quantitative distribution in single cells is not known (Tiffert & Lew 2003). This is particularly important in light of a significant cellular heterogeneity of RBCs (Wang et al. 2013). Most of the ratiometric Ca<sup>2+</sup> sensitive dyes including Fura-2 or Indo-1 that would allow quantitative Ca<sup>2+</sup> recordings are not usable in RBCs for 2 major reasons (i) UV illumination induces a severe autofluorescence and (ii) the haemoglobin interacts with the excitation as well as with the emission light resulting in altered spectral properties (Kaestner et al. 2004). Fluorescence lifetime imaging microscopy (FLIM) was proposed as an alternative and efficient tool to determine the absolute Ca<sup>2+</sup> concentration in RBCs because it is independent of the emitted fluorescence intensity (Minetti et al. 2013). We use time-correlated single photon counting (TCSPC) based FLIM (Sauer et al. 2014) to study numerous established and novel Ca<sup>2+</sup> sensitive dyes, such as Calcium-Green, Fura-Red, Fluo-4, Fluo-8 and Asante Calcium Red. Furthermore we established a calibration procedure that is independent of cellular regulation mechanisms (pH, ion concentration fluctuations) by permeabilisation of the plasma membrane and the utilization of dye salts. Thereby, we developed the methodological approach to quantitatively determine the Ca<sup>2+</sup> concentration in individual RBCs.

**P264**  
**Properties of novel voltage sensitive dyes in adult ventricular myocytes**

\*K. Nitzte<sup>1</sup>, Q. Tian<sup>1</sup>, L. M. Loew<sup>2</sup>, P. Yan<sup>2</sup>, P. Lipp<sup>1</sup>, L. Kaestner<sup>1</sup>  
<sup>1</sup>Saarland University, Molecular Cell Biology, Homburg, Germany  
<sup>2</sup>University of Connecticut Health Center, R.D. Berlin Center for Cell Analysis and Modeling, Farmington, United States

The gold standard for studying the electrical activity of excitable cells is the patch clamp technique either in voltage-clamp or current-clamp mode. The latter approach allows investigation of action potentials in excitable cells such as cardiac myocytes or neurones. These techniques though require an electrode to be inserted into the cells and to rupture a part of the cell membrane either mechanically or by means of artificial pores (perforated patch). In contrast, fluorescent dyes can help visualizing action potentials in a non-invasive manner. Fast voltage probes such as Di-8-Anepps integrate into cell membranes and sense changes in the transmembrane voltage, i.e. they change their spectral properties with changes in membrane potential. Using voltage clamp of isolated mouse ventricular myocytes in combination with spectrally resolved fluorescence photometry we investigated the efficiency of novel dyes that were designed to emit light shifted more to longer wavelengths of the spectrum than dyes available previously. Therefore we recorded both excitation and emission spectra upon defined changes in membrane voltage for detailed characterisation of different voltage probes. Our analysis of these novel voltage sensors revealed an interesting structure-function relationship. The linker length correlates with the membrane potential dependent shift of the emission spectra. Such optimized small molecule voltage probes will allow simultaneous ratiometric measurements of the membrane potential, the intracellular calcium concentration and contraction in cardiac myocytes with increased signal-to-noise ratios.

**P265**  
**Suitability of the micro-CT technique to analyze remodeling processes in carotid arteries of mouse**

\*C. Schürmann, Y. Yasar, R. Brandes  
Institut für Kardiovaskuläre Physiologie, Frankfurt am Main, Germany

The pathomechanisms underlying atherosclerosis and vascular remodeling are under intense research. Although animal model for these processes have been developed, non-invasive in vivo imaging technique in rodents are largely lacking. X-ray computed tomography (CT) is a nondestructive technique to visualize structures within solid objects. Especially for preclinical research, micro-CT scanners have a wide range of applications, which include: vasculature research, 3D bone analysis or soft tissue measurements after application of appropriate contrast agents. We hypothesized that in vivo micro-CT imaging is a suitable technique to study vascular luminal remodeling in small animals. This was studied after uni-lateral partial carotid artery ligation in hyperlipidemic ApoE knockout mice subjected to normal chow and

Western type high fat diet. AuroVist -15 nm nanoparticles were used as in vivo contrast agent using a Skyscan 1176 in vivo micro-CT applying a resolution of 18 µmeter in Voxel and a mean x-ray dose of 0.5 Gy. Mice were studied consecutively and at the end of the observation period animals were sacrificed, vessels were perfusion fixed and subjected to quantitative histology. On average µCT revealed a vascular lumen loss of 20% every week after ligation. The final vascular profile clearly correlates with the histology. Micro-CT scanners enable the assessment of the vasculature or vascular complications in vivo. Thereby, this technique gives new insights into disease progression under physiological conditions and works well in longitudinal studies.

**P266**  
**Does university entrance qualification reflect the performance in natural sciences?**

S. Wehlke, M. Stieg, B. Danz, D. Nafz, S. Werner, L. Solf, \*B. Nafz  
Charite Univ. med. Berlin, Deans office, Dep. of student affairs, Berlin, Germany

Due to legal reasons the overall performance presented at the university entrance qualification (OPQ), has to establish a major criterion during the election process of applicants who aspire to study medicine or dentistry in Germany (BVerfG 1972, 7.HRGÄndG 2004). On the other hand, insufficient knowledge of natural sciences has been shown to be a hallmark of students who leave university without graduation. In the light of more than 20 different major categories of university entrance qualifications we investigated to which extend the OPQ reflects performance in natural sciences. On the basis of the OPQ 1000 applicants were invited to a multiple choice questionnaire (MCQ). The MCQ was constructed to investigate skills in biology, chemistry, physics and mathematics. The applicants had to answer 80 questions within 90min. ~250000 answers were compared to the correct solutions to determine individual profiles of the applicants. A weighted sum of these results and the OPQ was calculated. The applicants were then ranked according to this sum and the best of them were elected to get university places. The mean performance (mean value of correct answers) was ~36 medicine (~31 dentistry). The MCQ induced a change of ~38% (50% dentistry) of the applicants between fail and pass respectively. In conclusion the OPQ is of limited use to determine performance in natural sciences. This can be markedly enhanced by a specific MCQ which establishes a cheap, fair, fast and legally valid alternative to selection interviews.

**P267**  
**Wiki-Scriptum: Interactive and adaptive modification of lecture scripts by students and their teacher**

\*T. Noack, R. Patejdl  
Universitätsmedizin Rostock, Oscar-Langendorff Institut für Physiologie, Rostock, Germany

How to learn best with the greatest effectiveness has been a matter of debate since a long time - even in academia. Strategies of the last century using mechanistic or electronic "learning machines" have not had the success as hoped. One great problem has always been the intellectual gateway between teacher and learner. It was hoped that at least the individual learning speed could be adapted best by e-learning. However, the speed is only one of several critical points in that gateway. Although e-learning tools are available, students prefer well structured and interesting lectures.

Such academic lectures use today electronic media like power point or blackboard. Both types can be used directly or by snapshots from the blackboard as electronic media. Using interactive communication between the students and the lecturer by internet, mail or smart phone during the lectures, a bidirectional communication line can be built up. Using such communication media, students can give their comments to those items which they feel to be most important for the next generation of students. Furthermore they can modify the sequence of content, add useful explanations or mark misunderstandings. Especially for medical students, who have to perceive an enormous amount of knowledge, e-learning programmes have shown in the past that the proper learning strategy is of great importance. With the "Tweedback" platform (Prof. Cap), the University of Rostock provides the hardware/software that enables such a new learning and teaching strategy. Such changes on the existing lecture scripts can be a useful tool for learning students.

**P268**  
**Monitoring breathing and heart rate in awake and anesthetized neonatal rodents: A novel method**

C. M. Zehendner, H. J. Luhmann, \*J.-W. Yang  
Institute of Physiology, Johannes Gutenberg-University, Mainz, Germany

Neonatal rodents, which compared to humans are born rather immature, are suitable models for studying early developmental processes during physiological and pathophysiological states. Breathing and heart rate are two basic parameters to monitor the general physiological condition. Here we present a simple setup and experimental procedures to monitor breathing rate by a piezoelectric transducer and heart frequency by electrocardiography in unrestrained awake or anesthetized neonatal rodents (C57/Bl6 mice and Wistar rats) between postnatal day 0 and 7. We show that heart rate increases both in rats and mice during the first postnatal week. Heart rate was significantly higher in mice than in rats but breathing rate did not differ between both species. Further our data indicate that the anesthetic agent urethane induces hypoventilation and consecutive respiratory acidosis in P6/7 mice and rats while heart rate remains unaffected. This urethane-induced hypoventilatory effect was also observed in P0/1 mice but not in P0/1 rats. Our data demonstrate the usefulness of monitoring cardio-respiratory parameters in newborn ro-

dents. Keeping cardio-respiratory parameters of neonates within a physiological range is an important issue to avoid experimental errors.

**P269**

**K-ras mutation detection from limited sample volumes by nested quantitative PCR**

\*T. Ehlert, P. Simon

Johannes Gutenberg-Universität Mainz, Sportmedizin, Mainz, Germany

**Question:** The detection of rare mutations from circulating cell free DNA (cfDNA) in blood plasma is an upcoming source of information when screening for diseases such as cancer. However, there are several obstacles when aiming at detecting mutated cfDNA fragments, like limited sample volume and low percentages of mutated fragments. Here we describe a highly sensitive and specific approach to extract a maximum of information out of a minimum of cfDNA sample. **Methods/Results:** We developed a nested real time PCR approach to specifically detect the seven most common K-ras mutations from low sample volumes. In the first round PCR, we performed 20 cycles amplifying a 110 bp fragment around the frequently mutated region of K-ras exon I, creating a stock for nearly unlimited second round PCRs. To accumulate the mutated fraction by more than 1000-fold, we added a wild type (WT) specific blocker oligonucleotide. The 50-fold diluted PCR-products were then amplified in a second round PCR using mutation specific forward primers. By combining WT blockers and mutation specific primers we could specifically detect down to 12 mutated fragments in a background of 30.000 WT fragments. **Conclusion:** We present a novel highly specific nested real time PCR approach for the detection of K-ras mutation status. By blocking WT-amplification we used a first round PCR to accumulate mutated DNA fragments followed by a specific detection step in a second round real time PCR. Our two-step procedure is optimized to warrant specific and sensitive detection of K-ras mutation status from minute amounts of sample volume.

**P270**

**Magnetic microbubble mediated lentiviral gene delivery to vascular cells**

\*Y. Stampnik<sup>1</sup>, F. Krötzl<sup>1</sup>, J. Pircher<sup>1</sup>, K. Zimmermann<sup>2</sup>, D. Eberbeck<sup>3</sup>, M. Wörnle<sup>4</sup>, M. Anton<sup>5</sup>, U. Pohl<sup>1</sup>, H. Mannell<sup>1</sup>

<sup>1</sup>Ludwig-Maximilians-University, Walter-Brendel-Centre for Experimental Medicine, Munich, Germany

<sup>2</sup>Institut für Pharmakologie und Toxikologie, Bonn University, Germany

<sup>3</sup>PTB, Berlin, Germany

<sup>4</sup>Ludwig-Maximilians-University, Nephrology, Medical Policlinic, Munich, Germany

<sup>5</sup>Klinikum rechts der Isar, TU, Institute of Experimental Oncology and Therapy Research, Munich, Germany

**Question:** Achievement of site-specificity and potent gene transfer is a great therapeutic challenge. Here we estab-

lished a new gene transfer technique by using magnetic microbubbles (MMBs) coupled to lentiviruses (LVs) for use in localised vascular gene transfer.

**Methods:** Magnetic moments of MMBs were measured by the magnetic responsiveness. Coupling of LVs containing a membrane GFP-fusion protein to MMBs was verified by flow cytometry. For determination of the transduction efficiency of LV-coupled MMBs in vitro and in vivo a lentiviral GFP-reporter construct was used. LV-coupled MMBs were targeted and disrupted by combined magnetic field (MF) and ultrasound (US; 1MHz, 2W/cm<sup>2</sup>, DC50%, 30sec) exposure. GFP expressing endothelial cells (EC) in vitro were quantified by flow cytometry. In vivo, microvessels of the dorsal skin of mice were targeted. Reporter gene expression (GFP) from organs was assessed by real-time PCR. Residual viral particle amount in body fluids was analyzed with p24 ELISA and cell culture. MNP biodistribution was measured by magnetic particle spectrometry.

**Results:** MMB were optimized to exhibit a magnetic moment of 103fA/m<sup>2</sup> (n=3) and high LV binding capacity (100% of LV bound; n=4). EC endocytosis of LV-MMB was clathrin independent (p<0.05; n=3). Simultaneous MF exposure and US-mediated disruption of LV-coupled MMBs strongly increased EC transduction in vitro compared to application of LV alone (31.8±1.7% vs. 1.8±0.5% GFP-expressing cells, respectively; p<0.05; n=4). Reporter gene expression was detected exclusively in the targeted dorsal skin of mice and not in other organs (n=4). MNP accumulation was detected mainly in lung and liver (19±4% and 41±9% of administered dose, respectively; n=5) 1h after treatment, which was reduced to 0.2±0.07% and 0.3±0.09% of administered dose, respectively, 96h after treatment (n=4). No residual LVs were detected in body fluids 48-72h after LV-MMB application (n=3).

**Conclusion:** Using the combination of magnetic targeting and US induced MB destruction, MMB allow for efficient and site-specific vascular gene transfer. Moreover, the coupled magnetic nanoparticles are effectively cleared from the organism, while reporter gene expression persists. Thus, the LV-associated MMB technology may represent a valuable tool for vascular gene therapy.

**P271**

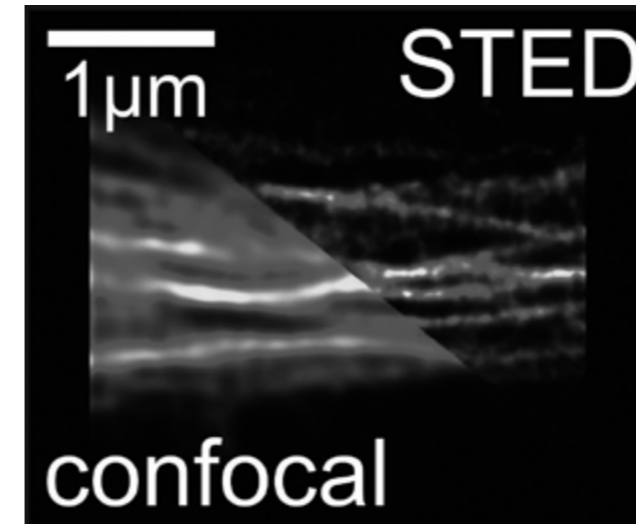
**The red fluorescent protein Tag-RFP-T is a suitable label for STED microscopy**

P. Hagemann, \*P. Happe

Ruhr-Universität Bochum, RUBION, Bochum, Germany

Fluorescent imaging of cellular structures is one of the major microscopy techniques used in the life sciences. However, the details that can be observed by fluorescent microscopy are limited due to the diffraction of light. Recently, various microscopy techniques have been developed which allow circumventing this limit by switching the fluorescent molecules between an on and an off state either direct or stochastically. Stimulated emission depletion (STED) microscopy (Hell and Wichmann, 1994) switches the fluorescent dye into a dark state by inducing stimulated emission

of the excited dye molecule at the periphery of the confocal excitation spot. Since in STED microscopy the resolution increases with increasing power of the laser beam used to induce stimulated emission, the dye molecules are exposed to light intensities which are approximately 1000fold the intensities used in confocal microscopy. Hence, bleaching of the dye molecules is a severe problem in STED microscopy. This is particularly important for live cell investigations where a fluorescent protein is added to the protein of interest by genetic modification. Fluorescent proteins show a much larger tendency to bleach than organic dye molecules, limiting the use of STED microscopy for live cell investigations. Here we tested whether Tag-RFP-T, a point mutant of Tag-RFP introduced by Shaner et al. (2008), is sufficiently photostable to allow sub-diffraction imaging by STED microscopy. We found that Tag-RFP-T allows sub-diffraction STED recordings with medium intensity of the laser beam inducing stimulated emission, yielding resolutions in the range of 100 nm.



**P272**

**Rapid prototype of a portable long-term live-cell imaging system for biomedical research and education**

\*S. Abolpour Mofrad<sup>1,2</sup>, M. Walzik<sup>1</sup>, V. Volmar<sup>1</sup>, T. Lachnit<sup>1</sup>, H. Bachmann<sup>1</sup>, D. Aschenbrenner<sup>1</sup>, O. Friedrich<sup>1,2</sup>, D. Gilbert<sup>1,2</sup>

<sup>1</sup>FAU Erlangen-Nuremberg, Institute of Medical Biotechnology, Erlangen, Germany

<sup>2</sup>Erlangen Graduate School in Advanced Optical Technologies, Erlangen, Germany

Time-resolved visualization and analysis of slow dynamic processes in living cells has revolutionized many aspects of in vitro cellular studies. However, existing technology applied in time-resolved life-cell microscopy is often bulky and stationary, costly, complicated to use, i.e. requires highly skilled staff for application and maintenance and hence, not readily applicable to a broad range of laboratories or even for educational purposes. The recent availabil-

ity of rapid prototyping technology, including 3D printers and microcontroller platforms makes it possible to quickly and easily engineer purpose-built alternatives to conventional research infrastructure which are low-cost and user-friendly.

We present a rapid prototype of a portable life-cell imaging system for time-resolved visualization of slow dynamic processes in living cells, which reduces the cost of acquisition to about one hundredth of the cost for conventional microscopes and can be readily available for other laboratories and also educational purposes. The device is made up of a microscope mounted on an automated stage and an incubator for maintaining optimal culture conditions. The system was constructed using a 3D-printer and off-the-shelf components, including a webcam-based microscope, temperature, gas and humidity sensors for environment control and open-source Arduino microcontroller boards for hardware control and data acquisition. A software interface was developed using LabVIEW and LabView interface for Arduino. We demonstrate its potential for biomedical use by long-term imaging of mammalian cell lines under conditions promoting and inhibiting cell growth, respectively and validate the ability to generate time-resolved data of similar quality to commercial microscope platforms, thus allowing analysis of slow dynamic processes in living cells.

**P273**

**Learning by doing with the virtual physiology series: Physiological and pharmacological in silico experiments**

\*H. A. Braun<sup>1</sup>, A. Tchaptchet<sup>1</sup>, J. dell Oro-Friedl<sup>2</sup>, D. Immer<sup>3</sup>, H. Schneider<sup>4</sup>, T. Braun<sup>5</sup>, S. Postnova<sup>6</sup>, O. Semyachkina-Glushkovskaya<sup>7</sup>, J. Schwabedal<sup>8</sup>, S. Wenzel<sup>9</sup>, K. Voigt<sup>1</sup>, M. C. Hirsch<sup>10</sup>

<sup>1</sup>University of Marburg, Institute of Physiology, Marburg, Germany

<sup>2</sup>University of Furtwangen, Furtwangen, Germany

<sup>3</sup>Entertrain, Mainz, Germany

<sup>4</sup>DAQ Solutions, Nehren, Germany

<sup>5</sup>motion design, Berlin, Germany

<sup>6</sup>University of Sydney, Sydney, Australia

<sup>7</sup>University of Saratov, Saratov, Russian Federation

<sup>8</sup>University of Atlanta, Atlanta, United States

<sup>9</sup>University of Giessen, Giessen, Germany

<sup>10</sup>Parmenides Foundation, München, Germany

The didactic concept of the Virtual Physiology series is different from typical in silico applications. The Virtual Physiology programs offer completely equipped laboratories on the computer screen with all necessary stimulation and recording devices to perform physiological and pharmacological experiments almost as in the real world. All settings of the devices are freely adjustable and mathematical algorithms guarantee for the appropriate reactions of the preparations, also considering their biological diversity. Hence, no student will have exactly the same results as another one. This didactic concept has been retained when the Virtual Physiology teaching tools recently have been reprogrammed as platform and resolution independent versions, extended by several new features and applications. The Virtual Physiology series simulates classical experi-

ments in life science education, e.g. with the isolated heart (SimHeart) and smooth muscle stripes of gut and blood vessels (SimVessel) as well as the traditional “frog experiments” on the gastrocnemius muscle (SimMuscle) and sciatic nerve (SimNerv). Two other teaching tools, SimPatch and SimNeuron, are simulating widely used experiments with current- and voltage/patch-clamp recordings that are too difficult to be physically carried out in conventional students' courses but can be performed in silico. Major emphasis thereby is laid on physiologically and methodologically appropriate realizations [1,2]. Fully functioning demo versions of the virtual labs can be downloaded from www.virtual-physiology.com

References:

- [1] Tchaptchet A, Postnova S, Finke C, Schneider H, Huber MT, Braun HA (2013): Modeling Neuronal Activity in Relation to Experimental Voltage-/Patch-Clamp Recordings. *Brain Res* 1536: 159-167
- [2] Braun HA (2013): Determinismus und Zufall in der Neurophysiologie und die Frage des freien Willens. In: *Homo Neurobiologicus - Ist der Mensch nur sein Gehirn*. Hrsg.: S. Höfling & F. Tretter. Hanns Seidel Stiftung, München, Argumente und Materialien zum Zeitgeschehen (AMZ) 87: 59-70



Figure: Examples from the Physiology series: Sim Heart (left) and Sim Nerv (right)

**P274**

**Novel automated technique to study ion channels in erythrocytes**

\*P. Petkova-Kirova, P. Lipp, L. Kaestner  
Saarland University, Molecular Cell Biology, Homburg, Germany

Red blood cells possess a diversity of membrane ion channels, pumps and transporters underlying their major function of gas transport but implicated also in important processes such as cell homeostasis, differentiation and death and intricately related to a number of blood diseases. Patch-clamp as a powerful tool to study ion transfer across membranes is however sparsely used with red blood cells. Major problems are their small size requiring high resistance pipettes with a specific shape of the tip, but mostly red blood cells deformability allowing them to easily squeeze through tiny capillaries but making every attempt to break their membrane a challenge. Further complication is a requirement for a high gigaohmic seal between the cell membrane and the pipette to avoid leak currents, which could otherwise be as big as the small currents of red blood cells. In the present study we report the use of an automated system, Patchliner (Nanion Technologies GmbH), to study whole cell currents in red blood cells. The

system is based on the employment of borosilicate glass chips, containing a micron-sized aperture, where a cell is automatically positioned by suction. The use of low resistance chips, 5-6MOhms (vs. 15-20 MOhms of conventional pipettes) and seal enhancing solutions greatly facilitates whole-cell recordings. The possibility for internal solution exchange and simultaneous measurements from up to 8 channels are further advantages. Automated and easy-to-do measurements will give further insight into red blood cells channels properties and functions and would help answer current questions in the field.

**P275**

**Optogenetic control of skeletal muscle: a new method to treat laryngeal paralysis**

\*T. Brueggemann<sup>1</sup>, T. van Bremen<sup>2</sup>, T. Send<sup>2</sup>, C. Vogt<sup>1</sup>, F. Holst<sup>1</sup>, A. Schröck<sup>2</sup>, P. Sasse<sup>1</sup>

<sup>1</sup>University of Bonn, Institute of Physiology I, Bonn, Germany

<sup>2</sup>University of Bonn, Department of Otorhinolaryngology/Head and Neck Surgery, Bonn, Germany

Bilateral laryngeal paralysis is a severe disease resulting in immobility of the vocal cords and life-threatening dyspnea. Until now tracheotomy or surgical removal of one vocal cord are the only available treatment options. Opening of the vocal cords by isolated electrical stimulation is problematic due to non-selective co-stimulation of antagonistic muscles, sensation of stimulations and corrosion of the electrodes (Zealer DL et al., *Laryngoscope* 2003). We therefore explored the possibility to stimulate selectively skeletal muscle cells by light and used for this purpose a transgenic mouse line expressing the light-sensitive cation channel Channelrhodopsin2 fused to EYFP under the control of the chicken- $\beta$ -actin promoter. Soleus muscles showed membrane-bound EYFP fluorescence and light-induced (470 nm) contractions in isometric force measurements. To determine the most effective stimulation pattern, single and repetitive tetanic light pulses were applied at various intensities (up to 7.0 mW/mm<sup>2</sup>), pulse durations (1-300 ms) and repetition frequencies (10-40 Hz). We found that using single light pulses, force was maximal (52.7 $\pm$ 3.4 mN, s.d., n=4) using 100 ms long pulses at 2.6 mW/mm<sup>2</sup>. In tetanus stimulations with repetitive light pulses, 5 ms long pulses at 30 Hz and 7.0 mW/mm<sup>2</sup> were most efficient and generated force of 69.1 $\pm$ 7.7 mN (sd, n=4), which amounted to ~70% of the force induced by electrical stimulation. We next investigated, whether light-induced opening of the vocal cords could be used in our transgenic mouse model and explanted for this purpose larynges and analyzed these ex vivo. Optical stimulation of the posterior cricoarytenoid muscle, that exclusively opens the vocal cords, was obtained by selective illumination of the postarytenoid region with a light guide ( $\varnothing$  400 $\mu$ m, NA=0.48, 470 nm). Tetanic contractions were induced by repetitive illumination with various pulse durations and repetition rates at 35.7 mW/mm<sup>2</sup>. We found that stimulation with 5 ms long light pulses at 40 Hz was most effective and led to an enlargement of the area between the vocal cords from 111 $\pm$ 54 to 495 $\pm$ 119

mm<sup>2</sup> which corresponds to an increase of 494 $\pm$ 119% (sd,n=3). Taken together, we provide evidence that optogenetic stimulation induces contractions of skeletal muscle and this approach could be an option in case of bilateral laryngeal paralysis.

**P276**

**Novel high throughput technique for measuring force generation in zebrafish larvae**

\*J. Eckhardt, M. Bitzer, R. Stehle, G. Pfitzer

Institute for vegetative Physiology, Köln, Germany

Introduction: Zebrafish larvae (ZL) emerged as valuable model organism for studying muscle development, knock down of muscle proteins and muscle-related chemical toxicity. Biomechanics of ZL has been investigated in organ bath using Krebs buffer (Dou et al., 2008) but not fresh water (FW), their natural habitat. Here, we developed a high-throughput technique for biomechanical investigation of ZL in FW. Methods: For isometric force measurements, the ZL is fixed between the head and the yolk bag with a nylon loop integrated into the force transducer (FT). The tail is mounted similarly at a fixed post. The attachment can be strengthened by histoacryl glue. This mounting procedure allows for high throughput measurements. The chamber system is temperature controlled and mounted on an inverted microscope. The sensitivity and the resonant frequency of the FT allows to study amplitude and kinetics of force generation. Results: Reproducible twitch contractions were elicited by electric field stimulation (1 Hz, 1.1 ms duration) and were respectively ~0.5 mN and ~1.12 mN in 2 and 3 post-fertilization ZL. Tetanic force elicited at 200 Hz was comparable to twitch force. Tetani resulted in a significant reduction in post-tetanic twitch force. Of note, our mounting procedure seals the interior of the ZL against the incubation medium. We found that this was essential for force generation in FW. Conclusion: Our study shows (i) the feasibility of high through-put biomechanical investigation of ZL, and (ii) raises the interesting possibility that tetanic contraction is not physiological in ZL. The underlying cause remains to be determined.

Renal functions II

**P277**

**Mitochondrial malfunction caused by protein mistargeting**

\*C. Broecker<sup>1</sup>, M. Reichold<sup>1</sup>, E. Klootwijk<sup>2</sup>, J. Reinders<sup>3</sup>, N. Assmann<sup>3</sup>, P. Oefner<sup>3</sup>, R. Kleta<sup>2</sup>, R. Warth<sup>1</sup>

<sup>1</sup>University Regensburg, Medical Cell Biology, Regensburg, Germany

<sup>2</sup>University College, Centre for Nephrology, London, United Kingdom

<sup>3</sup>University Regensburg, Functional Genomics, Regensburg, Germany

In 1992 Tolaymat et. al. described a family suffering from an unknown form of autosomal dominant renal Fanconi syndrome. However, the etiology was unclear. Recently, we succeeded in identifying a mutation in a gene coding for the peroxisomal protein enoyl-CoA hydratase/L-3-hydroxyacyl-CoA dehydrogenase (EHHADH). This protein is involved in the peroxisomal  $\beta$ -oxidation where it catalyzes two consecutive reactions. Using immunofluorescence we could observe that the mutated protein is imported into mitochondria of stably transfected inducible cells (LLC-PK1<sub>MUT</sub>) derived from the porcine proximal tubule (LLC-PK1). In contrast, cells overexpressing the wildtype protein (LLC-PK1<sub>WT</sub>) showed a normal localization to the peroxisomes. Respirometric measurements exhibited a 35% decrease in O<sub>2</sub> consumption in LLC-PK1<sub>MUT</sub> cells when stimulated with octanoyl-carnitine as a specific substrate for mitochondrial  $\beta$ -oxidation. Measurement of ATP content in these cells showed a significantly lower ATP/ADP ratio in LLC-PK1<sub>MUT</sub> cells. Furthermore, FAP has a 30% homology with HADHA, which is involved in mitochondrial  $\beta$ -oxidation as a part of the mitochondrial trifunctional protein complex (MTP). FAP co-immunoprecipitated with HADHB, the second component of the MTP. In addition, acyl-carnitine levels in the medium of LLC-PK1<sub>MUT</sub> cells were significantly elevated, pointing to a defect in mitochondrial  $\beta$ -oxidation. According to our hypothesis FAP is imported into the mitochondria where it is integrated into the MTP, thereby interfering with normal mitochondrial  $\beta$ -oxidation. As a consequence, ATP generation in proximal tubular cells is impaired leading to a defect in secondary active transport and thus to a renal Fanconi syndrome.

**P278**

**Low-dose nitrite improves renal tissue reoxygenation after ischemia**

\*K. Arakelyan<sup>1,2</sup>, K. Cantow<sup>1</sup>, M. Ladwig<sup>1</sup>, B. Flemming<sup>1</sup>, E. Seeliger<sup>1</sup>

<sup>1</sup>Charité - Universitätsmedizin Berlin, Institut für Vegetative Physiologie, Berlin, Germany

<sup>2</sup>Max Delbrück Center for Molecular Medicine, Berlin Ultra High Field Facility (B.U.H.F.F.), Berlin, Germany

**Questions:** Renal ischemia-reperfusion is one common cause of acute kidney injury. Postischemic hypoperfusion and hypoxia are pivotal in the pathophysiology of this inju-

ry. According to a new paradigm of hypoxic vasodilation, nitrite is reduced to vasodilatory nitric oxide by hemoglobin in hypoxic areas. We studied the potential of low-dose nitrite administration to improve postischemic hypoperfusion and hypoxia.

**Methods:** In anesthetized rats, arterial blood pressure, renal blood flow, cortical and medullary tissue  $pO_2$  and perfusion were monitored. Nitrite was infused throughout the experiment (0.172 mg/hour per kg BM for 10 min, followed by 0.057 mg/hour per kg BM). Control rats received isotonic saline. Nitrite's effect on hypoxic vasodilation was tested by a brief hypoxia. Then, the left kidney was exposed to 45 min of warm ischemia, followed by a reperfusion phase of 60 min.

**Results:** Low-dose nitrite did not result in hypotension during normoxic conditions but enhanced hypoxic vasodilation in renal and extrarenal vascular beds. In control rats, upon reperfusion cortical and medullary vasoconstriction resulted in slow  $pO_2$  recovery;  $pO_2$  remained 20-40% below the pre-ischemic level throughout the observation period. In the nitrite group, medullary and cortical  $pO_2$  was restored faster and reached values even above pre-ischemic level. This relied, in part, on improved reperfusion.

**Conclusion:** Low-dose nitrite alleviates renal tissue hypoperfusion and restoration of medullary and cortical tissue  $pO_2$  during the early reperfusion phase. Nitrite's beneficial effect relies, at least in part, on its reduction to nitric oxide in hypoxic tissue with ensuing vasodilation.

#### P279

##### Paracellular pathway properties of primary cultured in comparison to freshly isolated proximal tubules

\*A. Kliez, N. Himmerkus, S. Grüssel, V. Wulfmeyer, M. Bleich  
Christian-Albrechts-University of Kiel, Institute of Physiology, Kiel, Germany

**Question:** In the renal proximal tubule bulk reabsorption of water and electrolytes takes place via the paracellular pathway. The perception of this pathway has changed from an unregulated and passive transport route to being a highly regulated and adaptable player in epithelial transport. The selectivity of this pathway is mainly determined by the claudin composition of the tight junction. In the proximal tubule claudin-2, -10a, -11, -12 and -17 have been described. To investigate the regulation of proximal tubule claudin composition we established a primary cell culture (murine primary proximal tubular epithelial cells, mpPTEC) and compared the paracellular properties and claudin composition with native mouse proximal convoluted tubules (PCT).

**Methods:** Proximal tubular fragments were isolated enzymatically, manually sorted at high purity (mainly PCTs) and cultivated on transwell filter inserts. Electrophysiological properties of mpPTECs were measured in Ussing Chamber experiments and compared with measurements of microperfused freshly isolated proximal tubular segments. Immunofluorescence staining (IF) of mpPTECs and kidney

slices as well as qRT-PCR of mpPTECs and freshly isolated proximal tubules were performed to assess claudin expression.

**Results:** Transepithelial resistance was higher in mpPTECs ( $22.5 \pm 1.5$  Wcm<sup>2</sup>) in comparison to PCT ( $11.3 \pm 1.4$  Wcm<sup>2</sup>). The paracellular pathway in mpPTECs was slightly cation-selective ( $P_{Na^+}/P_{Cl^-}$ :  $1.9 \pm 0.2$ ) in comparison to native PCTs, which preferred anions ( $P_{Na^+}/P_{Cl^-}$ :  $0.67 \pm 0.05$ ). Native proximal tubules showed robust claudin-2 and claudin-10 staining in IF, whereas mpPTECs displayed only weak and inconsistent staining for claudin-2 and no staining for claudin-10. qPCR analysis of these claudins showed lower mRNA expression in mpPTECs for both claudins, however, a huge increase of the claudin 2/10a ratio from 2 to approx. 12.

**Conclusion:** Although the paracellular properties of the proximal tubule were conserved during our mpPTEC cultivation process with respect to the claudin-2 as proximal tubule specific claudin, the overall resistance increased and the selectivity changed from preference for anions to cations presumably, due to the change of claudin-2/10a ratio.

#### P280

##### Recovery of electrogenic transport and intracellular pH in isolated perfused thick ascending limb after metabolic ischemia

\*N. Himmerkus<sup>1</sup>, M. Bleich<sup>1</sup>, P. Steels<sup>2</sup>

<sup>1</sup>Christian-Albrechts-University of Kiel, Institute of Physiology, Kiel, Germany

<sup>2</sup>University Hasselt, Biomedical Research Institute, Diepenbeek, Belgium

**Question:** Ischemia/reperfusion (I/R) injuries are a common and severe problem in nephrology. One important feature of I/R is a drop in extracellular and intracellular pH ( $pH_e$ ,  $pH_i$ ) during ischemia and the respective recovery after reperfusion. We investigated the recovery of the thick ascending limb of loop of Henle (TAL) in electrogenic transport and  $pH_i$  under different extracellular pH conditions after metabolic ischemia (MI).

**Methods:** Freshly isolated TAL were microperfused and transepithelial voltage ( $V_{te}$ ) and resistance ( $R_{te}$ ) monitored parallel to  $pH_i$  using BCECF- microfluorimetry. NaCl transport was estimated by calculating the equivalent short circuit current ( $I_{sc}$ ). After an initial control period at  $pH_e$  7.4 MI was induced by 2 deoxy-glucose and cyanide for 5min and the subsequent washout and recovery period was investigated according to 3 different pHe protocols: (a) MI at  $pH_e$  6.8, 10 min recovery at  $pH_e$  7.4, (b) MI at  $pH_e$  6.8, 10 min recovery at  $pH_e$  6.8 followed by 5 min at  $pH_e$  7.4, (c) MI as well as 10 min recovery at  $pH_e$  7.4. Cell height at several positions along the tubule was measured before, during and after ischemia.

**Results:** We observed a fast  $I_{sc}$  recovery to  $30 \pm 6$  % of pre-ischemic  $I_{sc}$  after protocol (a) and to  $35 \pm 10$  % after protocol (b). Protocol (c) led to a recovery of  $72 \pm 10$  %. The initial fast drop in  $pH_i$  was comparable between groups, however, a  $pH_e$  of 7.4 during MI allowed a partial recovery already in the ischemic phase and a fast and robust

recovery ( $103 \pm 3$  %) in the wash-out phase in comparison to protocol (a) ( $96 \pm 2$  %). During the  $pH_e$  6.8 recovery phase of protocol (b)  $pH_i$  dropped again markedly and only showed full recovery in the additional  $pH_e$  7.4 wash-out phase ( $98 \pm 3$  %). In all cases cell height as a measure of cell swelling increased during MI and recovered afterwards. The time-point of regulatory cell volume decrease coincided with the beginning of  $I_{sc}$  recovery.

**Conclusion:** Physiological  $pH_e$  of 7.4 during the pathophysiological state of ischemia ameliorated the function of TAL after I/R injury indicating that acidic  $pH_e$  during ischemia is a deteriorating factor for transport recovery. Acidic  $pH_e$  in the reperfusion phase, however, altered the shape of  $pH_i$  recovery but did not influence the overall outcome.

#### P281

##### Functional relevance of connexin 40 in hyperplastic renin cells

\*C. Karger, A. Kurtz

Institute of Physiology, University of Regensburg, Regensburg, Germany

The gap junction protein connexin 40 (Cx40) has a major functional role in renin secreting cells of the kidney. Firstly, it is essential for a correct negative feedback control of renin secretion by the renal perfusion pressure. Loss of Cx40 function therefore leads to renin hypersecretion in vivo and to hypertension. Secondly, Cx40 is essential for correct position of renin secreting cells in the juxtaglomerular portion of afferent arterioles. Loss of Cx40 function therefore leads to ectopic displacement of renin secretion cells into the periglomerular interstitium. It is well known that genetic defects of the renin-angiotensin-aldosterone-system (RAAS) cause massive reactive hyperplasia of renin producing cells which are mainly located in the perivascular areas of afferent arterioles. The relevance of Cx40 for those hyperplastic renin secreting cells is yet unknown and was therefore investigated in this study. As a model for renin cell hyperplasia due to RAAS insufficiency we used mice with genetic deletion of aldosterone synthase (aldo-ko). Kidneys of those mice contain a more than ten-fold increased number of renin producing cells mostly in perivascular localization. To assess the function of Cx40 we used Cx40 gene deletion. We found that hyperplastic renin cells expressed Cx40 like the characteristic juxtaglomerular cells. Renin secretion from aldo-ko kidneys was inversely related to the renal perfusion pressure. This characteristic pressure control of renin secretion was completely absent in kidneys of aldo/Cx40 double-ko mice. Aldo-ko mice were found to be hypotensive in contrast to aldo/Cx40 double-ko mice where normal blood pressure was reestablished. While there was only minor increase in total renin mRNA we could observe a 2.5-fold increase in plasma renin concentrations in aldo/Cx40 double-ko compared to aldo-ko. Distribution of renin cells in aldo/Cx40 double-ko kidneys showed differences compared with aldo-ko kidneys. More precisely the renin producing cells in aldo-ko mice form multilayered cuff-like structures around afferent arterioles while renin cells in aldo/Cx40 double-ko are not restricted to the perivascular

area but in addition spread out into the tubular interstitium and the periglomerular region. Altogether, the sum of our findings suggests that Cx40 has the same functional relevance in hyperplastic renin cells as it has been recently established for juxtaglomerular cells.

#### P282

##### High K<sup>+</sup> intake in Na<sup>+</sup>-replete mice: Does it only look like an aldosterone-induced hypertension?

\*H. Vitzthum, P. Böttcher, A. Seniuk, H. Ehmke

UKE Hamburg, Department of Cellular and Integrative Physiology, Hamburg, Germany

Increasing K<sup>+</sup> intake stimulates aldosterone secretion. Consequently a high K<sup>+</sup> intake should be accompanied by an increased reabsorption of Na<sup>+</sup> and an elevated blood pressure, particularly if Na<sup>+</sup> intake is high. To gain insight into the physiological consequences of increased aldosterone secretion associated with high K<sup>+</sup> intake we investigated blood pressure, hormonal, and renal responses to a high K<sup>+</sup> intake (5%) in Na<sup>+</sup> replete (3% NaCl) mice. Mice receiving a high K-citrate diet had elevated blood pressure, an increased plasma aldosterone level and a decreased renal Na<sup>+</sup> excretion. Renal mRNA and protein expression of the epithelial Na<sup>+</sup>-channel ( $\beta$ -ENaC) and its activating kinase Sgk1 were increased after 10 days of high K<sup>+</sup> intake. Surprisingly, ENaC (amiloride) as well as mineralocorticoid receptor (spironolactone) antagonism failed to normalize blood pressure, suggesting the contribution of other, aldosterone-Sgk1-ENaC-independent mechanisms. To test the hypothesis, that the co-administered anion has a major impact on the responses to the high K<sup>+</sup> intake, we compared the effects of diets containing 5% K<sup>+</sup> together with either Cl<sup>-</sup>, citrate<sup>-</sup>, or HCO<sub>3</sub><sup>-</sup> for 10 days. Independent of the correspondent anion, in all groups a nearly identical increase in blood pressure was observed. Renal gene expression responses, however, markedly differed between the three high K<sup>+</sup> diet groups. While  $\alpha$ - and  $\beta$ -ENaC mRNA was upregulated in the K-citrate and KHCO<sub>3</sub> group, it did not change in the KCl group. Furthermore, we found an upregulation of the Na<sup>+</sup>-citrate-cotransporter NaDC1 mRNA in the high KCl group, as well as an upregulation of pendrin mRNA in the high KHCO<sub>3</sub> group. These findings indicate that in Na<sup>+</sup> replete mice a high K<sup>+</sup> diet induces blood pressure increase independent of both the co-administered anion and the aldosterone-Sgk1-ENaC-pathway.

#### P283

##### Insulin and dexamethasone increase cellular serum / glucocorticoid-inducible kinase 1 (SGK1) activity via different mechanisms in Na<sup>+</sup> absorbing mpkCCD cells

G. Watt<sup>1</sup>, D. Walker<sup>1</sup>, S. Land<sup>1</sup>, M. Bailey<sup>2</sup>, \*S. Wilson<sup>3</sup>

<sup>1</sup>University of Dundee, Division of Cardiovascular and Diabetes Medicine, Dundee, United Kingdom

<sup>2</sup>University of Edinburgh, University / BHF Institute for Cardiovascular Science, Edinburgh, United Kingdom

<sup>3</sup>University of Durham, School of Medicine, Pharmacy and Health, Stockton on Tees, United Kingdom

The regulated absorption of Na<sup>+</sup> within the cortical collecting duct determines the amount of Na<sup>+</sup> lost in the urine and this process is therefore critical to the control of whole body Na<sup>+</sup> and water balance and hence to the long term regulation of blood pressure. Previous studies of a Na<sup>+</sup> absorbing cell line derived from the mouse cortical collecting duct (mpkCCD cells) showed that insulin and dexamethasone both stimulate electrogenic Na<sup>+</sup> transport via mechanisms that involve an increase in the activity of serum / glucocorticoid-inducible kinase 1 (SGK1). In the present study we explore the mechanisms that underlie these increases in SGK1 activity. Western analyses / densitometry undertaken using phospho-peptide specific antibodies against an endogenous SGK1 substrate (NDRG1-Thr<sup>345/356/366</sup>) confirmed that dexamethasone (0.1 μM, 1 h, n = 5) and insulin (20 nM, 1 h, n = 7) do activate this regulatory kinase which is central to the control of Na<sup>+</sup> reabsorption. However, although earlier work shows that both responses are dependent upon PI3K activity (see e.g. MK Mansley & SM Wilson, Brit J Pharmacol 161, 571-588: 2010), dexamethasone did not alter the phosphorylation status of residues within an endogenous protein (PKB-Thr<sup>308</sup>, PKB-Ser<sup>473</sup>) that are phosphorylated in a PI3K-dependent manner. Insulin, on the other hand, consistently promoted phosphorylation of both residues. Moreover, analyses undertaken by quantitative, real time PCR (n = 6) showed that dexamethasone increase the abundance of mRNA encoding SGK1 to a level that was 43.9 ± 8.3 times greater than control level (P < 0.001) whilst whilst insulin had no discernible effect upon the expression of this mRNA species (1.03 ± 0.21 times control level, n = 6). These data therefore show that insulin and dexamethasone increase cellular SGK1 activity by different mechanisms since dexamethasone thus promotes SGK1 gene expression without activating PI3K, whilst insulin activates PI3K without evoking SGK1 gene expression. As anticipated by this model, cyclohexamide, an agent that blocks de novo protein synthesis, abolished the dexamethasone-induced activation of SGK1 (n = 5) but did not prevent the glucocorticoid-induced expression of the SGK1 gene (42.5 ± 4.4 times control, P < 0.001). However, we were surprised to find that cyclohexamide also disrupted the insulin-induced activation of PI3K / SGK1 (Fig. 1D). Both responses therefore depend upon protein synthesis.

**P284**

**Characterization of the apical K<sup>+</sup> conductance in different parts of the microdissected murine aldosterone-sensitive distal nephron**

<sup>\*V. Nesterov, C. Korbmacher</sup>

Institut für Zelluläre und Molekulare Physiologie, Erlangen, Germany

**Question:** The aldosterone-sensitive distal nephron (ASDN) comprises the late distal convoluted tubule (DCT2), the connecting tubule (CNT) and the entire collecting duct (CD). In the ASDN the key transport step for Na<sup>+</sup> absorption is the

amiloride sensitive epithelial sodium channel (ENaC), while K<sup>+</sup> secretion is mediated mainly by the Ba<sup>2+</sup> sensitive renal outer medullary K<sup>+</sup> channel (ROMK). Previously, we reported that ENaC activity in the late distal convoluted tubule/early connecting tubule (DCT2/CNT) was constitutively high and did not depend on circulating aldosterone, while in the late CNT/early cortical collecting duct (CNT/CCD) ENaC activity was aldosterone-dependent (Nesterov et al. 2012, Am J Physiol Renal Physiol 303: F1289-F1299). The known functional link between Na<sup>+</sup> absorption and K<sup>+</sup> secretion raises the question whether a similar heterogeneity also exists for the apical K<sup>+</sup> conductance in the ASDN.

**Methods:** Patch-clamp experiments were conducted using microdissected fragments of DCT2/CNT or CNT/CCD from mice maintained on standard diet. Tubular fragments were split open to gain access to the apical membrane with the patch pipette. Experiments were started in a high Na<sup>+</sup> bath solution and the amiloride-sensitive whole-cell current (ΔI<sub>ami</sub>) was determined at a holding potential of -60 mV. Subsequently, the Ba<sup>2+</sup> sensitive current (ΔI<sub>Ba(o/o)</sub>) was recorded in the outside-out configuration of the patch clamp technique using a high K<sup>+</sup> bath solution and a holding potential of -60 mV.

**Results:** In good agreement with our previous findings, ΔI<sub>ami</sub> was substantially larger in the DCT2/CNT (ranging from 65 to 334 pA, n=4) than in the CNT/CCD (ranging from 8.7 to 57 pA, n=6). Sizeable ΔI<sub>Ba(o/o)</sub> values ranging from 65 to 334 pA (n=4) were observed in outside-out patches from the DCT2/CNT. In contrast, in the CNT/CCD the values for ΔI<sub>Ba(o/o)</sub> did not exceed 4 pA. Single channel properties were consistent with those of typical ROMK channels.

**Conclusions:** The outside-out configuration of the patch clamp technique was used to demonstrate that the apical K<sup>+</sup> conductance is higher in the DCT2/CNT than in the CNT/CCD obtained from mice on a standard diet. This regional difference in K<sup>+</sup> conductance is reminiscent of that previously reported for the activity of ENaC in the ASDN. This supports the concept of a regional interdependence of Na<sup>+</sup> absorption and K<sup>+</sup> secretion in this nephron segment.

**P285**

**NFAT5-mediated expression of S100A4 contributes to proliferation and migration of renal carcinoma cells**

<sup>\*C. Küper<sup>1</sup>, F.- X. Beck<sup>1</sup>, W. Neuhofer<sup>1,2</sup></sup>

<sup>1</sup>LMU München, Physiologisches Institut, München, Germany

<sup>2</sup>LMU München, Med. Klinik und Poliklinik IV, München, Germany

**Question:** The osmosensitive transcription factor Nuclear Factor of Activated T-cells 5 (NFAT5) has been associated with the development of a variety of tumor entities, among them breast cancer, colon carcinoma, and melanoma. Especially the NFAT5-target gene S100A4 is a well-defined pro-metastatic factor. The aim of the present study was to evaluate, if NFAT5 and S100A4 are also involved in the development and progression of renal cell carcinoma (RCC).

**Methods:** CaKi-1 cells were used as in vitro model for clear cell RCC, the most common type of RCC, which originates from the proximal convoluted tubule. The non-cancerous

proximal tubule cell line HK-2 was used as control. Cellular NFAT5 activity was determined using a reporter vector. Expression of NFAT5 and NFAT5-target genes was measured by qRT-PCR and immunoblot. Expression of NFAT5 was blunted by transfection with a specific siRNA construct, and the effect of this maneuver on cell proliferation, cell survival and cell migration was assayed by MTT assay and in vitro wound healing assay, respectively.

**Results:** NFAT5 activity in CaKi-1 cells was several times higher compared to HK-2 cells. Osmotic stress conditions increased NFAT5 activity both in Caki-1 and HK-2 cells, again with significantly higher activities in Caki-1 cells. Analysis of NFAT5-regulating signaling pathways revealed that the Extracellular Regulated Kinase (ERK) is constitutively active in Caki-1, but not in HK-2 cells, and is partially responsible for the enhanced NFAT5 activity in CaKi-1 cells. The MAP kinases p38 and JNK are activated under osmotic-stress conditions and probably mediate upregulation of NFAT5 activity under these conditions both in CaKi-1 and HK-2 cells. siRNA-mediated knockdown of NFAT5 in Caki-1 cells reduced the expression of S100A4. This was accompanied by a significant decrease in cell proliferation and migration and a reduced cell survival under osmotic-stress conditions.

**Conclusions:** Taken together, our results indicate that NFAT5 induces S100A4 expression in CaKi-1 cells, thereby playing an important role for proliferation, migration, and cell survival of renal carcinoma cells.

**P286**

**The influence of stimulation of the cAMP pathway on paracellular permeability in the thick ascending limb (TAL)**

<sup>\*A. Plain, N. Himmerkus, M. Bleich</sup>

Christian-Albrechts-Universität zu Kiel, Physiologisches Institut, Kiel, Germany

**Question:** The TAL drives an important part of the reabsorption of divalent cations. This occurs through the cation selective paracellular pathway. Claudins determine the permeability and selectivity of this pathway. We wanted to study if cAMP pathway stimulation affects paracellular permeability in the TAL.

**Methods:** TALs from young mice (C57Bl/6J) were dissected for microperfusion with enzyme assistance. For stimulation we applied forskolin/IBMX, or arginine vasopressin (AVP). The experiments were performed acutely or after 30 min of preincubation. We measured transepithelial resistance and voltage (R<sub>te</sub>, V<sub>te</sub>), and calculated the equivalent short circuit current (I<sub>sc</sub>). From diffusion voltages across the paracellular pathway, we calculated the paracellular permeability (P) for Na<sup>+</sup>, Mg<sup>2+</sup> and Ca<sup>2+</sup>. Measurements were performed at 37°C with continuous perfusion at a constant perfusion pressure.

**Results:** Freshly isolated TAL segments (n=10) revealed characteristic transcellular properties (V<sub>te</sub> = 11 ± 2 mV; R<sub>te</sub> = 9 ± 2 Wcm<sup>2</sup>; I<sub>sc</sub> = 1338 ± 150 μA/cm<sup>2</sup>). Acute stimulation in the presence of furosemide (inhibition of transcellular transport) with an observation time of 10 to 12 minutes did

not result in any change in P<sub>Na</sub>. A second series of experiments was performed with unpaired preincubation for 30 min at 30°C, under control or stimulation conditions, respectively (n=8-11). Transcellular transport was not different between groups. Stimulation increased R<sub>te</sub> (AVP +68%; forskolin/IBMX +100%) and decreased P<sub>Na</sub> (AVP -40%; forskolin/IBMX -40%) while P<sub>Ca</sub> and P<sub>Mg</sub> remained unchanged in comparison to control. Interestingly, the diameter of TAL tubules incubated by either AVP or forskolin/IBMX was higher than control, indicating additional structural effects.

**Conclusions:** The paracellular permeability for cations in the TAL might be controlled by the cAMP pathway. The dependence on incubation conditions limits conclusions at this stage.

**P287**

**Glomerular injury and thrombotic microangiopathy in mice with impaired Gs-alpha/cAMP signaling in renin cells - possible role of VEGF**

<sup>\*P. Lachmann</sup>

Universitätsklinikum Carl G. Carus, TU Dresden, Nephrologisches Forschungslabor, Dresden, Germany

Renin lineage descendent cells are largely assembled in the glomerulus, the renal arteries and the collecting ducts of the mature mammalian kidney, while renin expression is restricted to the juxtaglomerular (JG) cells. The latter comprise only about 0,01 % of all renal cells. The G protein stimulatory alpha-subunit (Gs-alpha) generally mediates receptor-stimulated cAMP production and is known to increase renin synthesis. Thus, deficiency of Gs-alpha impairs renin production. Interestingly, the selective knockout of Gs-alpha in the renin cells of mice leads also to kidney malformations and renal failure. However, due to the developmental expression pattern of renin, these mice have diffuse Gs-alpha deficiency throughout the kidneys. Therefore, it remained unclear whether the impaired cAMP signaling in the JG cells is relevant for the pathogenesis of the kidney injury at all.

To address this issue we generated triple-transgenic mice with selective and inducible knockout of Gs-alpha in JG cells (termed JG-Gsalphasilenced mice). The JG-Gsalphasilenced and their control mice were followed-up for more than 24 weeks after the induction. The knockout was mapped exclusively to the JG cells. The JG-Gsalphasilenced mice excreted more osmolytes than the control group (mean±SEM 4964,4±520 μOsm/24 h vs 2801,7±410 μOsm/24 h, p=0,02 at the end of the experiment). Progressive albuminuria was observed in the JG-Gsalphasilenced, but not in the control mice (mean±SEM 201±55,7 μg/24 h vs 40±6,9 μg/24 h, p=0,039 at the end of the experiment). At the end of the observation period the JG-Gsalphasilenced mice had enlarged glomeruli with elevated injury score, thickened capillary basement membranes, enhanced matrix accumulation, and focal and segmental sclerosis. The structure of the glomerular filter of the Gsalphadeficient animals in electron microscopy was characterized by swollen endothelial cells, thickened glomerular basement mem-

branes and fibrin-like subendothelial deposits, all of which are typical signs of thrombotic microangiopathy (TMA). This phenotype is very similar to the one observed in mice with glomerular deficiency of vascular endothelial growth factor (VEGF). Therefore, we hypothesized that the knockout of Gsalpha diminished VEGF production in JG cells which then lead to glomerular damage and TMA. Moreover, it is known that VEGF is expressed in JG cells and we found that cAMP increases VEGF expression in cultured clonal renin-producing cells. In summary our data demonstrate that Gs-alpha deficiency in JG cells is sufficient to cause progressive renal damage with signs of TMA and thus may substantially contribute to the development of renal failure.

**P288**

**The role of BNP in the renal adaptation to loss of kidney tissue**

\*J. Staffel, A. Schreiber, D. Valletta, F. Schweda  
University of Regensburg, Physiology, Regensburg, Germany

**Question:** Unilateral nephrectomy (UNx) induces a rapid increase in the glomerular filtration rate (GFR) of the remaining kidney within days, so the GFR reaches up to 75% of the baseline values with two kidneys. Recent data of our group suggest that BNP might be the long-sought factor mediating this adaptation: 1. The rapid increase in the GFR is blunted in mice lacking the guanylylcyclase-A (GC-A), the common receptor for the natriuretic peptides ANP and BNP. 2. The plasma concentration of BNP, but not of ANP, is elevated in mice 3 days post UNx up to 110+14 pM. Whether this concentration of BNP is capable of stimulating the GFR is unknown and was investigated in the present study.

**Methods and Results:** Infusion of BNP at relevant in vivo concentrations resulted in concentration-dependent increases in renal perfusion and in GFR in isolated perfused kidneys from wildtype mice. These effects were absent in GC-A knockout mice. Likewise, infusion of BNP (1 ng / g body weight per minute) in anesthetized wildtype mice induced increases in the GFR as well as diuresis and natriuresis. Finally, a three-day infusion of exogenous BNP via osmotic minipumps in relevant post-UNx concentrations resulted in a significant elevation of the GFR (+20% vs. baseline). Moreover, the kidney weights of the mice infused with BNP were significantly higher compared with mice receiving 0.9% NaCl (vehicle control), indicating renal hypertrophy.

**Conclusions:** Our data show that BNP at concentrations that occur post-UNx is well capable of significantly enhancing kidney function. Together with our previous results, they clearly suggest that BNP mediates the rapid adaptation of kidney function to a loss of kidney tissue.

**P289**

**Natriuretic peptides buffer renovascular hypertension**

\*T. Demerath, J. Staffel, A. Schreiber, D. Valletta, F. Schweda  
University of Regensburg, Physiology, Regensburg, Germany

**Question:** The renin-angiotensin-aldosterone system and cardiac natriuretic peptides (atrial and B-type natriuretic peptide, ANP / BNP) are opposing control mechanisms for arterial blood pressure. Accordingly, an inverse relationship between the plasma concentrations of renin (PRC) and ANP exists in most circumstances. However, PRC and ANP levels are both elevated in renovascular hypertension. Because ANP can directly suppress renin release, we used ANP knockout mice (ANP<sup>-/-</sup>) to investigate whether high ANP levels attenuate the increase in PRC in response to renal hypoperfusion, thus buffering renovascular hypertension.

**Results and Conclusion:** ANP<sup>-/-</sup> mice were hypertensive and had reduced PRC compared with that in ANP<sup>+/+</sup> under control conditions. Unilateral renal artery stenosis (2-kidney, 1-clip, 2k1c) for 1 week induced similar increases in the blood pressure and in the PRC in both genotypes. Unexpectedly, the plasma BNP concentrations in ANP<sup>-/-</sup> significantly increased in response to 2k1c, potentially compensating for the lack of ANP. In fact, in mice lacking guanylyl cyclase A (GC-A<sup>-/-</sup>), which is the common receptor for both ANP and BNP, the renovascular hypertension was markedly augmented compared with that in GC-A<sup>+/+</sup>. However, the higher blood pressure of GC-A<sup>-/-</sup> was not caused by a disinhibition of the renin system because the PRC and renal renin synthesis were significantly lower in GC-A<sup>-/-</sup> than in GC-A<sup>+/+</sup>. Thus, natriuretic peptides buffer renal vascular hypertension via renin-independent effects, such as extracellular volume control or vasorelaxation. The latter possibility is supported by experiments in isolated perfused mouse kidneys, in which physiological concentrations of ANP and BNP elicited renal vasodilatation but did not suppress renin release.

Vascular functions and circulation II

**P290**

**Rigid nuclei of endothelial cells resist deformation induced by high loading forces**

\*I. Liashkovich, H. Oberleithner  
Institut für Physiologie II, Münster, Germany

Rapid changes of the macromechanical parameters in the vascular bed including blood flow and blood pressure re-

quire fast and well-orchestrated adjustments by the cellular components of the cardiovascular system. Endothelial cells are strategically positioned at the interface between blood and tissue to be able to rapidly respond to alterations of blood flow. However, the mechanisms of mechanosensing/mechanotransduction at the subcellular level are still unclear. Experimental evidence points towards the endothelial cell nucleus, bulging into the vessel lumen, as being directly involved in such processes. Therefore the aim of this work is to estimate the contribution of the nucleus to the overall mechanics of living endothelial cell. To address this question a novel combination of confocal laser scanning fluorescence microscopy with atomic force microscopy (AFM) was employed. This combination allows unprecedented precision of AFM probe positioning in 3D space. More importantly, confocal microscopy provides a coarse but reliable visual feedback of the extent of cellular deformation at a given loading force while AFM gives a precise readout of the forces and corresponding deformations. Previous reports indicate that the nucleus biochemically isolated from the cell appears to be the stiffest subcellular component. That is why a high loading force applied by the AFM probe onto the surface of a living endothelial cell was used during mechanical measurements. We reasoned that at such a high loading force (3 nN) the softer cellular structures like the glycocalyx (stiffness = 0.4 pN/nm) and the cortical actin cytoskeleton (stiffness = 1.7 pN/nm) are fully compressed leaving the nucleus responsible for bearing the excess load. Experimental data confirms that at the loading force of 3 nN the deformation of a living endothelial cell rarely exceeds 1.5 µm. If the nuclear stiffness were equal to or lower than the stiffness of the cortical actin network, we would expect the cell to be deformed by at least 2 µm. This indicates that the experimentally measured deformation of a living endothelial cell is at least 25% lower than what is expected from cortical actin network alone. We conclude that at such loading forces the cortical cytoskeleton is fully compressed and thus the mechanical strength is mainly provided by the nucleus.

**P291**

**Zyxin regulates vascular tone and smooth muscle cell phenotype in experimental hypertension**

\*S. Ghosh<sup>1</sup>, B. Kollar<sup>1</sup>, S. Suresh Babu<sup>1,2</sup>, A. Wojtowicz<sup>1,3</sup>, M. Cattaruzza<sup>1</sup>, M. Hecker<sup>1</sup>

<sup>1</sup>Institute of Physiology and Pathophysiology, Division of Cardiovascular Physiology, University of Heidelberg, Heidelberg, Germany

<sup>2</sup>University of British Columbia, Centre for Blood Research, Vancouver, Canada

<sup>3</sup>Centre Hospitalier Universitaire Vaudois, Department of Internal Medicine, Lausanne, Switzerland

**Question:** Vascular smooth muscle cells (VSMC) lining the blood vessel walls are exposed to increased wall tension or stretch in chronically elevated high blood pressure. This leads to a shift in phenotype of these cells eventually affecting arterial structure and tone. Zyxin, a focal adhesion protein capable of stretch-induced nuclear translocation,

affects the expression of several mechanosensitive genes. As such, we have analyzed changes in VSMC phenotype and vascular tone in zyxin-deficient mice in experimental hypertension.

**Method and Results:** Deoxycorticosterone acetate (DOCA)-salt treatment induced hypertension in wild type (WT) and zyxin-deficient (KO) mice which were analyzed in three separate series of experiments (animals aged 6, 12 and 18 months denoted as adult, old, very old, respectively). Both systolic and diastolic blood pressure failed to increase in very old KO but not WT animals. A lower resistivity of femoral arteries from these mice to blood flow (using ultrasound colour Doppler) in vivo and a poor myogenic response in situ further corroborated these findings. A reduced contractile response of these arteries to phenylephrine and endothelin-1 could be explained by lower mRNA expression of these receptors. Additionally, femoral arteries from DOCA salt-treated KO mice had a reduced networking of collagen I fibers possibly accounted for by the reduced expression of its crosslinking enzyme, transglutaminase 2. Aortic VSMCs from KO animals were pro-migratory, poorly contractile and highly proliferative in vitro, in line with the above findings.

**Conclusions:** Zyxin is a novel regulator of the phenotypic shift of VSMCs from a contractile to the synthetic phenotype in pathological vascular remodeling.

**P292**

**Effects of shear stress and aqueous cigarette smoke extract on the development of endothelial dysfunction and plaque stability**

\*S. Giebe<sup>1</sup>, C. Brunssen<sup>1</sup>, M. Brux<sup>1</sup>, N. Cockcroft<sup>2</sup>, K. Hewitt<sup>2</sup>, H. Morawietz<sup>1</sup>

<sup>1</sup>University Hospital Carl Gustav Carus, Division of Vascular Endothelium and Microcirculation, Dresden, Germany

<sup>2</sup>British American Tobacco, Group Research & Development, Southampton, United Kingdom

**Question:** Tobacco smoking is considered to support the development of atherosclerotic plaques. The rupture of an unstable atherosclerotic plaque leads to severe clinical complications. One of the first steps in the development of atherosclerosis is endothelial dysfunction. Endothelial dysfunction is associated with decreased bioavailability of nitric oxide, increased inflammation and a corresponding expression profile in the endothelial cells as the inner layer of the vessel wall. Local hemodynamic forces are key stimuli in this process. Low laminar flow is involved in the development of an unstable plaque phenotype, while high laminar flow supports a rather stable plaque composition. The molecular mechanisms controlling plaque stability in response to tobacco smoking remain largely unknown so far. Therefore, we exposed human endothelial cells to cigarette smoke extract (CSEaq) under normal and disturbed flow conditions and studied the molecular changes.

**Methods & Results:** Primary human endothelial cells (HUVEC) were stimulated with increasing dosages of CSEaq for 24 h. Cell viability was significantly reduced by CSEaq



in a dose-dependent manner. We investigated the impact of specific flow conditions and different doses of CSEaq using a cone-and-plate viscometer on the expression of atherosclerosis-related genes. High laminar shear stress of 30 dyn/cm<sup>2</sup> induced elongation of endothelial cells in the direction of flow. In addition, high laminar flow increased eNOS expression and NO release in a time-dependent manner. This increase was inhibited by CSEaq. Low laminar flow (1 dyn/cm<sup>2</sup>) showed no significant effect on eNOS expression and NO release. This might be directly linked to the development of endothelial dysfunction and an unstable plaque phenotype. The NRF2 antioxidative defense system was also induced by high laminar flow. NRF2 and NRF2 target genes HMOX1 and NQO1 were strongly activated by cigarette smoke. This upregulation was not affected by high laminar flow and might be a compensatory mechanism protecting the endothelial cells. Furthermore, we monitored the expression of proinflammatory genes. CSEaq strongly induced adhesion molecule ICAM-1 under static and flow conditions. Interestingly, VCAM-1 was unaffected by CSEaq. Induction of the major endothelial NADPH oxidase isoform NOX4 by CSEaq was prevented by high laminar shear stress. Catalase expression was not affected by shear stress and CSEaq, whereas CSEaq transiently increased SOD1 expression. Finally, we performed wound healing and monocyte adhesion assays under different flow conditions. Endothelial wound healing was significantly improved by atheroprotective high laminar flow, while low flow did not affect wound healing. Furthermore, high laminar shear stress decreased adhesion of monocytes to primary human endothelial cells, compared to low flow.

**Conclusions:** In this study, we suggest novel molecular mechanisms how tobacco smoking promotes the development of endothelial dysfunction. This can contribute to the formation of an unstable atherosclerotic plaque phenotype.

**P293**

**Influence of a mineralocorticoid receptor blockade on vascular function in atherosclerotic mouse models under high-fat diet**

\*J. Rissler<sup>1</sup>, C. Brunssen<sup>1</sup>, H. Langbein<sup>1</sup>, A. Hofmann<sup>1</sup>, A. Deussen<sup>2</sup>, M. Peitzsch<sup>3</sup>, P. Cimalla<sup>4</sup>, E. Koch<sup>4</sup>, G. Eisenhofer<sup>3</sup>, H. Morawietz<sup>3</sup>

<sup>1</sup>University Hospital Carl Gustav Carus, Division of Vascular Endothelium and Microcirculation, Dresden, Germany

<sup>2</sup>Medical Faculty Carl Gustav Carus, Department of Physiology, Dresden, Germany

<sup>3</sup>University Hospital Carl Gustav Carus, Institute of Clinical Chemistry and Laboratory Medicine, Dresden, Germany

<sup>4</sup>Medical Faculty Carl Gustav Carus, Department Clinical Sensing and Monitoring, Dresden, Germany

**Question:** An important step in the pathogenesis of atherosclerosis is the development of endothelial dysfunction. One well-established risk factor of endothelial dysfunction is consumption of high amounts of saturated fat. Recent studies reveal an endothelium-protective effect of blockade of the aldosterone-binding mineralocorticoid recep-

tor (MR). In this study, we analyzed the effects of high-fat diet (HFD) and MR blockade on metabolic parameters and endothelial function in C57BL6/J mice, the atherosclerosis model Low-Density Lipoprotein Receptor (LDLR<sup>-/-</sup>), the Lectin-like Oxidized Low-Density Lipoprotein-Receptor-1 (LOX-1)tg mice and their combination in LDLR<sup>-/-</sup>/LOX-1tg (LOLR) mice.

**Methods & Results:** Mice were fed a high-fat diet (HFD, with 60% energy from fat) and a standard diet (STD), or the corresponding interventional diet with the MR blocker eplerenone (200 mg\*kg BW<sup>-1</sup>\*d<sup>-1</sup>) for 20 weeks. The body weight and food uptake were documented weekly. Blood samples were taken for plasma analyses of the lipid profile. Fasting blood glucose levels were measured. Vascular function was evaluated by acetylcholine induced-vasorelaxation using Mulvany myograph in rings of thoracic aortas. Reactive oxygen species were determined by Luciferin-dependent chemiluminescence. Eplerenone was detected by high-performance liquid chromatography (HPLC). Aldosterone concentrations were measured by liquid chromatography-tandem mass spectrometry (LC-MS/MS). Feeding the HFD leads to increased energy uptake of all mice strains. After half of the feeding period, body weight of C57BL6/J animals fed the HFD + eplerenone was significantly lower than the HFD control group due to a lower energy uptake. Eplerenone was detectable in plasma and liver of C57BL6/J mice. Aldosterone concentrations increased in plasma of eplerenone-fed C57BL6/J mice. HFD-fed LOX-1- and LOLR-mice showed a decreased body weight reduction after 12 hours of fasting and an elevated fasting blood glucose level compared to STD-fed LOX-1- and LOLR-mice. Interestingly, treatment with eplerenone normalized blood glucose levels. LDLR<sup>-/-</sup>, LOX-1tg and LOLR-mice showed decreased endothelial function compared to C57BL6/J. Interestingly, all mice strains fed a HFD showed significantly weaker aortic pre-contraction in response to phenylephrine. In response to HFD we could observe a decreased endothelial function in C57BL6/J, LOX-1tg and LOLR mice. In these experiments, eplerenone shows beneficial effects. This could be due to the significantly reduced production of reactive oxygen species measured after eplerenone medication. All findings were independent of changes in vascular smooth muscle function. In addition, endothelial function was analysed by self-developed optical coherence tomography devices using flow-mediated vasodilation in the murine saphenous artery in vivo. Thus, feeding a HFD deteriorates endothelial function and metabolic activity of C57BL6/J, LOX-1 and LOLR mice.

**Conclusions:** In conclusion, our study provides improved understanding of the effects of MR inhibition on endothelial function and metabolic parameters.

**P294**

**Evidence for complex synaptic facilitation occurring in sympathetic varicosities of the rat vena cava**

\*R. Patejdl, H.- B. Heinrich, T. K. Noack

Universitätsmedizin Rostock, Institut für Physiologie, Rostock, Germany

**Question:** The tone of venous capacitance vessels is regulated to meet the circulation's demands for maintaining venous return. Sympathetic varicosities releasing Noradrenaline are an important element in this process. While some studies have faced the responses of the vena cava to externally added Noradrenaline and other substances, only little is known about the varicosities' dynamic function.

**Methods:** Mechanical responses of ring preparations of the abdominal vena cava from Wistar rats were studied using conventional organ bath technique. Various protocols of electric field stimulation (EFS) were applied to dissect neuronal and myogenic responses. Repetitive intermittent train stimulation over several minutes was engaged to study dynamic changes of synaptic function.

**Results:** Using single 2 second trains of pulses with a duration of 1ms produced mechanical responses that were virtually completely suppressed by TTX (10<sup>-7</sup> mol/l) or the alpha-1-Antagonist Urapidil (10<sup>-7</sup> mol/l). The amplitude of responses increased with the applied stimulus current and saturated at currents of 40mA. Repetitive train stimulation with 40mA each 10 seconds over 5 minutes resulted in a tetanization with a complex temporal pattern. Within the first minute, a marked mean increase in tension of 509% compared to single trains or trains applied at greater temporal with. The slope of tension during this initial tetanization increased after multiple repetitive train stimulations (mean 205%, SD 50%, n=5). Initial tetanization was followed by a phase of slow decline and merged into a phase of phasic oscillations at the frequency of single stimulus trains within the series.

**Conclusions:** Whereas the observed tetanization per se is likely to be the result of local accumulation of noradrenaline in the space surrounding the varicosity, the increasing slope of tetanization with repeated stimulation series can only be explained by dynamic changes in the behavior of the sympathetic varicosity. Repeated series stimulation leads to a facilitation of transmitter release, giving higher amounts of noradrenaline being released in response to a certain intensity of external EFS. EFS can be used as a tool to study the function of the autonomic nervous system via its effects on smooth muscle. Further detailed analysis of the response of sympathetic varicosities to EFS under various conditions may improve our understanding of the regulation of the venous capacitance system in health and disease.

**P295**

**Towards cell-specific targeting of proteasomes in cardiovascular cells**

\*S. Wieber<sup>1</sup>, B. Florea<sup>2</sup>, A. Wagner<sup>1</sup>, H. Overkleeft<sup>2</sup>, M. Hecker<sup>1</sup>, O. Drews<sup>1</sup>

<sup>1</sup>Institute of Physiology and Pathophysiology, Cardiovascular Research, Heidelberg, Germany

<sup>2</sup>University, Chemistry, Leiden, Netherlands

**Introduction:** Proteasome complexes are targeted in blood cells by cancer chemotherapeutics. Furthermore, their suitability as targets in cardiovascular disease is investigated.

Although proteasome assembly is heterogenic and cell-type dependent, it was not systematically analyzed in cardiovascular cells. Aim: of the study was to identify assembly of the proteasome with regard to its proteolytic subunits in cardiovascular cells.

**Methods and Results:** Proteasome assembly was mainly analyzed via fluorescent probes specifically targeting proteolytic subunits followed by non-denaturing and denaturing electrophoresis. Utilized in cytosolic extracts, these probes revealed that mixed assembly of constitutive and inducible proteasome subunits exists under non-stimulated conditions in all analyzed cell types. Notably, the percentage of inducible subunits was characteristic and observed in the following order from low to high: smooth muscle cells (SMC), endothelial cells (EC) and monocytes (MC). Since inducible subunits occupy the same space as their constitutive counterparts in assembled proteasomes, the order is reversed for the latter (e.g. subunit -81% β5 in MC vs. EC, p<0.01, n=4). The probes are based on the structure of proteasome inhibitors, mimicking proteasomal targeting by chemotherapeutics. To validate the results and consider the fact that intact cells differ in their susceptibility to proteasome inhibitors, the approach was optimized and standardized for cell culture conditions and perfused blood vessels. Indeed, proteasome assembly in living cells and tissue matched the in vitro results, but also revealed differences presumably superimposed by cell-dependent pharmacodynamics.

**Conclusion:** Assembly of proteasome complexes is characteristic for cardiovascular cell-types, which may prove advantageous to achieve more precise inhibitor-based therapy.

**P296**

**alpha-parvin regulates blood vessel stability in mice**

\*B. Pitter<sup>1</sup>, A. Fraccaroli<sup>1</sup>, H. Gerhardt<sup>2</sup>, U. Pohl<sup>1</sup>, E. Montanez<sup>1</sup>

<sup>1</sup>Walter-Brendel-Centre of Experimental Medicine, Ludwig-Maximilians-University, Munich, Germany

<sup>2</sup>Vascular Biology Laboratory, London Research Institute, Cancer Research UK, Lincoln's Inn Fields Laboratories, London, United Kingdom

During blood vessel development, endothelial cells (ECs) form cell-to-cell junctions maintaining vascular integrity. Here, we show that endothelial specific deletion of the focal adhesion protein alpha-parvin (alpha-pv) in mice results in vascular abnormalities, leading to hemorrhages and embryonic lethality. The vascular abnormalities are characterized by irregular vessel morphology, impaired vessel lumenization, vessel collapse and regression. Moreover loss of alpha-pv in ECs impairs the morphology of cell-to-cell junctions in vivo. Knockdown of alpha-pv in ECs impairs cell spreading, and perturbs organization of cortical actin filaments and maturation of adherent junctions. Our findings show that alpha-pv is essential to maintain vascular integrity during vessel development.

**P297**

**VEGF-A expression under prodiabetic conditions in human retinal and endothelial cells and the vitreous fluid of patients with type 2 diabetes**

\*H. Morawietz<sup>1</sup>, A. Frenzel<sup>1</sup>, A. Mieting<sup>1</sup>, W. Goettsch<sup>1</sup>, M. Valtink<sup>2</sup>, C. Roehlecke<sup>2</sup>, R. H. W. Funk<sup>2</sup>, K. A. Becker<sup>3</sup>, K. Engelmann<sup>3</sup>

<sup>1</sup>University of Technology Dresden, Div. of Vascular Endothelium and Microcirculation, Dresden, Germany

<sup>2</sup>University of Technology Dresden, Institute of Anatomy, Dresden, Germany

<sup>3</sup>Klinikum Chemnitz gGmbH, Department of Ophthalmology, Chemnitz, Germany

**Question:** Clinical complications of diabetes mellitus are retinal neovascularisation, proliferative vitreoretinopathy, or diabetic macular edema (DME). DME is the one of the leading causes of blindness in the industrial world. DME could be caused by abnormal vessel growth and increased vascular permeability due to elevated levels of Vascular Endothelial Growth Factor (VEGF) in the vitreous samples of diabetic patients. Inhibitors of VEGF are approved drugs for the treatment of Age Related Macular Degeneration. **Methods:** In this study, we established methods to study the expression of different VEGF isoforms by RT-PCR in human retinal and endothelial cells. Next, we established a co-culture of human retinal and endothelial cells. Finally, we analyzed the VEGF concentration in the vitreous fluid of patients with type 2 diabetes.

**Results:** VEGF-A 165A isoform was much higher expressed in retinal cells, compared to endothelial cells. Stimulation of retinal cells with high glucose levels as a diabetic model induced VEGF-A 165A in human retinal cells. Hydrogen peroxide as model of oxidative stress induced VEGF-A 165A expression in retinal cells as well. Glyoxal as a model of oxidative stress under diabetic conditions lead to an even more pronounced induction of VEGF-A 165A in human retinal and endothelial cells. In addition, we established for the first time a model of co-culture of human retinal and endothelial cells and can now analyze the impact of risk factors on vascular sprouting in this setting. In a clinical study, the VEGF concentration in the vitreous fluid of patients with type 2 diabetes showed a trend to be increased.

**Conclusions:** Our data suggest a novel mechanism how diabetes and oxidative stress induce VEGF-A and the ingrowths of novel blood vessels into the retina in diabetic retinopathy.

**P298**

**Phasic contractile activity in rat mesenteric arteries is due to cyclic release of noradrenaline from nerve varicosities**

K. Paul<sup>1</sup>, R. Patejdl<sup>1</sup>, \*T. Noack<sup>1</sup>

<sup>1</sup>Universitätsmedizin Rostock, Oscar-Langendorff Institut für Physiologie, Rostock, Germany

Time variant contractions of smooth muscle are addressed to spontaneous activity of the tissue. In intestinal smooth muscle, such phasic activity is reported as “Basal organ specific” and due to the activity of both, pacemaker cells

(interstitial Cajal cells, ICC) and smooth muscle cells. In some arterial vascular beds, phasic activity can be evoked and observed spontaneously or after depolarization. Using rat mesenteric arteries (0.4 mm inner diameter) in a myograph setup, regular tonic contractions were observed during application of a vasoconstrictor like noradrenaline or high potassium solution. Using electrical field stimulation (square pulses, 1 to 10 ms, 30 to 70 mA), single and rhythmical contractions could be observed. The frequency was typical for minute rhythm and it could be enhanced by the non-specific potassium channel blocker tetraethylammonium (TEA1-10 mM). On application of tetrodotoxin (TTX, 100 nM), the contractions which were elicited by field stimulation were abolished (more than 95%) and also those during TEA application. Analysis of the time course of the single contractions on 1 to 10 ms pulses demonstrated that direct muscle stimulation did not contribute to total activity (less than 10 %) under these conditions. Therefore, it is concluded that phasic contractile activity in arterial smooth muscle of rat mesenteric arteries is due to a rhythmical release of noradrenaline from nerve varicosities.

**P299**

**Low endothelial shear stress induces podosome formation via vascular endothelial growth factor receptor-2 stimulation**

\*T. Fey, U. Pohl, A. Dendorfer

LMU Munich, Walter-Brendel-Centre of Experimental Medicine, Munich, Germany

**Question:** Chronic changes in blood flow mediate vascular remodeling and angiogenesis. Podosomes are actin-rich cell adhesions which are associated with an enhanced local proteolysis of the extracellular matrix, an event being essential for remodelling processes. To delineate changes in podosome generation during remodelling, we studied the influence of different shear stress levels on podosome formation and on their matrix degradation capacity in endothelial cells. **Methods:** Human umbilical vein endothelial cells (HUVEC, passage 2 to 3) were grown on fluorescent gelatin (Oregon green-conjugated) whose structure was imaged by confocal microscopy. Gelatinolytic activity of HUVECs was quantified according to the number of circular gelatin defects. Shear stress was produced by unidirectional perfusion of a parallel plate flow chamber (Ibidi).

**Results:** Cells grown under static conditions expressed podosomes in circular arrangements (rosettes) that were associated with matrix metalloproteinase accumulation and focal gelatin degradation. HUVECs cultivated for 48 hours under static conditions formed podosome rosette imprints in a density of 196 per mm<sup>2</sup>. Exposure to shear stress significantly reduced the abundance of those ring-shaped gelatin defects. However, cells treated with very low shear (<math>1 \text{ dyn/cm}^2</math>) showed a significantly higher amount of rosette imprints compared to cells under higher shear stress (2-4 or 10  $\text{dyn/cm}^2$ ) (high shear 40, medium shear 43, low shear 78, n = 5). Stimulation of protein kinase C (PKC) significantly increased podosome formation. However, inhibi-

tion of PKC did not reduce podosome abundance under static conditions. In contrast, VEGF (vascular endothelial growth factor) receptor-2 inhibition significantly reduced podosome formation under static conditions by 85%. Furthermore, inhibition of main proteins of the VEGF pathway namely Src, PI3kinase and p38 contributed to the signal pathway as assessed by inhibitors. VEGF RNA and protein expression were highly increased in the static situation compared to high shear stress. External VEGF suppressed podosome rosette imprints only under high shear and not under static conditions. **Conclusions:** Thus podosome rosette formation and gelatinolytic activity of endothelial cells is locally inhibited under elevated shear stress. This VEGF receptor 2-mediated effect is due to a downregulation of endogenous VEGF levels by shear stress.

**P300**

**Assessment of the effects of tryptophan containing peptides from whey protein on vessel tone regulation and angiogenesis**

\*S. Khedr, M. Marten, A. Deußen

TU Dresden, Physiology, Dresden, Germany

**Introduction:** Approximately 50 % of the population of developed countries and an equally increasing fraction of the populations of developing countries exhibit arterial hypertension. Arterial hypertension may be seen as a pandemic disease. One potential approach of prevention would be the supplement of daily food with compounds that lower arterial blood pressure. Biologically active peptides obtained from milk proteins after being hydrolyzed proved to have an antihypertensive effect by acting as angiotensin converting enzyme (ACE) inhibitors. The most potent peptide has been isolated from whey protein (alpha-lactalbumin) and identified as isoleucine-tryptophan (IW). These peptides have other documented biological actions e.g. EW has an anti-angiogenic effect. Angiogenesis is pivotal for both physiological e.g. wound healing and pathological e.g. cancer processes. However, the underlying mechanisms as well as other biological actions are still unknown.

**Questions:** 1. Do tryptophan containing di-peptides differ in their biological actions with respect to relaxation of arterial vessels? 2. How do quantitative concentration-effect relationships differ for these peptides? 3. How do differences of the profile of action reflect the different molecular structures? 4. Do the biological actions require the intact peptide structure or are they shared with the hydrolysis product tryptophan?

**Methods:** IW and other peptides are tested for their ACE inhibiting potency against rabbit lung ACE and human plasma ACE. Measurement of ACE activity is performed using benzoyl-glycyl-histidyl-leucin (HHL) as substrate and its hydrolysis to hippuric acid and histidyl-leucin (HL) is assessed by HPLC. In addition the effects of tryptophan-containing peptides on sprouting by using fibrin gel bead assay were studied. Result: IW showed marked inhibitory potency on rabbit lung ACE and human plasma ACE in comparison to other peptides, however, this effect is modest in

comparison to captopril. On the other hand, EW showed a significantly higher anti-angiogenic effect which was marked by sprouting inhibition in fibrin gel bead assay in comparison to other peptides.

**Conclusion:** This study shows the novel ACE inhibitory, as well as, the anti-angiogenic effect of whey protein extracted peptides.

**P301**

**The extract of leaves of the Moringa tree is a modulator of smooth muscle tone**

C. Kupke, A. Steyer, J. Tödt, M. Werner, R. Patejdl, \*T. Noack

Universitätsmedizin Rostock, Oscar-Langendorff Institut für Physiologie, Rostock, Germany

Moringa oleifera is used commonly in wide parts of the world as food additive. A physiological effect however, is not documented. The dry leaf DMSO extract of Moringa was tested in rat gastric antrum, gastric fundus and portal vein preparations using conventional organ bath technique. 100 mg dry weight of Moringa leaves was added to 2 ml of DMSO. The mixture was agitated for 10 minutes and quantities were stored in the fridge (-20°C). After equilibration of the tissues, portal vein and gastric antrum showed regular spontaneous activity. The gastric fundus possessed only little tone. Using the extract in concentrations of 1.5 and 3 mg per 30 ml (organbath volume), basically no change of tone was observed. Using acetylcholine 0.1 and 1  $\mu\text{M}$  as preactivation, typically all three tissues showed their typical increase in activity. The cumulative addition of Moringa extract (1.5 and 3 mg per 30 ml) again showed only little effect. Using acetylcholine (0.1 nad 1  $\mu\text{M}$ ) and noradrenaline (0.2  $\mu\text{M}$ ), the addition of Moringa produced excitatory effects in gastric preparations and inhibitory action on the vessel. This behaviour can be mimicked by beta adrenergic inhibition by propranolol (1 to 10  $\mu\text{M}$ ). It is concluded, that Moringa, used as a food additive, might exert some of its effects by adrenergic receptor blockade.

**P302**

**Transport across the blood brain barrier with nanoparticle systems**

\*J. Hedrich<sup>1</sup>, D. Y. W. Ng<sup>2</sup>, M. Jansen<sup>1</sup>, T. Weil<sup>2</sup>, H. J. Luhmann<sup>1</sup>

<sup>1</sup>University Medicine Mainz, Institute of Physiology, Mainz, Germany

<sup>2</sup>University of Ulm, Institute of Organic Chemistry III, Ulm, Germany

The brain is the most challenging target of drug delivery, due to the fact that the blood brain barrier (BBB) protects the brain parenchyma from molecules of the blood stream and prevents delivery of most pharmaceuticals. This brain protective property is reached by the interplay of a dynamic system of highly differentiated cells of the neurovascular unit: brain capillary endothelial cells, pericytes, astrocytes and neurons. In this study we investigated nanoparticle systems to cross the BBB and target cells of the neurovascular unit. The uptake of the nanoparticles as investigated by live

cell imaging and immunohistochemistry followed by confocal imaging demonstrated that nanoparticles target cells of the neurovascular unit by the endosomal pathway. An in vitro cell culture transwell model was used to study a potential transcytotic passage of these nanoparticles across the endothelial monolayer. Transport studies revealed a charge dependent delivery of nanoparticles across the in vitro BBB. In addition the investigated nanoparticles present a high cellular compatibility. Even with nanoparticles concentration ten times above effective concentration no cytotoxic side effects or a disruption of the transendothelial resistance of the endothelial cell layer could be observed.

This work was financially supported by DFG (SFB 625) and a Stufe 1 grant, University Medical Center of the Johannes Gutenberg-University Mainz, to JH.

**P303**  
**Cell-specific and endothelium-dependent regulations of matrix metalloproteinase-2 in Rat Aorta**

\*I. Kopaliani, A. Deussen  
 TU Dresden, Physiology, Dresden, Germany

Aortic stiffness inevitably increases with age and considerably accelerates during hypertension. Chronic activation of angiotensin II (ANGII) and matrix metalloproteinase-2 (MMP-2) during hypertension contribute to increased aortic stiffness. We studied signalling mechanisms employed by ANGI in the regulation of latent and active forms of MMP-2 in rat aortic endothelial and smooth muscle cells, along with isolated rat aorta. Using western blotting, we demonstrate that ANGI (1 µmol/L) significantly (p<0.01) increases latent MMP-2 expression after 8 hours not only in endothelial and smooth muscle cells, but also in isolated rat aorta. We identified that ANGI acts via AT1 receptor activated cell-specific pathways. In endothelial cells, the JNK1 pathway is activated, whereas in smooth muscle cells the JAK2/STAT3 pathway. Results obtained in cell culture are in agreement with the results obtained in isolated aorta. However, active MMP-2 was not found under cell culture conditions, whereas in isolated aorta active MMP-2 was significantly (p<0.05) increased after stimulation with ANGI, as detected by gelatine zymography. This increase of MMP-2 activity was not inhibited by blocking pathways that control latent MMP-2 expression, but was abolished in the absence of endothelium. Our results demonstrate that ANGI regulates latent MMP-2 expression via cell-specific pathways in rat aorta. The endothelium plays an essential role in the activation of latent MMP-2. These findings offer new insights into molecular mechanisms potentially involved in aortic stiffness during hypertension and may lead to new strategies for inhibiting MMP-2 expression and activation in distinct cell types of the aortic wall.

**P304**  
**A model investigation upon the combined effect of shear and red blood cell distributions related trauma in rotary blood pumps**

\*A. Poorkhalil, K. Mottaghy  
 RWTH Aachen university, Institute of Physiology, Aachen, Germany

**Question:** Cell migration in physiological circulation is a well investigated phenomenon. In small capillaries, red blood cells (RBCs) migrate to the capillary center with a cell-free layer at the wall, known as “Fåhræus-Lindqvist effect”. This phenomenon occurs based on shear distribution and leads to a redistribution of RBCs forming “local Hct” values. Since the quantity of hemolysis is depends on Hct values, the consideration of this phenomenon is very important also in rotary blood pumps (RBP). This investigation should lead to the calculation of the relevant amounts of hemolysis produced in such pumps.

**Methods:** In order to change simultaneously the velocity profile and RBC distribution with modified cylindrical couette arrangements: coaxial cylinders are combined with thin blade allowing modeling of RBP blades. Model fluid and freshly drawn heparinized pig blood was sheared in different geometries and related hemolysis was measured.

**Results:** The results show two different hemolysis behaviors under same hemorheological condition and exposure time in couette devices with/ without blades. In the absence of blade, damage index increases almost linearly over time while surprisingly, in the higher shear regions, in the presence of the blade, damage index shows lower values. The model fluid confirms the results showing different “particle distribution” in the various compartments of the device.

**Conclusion:** It is concluded that the presented method, considering the cell distribution and shear distribution, delivers more realistic hemolysis results and therefore may lead to the design optimization of RBPs.

Transporters II

**P305**  
**Down-regulation of Na<sup>+</sup>-coupled glucose transporter SGLT1 by SPAK**

\*B. Elvira Jimenez, M. Bleuca, C. Munoz, E. Shumilina, F. Lang  
 University of Tuebingen, Department of Physiology, Tübingen, Germany

**Question:** Na<sup>+</sup>-coupled glucose transporter SGLT1 (SLC5A1) accomplishes concentrative cellular glucose uptake even at low extracellular glucose concentrations. The

present study explored whether SGLT1 activity is regulated by the WNK-dependent STE20/SPS1-related proline/alanine-rich kinase SPAK.

**Methods:** SGLT1 was expressed in *Xenopus* oocytes with or without additional expression of wild type SPAK, constitutively active <sup>CA</sup>SPAK, constitutively inactive <sup>CI</sup>SPAK or catalytically inactive <sup>KD</sup>SPAK and electrogenic glucose transport determined by dual electrode voltage clamp. SGLT1 activity was further determined by Ussing chamber experiments in jejunum of SPAK-deficient and wild type mice.

**Results:** In SGLT1-expressing oocytes, but not in oocytes injected with water, glucose addition induced an inward current (I<sub>g</sub>), which was significantly decreased following co-expression of wild-type SPAK and <sup>CA</sup>SPAK, but not <sup>CI</sup>SPAK or <sup>KD</sup>SPAK. Kinetic analysis revealed that SPAK decreased maximal I<sub>g</sub> without significantly modifying the glucose concentration required to trigger halfmaximal I<sub>g</sub> (K<sub>m</sub>). According to chemiluminescence, wild type SPAK but not <sup>KD</sup>SPAK decreased SGLT1 protein abundance in the oocyte cell membrane. Inhibition of SGLT1 insertion by brefeldin A (5 µM) resulted in a decline of I<sub>g</sub>, which was similar in the absence and presence of SPAK, suggesting that SPAK did not delay the retrieval of SGLT1 protein from the cell membrane but rather down-regulated SGLT1 by inhibiting carrier insertion into the cell membrane. Moreover, glucose-induced current was significantly lower in jejunum of wild-type mice compared to SPAK-deficient mice.

**Conclusions:** SPAK decreased SGLT1 protein abundance in the cell membrane, an effect requiring a WNK-dependent catalytic activity of SPAK, and thus impaired electrogenic glucose uptake.

**P306**  
**Role of Chorein in apoptotic cell death of therapy resistant human ZF rhabdomyosarcoma cells**

\*W. Yu<sup>1</sup>, S. Honisch<sup>1</sup>, A. Tsapara<sup>2</sup>, I. Alesutan<sup>1</sup>, F. Lang<sup>1</sup>, C. Stournaras<sup>1,2</sup>  
<sup>1</sup>University of Tuebingen, Department of Physiology, Tübingen, Germany  
<sup>2</sup>University of Crete Medical School, Department of Biochemistry, Heraklion, Greece

**Question:** Chorein, a protein encoded by VPS13A gene, defective in chorea-acanthocytosis (ChAc), is involved in neuronal cell survival as well as cortical actin polymerization of erythrocytes and blood platelets. In addition, chorein is expressed in human umbilical vein endothelial cells (HUVECs) regulating the cytoskeletal architecture and cell stiffness. In view of its anti-apoptotic effect in neurons, we explored whether chorein is expressed in cancer cells and has an impact on cancer cell survival and signaling.

**Methods:** RT-PCR was employed to determine transcript levels, specific siRNA's to silence chorein, FACS analysis to follow cell apoptosis and Western blotting to quantify protein expression and phosphorylation.

**Results:** RT-PCR analysis revealed differential expression profile of chorein in various cancer cell types. The protein was predominantly expressed in resistant tumor cell lines of low differentiation rate such as the human ZF rhabdomyosarcoma cells. Silencing of chorein in ZF rhabdomyo-

sarcoma cells induced potent early and late apoptosis and annexin-V binding reflecting phosphatidylserine translocation to the cell surface. In line with these findings, the ratio of phosphorylated (and thus activated) to total phosphoinositide 3 kinase (pPI-3K/PI-3K) was significantly reduced upon chorein silencing, implying inactivation of this crucial pro-survival signaling molecule. Moreover, chorein silencing diminished transcript levels and protein expression of anti-apoptotic BCL-2.

**Conclusions:** Chorein is expressed in various cancer cells, predominantly in therapy resistant tumor cells. Silencing of this protein promotes apoptotic cell death, mainly controlled by down-regulation of PI-3K activity and BCL-2 expression.

**P307**  
**Transporter-mediated replacement of extracellular glutamate for γ-aminobutyric acid in the developing murine neocortex**

\*P. Unichenko, H. J. Luhmann, S. Kirischuk  
 University Medical Center of the Johannes Gutenberg University Mainz, Institute of Physiology, Mainz, Germany

During early development, cortical neurons migrate from their places of origin to their final destinations where they differentiate and establish synaptic connections. Radially migrating cells move from deeper zone to the marginal zone, but they do not invade the latter. This “stop” function of the marginal zone is mediated by a number of factors, including glutamate and GABA, two main neurotransmitters in the central nervous system. In the marginal zone, GABA has been shown to be released via GABA transporters (GAT)-2/3, whereas glutamate transporters (EAATs) operate in the uptake mode. In this study GABAergic postsynaptic currents (GPSCs) were recorded from Cajal-Retzius cells in the marginal zone of murine neonatal neocortex using whole-cell patch-clamp technique. Minimal electrical stimulation was applied to elicit evoked GPSCs using paired-pulse protocol. We report that EAAT blockade with DL-TBOA, a specific non-transportable EAAT antagonist, abolishes constitutive GAT-2/3-mediated GABA release. In contrast to DL-TBOA, D-aspartate, an EAAT substrate, fails to block GAT-2/3-mediated GABA release. SNAP-5114, a specific GAT-2/3 antagonist, induced an elevation of intracellular sodium concentration ([Na<sup>+</sup>]<sub>i</sub>) under resting conditions and in the presence of D-aspartate, indicating that GAT-2/3 operates in reverse mode. In the presence of DL-TBOA, however, SNAP-5114 elicited [Na<sup>+</sup>]<sub>i</sub> decrease, demonstrating that GAT-2/3 operates in uptake mode. We conclude that EAATs via intracellular Na<sup>+</sup> signaling and/or cell depolarization can govern the strength/direction of GAT-mediated GABA transport.

**P308**

**Characterization of intestinal-specific NaPi-IIb/Slc34a2 deficient mice**

\*N. Hernando, K. Myakala, F. Simona, H. Murer, C. A. Wagner, J. Biber  
University Zurich-Irchel, Physiology, Zurich, Switzerland

Active transport of inorganic phosphate (Pi) across the intestinal epithelia is mediated by the Na/Pi-cotransporter NaPi-IIb (SLC34A2). In mice, the intestinal expression of NaPi-IIb is restricted to the brush border membrane (BBM) of ileum. Expression of NaPi-IIb mRNA is also detected in other tissues including lung and testis. Full ablation of NaPi-IIb is embryonically lethal whereas the global but inducible removal of the transporter in young mice leads to intestinal Pi loss and lung calcification. The aim of this work was to generate and characterize a non-inducible but intestinal-specific NaPi-IIb depleted mouse model. Depletion was achieved by crossing floxed-NaPi-IIb with villin-Cre transgenic mice. Intestinal-specific depletion was confirmed by quantifying the expression of the cotransporter mRNA on RNA samples extracted from ileum and lungs. We found that the constitutive ablation of NaPi-IIb in intestine results in viable pups. NaPi-IIb<sup>-/-</sup> mice are characterized by the complete absence of Na/Pi cotransport activity in BBM vesicles (BBMV) isolated from ileum, resulting in higher fecal loss of Pi. On the contrary, the urinary excretion of Pi is reduced in NaPi-IIb<sup>-/-</sup> animals, whereas the plasma levels of Pi are similar in wild type and NaPi-IIb deficient mice. The Na/Pi cotransport into renal BBMV as well as the expression of the renal Na/Pi-cotransporter NaPi-IIa is moderately increased in NaPi-IIb<sup>-/-</sup> females but not in males. The circulating levels of FGF23 are reduced in mutant mice, although this change reached statistical significance only in females. Osseal expression of FGF23 mRNA is also reduced in females but not in males. This data, together with the ratio of full-length FGF23 to cleaved FGF23, indicates that the reduced circulating levels of the hormone are probably due to reduced synthesis as well as increased degradation. In summary, intestinal ablation of NaPi-IIb results in fecal loss and reduced urinary excretion of Pi. The intestinal defect is fully compensated by the increased renal reabsorption. In females, this compensation associates with reduced levels of FGF23

**P309**

**Identification of phosphate regulated transcripts in ileum and renal proximal tubules**

\*T. Knöpfel, N. Kampik, N. Hernando, I. Rubio Aliaga, J. Biber, C. Wagner  
University of Zurich, Institute of Physiology, Zurich, Switzerland

Phosphate is a vital compound for every cell in order to maintain energy metabolism, cell signaling and structure. Two important organs in maintaining phosphate homeostasis are the intestine where phosphate from the nutrition gets absorbed and the kidney that reabsorbs filtered phosphate. Apical entrance of phosphate into intestinal and proximal tubular epithelial cells is well characterized, whereas basolateral efflux

mechanisms are poorly understood. The amount of Na-Pi cotransporters (members of the Slc34 family) expressed at the apical membrane is regulated by dietary phosphate intake by mechanisms, which are not fully understood. The aim of this project is to identify transcripts in ileum and renal proximal tubules regulated by dietary phosphate content. Identified genes may be involved in the transcellular transport of phosphate like the unknown basolateral transport pathway or contribute to adaption of apical phosphate uptake and metabolism. C57BL/6 male mice (8 weeks old) were fed a high (1.2%) or low (0.1%) phosphate diet for 3 days. Renal and intestinal adaption was confirmed by qPCR for known phosphate regulated transcripts including Slc34a2 and Cyp24a1. After the dietary adaptation, epithelial scrapings were prepared from the distal small intestine and micro-dissected renal proximal tubules were collected. The RNA isolated from these tissues was analysed using the RNA sequencing service provided by the Functional Genomics Center Zurich. Comparison of the transcriptome of low and high dietary phosphate conditions revealed 2029 genes to be differently (at least 2 fold changes) expressed in ileum and 327 in renal proximal tubules. Regulation of selected transcripts is currently being confirmed by qPCR and immunoblotting. Pathway analysis is performed and selected candidates for basolateral phosphate transporters will be expressed in *Xenopus laevis* oocytes.

**P310**

**Effect of rapid administration of phosphate in rats**

\*L. Thomas, C. Bettoni, U. Schnitzbauer, N. Hernando, C. Wagner, J. Biber  
University of Zurich, Institute of Physiology, Zurich, Switzerland

Extracellular phosphate (P<sub>i</sub>) is kept within a constant range by balanced intestinal absorption, deposition in soft tissues, bone resorption/deposition, and renal reabsorption. All these processes are controlled among other factors by PTH, 1,25-dihydroxy-vitamin D, and FGF-23. In addition, extracellular P<sub>i</sub> itself might control the above mentioned processes. The aim of this study was to analyze the response of hormones and P<sub>i</sub> transporters to rapid changes of extracellular Pi in rats upon intravenous or intragastric application of one bolus of Pi. Rats were fed for 5 days with low P<sub>i</sub> diet. Upon 12 hours fasting, rats were infused intravenously or gavaged with either sodium P<sub>i</sub> or saline. Blood and urine samples were collected at different time points and at the end of the experiment (4 hours post-application) several tissues (kidneys, femur, intestinal mucosa) were extracted. As expected, when sodium P<sub>i</sub> was infused into the femoral vein, there was a rapid increase in plasma P<sub>i</sub> concentration (two fold, within 10 minutes); then, it gradually decreased reaching normal values after two hours. Infusion with sodium P<sub>i</sub> increased urinary P<sub>i</sub> excretion (hundred fold) within 10 minutes; although the P<sub>i</sub> excretion decreased thereafter, it did remain higher than in control animals at the end of the experiment. By the end of the experimental protocol, only about 50 % of the infused P<sub>i</sub> was excreted in the urine. However, the remaining 50 % was not detected in the circulation since plasma P<sub>i</sub> normalized 2 hours post-in-

fusion. Plasma ionized Ca fell moderately (0.2 fold) after 10 min in the animals infused with sodium P<sub>i</sub>, and remained lower for the next hour. Infusion of sodium P<sub>i</sub> increased PTH (six fold) within 10 minutes, and the hormonal levels remained high until the end of the experiment. No changes in FGF23 and 1,25 Dihydroxy vitamin D levels were observed at any time point. All parameters remained constant in the saline-infused control rats. Our findings indicate that upon P<sub>i</sub> loading, normophosphatemia is quickly reestablished and that this is partially achieved by a massive and fast phosphaturic response. Increased PTH, but not FGF23 may contribute to phosphaturia. Moreover, organs other than kidney may also be involved in the P<sub>i</sub> normalization. These observations will be compared with data obtained in the gavage experiments.

**P311**

**The interaction between MCT4 and CAII is mediated by two glutamate residues in the C-terminal of MCT4**

\*S. I. Noor<sup>1</sup>, S. Dietz<sup>1</sup>, H. Heidtmann<sup>1,2</sup>, C. Boone<sup>3</sup>, R. McKenna<sup>3</sup>, J. W. Deitmer<sup>2</sup>, H. M. Becker<sup>1</sup>

<sup>1</sup>TU Kaiserslautern, Zoology/Membrane transport, Kaiserslautern, Germany

<sup>2</sup>TU Kaiserslautern, General Zoology, Kaiserslautern, Germany

<sup>3</sup>University of Florida, Department of Biochemistry and Molecular Biology, Florida, United States

The monocarboxylate transporters MCT1-4 mediate the H<sup>+</sup>-linked shuttling of lactate between glycolytic and oxidative cell types in different tissues like muscle and brain. Heterologous protein expression in *Xenopus* oocytes revealed that carbonic anhydrase isoform II (CAII), a ubiquitous enzyme catalyzing the reversible hydration of CO<sub>2</sub>, enhances transport activity of MCT1 and MCT4 but not of MCT2 (1-3). CAII-induced augmentation of transport activity via MCT1 and MCT4 is mediated by an intramolecular H<sup>+</sup>-shuttle within the CAII and does not depend on the catalytic activity of the enzyme (1, 2, 4). We have recently reported that the two glutamate residues E<sup>489</sup> and E<sup>491</sup>, flanking the acidic cluster E<sup>489</sup>EE within the MCT1 C-terminal mediate direct binding between MCT1 and CAII (5). Comparison of the protein sequence of MCT1 and MCT4 revealed several similar glutamic acid clusters within the C-terminal tail of MCT4, which could be potential binding sites for CAII. To identify the CAII binding site, truncation and single site mutations were introduced into the C-terminal tail of MCT4 and then heterologously expressed in *Xenopus* oocytes with and without CAII. Determination of transport activity with pH-sensitive microelectrodes revealed that deletion of the last 42 amino acids of the MCT4 C-terminal tail, as well as removal of the acidic cluster E<sup>431</sup>EE within the C-terminal, impaired augmentation of MCT4 transport activity by CAII. Exchange of both glutamate residues E<sup>431</sup> and E<sup>433</sup> by glutamine abolished the interaction between MCT4 and CAII, while exchange of any glutamate residue alone had no effect on the CAII-induced increase in MCT4 transport activity. These results suggest that modulation of MCT4 transport activity by CAII requires direct interaction be-

tween transporter and enzyme, which is mediated by the two glutamate residues E<sup>431</sup> and E<sup>433</sup>, flanking the acidic cluster E<sup>431</sup>EE within the C-terminal tail of MCT4.

This work was supported by the “Stiftung Rheinland-Pfalz für Innovation” (961-386261/957) and the “Research Initiative Membrane Biology”.

References

- [1] Becker HM & Deitmer JW (2008). J Biol Chem 283, 21655-21667.
- [2] Becker HM, Klier M & Deitmer JW (2010). J Membr Biol 234, 125-135.
- [3] Klier M, Schüler C, Halestrap AP, Sly WS, Deitmer JW & Becker HM (2011). J Biol Chem 286, 27781-27791.
- [4] Becker HM, Klier M, Schüler C, McKenna R & Deitmer JW (2011). Proc Natl Acad Sci U S A 08, 3071-3076.
- [5] Stridh MH, Alt MD, Wittmann S, Heidtmann H, Aggarwal M, Riederer B, Seidler U, Wennemuth G, McKenna R, Deitmer JW & Becker HM (2012). J Physiol 590, 2333-51.

**P312**

**Does Na<sup>+</sup>/K<sup>+</sup>ATPase regulation by thyroid hormone depend on Na<sup>+</sup>-influx through voltage-gated sodium channels?**

S. MohanaSundaram<sup>1,2</sup>, B. Igelhorst<sup>1</sup>, \*I. Dietzel-Meyer<sup>1</sup>

<sup>1</sup>Ruhr-University Bochum, Biochemistry II, Bochum, Germany

<sup>2</sup>International Graduate School for Neuroscience, Bochum, Germany

Thyroid hormone action is most commonly associated with a regulation of basal metabolic rate. 40% of resting metabolic rate, in turn, is consumed by Na<sup>+</sup>/K<sup>+</sup>-ATPases and consistent with this concept thyroid hormone has been found to regulate Na<sup>+</sup>/K<sup>+</sup>-ATPase activity as well as the synthesis of some of its subunits in a variety of tissues 1,2. An increase in overall Na<sup>+</sup>/K<sup>+</sup>-ATPase activity by thyroid hormone would stabilize resting membrane potentials and tentatively hyperpolarize cells, rendering them less excitable. Clinically, however, the opposite is observed: Hyperthyroidism leads to nervousness, restlessness, irritability and can sometimes even evoke epileptic seizures. This contradiction is resolved by the observation that hyperthyroidism leads to an up-regulation of the neuronal Na<sup>+</sup> current density which increases neuronal excitability3. Here we investigated whether the regulation of different Na<sup>+</sup>/K<sup>+</sup>-ATPase subunits in postnatal (p2-p4) rat neocortical cultures by thyroid hormone (Triodo-L-thyronine, T3) depends on Na<sup>+</sup>-influx through voltage-gated sodium channels. Mixed neuron/glia cell cultures were incubated with 30 nM T3 in the presence or absence of 50 nM tetrodotoxin (TTX) to block Na<sup>+</sup>-influx through voltage dependent Na<sup>+</sup> channels. Using western blots we found, that a pre- incubation with 30 nM T3 for 4 days significantly increased the expression of both, α1 and α2 subunits of the Na<sup>+</sup>/K<sup>+</sup>-ATPase leaving the expression of α3, as well as β1 and β2 subunits unaltered. If T3 treated cultures were co-incubated with TTX no significant changes in the expression of the Na<sup>+</sup>/K<sup>+</sup>-ATPase α1 and α2 subunits with respect to the control cultures were observed. We thus conclude, that, as already noticed in cultured myocytes4, the upregulation of Na<sup>+</sup>/K<sup>+</sup>-ATPase by T3 is reduced if the Na<sup>+</sup> influx into cells is blocked. Some

of the enhanced basal metabolic rate occurring in hyperthyroidism might thus be a consequence of an increased ATP consumption of the Na<sup>+</sup>pump in order to balance an increased intracellular Na<sup>+</sup> load.

1. Harrison, A. P., Clausen, T., A. J. & Metab,E. 274, 864-867 (2010).
2. Banerjee, B. & Chaudhury, S. Life sciences 71, 1643-54 (2002).
3. Hoffmann, G. & Dietzel, I. D. Neuroscience. 125, 369-379 (2004).
4. Brodie and Sampson, Endocrinology 123, 891-896 (1988).

**P313**  
**pH regulatory transporters in pancreatic ductal adenocarcinoma**

\*S. C. Kong  
University of Copenhagen, Department of Biology, Copenhagen, Denmark

Pancreatic Ductal Adenocarcinoma (PDAC) is among the most aggressive human malignancies, with a 5-year survival rate of 1-4%. Elucidation of specific molecular alterations in PDAC is urgently needed to devise new treatment strategies. Malignant tumors with rapid progression such as that in PDAC often undergo extensive metabolic changes resulting in increased acid production. We and others have shown in other cancers that this leads to the upregulation of acid extruding transporters, which in turn favors further cancer progression. The aim of our studies is to elucidate the regulation and roles of pH regulatory ion transporters in PDAC. We used qPCR to screen a panel of 4 human PDAC cell lines (AsPC-1, BxPC-3, Panc-1, MIAPaCa-2) against a normal human pancreatic ductal cell line (HPDE). Expression of mRNA levels by qRT-PCR showed that Na<sup>+</sup>/H<sup>+</sup> exchangers NHE1, NHE2 and/or NHE8 were overexpressed in 3 of 4 PDAC cell lines studied; the V-type H<sup>+</sup>-ATPase subunit a3 was strongly upregulated in all PDAC cell lines, while subunit b2 was slightly downregulated; all PDAC cell lines except BxPC-3 exhibited upregulation of either AE2 or AE3 Cl<sup>-</sup>/HCO<sub>3</sub><sup>-</sup> exchangers, and also the Na<sup>+</sup>-HCO<sub>3</sub><sup>-</sup> transporters SLC4A7 (NBCn1) and -A5 (NBCe2) were up-regulated in 2 of 4 PDAC lines. Surprisingly, the H<sup>+</sup>/lactate cotransporter MCT1 and MCT4 generally exhibited reduced expression levels in PDAC compared to HPDE. The protein levels of these transporters, as assessed by Western blotting and immunofluorescence analysis, generally corresponded to the mRNA levels. Involvement of the transporters in motility and invasiveness of PDAC cells were investigated by applying specific pharmacological inhibitors using scratch-wound assay and Boyden chamber assay. Interestingly, all PDAC cells exhibited an increase in both motility and invasiveness after being treated with NBC inhibitors, S0859, while PDAC cells treated with NHE inhibitor EIPA and the MCT1 and -2 inhibitor AR-C 155858 generally showed a slight decrease in motility and invasiveness. In conclusion, our results provide preliminary evidence for expression changes and functional implications of multiple pH regulatory transporters in PDAC. Ongoing experiments, including siRNA mediated

knock down and analyses of pH regulatory capacity, will provide further understanding of the roles of these transporters in PDAC.

**P314**  
**Expression and regulation of the NaPi-IIb phosphate transporter in kidney**

\*S. Motta, J. Biber, N. Hernando, C. A. Wagner  
University of Zürich, Physiology, Zürich, Switzerland

The sodium-dependent phosphate cotransporter NaPi-IIb (Slc34a2) is widely expressed. Its mRNA has been detected in intestine, testis, lung, liver, and more recently also in kidney. In mice, intestinal expression of NaPi-IIb is mainly found in the ileum, where it mediates the sodium-driven absorption of phosphate across the brush-border membrane. Mutations in NaPi-IIb in humans can lead to disorders such as pulmonary alveolar microlithiasis, and testicular microlithiasis. In the kidney, the main sodium-phosphate cotransporter is the proximal-tubular NaPi-IIa (Slc34a1), which is responsible for 80% of phosphate reabsorption from the primary urine; also NaPi-IIc (Slc34a3) is expressed in kidney. Intestinal NaPi-IIb is considered one of the players responsible for phosphate homeostasis, however little is known about its role in kidney. The aim of this project is to clarify the expression and the potential regulation of NaPi-IIb in kidney. We analyzed the expression of NaPi-IIb, at mRNA and protein levels, in kidneys of mice, rats, and humans. Wild-type mice and rats, as well as several mice knockout (renal NaPi-IIc inducible knockout mice, and intestinal NaPi-IIb conditional knockout mice) were used. In addition, wild-type mice and rats fed with high and low phosphate diets were investigated. The collected data show a clear NaPi-IIb mRNA expression in kidneys of mice, rats and humans. However, no regulation was seen in knockout mice or in mice treated with different phosphate diets. Although Westernblots failed to detect the presence of the NaPi-IIb protein in mice renal samples, immunofluorescence analysis suggested the expression of the protein in a small subset of tubules. Ongoing studies should clarify the identity of these segments. So far, the expression of the NaPi-IIb protein in rat and human kidneys could not be analyzed due to the absence of specific antibodies. In conclusion, NaPi-IIb mRNA was found in kidneys of the three species investigated, and further studies should clarify its presence at the protein level and function.

**P315**  
**A sticky relationship: The Na<sup>+</sup>/H<sup>+</sup> exchanger NHE1 regulates cell-cell adhesion of melanoma cells**

\*F. T. Ludwig, M. Wälte, F. Frontzek, S. Sargin, H. Schillers, A. Schwab, C. Stock  
University Hospital Münster, Institute of Physiology II, Münster, Germany

Metastasis requires the detachment of tumor cells from the primary tumor caused by loss of cell-cell adhesion as well

as tumor cell migration and invasion promoted by balanced cell-matrix adhesion. The Na<sup>+</sup>/H<sup>+</sup> exchanger NHE1 affects integrin-mediated cell-matrix adhesion via two independent mechanisms: (i) cytoskeletal anchoring and (ii) local pH-regulation. In the present study we tested whether cell-cell adhesions mediated by adherens junction proteins can also be modulated by the presence and/or the activity of NHE1. Experiments were performed on human melanoma cells (MV3) transfected with an empty or an NHE1 expression vector, NHE1-deficient cells and NHE1-deficient cells rescued by NHE1 transfection. The adhesion force between pairs of single cells of the same clone was assessed by employing Atomic Force Microscopy (AFM). The cell-cell adhesion force was high in NHE1-deficient cells and low in NHE1-overexpressing cells. In contrast, pharmacological inhibition of NHE1 function in NHE1-overexpressing cells did not cause an increase in cell-cell adhesion; instead, it decreased the cell-cell adhesion force even further. Thus, in MV3 cells NHE1 expression and ion translocation affect the stability of adherens junctions differently. We conclude that sheer presence of NHE1 promotes metastasis by facilitating the cells' detachment from the primary tumor while its activity supports directional migration and invasion into the extracellular matrix. The mechanism by which the activity of NHE1 affects cell-cell adhesion needs to be elucidated in further experiments.

**P316**  
**pH-dependent endocytosis in tumor cell lines**

\*D. Gündel<sup>1</sup>, M. Allmeroth<sup>2</sup>, R. Zentel<sup>2</sup>, O. Thews<sup>1</sup>  
<sup>1</sup>Martin-Luther-Universität, Julius-Bernstein-Institut, Halle, Germany  
<sup>2</sup>Johannes Gutenberg-University, Institute for Organic Chemistry, Mainz, Germany

Because of an increased glycolytic metabolism in tumors, the extracellular pH is markedly lower (5.5-7.0) than in normal tissues (7.0-7.4). New chemotherapeutic concepts using macromolecular drug carriers rely on the endocytotic uptake of these nanoscaled molecules into the tumor cells. Therefore, the aim of the present study was to analyze, whether the tumor pH might be a critical point for the endocytotic uptake of drugs during cancer therapies. The rat prostate carcinoma cell line Dunning AT-1 and the mammary carcinoma cell line Walker-256 were investigated for endocytotic uptake at different pHs. Cellular uptake of fluorescence labeled 10 kDa dextran, a marker for endocytosis, was compared with the uptake of drug nanocarriers poly-N-(2-Hydroxypropyl)methacrylamides (pHPMAs). Experiments were performed in bicarbonate buffered HEPEs- and MES-Ringer adjusted to the desired pH. To investigate, whether endocytosis depends on intracellular or extracellular acidity a lactate-Ringer in combination with an anion exchange inhibitor (DIDS) was used in order to solely acidify the intracellular compartment. The uptake of dextran as well as of pHPMAs was tumor cell line specific with endocytosis in Walker-256 being 5-times higher than in AT-1 cells (at pH 7.4). In AT-1 cells the cellular binding and the subsequently endocytosis of dextrans seems to be

pH dependent. The endocytosis of pHPMAs additionally depended on their polymer structure. An acidic intracellular pH in Walker-256 cells seems to improve endocytosis of dextran. These results indicate that the endocytosis of tumor cells seems to be pH-dependent and may limit the efficacy of nanoscaled drug carriers in acidotic tumors.

Oxygen metabolism / hypoxia / ROS II

**P317**  
**Advanced ROS/redox imaging based on genetically-encoded probes, ratiometric 2-photon microscopy and fluorescence-lifetime imaging**

\*M. Müller, K. Kizina, G. Bao  
Universitätsmedizin Göttingen, Zentrum Physiologie und Pathophysiologie, Göttingen, Germany

Reactive oxygen species (ROS) contribute to cellular signaling and neuropathology. Accordingly, there is tremendous interest in quantitative recordings of their cellular dynamics. Previously, organic dyes served to rate ROS formation, but they respond irreversibly and report oxidation only. Meanwhile, genetically-engineered optical redox sensors are available, which derive from fluorescent proteins. We characterized HyPer and roGFP1; both are ratiometric by excitation and respond reversibly to redox changes. HyPer is a circularly permuted YFP inserted into a prokaryotic H<sub>2</sub>O<sub>2</sub>-sensitive transcription factor; roGFP1 is a modified GFP with reactive thiols. Lipofected mouse hippocampal cell cultures expressed these sensors cytosolically; nuclear counter-labeling confirmed that only HyPer spared the nucleus. 2-photon excitation spectra show broad absorption for both sensors rather than distinct peaks. Ratiometric 2-photon excitation revealed an increased fluorescence ratio of HyPer [920/760 nm] upon oxidation by H<sub>2</sub>O<sub>2</sub>, but less consistent responses to reduction by DTT. In contrast, the roGFP1 ratio [740/910 nm] increased upon oxidation and decreased upon reduction. Fluorescence-lifetime imaging (time-domain FLIM) of HyPer and roGFP1 yielded monoexponential decays with τ=1.3 ns and τ=2.3 ns, respectively. The fluorescence-lifetime of HyPer was decreased by H<sub>2</sub>O<sub>2</sub>, but failed to respond reliably to DTT. RoGFP1 responded to oxidation and reduction, showing decreased and increased fluorescence-lifetimes, respectively. In conclusion, both sensors are clearly superior to organic ROS-sensitive dyes. They are suited for ratiometric 2-photon imaging and FLIM, the latter of which may facilitate quantitative assays.

This extends the use of both sensors to more complex preparations, paving the way for future analyses in redox-sensor mouse models.

Supported by the Center for Nanoscale Microscopy and Molecular Physiology of the Brain (CNMPB)

**P318**  
**Relation between NO<sub>x</sub> concentration in plasma and red cells during acute hypoxia**

\*M. Maassen<sup>1</sup>, M. Nacke<sup>2</sup>, K. Suetmoeller<sup>2</sup>, H. Starke<sup>2</sup>, D. Tsikas<sup>3</sup>, N. Maassen<sup>2,1</sup>

<sup>1</sup>Leibniz University Hannover, Institute for Sport Science, Hannover, Germany

<sup>2</sup>Medical School Hannover, Institute for Sportmedicine, Hannover, Germany

<sup>3</sup>Medical School Hannover, Institute for Clinical Pharmacology, Hannover, Germany

**Question:** To investigate the relation between NO<sub>x</sub> concentration and oxygen saturation in vivo we performed experiments under acute hypoxia.

**Methods:** 5 subjects served as controls under normoxia. To vary the SO<sub>2</sub> 12 subjects were connected to the "Hypoxicator GO2Altitude®" (BIOMEDTECH, Melbourne, Australia). The relative oxygen concentration in the inspired gas was stepwise reduced from 21% to 9%. In parallel blood samples were taken from a cubital vein. Acid base status was measured by an ABL 520. In plasma and haemolysate [NO<sub>2</sub>] and [NO<sub>3</sub>] were determined by GC-mass-spectroscopy. In the hypoxia trial additionally [Lac] was determined. No prescription related to food intake was given.

**Results:** Normoxia: [NO<sub>2</sub>-] and [NO<sub>3</sub>-] in plasma did not change significantly over time.

**Hypoxia:** In plasma the decrease in [NO<sub>2</sub>-] failed to reach significance (p>0.08) but was significantly correlated to a decrease SO<sub>2</sub> (p<0.008). [NO<sub>3</sub>-] decreased significantly during the experiment (p<0.05). The change in [NO<sub>3</sub>] correlated to SO<sub>2</sub> (p<0.04). [NO<sub>3</sub>-]<sub>kgH<sub>2</sub>O</sub> in red cells did not change during the experiments and was not related to SO<sub>2</sub>. Intracellular [NO<sub>3</sub>-]<sub>kgH<sub>2</sub>O</sub> was significantly lower than in plasma (p<0.002) and lower than expected from the Donnan-equilibrium. Instead, the distribution of NO<sub>2</sub> between the intra- and extracellular space is close to the Donnan-equilibrium. [NO<sub>2</sub>] in red cells increased significantly (p<0.05) with decreasing SO<sub>2</sub>.

**Conclusion:** The results show that NO<sub>2</sub> might be passively distributed between plasma and red cells. The decrease in plasma [NO<sub>3</sub>] might point to an extracellular nitrate-reductase-activity which might be oxygen dependent.

**P319**  
**The tyrosine phosphatase SHP-2 is an important factor for HIF-1α stabilisation and hypoxic angiogenesis**

\*H. Mannell<sup>1</sup>, Y. Stampnik<sup>1</sup>, M. Anton<sup>2</sup>, K. Zimmermann<sup>3</sup>, U. Pohl<sup>1</sup>, F. Krötz<sup>4</sup>

<sup>1</sup>Walter Brendel Centre, Munich, Germany

<sup>2</sup>Institut für Experimentelle Onkologie und Therapieforschung, TU, Munich, Germany

<sup>3</sup>Institut für Pharmakologie und Toxikologie, Bonn University, Bonn, Germany

<sup>4</sup>Invasive Cardiology, Starnberg Clinic, Munich, Germany

**Question:** We previously demonstrated the importance of the tyrosine phosphatase SHP-2 for growth factor dependent angiogenesis. Here we studied whether SHP-2 influences hypoxic angiogenesis and HIF-1α signalling in endothelial cells.

**Methods:** Overexpression of wild type (SHP-2 WT), catalytically inactive (SHP-2 CS) or constitutively active (SHP-2 E76A) SHP-2 in human microvascular endothelial cells (HMEC) was achieved by lentiviral transduction. HIF-1α dependent angiogenesis in vivo was assessed by wound healing in the mice dorsal skin. Vessel sprouting was assessed by the aortic ring assay. Cells and isolated aortae were exposed to hypoxia (95% N<sub>2</sub>, 5% CO<sub>2</sub>). Proliferation was assessed by MTT reduction. HIF-1α protein levels and hydroxylation were detected by western blot. HIF-1α mRNA levels were quantified using real-time PCR.

**Results:** Compared to SHP-2 WT, expression of constitutively active SHP-2 enhanced proliferation by 57±10% (24h, p<0.05, n=8). After hypoxia exposure, vessel sprouting ex vivo (24h, p<0.05, n=5) as well as hypoxia inducible factor 1α (HIF-1α) protein levels (4h, p<0.05, n=4), but not mRNA levels (4h, n=3), were enhanced by 5-fold and 1.3-fold respectively in cells expressing constitutively active SHP-2. Moreover, expression of constitutively active SHP-2 in wounds in vivo increased the rate of vascular wound closure (90±10% closure compared to 65±24% in SHP-2 WT, n=2). In contrast, expression of catalytically inactive SHP-2 impaired hypoxic proliferation by 20±5% (24h, p<0.05, n=8) as well as ex vivo vessel sprouting after hypoxia exposure (24h, p<0.05, n=4) compared to SHP-2 WT. In addition, in cells with non functional SHP-2 hypoxic HIF-1α protein accumulation (4h, p<0.05, n=4) was reduced and an increase in hydroxylated HIF-1α was observed (4h, n=3, p<0.05). However, the reduction in HIF-1α protein was rescued by treatment with proteasomal inhibitors (MG132 or Epoximycin, n=3, 4h).

**Conclusion:** SHP-2 affects angiogenesis during hypoxic conditions, which may partly be due to HIF-1α protein stabilisation. Thus, controlled induction of SHP-2 catalytic activity may be a therapeutic target for angiogenesis induction in ischemic conditions.

**P320**  
**Age-related changes in the mouse brain hippocampus**

G. Reichart<sup>1</sup>, \*J. Mayer<sup>1</sup>, \*T. Tokay<sup>1</sup>, S. Ibrahim<sup>2</sup>, S. Baltrusch<sup>3</sup>, R. Köhling<sup>1</sup>

<sup>1</sup>Rostock University Medical Center, Oscar Langendorff Institute of Physiology, Rostock, Germany

<sup>2</sup>University of Lübeck, Department of Dermatology, Lübeck, Germany

<sup>3</sup>Rostock University Medical Center, Institute of Medical Biochemistry and Molecular Biology, Rostock, Germany

In view of an ageing population, age-related cognitive dysfunctions increasingly are in the focus of research. As the hippocampus plays an important role in the consolidation of information from short-term to long-term memory and spatial navigation we analysed hippocampal learning- and plasticity-related parameters in mice at different age-groups (3, 6, 12 and 24 months). One hypothesis for the mechanism of ageing is based on mitochondrial free radical production. Since it is known that increases in reactive oxygen species (ROS) can lead to tissue dysfunction, we analysed mitochondrial superoxide production. We found that mitochondrial superoxide levels are clearly age-dependent. They reach a maximum in middle-aged mice (6 to 12 months) and stay like this during the following lifetime. Because an increase of ROS can lead to cell death, we furthermore investigated changes in cell numbers and composition. We found that the ratio between neurons and astrocytes also changes age-dependently. To check the physiological impact of these alterations on the cellular level, we analysed synaptic plasticity in vitro using field potential recording of long-term potentiation (LTP) as well as in vivo spatial learning performance in the Morris water maze. Interestingly we could not find age-related changes in LTP of synaptic transmission whereas in vivo learning performance correlates with both superoxide levels and astrocyte-to-neuron ratio during ageing.

**P321**  
**Mononuclear blood cells of professional oxygen-divers show significant less DNA damage after ex-vivo exposure to hyperbaric hyperoxia, this adaptation is reversible**

J. Witte<sup>1</sup>, D. Weyer<sup>2</sup>, W. Kähler<sup>1</sup>, T. Wunderlich<sup>1</sup>, \*A. Koch<sup>1</sup>

<sup>1</sup>German Naval Medical Institute, Maritime Medicine, Kronshagen, Germany

<sup>2</sup>Armed Forces Hospital, Ulm, Germany

**Introduction:** With the Comet Assay an oxygen-dose and exposure-time dependence of DNA damage could be shown for „ex vivo“ hyperoxia exposed cells that have never before been exposed to hyperoxia. Little is known about adaptation to repetitive exposures to hyperoxia in professional oxygen diving.

**Methods:** Freshly isolated PBMCs (peripheral mononuclear blood cells) from active professional oxygen divers (n=18) of the German Navy, with a break in diving activity less than 21 days (n=18), more than 21 days (n=18), and from non-diving controls (n=12) were exposed to hyperbaric hyperoxia of 100% oxygen at a pressure of 4,0 bar in a 96µl Microwellplate at 37-38° Celsius up to 6.5 hours of exposure-time. DNA damages were visualized hourly using the alkaline Comet Assay (single cell gel electrophoresis) and with analysis of the tailmoment and the Yes/No-scor-

ing method out of 200 cells (Comet Assay IV- software). **Results:** PBMCs of active oxygen divers showed significantly less "ex vivo"-inducible DNA-damages compared to the controls in the Yes/No-scoring (significant lower slope in the linear regression analysis, p<0.001). After a break <21 days results were similar to active divers (p<0.001), but not after >21 days break: no longer significant lower slope compared to controls. Tailmoments showed inconclusive results due to huge standard deviations.

**Conclusion:** PBMCs of active oxygen divers adapt to repetitive hyperoxia with lower percentage of damaged cells in the Comet Assay after ex-vivo hyperoxic stress. This adaptation seems to be only temporary.

**P322**  
**Androglobin, the latest addition to the globin family plays a role during spermatogenesis**

S. Santambrogio<sup>1</sup>, A. Fabrizius<sup>2</sup>, A. Bracke<sup>3</sup>, A. Lelli<sup>1</sup>, S. Claus<sup>2</sup>, B. Ebner<sup>2</sup>, F. Germani<sup>3</sup>, L. Moens<sup>3</sup>, S. Dewilde<sup>3</sup>, T. Hankeln<sup>2</sup>, R. Wenger<sup>1</sup>, \*D. Hoo-gewijs<sup>1</sup>

<sup>1</sup>University of Zurich, Institute of Physiology, Zurich, Switzerland

<sup>2</sup>Johannes Gutenberg-University, Institute of Molecular Genetics, Mainz, Germany

<sup>3</sup>University of Antwerp, Department of Biomedical Sciences, Antwerp, Belgium

Hemoglobin and myoglobin represent the two most-established and well-studied heme-containing oxygen binding proteins. The post-genomic era revealed the presence of additional mammalian globin types, including neuroglobin and cytoglobin. We recently reported the identification of a new metazoan globin lineage, consisting of large chimeric proteins with an N-terminal cysteine protease domain and a central globin domain, named androglobins (Adgbs), because of their specific expression in testis tissue in human, mice and zebrafish. Intriguingly, this new member of the globin family is evolutionary ancient and extremely conserved, being present in mammals, vertebrates, more basal animal clades and even unicellular organisms. Hexacoordination of the Adgb heme iron and lack of transcriptional induction in hypoxia suggest a function independent of classical O<sub>2</sub> supply. Adgb expression is associated with postmeiotic stages of spermatogenesis. Furthermore, analysis of a newly generated Adgb knock out mouse model indicates a crucial role in reproduction in line with the observation of higher Adgb expression levels in spermatozoa from fertile vs. infertile males.

**P323**  
**Oxidative energy metabolism during different hippocampal network activity states**

\*J. Schneider<sup>1,2</sup>, N. Berndt<sup>3</sup>, I. Papageorgiou<sup>1,2</sup>, H.- G. Holzhütter<sup>3</sup>, O. Kann<sup>1,2</sup>

<sup>1</sup>Interdisciplinary Center for Neurosciences (IZN), Universität Heidelberg, Heidelberg, Germany

<sup>2</sup>Institute of Physiology and Pathophysiology, Universität Heidelberg, Heidelberg, Germany

<sup>3</sup>Institute of Biochemistry, Charité-Universitätsmedizin Berlin, Berlin, Germany

**Question:** The brain has a high energy expenditure and critically depends on oxidative phosphorylation in mitochondria. However, little is known about energy expenditure at specific activity states in local neuronal networks. We addressed this issue in subfield CA3 of acute slices from the mouse hippocampus under well-defined recording conditions.

**Methods:** We combined recordings of local field potential (LFP) and interstitial partial oxygen pressure (pO<sub>2</sub>) during different specific activity states, namely (i) gamma oscillations (GAM, 30-100 Hz) as induced by cholinergic receptor activation, (ii) recurrent sharp wave-ripple complexes (SPW-Rs), (iii) spontaneous asynchronous network activity (SPON), (iv) isoflurane-induced anesthesia (ISO), and (v) the absence of action potentials. Oxygen consumption rates were estimated by pO<sub>2</sub> depth profiles with high spatial resolution and a mathematical model that considers convective transport, diffusion and activity-dependent consumption of oxygen.

**Results:** (1) The oxygen consumption rate was highest during gamma oscillations by a factor of 2.14 on average. (2) Oxygen consumption rates during sharp wave-ripple complexes, spontaneous asynchronous network activity and anesthesia did not significantly differ. (3) For gamma oscillations and sharp wave-ripple complexes, there was a positive correlation between oxygen consumption rates and the oscillation amplitude in the local field potential. (4) Overall, oxygen consumption rates showed a positive correlation to action potential generation during the different activity states.

**Conclusions:** We conclude that in local hippocampal networks the oxygen consumption rate may vary by a factor of two during specific activity states and anesthesia, which depends on the degree of both postsynaptic potentials and action potentials.

### P324

#### Effects of acute and chronic oxidative stress on mitochondrial function and energy metabolism

\*A. Pfeiffer<sup>1</sup>, M. Jaeckel<sup>2</sup>, J. Lewerenz<sup>3</sup>, R. Noack<sup>1</sup>, A. Pouya<sup>1</sup>, T. Schacht<sup>1</sup>, C. Hoffmann<sup>1</sup>, J. Winter<sup>4</sup>, S. Schweiger<sup>4,5</sup>, M. K. E. Schäfer<sup>2,5</sup>, A. Methner<sup>1,5</sup>

<sup>1</sup>University Medical Center of the Johannes Gutenberg-University, Neurology, Mainz, Germany

<sup>2</sup>University Medical Center of the Johannes Gutenberg-University, Anesthesiology, Mainz, Germany

<sup>3</sup>University of Ulm, Neurology, Ulm, Germany

<sup>4</sup>University Medical Center of the Johannes Gutenberg-University, Inst. of Human Genetics, Mainz, Germany

<sup>5</sup>Focus Program Translational Neuroscience (FTN) of the Johannes Gutenberg-University, Mainz, Germany

Mitochondria, the powerhouses of the cell, are influenced by oxidative stress. An excellent model system for studying oxidative stress is the hippocampal cell line HT22 missing ionotropic glutamate receptors. In these cells, extracellular glutamate blocks the glutamate/cystine antiporter system x<sub>c</sub><sup>-</sup> resulting in cellular glutathione depletion causing an increase in reactive oxygen species and mitochondrial dysfunction leading to cell death. We analyzed the effects of acute and chronic oxidative stress on mitochondrial function and energy metabolism by studying the mitochondrial shape and respiration in glutamate-resistant and -sensitive cells. Mitochondria of the glutamate-resistant HT22R cells displayed a less fragmented morphology, while acute oxidative stress induced no changes in mitochondrial morphology of the glutamate-sensitive parental HT22S cell line. High-resolution respirometry suggested a reduction in mitochondrial respiration in HT22R and an increase in glutamate-sensitive HT22S cells after induction of oxidative stress. In comparison to a reduced respiration of glutamate-resistant cells, mitochondrial calcium and mitochondrial superoxide production was enhanced and the oxidative phosphorylation capacity was increased in HT22R cells. A resistance to the ATP synthase-inhibitor oligomycin, a sensitivity to the glycolysis-inhibitor deoxyglucose, a strong increase in cytosolic hexokinase 1 and 2, a reduced lactate production as well as an enhanced activity of glucose-6-phosphate dehydrogenase suggest that glutamate-resistant HT22R cells metabolize most available glucose in the pentose phosphate pathway to increase glutathione recovery. These results imply that metabolic and mitochondrial adaptations play an important role in resistance against chronic oxidative stress and mitochondrial function is influenced by acute oxidative stress.

### P325

#### Modification of the assembly process of hypoxia inducible factors

\*I. Pisarenko, A. Bernardini, T. Otto, J. Hu, J. Fandrey  
Institute of Physiology, Essen, Germany

**Question:** Hypoxia-inducible transcription factor (HIF) complexes regulate expression of genes responsible for cellular adaptation to hypoxia, e. g. endothelial growth factor (VEGF), erythropoietin and glucose transporter [1]. HIFs are heterodimers and consist of a labile, O<sub>2</sub>-sensitive- $\alpha$ -subunit and a stable  $\beta$ -subunit. Both subunits belong to the family of basic helix-loop-helix proteins containing a Per-ARNT-Sim domain. 3 HIF- $\alpha$  isoforms have been identified in humans: HIF-1 $\alpha$ , HIF-2 $\alpha$ , and HIF-3 $\alpha$  [2]. The interdependencies between different HIF subunits forming either functional or nonfunctional homo- or heterodimers are not yet fully understood. Therefore this research project will focus on the assembly mechanisms of HIF complexes.

**Methods:** To analyze molecular interactions of HIF subunits, Fluorescence Resonance Energy Transfer (FRET) microscopy is applied. For that purpose plasmid DNA encoding different HIF subunits fused to either enhanced cyan fluorescent protein (ECFP) or enhanced yellow fluorescent

protein (EYFP) should be transfected into human tumor cells, e. g. osteosarcoma cells (U2OS). 24 h after transfection FRET microscopy is applied.

**Results:** Random FRET signal was detected in osteosarcoma cells (U2OS) transfected with plasmids that express the fluorophores ECFP and EYFP only. Further experiments will be done in short to determine the interactions between different protein subunits.

**Conclusions:** The confocal microscopy system for FRET was successfully tested on different plasmid constructs earlier and should provide reliable results for the examination of the assembly process of different HIF subunits.

[1] Déry M-A. C et al., 2005; The International Journal of Biochemistry & Cell Biology 37: 535-540.

[2] Fandrey J et al., 2006; Cardiovascular Research 71: 642-651.

### P326

#### Analysis of 5' regulatory sequences of the human NADPH oxidase 4 gene in endothelial cells

\*F. Engelmann, C. Brunssen, M. Brux, H. Morawietz

University Hospital Carl Gustav Carus, Division of Vascular Endothelium and Microcirculation, Dresden, Germany

**Question:** The role of different NADPH oxidase (NOX) isoforms in cardiovascular physiology and pathophysiology is highly controversial. While the increased formation of superoxide anions by NOX enzymes is considered to be deleterious in the cardiovascular system, recent evidence support a vasoprotective role of the mainly H<sub>2</sub>O<sub>2</sub> producing isoform NOX4. Especially, regulation of NOX4 and formation of reactive oxygen species is involved in NO release. Previously we could show, that NOX4 is the major endothelial NOX isoform and constitutively active. In addition, we could show regulation of human NOX4 promoter via an antioxidative response element (ARE)-like/Oct-1 binding site. Besides these findings, the molecular mechanisms controlling the high and constitutive basal expression of NOX4 remain largely unknown so far. Therefore, we performed deletion analysis of 5' regulatory sequences of the human NOX4 gene using Dual-Luciferase Reporter Assay System in human endothelial and embryonic kidney cells.

**Methods & Results:** For functional analysis of 5' regulatory sequences of the human NOX4 promoter, a 1494 bp fragment upstream of human NOX4 translation start point was cloned. This fragment includes 1255 bp of putative NOX4 promoter and 239 bp of first exon until ATG (-1255/+239, ATG = position 239). This fragment was linked to reporter gene firefly luciferase (pGL4.10[luc2] reporter vector) and different deletion constructs of this NOX4 promoter fragment were generated. Human endothelial (HMEC-1) and human embryonic kidney cells (HEK 293T) were transfected and promoter activity was measured by Dual-Luciferase Reporter Assay System. Thereby, constitutive active co-reporter pGL4.74[hRluc/TK] was used for normalisation of transfection efficiency. -1255/+239 NOX4 promoter construct showed high basal activity compared to empty pGL4.10[luc2] reporter vector in both cell types (HMEC-

1 = 4,5±0,6; HEK 293T = 9,7±1,3). No changes for basal activity were determined for various deletion constructs within the range between -1255/+239 and +1/+239. A decreased basal activity was measured for +119/+239 NOX4 promoter construct. This indicates binding sites for transcriptional activators in between the range of +1/+239 and +119/+239. Further deletion of NOX4 promoter fragment leading to complete loss of basal activity in both cell types (+234/+239 NOX4 promoter construct), indicating additional binding sites for transcriptional activators within this range. In silico analysis by MatInspector software tool supporting putative binding sites of transcriptional activators within the given ranges of the NOX4 promoter fragment.

**Conclusions:** Our data suggest, that binding sites of transcriptional activators controlling basal NOX4 transcriptional activity are located in the 239 bp downstream of the transcription start site of the human NOX4 gene.

### P327

#### The serum and glucocorticoid inducible kinase-1 is a pleiotropic regulator of hypoxia-inducible factor-1 $\alpha$ in the hypoxic vascular response

A. Petry<sup>1</sup>, I. Diebold<sup>1</sup>, S. Belaiba<sup>1</sup>, D. Kracun<sup>1</sup>, F. Lang<sup>2</sup>, \*A. Görlach<sup>1</sup>

<sup>1</sup>German Heart Center Munich at the TU Munich, Experimental and Molecular Pediatric Cardiology, München, Germany

<sup>2</sup>University Tübingen, Institute for Physiology, Tübingen, Germany

Hypoxic stress is essentially involved in the pathogenesis of many disorders including cardiovascular and pulmonary disease. A key regulator of the cellular response to hypoxia is hypoxia-inducible factor-1 (HIF1). The serum- and glucocorticoid-inducible kinase-1 (Sgk1) confers cell survival under various triggers of cell stress. Nothing is known, however, about the interaction of Sgk1 and HIF1. We hypothesized that Sgk1 plays a role in the vascular response to hypoxia by controlling HIF1. Hypoxia increased expression and activity of Sgk1 in pulmonary vascular cells, and forced expression of Sgk1 enhanced HIF1 $\alpha$  levels. Conversely, expression of kinase-deficient Sgk1 diminished hypoxic HIF1 activity and HIF1 $\alpha$  expression. Similarly, hypoxic HIF1 $\alpha$  induction was blunted in cells and tissues derived from sgk1<sup>-/-</sup> mice. Detailed analysis revealed several pathways orchestrated by Sgk1 to induce HIF1 $\alpha$ : Sgk1 directly interacted with pVHL to diminish HIF1 $\alpha$  degradation. Sgk1 interacted also with GSK3 $\beta$  to prevent HIF1 $\alpha$  degradation by the ubiquitin ligase Fbw7. Sgk1 interacted with HDM2 to repress p53 while promoting HIF1 $\alpha$  levels. Sgk1 activated the NF $\kappa$ B pathway to enhance HIF1 $\alpha$  transcription. Functional studies demonstrated a requirement of Sgk1 for vascular proliferation and vessel sprouting. Importantly, sgk1<sup>-/-</sup> mice were protected against the development of hypoxia-induced pulmonary vascular remodeling. In summary, Sgk1 is a novel oxygen-sensitive kinase which controls HIF1 $\alpha$  and the HIF pathway by orchestrating major cellular pathways to promote vascular adaptation to hypoxia. Targeting Sgk1 may thus be a novel therapeutic option for hypoxia-associated diseases such as pulmonary vascular remodeling.

P328

**Hypoxia-induced carbonic anhydrase IX enhances lactate transport in human breast cancer cells by a non-catalytic mechanism**

\*S. Jamali<sup>1</sup>, M. Klier<sup>1,2</sup>, B. Wardas<sup>1</sup>, R. McKenna<sup>1,3</sup>, J. W. Deitmer<sup>2</sup>, H. M. Becker<sup>1</sup>

<sup>1</sup>Technical University of Kaiserslautern, Division of Zoology / Membrane Transport, FB Biology, Kaiserslautern, Germany

<sup>2</sup>Technical University of Kaiserslautern, Division of General Zoology, FB Biology, Kaiserslautern, Germany

<sup>3</sup>University of Florida, Biochemistry and Molecular Biology, Gainesville, United States

Local hypoxia, which arises from elevated respiration and/or inadequate blood supply is a hallmark of most solid tumors and is associated with poor prognosis. Hypoxia affects many important processes in tumor metabolism and promotes malignant progression by alteration of glycolysis, followed by increased acid extrusion. We examined the effect of hypoxia on lactate flux and intracellular pH regulation, using MCF-7 cells as a model system. Cells were cultivated under normoxic (21% O<sub>2</sub>) or hypoxic (1% O<sub>2</sub>) conditions for 1-3 days. Expression levels of proteins involved in metabolite transport and acid/base regulation were measured by quantitative real-time PCR and Western blot analysis. Monocarboxylate transporter (MCT)-mediated changes in intracellular H<sup>+</sup> concentration were measured with H<sup>+</sup>-sensitive dyes. Hypoxia resulted in a robust increase in the expression level of the cancer-specific carbonic anhydrase CAIX, while leading to only moderate changes in the expression of MCT1 and MCT4. Nevertheless, hypoxia caused a significant increase in MCT-mediated H<sup>+</sup> flux, both in the presence and absence of CO<sub>2</sub>/HCO<sub>3</sub><sup>-</sup>. The increase in MCT activity was insensitive to inhibition of CA catalytic activity with ethoxzolamide (EZA). However, knock-down of CAIX with siRNA abolished the hypoxia-induced increase in MCT activity. These results indicate that hypoxia-induced CAIX may enhance transport activity of MCT by a non-catalytic mechanism. To analyze the mechanism further, we heterologously co-expressed CAIX with MCT1 and MCT4 in *Xenopus* oocytes. Coexpression of MCT1/4 with CAIX resulted in a twofold increase in MCT transport activity, as measured by the rate of change in [H<sup>+</sup>]<sub>i</sub> in oocytes during application of lactate. The CAIX-mediated increase in transport activity persisted in the absence of CO<sub>2</sub>/HCO<sub>3</sub><sup>-</sup> and was insensitive to inhibition of CA with EZA. However, mutation of the intramolecular H<sup>+</sup> shuttle in CAIX, H200, abolished the functional interaction between MCT1/4 and CAIX. The mechanism appears to resemble the interaction between MCT1/4 and CAII/CAIV, which may operate as proton-collecting antennae for the transporters (Becker et al., 2011, Proc. Natl. Acad. Sci.; Klier et al., J. Biol. Chem., in press). Our results indicate that CAIX, the expression of which is a hallmark in many cancer cells, especially under hypoxic conditions, can enhance lactate transport across the cell membrane by a non-catalytic mechanism, possibly by operating as an extracellular proton-collecting/distributing antenna for MCT1/4.

P329

**Phosphatase and tensin homolog up-regulates the gene expression of hypoxia-inducible factor-2α in glioblastoma cells**

\*W. Sun, W. Jelkmann, R. Depping

University of Lübeck, Institute of Physiology, Lübeck, Germany

Glioblastoma is the most common and most aggressive primary brain tumor in adults. Advanced glioblastomas mostly contain hypoxic areas due to the rapid cell proliferation and inadequate vascularisation. Hypoxia-inducible factor (HIF) is a dimeric transcription factor which mediates the primary cellular responses to hypoxia. HIF consists of an oxygen-labile α-subunit (HIF-1α, -2α) and a stable β-subunit (ARNT). Although HIF-1α and HIF-2α share several redundant functions, they also exhibit unique activities by regulating unique target genes. Phosphatase and tensin homolog (PTEN) is a phosphatase which preferentially dephosphorylates phosphoinositide substrates. Mutations and deletions of PTEN gene were frequently observed in glioblastomas. PTEN was discussed to suppress glioblastoma growth by inhibiting the proliferation of glioblastoma cells. Activation of PTEN pathway has represented a therapeutic option for glioblastomas. In this study, we found that in the PTEN-deficient glioblastoma cells, overexpression of PTEN caused a significant increase of HIF-2α mRNA. The gene expression of glucose transporter 1 (GLUT1) and amphiregulin (AREG) was up-regulated in the cells overexpressed with PTEN. Our findings suggest a biphasic role of PTEN in regulating the progression of glioblastomas. The mechanisms and the clinical implications of this biology need to be further studied.

P330

**Mitochondrial respiration in different neuronal cell lines and murine cortical neurons under hypoxia**

\*M. Jaeckel<sup>1</sup>, A. Pfeiffer<sup>2</sup>, C. Stihl<sup>1</sup>, A. Methner<sup>2</sup>, M. K. E. Schäfer<sup>1</sup>

<sup>1</sup>Universitätsmedizin Mainz, Anesthesiology, Mainz, Germany

<sup>2</sup>Universitätsmedizin Mainz, Neurology, Mainz, Germany

Hypoxia is a critical event to neurons following stroke or cardiac arrest and often leads to severe disability or death. Mitochondrial dysfunction has been proposed to play a pivotal role in hypoxia-dependent loss of neuronal tissue. Although neuronal cell lines and primary neuronal cultures have been widely used to elucidate molecular mechanisms underlying hypoxia-induced cell death, the differences and commonalities of mitochondrial respiration and energy metabolism in commonly used neuronal cell lines and primary neuronal cultures are unknown. We here investigated mitochondrial respiration by high resolution respirometry (Oxygraph-2k, Oroboros Instruments, Austria), determination of lactate dehydrogenase (LDH) levels and expression profiling of several molecular markers in the murine derived neuronal cell lines NSC34, N2A, HT22S (sensitive to oxidative stress) and HT22R (resistant to oxidative stress) as well as in primary cortical neurons under normoxic and hypoxic (1 % oxygen) conditions. Our results show substantial dif-

ferences in the oxygen consumption rate (OCR) related to the oxidative phosphorylation system in different cell types. The OCR varied under basal conditions as well as in different metabolic states induced by defined substrate control and use of inhibitory drugs. Hypoxia experiments revealed a different susceptibility towards hypoxic conditions in different cell-types in relation to their oxidative phosphorylation system. These findings confirm the diversity and complexity of cell respiration in different neuronal cell lines and primary cortical neurons under normoxic and hypoxic conditions. Elucidating the mechanistic commonalities and differences may help to gain further understanding of hypoxia-dependent neuronal tissue loss.

**Gastrointestinal functions and endocrine systems**

P331

**Vitamin D-role in endometriosis**

\*R. Vatakencherry<sup>1</sup>, S. L<sup>1</sup>, R. K<sup>2</sup>, S. Krishnan<sup>3</sup>

<sup>1</sup>Amrita Institute of Medical Sciences, Physiology, Kochi, India

<sup>2</sup>Amrita Institute of Medical Sciences, Gynaecology, Kochi, India

<sup>3</sup>Amrita Institute of Medical Sciences, Biochemistry, Kochi, India

**Background:** Endometriosis is a gynaecological condition in which cells in the endometrium appear and flourish outside the cavity of uterus, mostly on the ovaries. Since Vitamin D is an immunomodulator, it may have a role in the pathogenesis of endometriosis.

**Objective:** To study the role of vitamin D as a risk factor for endometriosis. **Materials and methods:** Sixty women with endometriosis and sixty women without endometriosis (age group-20 to 40 years) attending Gynaecology Out patient department of Amrita Institute of Medical Sciences; Kochi from October 2012 to March 2013 were enrolled in the case control study. Serum levels of 25 Hydroxy Vitamin D were assessed.

**Results:** Sixty women with endometriosis and sixty women without endometriosis were recruited. Mean(±S.D)levels of 25 Hydroxy Vitamin D in women with and without endometriosis were 9.1±3.97ng/ml and 20.51±6.59ng /ml respectively (p value=<0.001).Statistically significant lower levels of Vitamin D was observed in women with endometriosis.

**Conclusion:** Women with endometriosis are found to have lower levels of Vitamin D when compared to women without endometriosis.

P332

**Thyroid autoimmunity in endometriosis**

\*R. Vatakencherry<sup>1</sup>, S. L<sup>1</sup>, R. K<sup>2</sup>, S. Krishnan<sup>3</sup>

<sup>1</sup>Amrita Institute of Medical Sciences, Physiology, Kochi, India

<sup>2</sup>Amrita Institute of Medical Sciences, Gynaecology, Kochi, India

<sup>3</sup>Amrita Institute of Medical Sciences, Biochemistry, Kochi, India

**Background:** Endometriosis is a gynaecological condition in which cells in the endometrium appear and flourish outside the cavity of uterus, mostly on the ovaries. Endometriosis shows elevated levels of cytokines, decreased apoptosis and cell mediated abnormalities. Women with endometriosis may have higher rates of autoimmune disorders including hypothyroidism. Objective: To compare the prevalence of hypothyroidism and autoimmune thyroid disease(AITD) between married women with endometriosis and married women without endometriosis.

**Materials and Methods:** One hundred and fifty married women (age group-20-40 years) with endometriosis (study group) and one hundred and fifty married women (age group-20-40 years) without endometriosis (control group) attending Gynaecology Out patient department of Amrita Institute of Medical Sciences; Kochi; Kerala; South India from October 2012 to August 2013 were enrolled in the cross-sectional study. Serum levels of thyroid stimulating hormone(TSH), free thyroxine (T4) were evaluated. Sixty married women was randomly selected from both study and control group and anti-thyroperoxidase (anti-TPO) antibody titre was evaluated. Statistical Analysis: Statistical Analysis was done using IBM SPSS Statistics 20.0. Pearson's chi-square test was applied to test the relationship between two categorical variables. P-value of <0.05 were considered as statistically significant.

**Results:** Prevalence of hypothyroidism in married women with and without endometriosis were 66.67%(100) and 20%(30) respectively. Among sixty women with endometriosis, 78.33%(47) were hypothyroid and high anti-TPO titre was found in 97.9%(46) of hypothyroid women with endometriosis. Among sixty women without endometriosis, 13.3%(8) were hypothyroid and high anti-TPO titre was found in 12.5%(1) of hypothyroid women without endometriosis. (pvalue=<0.001).

**Conclusion:** Prevalence of hypothyroidism and autoimmune thyroid disease[AITD] was high in endometriosis when compared to control group. Screening for thyroid diseases in endometriosis is indicated.

P333

**Anoctamins form the intestinal secretory Ca<sup>2+</sup> dependent Cl<sup>-</sup> channel**

\*D. Faria<sup>1</sup>, B. Skryabin<sup>2</sup>, J. Rock<sup>3</sup>, K. Kunzelmann<sup>1</sup>, R. Schreiber<sup>1</sup>

<sup>1</sup>University of Regensburg, Regensburg, Germany

<sup>2</sup>University of Münster, Münster, Germany

<sup>3</sup>University of San Francisco, San Francisco, United States

Electrolyte secretion in the intestine requires Cl<sup>-</sup> channels in the apical membrane of epithelial cells. Electrolyte secretion is controlled by a number of hormones leading to



increase in either intracellular cAMP or Ca<sup>2+</sup>, with consecutive activation of cystic fibrosis transmembrane conductance regulator (CFTR) or Ca<sup>2+</sup> activated Cl<sup>-</sup> channels (CaCC). While the contribution of CFTR to intestinal Cl<sup>-</sup> secretion is well defined, controversial results have been reported for CaCC, which, however, has now been identified as anoctamin 1 (TMEM16A; Ano1). We earlier reported that neonatal mice lacking expression of Ano1 do not show Ca<sup>2+</sup> dependent Cl<sup>-</sup> secretion in airways, salivary glands, and distal colon. We also provided evidence for a role of Ano1 in secretory diarrhea induced by the rotavirus toxin NSP4. However, Ano1 null mice are severely ill and die within 3 days after birth. In the present report we examined the effects of tissue specific knockouts of Ano1 and Ano10 in intestinal epithelial cells, and assessed the effects of a conventional Ano6 knockout on mouse intestinal Ca<sup>2+</sup>-dependent Cl<sup>-</sup> secretion. The results establish a clear role of Ano1 for Ca<sup>2+</sup> dependent Cl<sup>-</sup> secretion in mouse large intestine, while Ano10 appears to be in charge of Ca<sup>2+</sup> dependent Cl<sup>-</sup> secretion in the small intestine.

**P334**  
**Modulation of beta-cell function and glucose homeostasis by the bile acid farnesoid X receptor (FXR)**

\*B. Schittenhelm<sup>1</sup>, M. Düfer<sup>2</sup>, V. Kähny<sup>1</sup>, R. Wagner<sup>1</sup>, P. Krippeit-Drews<sup>1</sup>, G. Drews<sup>1</sup>

<sup>1</sup>Institute of Pharmacy, University of Tübingen, Department of Pharmacology, Toxicology and Clinical Pharmacy, Tübingen, Germany

<sup>2</sup>Institute of Pharmaceutical and Medical Chemistry, University of Münster, Department of Pharmacology, Münster, Germany

**Question:** Development of type-2 diabetes mellitus coincides with alterations in the size and composition of the bile acid (BA) pool. We used in vitro and in vivo (gluco)lipotoxicity (GLT) models to investigate how addition of chenodeoxycholic acid (CDC) affects glucose homeostasis.

**Methods:** Wild type (WT) and FXR-knockout (FXR-KO) islets were exposed to GLT medium (25mM glucose, 100µM palmitate, n=4). Insulin release and content was quantified by radioimmunoassay. High fat diet (HFD) was applied for 12 weeks (n=7-10). Insulin sensitivity and glucose tolerance were determined after i.p. insulin and glucose injection. Morphometric analysis was carried out on slices of paraffin-embedded pancreatic tissue by immunostaining of insulin and glucagon (n=3).

**Results:** In contrast to islets of FXR-KO mice, GLT medium (24 h) significantly lowered insulin content of WT islets. Addition of CDC (48 h) restored insulin content in WT islets kept in GLT medium and led to improved glucose-stimulated insulin secretion. In vivo CDC supplementation protected against HFD-induced impairment of fasting glucose concentration and glucose tolerance in WT mice and additionally improved these parameters in FXR-KO mice. These effects were not due to differences in body weight or insulin resistance. Histologically, beta-cell size did not differ between FXR-KO and WT under HFD but the num-

ber of beta-cells was augmented compared to control diet, indicating a compensatory hyperplasia. Interestingly, CDC supplementation prevented this hyperplasia.

**Conclusion:** Under GLT conditions -opposed to normal nutrient intake- lack of FXR ameliorates glucose homeostasis. Moreover, CDC exerts beneficial effects on glucose tolerance beyond FXR activation.

**P335**  
**Loss of carbonic anhydrase IX expression impairs gastric mucosal defence against luminal acid**

\*T. Li<sup>1</sup>, X. Liu<sup>1</sup>, A. Singh<sup>1</sup>, B. Riederer<sup>1</sup>, B. Tuo<sup>2</sup>, G. Gros<sup>3</sup>, H. Bartels<sup>4</sup>, U. Seidler<sup>1</sup>

<sup>1</sup>Hannover Medical School, Gastroenterology, Hannover, Germany

<sup>2</sup>ZunYi Medical College, Gastroenterology, ZunYi, China

<sup>3</sup>Hannover Medical School, Physiology, Hannover, Germany

<sup>4</sup>Hannover Medical School, Anatomy, Hannover, Germany

**Question:** The exoenzyme carbonic anhydrase IX is strongly expressed in tumours. In normal tissues, CA IX is expressed during embryogenesis but downregulated postnatally, except in the stomach. So the physiological function of CAIX in the stomach is need to be elucidated.

**Methods:** We studied the cellular differentiation pattern and acid secretory capacity in gastric mucosa from CAIX KO and WT mice at age 8 days to 1,3,6,9,12 months. Surface pH and mucus layer thickness, as well as the ability of the surface epithelial cells to withstand a luminal acid load was assessed in young adult CAIX KO and WT mice by in vivo two photon microscopy.

**Results:** CAIX KO gastric mucosa developed a unique phenotype with a gradual expansion of the surface cell zone, and regression of the parietal cell zone to the lower gland area. Concomitantly, the acid secretory capacity, which was normal at young age, declined. HCO<sub>3</sub><sup>-</sup> output into the lumen and mucus layer thickness were not significantly different between CAIX KO and WT. However, the ability of the surface cells to withstand a luminal acid load, as well as to maintain a more alkaline surface pH than the luminal pH, was significantly impaired in CAIX KO compared to WT stomach.

**Conclusions:** We speculate that the CAIX at the basolateral membrane of the gastric surface cells rapidly converts extruded protons with blood-borne HCO<sub>3</sub><sup>-</sup> to CO<sub>2</sub> and thus augments interstitial buffer capacity, surface cell pH regulation, and maintenance of the pH microclimate in the mucus layer.

**P336**  
**Niclosamide regulates the Caco-2 intestinal epithelial tight junction barrier**

\*M. R. Lornejad-Schäfer, J. Weidinger, C. Schäfer  
BioMed-zet Life Science GmbH, Linz, Austria

**Question:** Colorectal cancer is the leading cause of cancer death worldwide. Niclosamide is an anthelmintic drug

approved for human use that has recently been found to be active against colon cancer spreading, because it inhibits the S100 calcium binding protein A4 (S100A4) which is involved to the formation of cancer metastasis (Helfman et al. 2011). How niclosamide influences the human intestinal epithelium may be important for the bioavailability of co-administered or following substances (drugs, nutrients). Therefore, our aim was to investigate the side effect of niclosamide on the tight junction protein complex in the differentiated Caco-2 barrier model.

**Methods:** Caco-2 cells were differentiated for 21 days, followed by 10 µM niclosamide treatment for 3h, 6h and 24 h. The rate of cell cytotoxicity of niclosamide was determined using LDH assay. The cell transepithelial electrical resistance (TER) was measured using impedance (Z) measurement. Membrane permeability was tested by selective transport of small Fluorescein thiocarbonyl (FITC)-dextran (3-5 kDa). The expression of ZO-1 and Occludin were investigated by western blotting and the localization and distribution of ZO-1 was tested by immunofluorescence. **Results and Discussion:** 10 µM Niclosamide increased the membrane permeability of small molecules (3-5 kDa FITC-Dextran) time-dependently (3h, 6h, and 24h). The membrane integrity (TER value) decreased after 6h and 24h incubation time, but not after 3h. Furthermore, 10 µM niclosamide increased the protein expression of Occludin in a time-dependent manner. However, the expression of ZO-1 was upregulated only after short incubation time (3h) and downregulated after long incubation time (6h, and 24h). In summary, we have shown that niclosamide affected the tight junction protein complex members, ZO-1 and Occludin, which are required for the maintenance of membrane integrity and the regulation of the selective intestinal epithelial barrier through the paracellular transport pathway.

**Conclusion:** Altogether, niclosamide can change the intestinal barrier properties and may increase the bioavailability of co-administered or following substances. Therefore, the understanding of niclosamide effects on the intestinal barrier can help to find the appropriate dose for therapeutic applications against colon cancer.

Keywords: niclosamide, colon cancer, tight junction, barrier model, membrane integrity, paracellular transport pathway

Ref. David M. Helfman. Niclosamide: An Established Anthelmintic Drug as a Potential Therapy Against S100A4-Mediated Metastatic Colon Tumors. Advance Access publication on June 17, 2011

**P337**  
**Membrane androgen receptor activation inhibits the tumorigenic gene products c-Src, β-catenin and GSK-3β in colon tumor cells**

\*S. Honisch<sup>1</sup>, S. Gu<sup>1</sup>, M. Kounenidakis<sup>2</sup>, S. Alkahtani<sup>2,3</sup>, S. Alarifi<sup>2,3</sup>, K. Alevizopoulos<sup>2</sup>, F. Lang<sup>1</sup>, C. Stournaras<sup>1,2</sup>

<sup>1</sup>University of Tuebingen, Department of Physiology, Tübingen, Germany

<sup>2</sup>University of Crete Medical School, Department of Biochemistry, Heraklion, Greece

<sup>3</sup>King-Saud-University, Department of Zoology, Science College, Riyadh, Saudi Arabia

**Question:** Functional membrane androgen receptors (mARs) have been recently described in colon tumor cells and tissues. Their activation by specific testosterone conjugates (TAC) down-regulates PI-3K/Akt pro-survival signaling and triggers apoptosis both, in vitro and in vivo. The present study explored the regulation of gene products implicated in the tumorigenic activity of Caco2 colon cancer cells. **Methods:** RT-PCR was employed to determine transcript levels, Western blotting to quantify protein expression and phosphorylation, and confocal laser scanning microscopic analysis to localize proteins. **Results:** mAR activation significantly decreased Tyr-416 phosphorylation of c-Src, an effect evident 30 min upon testosterone treatment and persisting for at least 12 hours. In line with the reported down-regulation of the PI-3K/Akt pathway in testosterone-treated colon tumors, GSK3-β was phosphorylated after long term stimulation of the cells with TAC. mAR decreased β-catenin transcripts, implying the involvement of this proto-oncogene in mAR-induced pro-apoptotic signaling. β-catenin colocalized with actin cytoskeleton in testosterone-treated Caco2 cells and may thus participate in the reported modulation of cytoskeletal dynamics in mAR-stimulated Caco2 cells. **Conclusions:** mAR activation triggers the tumorigenic gene products c-Src, GSK3-β and β-catenin, thus facilitating the pro-apoptotic response in colon tumors.

**P338**  
**Cushing's syndrome: Development of highly potent and selective steroid 11β-hydroxylase inhibitors of the (Pyridylmethyl)pyridine type**

J. Emmerich<sup>1</sup>, Q. Hu<sup>1</sup>, \*N. Hanke<sup>2</sup>, R. W. Hartmann<sup>1</sup>

<sup>1</sup>Pharmaceutical and Medicinal Chemistry, Saarland University and Helmholtz Institute for Pharmaceutical Research Saarland (HIPS), Saarbrücken, Germany

<sup>2</sup>ElexoPharm GmbH, Preclinical Drug Development, Saarbrücken, Germany

Potent and selective steroid 11β-hydroxylase (CYP11B1) inhibitors could be promising therapeutics for the treatment of Cushing's syndrome. Optimization of compound 1 (5-((1H-imidazol-1-yl)methyl)-2-phenylpyridine) led to compound 44 (5-((5-methylpyridin-3-yl)methyl)-2-phenylpyridine) with a 50-fold improved IC<sub>50</sub> value of 2 nM toward human CYP11B1 and an enhanced inhibition of the rat enzyme (rCYP11B1 IC<sub>50</sub> = 2440 nM) compared to compound 1 (rCYP11B1 IC<sub>50</sub> > 10000 nM). Furthermore, selectivities over human aldosterone synthase (CYP11B2), 17α-hydroxylase (CYP17) and aromatase (CYP19) were observed, as well as satisfying metabolic stability not only in human and rat plasma, but also with liver S9 fraction of these two species. Investigation of cytotoxicity in HEK293 cells and inhibition of hepatic cytochrome P450 metabolic enzymes

CYP2A6 and CYP3A4 showed that compound 44 fulfills first safety criteria and can be considered for further in vivo evaluation in rats.

**P339**

**Carbonic anhydrase II is an essential, external CO<sub>2</sub>-independent, component of the gastric acid secretory machinery in mice**

\*T. Li<sup>1</sup>, X. Liu<sup>1</sup>, B. Riederer<sup>1</sup>, B. Tuo<sup>2</sup>, K. Herzig<sup>3</sup>, G. Gros<sup>4</sup>, H. Bartels<sup>5</sup>, U. Seidler<sup>1</sup>

<sup>1</sup>Hannover Medical School, Hannover, Germany

<sup>2</sup>ZunYi Medical College, Gastroenterology, Zunyi, China

<sup>3</sup>Oulu University, Department of Physiology and Biocenter of Oulu, Oulu, Finland

<sup>4</sup>Hannover Medical School, Physiology, Hannover, Germany

<sup>5</sup>Hannover Medical School, Anatomy, Hannover, Germany

**Question:** An acid inhibitory effect of carbonic anhydrase (CA) inhibitors is known, but the molecular mechanisms have been controversially discussed. The gastrointestinal tract expresses a large number of CAs. We therefore sought to establish the specific isoform (if any), and to get insight into the molecular action of gastric carbonic anhydrases by studying available knockout mice of the stomach-expressed CAs.

**Methods and Results:** The isolated gastric mucosa of CA II-deficient and WT mice from newborn to adult age were mounted in Ussing chambers and basal, as well as agonist-induced acid secretory rates were measured, in the presence and absence of CO<sub>2</sub>/HCO<sub>3</sub><sup>-</sup>, and the presence and absence of either selective or complete inhibition of all CAs. The results demonstrated that basal acid output was low and not different between CAII KO and WT mucosae, while the achievement of maximal acid secretory rates was already strongly compromised at birth, and progressed with age in CAII KO mucosae. Parietal cell mass was increased, and electron microscopical examination revealed a healthy, but fully stimulated parietal cells in the CAII-deficient mucosae even in the absence of external stimulation. External CO<sub>2</sub> was not required to achieve maximal acid secretory rates, and high concentrating of proton carrying buffers were not able to rescue the phenotype in either neonatal or adult mucosa. Other CA KO mice(9,4,14) did not display this phenotype.

**Conclusions:** CAII and endogenous CO<sub>2</sub> is absolutely required, as well as sufficient, to shuttle the protons from the mitochondria to the proton pump.

**P340**

**A study of ruminal ammonia transport with implications for understanding the gastrointestinal recycling of nitrogen**

J. Rosendahl, J. R. Aschenbach, \*F. Stumpff

Freie Universität Berlin, Institut für Veterinär-Physiologie, Berlin, Germany

**Introduction:** In gastrointestinal recycling of nitrogen, urea is secreted into the gut, microbially converted to ammonia,

reabsorbed and detoxified to urea that is again secreted. Since large quantities of energy are lost in the process, more information is needed about the transport proteins involved. In addition, no information on the ratio of NH<sub>3</sub> and NH<sub>4</sub><sup>+</sup> appearing serosally is available.

**Methods:** Bovine ruminal epithelium was measured in Ussing chambers. The mucosal buffer contained 0 mmol·l<sup>-1</sup>, 10mmol·l<sup>-1</sup> or 40 mmol·l<sup>-1</sup> NH<sub>4</sub><sup>+</sup>; pH was set to 6.4 (100% O<sub>2</sub>, MES/Tris). The serosal buffer contained no NH<sub>4</sub><sup>+</sup>; pH was 7.4 (100% O<sub>2</sub>, no additional buffer). Serosal pH and appearance of ammonia were measured using ion sensitive macroelectrodes. The electrophysiological parameters were followed throughout.

**Results:** Currents induced by apical NH<sub>4</sub><sup>+</sup> (40 mmol·l<sup>-1</sup>) could be partially blocked by ipsilateral application of 100 μmol·l<sup>-1</sup> capsaicin (n = 6; p = 0.02). Appearance of serosal NH<sub>4</sub><sup>+</sup> increased with increasing apical NH<sub>4</sub><sup>+</sup> (76 μmol·l<sup>-1</sup>·h<sup>-1</sup> serosal NH<sub>4</sub><sup>+</sup> per mmol·l<sup>-1</sup> NH<sub>4</sub><sup>+</sup> apically applied), with serosal NH<sub>4</sub><sup>+</sup> reaching levels of 8 ± 2 mmol·l<sup>-1</sup> at 40 mmol·l<sup>-1</sup> NH<sub>4</sub><sup>+</sup> after 2.5 hours of incubation (N = 8; n = 40). Serosal pH did not change significantly.

**Conclusion:** The data confirm a previous study suggesting that the ruminal absorption of NH<sub>4</sub><sup>+</sup> is sensitive to modulators of TRP channels and that, in net terms, ammonia is absorbed through the ruminal epithelium in the protonated form. We suggest that nitrogen recycling may contribute to the pH homeostasis of both the epithelium and luminal content.

Grants: DAAD

**P341**

**Determination of the buffer value of ruminal fluid using a variation of the Astrup technique**

K. T. Hille<sup>1</sup>, S. K. Hetz, J. Rosendahl<sup>1</sup>, H.- S. Braun<sup>1</sup>, M. Grunau<sup>1</sup>, J. R. Aschenbach<sup>1</sup>, \*F. Stumpff<sup>1</sup>

<sup>1</sup>Freie Universität Berlin, Institut für Veterinär-Physiologie, Berlin, Germany

<sup>2</sup>Humboldt Universität zu Berlin, Tierphysiologie, Berlin, Germany

**Introduction:** Despite the importance of adequate buffering of ruminal contents for the health of ruminants, the relevant buffering constants have never been stringently determined. We therefore examined the variables and constants of the Henderson-Hasselbalch equation to calculate buffer value using a variation of the Astrup technique. Method: Ruminal fluid was taken from two fistulated cows on different days (n = 24) and immediately frozen in liquid N<sub>2</sub> to terminate further fermentation. After thawing and equilibration with different partial pressures of CO<sub>2</sub> (P(CO<sub>2</sub>)) at 38°C for one hour, the pH of the samples was measured. Thereafter, [CO<sub>2</sub>]<sub>tot</sub> in fluid was determined by conversion into gaseous CO<sub>2</sub> by acidification (H<sub>2</sub>SO<sub>4</sub>), which was analyzed via infrared spectrometry using a Foxbox™ in a closed system. The pK and Henry's constant (a) of each sample was determined from the equation, the Henderson-Hasselbalch equation and the measured pH.

**Results and Conclusion:** Despite dramatic differences in composition, the solubility of CO<sub>2</sub> in ruminal fluid was found

to be similar to that of plasma (α = 0.229 ± 0.062 mmol/(l·kPa)). The pK value was 6.21 ± 0.16. Buffer values were determined from the slope of the buffer line in a Davenport diagram and ranged from 5 to 15 meq/(l·pH), indicating a low non-bicarbonate buffer capacity in the physiological pH range. From the pK and pH measured, we consider the rumen fluid as a buffer system which is mostly controlled by bicarbonate. Equations found for determining the acid-base status of blood are transferable to ruminal fluid.

grants: European Social Fund; German Ministry of Economics and Technology

Ion channels III

**P342**

**Identification of domains that localize stomatin to the cell surface and permit inhibition of ASIC3 activity**

\*V. Schwartz, H. Siebertz, S. Gründer

Institute of Physiology of RWTH Aachen University, Aachen, Germany

Stomatin is a ubiquitously expressed integral membrane protein which was originally isolated from erythrocyte membranes. It is known to interact with acid-sensing ion channel 3 (ASIC3), a proton-gated Na<sup>+</sup> channel of the DEG/ENaC family, and to inhibit its currents. Interestingly, we found that stomatin like protein-3 (SLP-3) - a stomatin related protein with a high degree of sequence similarity - does not affect ASIC3 activity. We asked whether the differential effect of stomatin and SLP-3 on ASIC3 activity is due to a different cellular localization of the two proteins. In fact in transfected HeLa cells, stomatin mainly localized to the plasma membrane while SLP-3 localized to Rab11-positive vesicles. To determine which domains of stomatin define its membrane localization and which domains are essential for ASIC3 inhibition, we generated chimeras between stomatin and SLP-3. Electrophysiological measurements suggest that in addition to the extreme C-terminal domain of stomatin, several residues within the central domain of stomatin (aa113-158) are essential for its inhibitory effect. Using confocal microscopy of fluorescently labeled chimeras, we observed that these domains of stomatin are also important for its localization at the plasma membrane. In conclusion, our findings identify regions important for localization of stomatin to the plasma membrane and suggest that SLP-3 does not inhibit ASIC3 because it does not localize to the cell surface.

**P342b**

**The NCI-H295R cell line as in vitro model of hyperaldosteronism lacks functional KCNJ5 (GIRK4; Kir3.4) channels**

\*M.- C. Kienitz<sup>1</sup>, E. Mergia<sup>2</sup>, L. Pott<sup>1</sup>

<sup>1</sup>Ruhr-Universität, Institut für Physiologie, Bochum, Germany

<sup>2</sup>Ruhr-Universität, Abteilung für Pharmakologie und Toxikologie, Bochum, Germany

Primary aldosteronism, a major cause of secondary (non-essential) hypertension, is characterized by increased constitutive secretion of aldosterone (Ald). It is either caused by adrenal hyperplasia or by Ald-producing adenoma (APA). Recently, somatic and germline gain-of-function mutations in the KCNJ5 gene have been identified as a major common cause of APA<sup>1</sup>. KCNJ5 encodes for an inward-rectifying K<sup>+</sup> channel subunit (Kir3.4; GIRK4). In the heart, where this type of channel has first been identified, the functional channel is a tetrameric complex of GIRK4 (KCNJ5) and GIRK1 (KCNJ3) in a 2:2 stoichiometry. Identification of a membrane current related to GIRK channels in Ald-producing cells thus far is lacking. NCI-H295R, a human cell line derived from an adrenocortical adenoma, is the most frequently used cellular model for in vitro studies related to regulation of Ald-synthesis<sup>2</sup>. Because of the emerging but undefined role of KCNJ5 (GIRK4) in regulating synthesis of Ald, we aimed at identifying basal (agonist-independent) and G protein-activated macroscopic current carried by GIRK4 in this exemplary cell line. Tertiapin-Q (T-Q), the potent GIRK-specific blocking peptide did not affect basal (background) current. Neither loading of cells with GTP-γ-S via the patch-clamp pipette nor agonist stimulation of a transfected adenosine G<sub>βγ</sub>-coupled A1-adenosine receptor resulted in activation of current. In contrast, these maneuvers in cells co-transfected with KCNJ5 resulted in robust activation of basal and adenosine-activated TQ-sensitive inward-rectifying current. These data are in support of the notion that H295R cells cultured under standard conditions do not express functional GIRK channels. This is unreckoned, since GIRK4 protein can be detected in Western blots of H295R homogenates. We suggest that GIRK4 protein in Ald-producing cells might serve a so far unknown function, unrelated to forming G<sub>βγ</sub>-activated channels.

<sup>1</sup>Mulatero et al.(2013) Nat. Rev. Endocrinol. 9: 104 - 112 <sup>2</sup>Lichtenauer et al.(2013) Horm. Metab. Res. 2: 124-129

**P343**

**Familial hemiplegic migraine due to a novel Nav1.1 mutation L1613P**

\*C. Fan, F. Lehmann-Horn, K. Jurkat-Rott

Ulm University, Division of Neurophysiology, Ulm, Germany

Question: Familial hemiplegic migraine (FHM) is a rare autosomal dominant migraine subtype with aura associated with reversible hemiparesis. It is caused by missense mutations in genes of CACNA1A (FHM1), ATP1A2 (FHM2) and SCN1A (FHM3). Moreover, all 3 types of FHM showed associated epilepsy. SCN1A is a well-known epilepsy gene with

over 100 known mutations, while till now only fewer FHM3 mutations have been identified. The aim of this study was to explore the clinical, genetic and pathogenesis features of a FHM family. Method: Four FHM patients in this family were enrolled in this study and the clinical features were analyzed. Genomic DNA was extracted from blood samples of the patients and screened for SCN1A mutations. SCN1A together with the auxiliary subunits  $\beta 1$  and  $\beta 2$  were cotransfected in human TSA 201 cells. Standard whole-cell patch clamp was employed for electrophysiological characterization of sodium channels. Results: Here we report an identification of a novel SCN1A L1613P mutation in a three-generation family with four patients present with both FHM and epilepsy. Whole-cell patch clamp recordings showed depolarization induced persistent currents for L1613P, which is TTX sensitive, indicating disturbed inactivation. Conclusion: The present study provides further evidence that SCN1A mutations can cause both FHM and epilepsy, and we propose that inactivation changes in L1613P might be involved in the pathomechanisms of both FHM and epilepsy.

**P344**

**Tauro-conjugated bile acids activate the human epithelial sodium channel in its  $\alpha\beta\gamma$  subunit configuration**

\*A. Ilyashkin, S. Haerteis, C. Korbmayer, A. Diakov

<sup>1</sup>Friedrich-Alexander-Universität Erlangen-Nürnberg (FAU), Institut für Zelluläre und Molekulare Physiologie, Erlangen, Germany

**Question.** The epithelial sodium channel (ENaC) plays a pivotal role in regulating sodium absorption in several epithelial tissues including the distal colon. Recently, it has been reported that bile acids activate rat ENaC (Wiemuth D. et al., Pflügers Arch 2013). The aim of the present study was to confirm a stimulatory effect of bile acids on heterologously expressed human ENaC. Tauro-cholic (t-CA), tauro-deoxycholic (t-DCA) and tauro-chenodeoxycholic (t-CDCA) acids are relevant bile acids in the human gastrointestinal tract and may affect ENaC activity in the colon. Therefore, we investigated the effect of these bile acids on human  $\alpha\beta\gamma$ ENaC.

**Methods.** Human  $\alpha\beta\gamma$ ENaC was heterologously expressed in *Xenopus laevis* oocytes. To determine ENaC activity, amiloride (2  $\mu$ M)-sensitive whole-cell currents ( $\Delta I_{ami}$ ) were measured using the two-electrode voltage-clamp technique.

**Results.** We demonstrated that t-CDCA activates human  $\alpha\beta\gamma$ ENaC in a concentration-dependent manner with an EC50 of about  $5 \times 10^{-5}$  M. Applied in a concentration of 250  $\mu$ M, t-CA, t-DCA or t-CDCA significantly increased  $\Delta I_{ami}$  in  $\alpha\beta\gamma$ ENaC expressing oocytes by a factor of  $1.7 \pm 0.1$  ( $n=23$ ,  $p<0.001$ ),  $2.2 \pm 0.2$  ( $n=21$ ,  $p<0.001$ ) or  $1.5 \pm 0.1$  ( $n=20$ ,  $p<0.001$ ), respectively.

**Conclusions.** In conclusion, our data demonstrate that several tauro-conjugated bile acids (t-CA, t-DCA, and t-CDCA) can activate human  $\alpha\beta\gamma$ -ENaC in physiological-

ly relevant concentrations. Therefore, this mechanism may contribute to the regulation of ENaC mediated sodium transport in human distal colon.

**P345**

**Loss of function through heteromerisation - a novel disease mechanism for EAST syndrome**

\*A. Zdebik<sup>1</sup>, S. Parrock<sup>1</sup>, N. Issler<sup>2</sup>, S. Amin-Rasip<sup>1</sup>, R. Kleta<sup>1,2</sup>, D. Bockenhauer<sup>2</sup>

<sup>1</sup>UCL, Neuroscience, Physiology and Pharmacology, London, United Kingdom

<sup>2</sup>UCL, Institute of Child Health, London, United Kingdom

**Question:** We investigated several new mutations in KCNJ10 identified in patients with EAST syndrome characterised by Epilepsy, Ataxia, Sensorineural hearing loss and renal Tubulopathy. Of note, p.A167V, previously described only in heterozygous state, was found in homozygous state in siblings from two families with atypical EAST syndrome. The mutation has been described as partially functional by others.

**Methods:** Heterologous expression in *Xenopus* oocytes

**Results:** We confirmed that KCNJ10 A167V mutant channels are functional on their own - with about 70% residual activity. This is above the level expected in heterozygous carriers of a loss of function mutation. To solve this genetic dilemma, we co-expressed KCNJ10 WT and A167V with its known interaction partner KCNJ16. While KCNJ10/16 heteromers showed strongly inwardly rectified currents sensitive to barium, currents were completely abolished in oocytes expressing KCNJ10 A167V/KCNJ16 heteromeric channels.

**Conclusions:** The mutation p.A167V has previously been thought to cause EAST syndrome only when paired with another, more severe mutation due to its large residual activity. We now show that co-expression with its known interaction partner KCNJ16 leads to loss of function. As KCNJ10 shows complete overlap in expression in kidney DCT, but not in some glial cells, an incomplete EAST phenotype can be expected.

**P346**

**Co-operative endocytosis of the potassium channel TASK-1 and the SNARE protein syntaxin-8**

\*V. Renigunta, T. Fischer, M. Zuzarte, S. Kling, X. Zou, K. Siebert, M. M. Limberg, S. Rinné, N. Decher, G. Schlichthörl, J. Daut

Institut für Physiologie und Pathophysiologie, Zellphysiologie, Marburg, Germany

**Question.** It is still unclear to what extent membrane proteins determine the itinerary and the destination of the transport vesicles in which they reside. In many cases the intracellular traffic of membrane proteins is controlled by specific interacting proteins. We found that the endosomal SNARE protein syntaxin-8 interacts with the potassium channel TASK-1 and studied the functional relevance

of this interaction. **Methods.** Syntaxin-8 and TASK-1 were co-expressed in *Xenopus* oocytes and in mammalian cell lines. Surface expression, subcellular localisation and endocytosis of TASK-1 and syntaxin-8 were studied using voltage clamp, systematic mutagenesis, live-cell fluorescence imaging, TIRF microscopy and antibody-based surface expression and endocytosis assays.

**Results.** Co-expression of syntaxin-8 caused a four-fold reduction in TASK-1 current, a marked reduction in the expression of TASK-1 at the cell surface and an increase in the rate of endocytosis of the channel. The stimulatory effect of the SNARE protein on the endocytosis of the channel was abolished when both an endocytosis signal in TASK-1 (YAEV300-303) and an endocytosis signal in syntaxin-8 (DQRQNLL77-83) were mutated. A syntaxin-8 mutant which cannot assemble with other SNARE proteins had virtually the same effects as wild-type syntaxin-8. TIRF microscopy showed formation and endocytosis of vesicles containing fluorescence-tagged clathrin, TASK-1 and/or syntaxin-8.

**Conclusions.** Our results suggest that the unassembled form of syntaxin-8 and TASK-1 are internalised via clathrin-mediated endocytosis in a co-operative manner. This implies that syntaxin-8 regulates the endocytosis of TASK-1, and vice versa. In addition, our study shows that SNARE proteins can have functions unrelated to membrane fusion.

**P347**

**Activity of voltage-gated calcium channels controls ATP-sensitive potassium (K-ATP) channels in dopamine substantia nigra neurons**

\*S. Kutterer, J. Roepfer

Goethe University Frankfurt, Neurophysiology, Frankfurt, Germany

The firing frequencies and patterns of dopamine (DA) substantia nigra (SN) neurons are critical for striatal DA release, which in turn controls action selection and motor behavior. In rostro-medial DA SN neurons, co-activation of NMDA-receptors and K-ATP channels is necessary and sufficient to generate burst firing and activate exploratory behavior in a novel environment (Schiemann et al., 2012). However, the upstream mechanisms to control the physiological activity of K-ATP channels in DA SN neurons are unknown. To investigate the mechanisms of K-ATP channel activity under physiological conditions, we recorded pacemaker firing and single K-ATP channel activity in parallel, using somatic cell-attached patch-clamp recordings on DA SN neurons in brain slices from adult mice (> 8 weeks). At the end of on-cell recording, the whole-cell configuration was established to fill the neurons with neurobiotin for post-hoc immunohistochemical and morphological identification. We further performed gramicidine perforated patch clamp recordings to study the contribution K-ATP channels to the membrane potential changes during pacemaker activity in metabolically intact cells. We detected spontaneous openings of single K-ATP channels in rostro-medial SN neurons. These channels were not observed in the presence of 1  $\mu$ M glibenclamide or in the Kir6.2 knockout mouse. We pharmacologically inhibited pacemaker-related voltage-gated so-

dium or calcium channels to study their roles for upstream control of K-ATP channel activity. While inhibition of sodium channels with 300 nM tetrodotoxin (TTX) had little effect on the open probability of K-ATP channels in DA SN neurons, the inhibition of both voltage-gated L-type calcium channels with isradipine (300 nM) and T-type calcium channels with NNC 55-0396 (30  $\mu$ M) dramatically reduced the mean K-ATP channel open probability. Also, we observed a decrease in pacemaker precision after pharmacological activation of K-ATP channels with NN414 (10  $\mu$ M), whereas K-ATP channel inhibition with tolbutamide (100  $\mu$ M) or inhibition of T-Type calcium channels increased pacemaker precision. Our results demonstrate the functional coupling of voltage-gated calcium channels and K-ATP channels in metabolically intact DA SN neurons. Opening of K-ATP channels in turn might facilitate recovery from inactivation of voltage-gated calcium channels, decrease pacemaker precision, and thereby might facilitate burst firing in vivo similar to SK channel inhibition.

**P348**

**Agonists binding nicotinic receptors elicit specific channel opening patterns at  $\alpha\gamma$  or  $\alpha\delta$  sites**

\*M. Heckmann, P. Stock, D. Ljaschenko, J. Dudel

Universität Würzburg, Physiologie, Würzburg, Germany

'Embryonic' muscle type nicotinic acetylcholine receptor/channels (nAChRs) bind ligands at interfaces of  $\alpha$ - and  $\gamma$ - or  $\delta$ -subunits.  $\alpha\gamma$ - and  $\alpha\delta$ -sites differ in affinity but their contributions in opening the channel remained elusive. We compared high resolution patch-clamp currents evoked by epibatidine (Ebd), carbamylcholine (CCh) and acetylcholine (ACh). Ebd binds with 75-fold higher affinity at  $\alpha\gamma$ - than at  $\alpha\delta$ -sites whereas CCh and ACh prefer  $\alpha\delta$ -sites. Similar short ( $\tau_{O1}$ ), intermediate ( $\tau_{O2}$ ) and long types of openings ( $\tau_{O3}$ ) were observed with all three agonists.  $\tau_{O2}$  openings were maximally prevalent at low Ebd concentrations, binding at  $\alpha\gamma$ -sites. Vice versa,  $\tau_{O1}$  openings appear to be generated at  $\alpha\delta$ -sites. In addition two types of bursts appeared: Short bursts of on average 0.75 ms ( $\tau_{B1}$ ) that should arise from the  $\alpha\gamma$ -site, and long bursts of 12 to 25 ms ( $\tau_{B2}$ ) durations arising from double liganded receptors. Limited by the temporal resolution, the closings within bursts were invariant at 3  $\mu$ s. Corrected for missed closings, in case of ACh the openings within long bursts lasted 170  $\mu$ s, those in short bursts about 30  $\mu$ s. Blocking  $\alpha\delta$ -sites with  $\alpha$ -conotoxin M1 (CTx) eliminated both  $\tau_{O1}$  and  $\tau_{B2}$  and left only  $\tau_{O2}$  and the short  $\tau_{B1}$  bursts, as expected. Furthermore we found desensitization when the receptors bind ACh only at the  $\alpha\gamma$ -site. When CTx was applied to 'embryonic' mouse endplates, monoquantal current rise times were increased, and amplitude and decay time constants were reduced, as expected. Thus the  $\alpha\gamma$ - and  $\alpha\delta$ -site of nAChRs elicit specific channel opening patterns.

**P349**

**The extraordinary biophysical properties of the KCNQ-conductance  $I_{K_n}$  in cochlear outer hair cells**

\*M. Dierich, D. Oliver, M. G. Leitner

Institute of Physiology and Pathophysiology, Philipps-University Marburg, Neurophysiology, Marburg, Germany

Cochlear outer hair cells (OHCs) constitute the cellular basis of cochlear amplification and are characterised biophysically by the potassium conductance  $I_{K_n}$ . Recently, voltage-gated KCNQ4 (Kv7.4) channel subunits were identified as component of the native current. The importance of KCNQ4 is highlighted by loss-of-function mutations that disrupt  $I_{K_n}$  and cause human hereditary deafness (DFNA2). However,  $I_{K_n}$  in OHCs displays extraordinary biophysical properties that cannot be reproduced by heterologously expressed KCNQ4. Strikingly, the voltage dependence of  $I_{K_n}$  is shifted by -60 mV strongly suggesting OHC-specific, yet unidentified, modulation of  $I_{K_n}$ . We performed patch clamp experiments on isolated OHCs and analysed biophysical properties of  $I_{K_n}$  in comparison to KCNQ4 in an expression system.  $I_{K_n}$  activated at hyperpolarised voltages and was sensitive to KCNQ-specific inhibitors. Both currents were inhibited by neomycin-induced reduction of phosphatidylinositol-(4,5)-bisphosphate, but the sensitivity of  $I_{K_n}$  was significantly lower. Also, the sensitivity of  $I_{K_n}$  towards chemical KCNQ channel openers (e.g. retigabine) was reduced. In contrast to heterologous KCNQ4, voltage dependence and current amplitudes of  $I_{K_n}$  were not modulated by oxidizing-conditions or alkylating substances. Since in OHCs  $I_{K_n}/KCNQ4$  appears to be involved in the regulation of  $K^+$  homeostasis, we also tested for current modulation through extracellular  $K^+$  levels. Surprisingly, elevated extracellular  $K^+$  shifted the voltage-dependence to hyperpolarised potentials, and enhanced relative current amplitudes of  $I_{K_n}$  exclusively. Our findings add to the extraordinary biophysical properties of  $I_{K_n}$  in OHCs and suggest the involvement of OHC-specific components apart from KCNQ4 to the native conductance.

Supported by a research grant of the UKGM to M.G.L.

**P350**

**TMEM16A (ANO1) in human pancreatic ductal adenocarcinoma (PDAC) cells**

\*D. Sauter<sup>1</sup>, I. Novak<sup>2</sup>, S. Pedersen<sup>1</sup>, E. Larsen<sup>2</sup>, E. Hoffmann<sup>1</sup>

<sup>1</sup>Section for Cell and Dev. Biology, University of Copenhagen, Copenhagen, Denmark

<sup>2</sup>Section for Molecular and Integrative Physiology, Dept. of Biology, University of Copenhagen, Copenhagen, Denmark

In the last decade, it was found that ion channels are also involved in the pathogenesis of cancer. TMEM16A is a recently identified  $Ca^{2+}$ -activated  $Cl^-$  channel (CaCC) that is upregulated in several tumors. TMEM16A is involved in cell proliferation in some tumors and was therefore suggested as a new target in cancer therapy. Present study is to validate the significance of TMEM16A in PDAC behavior.

We performed qPCR measurements on different pancreatic cancer cell lines (Capan-1, AsPC-1, BxPC-3) and compared the results to a human pancreatic ductal epithelium (HPDE) cell line. All cancer cell lines showed an upregulation of TMEM16A mRNA levels. Expression was confirmed on protein level using Western Blot. Whole-cell patch-clamp recordings identified large  $Ca^{2+}$  and voltage - dependent  $Cl^-$  currents in PDAC cells that were almost completely abolished upon siRNA knock-down of TMEM16A. Surprisingly, application of the TMEM16A inhibitors T16A<sub>inh</sub>-A01 (20  $\mu$ M), CaCCi<sub>inh</sub>-A01 (20  $\mu$ M) and NS3728 (10  $\mu$ M) attenuated this current only partially. We further assessed the functional role of TMEM16A in cellular proliferation and migration. CaCCi<sub>inh</sub>-A01 and NS3728 decreased proliferation in all PDAC and control cells tested by 40%. This effect was not observed in TMEM16A knock-down cells. In an ongoing study we subjected PDAC cells to the inhibitors in a scratch assay. Application of T16A<sub>inh</sub>-A01 resulted in a 50% decrease in wound closure after 36h. In conclusion, we find that TMEM16A is highly unregulated in PDAC cells and that it is likely to have an important role in cell behavior.

**P351**

**Effects of lung adenocarcinoma on sodium transport of healthy alveolar epithelial cells**

\*E. Ermis Kaya<sup>1,2,3</sup>, E. Baloglu<sup>1,3</sup>, M. Meister<sup>4,3</sup>, S. Cebesoy<sup>2</sup>, H. Mairbaeurl<sup>1,3</sup>

<sup>1</sup>Heidelberg University Medical Clinic VII, Sportmedicine, Heidelberg, Germany

<sup>2</sup>University of Ankara, Science Faculty, Biology Department, Ankara, Turkey

<sup>3</sup>German Center for LUNG Research (DZL-TLRC-H), Heidelberg, Germany

<sup>4</sup>University of Heidelberg, Throat Clinic, Section Translational Research, Heidelberg, Germany

**Question:** Lung cancer is an aggressive cancer type. There is evidence that cancer cells affect signaling pathways of surrounding cells, which at that point often appear histologically healthy, a finding termed "cancerization field effect". Based on this interaction we ask the question whether cancer cells growing in close vicinity of healthy tissue affect the barrier function of supposedly healthy alveolar epithelium.

**Methods:** Primary human alveolar epithelial cells (hATII) were isolated from lung tissue from healthy regions of patient-lungs after lobotomy. hATII cells were grown on transwell filters in co-culture with A549 adenocarcinoma cells or with conditioned media from A549 cells. Effects on hATII cell growth were measured with crystal violet, ion transport was determined in Ussing chambers. The transepithelial electrical resistances (TEER) were measured as indicator of barrier tightness.

**Results:** When cultured with A549 conditioned media the growth of hATII was impaired after 3 days exposure. Nevertheless, transport via Na-channels and Na/K-ATPase tended to be increased. Co-culturing hATII with A549 cells increased ion transport after 24h but longer exposures de-

creased both Na-channels and Na/K-ATPase. TEER tended to be increased by culturing hATII with A549 conditioned media when compared with co-culturing with A549 cells.

**Conclusion:** These results indicate that direct contact and conditioned media modify healthy hATII  $Na^+$ -transport differently. Likely due to soluble factors released upon interaction of cancer cells and hATII that stimulate cell growth and metabolic effects causing impaired function.

**P352**

**HIF-2 $\alpha$  is involved in the decreased activity of ENaC in hypoxic alveolar epithelial cells**

\*E. Baloglu<sup>1,2</sup>, K. Velineni<sup>1,2</sup>, H. Mairbaeurl<sup>1,2</sup>

<sup>1</sup>University of Heidelberg, Internal Medicine VII, Heidelberg, Germany

<sup>2</sup>German Center for Lung Research (DZL-TLRC-H), Heidelberg, Germany

**Question:** Alveolar epithelium plays a central role in maintaining optimal gas exchange and fluid transport via epithelial Na Channels (ENaC). Hypoxia of the alveolar epithelium such as in pulmonary edema decreases the expression and activity of ENaC to be able to maintain cellular ATP demand and cell survival. Here we asked whether HIF is involved in the regulation of ENaC expression and activity in hypoxia.

**Methods:** HIF-1 $\alpha$  and HIF-2 $\alpha$  were silenced in primary rat alveolar epithelial cells by adenoviral transfer of shRNAs. Cells were exposed to hypoxia (1.5%) for 2-48h and hypoxia mimetic cobalt for 24h. ENaC activity was measured in Ussing chambers, mRNA by RT qPCR and protein expression by western blot.

**Results:** mRNA expression of ENaC subunits was decreased at 24h hypoxia, which was not affected by silencing HIFs. 24h of incubation with cobalt did not decrease the ENaC mRNAs. Hypoxia decreased ENaC activity by time dependent manner which was already evident after 2h of hypoxia. Silencing HIF-2 $\alpha$  significantly prevented some of the decreased ENaC activity after 24h of hypoxia. In contrast, HIF-1 $\alpha$  silencing enhanced ENaC inhibition after 48h.

**Conclusion:** These data show a fast and persisting inhibitory effect of hypoxia on ENaC activity, which is not explained by altered ENaC mRNA expression. However, the partial prevention by HIF-2 $\alpha$  silencing and the enhancement of inhibition by HIF-1 $\alpha$  silencing indicate that inhibition is caused at the post-transcriptional level part of which depends on the presence of HIFs.

This project was funded by the German Research Foundation.

**P353**

**Hypoxia decrease Na/K-ATPase transcription and activity by HIF dependent manner**

\*E. Baloglu<sup>1,2</sup>, K. Velineni<sup>1,2</sup>, H. Mairbaeurl<sup>1,2</sup>

<sup>1</sup>University of Heidelberg, Internal Medicine VII, Heidelberg, Germany

<sup>2</sup>German Center for Lung Research (DZL-TLRC-H), Heidelberg, Germany

**Question:** Active Na transport in alveolar epithelial cell occurs by the entry of  $Na^+$  via apical located amiloride sensitive  $Na^+$  Channels and is pumped out by the basolateral Na/K-ATPase. Thus, the intact Na/K-ATPase is essential for preventing alveolar fluid accumulation. Ischemia and reperfusion injury, in-vivo and in-vitro hypoxia impair Na/K-ATPase activity, leading pulmonary edema. It is not known whether the decreased Na/K-ATPase activity in hypoxia involves HIF signaling. **Methods:** HIF-1 $\alpha$  and HIF-2 $\alpha$  were silenced in primary rat alveolar epithelial cells by adenoviral transfer of shRNAs. Cells were exposed to hypoxia (1.5%) for 24-48h. mRNA of  $\alpha$ 1- and  $\beta$ 1-Na/K-ATPase was measured by RT qPCR. Na/K-ATPase activity was measured in Ussing chambers after permeabilization of apical membranes with Amphotericin B. Thus, the measured activity represents the capacity and membrane-expression of the pump. **Results:** Decreased the mRNA expression of  $\alpha$ 1- and  $\beta$ 1-Na/K-ATPase in hypoxia was almost completely prevented by silencing HIF-1 $\alpha$  and HIF-2 $\alpha$ . Hypoxia decreased Na/K-ATPase activity. Silencing HIFs partially prevented some of this inhibition after 24h and 48h of hypoxia.

**Conclusion:** These data show that the decrease in Na/K-ATPase mRNA but not the plasma membrane expression and activity in hypoxia is under the control of HIF-1 $\alpha$  and HIF-2 $\alpha$ . These results indicate that Na/K-ATPase activity is reduced in hypoxia by the limited translation rates because hypoxia reduces ATP consuming events such as protein synthesis.

This project was funded by the German Research Foundation.

**P354**

**Altered firing activity of renal afferent neurons originates from the clipped kidney in the 2Kidney/1Clip model of hypertension**

\*W. Freisinger<sup>1,2</sup>, A. Karl<sup>2</sup>, T. Ditting<sup>2</sup>, S. Heinlein<sup>2</sup>, R. Schmieder<sup>2</sup>, K.-F. Hilgers<sup>2</sup>, R. Veelken<sup>2</sup>

<sup>1</sup>Universitätsmedizin Mainz, 1. Medizinische Klinik, Mainz, Germany

<sup>2</sup>University Erlangen-Nürnberg, Medizinische Klinik 4-Nephrologie, Erlangen, Germany

**Question:** Renal afferent neurons are peculiar showing predominantly tonic firing pattern upon depolarizing current injection, most likely due to specific expression of voltage gated sodium channels. Recently, we found that this firing was decreased in the 2Kidney/1Clip model of hypertension. The aim of this study was to investigate whether this decrease is found in all renal afferent neurons or if it is associated either to the clipped or to the non-clipped side.

**Methods:** Clipping of the renal artery induced hypertension in male Sprague-Dawley rats. Dil-labeling allowed the identification of dorsal root ganglion (DRG) neurons (Th<sub>11</sub>-L<sub>2</sub>) with projections either to the clipped or to the unclipped kidney. Current clamp was used to characterize neurons according to their firing response upon stimulation as "tonic", i.e. sustained action potential (AP) firing or as "phasic", i.e. showing

**Results:** Renal DRG neurons of hypertensive animals showed a significant decrease of tonic firing (44,3% [39/88] vs. 59,5% [50/84])

**Conclusion:** We found that the significantly decreased firing in afferent renal neurons in the 2Kidney/1Clip model of hypertension seems to originate from the clipped kidney. So far, the mechanisms causing the “switch” from tonic to phasic firing in the neurons of the clipped kidney, e.g. modulation of the voltage gated sodium channels, need further elucidation.

**P355**

**TREK-1 currents in rat ventricular cardiomyocytes**

\*M. Bodnár, J. Daut

Institute of Physiology and Pathophysiology, University of Marburg, Marburg, Germany

TREK-1 channels are expressed in the heart of many vertebrates including homo sapiens. Due to their dependence on mechanical stimulation TREK-1 channels may play a major role in human cardiac physiology and pathophysiology. As a first step towards the elucidation of their physiological role in the heart we tried to give a quantitative description of TREK-1 currents in rat cardiomyocytes. Whole-cell patch-clamp measurements were performed in isolated rat ventricular cardiomyocytes; a suitable voltage protocol and a blocker cocktail were used to separate the TREK-1 current from other current components. Since TREK-1 channels are known to be much more temperature sensitive than other potassium channels we studied the temperature sensitive outward current component at positive potentials in the presence of the blocker cocktail. It showed the outward rectification typical for TREK-1 and had an amplitude of ~1.0 to 1.5 pA/pF at +30 mV. It could be inhibited via the PKA signalling pathway. The outward current at 37 °C could also be inhibited by application of 400 µM quinidine, as previously described for TREK-1 channels. The quinidine-sensitive current measured at 37 °C was 1.0 to 2.0 pA/pF. In conclusion, the quinidine and temperature sensitive outward current component measured was probably mainly carried by TREK-1 channels. The putative TREK-1 current (~1.5 pA/pF) was found to be about five-fold larger than the current carried by TASK-1 channels at room temperature (~0.3 pA/pF). The modulation of TREK-1 channels via adrenergic receptors may play an important role in the regulation of action potential duration.

**P356**

**Effects of SGK3 on the intracellular traffic of the inward rectifier channel Kir2.2**

\*K. Grothus, R. Preisig-Müller, J. Daut

Institut für Physiologie und Pathophysiologie, AG Zellphysiologie, Marburg, Germany

Inwardly rectifying potassium channels stabilize the resting membrane potential of many cell types including car-

diac myocytes and neurons. We found that coexpression of Kir2.2 with serum- and glucocorticoid-inducible kinase 3 (SGK3) in *Xenopus laevis* oocytes caused a significant increase of both current amplitude and surface expression of the channel. These results were confirmed in a mammalian expression system (COS7 cells), where a constitutively active mutant of SGK3 (but not the corresponding mutant of SGK1) increased the surface expression of Kir2.2 by 80 %. Live cell imaging showed extensive colocalization of Kir2.2 with SGK3 in endosomal structures, while no colocalization was observed with SGK1. Both Kir2.2 and SGK3 were coexpressed with Rab4, Rab5, Rab7 and Rab11, which served as markers for early endosomes, late endosomes, a fast recycling pathway and recycling endosomes, respectively. SGK3 was localized to Rab5- and Rab7-positive vesicles. Kir2.2 was predominantly localized to Rab7 containing vesicles but also showed some colocalization with Rab5. SGK3 is localized to PI3P-containing membranes due to a PX domain in its N-terminus. A mutation in the PX domain abolished its endosomal localization and significantly reduced the effect of the kinase on the surface expression of Kir2.2. In conclusion, our results show that coexpression with SGK3, but not SGK1, increases the copy number of Kir2.2 channels in the plasma membrane. Kir2.2 and SGK3 are colocalized in the early and late endosomal compartment and this colocalization may be involved in mediating the effect of the enzyme on the surface expression of the channel.

**P357**

\*C. Holzmänn, T. Kilch, S. Kappel, A. Armbrüster, V. Jung, M. Stöckle, I. Bogeski, E. C. Schwarz, C. Peinelt

<sup>1</sup>Universität des Saarlandes, Institut für Biophysik, Homburg, Germany

<sup>2</sup>Universität des Saarlandes, Klinik für Urologie und Kinderurologie, Homburg, Germany

Calcium signals are involved in a plethora of cellular functions. Store operated calcium entry (SOCE) was shown to be an important mechanism in calcium signaling in several cell types. However, how the STIM and Orai proteins that mediate SOCE are involved in regulating cellular functions of prostate epithelial cells is still unknown. We have recently developed a cell culture method to isolate primary human prostate epithelial cells and we conducted reverse transcriptase real-time PCR, siRNA-knockdown assays, patch-clamp, calcium-imaging (Fura-2AM) and quantification of PSA secretion (prostate specific antigen) to investigate the role of SOCE/ $I_{CRAC}$  in primary cells and different prostate cancer cell lines. We also characterise the differential role of Orai isoforms 1 and 3 in those cells and we describe dihydrotestosterone as a rapid activator of SOCE in prostate epithelial cells. Our results point to an essential role of Orai proteins in prostate epithelial cells where they form functional channels mediating SOCE. Our findings also indicate that Orai3 subunits modulate the pharmacological profile of CRAC channels. In addition we show that dihydrotestosterone rapidly activates calcium influx by store depletion

and influences secretion of PSA. The fast kinetic of these DHT-effects can not be explained by changes in gene expression.

**P358**

**Searching for fluorescence labeled ATP derivatives as P2X channel agonists**

\*T. Suchanke, T. Schwabe, T. Zimmer, F. Schwede, K. Benndorf

<sup>1</sup>University Hospital Jena, Friedrich Schiller University Jena, Institute of Physiology II, Jena, Germany

<sup>2</sup>BIOLOG Life Science Institute, Bremen, Germany

P2X receptors are cation-permeable, ligand-gated ion channels. They are involved in synaptic transmission and modulation, but are also expressed in many non-neuronal cell types to mediate e.g. smooth muscle contraction, secretion, and immune modulation. P2X receptors consist of three subunits for which seven isoforms have been identified (P2X1-7). These subunits can form either homotrimeric (except P2X6) or heterotrimeric channels, exhibiting different pharmacological and electrophysiological properties. Each subunit comprises two transmembrane domains and a large extracellular loop. N- and C-terminus are located intracellularly. For the homotrimeric P2X4 receptor the structure has been identified in an open and a closed conformation. To better understand the gating kinetics of P2X receptors, conjoint measurement of ligand binding and activation gating is promising by using confocal patch-clamp fluorometry. Herein we tested fluorescence labeled ATP derivatives for their effects on the activity of P2X2 receptors in inside-out patches of *Xenopus* oocytes. The dyes Cy3, DY547, and Bodipy were coupled to the positions 2 or 8 of the adenine moiety or to 2'/3' of the ribose moiety. The result was that none of the compounds is a full agonist but that some of the compounds led to partial activation with efficiencies <50%. At present it remains open whether there is enough space in or at the binding pocket for a fluorophore moiety in addition to the ligand ATP to design a fluorescent ligand that is appropriate for confocal patch-clamp fluorometry.

**P359**

**Small molecule rescue of impaired protein stability in the ADPKD PKD2-D511V patient mutation**

\*A. Hofherr, C. Wagner, M. Köttgen

<sup>1</sup>University Medical Centre Freiburg, Nephrology and General Medicine, Freiburg im Breisgau, Germany

<sup>2</sup>University Hospital Heidelberg, Heidelberg, Germany

**Question:** Autosomal dominant polycystic kidney disease (ADPKD) is the most common lethal monogenetic disorder in humans. Mutations in PKD2 account for approximately 15 % of cases. PKD2 encodes the transient receptor channel polycystin-2 (TRPP2), a non-selective Ca<sup>2+</sup>-permeable cation channel. The ADPKD Mutation Database lists a total of 268 unique PKD2 mutations, including 77 frame-shift, 42

non-sense and 37 splice mutations as well as 26 substitutions. A particular difficulty presents the accuracy of discrimination between pathogenic nucleotide substitutions and harmless sequence variants based on in silico predictions. Rather little experimental data investigating the disease mechanism of PKD2 mutations is available.

**Methods:** Here we analyse the biochemical properties of the pathogenic missense variant PKD2-D511V, which has been previously characterised as a channel-dead mutant. Cellular expression systems and a *D. melanogaster* PKD2-D511V model are used for in vitro and in vivo studies respectively.

**Results:** The D511V mutation causes significantly reduced (~85.2 %) TRPP2 expression compared to wild-type protein in heterologous cell culture systems, despite similar mRNA levels. The mutant protein is degraded in lysosomes. Inhibition of lysosomal degradation by chloroquine increases TRPP2 protein levels to 1461 %, whereas incubation with the proteasome inhibitor MG132 has no effect. Notably, incubation of cells expressing TRPP2<sup>D511V</sup> with an FDA-approved small molecule results in a significant rescue of reduced expression levels. To assess the in vivo relevance of this chemical rescue of TRPP2<sup>D511V</sup> protein levels, we introduced the corresponding mutation into the *D. melanogaster* PKD2 homolog (Amo-D627V). We show, that this transgene is pathogenic: 1) it does not rescue the PKD2 knock-out phenotype; and 2) protein expression is likewise reduced compared to wild-type TRPP2 in vivo.

**Conclusions:** Taken together, the D511V mutation causes lysosome-mediated TRPP2 protein instability, which can be rescued by small molecules in vitro. Future studies will have to show whether this chemical rescue of protein instability results in increased TRPP2 function in vivo. The *D. melanogaster* model mimicking PKD2-D511V will be a valuable tool to test this hypothesis.

**P360**

**Hydrogen sulfide decreases β-agonist stimulated lung liquid clearance by inhibiting cAMP regulated transepithelial sodium absorption**

\*A. Agné, J.- P. Baldin, M. Orogo-Wenn, L. Wichmann, D. Walters, M. Althaus

<sup>1</sup>Justus-Liebig University, Institute of Animal Physiology, Gießen, Germany

<sup>2</sup>St. George's University of London, Division of Clinical Sciences, London, United Kingdom

**Question:** Hydrogen sulfide (H<sub>2</sub>S) is a signalling molecule which interferes with ion channels. In lungs, sodium channels facilitate the clearance of sodium and, consequently, liquid across the pulmonary epithelium. This clearance is regulated by β-adrenergic agonists. This study investigated if H<sub>2</sub>S interferes with the adrenergic regulation of pulmonary epithelial sodium channels.

**Methods:** Liquid clearance was measured by monitoring liquid volume in rat lungs in situ. Epithelial sodium absorption was measured across human pulmonary epithelial cells (H441) in Ussing chambers.

Cellular ATP concentrations were measured with a luminescence assay.

**Results:** In rat lungs, the  $\beta$ -adrenergic agonist terbutaline increased lung liquid clearance. This effect was inhibited by the H<sub>2</sub>S-releasing salt Na<sub>2</sub>S (50  $\mu$ M).  $\beta$ -adrenergic agonists increase liquid absorption by an adenylate cyclase/cAMP mediated increase in epithelial sodium channel (ENaC) activity. Activation of the adenylate cyclase/cAMP pathway by forskolin (5  $\mu$ M) and IBMX (100  $\mu$ M) increased amiloride-sensitive ENaC currents in H441 cells. This was completely blocked by Na<sub>2</sub>S in a dose dependent manner (5-50  $\mu$ M). H<sub>2</sub>S did not impair cellular energy metabolism as ATP concentrations remained unchanged in the presence of Na<sub>2</sub>S (250  $\mu$ M). H<sub>2</sub>S is known to modify thiol groups by a mechanism referred to as S-sulfhydration. The thiol-modifying agent N-ethyl maleimide (50  $\mu$ M) mimicked the effect of Na<sub>2</sub>S and blocked forskolin/IBMX-induced ENaC activation in H441 cells.

**Conclusion:** These data indicate that H<sub>2</sub>S inhibits  $\beta$ -adrenergic agonist stimulated lung liquid clearance. This is due to inhibition of the adenylate cyclase/cAMP signalling pathway by a mechanism which likely involves a thiol modification by H<sub>2</sub>S.

**P361**

**Luminal acetylcholine induces a current increase in porcine airway epithelium - no evidence for the activation of CFTR**

\*N. Ditttrich<sup>1</sup>, W. Claus<sup>1</sup>, W. Kummer<sup>2</sup>, M. Fronius<sup>1,3</sup>

<sup>1</sup>Justus-Liebig-University Giessen, Institute of Animal Physiology, Giessen, Germany

<sup>2</sup>Justus-Liebig-University Giessen, Institute of Anatomy and Cell Biology, Giessen, Germany

<sup>3</sup>University of Otago, Department of Physiology, Dunedin, New Zealand

The cystic fibrosis transmembrane conductance regulator (CFTR) is crucial for airway fluid homeostasis and malfunction is associated with the phenotype of cystic fibrosis lung disease. Luminal acetylcholine (ACh) has been identified to activate Cl<sup>-</sup> secretion in airway epithelia - indicating that the CFTR participates in this effect. The present study investigates whether the CFTR is a putative target of luminal ACh in the airways of pigs. Porcine tracheal preparations were mounted in Ussing-chambers for transepithelial short-circuit-current (I<sub>sc</sub>) recordings. ACh (100  $\mu$ M) was applied from the luminal side. CFTR-dependent Cl<sup>-</sup> secretion was induced by increasing cAMP levels using IBMX (100  $\mu$ M) and forskolin (10  $\mu$ M) in the presence of amiloride (10  $\mu$ M). GlyH-101 (50  $\mu$ M) was applied to determine CFTR-mediated currents. Luminal application of ACh significantly increased the I<sub>sc</sub> (before: 36.0 $\pm$ 2.9  $\mu$ A/cm<sup>2</sup>; peak: 46.1 $\pm$ 3.8  $\mu$ A/cm<sup>2</sup>; p<0.001; n=35). Under control condition the IBMX/forskolin-activated current ( $\Delta I_{I/F}$ ) was 32.4 $\pm$ 6.4  $\mu$ A/cm<sup>2</sup> (n=6). In contrast, in the presence of GlyH-101  $\Delta I_{I/F}$  was significantly reduced ( $\Delta I_{I/F}$ : 13.1 $\pm$ 3.7  $\mu$ A/cm<sup>2</sup>; p<0.01; n=6), demonstrating that a substantial portion of the  $\Delta I_{I/F}$  is CFTR dependent. However, the effect of luminal ACh was not altered in presence of the CFTR inhibitor GlyH-101 ( $\Delta I_{ACh}$ : 11.3 $\pm$ 2.3; n=5) compared to control measurements ( $\Delta I_{ACh}$ :

10.1 $\pm$ 2.2; n=5). Luminal ACh activates ion transport processes in porcine airway epithelium, pointing to the existence of a non-neuronal cholinergic system in the airways. The observed effect does not involve CFTR-dependent Cl<sup>-</sup> secretion and the targets responsible for this effect are still to be identified.

**Ion channels IV**

**P362**

**Hypomethylation of the KCNN4 promoter correlates with increased KCa3.1 channel expression in highly metastatic NSCLC cells and a poor prognosis in lung cancer**

\*E. Bulk<sup>1</sup>, C. Rohde<sup>2</sup>, E. Schmidt<sup>2</sup>, A. Hascher<sup>2</sup>, H.-U. Klein<sup>3</sup>, M. Dugas<sup>3</sup>, C. Müller-Tidow<sup>2</sup>, A. Schwab<sup>1</sup>

<sup>1</sup>University of Muenster, Institute of Physiology II, Muenster, Germany

<sup>2</sup>University of Muenster, Department of Medicine, Hematology and Oncology, Muenster, Germany

<sup>3</sup>University of Muenster, Institute of Medical Informatics, Muenster, Germany

Lung cancer is one of the leading causes of cancer-related death worldwide. The prognosis is very poor with a 5-year survival rate of non-small cell lung cancer (NSCLC) patients in advanced stages of ~10 % due to the early development of metastasis. Within the last years it became apparent that epigenomic changes, such as DNA methylation have an important share in shaping the metastatic phenotype of cancer cells by regulating gene expression. However, so far there is only limited knowledge about the identity of these "prometastatic genes" whose expression is regulated by methylation. Here, we identified the genomic promoter region of the K<sup>+</sup>-channel K<sub>Ca</sub>3.1 (KCNN4) to be hypomethylated in a highly aggressive metastatic NSCLC cell line. Accordingly, K<sub>Ca</sub>3.1 channel expression was upregulated in these cells. K<sub>Ca</sub>3.1 channels are functionally relevant since their blockade with TRAM-34 leads to an inhibition of migration, proliferation and reduces the Ca<sup>2+</sup> influx. Furthermore, we found in a large cohort of lung adenocarcinoma patients that decreased DNA methylation within the KCNN4 promoter region is associated with a poor prognosis of these patients. This finding correlates with increased K<sub>Ca</sub>3.1 expression levels in NSCLC patients with a low survival rate. In conclusion, our findings reveal that epigenetically regulated K<sub>Ca</sub>3.1 channel expression not only supports the prometastatic behavior of NSCLC cells, but that the hypomethylation within the KCNN4 promoter region has strong predictive value in patient prognosis.

**P363**

**Functional coupling of the mitochondrial Ca<sup>2+</sup>-sensitive K-channel to the respiratory chain**

P. Bednarczyk, \*D. Siemen, A. Szewczyk

Otto-von-Guericke-University, Dept. of Neurology, Magdeburg, Germany

Potassium channels as present in the plasma membrane of various cells have also been found in the inner mitochondrial membrane. Potassium channels have been proposed to regulate the mitochondrial membrane potential, respiration, matrix volume and Ca<sup>2+</sup>-ion homeostasis. It has been suggested that mitochondrial potassium channels participate in ischemic preconditioning and neurodegenerative disorders. Calcium sensitive K-channels of the BK-type (mtBK) keep the permeability transition pore closed which is opened during apoptosis. We measured single channel currents of mtBK by patch-clamping mitoplasts isolated from an astrocytoma cell line. Mitoplast were prepared in hypotonic solution causing unfolding of the inner membrane thus breaking the outer membrane. Isotonicity was restored by adding a hypertonic solution. Potassium currents were recorded with a mean conductance of 290 pS in symmetrical 150 mM KCl solution. The channel was activated by Ca<sup>2+</sup> and inhibited irreversibly by iberiotoxin, a selective inhibitor of the BK<sub>Ca</sub> channel. Substrates of the respiratory chain like succinate decreased the activity of the channel. The effect was abolished by cyanide and antimycin, being inhibitors of respiratory chain. Our findings indicate that the mtBK has properties similar to its counterpart in the plasma membrane. It is present in human astrocytoma mitochondria and can be stimulated by redox status of the respiratory chain (Bednarczyk et al., 2013, PLOS One 8(6):e68125).

We appreciate support by Warsaw University of Life Sciences - SGGW, by the Polish Mitochondrial Network Mi-toNet.pl, and by DZNE.

**P364**

**Gap junction hemichannels are responsible for the anion permeability of the granulosa cells and are regulated by P2Y<sub>2</sub> and P2Y<sub>4</sub> receptors**

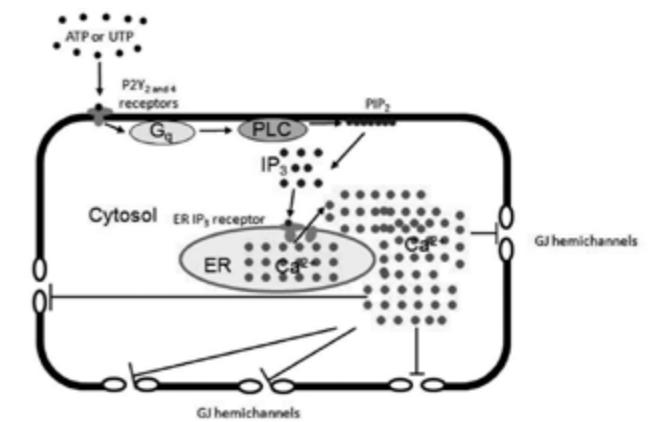
N. Dilger<sup>1</sup>, W. Bintig<sup>2</sup>, \*A. Ngezahayo<sup>1</sup>

<sup>1</sup>Leibniz Universität Hannover, Institut für Biophysik, Hannover, Germany

<sup>2</sup>Charité, Berlin, Germany

The rat GFSHR-17 granulosa cells express FSH receptor and were therefore proposed as a suitable in vitro model to analyse the developmental physiology of the follicle. Perforated patch-clamp experiments revealed that the cells had a membrane potential of -40 mV. Application of ATP (10  $\mu$ M) induced a transient increase of the intracellular concentration of free Ca<sup>2+</sup> ([Ca<sup>2+</sup>]<sub>i</sub>) which induced a hyperpolarisation of the cells to lower than -60 mV. The use of UTP and blockade of the IP<sub>3</sub> pathway cascade showed that ATP affected the [Ca<sup>2+</sup>]<sub>i</sub> by activation of P2Y<sub>2</sub> and P2Y<sub>4</sub> receptors and that the Ca<sup>2+</sup> signals was a required and sufficient prerequisite for the hyperpolarization of the cell membrane. Pharmacological experiments showed that the membrane

voltage of the cells was controlled by chloride permeability, which was reduced by Ca<sup>2+</sup> released in response to stimulation of the P2Y<sub>2</sub> and P2Y<sub>4</sub> receptors. Chloride channels are normally activated by Ca<sup>2+</sup>, therefore the observed chloride permeability was due to other channels than Cl<sup>-</sup> channels. A combination of electrophysiology, pharmacology and molecular biology revealed that the chloride permeability was related to gap junction hemichannels expressed by the GFSHR-17 cells. The role of gap junction hemichannels in secretion of the antral fluid during follicular development is proposed.



**P365**

**A novel mechanism of voltage sensing and gating in K2P potassium channels**

\*M. Schewe<sup>1</sup>, M. Rapedius<sup>1</sup>, E. Nematian-Ardestani<sup>1</sup>, T. Linke<sup>2</sup>, K. Bendorff<sup>2</sup>, S. J. Tucker<sup>3</sup>, T. Baukrowitz<sup>1</sup>

<sup>1</sup>University of Kiel, Institute of Physiology, Kiel, Germany

<sup>2</sup>University of Jena, Institute of Physiology II, Jena, Germany

<sup>3</sup>University of Oxford, Department of Physics, Oxford, United Kingdom

Two-pore domain (K2P) potassium channels are important regulators of cellular electrical excitability integrating a wide range of stimuli including phosphorylation, various lipids, temperature, intracellular/extracellular pH and membrane voltage. Here we investigated the mechanism of voltage sensing/gating in K2P channels. We show that TASK-3 and TRAAK are mostly closed at the resting membrane potential but become strongly activated by depolarisation similar to classical Kv channels. Moreover, strong voltage activation was also seen for other K2P channels such as TREK-1, TREK-2, TRESK and TALK-2, however, only when intracellular K<sup>+</sup> was replaced by other permeant ions such as NH<sub>4</sub><sup>+</sup>, Cs<sup>+</sup> or Rb<sup>+</sup>. Strikingly, voltage activation was abolished upon intracellular Na<sup>+</sup> or NMDG<sup>+</sup> replacement suggesting that movements of permeant ions in the electric field focused in the selectivity filter power voltage gating and, thus, are likely to represent the gating charge in K2P channels. Indeed, mutations in the selectivity filter, experiments with high affinity pore blockers and cysteine modification establish the selectivity filter as the voltage gate.

Furthermore, voltage activation in K2P channels exhibits distinct functional features compared to classical Kv channel gating as the V<sub>1/2</sub> for voltage activation was strictly coupled to the K2P channel reversal potential and the kinetics of voltage gating were largely voltage-independent. The latter finding suggests a voltage-dependent fast multi ion binding step to a non-conductive but ion accessible selectivity filter and a second slower voltage-independent gating step leading to the conductive state of the selectivity filter. These findings demonstrate a novel concept of voltage sensing in K<sup>+</sup> channels and point to a new role of K2P channels in cell excitability as the strong voltage dependence would enable K2P channel to contribute significantly to the repolarisation phase of neural (e.g. TRAAK) or cardiac (e.g. TASK-3) actions potentials.

**P366**

**Activation of TGR5 stimulates TRPA1 in the *Xenopus laevis* oocyte expression system**

\*M. Krappitz<sup>1</sup>, S. Haerteis<sup>1</sup>, T. Lieu<sup>2</sup>, N. Bunnett<sup>2</sup>, C. Korbmacher<sup>1</sup>

<sup>1</sup>Friedrich-Alexander-Universität Erlangen-Nürnberg (FAU), Institut für Zelluläre und Molekulare Physiologie, Erlangen, Germany

<sup>2</sup>Monash University, Monash Institute of Pharmaceutical Sciences, Melbourne, Australia

**Question:** TGR5 (also known as GPR131 or GpBAR1), a G protein-coupled plasma membrane receptor for bile acids, has a wide range of (patho-)physiological functions. For example, it induces hyperexcitability in dorsal root ganglia and plays a major role in bile acid induced histamine-independent itch and analgesia. Another component contributing to histamine-independent itch is the non-selective, calcium-permeable cation channel TRPA1 (transient receptor potential cation channel, subfamily A, member 1) (Wilson et al., Nat Neuroscience, 2011). Interestingly, TRPA1 and TGR5 are co-expressed in dorsal root ganglia (Alemi et al., J Clin Invest, 2013). Therefore, the aim of the present study was to investigate whether activation of TGR5 modulates TRPA1 function in the *Xenopus laevis* oocyte expression system.

**Methods:** Whole-cell currents were measured in *Xenopus laevis* oocytes expressing human TRPA1 or TRPA1/TGR5 using the two-electrode voltage-clamp technique. The TRPA1 activator allyl isothiocyanate (AITC, 50 μM) and the selective TRPA1 inhibitor HC030031 (15 μM) were used as tools to activate and inhibit TRPA1 currents, respectively. TGR5 was activated by deoxycholic acid (DCA, 0.5 mM).

**Results:** Application of AITC to oocytes expressing TRPA1 or TRPA1/TGR5 elicited a transient inward current sensitive to HC030031 consistent with functional TRPA1 expression. In contrast, AITC had no significant effect in non-injected control oocytes. To activate TGR5, oocytes co-expressing TRPA1/TGR5 were exposed for 30 seconds to DCA prior to the application of AITC. This resulted in a ~40% increase of the AITC elicited TRPA1 current response compared to that observed in matched TRPA1/TGR5 co-expressing oocytes not treated with DCA. In contrast, DCA did not increase the AITC current response in oocytes expressing TRPA1 alone. This indicates that the stimulatory effect of

DCA on TRPA1 depends on the co-expression of TGR5. **Conclusion:** Our results indicate that activation of TGR5 by bile acids stimulates TRPA1 channels in the *Xenopus laevis* oocyte expression system. This mechanism of TGR5-mediated TRPA1 regulation by bile acids may also be relevant in native tissues co-expressing TRPA1 and TGR5, e.g. in dorsal root ganglia.

**P367**

**Auditory profile of Cav 2.3 mice using auditory brainstem response (ABR) analysis**

\*A. Lundt<sup>1</sup>, T. Kahl<sup>2</sup>, A. Papazoglou<sup>1</sup>, K. Broich<sup>3</sup>, M. Weiergräber<sup>1</sup>

<sup>1</sup>Federal Institute for Drugs and Medical Devices, Cellular and Systemic Neuropsychology, Bonn, Germany

<sup>2</sup>University of Bonn, Zoology, Bonn, Germany

<sup>3</sup>Federal Institute for Drugs and Medical Devices, Vice President, Bonn, Germany

Voltage-gated Ca<sup>2+</sup> channels are functional key elements in the auditory system. The 1.3 voltage-gated calcium channel is expressed in the outer hair cells of the organ of Corti. Systemic ablation of the Ca<sub>v</sub>1.3 (α1D) subunit has been shown to cause congenital deafness associated with cochlear pathomorphology. Although Ca<sub>v</sub>2.3 R-type Ca<sup>2+</sup>-channels are also expressed in outer hair cells of the organ of Corti, their functional impact in the auditory tract is still unclear. In order to evaluate the role of Ca<sub>v</sub>2.3 channels in the auditory neural pathway, we performed auditory brainstem response (ABR) recordings in Ca<sub>v</sub>2.3 deficient mice aged 5-50 weeks. ABR recordings are a common tool to investigate hearing impairments in humans as well as in animal models. ABR recordings were performed on anesthetized(ketamine/xylazine, 100/10 mg/kg i.p.) animals and electrodes were placed subcutaneously axial and rostral from the pinnae. Broadband clicks and tone bursts (1-78 kHz) with ascending sound pressure levels (0-90 dB) were applied as auditory stimuli to create an auditory profile including general auditory activity, hearing range and threshold. Latency, amplitude and attendance of ABR components were used to detect differences in hearing and possible deficits in the neural pathway. We compared male and female C57BL/6J and Ca<sub>v</sub>2.3 wild-type, heterozygous and knock-out mice. Our results illustrate that although Ca<sub>v</sub>2.3knock-out mice do not suffer from congenital deafness, Ca<sub>v</sub>2.3 voltage-gated Ca<sup>2+</sup>-channel may play an exceptional role in the auditory pathway.

**P368**

**Contributions of the transmembrane pore domains to the gating mechanisms in TREK-1 channels**

\*F. Schulz<sup>1</sup>, M. Rapedius<sup>1</sup>, P. L. Piechotta<sup>2</sup>, E. Nematian-Ardestani<sup>1</sup>, M. Schewe<sup>1</sup>, S. Tucker<sup>3</sup>, T. Baukrowitz<sup>1</sup>

<sup>1</sup>CAU Kiel, Institute of Physiology, Kiel, Germany

<sup>2</sup>University of Jena, Institute of Physiology, Jena, Germany

<sup>3</sup>University of Oxford, Department of Physics, Oxford, United Kingdom

Two-pore domain (K<sub>2p</sub>) potassium channels are important regulators of cellular electrical excitability and are capable of integrating a wide range of signalling pathways such as phosphorylation, various lipids, intracellular pH, anesthetics and mechanosensitivity. The structural basis and molecular mechanisms underlying the various regulatory mechanisms in K2P channels are just starting to emerge. We have previously reported that the TREK-1 primary gating mechanism reside close to, or within the selectivity filter and does not involve gating at the cytoplasmic bundle crossing as seen in e.g. voltage activated K<sup>+</sup> or Kir channels. However, it remains poorly understood how the large number of cellular factors can transfer their regulatory inputs from the cytosolic domains towards the selectivity filter to gate TREK-1 channels. Here we employed high affinity pore blockers and cysteine modification to gain insights into the coupling mechanisms between the intracellular C-terminal domains and the selectivity filter gate. Further, we also used this approach to explore the structural basis of interaction for different TREK-1 pharmacophores such as fluoxetine. Our findings suggest an unusual pore accessibility profile to chemical cysteine modification, which identifies the transmembrane helices as dynamic and gating sensitive domains. We propose a model where C-terminal gating signals are transduced via subtle movements of the transmembrane helices to the selectivity filter gate without large changes in pore opening diameter.

**P369**

**Towards a strategy to treat virus-induced arrhythmias**

\*M. Rohrbeck<sup>1</sup>, K. Steinke<sup>2</sup>, F. Sachse<sup>3</sup>, N. Strutz-Seebohm<sup>1</sup>, U. Henrich<sup>2</sup>, L. Pott<sup>4</sup>, E. Schulze-Bahr<sup>1</sup>, F. Lang<sup>5</sup>, K. Klingel<sup>6</sup>, G. Seebohm<sup>1</sup>

<sup>1</sup>University Hospital Münster, Department of Cardiovascular Medicine, Institute for Genetics of Heart Diseases (IfGH), Münster, Germany

<sup>2</sup>Ruhr University Bochum, Department of Biochemistry I, Cation Channel Group, Bochum, Germany

<sup>3</sup>University of Utah, Department of Bioengineering, Salt Lake City, United States

<sup>4</sup>Ruhr University Bochum, Department of Cellular Physiology, Bochum, Germany

<sup>5</sup>University of Tuebingen, Department of Physiology I, Tuebingen, Germany

<sup>6</sup>University of Tuebingen, Department of Molecular Pathology, University Hospital of Tuebingen, Germany

Coxsackie viruses of type B (CVB) infections can induce severe forms of acute and chronic myocarditis and are often accompanied by ventricular arrhythmias and sudden cardiac death. Recently, we analyzed the mechanisms underlying the development of virus-induced, life-threatening arrhythmias. Viral proteins can modulate ion channel trafficking and increase the proarrhythmic potential whereas the modulation of K<sub>v</sub>7.1/KCNE1 channels seems to be of highest relevance. If these effects have been a motor for genetic selection and can pharmacologically be modulated remains enigmatic. In the poster, we show that the anti-viral compound AG7088 which is currently in clinical development did not prevent these effects on channels. Further, we

show that the common Asian polymorphism K<sub>v</sub>7.1-P448R is a genetic determinant potentially preventing CVB3-induced effects in vitro. This study provides novel data which support that pharmacological targeting or genetic variation of K<sub>v</sub>7.1/KCNE1 channel trafficking could help to develop therapeutic strategies for viral induced arrhythmia treatment.

**P370**

**Progesterone, 4-amino pyridine (4-AP) and quinidine activate voltage-dependent cation channels in human spermatozoa**

S. Mansell<sup>1</sup>, S. Publicover<sup>2</sup>, C. Barratt<sup>1</sup>, \*S. Wilson<sup>3</sup>

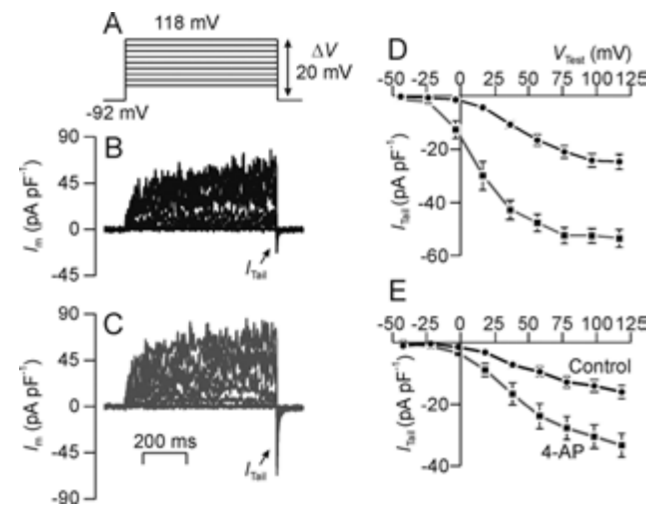
<sup>1</sup>University of Dundee, Division of Cardiovascular and Diabetes Medicine, Dundee, United Kingdom

<sup>2</sup>University of Birmingham, School of Biosciences, Birmingham, United Kingdom

<sup>3</sup>University of Durham, School of Medicine, Pharmacy and Health, Stockton on Tees, United Kingdom

Once in the female reproductive tract, spermatozoa undergo poorly understood maturation changes that lead to the acquisition of fertilizing capacity. The high levels of progesterone encountered as sperm approach the egg thus promote Ca<sup>2+</sup> entry by activating spermatozoon cation channels (CatSper) and thus trigger a transition to 'hyperactive' motility (Lishko et al, Nature 471, 387-392: 2011; Strünker et al, Nature 471, 382-386: 2011). However, 4 amino pyridine (4-AP) also induces hyperactivation of the mechanism underlying this response is poorly understood (Almasmari et al, J Biol Chem 288, 6248-6258: 2013). To define the effects of progesterone and 4-AP upon human spermatozoa, we now explore the effects of these agents upon the conductive properties of these cells. Spermatozoa from normal donors were held under voltage clamp in the whole cell recording configuration using pipette / bath solutions that maintained quasi-physiological ionic gradients; internal pH and [Ca<sup>2+</sup>] were 7.4 and 0.1 μM respectively. Leak / capacitative currents were subtracted from all records. The holding potential was normally -92 mV. Depolarizing voltage steps (Fig 1A) normally evoked outward current that developed over ~200 ms (Fig 1B) that are predominantly due to K<sup>+</sup> exiting the cell via a conductance with relatively poor (~7 fold) K<sup>+</sup> vs. Na<sup>+</sup> selectivity (Data presented at Dresden meeting). Repolarization to -92 mV induced a transient inward current (Fig 1B) whose magnitude was dependent upon V<sub>Test</sub> (Fig 1D). This 'tail' current (I<sub>tail</sub>) must reflect ionic currents through channels activated during depolarization, and ionic substitution experiments showed that these channels were permeable to Na<sup>+</sup>, K<sup>+</sup> and Ca<sup>2+</sup>. Analysis of I<sub>tail</sub> - V<sub>Test</sub> relationship showed that the potential needed for half maximal activation (V<sub>50</sub>) was ~22 mV (Fig 1D). Progesterone (0.5 μM, 2 - 3 min) had no effect upon the outward K<sup>+</sup> current but augmented I<sub>tail</sub> (Fig1C, D) and caused a hyperpolarising shift in V<sub>50</sub> (Fig 1D). 4-AP (2 mM, 2 - 3 min) also had no effect upon the outward K<sup>+</sup> current and enhanced I<sub>tail</sub> although, in contrast to the response to progesterone,

4-AP did alter  $V_{50}$  (Fig 1E). Moreover, although quinidine blocked the voltage-induced outward  $K^+$  current, it mimicked the effects of 4-AP upon  $I_{tail}$ . Spermatozoa therefore express voltage-activated cation channels that are activated by progesterone, 4-AP and quinidine. Since these substances all caused hyperactivation these channels may be important to the control of motility.



**P371**  
**Specific Targeting of Kv7.1/KCNE1 channel complexes**

\*E. Wrobel, N. Strutz-Seeböhm, G. Seeböhm  
Uniklinikum Münster, Institut für Genetik von Herzkrankungen, Münster, Germany

**Background:** The voltage-gated potassium channel  $\alpha$ -subunit Kv7.1 is expressed in several human tissues including heart, epithelia and smooth muscle. To fulfill its physiological functions Kv7.1 is co-assembled with different members of the KCNE  $\beta$ -subunit family. Best studied is the molecular basis of interactions between KCNE1 and Kv7.1, which, together, supposedly form the channel complex underlying native cardiac I(Ks) current. Besides biophysical effects the pharmacology of Kv7.1 is modulated by KCNE1. A novel compound reported to potently inhibit cardiac I(Ks) is JNJ303. This substance evoked unprovoked torsades de pointes arrhythmias in vivo in an anesthetized dog model.

**Methods:** The aim of the present study was to gain deeper insights into the molecular mechanisms underlying JNJ303 inhibition of Kv7.1/KCNE1 channels. Therefore, we expressed these channels in *Xenopus laevis* oocytes and tested their sensitivity to JNJ303 using two-electrode voltage clamp (TEVC). To determine the putative binding site of this inhibitor we used site-directed scanning mutagenesis combined with electrophysiology and molecular docking.

**Results:** Here, we present data on a highly potent Kv7.1/KCNE1 inhibitor. This compound blocks Kv7.1/KCNE1 channels by modulating channel gating. Using different approaches we localized the putative drug receptor of JNJ303 to the pore region, especially, the S6 transmembrane segment of Kv7.1. In the future the growing knowl-

edge of inhibitor binding sites may help us to design novel specific ion channel modulators or to prevent unwanted binding to channels like Kv7.1/KCNE1 during early drug development.

**P372**  
**Functional characterization of novel HCN4 mutations associated with cardiac arrhythmia**

\*M. Moeller<sup>1</sup>, E. Wrobel<sup>1</sup>, N. Strutz-Seeböhm<sup>1</sup>, E. Schulze-Bahr<sup>1</sup>, G. Seeböhm<sup>1</sup>  
<sup>1</sup>Institute for Genetics of Heart Diseases, Department of Cardiovascular Medicine, Münster, Germany

**Background:** The hyperpolarization-activated cyclic nucleotide-gated channel 4 (HCN4) is thought to play a critical role in generating the spontaneous sinus node action potential and in accelerating the heart rate during sympathetic drive. The relevance of HCN4 channels to pacemaking has been further supported by the discovery of four loss-of-function mutations (S672R, 573X, 695X, D553N) in patients suffering from inherited sinus bradycardia. All of these mutations are mainly located in the C-terminus of HCN4 and exhibit their dominant-negative effect by altering voltage-dependence of channel activation, decreasing channels cAMP-sensitivity or leading to a mis-trafficking of channel proteins. In this study, we identified and analyzed five novel HCN4 mutations in patients suffering from sinus node dysfunction, dyspnea and atrial fibrillation.

**Methods:** To study the biophysical properties of the five novel HCN4 mutants, these channels were expressed in *Xenopus laevis* oocytes and analyzed using two-electrode voltage clamp (TEVC). Further, membrane expression of the mutated channels was studied using Western Blot and Immunodetection.

**Results:** Here, we report that two HCN4 channels carrying a point mutation in S4 and in the pore-domain mediated If-like currents that were significantly decreased compared to wildtype channels and therefore result in channels loss-of-function. Additionally, co-expression experiments indicate a dominant-negative effect of one specific point mutation on wild-type subunits. Taken together, our data indicate that disease associated mutated HCN4-channels show altered biophysical properties.

**P373**  
**Impact of a Kv7.1-channel key residue in complex cardiac disease**

\*I. Rothenberg<sup>1,2</sup>, N. Strutz-Seeböhm<sup>2</sup>, E. Schulze-Bahr<sup>2</sup>, N. Schmitt<sup>3</sup>, G. Seeböhm<sup>2</sup>

<sup>1</sup>Faculty of Chemistry and Biochemistry, Ruhr University Bochum, Department of Biochemistry I – Cation Channel Group, Bochum, Germany

<sup>2</sup>Institute for Genetics of Heart Diseases (IfGH), University Hospital Münster, Department of Cardiovascular Medicine, Münster, Germany

<sup>3</sup>Faculty of Health and Medical Sciences, University of Copenhagen, Department of Biomedical Sciences, Copenhagen, Denmark

**Background:** Kv7.1 belongs to the family of voltage-gated potassium channels and is expressed in several tissues throughout the human body. The Kv7.1  $\alpha$ -subunit, assembled with the KCNE1  $\beta$ -subunit, forms a channel complex constituting the cardiac delayed rectifier current  $I_{Kr}$ .  $I_{Kr}$  plays a critical role in repolarization of the cardiac tissue terminating the action potential. The physiological relevance of this channel is further underlined by the observation that mutations in its gene KCNQ1 are associated with cardiac disorders like short QT syndrome (SQTS) or long QT syndrome (LQTS). In this study, we analyzed the relevance of Kv7.1 residue A287 which was identified in patients suffering from cardiac arrhythmias and atrial fibrillation.

**Methods:** To gain deeper insights into the molecular mechanism leading to channel dysfunction, the alanine residue at position 287 was systematically exchanged to different amino acids. The resulting channel complexes were studied using two-electrode voltage clamp method (TEVC). In addition, surface membrane expression of these mutant channels was determined using Western Blot analysis.

**Results:** Electrophysiological measurements indicated that the specific physico-chemical nature of this residue determines function of channels. Both, gain-of-function and loss-of-function of A287 mutants were found which helps to explain the complex clinical findings.

**P374**  
**Tonic GABA controls excitability in a central auditory nucleus**

\*A. Fischer, E. Friauf  
TU Kaiserslautern, Biology, Kaiserslautern, Germany

Neurons of the lateral superior olive (LSO), a brainstem nucleus involved in sound source localization, integrate excitatory and inhibitory inputs from the ipsi- and contralateral ear, respectively. Interaural level differences consequently become encoded as discharge rate of LSO neurons. Although contralateral synaptic inhibition is mediated by glycine and ipsilateral excitation by glutamate, both inputs are tonically balanced via presynaptic GABA<sub>B</sub>Rs by ambient GABA (Magnusson et al., 2008). In neonates, activation of postsynaptic GABA<sub>B</sub>Rs causes long-term depression of inhibitory inputs (Chang et al., 2003). Thus, GABA plays a crucial role in synaptic transmission in the LSO. However, nothing is known about GABA-mediated tonic inhibition through extrasynaptic receptors in this nucleus. Therefore, we asked two questions. 1. Do LSO neurons exert extrasynaptic GABAergic inhibition? 2. If so, does tonic inhibition by GABA influence excitability? Although recordings from patch-clamped LSO neurons displayed no GABA-mediated synaptic transmission, puff application of exogenous GABA resulted in robust GABA<sub>A</sub>R-mediated currents. Hence, LSO neurons do express functional extrasynaptic GABA<sub>A</sub>Rs. Tonic inhibition under physiological GABA concentrations efficiently suppressed neuronal spiking caused

by supra-threshold current injections of control recordings. As this shift of excitability was accompanied by a decrease in overall membrane resistance, we argue that tonic GABA strongly facilitates shunting inhibition. Taken together, we extend the previously described role of GABA in the LSO from a purely synaptic point of view to an overall modulator of neuronal excitability.

**P375**  
**Functional characterization of heteromeric TRPV channels**

\*S. Cordeiro, N. Hering, T. Baukrowitz  
Christian-Albrechts-University Kiel, Institute of Physiology, Kiel, Germany

TRPV channels are a subfamily of the transient receptor potential (TRP) channel family that can be further subdivided into two subgroups, TRPV1-4 and TRPV5-6. TRPV 1-4 channels are non-selective cation channels that are regulated by a variety of stimuli including heat, vanilloids, osmotic stress, voltage and low extracellular pH but differ substantially in their respective sensitivity to the different stimuli. It is well known that some TRP channels can form heteromeric channels. However, for the TRPV channel subgroup the formation of heteromeric tetramers is still under debate. To this end we constructed dominant-negative mutants of different TRPV channel subunits and co-expressed them with the different TRPV WT subunits in *Xenopus* oocytes and HEK293 cells for electrophysiological characterization. Furthermore, we constructed the following concatamers: TRPV1-TRPV1, TRPV1-TRPV2, TRPV1-TRPV3, and TRPV1-TRPV4 to study heteromeric TRPV channels with fixed stoichiometry. We show that some TRPV channels (e.g. TRPV1 and TRPV2) form heteromeric channels with properties different to respective homomeric channels. The physiological and functional consequences of heteromeric TRPV channels will be discussed.

**P376**  
**Dystrophin deficiency leads to drastic weakness of mdx diaphragm muscle, but has little influence on soleus muscle force**

\*Y. Zhang<sup>1</sup>, J. Zschüntzsch<sup>2</sup>, J. Schmidt<sup>2</sup>, H. Brinkmeier<sup>1</sup>  
<sup>1</sup>University of Greifswald, Institute of Pathophysiology, Greifswald, Germany  
<sup>2</sup>University of Goettingen, Institute of Neurology, Goettingen, Germany

**Objective:** Duchenne muscular dystrophy and the homologue mouse model mdx are characterized by fiber degeneration, regeneration and fibrosis in most skeletal muscles. In mice, dystrophin deficiency causes a rather mild phenotype compared to humans. Only aged mdx mice develop fibrosis and weakness in some of their muscles. Nevertheless, most studies on mdx muscular dystrophy are performed with young or just adult animals. To provide a basis for studies on aged mdx mice, we investigated force characteristics and histological features of diaphragm and soleus muscles of 18 month old mdx and wildtype mice.



**Methods:** Isometric force of soleus muscles and segments of diaphragms (DIA) from wildtype (WT) and mdx mice was tested in vitro at 25 °C. Electrical stimulation protocols allowed us to record single twitches, maximum tetanic forces (at 120 Hz) and muscle fatigue. The histological analysis of muscle cross sections included H&E, Sirius Red and myosin-ATPase stainings.

**Results:** Twitch force and maximal tetanic force were drastically reduced in aged mdx DIA, but not in M. soleus. Specific maximal tetanic force of mdx DIA segments (at 120 Hz stimulation) was on average  $47.0 \pm 3.6$  mN/mm<sup>2</sup> (WT:  $142 \pm 12$  mN/mm<sup>2</sup>, mean  $\pm$  SEM, n = 8 and 10, respectively). When the same test was applied to mdx soleus muscle, force reduction was only 10% compared to WT. The absolute force of mdx soleus muscles was even higher than that of WT animals due to muscle hypertrophy. Kinetics of twitches and tetani were not altered for both mdx muscles. However, when we studied muscle fatigue, a strongly reduced fatigability of mdx DIA was observed. After 300 s of sustained repetitive stimulation, force reduction was on average 62% for WT muscle, but only 24% for mdx muscle (n = 8 vs. 10). The data are in agreement with a shift to fast twitch oxidative fibers (type IIA) in aged mdx DIA. Histological data on muscle fiber types are in preparation.

**Conclusion:** Dystrophin deficiency has highly differential effects on mouse muscles. Muscle weakness becomes obvious only in aged mdx diaphragm, but not in M. soleus. The differential response of human and mouse muscles to the lack of dystrophin should be kept in mind when experimental treatment is studied in mdx mice.

**P377**

**TRPV channels are regulated by the intracellular pH**

\*N. Hering, S. Cordeiro, T. Baukrowitz

Institute of Physiology, Workgroup Baukrowitz, Kiel, Germany

TRPV channels (Transient Receptor Potential Vanilloid) are a subfamily of the TRP family. TRPV channels can be subdivided into two subgroups, TRPV 1-4 and TRPV 5/6. TRPV 1-4 channels are non-selective cation channels that are activated by a variety of stimuli including heat, vanilloids, osmotic stress and low extracellular pH. Here we investigated TRPV1, TRPV2, TRPV3 and TRPV4 channels expressed in *Xenopus* oocytes using the patch-clamp-technique in the inside-out configuration. It is well accepted that TRPV1 channels are activated by low extracellular pH<sub>extra</sub> but the effect of changes in the intracellular pH<sub>intra</sub> led to inconsistent results. Here we show that TRPV1 is activated by acidic pH<sub>i</sub> with an even stronger potency than by the TRPV channel activator 2-APB. The pH<sub>i</sub> activation occurred within the physiological/pathophysiological pH range with an EC<sub>50</sub> of  $6.6 \pm 0.1$ , a Hill coefficient of  $3 \pm 0.5$  and maximal activation at pH6. Similar to TRPV1 pH<sub>i</sub> activation was also seen for TRPV2 and TRPV3 channels and, thus, pH<sub>i</sub> activation appears to be a general property of the TRPV 1-4 subgroup. Furthermore, data on the molecular mechanism underlying pH<sub>i</sub> activation in the TRPV1 channel will be presented.

**P378**

**Investigating the oligomerisation behaviour of connexins by building concatemeric connexins**

\*P. Schadzek<sup>1</sup>, B. Schlingmann<sup>2</sup>, A. Ngezahayo<sup>1,3</sup>

<sup>1</sup>Leibniz University Hannover, Institute of Biophysics, Hannover, Germany

<sup>2</sup>Emory University School of Medicine, Department of Pulmonary, Allergy and Critical Care Medicine, Atlanta, United States

<sup>3</sup>University of Veterinary Medicine Hannover, Center for Systems Neuroscience, Hannover, Germany

Gap junction channels are composed of two connexons or hemichannels, which consist of six protein subunits, called connexins (Cx). Formation of gap junction between cells is a complex process in which homomeric (one Cx type) and heteromeric (more than one Cx type) connexons were proposed, as well as homotypic (two equal homomeric connexons), heterotypic (two different homomeric connexons) and heteromeric heterotypic (two heteromeric connexons) gap junction channels. We generated eGFP labelled hCx46 and concatemeric hCx46-hCx46 mutant called tandem and expressed them in gap junction deficient HeLa cells to analyse their capacity to form functional gap junction channels. Western blot experiments showed that the tandem was expressed as one single protein with the expected size. Confocal laser scanning microscopy revealed that the tandem formed gap junction plaques similar to those of the hCx46. Dye transfer experiments revealed that both tandem and hCx46 formed metabolically coupled gap junction channels. The experiments show that the concatemericization of a connexin does not alter the capacity of the connexin to form functional gap junction channels. Experiments using *Xenopus* oocytes expressing different connexins, have confirmed the formation of heterotypic gap junction channels. Moreover, it was found that not every combination of connexins leads to functional gap junction channels, suggesting complex Cx-Cx specificity. So far, evidence for formation of functional heteromeric connexons could not be conclusively found. Our results constitute a first attempt to analyse the formation of heteromeric connexons. They open up the possibility of studying interaction specificity between connexins during formation of gap junction channels.

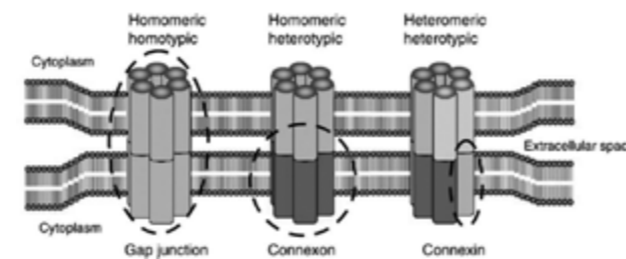


Figure 8 | Different level of connexin organisation in gap junction channels.

**P379**

**Regulation of functional TREK-1 channel expression by TWIK-1**

\*E. Nematian Ardestani, M. Musinszki, T. Baukrowitz

Institute of Physiology Kiel, Kiel, Germany

Two-pore domain (K2P) potassium channels form a family of 15 members that are important regulators of cellular electrical excitability. The formation of heteromeric channels between the different K2P channels is currently poorly understood. Here we investigated whether the expression of TREK-1 channels is effected by the presence of TWIK-1 channels since both channels are found to co-localize in various cells such as astrocytes. Expression of TREK-1 and TWIK-1 channel was investigated in inside-out patches excised from *Xenopus* oocytes as well as by fluorescence microscopy subsequent to immunostaining. We found that TREK-1 generated large currents while for TWIK-1 channels no currents were detectable consistent with previous reports demonstration of TWIK-1 retention in intracellular compartments. Co-expression of TREK-1 and TWIK-1 resulted in largely reduced TREK-1 currents and TREK-1 localisation changed from the plasma membrane to intracellular compartments while e.g. TRESK currents were unaffected by TWIK-1 expression. Further, TREK-1 co-expression with a double TWIK-1 mutant (I293A, I294A) removing the TWIK-1 retention signal resulted in TREK-1 and TWIK-1 currents with clearly different properties but, surprisingly, no channels with novel properties indicating the formation of functional TREK-1/TWIK-1 heteromers were observed. These results suggest that TREK-1 and TWIK-1 can interact in internal compartments resulting in the retention of TREK-1 in the presence of TWIK-1. However, when TWIK-1 retention is removed in the TWIK-1 double mutant TREK-1 and TWIK-1 are processed separately to the plasma membrane. Our findings indicate that the interaction of TREK-1 and TWIK-1 might represent a possible mechanism to control TREK-1 currents in cells.

**P380**

**Involvement of gap junction hemichannels in GFSHR-17 granulosa cells during folliculogenesis**

\*N. Dilger<sup>1</sup>, W. Bintig<sup>2</sup>, A. Ngezahayo<sup>1</sup>

<sup>1</sup>Leibniz University Hannover, Institute of Biophysics, Hannover, Germany

<sup>2</sup>Charité - Universitätsmedizin Berlin, Cellular and Molecular Neurobiology, Berlin, Germany

The granulosa like GFSHR-17 cells express the FSH receptor. They were proposed as an in vitro model to study the physiology of follicular maturation. Using the whole-cell patch-clamp configuration, we showed that the GFSHR-17 cells have a resting membrane potential of about -30 mV. Application of voltage pulses between -120 mV and 90 mV evoked a strong outward current and a low inward current. In the presence of the non-specific gap junction inhibitor carbenoxolone (CBX) the membrane potential was strongly reduced. CBX as well as the Cx43 specific mimetic peptide 43Gap26 significantly decreased the outward currents.

Previously, we proposed that a P2Y<sub>2</sub> and P2Y<sub>4</sub> regulated chloride permeability in GFSHR-17 cells could be a key mechanism for the secretion of follicular fluid during follicular maturation. ATP stimulates these P2Y receptors, which could lead to an increasing intracellular Ca<sup>2+</sup> concentration and thus could close the gap junction channels. Consequently ATP treatment should lead to a transient hyperpolarisation of the cell, which we were able to show. Here we provide evidence that the chloride permeability of the GFSHR-17 granulosa cells is related to gap junction hemichannels, which are closed by Ca<sup>2+</sup> released by stimulation of the P2Y<sub>2</sub> and P2Y<sub>4</sub> receptors.

**P381**

**The Y39 in N-terminal unique region of NBCe1B plays an inhibitory role of NBCe1 electrogenicity**

\*J. Xu<sup>1</sup>, H. Ji<sup>1</sup>, S. Yeruva<sup>1</sup>, B. Riederer<sup>1</sup>, M. Soleimani<sup>2</sup>, U. Seidler<sup>1</sup>

<sup>1</sup>Image Hannover Medical School, Gastroenterology, Hepatology and Endocrinology, Hannover, Germany

<sup>2</sup>University of Cincinnati, Center on Genetics of Transport and Epithelial Biology, Cincinnati, Ohio, United States

**Question:** The sodium bicarbonate cotransporter NBCe1 is crucial to the reabsorption of HCO<sub>3</sub><sup>-</sup> in the kidney and for the secretion of HCO<sub>3</sub><sup>-</sup> in pancreatic ducts. The two major isoforms NBCe1A (kidney) and B (pancreatic) exhibit differential electrogenicities. It is hypothesized that there is an inhibitory mechanism in the unique N-terminal region of NBCe1B (Boron, et al., J Exp Biol 2009).

**Methods:** The aim of the current study was to identify such inhibitory component(s). Various NBCe1 mutants were generated by site-directed mutagenesis, and pH<sub>i</sub>-recovery (when expressed in HEK 293 cells) in the presence of HCO<sub>3</sub><sup>-</sup> was analysed.

**Results:** The rates of pH<sub>i</sub>-recovery from acidosis were measured in BCECF-loaded transfected HEK293 cells in the presence of sodium and bicarbonate, with 1 mM amiloride to inhibit NHEs. pH<sub>i</sub> recovery rate was significantly lower in HEK293 cells transfected with NBCe1B than that in the cells transfected with NBCe1A. A deletion of a.a. from delta 31 to 41 resulted in disinhibition of NBCe1B activity. (n= p<0.05). Furthermore, the specific pointed-mutation Y39A (changing tyrosine to alanine) in NBCe1B disinhibited NBCe1B activity (NBCe1B Y39A, n=11, p<0.05). The pH<sub>i</sub> recoveries from acidosis in HEK293 cells with NBCe1 wild type and mutant expression were abolished in the presence of 0.2 mM DIDS.

**Conclusion:** As previously shown for *Xenopus* oocytes, NBCe1B also displays less HCO<sub>3</sub><sup>-</sup> transport activity than NBCe1A under Vmax conditions in the HEK293 expression system. Mutating the amino acid residue Y39 of the N-terminal unique domain of NBCe1B noticeably increase its activity, demonstrating that amino acid residue tyrosine at 39 of NBCe1B is a component involved in inhibitory mechanism of in the unique N-terminal region of NBCe1B.

P382

**Investigating the role of the tetradic arrangement of DHPRs in skeletal muscle excitation-contraction coupling**

A. Polster<sup>1</sup>, N. F. Linde<sup>2</sup>, D. Filipova<sup>2</sup>, A. Walter<sup>2</sup>, K. G. Beam<sup>1</sup>, \*S. Papanopoulos<sup>2</sup>

<sup>1</sup>University of Colorado, Physiology and Biophysics, Aurora-Denver, United States

<sup>2</sup>Medical Faculty of the University of Cologne, Institute of Vegetative Physiology, Cologne, Germany

Excitation-contraction coupling (ECC) in skeletal muscle is characterized by a unique mode of coupling the electrical signal (action potential, depolarization) to Ca<sup>2+</sup> release from sarcoplasmic reticulum (SR): Experimental evidence suggests that the voltage-gated Ca<sup>2+</sup> channel Dihydropyridine receptor (DHPR), anchored in the surface/t-tubular membrane, acts primarily as voltage-sensor, mechanically transmitting the depolarization-induced conformational changes to the Ca<sup>2+</sup> release channel of the SR membrane, the type 1 Ryanodine receptor (RyR1). Ultrastructural studies, by demonstrating a regular arrangement of DHPRs in groups of four (tetrads), are in favor of a model according to which the homotetrameric symmetry of a single RyR1, by mechanical coupling to four DHPRs, imposes the tetradic arrangement of the latter. Interestingly, ultrastructural studies also reveal the abundant presence of incomplete tetrads, especially during muscle differentiation. One question arising is therefore, what exactly is the mode of operation of the tetradic arrangement? Specifically, does proper conformational coupling between the RyR1 and the DHPR (ore more precise, the DHPR a<sub>1s</sub> subunit) require the presence of all four DHPR:RyR1 interactions in the tetrad or could even a single DHPR initiate RyR1 opening. In the latter case, the additional DHPR:RyR1 interactions within the tetrad could serve as safety mechanism to guarantee reliable RyR1 gating when other DHPRs within the same tetrad fail. Since these questions are very difficult to address via expression of single DHPR a<sub>1s</sub> subunits, over a broad range of DHPR activation. We here describe a way to experimentally dictate the composition of individual tetrads by designing DNA plasmids for the expression of fluorescently labeled a<sub>1s</sub> multimers, encoding up to four covalently linked subunits (a<sub>1s</sub>-a<sub>1s</sub>-a<sub>1s</sub>-a<sub>1s</sub>). Upon expression of the constructs in dysgenic (=no endogenous a<sub>1s</sub>) myotubes, these constructs (a) prevailed as stable fusions, (b) displayed moderate to proper trafficking, (c) displayed moderate to normal L-type Ca<sup>2+</sup> currents and, most importantly, (d) were able to reconstitute ECC, as demonstrated by the presence of Ca<sup>2+</sup> transients and cell twitches. Western Blot analysis of these multimeric a<sub>1s</sub> constructs, expressed in the dysgenic GLT cell line, is under way. As is ultrastructural analysis, aiming to elucidate the arrangement of the multimers in subcellular regions of DHPR:RyR1 interaction.

---

---

---

---

---

---

---

---

---

---

---

---

---

---

---

---

---

---

---

---

---

---

---

---

---

---

---

---

---

---